Department of Chemistry

Antiprotozoals based on the inhibition of *N*-Myristoyltransferase

Robert Alexander Norman Clegg

This thesis is presented for the Degree of
Doctor of Philosophy
of
Curtin University

May 2018

Abstract

Malaria and Human African Trypanosomiasis are vector borne protozoan parasitic diseases. Resistance to current treatments is widespread with many historical treatments becoming obsolete and ineffective or contain impracticable treatment regimes. *N*-Myristoyltransferase (NMT) inhibition is being targeted towards such diseases. This project developed a structure-activity investigation into transition state mimetic inhibitors of NMT and demonstrated their activity towards *T. brucei and* two strains of *P. falciparum.*

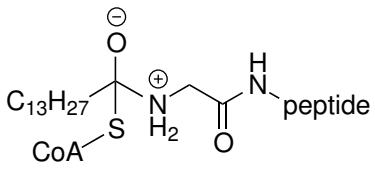

1

CoA-Myristoyl-peptide NMT intermediate

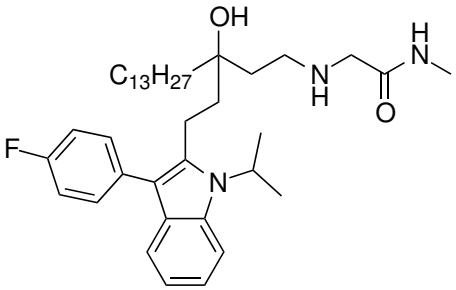

4

Potential NMT transition state mimetic

The initial investigation synthesised a simplified transition state mimetic **108** from myristic acid using protecting group strategies. The hydroxyamine scaffold contained on hydroxyamine **109** was consequently present in numerous other derivatives. The structure-activity investigation successfully demonstrated that the activity towards *T. brucei and P. falciparum* is due to the key features of the hydroxyamine **109**.

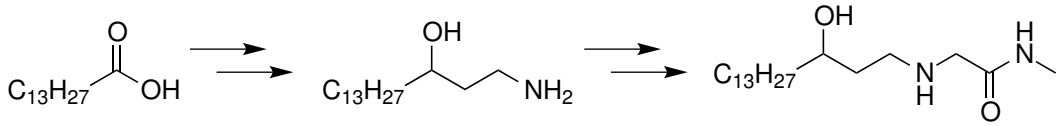

7 **109** **108**

		SI		SI
T.brucei IC_{50}:	0.27 ± 0.01 µM	83	0.30 ± 0.01 µM	>167
P.falciparum TM4 IC_{50}:	20.2 ± 0.95 µM	1.1	> 50 µM	-
P.falciparum K1CB1 IC_{50}:	20.8 ± 2.38 µM	1.1	> 50 µM	-
VERO IC_{50}:	22.3 ± 1.09 µM	-	>50 µM	-

The project investigated the introduction of fragments from HMG-reductase inhibitors into the hydroxyamine scaffold. A cerium acetylide addition reaction was used to gain access to a series of tertiary alcohol derivatives and reductive aminations to make the amine derivatives. Early synthetic HMG-reductase inhibitors were incorporated to investigate their activity towards *T. brucei and P. falciparum* by inhibition of NMT.

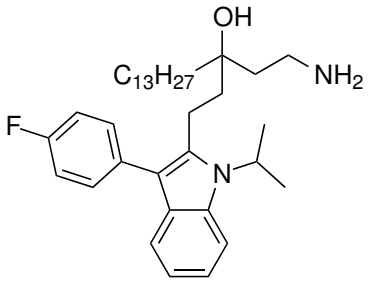

116

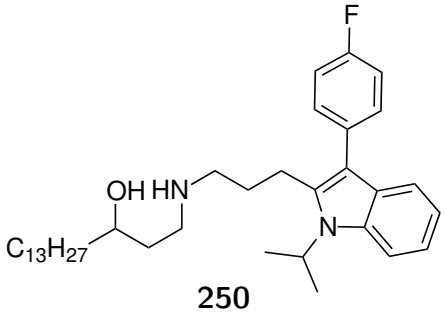

250

	116	SI	**250**	SI
T.brucei IC_{50}:	2.75 ± 0.21 µM	8.8	19.2 ± 1.33 µM	1.2
P.falciparum TM4 IC_{50}:	24.2 ± 3.60 µM	1.0	8.42 ± 3.76 µM	2.8
P.falciparum K1CB1 IC_{50}:	14.4 ± 4.57 µM	1.7	3.49 ± 1.01 µM	6.7
VERO IC_{50}:	24.3 ± 2.1 µM	-	23.5 ± 1.58 µM	-

Derivatives were also developed that included alkene and phenoxy variation of the myristoyl chain, which built on the chemistry used to generate the hydroxyamine **109**. However, derivatisation did not improve the selectivity and potency profile of the parent hydroxyamine **109**.

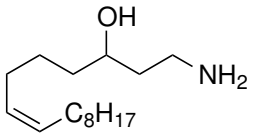

263

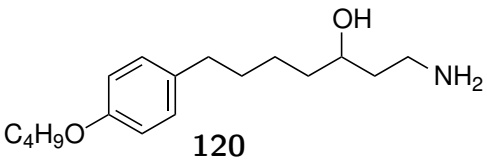

120

	263	SI	**120**	SI
T.brucei IC_{50}:	3.12 ± 0.05 µM	>16	2.79 ± 0.21 µM	>18
P.Falciparum TM4 IC_{50}:	21.0 ± 2.79 µM	>2.4	21.1 ± 3.42 µM	>2.4
P.Falciparum K1CB1 IC_{50}:	17.5 ± 2.25 µM	>2.9	22.4 ± 3.06 µM	>2.2
VERO IC_{50}:	>50 µM	-	>50 µM	-

Acknowledgements

I must truly thank both my parents for giving me the foundation as to hold enough thoughts, for long enough, to be able to progress through the complexity.

I would not have achieved higher level understandings without the true educators in my life. I have enormous gratitude these educators; Nicole Caporn, my high school chemistry teacher, who successfully sparked scientific curiosity which I hope will never cease. Mauro Mauroceno, my co-supervisor for helping me in developing and applying the curiosity throughout my tertiary level education and Alan Payne my primary doctorate supervisor for countless hours of patient complex discussion, scientific rigour and proofing that has help me enormously through the ideas contained in this thesis. All have contributed to the building of a set of professional skills that both continue to grow and will be near imposable to lose.

I must acknowledge the relationships that have inherently suffered as a result of the completion of this doctorate. I will be eternally grateful for the continuous support, often though the acceptance of my absence, or the countless hours that my friends, both professional and personal, and family who have listened, I am however the most grateful for those who refused to listen too much.

I would also like to acknowledge some of my less scientific attributes to my Uncle, Alan Geoffrey Read, who sadly passed during the completion of this thesis. He was a true adventurer, with logic that surpasses no other and is missed by his friends and family.

Contents

List of abbreviations

2M2B	2-methyl-2-Butene
ATR	Attenuated total reflectance
Bn	Benzyl
br	Broad
CoA	Co-Enzyme A
CDI	carbonyl diimidazole
$CDCl_3$	Deuterated chloroform
CBz	Carboxybenzyl
d	Doublet
dd	Doublet of doublets
ddd	Doublet of doublets of doublets
dt	Doublet of triplets
DCE	1,2-Dichloroethane
DCM	dichloromethane
DIPEA	disopropylethylamine
DMSO	Dimethyl sulfoxide
DMF	*N*,*N*-Dimethylformamide
EC_{50}	Half maximal effective concentration
Eq.	Equilivents
EtOAc	Ethyl Acetate
EtOH	Ethanol
ESI	Eletrospray Ionisation
h	Hour(s)
HMDS	Hexamethyldisilazane
HRMS	High Resolution Mass Spectrometery
HDL	High Density Lipoproteins
KTA	Potassium *tert*-Amylate
LDL	Low Density Lipoproteins
IBX	2-Iodoxybenzoic acid
IR	Infrared

J	Coupling Constant
IC_{50}	Half maximal inhibitory concentration
PCC	Pyridinium chlorochromate
ppm	Parts per million
Py	pyridine
Ph	Phenyl
PS	Petrolium sports
q	Quartet
RT	Room temperature
s	Singlet
t	Triplet
td	Triplet of doublets
TBAF	*tert*-Butyldimethylsilyl
Tol	Toluene
TEA	Triethylamine
TMS	Trimethylsilyl
THF	Tetrahydrofuran
TLC	Thin layer chromatography
tt	Triplet of triplets
TBAB	Tertbutyl ammonium bromide

Chapter 1

Introduction

The inhibition of *N*-Myristoyltransferase (NMT) is being targeted as treatments for fungal, protozoan and viral diseases. NMT uses a myristoylated Co-enzyme A (CoA) substrate during it catalytic cycle. The transition state intermediate **1** present during the catalytic cycle is shown in Figure 1.1. A compound that mimics **1** would give rise to a new group of inhibitors that combine three aspects of the intermediate; the peptide, CoA and myristoyl chain. Mimetics of CoA are known, and have been used in the inhibition of 3-hydroxy-3-methylglutaryl-CoA (HMG-CoA) reductase to control cholesterol biosynthesis. This led to the development of the HMG-reductase inhibitors, the statins, that are HMG-CoA **2** mimetics and blockbuster pharmaceutical drugs. Statins (e.g. fluvastatin **3**) contain two regions; a HMG mimetic and a hydrophobic portion that binds into an area of HMG-CoA reductase where Co-Enzyme A would be located. The purpose of this project is to develop a NMT transition state mimetic which may incorporate aspects of the statins and applying them towards the inhibition of NMT. The hypothetical compound **4** combines critical areas of the myristoyl-CoA intermediate **1** with fluvastatin. This project will investigate the structure-activity relationships of compounds such as **4** in relation to activity against *T. brucei* and *P. falciparum.*

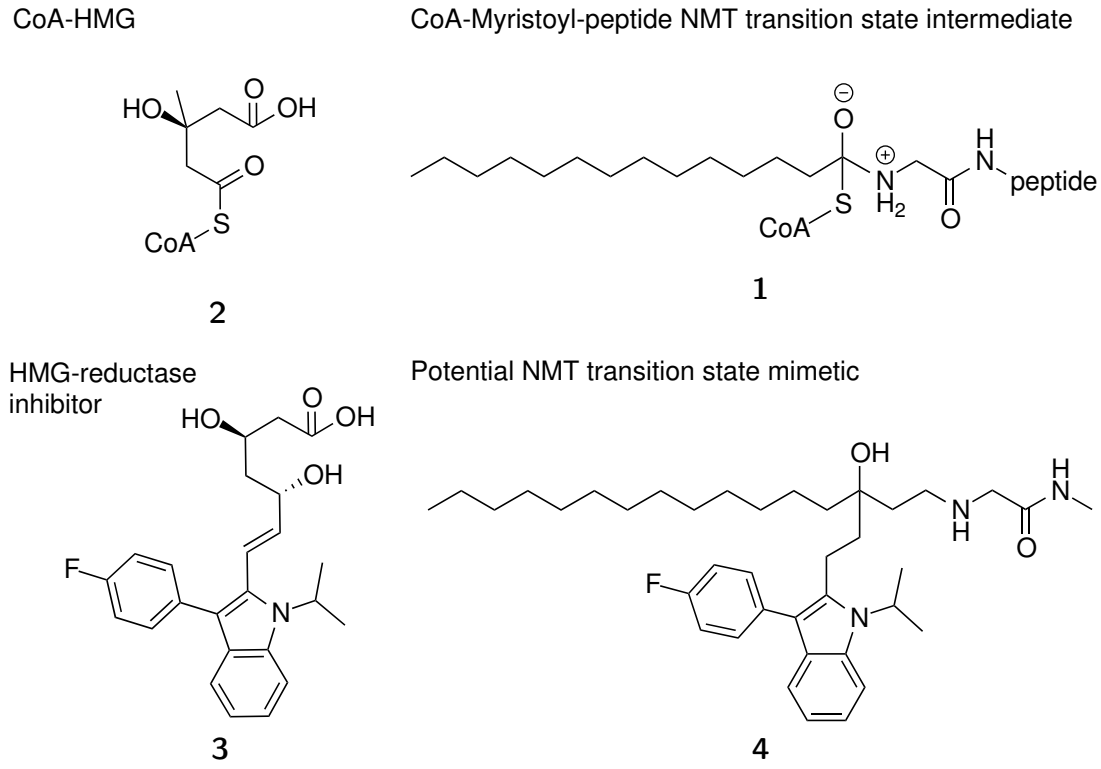

Figure 1.1: Introduction

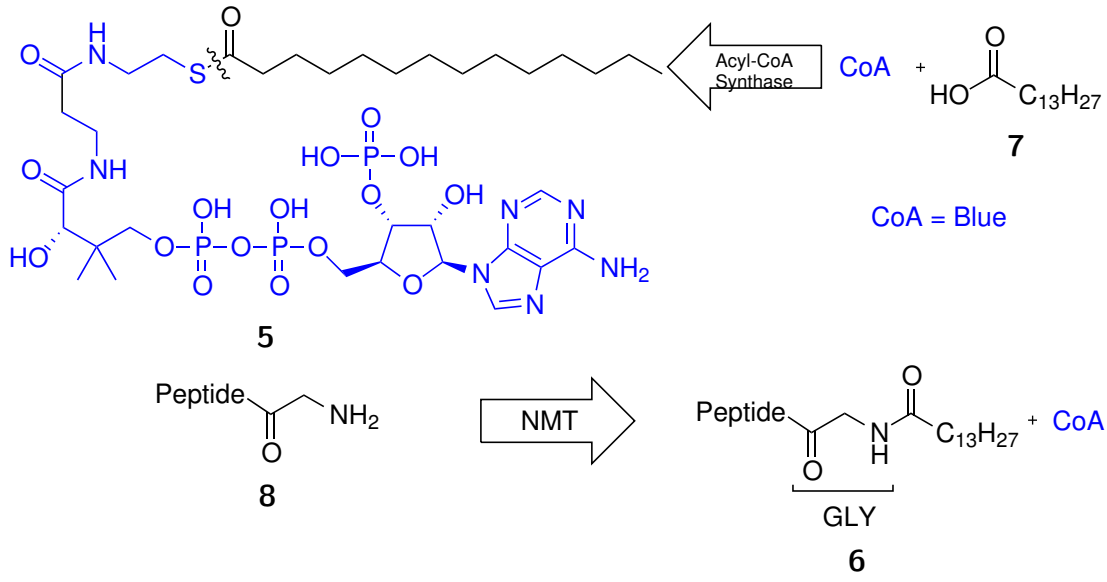

Figure 1.2: The reaction catalysed by NMT and the formation of its substrate Myristoyl-CoA **5** catalysed by Acyl-CoA synthase

1.1 *N*-Myristoyltransferase (NMT)

N-Myristoyltransferases are enzymes responsible for modifying specific proteins by covalent attachment of myristic acid (Figure 1.2). *N*-Myristoylation occurs at the glycinyl *N*-terminus of specific targeted peptides **8**. Myristoyl-CoA, the NMT substrate, is the product of the substitution reaction between CoA and Myristic acid, catalysed by Acyl-CoA synthase. NMT catalyses thioester cleavage of Myristoyl-CoA **5** and directs the substitution of the peptide substrate. Although the biological functions of myristoylated peptides are complex, it is well understood that the hydrophobic myristoyl chain can anchor the peptide into the lipid bilayer.

NMT exists in all eukaryotic cellular organisms[1] and are related to the GCN5 superfamily of enzymes.[2,3] Significant genetic variance exists between species expressing NMT with significant genetic variation depending on the source organism. As a consequence of genetic variation, NMT inhibitors have been widely studied in an effort to exploit selectivity towards various therapeutic targets, without adverse human toxicity. Currently there are no licensed NMT inhibitors in the clinical domain.

NMT was first isolated from *Saccharomyces cerevisiae* and its catalytic kinetics were established using reverse phase HPLC.[4] Rudnick *et al.* showed that myristoyl-CoA binds to NMT prior to the peptide recognition. After catalysis NMT has little affinity for CoA, releasing it before the myristoylated peptide. The mechanistic study confirmed the stability of NMT-Myristoyl-CoA complex and its Bi-Bi ordered mode of action (Figure 1.3). The first three dimensional structure of *Candida albicans* NMT (caNMT[5]) was resolved in 1998 closely followed by *Saccharomyces cerevisiae* NMT (scNMT[6]) and provided the first structural analysis and mechanistic description of the catalytic mode of action of NMT.

The active site of NMT contains 4 distinct regions that act synergistically (Figure 1.4A). A deep hydrophobic pocket extends the length of NMT and provides internalisation and stabilisation of the myristoyl chain. Bhatnagar *et al.* crystallised ScNMT with *S*-(2-oxo)pentadecyl-CoA **9** (originally synthesised by Zheng *et al.*[7]) . *S*-(2-oxo)pentadecyl-CoA **9** has a non-cleavable methylene between car-

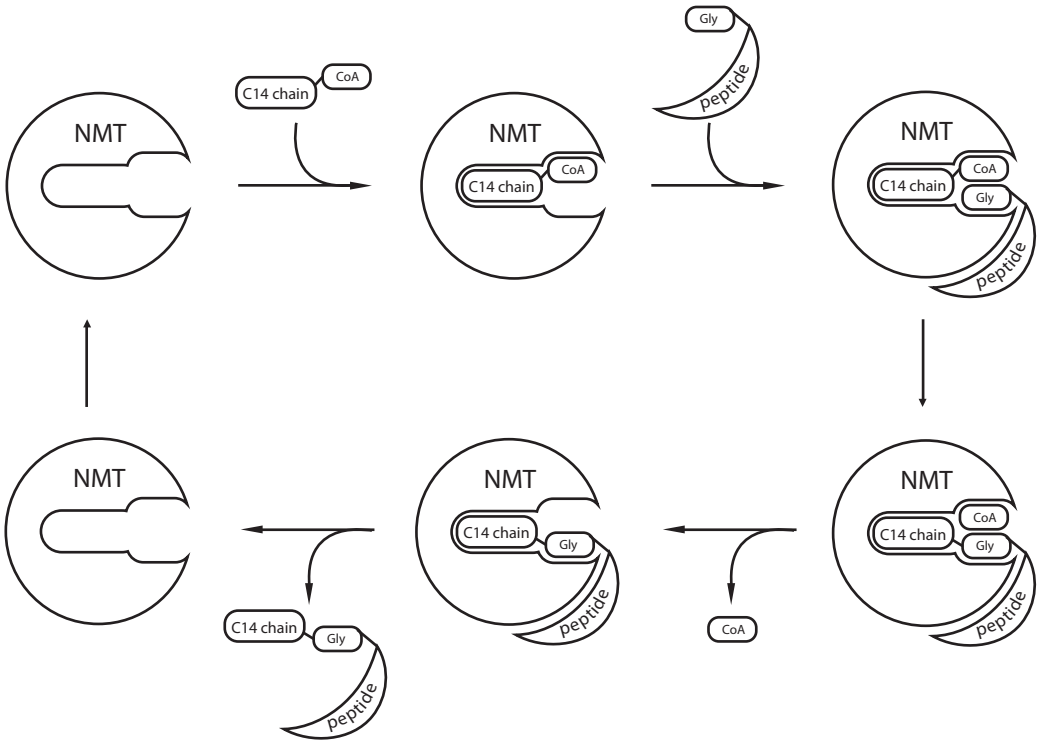

Figure 1.3: Sequential Ordered Bi-Bi Mechanism of *N*-myristoyltransferase[4]

bonyl and sulphur atoms of the thioester contained on myristoyl-CoA and is a potent inhibitor of NMT (Figure 1.4C). The hydrophobic residues and the distinctive bent shape of the myristoyl pocket, along with the Co-A portion were identified by understanding the binding mechanism of *S*-(2-oxo)pentadecyl-CoA **9** (Figure 1.4C). The selectivity of NMT to C14 fatty acids was attributed to Van der waals interactions between the Trp 200 and His 201 residues at the end of the hydrophobic pocket. A conformational change was proposed during the myristoyl CoA binding event that would enable peptide recognition and catalysis.

*Sc*NMT induces the nucleophilic addition-elimination reaction by carbonyl activation of the thioester on myristoyl-CoA, through hydrogen bonding with the amide groups of Phe 170 and Leu 171 residues within a oxyanion hole (Figure 1.5A). Bhatnagar *et al.* also provided evidence of the role of the carboxylate C-terminus of *Sc*NMT, through activation by deprotonation of the N-terminus of GLY peptide substrate (Figure 1.5A) and enhancing its reactivity by improving its nucleophilicity.

*Sc*NMT was widely studied and later Farazi *et al.* confirmed the mechanism

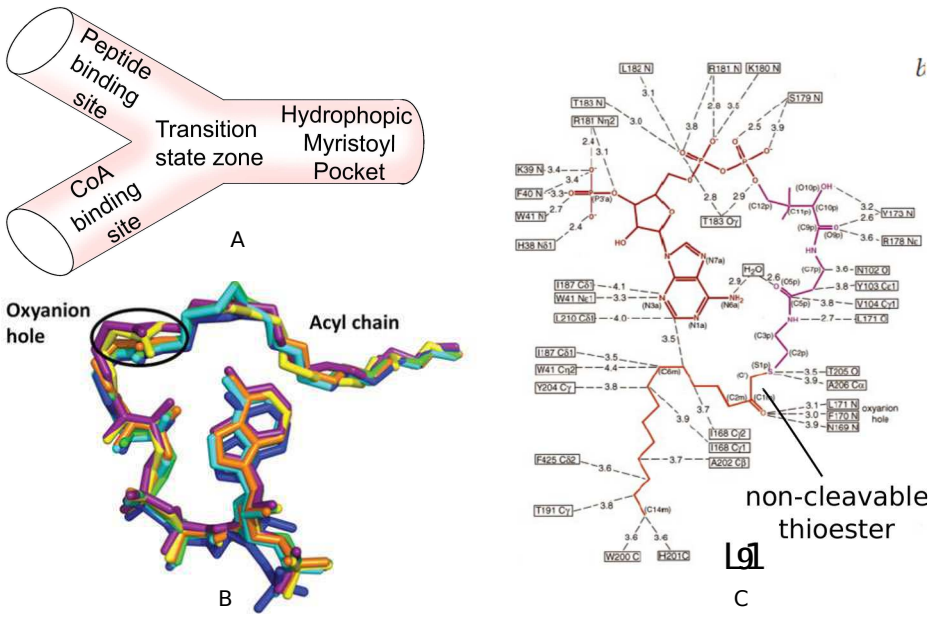

Figure 1.4: A) A schematic of the active site of NMT; B) Compariason of Myristoyl-CoA conformation from differant source organisms[8] (reproduced); C) Structural binding mechanism of myristoyl CoA[7](reproduced).

by describing an Ab loop conformation change, after the Myristoyl-CoA binding event.[9] This conformational change frees a portion of the peptide binding site, confirming the Bi-Bi mechanism previously reported. Farazi *et al.* also expanded that structural mechanism of action by describing the stabilisation effects caused by residues Asn 169 and Thr 205 after the peptide substrates glycine N-terminus is activated by deprotonation (Figure 1.5A). Wu *et al.* later described the importance of the N-terminus region of NMT though stabilisation effects of the Ab loop conformation change after myristoyl-CoA binding, and the specific N-terminus region interactions that *Sc*NMT has with Myristoyl-CoA.[10] Several crystal structures of NMT have been published from different organisms, but even with significant genetic variations existing between NMT from different organism little differences are observed in the binding mechanism and conformation of myristoyl-CoA (Figure 1.4B).

NMT myristoylates numerous peptide substrates which have a wide range of secondary functions. The NMT-peptide substrate recognition event mechanism is significantly more complex compared with NMT-myristoyl-CoA recognition and varies greatly between NMTs from different organisms. Evidence that myristoylation is totally selective to the Glycine N-terminus substrate was provided by

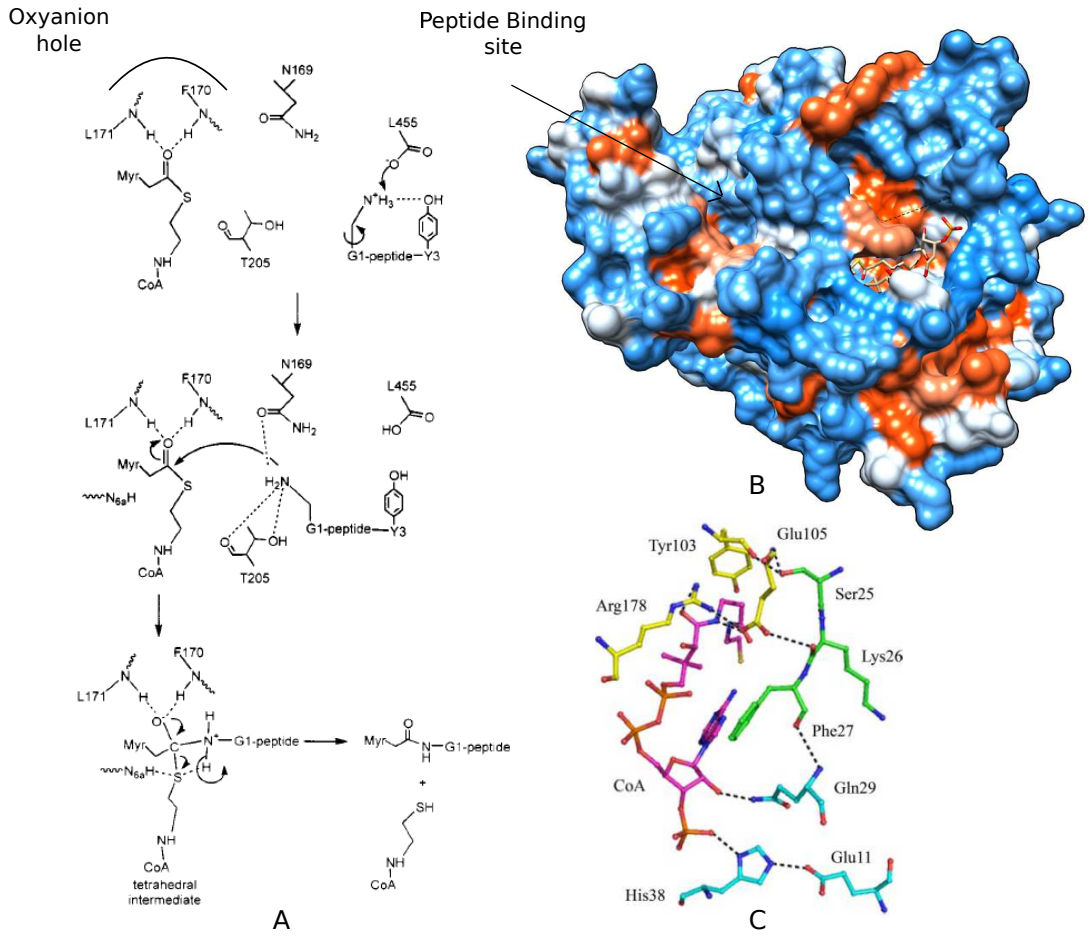

Figure 1.5: A) Structural enzymatic mechanism of ScNMT (reproduced[9]); B) Crystal structure containing Myristoyl-CoA **5** of ScNMT from 2P6E[10]; C) Full describtion of Myristoyl-CoA **5** binding mechanism (reproduced[10]).

synthetic octapeptide studies[11] and significant genetic similarities exist in NMT between species in the peptide substrate binding region.[12] Peptidic inhibitors and their mode of action will be discussed in some detail, but full analysis of the peptide substrate recognition events is outside the scope of this project.

1.2 Applications of preclinical NMT inhibitors

Historically, inhibitors of NMT have been developed as anti-fungal agents. Research has progressed in the development of NMT inhibitors towards a variety of other targets including, but not limited to protozoan, viral and fungal infections. Other inhibitors of NMT are beyond the scope of this project. No clinically available NMT inhibitors are licensed and a new clinically available NMT inhibitor would be a new class of medicine.

Fungal infections

The kingdom of fungi has been estimated, with significant debate, to contain 1.5 million species.[13] Approximately 70,000 species have been formally characterised with about 300 being virulent to humans[14] with risks postulated to increase with rises in global ambient temperatures.[15] *Cryptococcal meningitis* is caused by the fungi *Cryptococcus* and results in 625,000 deaths each year mainly occurring in sub Saharan Africa.[16,17] Histoplasmosis is a opportunistic fungal infection caused by *Histoplasma capsulatum* that has a mortality rate of 20 - 40% in immunocompromised patients, often misdiagnosed as tuberculosis.[18] Fungal infections are harder to treat than bacterial as both fungal and human cells are eukaryotic, often leading to excessive toxicity.

There are four major classes of anti-fungals that are clinically utilised. The polyenes were developed early and include amphotericin B **10**, also active against Leishmaniasis, which shows activity by disrupting fungi membrane functions. Naftifine **11** is a member of the allyl amine class of anti-fungals which show activity by inhibition of the fungal enzyme squalene epoxidase, but toxic metabolites of naftifine limit its use to topical applications. The azoles are the largest

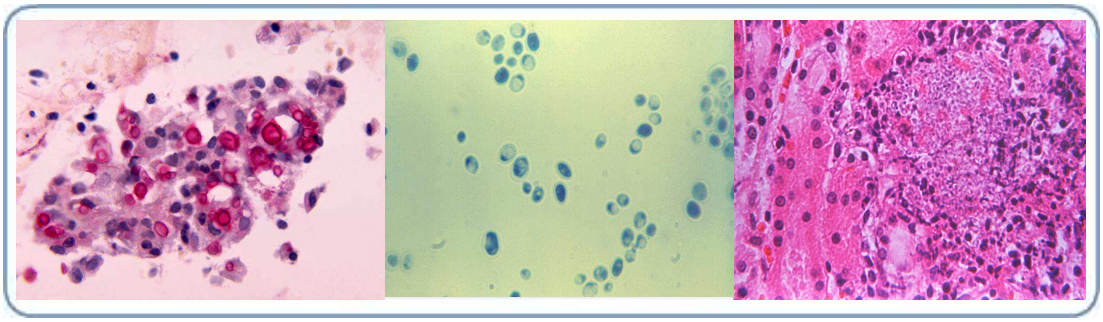

Figure 1.6: Left: *Cryptococcosis* of the lung using mucicarmine stain. Centre: *Candida albicans* fungal organisms. Right: Histopathologic changes associated with a fungal infection with *Candida albicans*. (reproduced[19]).

class exemplified by fluconazole **12** which disrupts ergosterol biosynthesis through inhibition of the 14α-demethylase. Caspofungin **13**, within the newly developed Echinocandin class of anti-fungals, disrupt cell wall biosynthesis through inhibition of the enzyme β-1,3-glucan synthase.[20] Early NMT inhibitors have been demonstrated as anti-fungal agents.

Myristic acid analogues show moderate anti-fungal properties (Table 1.2.1). 4-Oxatetradecanoic acid **14** was found to have fungicidal properties and its mechanism of action was determined by efficient incorporation into peptides, disrupting downstream functions.[21] 2-substituted myristic analogues **15**, **16**, **17** and **18** were shown to have anti-fungal activity.[22] The mechanism of action was not demonstrated but competitive inhibition is plausible. 2-Methoxymyristric acid **19** was also shown to be an anti-fungal agent but its mechanism of action was also never concluded.[23,24]

Peptomimetics targeting the peptide binding site were based on the octapeptide substrate **22**.[25] A series of NMT inhibitors were developed as anti-fungals with structures exemplified by the dipeptide **23**.[26] The dipeptide **23** shows over 200-fold selectivity to *Ca*NMT compared to HsNMT but had a low *in vivo* toxicity towards to *C. albican*s despite nano-molar potency to *Ca*NMT.[27] It was postulated that compounds such as **23** suffered from transport or metabolism difficulties. The peptidic backbone contained on **23** was modified and **24** was developed.[28] The amide **24** reserved the key structural features of **23** and improved its *in vivo* activity. Other strategies towards NMT inhibition were also being explored as anti-fungal agents.

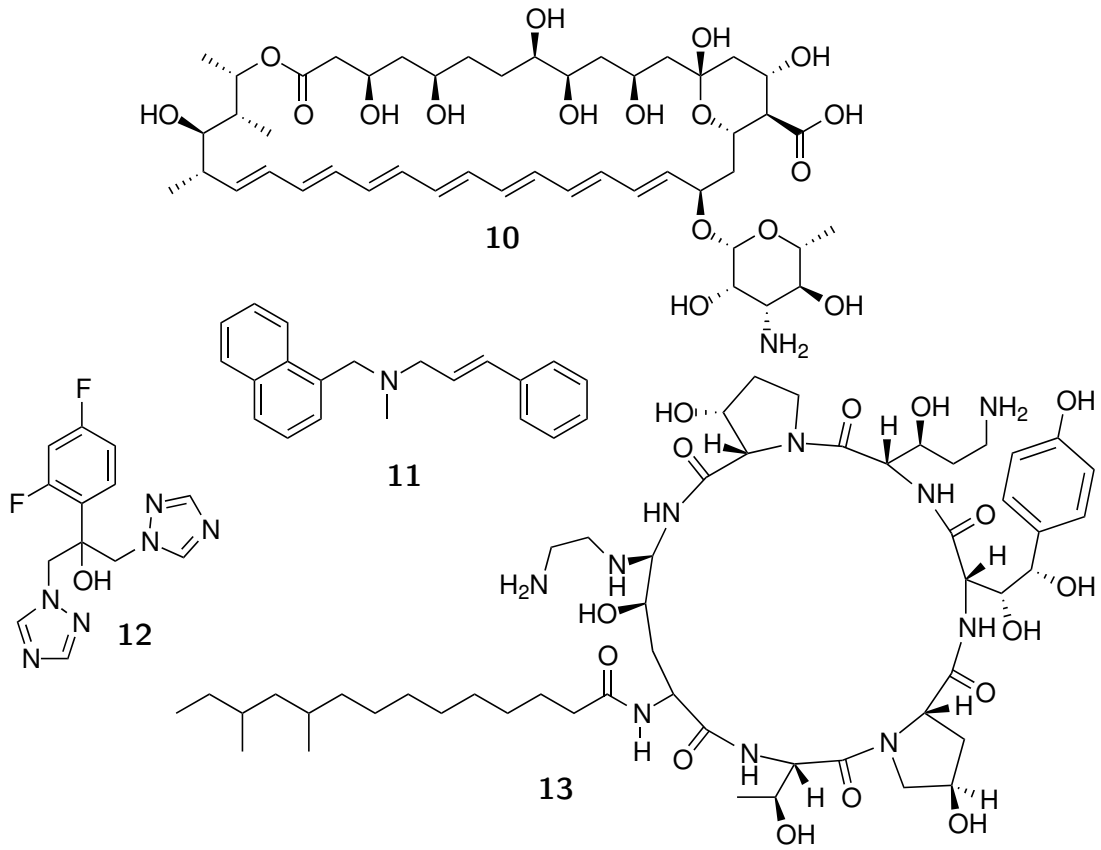

Figure 1.7: Commonly utilised antifungals amphotericin B**10**, naftifine **11**, fluconazole **12** and caspofungin **13**.

Table 1.2.1: Analogues of myristic acid with anti-fungal properties.[22–24]

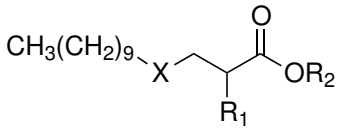

Myristic acid analogue	X	R_1	R_2	MIC (mM) *C.albicans*	MIC (mM) *N.neoforms*
14	O	H	H	ND	ND
15	CH_2	OH	H	>5	>5
16	CH_2	Br	H	0.04	0.02
17	CH_2	Cl	H	0.59	0.04
18	CH_2	Br	CH_3	>5	1.9
19	CH_2	OCH_3	H	0.11	0.11
20	O	OCH_3	H	3.5	0.08
21	S	OCH_3	H	1.24	1.24

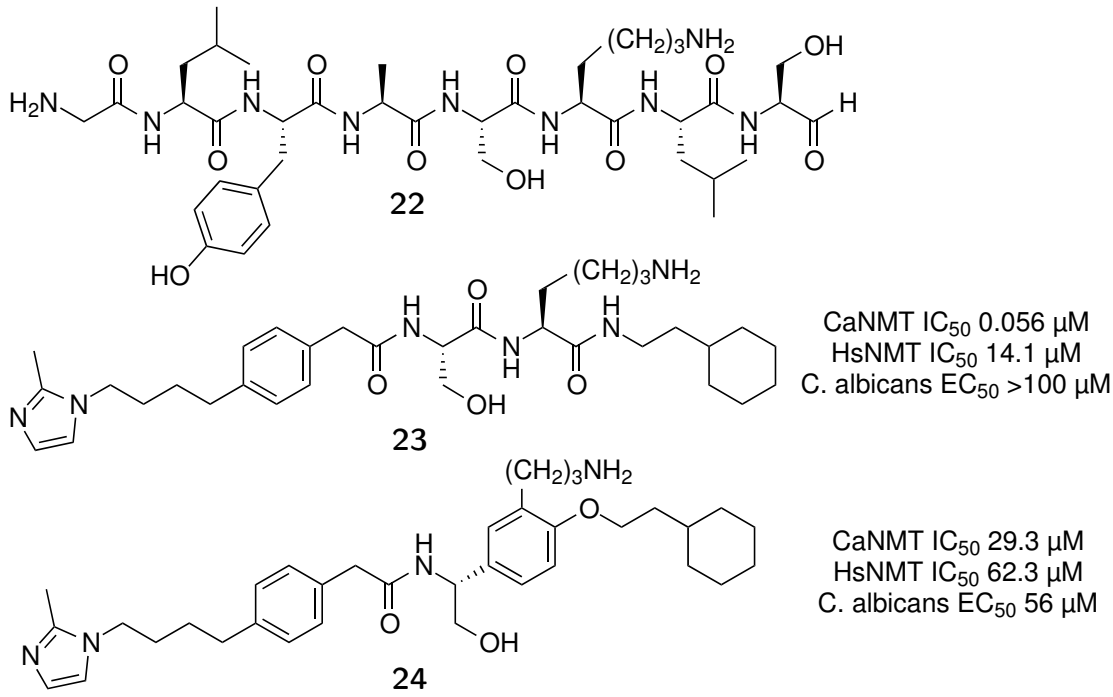

Figure 1.8: Peptomimetic inhibitors of NMT.[25,27,28]

The benzofuran **25** was discovered through an industry screening of *Ca*NMT inhibitors.[29] The known beta-blocking activity of **25** was removed by elimination of its ß-amino alcohol moiety. The new lead **26** had sub micro-molar activity, excellent *in vitro* selectivity and showed promising anti-fungal activity against *C.albicans* achieving *in vitro* activities similar to the fluconazole. The crystal structure of *Ca*NMT containing a benzofuran inhibitor was solved and it linked the importance of the amine containing C4 side chain with specific peptide residues.[30] The low *in vivo* activity of **26** was attributed to a short half life due to its hydrolysable ester.[31] Swapping the C1 substitution to a non-hydrolysable ether exemplified in **27** improved the half life and potency. Despite the nano-molar potency and excellent selectivity **27** showed a modest *in vivo* anti-fungal activity with ED_{50} 7.1 mg/kg compared to that fluconazole ED_{50} of 0.5 mg/kg in the same rat model.[32,33]

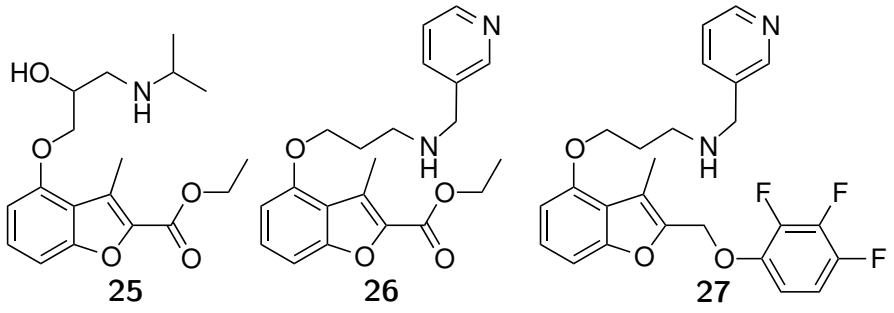

Figure 1.9: CaNMT inhibitors developed as antifungal agents.[30–33]

Protozoan Infections

Human African Trypanosomiasis

Human African Trypanosomiasis (HAT), or sleeping sickness, is a parasitic disease caused by infection with the protozoa *Trypanosoma brucei* (*T.b*) *gambiense* or *T.b. rhodesiense*. HAT occurs in 36 sub-Saharan African countries and *T.b gambiense* is responsible 98 % of reported cases.[34] The primary vector of the disease is infection from the bite of an infected tsetse fly. The first clinical symptoms occur 1-2 years from infection and if left untreated can cause death in about 3 years.[35] Recurring outbreaks have occurred in the past century with the most recent epidemic coming to a end in the late 1990s and in 2009 worldwide cases dropped below 10 000. The decline in cases was confirmed with only 6314 reported in 2013.[34] Despite the gradual decline in the number of reported cases several gaps exist in the current clinical strategy for the treatment of HAT.

Stage one treatments, effective before *Trypanosoma brucei* crosses the blood-brain barrier, are limited with only suramin **28** effective against *T.b. rhodesiense* and Pentamidine **29** against *T.b. gambiense*. Suramin **28** has excessive toxicity[37] and pentamidine **29** is the preferred treatment at the early stages of infection. Stage two treatments, applied once *Trypanosoma brucei* crosses the blood-brain barrier, require alternative clinical strategies. Melarsoprol **30**, an arsenic containing compound is the first line treatment against *T.b. rhodesiense* despite

Figure 1.10: Trypanosoma brucei in thin blood smears stained with giemsa. Center: A close up of a tsetse fly (reproduced[36]).

excessive toxicity and being fatal in a small number of treatments. Eflornithine **31** is significantly less toxic but is only effective against *T.b. gambiense*. In 2009, co-administered intravenous eflornithine **31** with oral nifurtimox **32** (*Trypanosoma cruzi* / Chagas treatment) was approved for clinical use. The combination therapy is now listed on the WHO list of essential medicine and treatment kits are donated by Sanofi and Bayer. The use of melarsoprol-free treatment has increased the price of treatment from $30 USD in 2001 to $440 in 2010 which may hinder treatments in the future.[38] Phase 1 trials of acoziborole **33** are complete and are continuing though the development pipeline. Phase 3 clinical trials of Fexinidazole **34** confirmed it is safe and effective and is currently awaiting submission to the European Medicines Agency.[39]

The myristic acid analogue **35** was discovered to have selective toxicity to HAT.[40] As a result a further 244 myristic acid analogues were synthesised and revealed 20 with high HAT toxicity.[41] A thioether or ether was present in many of the structures exemplified in compounds **36** and **37** in Figure 1.12. The ether functional group was also present combined with aromatic systems in **38** and **39** and also as the ester **40**.

The mode of action of myristic analogues were unresolved with several complex mechanisms postulated by Doering.[40,41] The analogues may disrupt the action of Acyl-CoA synthase, the enzymatic step before myristoylation. Another possibility is the analogues could have activity by disrupting homoeostasis though modified myristoylation of peptide substrates. Alternatively the myristic acid analogues could competitively inhibit NMT though improved binding efficiency inside the hydrophobic pocket. Incorporation of functional groups, into the myristoyl chain,

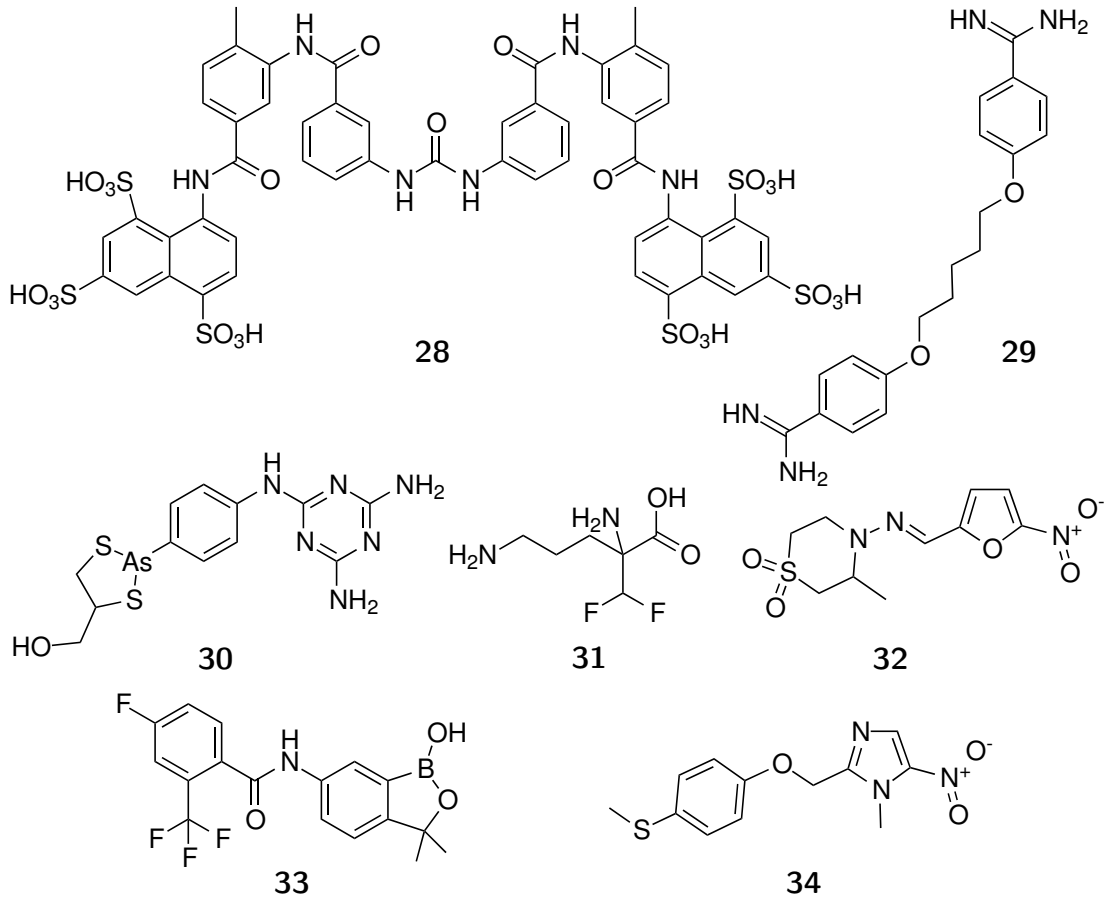

Figure 1.11: Clinically available HAT treatments. Stage 1 effective suramin **28** and pentamidine **29**. Stage 2 effective melarsoprol **30**, eflornithine **31** and nifurtimox **32** used as a combination therapy with eflornithine **31**. Stage 2 clinical cadidates **34** and **33**

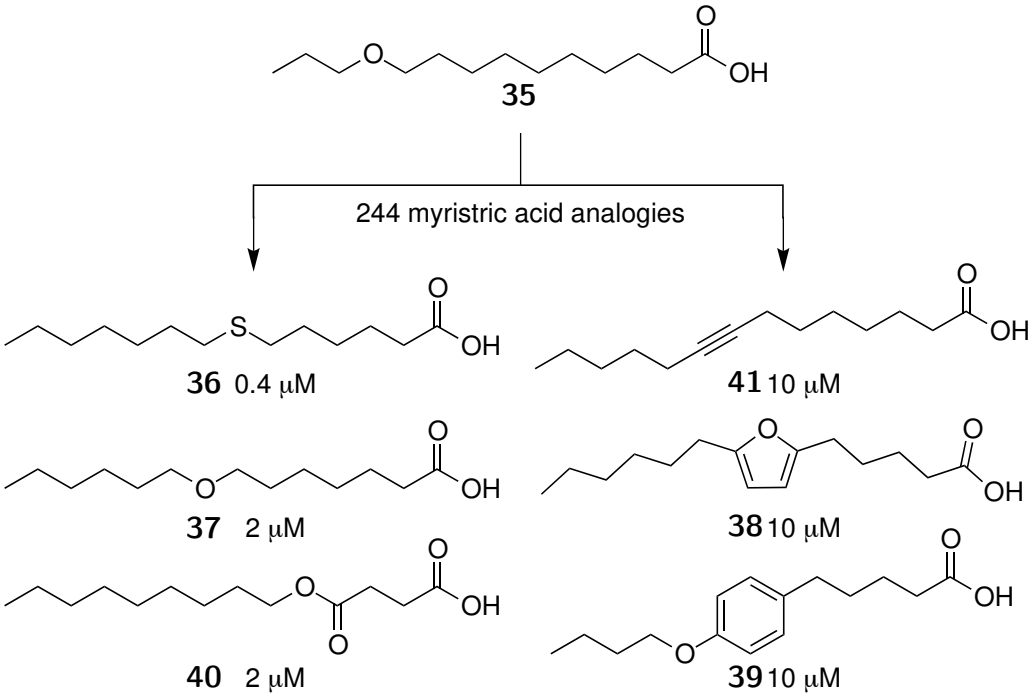

Figure 1.12: Early analogues of myristric acid activity against HAT

that aid competitive selective binding to NMT would benefit the inhibitor potency of a transition state mimetic. A combination of mechanisms of toxicity towards HAT was not dismissed by Doering. NMT inhibitors that specifically target *T. brucei* later reemerged.

The genome of *Trypanosoma brucei* was sequenced and *Trypanosoma brucei* NMT (*Tb*NMT) successfully purified.[42] Several anti-fungal NMT inhibitors, exemplified by **42** and **43** in **44** were shown to inhibit *T. brucei* NMT (*Tb*NMT).[43,44] Piggybacking the inhibitory properties from anti-fungal compounds developed at Pfizer provided starting points for inhibition of *Tb*NMT, as a new potential mechanism for clinical treatment of HAT. These hits against *Tb*NMT were interesting but were never optimised as other more promising novel *Tb*NMT inhibitors as a potential for HAT treatments evolved.

A focused library of 62000 compounds were used in high throughput screen for inhibition of *Tb*NMT and many consequently showed *T. brucei* activity.[45] Figure 1.14 shows the pyrazole sulphonamide **45** which was the initial hit from the campaign and showed micro molar IC_{50} *Tb*NMT with promising selectivity. The hit was optimised to give **46** with nanomolar activity and 100 fold selectivity.[46,47] As *Trypanosoma brucei* crosses the blood brain barrier, **46** was optimised further

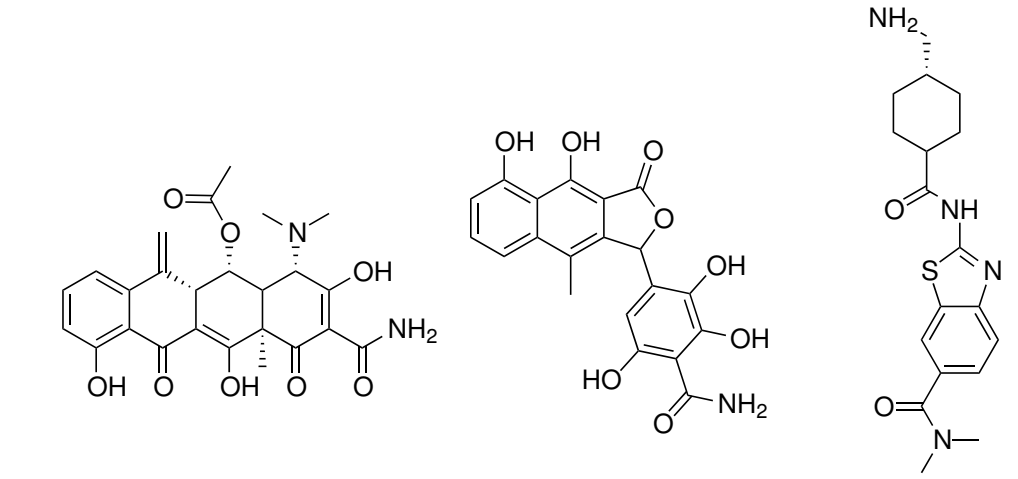

Figure 1.13: Antifungal inhibitors demonstrated to show *Tb*NMT inhibition and activity towards *T.brucei*.[43]

to have bioavailability at the infection site.[48] The inhibitor binding mechanism of **47** was proposed by co-crystallisation in *Leishmania major* NMT (*Lm*NMT) and confirmed that its binding site was within the peptide binding site area of NMT. Currently, there are no clinically available *Tb*NMT inhibitors with applications towards Human African Trypanosomiasis.

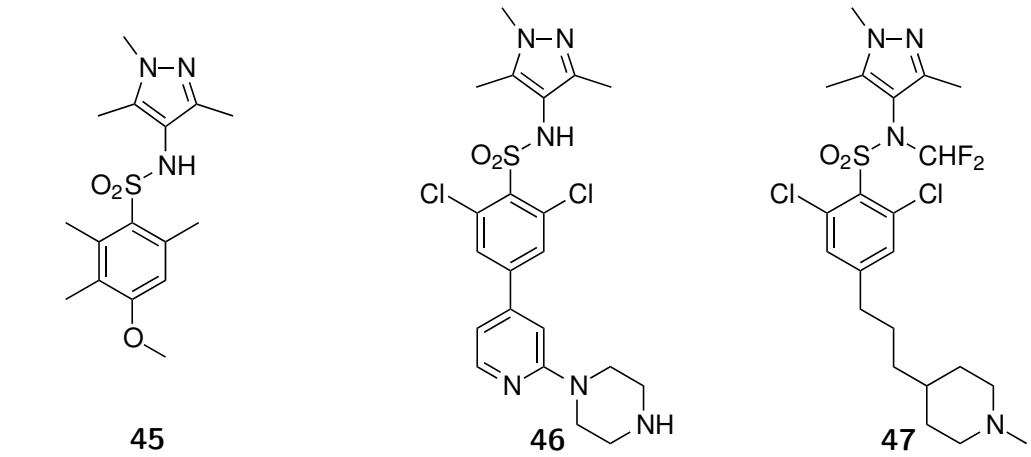

Figure 1.14: TbNMT inhibitors with *in vitro* activity against *T.brucei*[45–48]

Malaria

Approximately half of the worlds population is at risk from infection of *Plasmodium* parasites that cause malaria. There are four species of protozoa; *Plasmodium falciparum*, *vivax*, *malariae* and *ovale* that are transmitted though the bite of the *Anopheles* mosquitoes. It is estimated that in 2013 about 198 million cases of malaria occurred worldwide and these led to the deaths of approximately 584 000 people.[49]

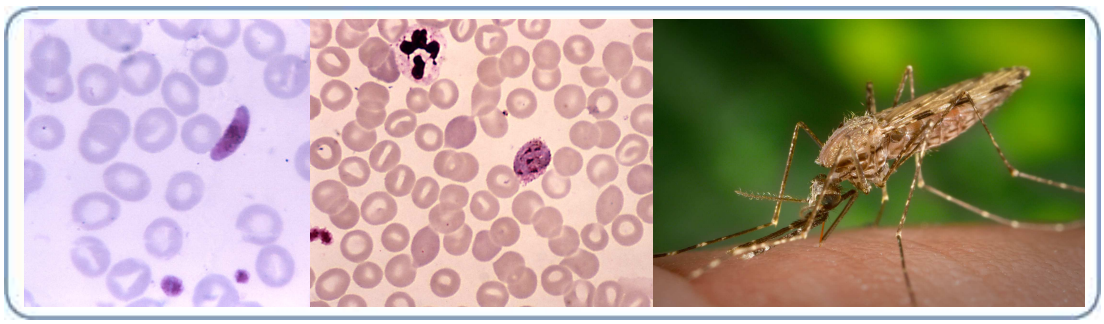

Figure 1.15: Left: *Plasmodium falciparum* in human host; Centre: Immature *P.Vivax* in human host; Right: Feeding female anopheles quadriannulatus mosquito. (Reproduced[19])

There is a wide range of treatments clinically available for treatment (chloroquine **48**) and prevention (doxycycline **49**) of malaria. The prevalence of parasitic res-

istance to chloroquine, and others within its class, lead to the development of combination therapies such as malerone (atovaquone **50** and proguanil **51**). Although malaria is considered preventable and curable, the latest class of antimalarials developed from artemisinin **52** are now showing significant geographic patterns of resistances.[50,51] Development of new classes of anti-malarials are needed to combat and treat life threatening multidrug resistant *Plasmodium* infections.

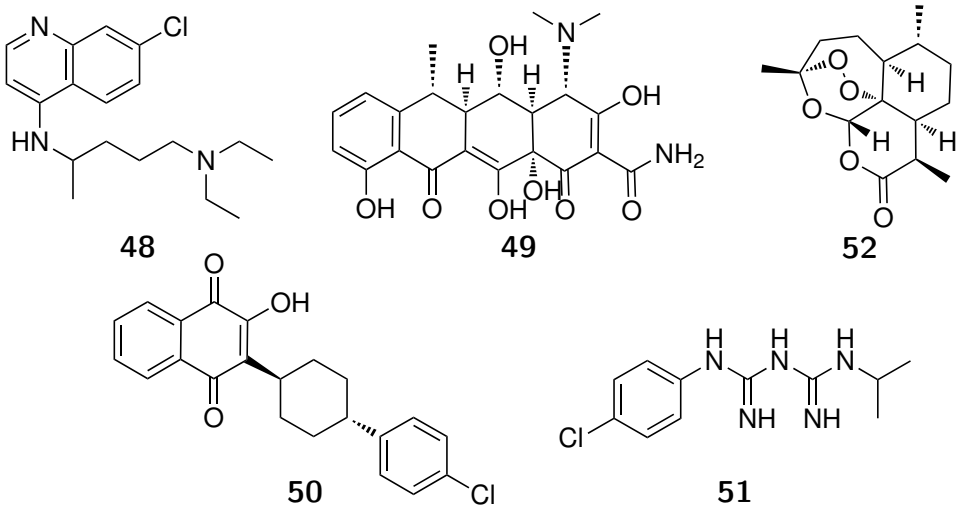

Figure 1.16: Examples from the major classes of clinically avaible malaria treatment including chloroquine **48**, doxycycline **49**, artemisinin **52** and malerone (atovaquone **50**/proguanil **51**).

The benzothiazole **44** is a anti-fungal that showed inhibition of TbNMT (Figure 1.13).[43] Using the same 'piggy-backing' approach, *P. falciparum* NMT (*Pf*NMT) was targeted *in vitro*.[52,53] Industry developed anti-fungals showed *in vitro Pf*NMT inhibition. The benzothiazole **44** is a selective inhibitor of *Pf*NMT over *Hs*NMT. Analogues of the benzothiazole **44**, namely **53** and **54** showed good potency with *in vitro Pf*NMT IC_{50} below 30 µM.[54] Piggy-backing structure based activity from anti-fungals provided evidence for commissioning a screen of *Ca*NMT inhibitors towards PfNMT.

The benzofuran **26** (RO-09-4609) shows a micro-molar inhibitory activity in *Pf*NMT. It was developed at Roche as a *Ca*NMT inhibitor which showed low micromolar anti-fungal activity against *C. albicans* (Figure 1.18).[30–32] The activity of **26** in *Pf*NMT was significant and led to the synthesis of **55** that contained the 4-piperinol and benzyl oxadiazole systems that improved potency while conserving selectivity.[55] The benzofuran core was modified and consequently **56**

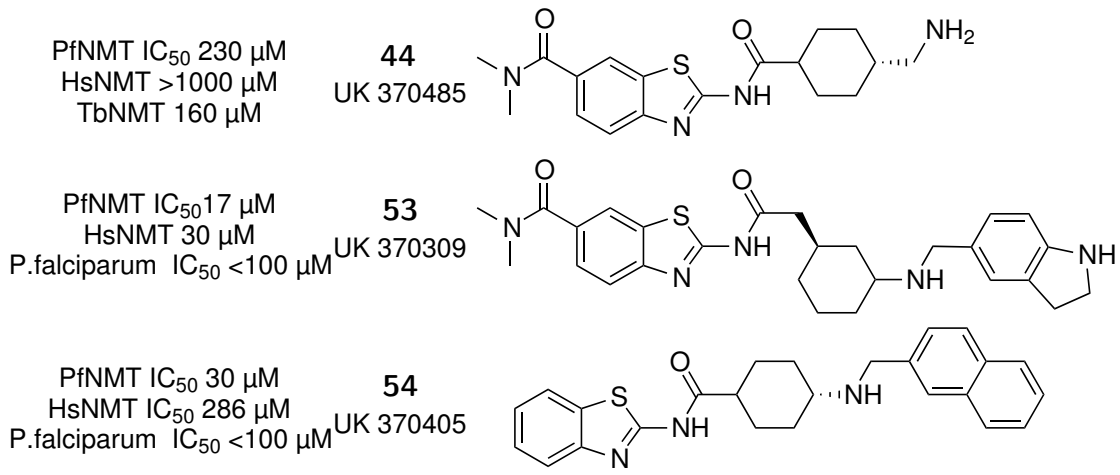

Figure 1.17: PfNMT inhibitors **44**, **53** and **54**[54]

showed nanomolar activity.[56] Figure 1.18 shows the redevelopment of the *Ca*NMT anti-fungal inhibitor **26** towards PfNMT and consequently showed sub micro-molar *in vivo* activity against *P. falciparum.*

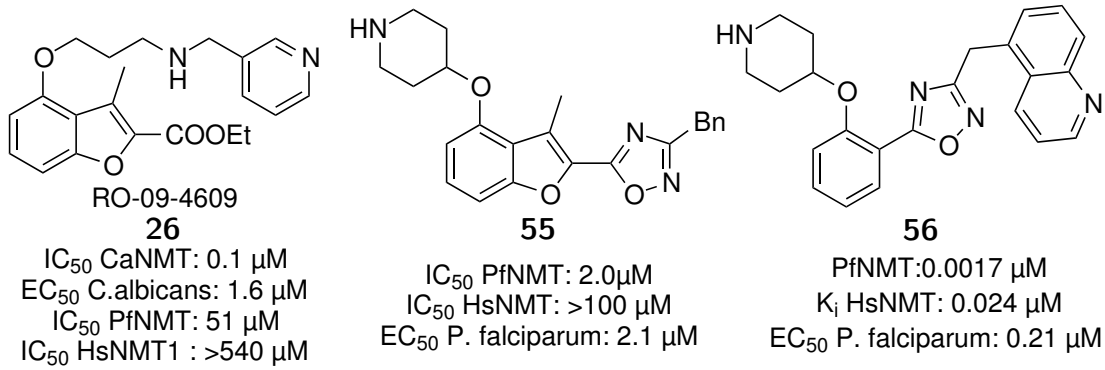

Figure 1.18: Sucsessive generations PfNMT benzofuran inhibitors[55,56]

Compound **57** replaces the benzofuran scaffold of **26** with a benzothiophene scaffold (Figure 1.19).[57] The benzothiophene **57** contains the 4-piperinol fragment found in the later generation benzofuran inhibitor **55** and a child inhibitor **56** shown in Figure 1.18. The 4-piperinol ring is structurally similar to the piperazine ring contained on HAT inhibitor **46** discussed previously. The inhibitor **46** shows a nano molar activity against PfNMT. Its 1,3,5-trimethylpyrazole fragment was incorporated into **58** which also combined the 4-piperinol and oxadiazole fragments of **55** (Figure 1.18) with the benzothiophene scaffold leading to selective sub micro-molar *in vivo* activities. The binding mode of **46** and **58** were found experimentally to be closely related.[58] Incorporation of the 1,3,5-trimethylpyrazole,

developed from a *Trypanosome* research stream,[46–48] was a successful mechanism for provision of a potent inhibitor of *Plasmodium* NMT.

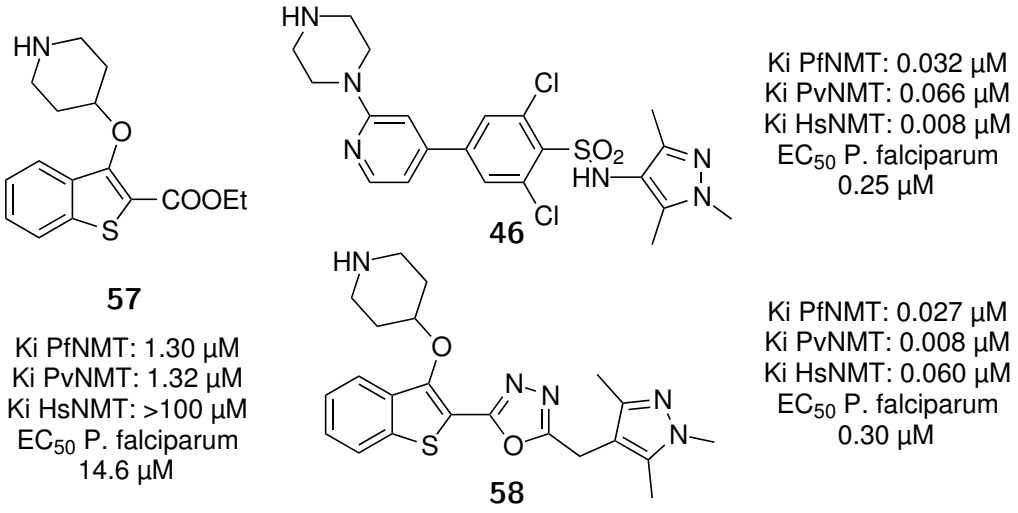

Figure 1.19: Benzothiophene inhibitors of PfNMT.[57,58]

MRT00057965 **59** is a quinoline based inhibitor that shows micro-molar activity against *Plasmodium vivax* NMT (*Pv*NMT).[59] It was discovered during a HTS campaign towards protozoa NMT and is structurally different from the benzofuran and benzothiophene inhibitors previously discussed. The original hit was optimised to give **60** by introducing a ester into position 3 of the quinoline backbone. Compound **60** is structurally similar to **57** shown in Figure 1.19. It was shown to be more selective for *Pv*NMT over *Hs*NMT than the lead **59**. Incorporation of the pyridinyl-3-propylamine fragment contained in **61** showed some similarities to the anti-fungal **26** shown in Figure 1.18. Nanomolar activity of **61** was achieved but high selectivity compared to *Hs*NMT is yet to be accomplished on the quinoline series.[60]

A myristoylation assay was performed using a HTS of Pfizers Global Diverse Representative set of 150000 compounds against NMT isolated from *P. falciparum*, *L. donovani* and *H.sapien.*[61] The screen revealed several novel scaffolds as starting points for further medical chemistry campaigns including the PF-03531814 **62**, PF-02378143 **63**, PF-03665853 **64** and CP-854190 **65** (Figure 1.21). **62** is an azetidinopyrimidine, a class that showed 9 other hits of similar structure and some having a SAR profile selective to *Pf*NMT over *Hs*NMT. The aminomethylindazole class, represented by **63** had 15 related compounds with selective SAR

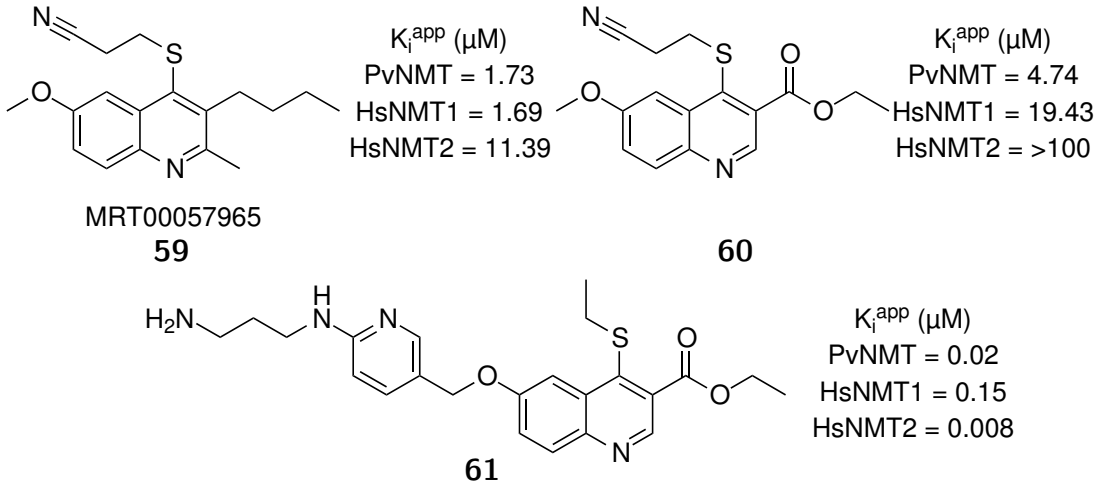

Figure 1.20: Quinoline based PvNMT inhibitors.[59,60]

*Pf*NMT profiles. The glycinyl 3-aminopyrrolidine **65** showed 30 hits. **64** is a representative benzimidazolemethylamine, a class which showed 47 hits in the screen. All represent novel scaffolds requiring further development as potential selective NMT inhibitors targeting *P. falciparum* and *L. donovani*.

Inhibitors that target NMT have been demonstrated to show excellent potential as a novel class of medicine for clinical treatment of protozoan infections. NMT inhibitors are not limited to protozoan applications, but this is beyond the scope of this project. Specifically, the scope of this thesis is *in vivo* activity towards *T. brucei rhodesience* and TM4/8.2 and K1CB1, a sensitive and multi-drug resistant strains of *P. falciparum*. The development of NMT inhibitors has been demonstrated through a piggybacking approach by redesigning the activity of anti-fungal NMT inhibitors toward *P. falciparum*. This project will explore piggy backing the NMT inhibitory activities of fragments from alternative sources, in particular HMG-CoA reductase inhibitors or the statins.

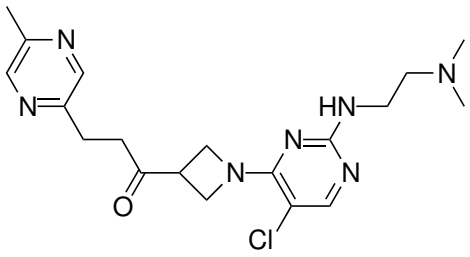

62

PF-03531814

IC_{50} (μM)
PfalNMT = 0.48
TbNMT = >80
HsNMT1 = 70.0
HsNMT2 = 76.0

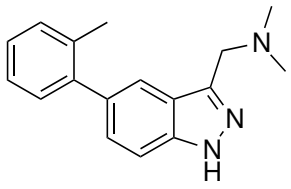

63

PF-02378143

IC_{50} (μM)
PfalNMT = 2.54
TbNMT = >80
HsNMT1 = 38.9
HsNMT2 = 56.3

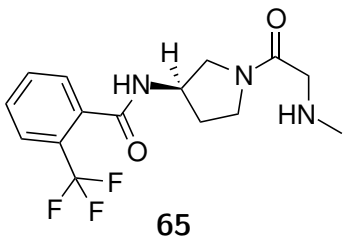

65

CP-854190

IC_{50} (μM)
PfalNMT = 1.72
TbNMT = >80
HsNMT1 = 0.57
HsNMT2 = 1.59

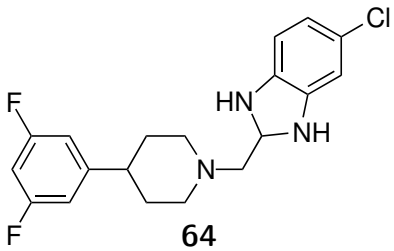

64

PF-03665853

IC_{50} (μM)
PfalNMT = 0.91
TbNMT = 35.4
HsNMT1 = 0.51
HsNMT2 = 0.56

Figure 1.21: Novel scaffolds identified from HTS screening against *P. falciparum* and *T. brucei* NMT

1.3 HMG-CoA reductase and heart disease

Coronary heart disease is characterised by cholesterol rich atherosclerotic arterial deposits that block blood flow to the heart (Figure 1.22). Heart disease is the leading cause of death in the US[62], UK[63] and Australia.[64] The primary symptoms are angina, heart attacks and heart failure which are life threatening if left untreated. The major underlying physiological cause of heart disease is an excess of cholesterol in the bloodstream either from diet or excessive biosynthesis.

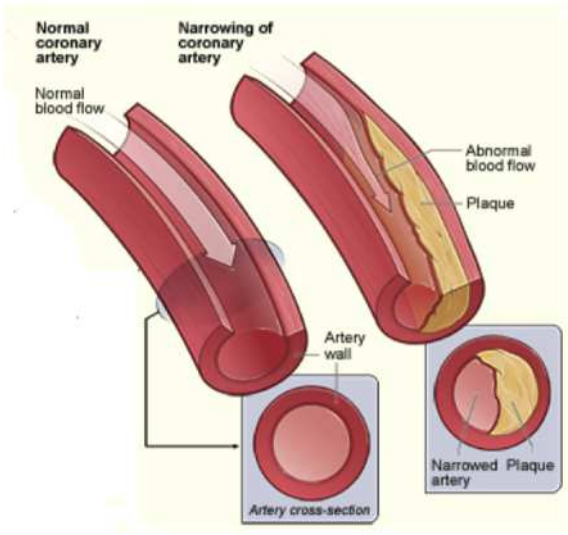

Figure 1.22: Atherosclerotic arterial deposits. (reproduced[62]

Before clinical manifestations of heart disease occur, physicians diagnose heart disease by measuring levels of Low and High Density Lipoproteins bound cholesterol (LDL/HDL). LDL levels are key indicators of heart disease along with several other risk factors including cigarette smoking, hypertension, diabetes mellitus, obesity, lifestyle and family history. Treatment of coronary heart disease before clinical intervention includes modification of lifestyle to include regular exercise, balanced diet, abstaining from smoking and controlling alcohol intake. If lifestyle changes are not successful then clinical intervention is required to lower LDL levels.[65]

Cholesterol is an essential molecule in mammals, helping to regulate cell membrane fluidity. It is also the precursor to the steroid hormones which regulate an extensive range of biological functions. Cholesterol is a biologically fundamental molecule, yet high concentration of cholesterol lead to atherosclerotic deposition

in arteries and consequently increase health risks. Mammals obtain cholesterol either though ingestion or by biosyntheses from acetyl-CoA. Biosynthesis of cholesterol from acetyl-CoA occurs through a process of more than 20 bio-synthetic steps (simplified pathway Scheme 1.1).

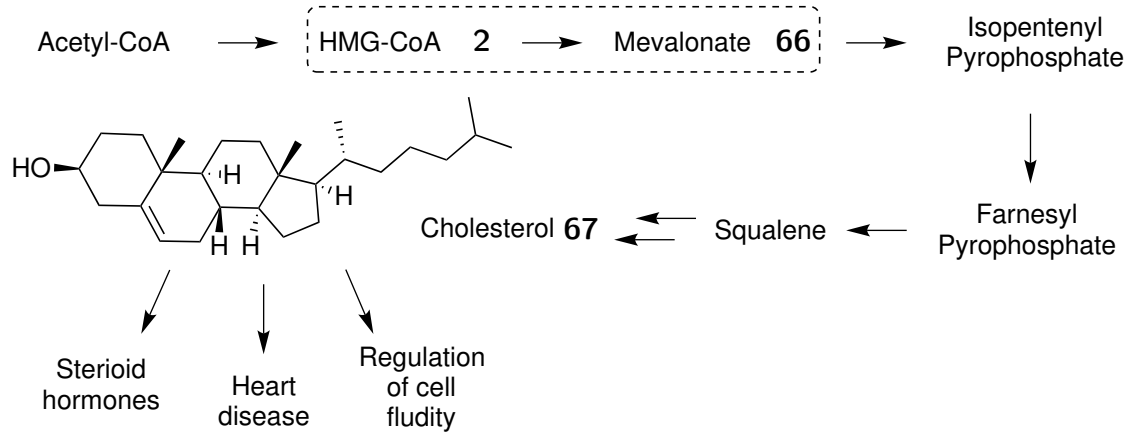

Scheme 1.1: Simplified cholesterol biosyntheses from acetyl-CoA.

Cholesterol biosynthesis inhibition was demonstrated in the 1960s as an effective means to lowering plasma cholesterol in mammals.[66] Cholesterol biosynthesis inhibition is today the primary clinical mechanism for the treatment of heart disease. LDL Cholesterol levels are lowered by inhibiting a single biosynthetic step. Clinical HMG-reductase inhibitors are known as the statins. By lowering LDL cholesterol biosynthesis in the blood, it reduces the deposition of cholesterol as arterial deposits, thus lowering the risk of developing life threatening symptoms.

HMG-reductase inhibitors and the first Statins

Cholesterol synthesis occurs in every cell in the body. The rate limiting step during biosynthesis is the reduction of HMG-CoA to Mevalonate (Scheme 1.2). Mammalian HMG-CoA reductase is a 97 kDa glycoprotein anchored to the endoplasmic reticulum membrane and contains 8 active sites.[67] HMG-CoA reductase catalyses the reduction of HMG-CoA **2** through stabilisation of the natural substrate, intermediates and guiding two equivalents of NADPH sequentially into the active site.[68–70] Inhibition of HMG-CoA reductase became a target for lowering cholesterol in the 1960's.[71]

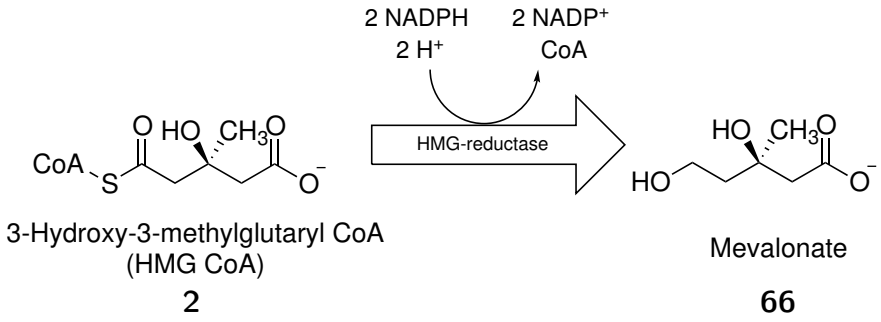

Scheme 1.2: Emzyme catalysed reduction of HMG-CoA

Compactin, **68**, was the first HMG-CoA inhibitor pharmacophore discovered in the early 1970s in broths of *Penicillium brevicompactum*[72] and *Penicillium citrinum.*[73] Scheme 1.3 shows the prodrug compactin **68** conversion from a lactone into its active ring open form **69**. The active form contains a HMG emulating hydrophilic moiety (outlined) and a hydrophobic portion which is replacing the CoA fragment of the natural CoA substrate. Compactin entered clinical trials as a pro drug in 1978, but was never marketed.[74]

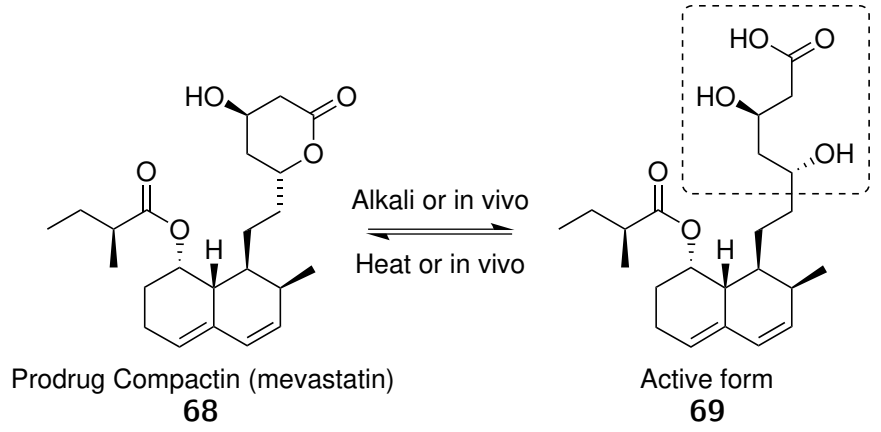

Scheme 1.3: Compactin (prodrug) and active form.

Although compactin **68** was clinically unsuccessful it served as a scaffold for the generation and investigation of structurally similar derivatives. This lead to three compounds approved for clinical use; lovastatin **70** (1987), pravastatin **72** (1989) and the semi synthetic simvastatin **71** (1991). The first statins had structures almost identical to compactin and were clinically and commercially enormously successful. As a consequence the prescription and world sales of simvastatin **71** reached US$5.9 billion shortly before its patent expired in 2004.[75] Competition from generic manufacturers of simvastatin **71** dropped the price to approximately

$361 million in the US alone in the 12 months prior to the 31st March 2010.[76]

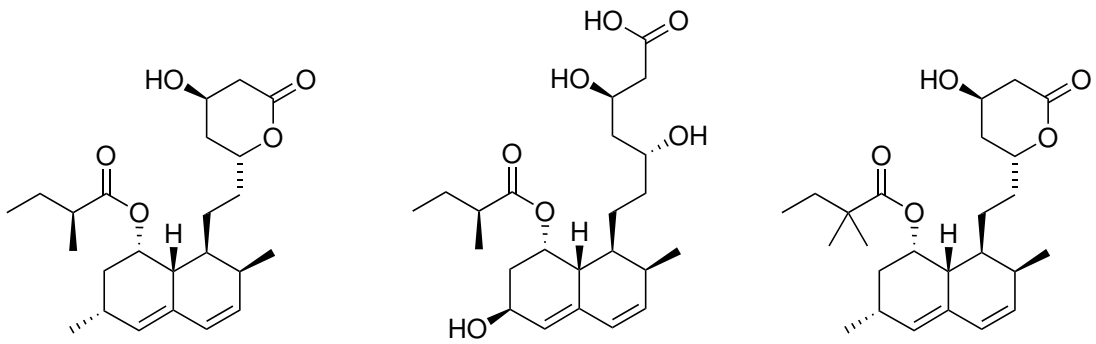

Lovastatin **70** | Pravastatin **72** | Simvastatin **71**

Figure 1.23: First generation clinical HMG-reductase inhibitors.

Development of the synthetic statins, structural mode of action and clinical trials

As the early statins were progressing though clinical trials, the development of synthetic HMG-CoA reductase inhibitors intensified. New analogues based on a substituted decalin ring structure were difficult to access. Consequently, detailed development began into fully synthetic inhibitors. Sato *et al.* demonstrated that cholesterol biosynthesis could be inhibited using a simple hydrophobic fragment such as **73** (Figure 1.24).[77] This work highlighted that the complexity of the decalin ring in compactin **68** was not required. Since analogues of the lactone **73** were significantly easier to prepare, it was used as a starting point for numerous medicinal chemistry campaigns.

The development of synthetic statins progressed by understanding the structural requirement for binding to HMG-CoA reductase. Nakamura *et al.*[78] described the inhibition constants of HMG-CoA and several compactin fragments with HMG-CoA reductase (Table 1.3.1). **74** showed no inhibition of HMG-CoA reductase and demonstrated the importance of the HMG mimetic fragment. No synergistic inhibition was observed, indicating that compactin interacted with a single site. Mevalonate **66** showed activity in the same order of magnitude as dihydroxy-valerate **75**. Nakamura *et al.* showed the importance of a hydrophobic pocket close to the binding site of CoA substrate, and adjacent to the HMG binding

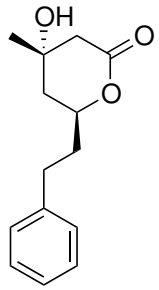

73

Cholesterol Biosynthesis

IC_{50} = 40 μM

Figure 1.24: A chloresterol biosynthesis inhibitor **73** reported by Sato.[77]

site. Nakamura *et al.* reported the structure of **76** which used a 2,4-dichloro-6-hydroxy phenyl substitution to space-fill the pocket. **76** was demonstrated to have a dissociation constant on par with compactin.

At the same time Stocker *et al.* reported the structure activity relationship of the first generation of synthetic HMG-reductase inhibitors.[79] Stocker *et al.* reported the inhibition results of lactone **76** with many other derivatives. The suite of analogues prepared eventually identified key features required for inhibition and demonstrated that a phenol was not essential. The activity of the styrene **77** which contains a *trans*-ethylene linker gave similar activity compared to its ethyl linked derivative **78**. The *trans*-ethylene linker was demonstrated as superior in companion series and is consequently seen downstream in the development of further statins. One of the key outcomes of the project was the resolution of diastereoisomers and enantiomers contained in **77**.

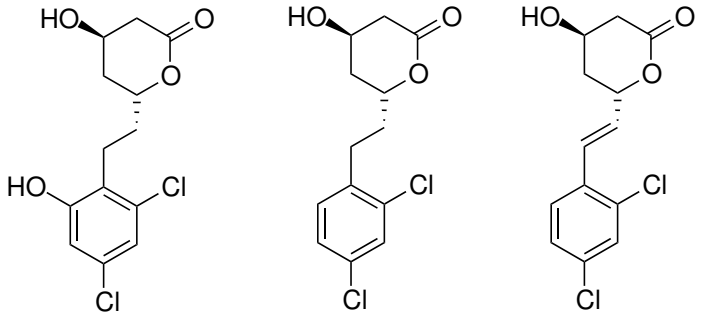

IC_{50} = 7.9 μM **76**

IC_{50} = 15.2 μM **78**

IC_{50} = 22 μM **77**

Figure 1.25: The first generation of synthetic HMG-CoA reductase inhibitors.

Table 1.3.1: Dissociation constants determined by Nakamura.[78]

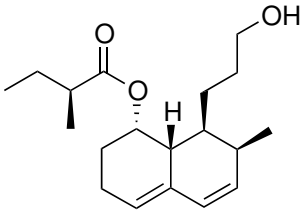

74

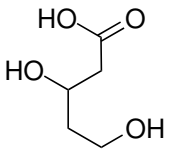

75

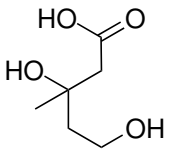

66

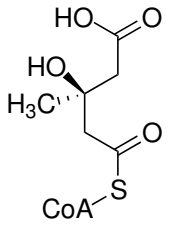

2

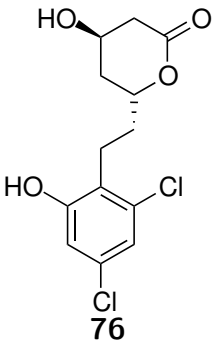

76

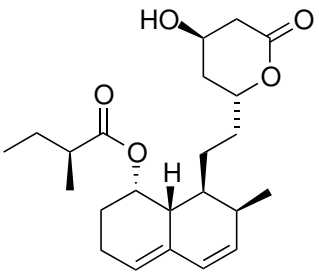

69

Compound	Dissociation Constant (M)
74	no inhibition
mixture **74** and *DL*-3,5-dihydroxyvalerate **75**	21 x 10^{-3}
DL-mevalonate **66**	4 x 10^{-3}
DL-3,5-dihydroxyvalerate **75**	21 x 10^{-3}
HMG-CoA **2**	0.6 x 10^{-6}
76	0.28 x 10^{-9}
Compactin **69**	0.24 x 10^{-9}

Scheme 1.4 shows the synthesis of the mixture of diastereoisomers **77** and **79** generated in 4 steps from 2,4-dichlorobenzaldehyde. The aldol condensation between acetaldehyde and 2,4-dichlorobenaldehyde **80** was complete in two steps. Under basic conditions acetaldehyde and the benzaldehyde **80** gave the aldol product, which was dehydrated using acetic anhydride to give **81** in excellent yield. Methyl acetoacetate was sequentially deprotonated using NaH and *n*-BuLi before being added to the aldehyde **81** to give **82** in near quantitive yield. After reduction of the ketoalcohol **82** using sodium borohydride, hydrolysis and lactonisation of the ester **83** generated a mixture of lactone diastereoisomers **77** and **79** which were separated by chromatography. The two enantiomers of the active diastereoisomer **77** were then separated by chiral amide derivatisation using (*R*)-(+)-α-methylbenzylamine and column chromatography. Hydrolysis of individual chiral amide derivatives **84** and **85** prior to lactone recyclisation gave the enantiomers **86** and **87** respectively. Only **86** was found to be an active HMG-reductase inhibitor offering critical information regarding the active site of HMG-reductase.

As the drug discovery process progressed a biphenyl system replaced the simple aryl ring contained in the lactone **77**.[80,81] A 4'-methylbiphenyl ring in the lactone **88** led to nanomolar inhibition of HMG reductase, and was later replaced with a 4'-fluorobiphenyl system contained in the lactone **89**. The 4'-fluorophenyl moiety features in current commercially available synthetic statins. The lactone **90** replaces the chlorine substituents with methyl groups to fill the hydrophobic pocket in HMG reductase.

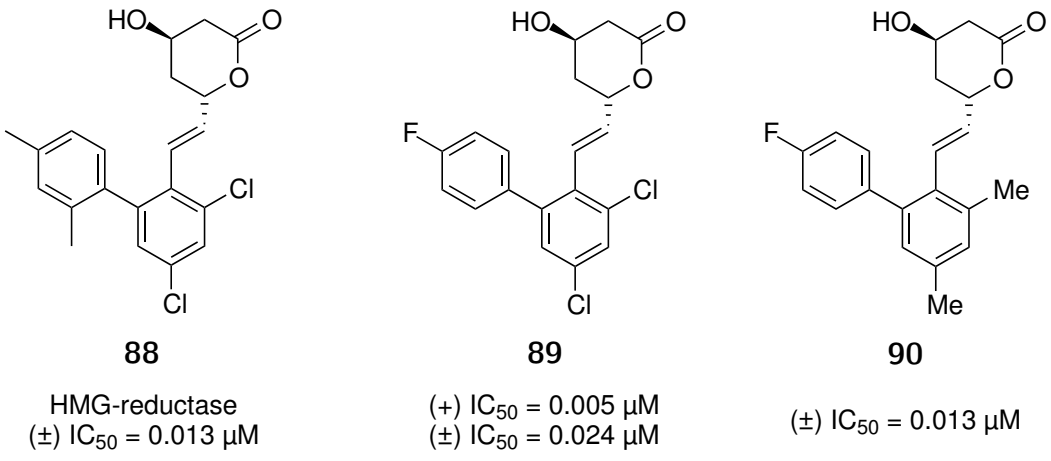

88

HMG-reductase
(±) IC_{50} = 0.013 μM

89

(+) IC_{50} = 0.005 μM
(±) IC_{50} = 0.024 μM

90

(±) IC_{50} = 0.013 μM

Figure 1.26: The second generation of synthetic HMG-CoA reductase inhibitors.

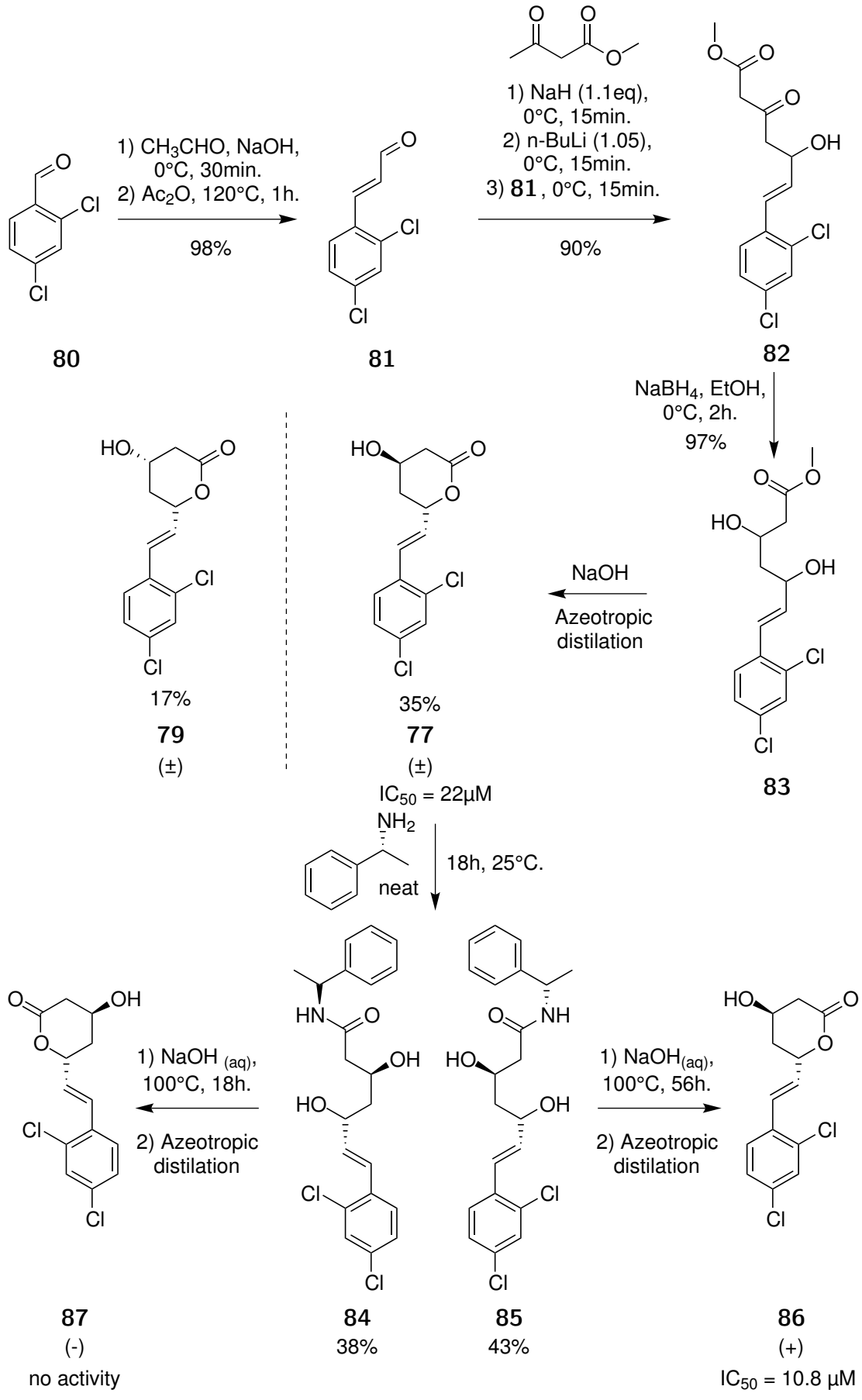

Scheme 1.4: Synthesis and isolation of the racemic mixture of **77** and seperation of its enantiomers **87** and **86**.

Synthesis of many of the substituted biphenyl analogues, including **89**, was performed in 6 steps (Scheme 1.5). The biphenyl system was formed using a CH activation strategy. The benzyl imine **91** was generated by a condensation reaction between 2,4-dichlorobenzaldehyde **80** and aniline. The newly formed imine directed the palladium CH insertion to give the palladacycle **92** in quantitative yield. Reaction with 4-fluorophenylmagnesium bromide then gave the desired biphenyl **93** from which the HMG emulating fragment was installed using the same strategy described in Scheme 1.4.[80]

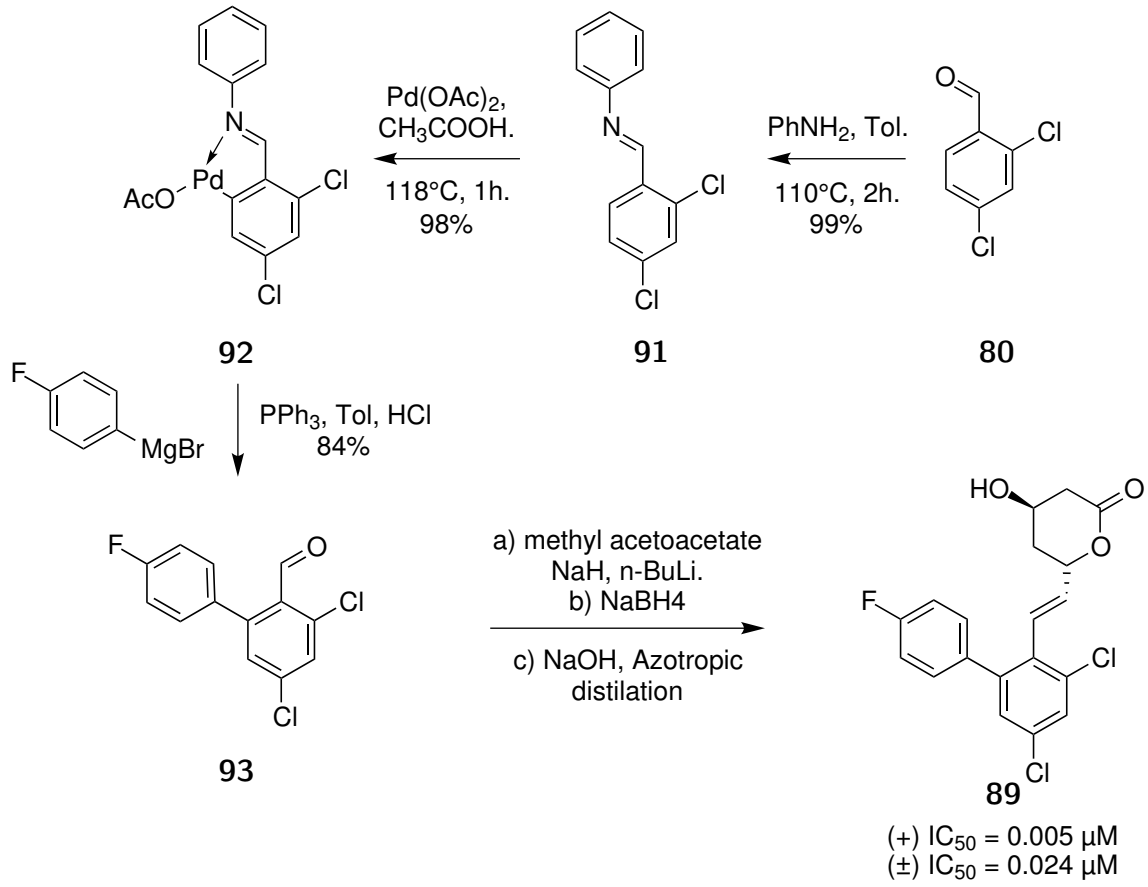

Scheme 1.5: Formation of the biphenyl system contained on **89**.[80]

The majority of the medicinal chemistry performed during the development of the synthetic statins remains unreported. Figure 1.27 shows the pyrrole **94** which has an isopropyl substitution and was reported by Roth *et al.*[82] The isopropyl substitution is a core feature of many of the clinical synthetic statins marketed today. Fluvastatin **3** has an 4-fluorophenyl and an isopropyl substituted indole core with a *trans*-ethylene linker. Fluvastatin **3** has all of the core features previously discussed and was commercially licensed as a HMG-reductase inhibitor in

1993.

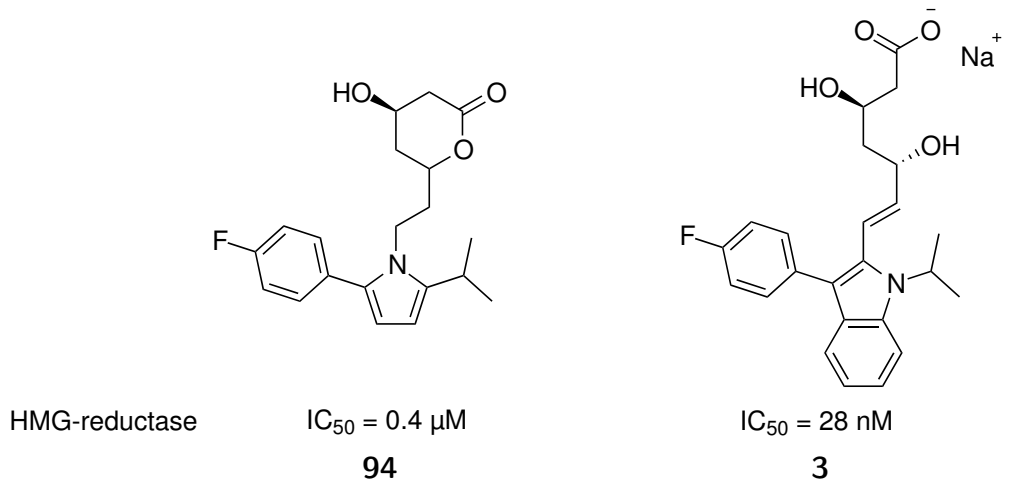

Figure 1.27: Introduction of the isopropyl pyrrole substitution shown in **94**[82] which is structurally similar to fluvastatin **3**.

The process used to manufacture fluvastatin is shown in Scheme 1.6. The key feature of the synthesis is that it generates the *syn*-diol of **3** without need for chromatography and uses fluorobenzene **95** as the starting material. The indole **96** is formed using a Bishler-indole synthesis between **97** and **98**. A formylation of the indole **96** uses *N*-methyl-*N*-phenyl-3-aminoacrolein **99** and gives **100** as a single isomer. Introduction of the HMG emulating fragment was performed using *tert*-butyl acetoacetate to give **101** in the same manner as Scheme 1.4. The key stereoselective reduction uses diethylmethoxyboron as a covalently bound chelation agent to activate the beta ketone and guide the hydride addition to generate *syn*-diol **102** in 99:1 *syn*:*anti* purity. Hydrolysis of the ester and conversion to its sodium salt generates fluvastatin in 6 steps.[83]

The absolute three dimensional shape of the active site of HMG-CoA reductase, containing its natural substrate HMG-CoA, was not reported until after a large majority of the statins were approved or in late stage clinical trials.[70] The research and development of statins was thus achieved using traditional medicinal chemistry permutations without a complete understanding of the interactions with HMG-CoA reductase. Crystallisation of HMG-CoA containing the statins offered the first complete explanation to the statins mechanism of binding towards the active site of HMG-CoA reductase.[84] Istvan *et al.* described the hydrophilic region of HMG-CoA reductase which shared several polar interactions with the

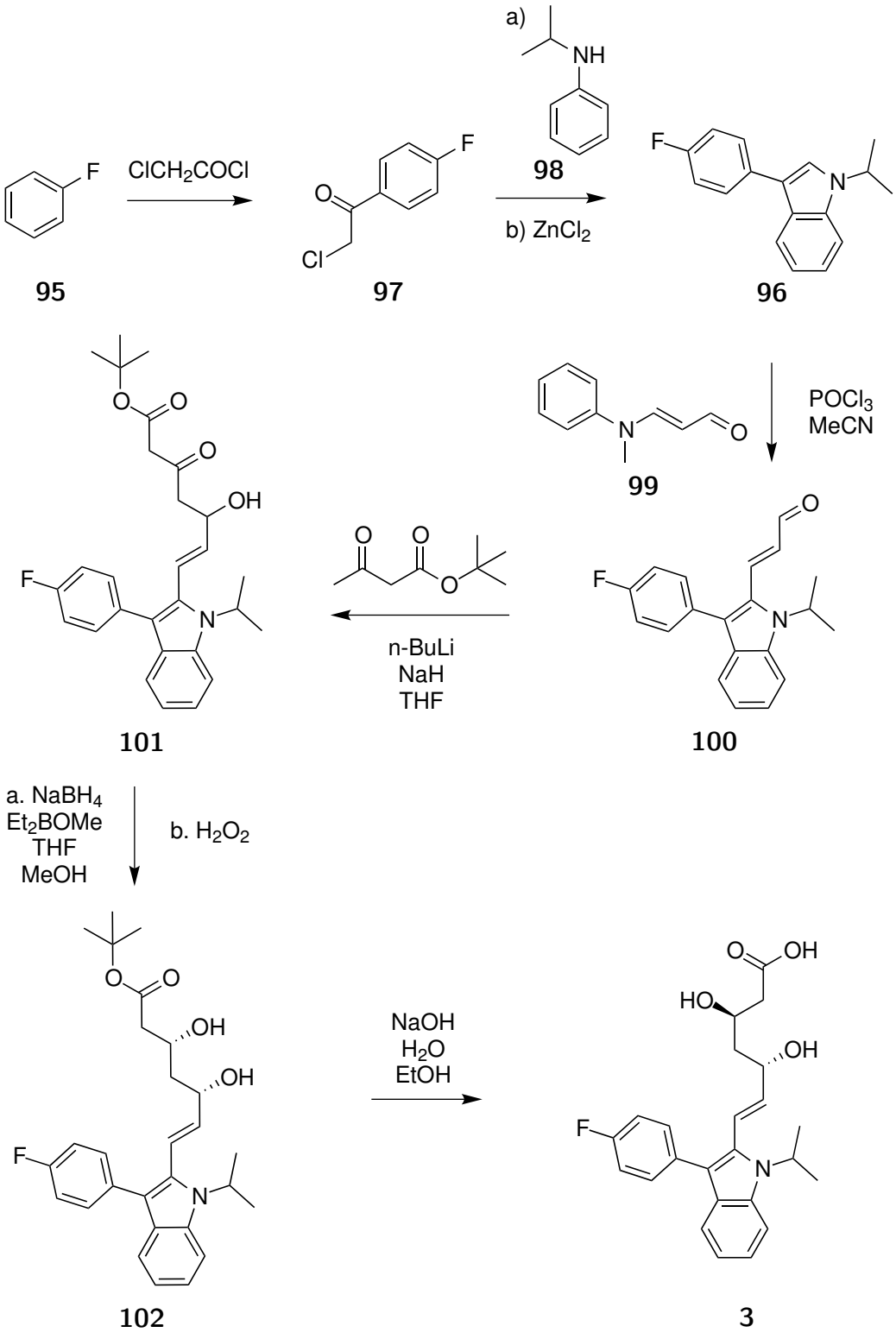

Scheme 1.6: Commercial manufacture of fluvastatin.

HMG moiety on the statins exemplified by fluvastatin in Figure 1.28. These interactions include a hydrogen bond network of Glu^{559} and Asp^{767} to the O5 hydroxyl group of fluvastatin and a salt bridge between the terminal carboxylate of the HMG moiety with Lys^{735}. The second region Istvan *et al.* described involved the hydrophobic side chains of residues Leu^{562}, Val^{683} , Leu^{853}, Ala^{856} and Leu^{857}, that participate in Van der Waals interactions with the hydrophobic areas of statins. Istvan *et al.* highlighted the importance of the 4'-fluoro position and its polar interaction with Arg^{590} and a binding mechanism present in all the synthetic statins.

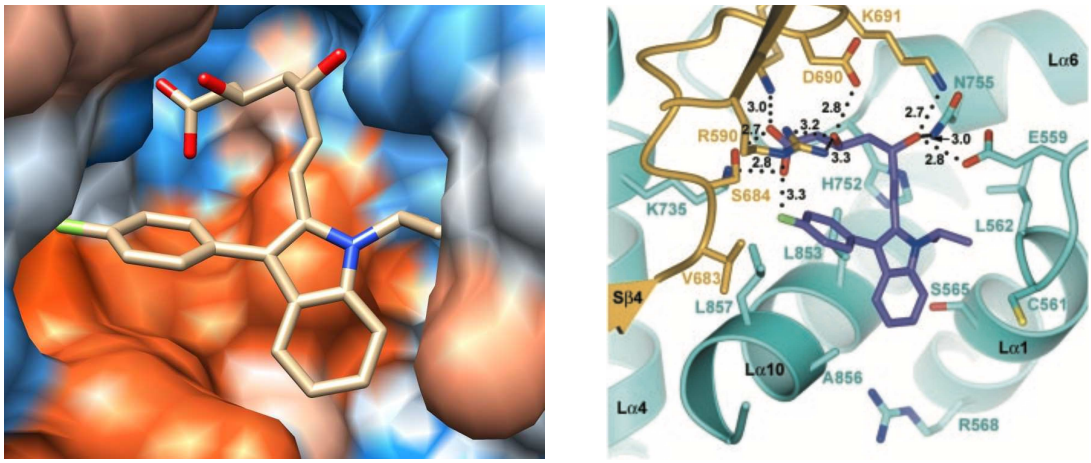

Figure 1.28: Crystal structure of fluvastatin bound to HMG-CoA reductase. (reproduced[84])

Figure 1.29 shows the four fully synthetic statins which are clinically available for treatment of heart disease. All of the statins have similar structural features, discussed previously, that inhibit HMG-reductase. Widespread scepticism about cholesterol biosynthesis inhibition and postulated long term side effects remained long after the first statins were licensed. It was not until large scale phase 4 clinical trials were performed as post marketing surveillance that statins were finally confirmed to be clinically safe and effective. Scandinavian Simvastatin Survival Group involved over four thousand patients and linked the use of statins to the successful lowering of LDL cholesterol resulting in the reduction in heart attacks without major presence of side effects.[85]

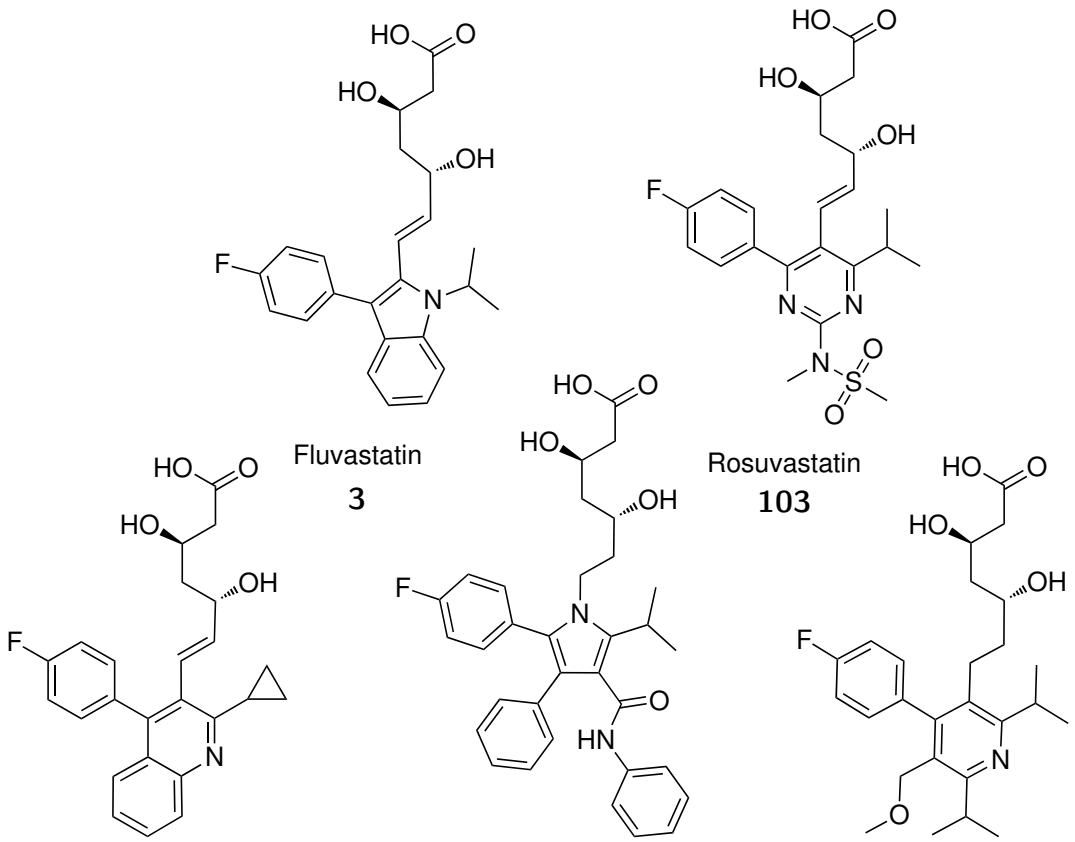

Figure 1.29: Commercially available synthetic statins

1.4 Aims

Incorporation of HMG-CoA reductase inhibitors towards NMT transition state mimetics

This project will investigate the potential of designing NMT inhibitors, through synthesis, that include fragments from the HMG-CoA reductase inhibitors. Inclusion of statin fragments into myristic structures could initiate a novel mode of inhibition of NMT with potential applications towards *T. brucei* and *P. falciparum*. Similarly the investigation will also include the incorporation of features developed previously as myristic acid analogs as to explore the structure-activity dependency of the myristic chain.

The hypothetical NMT inhibitor **107** shows the 4 key aspects to be explored in the scope of this structure-activity investigation. Firstly **107** contains a non-cleavable linker housed between the myristic chain and the peptide glycine N-terminus. The inhibitor **107** also incorporates a fluvastatin fragment. The application of statin fragments towards NMT is one of the major scientific outcomes to be explored in this investigation. Lastly **107** contains a myristic chain analog that contains a phenoxy fragment inspired from a myristic acid analog which has a demonstrated HAT toxicity (see Figure 1.12). The investigation will approach each segment individually so to build a clear understanding the structure activity dependency of the key elements towards *T. brucei* and *P. falciparum*.

In Chapter 2, the structure-activity investigation will commence through synthesis of a simplified version of **107**. The initial target **108** contains a non cleavable 3-hydroxy amine system with a glycine substitution. A non-cleavable myristoyl-CoA analogue was previously demonstrated as a potent NMT inhibitor (see Figure 1.4). It is postulated that a similar strategy in a transition state mimetic may improve potency by resisting metabolism. The intermediate **109** does not contain a substituted amine or a functionalised myristoyl chain, and thus provides a baseline toxicity against *T. brucei* and *P. falciparum* and an initial proof of concept. Amine substitutions, generalised in **110**, will provide information about favourable substitutions that improve the potency and selectivity

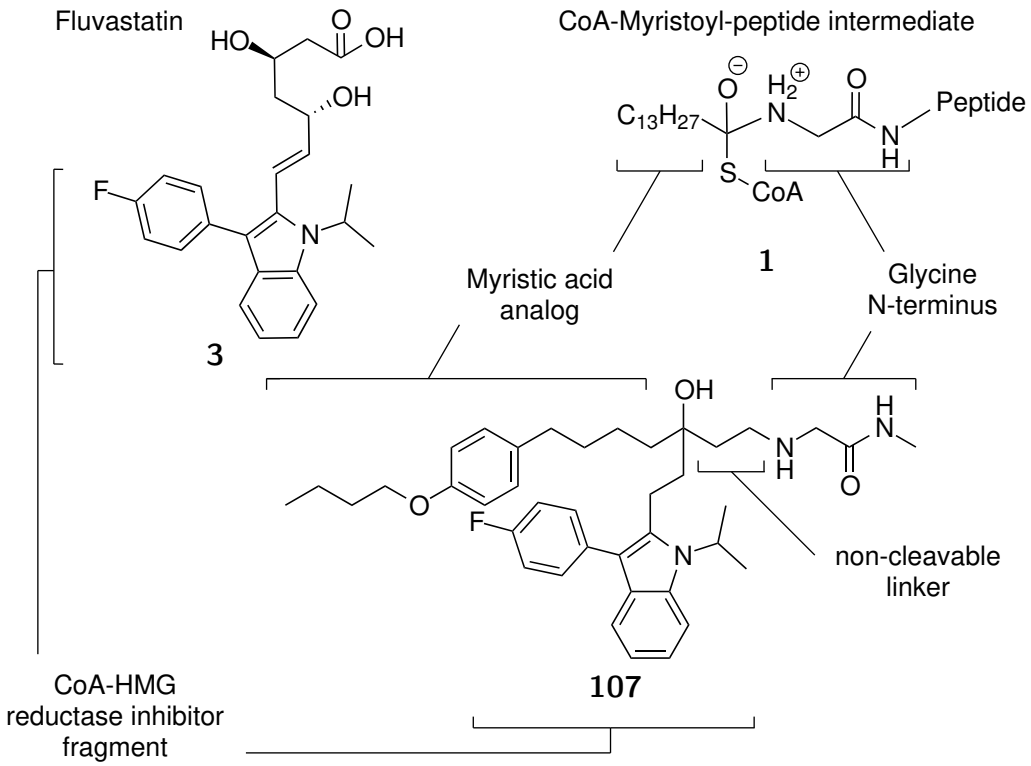

Figure 1.30: The hypothetical inhibitor **107** showing key aspects of the SAR invesagation.

profiles against *T. brucei* and *P. falciparum*.

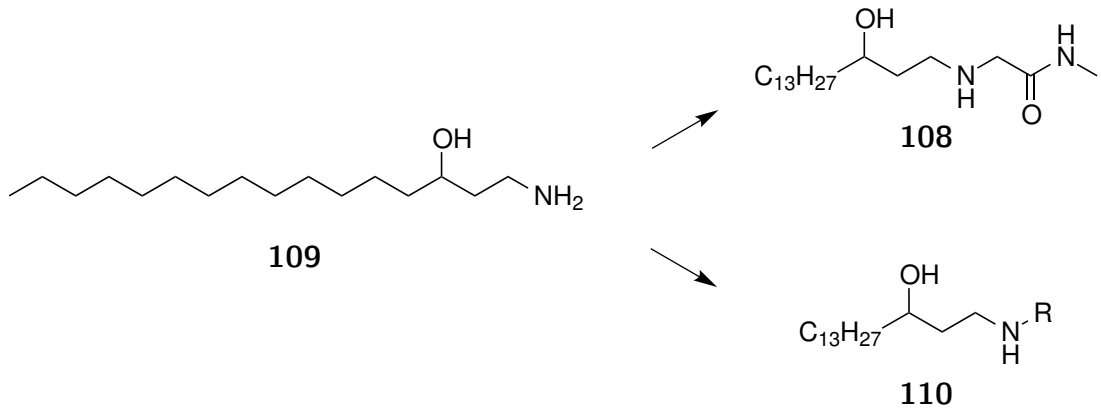

Figure 1.31: Inital target **108** from its key intermediate **109** used for further derivatation.

Synthesis of the key intermediate **109** is proposed from ethyl myristate **111**. The linker length between the hydroxyl and amine functional groups will be explored though the synthesis of two variations of **109**. Synthesis of the C1 hydroxyamine **112** is proposed via the cyanohydrin **113**. Conversely, synthesis of the C3 hydroxy amine **114** is proposed from from its alkyne **115**.

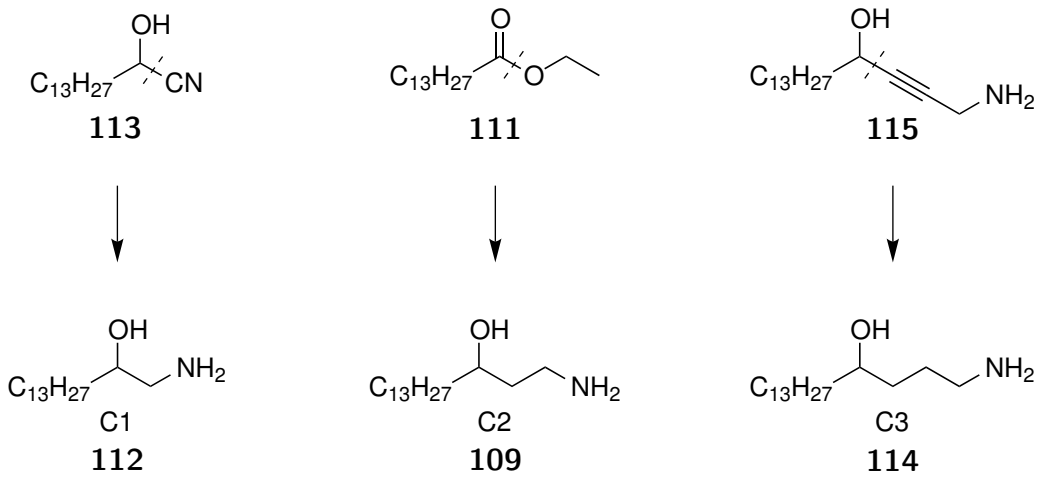

Figure 1.32: Investagation into the structure activity dependency of the hydroxy-amine linker.

Chapter 3 will investigate the incorporation of statin fragments into NMT memetic inhibitors. Baseline activity towards *T. brucei* and *P. falciparum* will be provided by the hydroxyamine **109**. The structure activity investigation will then functionalise the hydroxyamine **109** with statin fragments and make an assessment of the effects towards *T. brucei* and *P. falciparum* toxicity. Figure 1.33 illustrates two targets **116** and **117** which incorporate a fluvastatin fragment into **109**. The target **116** illustrates the structure-activity investigation though the incorporation of a fluvastatin fragment as a tertiary alcohol. Conversely **117** illustrates another structure-activity investigation strategy by incorporation of the fluvastatin fragment through an amine substitution. The two targets **116** and **117** illustrate the strategic investigation into the two potential CoA binding areas of NMT, accessible by adding complexity to the hydroxyamine **109**.

The structure-activity investigation will develop two series of compounds. The first series of compounds will incorporate several increasingly complex statin fragments as tertiary alcohols (Figure 1.34). The second series will investigate the activities of compounds with the same fragments installed as amine substitutions. Analysis of the potency and selectivity profiles of each compound set **118** and **119** against *T. brucei* and *P. falciparum*, and comparison with the unsubstituted hydroxy amine **109** will offer information to the dependency of the statin fragments to binding efficiency with NMT.

Chapter 4 will focus on the structure activity investigation of the myristic chain.

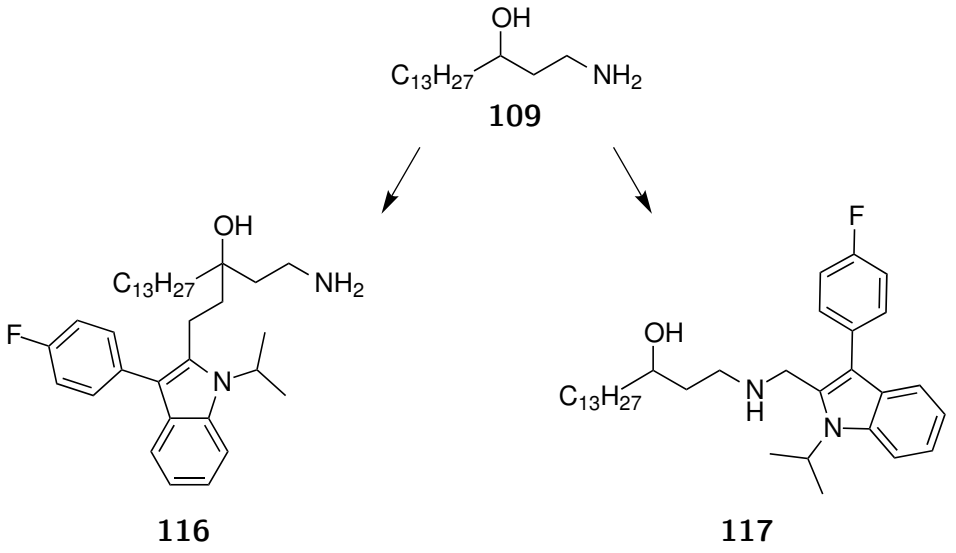

Figure 1.33: Investagation into the structure activity dependency of statin fragment.

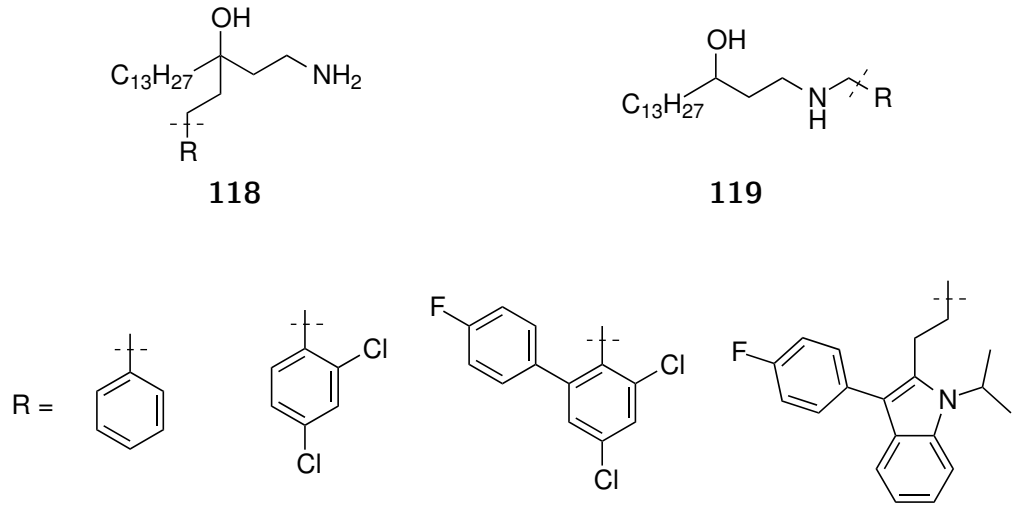

Figure 1.34: Introduction of statin fragment to the parent hydroxyamine **109**.

Several myristic acid analogues have been demonstrated to show anti-HAT and anti-fungal activity. If a myristic acid analogue shows activity though competitive inhibition, incorporating the chain functionality from the myristic acid analogues would improve the potency and selectivity profiles of mimetic inhibitors. Two myristic chain functionalised targets are shown in Figure 1.35. The first target **120** incorporates a phenoxy fragment at the C6 position of myristoyl chain contained on**109**. The second target **121** incorporates a *cis*-alkene at the C5 position of the myristoyl chain. The aim of both targets is to explore whether functionalisation of the chain leads to improved binding efficiency towards NMT and a improved potency and/or selectivity profile towards *T. brucei* and *P. falciparum.*

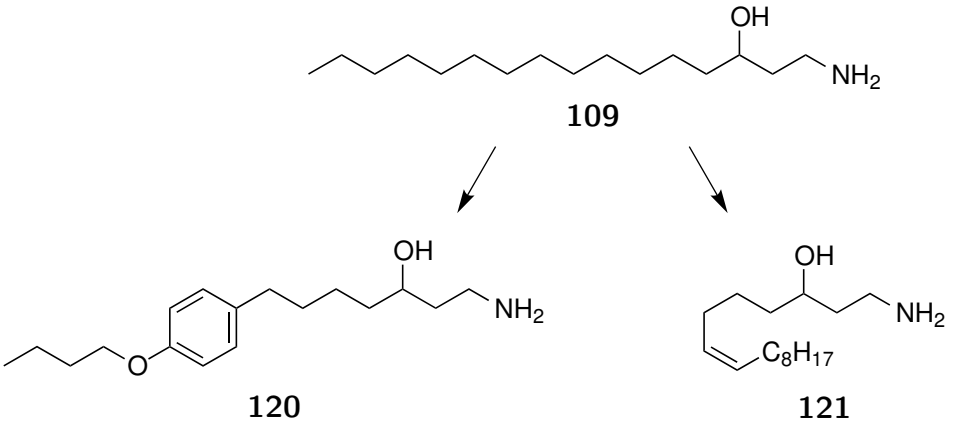

Figure 1.35: Investagation into the structure activity dependency the myristoyl chain.

Chapter 2

Myristoyl-Peptide Mimetics

2.1 Linear synthesis of proposed NMT inhibitor 108

Two targets were envisaged for the proof of concept studies for the proposed NMT inhibitors, namely the amines **122** and **108**. These amines are reminiscent of the tetrahedral intermediate **123** formed in the reaction catalysed by NMT. The amines **122** and **108** contain a 13 carbon chain and a charged glycine subunit mimicking the myristic acid and the peptide chain respectively. A CoA-emulating moiety was not used initially as to provide baseline activity during biological assessments for this potential binding motif. The target **108** was favoured over **122**, because **122** was thought to be susceptible to glycolytic cleavage in the cell. Unlike **122**, the extra methylene in **108** provided a non-cleavable linker and thus postulated to reduce metabolic deactivation.

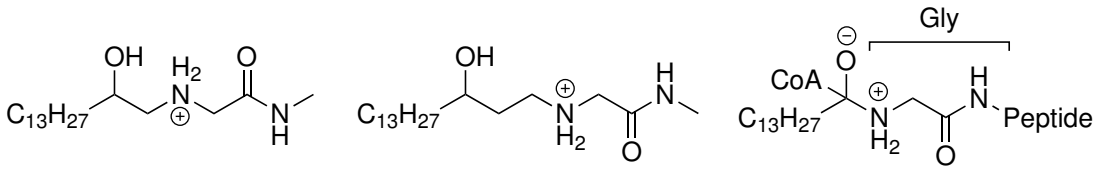

122 **108** **123**

Figure 2.1: The initial transition state mimetics **122** and **108** and the transition state of NMT **123**

The proposed synthesis of **108** from myristic acid **7** is shown in Scheme 2.1.

The esterification of myristic acid **7** followed by a Claisen condensation with acetonitrile should produce the ketonitrile **124**. Reduction of the ketonitrile **124** to the amine **109** could be performed using a metal hydride reduction to give the hydroxyamine **109**. Then attachment of methyl glycine, using **125**, would generate **108** in a relatively short synthesis.

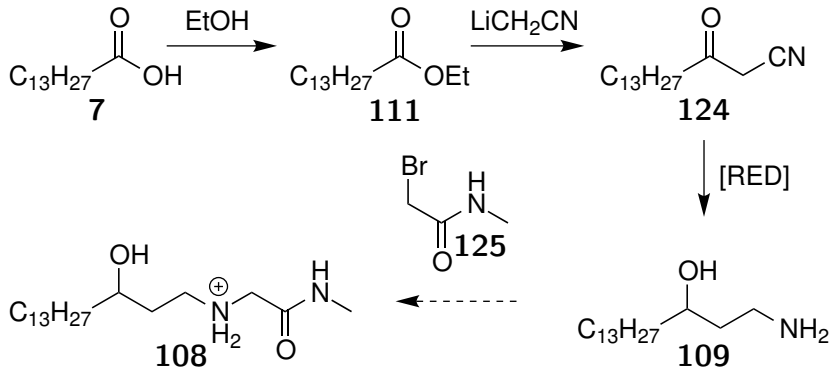

Scheme 2.1: Proposed synthesis of target **108**

Ethyl myristate **111** was prepared using a Fisher esterification (Scheme 2.2).[86] A solution of myristic acid and sulphuric acid in ethanol was heated under reflux for 24 hours to give the ester in good yield after vacuum distillation. After some experimentation, the conversion of the ester to the ketonitrile **124** was accomplished. However, to obtain good yields, strict anhydrous conditions were required (Scheme 2.2). The nucleophile for this reaction was lithioacetonitrile and was prepared by treating anhydrous acetonitrile with *n*-butyllithium at -84°C.[87–89] Good yields of **124** were obtained when the ester **111** was treated with two equivalents of lithioacetonitrile at -45°C. An excess of base was used as a precaution to ensure the ketonitrile **124** was sequestered as the enolate **126** avoiding significant generation of the double addition product **127**, which was not observed in the reaction (Scheme 2.3).

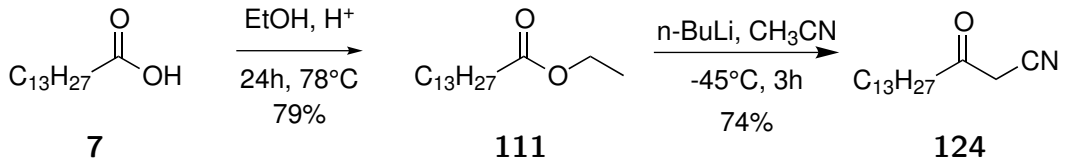

Scheme 2.2: Generation of the ketonitrile **124**

The high solubility of the unreacted starting material **111** and other by-products

in petrol was exploited in the purification of **124**. Trituration of the crude residue with petrol gave the pure ketonitrile in good yield (Scheme 2.2). The ^{1}H NMR spectrum of the ketonitrile **124** contained the key singlet at 3.43 ppm (2H) assigned to the methylene between the nitrile and carbonyl groups. A triplet at 2.61 ppm (2H) was assigned to the methylene on the alkyl chain adjacent to the ketone. The ^{13}C NMR spectrum contained the expected 16 signals and the presence of a ketone and nitrile functional groups confirmed by the signals at 197.7 and 114.0 ppm respectively. The presence of the nitrile and carbonyl was also confirmed by their respective absorbances at 2259 and 1716 cm^{-1} in the IR spectrum. With sufficient quantities of the ketonitrile **124** in hand, the reduction of the nitrile and ketone functional groups were explored.

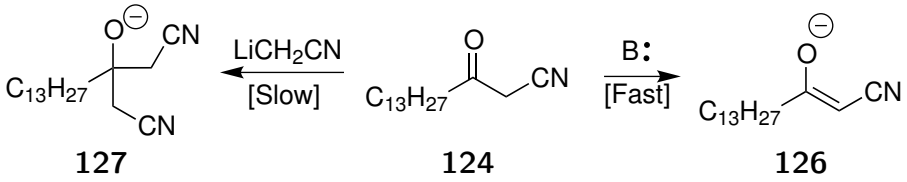

Scheme 2.3: Potential side reaction of ketonitrile generation

Cobalt boride is a mild reducing reagent used to convert nitriles to amines[90,91] and was expected to generate the hydroxamine **109** from the ketonitrile **124**. When the ketonitrile **124** was exposed to cobalt boride, generated *in situ* by reacting cobalt chloride and sodium borohydride, a new product was isolated (Table 2.1.1). The crude isolated material had no starting material by TLC and showed a new highly polar spot expected for the hydroxyamine **109**. The ^{1}H NMR spectrum of this crude material also confirmed consumption of the starting material and broad new signals at 3.80, 3.13 and 2.85 ppm which suggested the 1,3-hydroxyamine system of **109**. Despite the evidence of a successful reduction, performing this reaction on a large scale (>500 mg) was problematic. Acidic conditions were required to remove excess cobalt boride. This led to protonation of the amine, essentially forming a surfactant which led to emulsions. Under basic conditions, the hydroxamine **109** became an excellent ligand for the cobalt ion, leading to broad NMR signals. As a consequence, this reaction was impractical and an alternative reduction procedure was explored.

Lithium aluminium hydride in THF has been used to reduce nitriles to amines[92]

Table 2.1.1: Reduction of the ketonitrile **124**

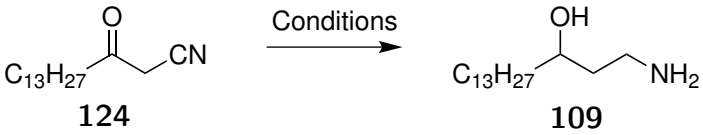

124 **109**

conditions	**109**
$CoCl_2$, $NaBH_4$, EtOH, RT, 1h, HCl workup.	56% (impure crude)
$LiAlH_4$, THF, 3h, RT.	55% purified.

and was successfully employed in the generation of the hydroxamine **109**. A crystallisation workup was applied by sequential addition of water and sodium hydroxide solution which precipitated the bulk of the lithium/aluminium salts which were removed by filtration. Subjecting the crude material to column chromatography gave the desired hydroxamine **109** in reasonable yields (Table 2.1.1). The ^{13}C NMR spectrum of the isolated product possessed considerable signal overlap around 30 ppm because of the similarity of chemical shifts contained in the myristoyl chain. Similar signal overlap occurs in a large majority of the compounds containing the myristoyl chain (e.g. ethyl myristate **111**[93]) and consequently the number of carbon signals reported in the experimental does not equal the number of carbons that theoretically have independent chemical shifts. The ^{1}H NMR spectrum of **109** contained a broad signal at 3.80 ppm assigned to the methine with a hydroxyl substitution. A new stereocenter led to two doublet of triplets at 3.13 and 2.85 ppm and assigned to the methylene protons with an amine substitution. Reduction was confirmed by the absence of the nitrile and carbonyl ^{13}C NMR signals and the presence of a hydroxyl substituted methine signal at 73.4 ppm.

Conversion of the 3-hydroxyamine **109** to the target **108** was expected via a substitution reaction as per Scheme 2.1. 2-Bromo-*N*-methylacetamide **125** was required to prepare the target **108** from the amine **109**, and was made by a substitution reaction, using 2-bromoacetyl bromide and methylamine hydrochloride (Scheme 2.4).[94,95] The deprotonation of methylamine hydrochloride with sodium hydroxide generated methyl amine, an excellent nucleophile, which quickly perfored a substitution with the acid bromide **128** to give **125** in good yield. Attempts to purify **125** by vacuum distillation[94] were unsuccessful due to thermal

decomposition of **125**. Nevertheless, the crude material obtained after workup was used in the subsequent reactions with the hydroxyamine **109**.

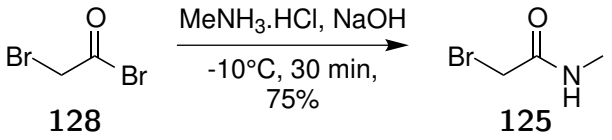

Scheme 2.4: Generation of the glycyl derivative **125**

Conversion of the hydroxyamine **109** to the glycine target **108** required the mono-substitution with 2-bromo-*N*-methylacetamide **125**. The amine functional group contained on **109** is inherently a better nucleophile than its hydroxyl functional group. A alkylation reaction with **125** was expected to preferentially derivatise the amine to give **108**. However, when a mixture of 3-hydroxyamine **109**, bromide **125** and potassium carbonate was heated under reflux, this gave the double substitution product **129** (Table 2.1.2). Figure 2.2 shows the expanded ^{1}H NMR spectrum of **129** which provided sufficient information to assign the unwanted double substitution product. Two key signals visible at 3.19 ppm (4H) and 2.81 ppm (6H) were assigned to the respective alkyl protons ② and ③ shown in Figure 2.2. **129** was isolated instead of the target **108** as it contains a free amine available for a second substitution with the bromide **125**. The inherent preference of the alkylation reaction to form the double substituted product **129** implies that the first substitution is slow with respect to the second (Table 2.1.2).

Table 2.1.2: Relative reaction rate for competing substitution reactions

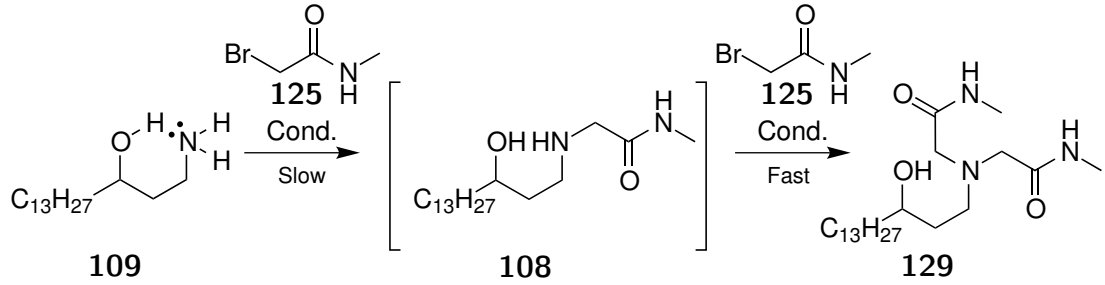

Conditions	**108**:**129**
1 eqv **125**, K_2CO_3, THF, 66°C, 48h.	0 : 100*
1 eqv **125**, K_2CO_3, DMSO, 66°C, 24h.	0 : 100
1 eqv **125**, K_2CO_3, DMF, 66°C, 24h.	0 : 100
1 eqv **125**, CsOH, 4A-MS, DMF, 25°C, 60h.	complex mixture

*__129__ was isolated 45% yield based on **125**

Attempts were made to optimise the reaction to isolate the mono-substitution product **108**. Experiments were conducted using DMSO or DMF as the solvent, however the exclusive formation of the double addition product was again observed in both cases. These attempts were performed to investigate if a rate change of the first substitution, with respect to the second substitution, could be induced by using more polar and protic solvents. No changes were noted and formation of the undesired double substitution product **129** was observed. A method for mono-substitution of primary amines using caesium hydroxide and 4Å-MS was reported by Salvatore.[96] According to the authors, the caesium cation under anhydrous conditions leads to chelation with amine thus affecting its reactivity.[97] However, when **109** and **125** were stirred with caesium hydroxide in DMF for 60 hours **129** was formed as part of a complex mixture and consequently a protection strategy for the synthesis of the mono substitution product **108** was envisioned.

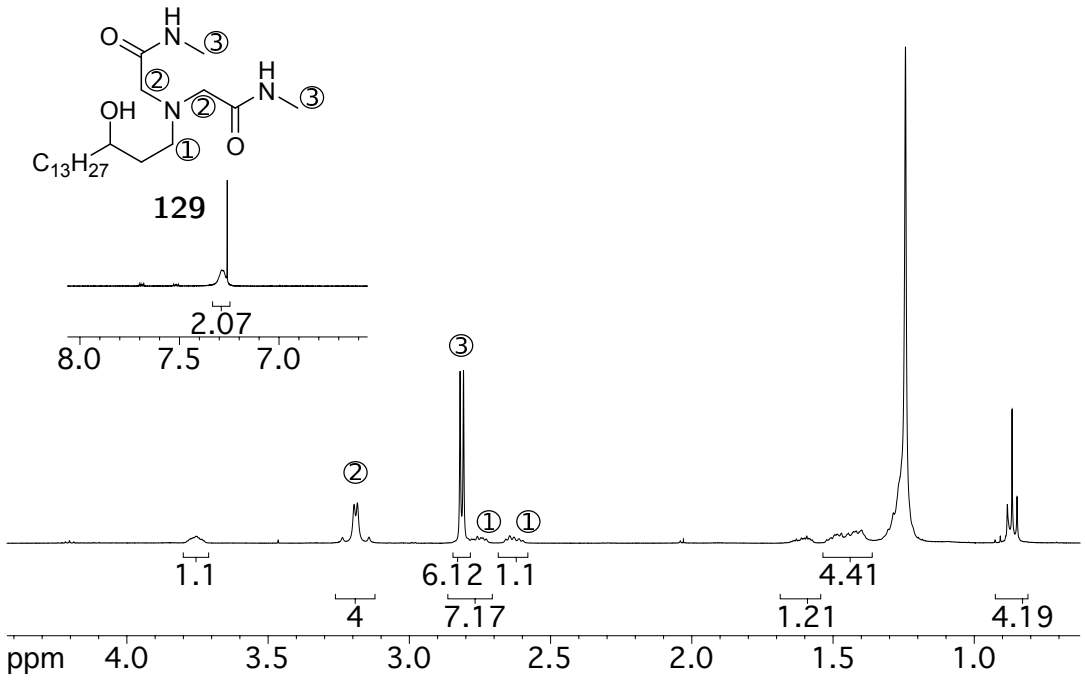

Figure 2.2: Double substitution product obtained from direct alkalation

2.1.1 Carbamate protective strategies

In light of the inherent reactivity of the hydroxyamine **109** towards double substitution, a protection strategy towards **108** was pursued. Carbamates are standard protective groups for amines and several installation and deprotective methods are available.[98] The conversion of the amine to a carbamate **130** is possible though a substitution reaction. Scheme 2.5 pivots on conditions that promote carbamate substitution reported by Salvatore.[99] Application of these conditions should promote the acylation reaction between **130** and the methyl glycine fragment **125**. Deprotection of **131** would generate the target **108**.

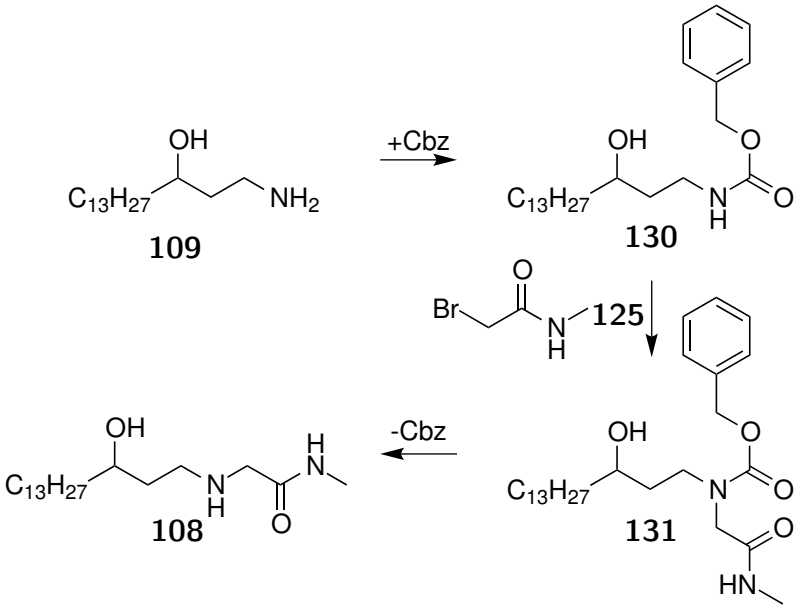

Scheme 2.5: Proposed mono-substitution of **109** via benzyl carbamate protection

The hydroxyamine **109** was converted to its benzyl carbamate derivative **130** in good yield using benzyl chloroformate and a non-nucleophilic base, DIPEA (Scheme 2.6).[100] The ^{1}H NMR spectrum of the carbamate showed a distinct benzyl singlet at 5.12 ppm and a multiplet in the aromatic region integrating to 5 hydrogens. The ^{13}C NMR spectrum also showed 4 new aromatic signals and **130** was confirmed by the presence of new carbamate and benzyl signals at 157.3 and 66.9 ppm respectively.

Salvatore reported using caesium carbonate under phase transfer conditions to improved the inherently low nucleophilicity of the carbamate nitrogen.[99] Follow-

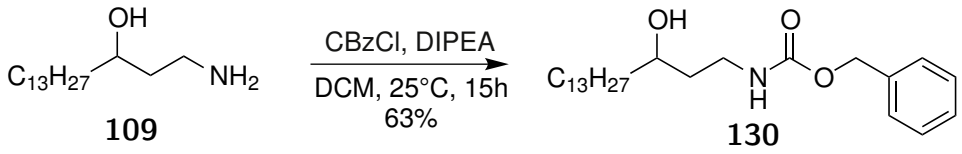

Scheme 2.6: Benzyl carbamate protection of **109**

ing the same conditions the benzyl carbamate **130** and **125** were stirred with TBAI and caesium carbonate in DMF at room temperature (Scheme 2.7). The expected product **131** was not isolated from the reaction mixture, instead two new compounds **132** and **133** were isolated in trace quantities and characterised by NMR spectroscopy.

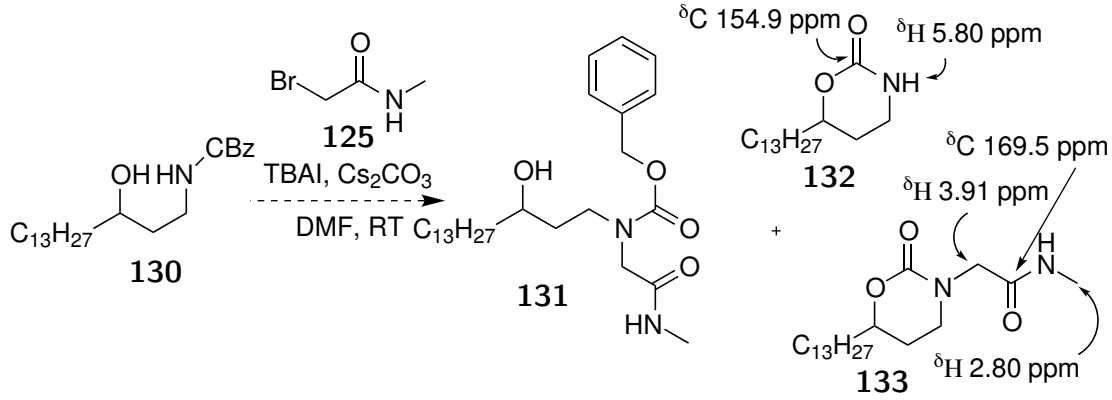

Scheme 2.7: By-products isolated from the substitution of **130**

The NMR spectra of the two isolated products **132** and **133** were notable in the absence of a benzyl group. Compound **132** contained a new carbamate carbonyl signal at 154.9 ppm and a signal at 5.80 ppm indicative of a carbamate proton (Scheme 2.7). Compound **133** contained an amide carbonyl signal at 169.5 ppm and a carbamate carbonyl signal at 155.0 ppm. The ^{1}H NMR spectrum of **133** did not contain a carbamate proton signal at 5.80 ppm instead new signals at 3.91 and 2.80 ppm indicated the presence of the methyl glycine fragment.

The proposed mechanism for the formation of **132** and **133** is shown in Scheme 2.8. The first step is the deprotonation of the hydroxyl group contained on **130** to give the anion **134**. The alkoxide anion **134** is a excellent nucleophile and performs an intramolecular nucleophilic substitution via the tetrahedral intermediate **135** to give the cyclic carbamate **132**. Subsequent deprotonation of **132** generates the alkoxide **136** capable of a substitution reaction with **125** leading to the genera-

tion of **133**. These by-products inspired the development of alternative methods to generate **132** directly from the free hydroxyamine **109** and its subsequent alkylation.

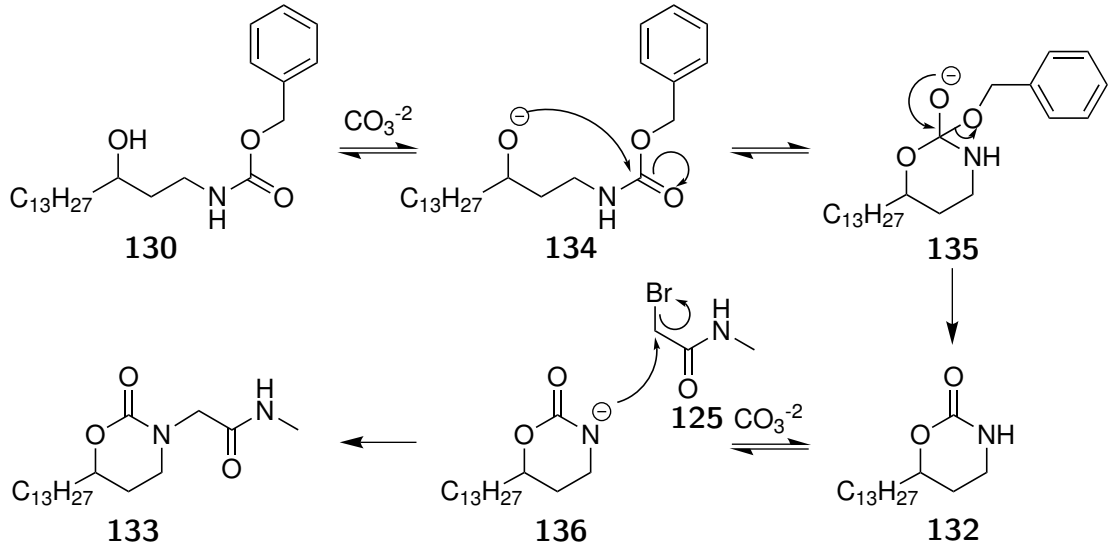

Scheme 2.8: Cyclic carbamate formation and alkylation

As the cyclic carbamate **132** is also effectively a protecting group, its direct formation was investigated (Scheme 2.9). The formation of cyclic carbamates from 1,3-hydroxyamines are readily performed using a variety of reagents such as phosgene, carbon monoxide, carbonate esters and carbonyldiimidazole (CDI).[98] Substitution of the cyclic carbamate **132** with the methyl bromoacetate **125** would be promoted through the use of a strong base. Hydrolysis of the carbamate on **133** would generate the target **108**. The first step required carbamate cyclisation and as carbonyldiimidazole was available, this reagent was tested for the synthesis of **132**.

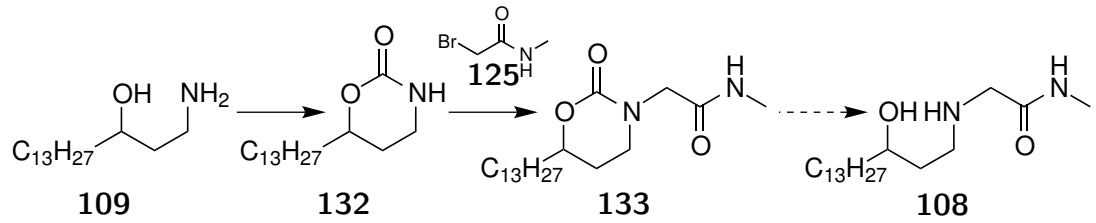

Scheme 2.9: Dual alcohol and amine protection via cyclic carbamate formation

The conversion of the hydroxyamine **109** to the cyclic carbamate **132** was achieved using two equivalents of CDI in THF at reflux (Scheme 2.10).[101,102] The mater-

ial isolated was significantly less polar that the starting material. The ^{1}H NMR spectrum of **132** contained a 2 proton multiplet at 3.35 ppm and shifts in the hydroxyl substituted methine signals were witnessed. A new carbamate N-H signal of **132** was visible at 5.35 ppm (Figure 2.3) with the remaining NMR signals matching that obtained from Scheme 2.7.

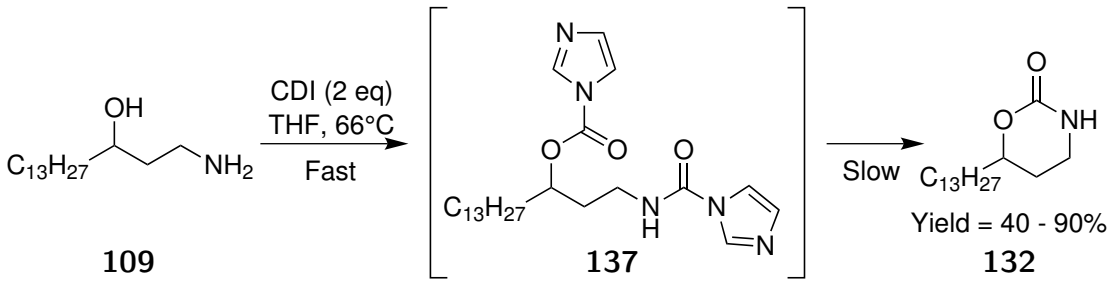

Scheme 2.10: Posibile intermediates during reaction using CDI

Unfortunately repeating the reaction under the same conditions gave inconsistent yields, ranging from 40 to 90%. To gain further insights, the reaction was periodically monitored using ^{1}H NMR (Figure 2.3). After 3 hours the reaction mixture ② showed complete consumption of the starting material ①. The reaction mixture ② shows new downfield signals indicating the formation of the intermediate **137**. After heating ③ shows a mixture of the intermediate **137** and the desired carbamate **132**. ④ was obtained after prolonged heating and workup. The variable yields were attributed to removal of the intermediate **137** during an acidic workup. After some experimentation, the optimised conditions used single equivalent of CDI in THF and held at reflux for 6 hours. Repeatable excellent yields were obtained and shorter reaction times were observed with no further purification required beyond an acidic workup.

When an alkylation reaction was performed by sequential deprotonation of the acidic amide of **132** using sodium hydride, followed by addition of 2-bromo-*N*-methylacetamide **125** and heating under reflux, two products were obtained in low yield (Scheme 2.11). The first product was identified as **133** and its ^{1}H NMR spectrum was identical to the product originally isolated in Scheme 2.7. The second major product **138** required careful NMR analysis to confirm its structure.

Figure 2.4 shows an expanded overlay of the ^{1}H NMR spectra for **133** and **138**.

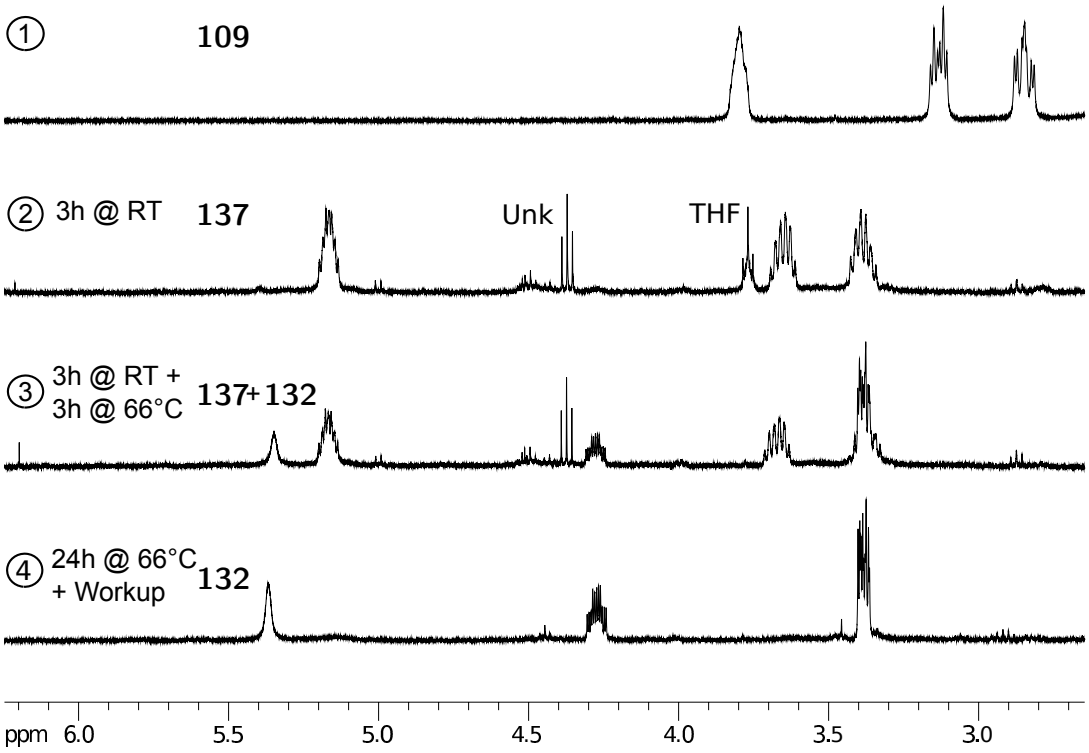

Figure 2.3: Monitoring Scheme 2.10 by ^{1}H NMR spectrometry.

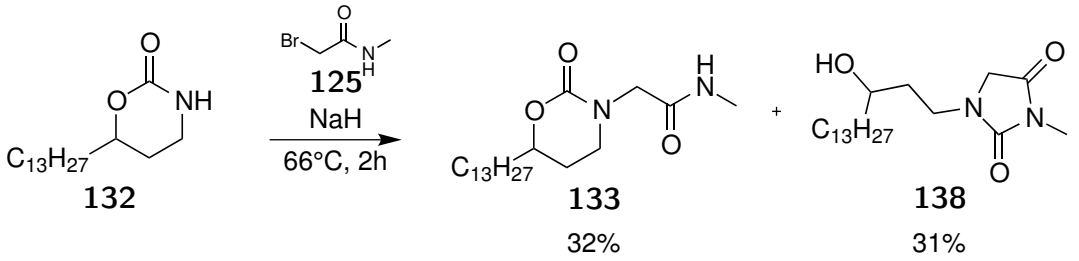

Scheme 2.11: Alkylation of cyclic carbamate

Interestingly **138** no longer possesses a downfield amide signal at 6.46 ppm. The imidazolium ring structure of **138** was primarily assigned as the methyl signal appeared appeared as a singlet at 3.02 ppm. Two carbonyl signals remained 170.2 and 157.7 ppm in the ^{13}C NMR spectrum of **138**, as did the indicative AB pattern in the ^{1}H NMR spectrum. A shift of the hydroxyl substituted ^{13}C carbon signals from 78.0 ppm in **133** to 68.8 ppm in **138** confirmed the cleavage of the carbamate, a change mirrored in the ^{1}H NMR spectra.

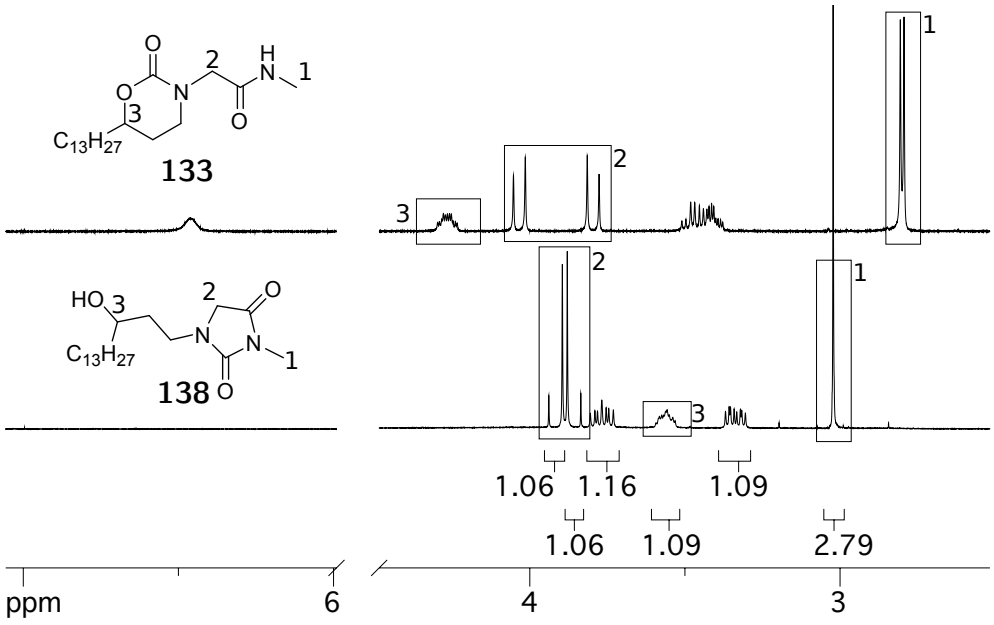

Figure 2.4: Overlay of the ^{1}H NMR spectra of compounds **133** and **138**.

The proposed mechanism for the formation **138** from **133** under basic conditions is shown in Scheme 2.12. Sodium hydride can deprotonate the glycyl amide in **133**, resulting in the anion **139** capable of intramolecular reaction to give the alkoxide **140** that generates **138** after workup. The formation of **140** is favoured over **139** though stability gained by the formation of a urea. Despite the formation of the by-product **138**, sufficient quantities of **133** were obtained to enable the investigation of the hydrolysis of its carbamate.

Standard conditions for hydrolysis of cyclic and acyclic carbamates employ basic conditions and can be performed using a number of weaker bases such as potassium *tert*-butoxide, barium hydroxide, caesium carbonate or lithium hydroxide.[98] When **133** was treated with lithium hydroxide in wet methanol (Table 2.1.3), the urea **138** was isolated as the product. A similar observation was made with

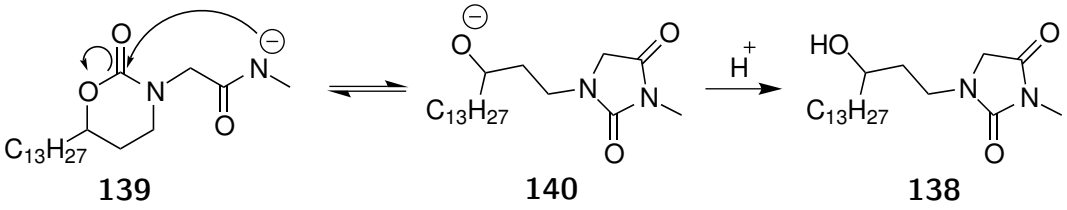

Scheme 2.12: Formation of unwanted imidiazolium alcohol **138**.

caesium carbonate and thus further hydrolysis experiments of **133** under basic conditions were abandoned.

Table 2.1.3: Carbamate de-protection trials

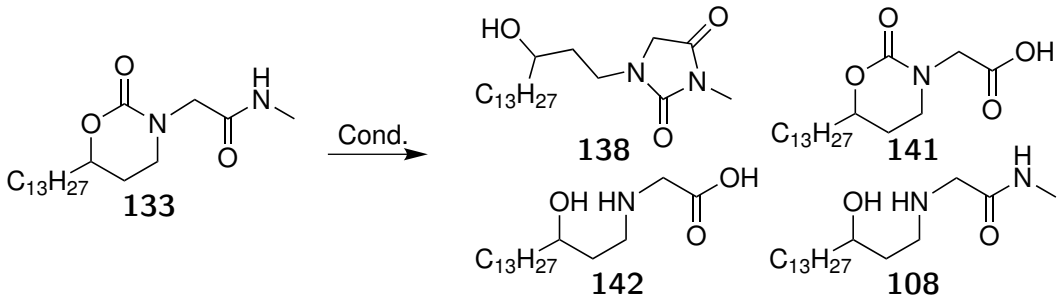

Conditions	**133**	**138**	**141**	**142**	**108**
LiOH, H_2O/MeOH, 25°C, 15h.	Minor	Major	-	-	ND
Cs_2CO_3, H_2O/MeOH, 25°C, 15h.	Minor	Major	-	-	ND
CH_3COOH, HBr	Recovered	-	ND	ND	ND
TFA, $CHCl_3$, 61°C, 15h.	Recovered	-	ND	ND	ND
~1M HCl, H_2O/MeOH, 25°C, 24h.	Recovered	-	ND	ND	ND
~6M HCl, H_2O/MeOH, 55°C, 15h.	Minor	-	Major	ND	ND

Examples of carbamate hydrolysis under acid conditions were not prevalent in the literature for systems such as **133**.[98] Acidic conditions have been used to cleave methyl and ethyl carbamates a reagent such as hydrobromic acid in acetic acid. No change to the TLC was seen on exposure of **133** to hydrobromic acid in acetic acid. Exposure of **133** to trifluoroacetic acid also showed no change in TLC (Table 2.1.3). Forcing conditions were applied by reacting **133** with hydrochloric acid, at elevated temperatures. Under these conditions a new product was observed by NMR spectroscopy (Figure 2.5). The ^{1}H NMR spectrum show a upfield shift from 3.90 ppm in **133** to 4.10 in **141** combined with a significant change to is AB coupling pattern. With the AB pattern intact it was probable the trigonal planar carbamate was still present and this was confirmed by two new carbonyl signals and matching oxygen substituted signal. Carbamate hydrolysis

was excluded as no hydroxyl substituted ^{13}C signal was present around 72 ppm expected from a secondary alcohol. Amide hydrolysis was confirmed by the lack a of matching ^{1}H methyl signal at approximately 2.8 ppm and the lack of a ^{13}C signal at 27.40 ppm. The liability of amide cleavage over carbamate cleavage was a major synthetic obstacle while utilising the cyclic carbamate as a protective group.

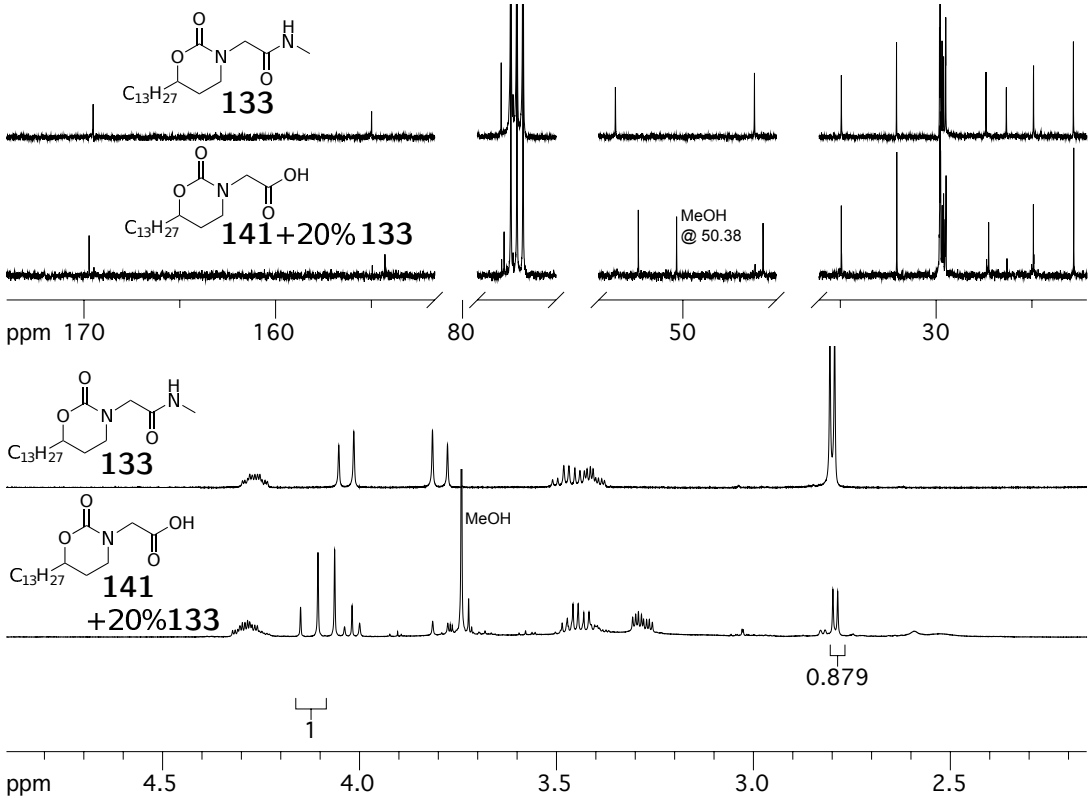

Figure 2.5: ^{1}H and ^{13}C NMR spectra overlays of crude reaction mixture containing **141** with its precursor **133**

The cyclic carbamate **132** allows for mono-substitution to give **133** (Scheme 2.11). However, the use of a cyclic carbamate protective system gave rise to a new synthetic obstacle as standard deprotection methods, under basic conditions, led to the generation of the undesired rearrangement product **138** (Table 2.1.3). The lability of the glycyl amide bond in preference to the carbamate amide bond under acidic conditions led to a synthetic dead end. The incompatibility of **133** with basic conditions, and the lability of the glycyl amide bond, were critical obstacles in the efforts to generate the target **108**. Protection methods that would effectively mask the reactivity of the acidic amide contained on **133** enabling carbamate hydrolysis under basic conditions were then explored.

2.1.2 Benzyl acetamide protection strategies

To circumvent the base catalysed rearrangement of **133** to **138** seen in the previous section the use of a benzyl protected acetamide **143** was investigated (Scheme 2.13). Substitution of **132** with **143** would generate tertiary amide **144** and hydrolysis of **144** prior to debenzylation would give access to the target **108**. Scheme 2.13 pivots on amide debenzylation which are well reported in the literature.[98]

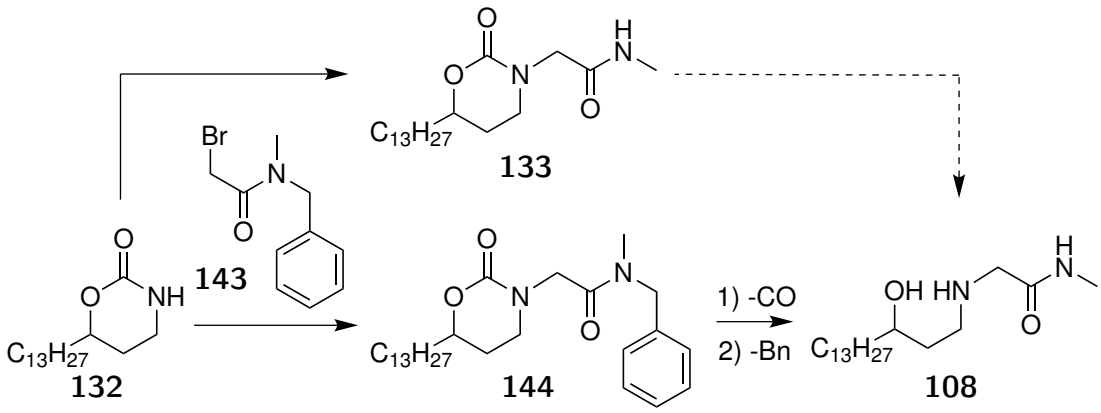

Scheme 2.13: Alternative synthesis of **108** amenable to basic hydrolosis conditions

The proposed synthesis of the bromide fragment **143** used 2-bromoacetyl bromide **128** akin to Scheme 2.4, except *N*-methylbenzylamine **145** was to be used instead of methylamine hydrochloride. *N*-Methylbenzylamine **145** was made from benzyl bromide **146**. A substitution reaction between methylamine and benzyl bromide in methanol was performed at room temperature (Scheme 2.14). A 1:1 molar mixture of **145**:**147** was obtained despite using 13 equivalents of methyl amine. The mixture was used in the next step without purification.

The next synthesis step was the alkylation of *N*-methylbenzylamine **145** with 2-bromoacetyl bromide. The crude mixture containing *N*-methylbenzylamine **145** was exposed to bromoacetyl bromide in dry DCM at 0°C (Scheme 2.14) using triethylamine as an acid scavenger. Purification of the reaction mixture was achieved by an acidic work up and column chromatography to give **143** in low yield over two steps. The ^{1}H NMR spectrum showed a number of rotamer signals expected for a tertiary amide and contained a benzyl signal at 4.60 ppm (Figure 2.6). The ^{13}C NMR spectrum mirrored the rotamer splitting trend and

contained a key carbonyl signal at 167.0 ppm indicative of amide substitution. The ^{1}H NMR spectrum matched those reported by Cappelli[103] and a sample was obtained with an acceptable purity for the following reaction. The low yield was attributed to utilising a crude mixture as the starting material but sufficient quantities of **143** were obtained by synthesis on the large scale.

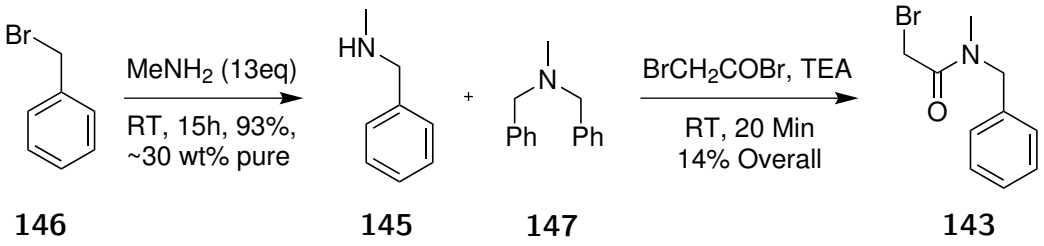

146 **145** **147** **143**

Scheme 2.14: Two step formation of 2-bromo-*N*-methyl-*N*-benzyl acetamide

The cyclic carbamate **132** was reacted with the bromide **143** using sodium hydride in THF (Scheme 2.15). The reaction proceed smoothly without the formation of the by-product **138** and gave **144** in high yield. The ^{1}H NMR spectrum contained signals at 4.34, 3.50 and 3.33 ppm from the protons adjacent to the carbamate system. **144** had overlapping signals centered around 4.19 ppm containing the AB pattern caused by substitution of the trigonal planar carbamate system and splitting from rotamers induced by the benzyl acetamide sytem. Consequently the ^{13}C NMR spectrum was also complex. The key amide carbonyl signal was present at 168.1 ppm and complemented by a carbamate carbonyl at 154.6 ppm. Sufficient quantities of **144** were obtained to perform deprotective carbamate trials.

Hydrolysis of the cyclic carbamate **144** using lithium hydroxide in wet ethanol proceeded smoothly in good yield to give the secondary amine **148** (Scheme 2.15). The new product **148** no longer contained a typical carbamate carbonyl signal at around 155 ppm and the hydroxy substituted ^{13}C signal shifted from 77.8 ppm in **144** to 73.2 ppm. Hydrolysis was also confirmed as the ^{1}H NMR hydroxyl substituted methine signal showed a shift to 3.79 ppm in **148**. A single carbonyl signal, present as a rotamer pair at 171.3 and 170.9 ppm, was characteristic of the tertiary amide present on **148**. A successful hydrolysis of **144** under basic conditions was attributed to the benzyl protection of the acidic amide thus

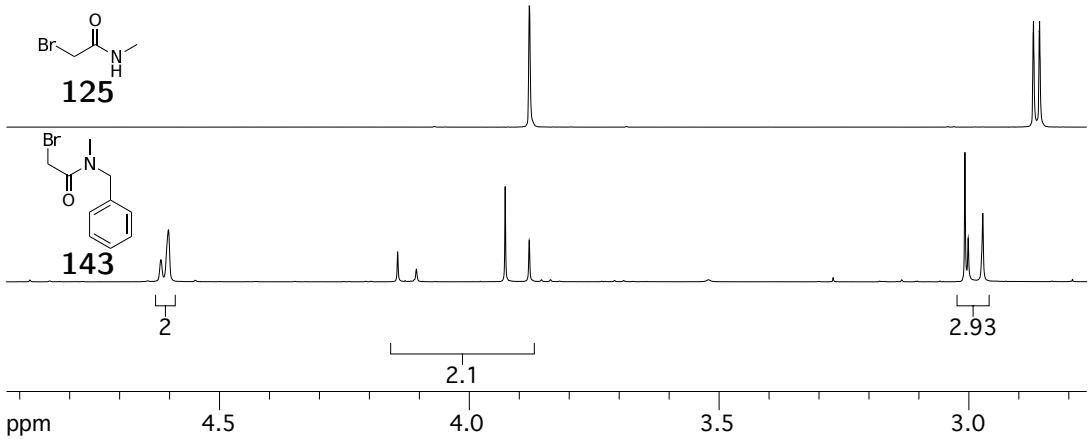

Figure 2.6: Rotamer signals in the ^{1}H NMR spectrum of **143** and comparason with 2-bromo-*N*-methylacetamide **125**

circumventing the unwanted cyclisation product **138** in Scheme 2.15.

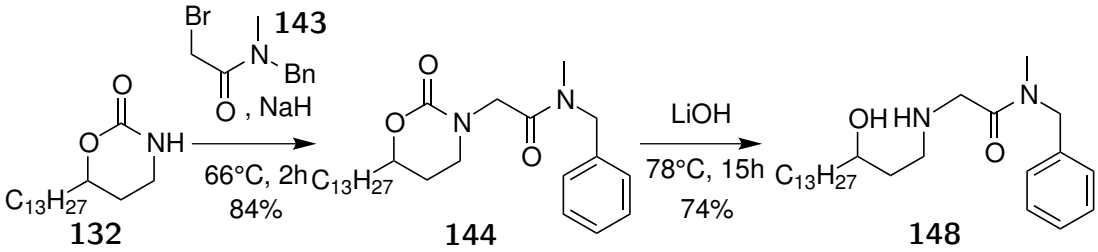

Scheme 2.15: Substution of the cyclic carbamate **132** with 2-bromo-*N*-methyl-*N*-benzylacetamide **143** and carbamate deprotection under basic conditions

With the isolation of **148**, a single debenzylation step was required to convert **148** to the desired transition state mimetic **108**. Initial debenzylation attempts using palladium on carbon and acetic acid under a hydrogen atmosphere were unsuccessful (Table 2.1.4).[98] Birch reductions were often reported for debenzylation reactions.[104] When **148** was exposed to sodium metal in condensed ammonia at -84°C, a new material was isolated that no longer contained aromatic signals in the ^{1}H or ^{13}C NMR spectra. Debenzylation was also confirmed by the disappearance of the ^{1}H NMR benzyl rotamer signals at 4.60 and 4.47 ppm. Restoration of a secondary amide led to a new broad ^{1}H NMR signal at 6.89 ppm and confirmed by a ^{13}C NMR amide carbonyl signal at 171.7 ppm. Sufficient quantities of the target **108** were obtained for biological testing, therefore no optimisation studies were performed to improve the yield of this reaction.

Table 2.1.4: Deprotective debenzylation of **148** using a Birch reduction.

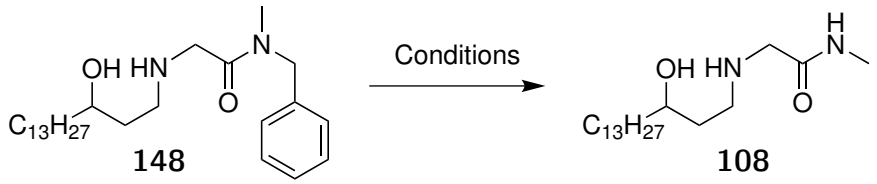

148 **108**

Conditions	Conversion **148**:**108**	Yield **108**
CH_3COOH, Pd/C, H_2, 48h.	100:0	-
Na, NH_3, -84°C, 20 min.	33:67	30%

2.1.3 Benzyl amine protective strategies

An alternate strategy to the synthesis of the mimetic **108** was investigated. Scheme 2.16 is a concise benzyl protective pathway that inherently avoids the formation of the double substitution byproducts (Table 2.1.2) and complications arising from the use of cyclic carbamates (Scheme 2.11). The benzyl group could be installed using a reductive amination of benzaldehyde. A benzyl protective group is superior to a carbamate system as it leaves the reactivity of the amine intact. A substitution reaction between **149** and **125** would generate the tertiary amine **150**. Removal of the benzyl protection group would generate **108** in significantly less steps compared to Scheme 2.13 which was used previously. Other alkyl halides could be used instead of **125** to generate further secondary amine analogues.

A simple method for the preparation of the benzyl protected amine **149** was adopted from the literature.[105] When the amine **109** was stirred with benzaldehyde in a mixture of DCM:THF 5:1 using anhydrous magnesium sulphate, the hydroxyamine **109** was completely converted to the imine which was then reduced with sodium borohydride in methanol to give the amine **149** in excellent yield. New aromatic signals were present in both the ^{1}H and ^{13}C NMR spectra of the amine **149**. The benzyl ^{1}H NMR AB signal overlapped with the hydroxy substituted signal at 3.77 ppm. Benzylation was confirmed by a new ^{13}C signal at 54.0 ppm.

Substitution reactions using **149** were tested to take advantage of the reactivity of the amine. When the amine **149**, 2-bromo-*N*-methylacetamide **125** and

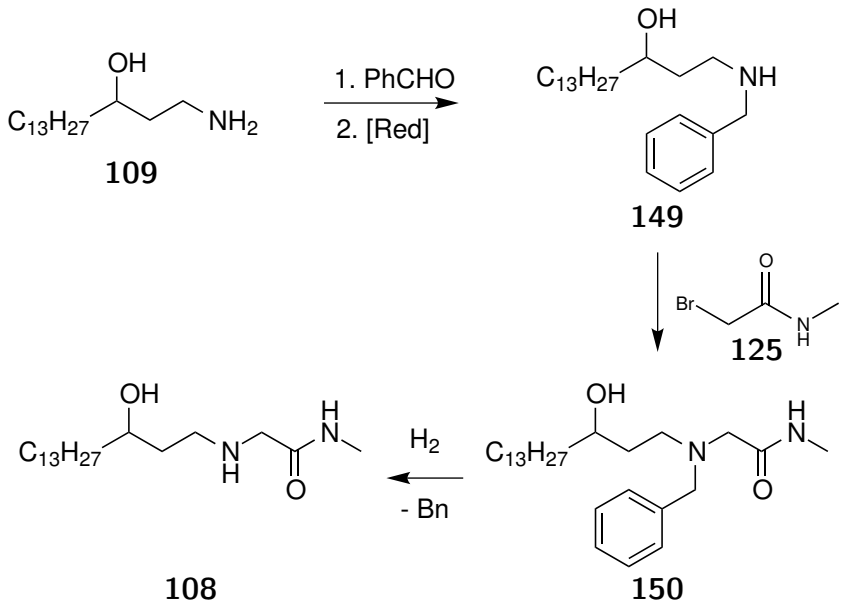

Scheme 2.16: Synthesis via protective benzylation using reductive amination

Table 2.1.5: Reductive amination prior to substitution iterations

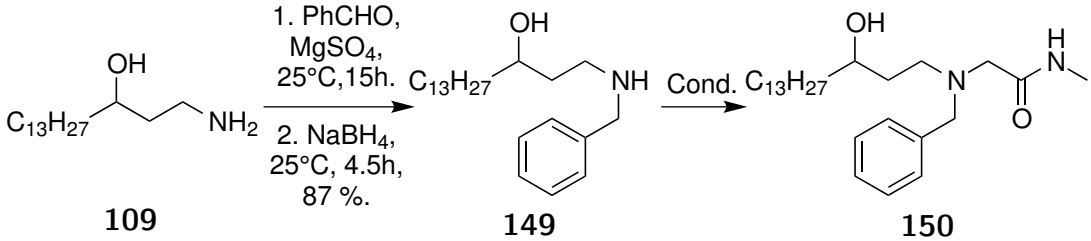

Conditions	**150**
125, K_2CO_3, THF, 25°C, 96 h.	41 % Purified
125, K_2CO_3, THF, 66°C, 15 h.	64 % Conversion
125, DIPEA, DMF, 70°C, 15 h.	69 % Purified

potassium carbonate were stirred at room temperature, the reaction proceeded slowly. Heat was required to increase the reaction rate (Table 2.1.5). When the substitution reaction was performed using DIPEA in DMF, the tertary amine **150** was isolated in good yield. The ^{1}H NMR spectrum of **150** contained an AB pattern at 3.1 ppm complemented by an apparent doublet at 2.79 ppm indicative of the methyl amide rotamer. The ^{13}C spectrum had a amide carbonyl present at 171.5 ppm and the tertiary amine system had 3 signals present between 50 - 60 ppm.

Debenzylation of the benzylamine **150** was expected to generate the target mimetic **108**. Standard hydrogenolysis using palladium on carbon proved unsuccessful and resulted in complex mixtures. Birch conditions resulted in recovery of the starting material (Table 2.1.6). A hydrogen transfer method using palladium on carbon and formic acid in methanol at room temperature gave excellent results.[106] The reaction showed complete consumption of the starting material **150** to give **108** in excellent yield. Scheme 2.16 proved synthetically beneficial as it allows access to secondary amines using mild reaction conditions.

Table 2.1.6: Deprotective amine debenzylation

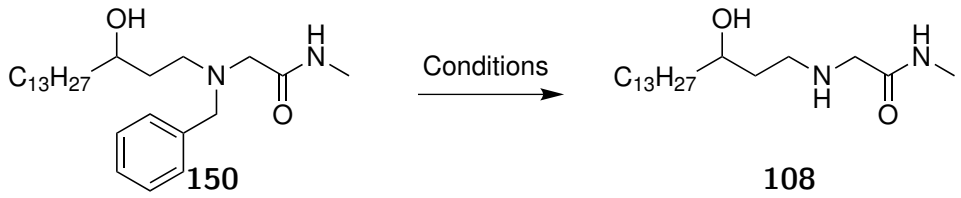

150 **108**

Conditions	**108**
Pd/C, H_2, EtOH, 25°C, 15h.	Complex mixture
Na, NH_3, *t*-BuOH, -84°C, 30 min.	SM recovered
Pd/C, 5% Formic acid in MeOH, 25°C, N_2, 15h.	68 % Purified

2.2 Structure activity relationship of 109

An investigation into the structure-activity relationship of the hydroxyamine **109** was proposed. Several aspects of the amine **109** are synthetically accessible. Changing the linker length will provide information about its structure activity dependency. Substitution of the hydroxyl group will help provide information into its mode of action, as well as investigate favourable amine substitutions that may improve its activity. Amine derivatisation, using chemistry explored previously, was hoped to improve the potency profile of the parent hydroxamine **109**.

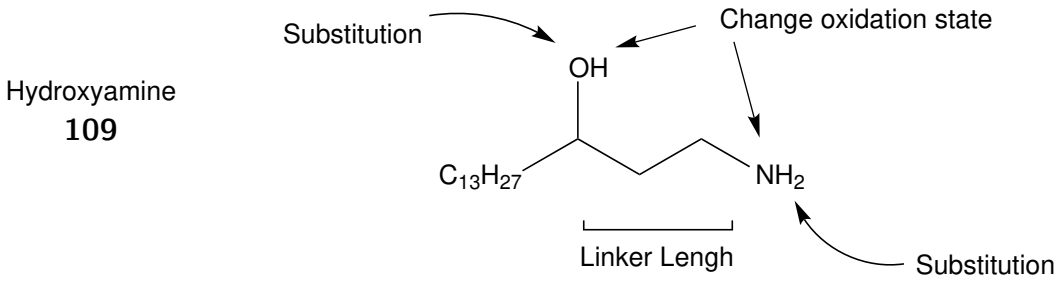

Figure 2.7: Structure-Activity investagation.

2.2.1 Variation of amine linker length

Investigating the structure-activity dependancy of the carbon linker bridge between hydroxy and amine functional groups led to two new targets **112** and **114** (Figure 2.8). Synthesis of the C1 and C3 hydroxyamines **112** and **114** would give critical information about the importance of the linker length towards potency. Synthesis of the new targets required separate synthetic strategies before a reduction to their successive amines.

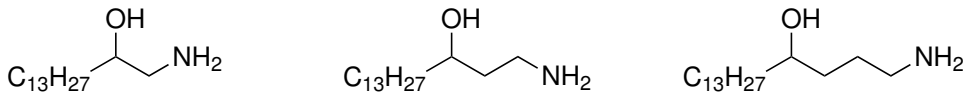

112 **109** **114**

Figure 2.8: new respective C1 and C3 linker targets **112** and **114**

The synthesis of the C1 hydroxyamine **112** was proposed by reduction of the cyanohydrin **113** (Scheme 2.17). A method was reported by Chandia[107] for cyanohydrin formation which was adapted for myristic aldehyde. Myristic aldehyde **151**

was exposed to sodium sulphite prior to addition of sodium cyanide. The sulphite adduct activates nucleophilic addition of cyanide to form **113**. The myristic sulphite adduct was extremely insoluble in both aqueous and organic solvents. The biphasic mixture limited the reaction rate and mechanical dispersion to reduce the particle size of the precipitated adduct was required, and produced a visible change as the cyanide addition proceeded. An extractive workup isolated the desired cyanohydrin from excess inorganic salts and the crude material was purified by column chromatography. The key ^{13}C NMR signals at 120.1 and 61.6 ppm were attributed to their respective nitrile and alcohol substituted carbons. The ^{1}H NMR spectrum did not contain a aldehyde signal which was replaced by a downfield triplet at 4.47 ppm. The introduction of the cyanohydrin system also resulted in a hydroxyl and nitrile stretch at 3395 and 2253 cm^{-1} respectively.

The same method previously used to reduce nitriles in Table 2.1.1 was applied to the cyanohydrin **113**. When the cyanohydrin **113** was reacted with lithium aluminium hydride, the starting material was consumed and a new polar compound was isolated. The ^{13}C NMR spectrum contained no nitrile signal. The ^{1}H NMR spectrum showed a clear ABX pattern, a pair of doublet of doublets at 2.66 and 2.51 ppm, due to the 2-hydroxyamine system. With the C1 hydroxyamine **112** isolated, attention was focused on a synthetic strategy towards the C3 target **114**.

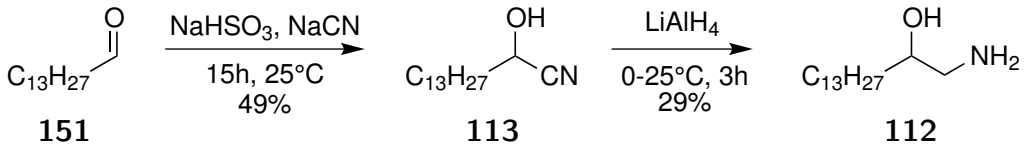

151 **113** **112**

Scheme 2.17: Synthesis of the C1 linker

Propargylamine could be used to incorporate the 3 carbon unit in the hydroxyamine **114**. Protection of propargylamine was required as to mask the inherent reactivity of the amine functional group (Scheme 2.18). The addition of lithiated TMS protected propargyl amine **152** to myristoyl aldehyde, after quenching with TMSCl, would generate the alkyne **153**. Hydrogenation of the alkyne in **153** over palladium was expected to give **154**, that upon deprotection would yield the C3 target **114** .

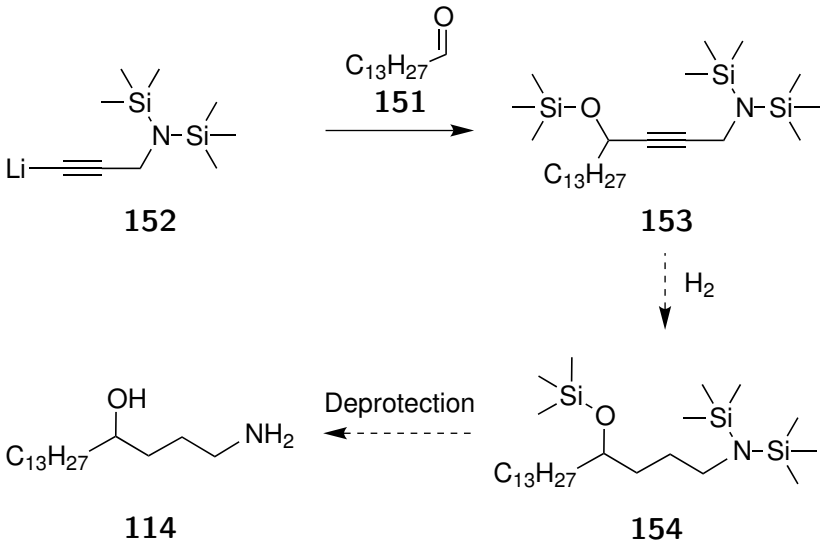

Scheme 2.18: Synthesis of the C3 linker

TMS protected propargylamine **155** was prepared by a method developed by Corriu.[108,109] The procedure involved the deprotonation of two equivalents of HMDS with *n*-butyllithium, followed by the addition of propargyl bromide. This method successfully generated gram quantities of **155** after a buffered quench and purification by distillation (Scheme 2.19). **155** was isolated with a 15% mol impurity of HMDS . Unfortunately, *N,N*-bis(trimethylsilyl)propargylamine **155** was found to significantly degrade, even when stored at -20°C. To address this issue a one pot addition reaction that immediately utilises **152** was explored.

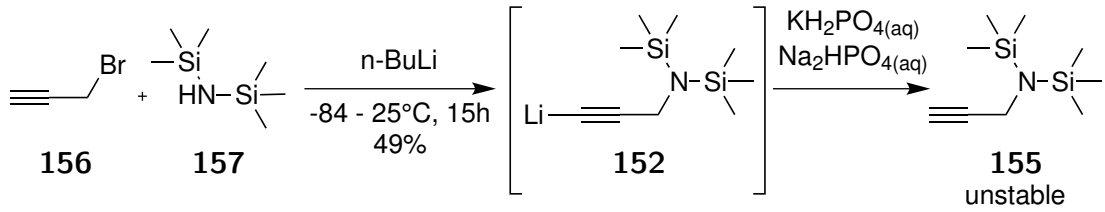

Scheme 2.19: Synthesis of TMS protected amine

Corriu detailed a single pot substitution, addition and protection procedure in the same paper.[108] The sequential synthesis avoided the isolation of **155**, instead the anionic intermediate **152** was immediately reacted with myristic aldehyde **151**. The alkoxide addition product was then protected with TMSCl to give **153** (Scheme 2.20). The crude isolated material showed complete consumption of the myristic aldehyde **151** in the ^{1}H and ^{13}C NMR spectra. The ^{1}H NMR spectrum showed a triplet of triplets at 4.46 ppm and doublet at 3.55 ppm indicative of the

propargyl alcohol/amine system, confirmed by respective ^{13}C signals at 63.3 and 39.5 ppm. The substituted alkyne was confirmed by two downfield alkyne signals at 86.2 and 84.0 ppm. The presence of two distinct types of trimethylsilyl group was confirmed by two singlets in the ^{1}H NMR spectrum with a 1:2 integration ratio at 0.26 and 0.24 ppm. The purity of the crude product was acceptable and further purification, beyond extended periods under reduced pressure removing the volatile starting materials and intermediates, was avoided due to the expected instability of **153** on silica gel.

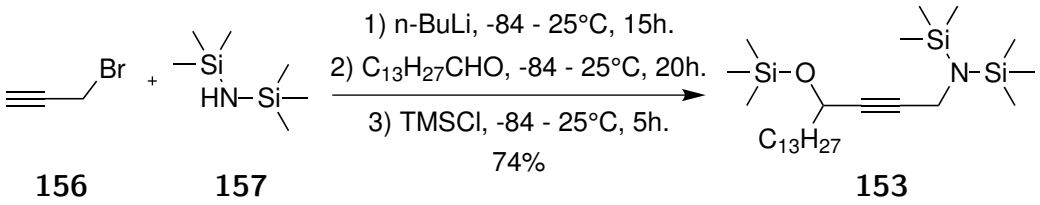

156 **157** **153**

Scheme 2.20: Squential addition reaction to generate **153**

Methods for the hydrogenation of the alkyne were investigated using standard hydrogenation techniques. Scheme 2.21 shows the outcome of a hydrogenation using hydrogen and palladium on carbon on the TMS protected alkyne **153**. Palladium(0) is often poisoned by amines and it was hoped that hydrogenation would proceed smoothly if the TMS protective groups remained. The starting material was consumed but the alkene **158** was isolated instead of the desired alkane **154**. The ^{1}H NMR spectrum possessed two clear alkene signals at 5.46 and 5.34 ppm. The *Z*-isomer was assigned as the two vinylic hydrogens had a coupling constant of 11.0 Hz. Isolation of a single isomer was confirmed as only two downfield alkene signals were present at 134.8 and 132.9 ppm in the ^{13}C NMR spectrum. The TMS protection groups remained intact as the ^{1}H integration ratio of 9:18 remained for the two signals at 0.21 and 0.20 ppm. The generation of **158** proved to be interesting, repeatable and convenient result as TMS deprotection would make **159** available for biological assessment.

The alkene **158** was deprotected using TBAF to give the aminoalcohol **159** in modest yield. The low yield was attributed to the extensive purification required to remove TBAF from the polar hydroxyamine **159**. The ^{1}H NMR spectrum of **159** no longer possessed signals at 0.22 and 0.20 ppm indicating the absence of

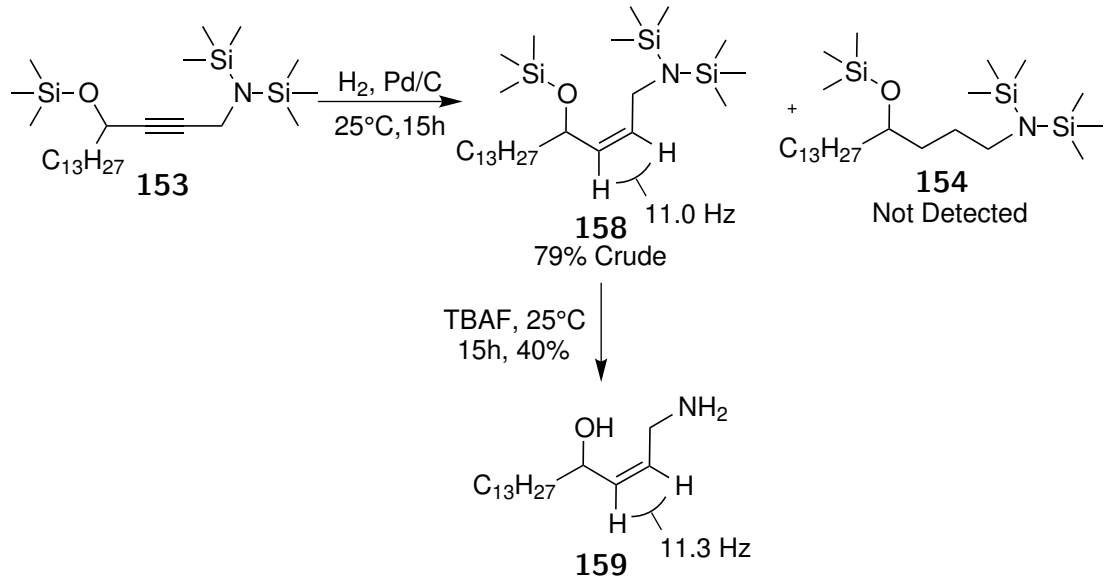

Scheme 2.21: Deprotection and hydrogenation stratergy utilised to isolate the C3 alkene **159**

TMS groups. Cleavage of the TMS groups allowed access to the novel alkene **159** for biological assessment. The deprotection of **153** prior to the hydrogenation should generate **114** via the alkyne **160**. This pathway was pursued as it would generate **115** for potency testing.

When **153** was treated to TBAF at room temperature (Scheme 2.22), removal of the TMS groups was observed and **160** was isolated in good yield. **160** was then exposed to palladium on carbon under a hydrogen atmosphere (Scheme 2.22) and the alkyne was reduced to the alkane **114** in good yield. The hydrogenation of the alkyne was confirmed as no downfield signals of either the alkene **159** or alkyne **115** were present in the ^{1}H and ^{13}C NMR spectra. A ^{1}H NMR multiplet at 3.55 ppm was assigned to the hydroxy substituted methine and a pair of multiplets at 2.40 and 2.24 ppm from the propargylamine. The ^{1}H and ^{13}C NMR spectra were similar to that obtained for **109**.

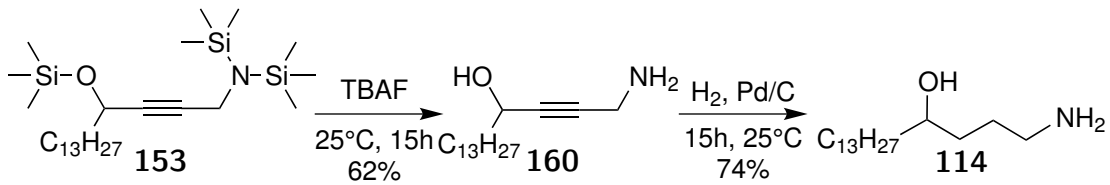

Scheme 2.22: Deprotection and hydrogenation stratergy utilised to isolate the C3 linked alkyne **115** and its saturated analogue **114**

With the isolation of the C3 linked hydroxyamine **114** complete, the desired series shown in Figure 2.8 was finalised. Two new compounds, **115** and **159** were isolated and used to expand the structure-activity relationship introduced from the inherent rigidity associated with the alkene and alkyne functional groups.

2.2.2 Aromatic amine derivatives

New amines **161** and **162** were envisioned to expand the structure-activity relationship study of the hydroxyamine **109** (Scheme 2.23). Incorporation of a 3-phenyl ethyl group to the hydroxyamine **109** adds a longer linker compared to the benzyl amine **149** generated previously (Table 2.1.5). The synthesis of **161** was envisioned by a reductive amination of the hydroxyamine **109** with 3-phenylpropanal **163**. The biphenyl derivative **162** aimed to determine the effect of a large hydrophobic group on potency. Synthesis of **162** was proposed by hydrolysis of the carbamate precursor **164**.

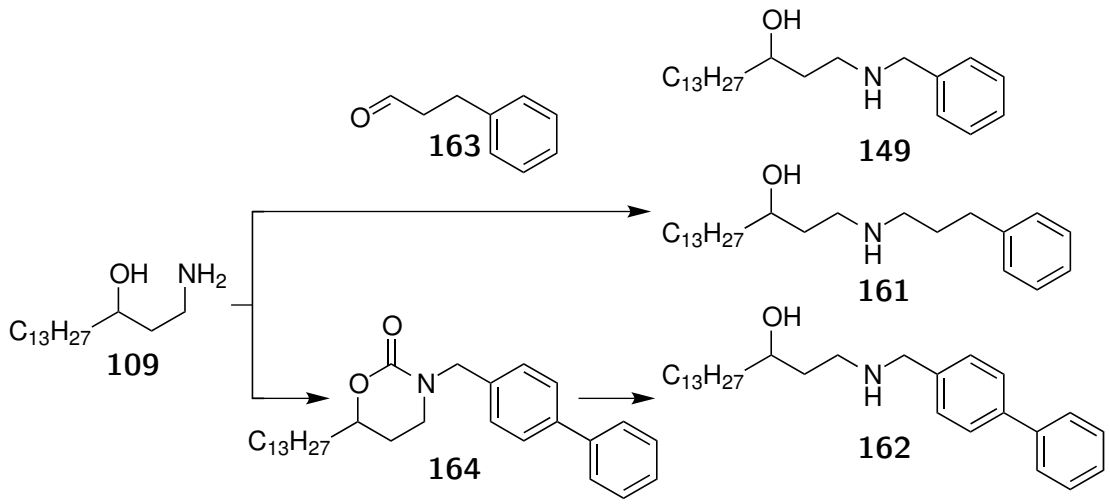

Scheme 2.23: New aromatic targets

The reductive amination, using 3-phenylpropanal **163**, proceeded using conditions described previously in Table 2.1.5 (Scheme 2.24). The hydroxyamine **109** and 3-phenylpropanal **163** were stirred with magnesium sulphate for 15 hours before exposure to sodium borohydride. **161** was isolated in low yield and contained 4 new aromatic ^{13}C NMR signals between 142.0 and 126.0 ppm. The methylene carbons adjacent to the amine were assigned to the two ^{13}C NMR signals at 49.26 and 49.18 ppm. The propyl chain appeared as a multiplet of overlapping ^{1}H NMR

signals between 2.54 and 2.77 ppm. Attention then shifted towards the synthesis of **164**, the precursor of **162** shown in Scheme 2.23.

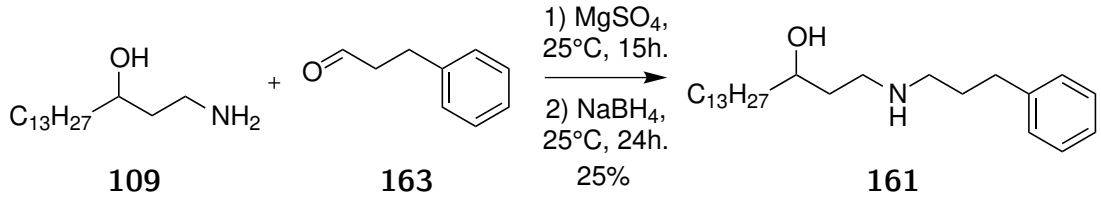

109 **163** **161**

Scheme 2.24: Generation of **161** by reducive amination

The carbamate precursor **164** was generated using a alkylation reaction of the carbamate **132** with 4-(chloromethyl)1,1'-biphenyl **165** (Scheme 2.25). When the carbamate **132**, the chloride **165** and a catalytic amount of sodium iodide were stirred with NaH in THF for 90 hours at 25°C, a new non-polar compound was isolated with a ^{13}C NMR spectrum containing the 8 signals assigned to the biphenyl system and a signal at 154.4 ppm indicative of carbamate carbonyls. The ^{1}H NMR spectrum contained an AB pattern at 4.65 and 4.56 ppm assigned to each of the benzylic protons. ^{1}H NMR signals at 4.25 and 3.25 ppm were characteristic of the oxazolidone system. Hydrolysis of the carbamate used conditions described previously (Table 2.1.3). A solution of the carbamate **164** and lithium hydroxide in wet ethanol was heated to 150°C for 2 hours using microwave irradiation. A new polar compound was isolated which no longer contained a carbonyl signal in the ^{13}C NMR spectrum. The loss of the carbamate was also mirrored by the shifting of the ^{1}H NMR benzyl protons to 3.94 and 3.87 ppm.

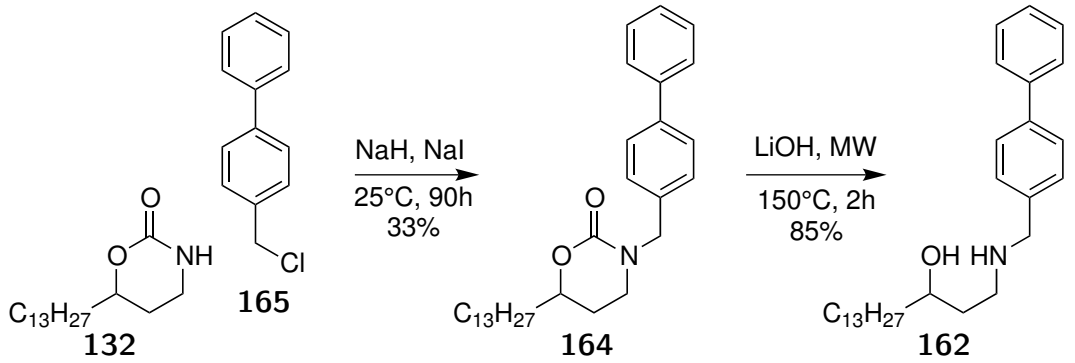

Scheme 2.25: Synthesis of **162** from the carbamate **132**

2.2.3 Selective amine and hydroxyl inactivation

Further targets were designed to probe the structure-activity of the dependency on the hydroxy and amine functional groups. The first target, the 3-hydroxynitrile **166**, is designed to probe the structure activity dependency of the amine contained on its free amine **109**. A similar comparison, between the masked hydroxy target **167** and the free hydroxyamine **109**, provided the structure-activity relationship of the hydroxy functional group. A method to generate the targets **166** and **167** was investigated.

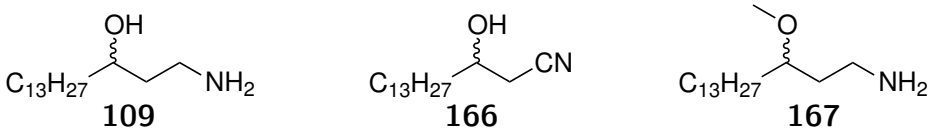

Figure 2.9: New respective deactivated amine and hydroxyl targets **166** and **167**

The hydroxynitrile **166** is an intermediate in the synthesis of the methoxyamine **167**. Scheme 2.26 shows the synthesis of **167** from the ketonitrile **124**. A selective reduction of the ketonitrile **124** would generate the hydroxynitrile **166**. Methylation of the hydroxyl group in **166** would generate the ether **168** which could then be reduced to the amine **167**.

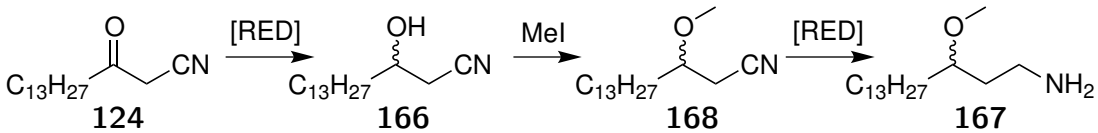

Scheme 2.26: Selective reduction of ketone, followed by methylation and subesquent reduction to generate **167** via **166**

The selective carbonyl reduction was achieved by exposure of **124** to sodium borohydride at room temperature (Scheme 2.27). No ^{13}C NMR carbonyl signal at 197.5 ppm was present, being replaced by a signal at 68.0 ppm, characteristic of hydroxyl substitution. Reduction was confirmed since the ^{1}H NMR methylene adjacent to the nitrile appeared as singlet in the starting material at 3.44 ppm and now appeared as multiplet at 2.52 ppm. No carbonyl signal was present in the IR spectra at 1716 cm^{-1} which was replaced by a hydroxyl signal at 3372 cm^{-1}. With the successful isolation of the first target, methylation of the hydroxy group contained on **166** was investigated.

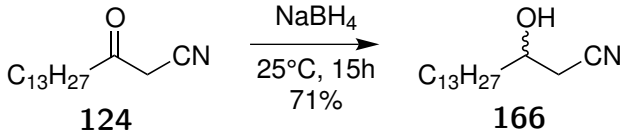

124 **166**

Scheme 2.27: Selective carbonyl reduction of the ketonitrile **124**

An initial attempt to methylate the hydroxyl group on **166** was performed by deprotonation with sodium hydride in methyl iodide at room temperature (Scheme 2.28). The starting material was consumed and two new products, **169** and **170** were isolated. **169** and **170** contained alkene signals that were matched with the vinylic nitriles reported by Bai.[110] The ^{13}C spectra each contained a pair of downfield alkene signals and a mechanistic explanation accounting for the formation of **169** and **170** was proposed in Scheme 2.29.

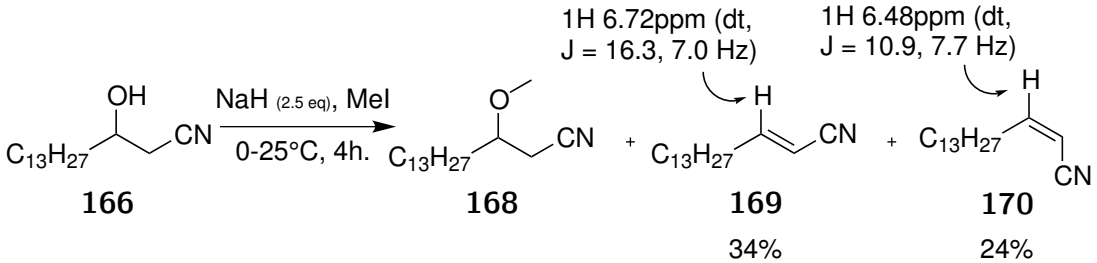

166 **168** **169** **170**

34% 24%

Scheme 2.28: Methylation attempt using sodium hydride.

The use of excess sodium hydride led to deprotonation and formation of the two nitrile anion conformers **171** and **172** (Scheme 2.29). Each conformer then undergoes a methoxy elimination to generate the isomers **169** and **170**. Milder conditions were investigated to avoid generation of the undesired alkenes.

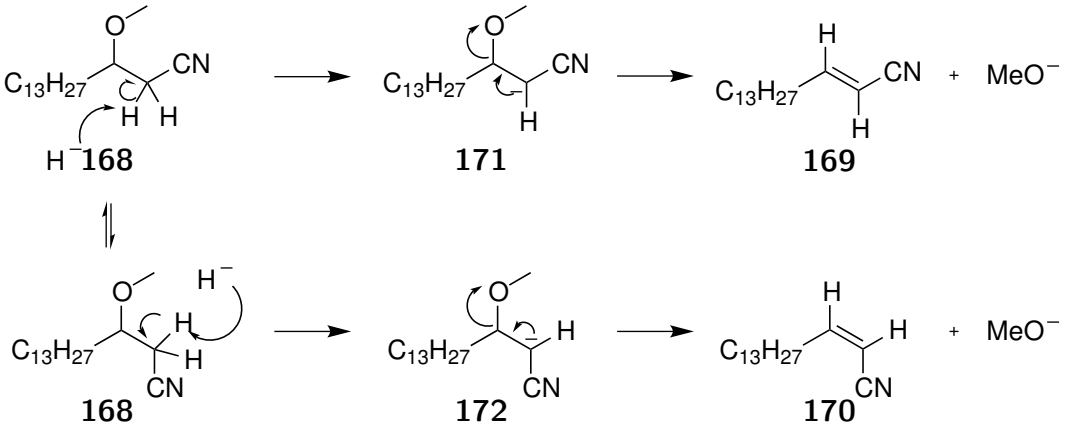

Scheme 2.29: Formation of the alkenes **169** and **170**.

A method was reported by Paz that used silver oxide to aid methylation in a 3-hydroxy nitrile system.[111] The 3-hydroxynitrile **166** was exposed to silver oxide and methyl iodide in DMF at 100°C. The non-polar elimination products **169** and **170** were witnessed by TLC. Consequently the 3-hydroxynitrile **166** was exposed to silver oxide and neat methyl iodide and stirred in a sealed vessel for 5 days. The starting material was consumed and no elimination products **169**/**170** were present by TLC or NMR. The ^{1}H NMR spectra showed a new methoxy signal at 3.40 ppm and the hydroxy substituted methine signal shifted from 3.94 ppm in **166** to 3.44 ppm. Substitution was confirmed by the new methoxy signal at 57.5 ppm in the ^{13}C NMR spectrum.

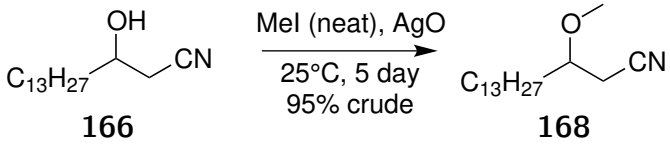

Scheme 2.30: Methylation of **166**

The 3-methoxynitrile **168** was exposed to lithium aluminium hydride at room temperature (Table 2.2.1). A complex mixture was obtained and an alternative reduction method using cobalt boride was applied. Sodium borohydride was added to a solution of 3-methoxynitrile **168** and cobalt chloride mirroring conditions used previously (Table 2.1.1). The ^{13}C NMR spectrum of **167** no longer showed a nitrile signal. A ^{1}H NMR spectrum of **167** showed the amine substituted methine triplet at 2.78 ppm and methoxy singlet at 3.30 ppm.

Table 2.2.1: Reduction of the 3-methoxynitrile **168**

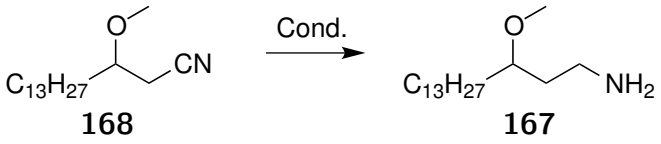

168 **167**

Conditions	Yield
$LiAlH_4$, 25°C, 2h.	Complex mixture
$CoCl_2$ (2 eq), $NaBH_4$ (10 Eq), 0 - 25°C, 3h.	32 %

2.3 *in vitro* Protozoan toxicity

Development of the structure-activity relationship began by toxicological assessment of 6 compounds, either synthesised in this chapter or available off the shelf, against *T.brucei rhodesience* and *P.falciparum* (Figure 2.10). The assays were conducted by Prof. Sumalee Kamchonwongpaisan at the National Centre for Genetic Engineering and Biotechnology, Thailand. The initial assessment was promising with the hydroxyamine **109** showing selective sub-micro molar activity towards *T.brucei rhodesience*. A series of control compounds were tested to check that the potency was due to the hydroxyamine feature. Myristic acid **7** did not show any toxicity towards *T.brucei or P.falciparum* as it is a natural substrate. Hexadecylamine **173** is identical to the hydroxyamine **109** except the hydroxyl group is absent. **173** was 2 orders of magnitude less potent than **109**, showing the critical role of the hydroxyl group in a hydrogen bonding interaction.

Interestingly methylation of the hydroxyl group had little effect upon activity towards *T.brucei rhodesience* but it significantly improved selectivity. **167** showed the same activity towards *T.brucei rhodesience* as its free hydroxyamine counterpart **109**. This trend indicated that the oxygen may be acting as a hydrogen bond acceptor in *T.brucei rhodesience*, and hence potency was uninfluenced by methylation. This trend was again observed with the activity of **167** towards *P.falciparum* which was the same when compared to its unsubstituted counterpart **109**. Methylation of the hydroxyl group of **109** validated the idea of hydroxyl substitution for a starting point for further structure-activity relationship investigations.

The structure-activity dependency on the amine was demonstrated to be very

high. When the amine was masked as a nitrile in **166**, the activity drops significantly when compared with the free amine **109**. The potency and selectivity remained unchanged when the hydrochloride of **109** was assessed indicating buffering in biological media was likely. The importance of the hydroxyl and amine functional groups was validated, consequently became primary features of all remaining compounds.

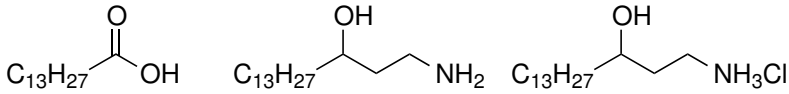

	7	**109**	SI	**174**	SI
T.brucei IC_{50}:	>100 µM	0.27 ± 0.01 µM	83	0.27 ± 0.01 µM	83
P.Falciparum TM4 IC_{50}:	> 100 µM	20.2 ± 0.95 µM	1.1	4.96 ± 1.66 µM	4.5
P.Falciparum K1CB1 IC_{50}:	> 100 µM	20.8 ± 2.38 µM	1.1	16.15 ± 1.81 µM	1.4
VERO IC_{50}:	>100 µM	22.3 ± 1.09 µM	-	22.5 ± 0.8 µM	-

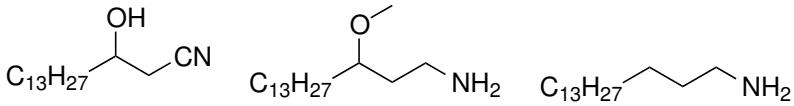

	166	SI	**167**	SI	**173**	SI
T.brucei IC_{50}:	20.94 ± 0.48 µM	4.8	0.32 ± 0.02µM	156	20.21 ± 0.52 µM	2.5
P.Falciparum TM4 IC_{50}:	> 100 µM	-	21.3 ± 3.29 µM	2.3	>50 µM	-
P.Falciparum K1CB1 IC_{50}:	> 100 µM	-	24.6 ± 1.44 µM	2.0	>50 µM	-
VERO IC_{50}:	>100 µM	-	>50 µM	-	>50 µM	-

Figure 2.10: Inital activities of selected compounds againsed *T. brucei rhodesience*

Having shown the hydroxyamine **109** was a good lead, a series of compounds was developed to investigate the structure activity dependency of carbon linker between hydroxyl and amine functional groups. Compounds **112** and **109**, with a one or two carbon linker, showed very similar activities towards *T.brucei rhodesience* and *P.falciparum.* Increasing the linker length beyond two carbons saw a overall drop in activity. Since molecules containing a three carbon linker, namely hydroxy amines **114**, **159** and **160**, did not improve potency inclusion into later generations of compounds was avoided. The results also validate the use of a 2 carbon linker as opposed to a one carbon linker.

Figure 2.12 shows the selectivity index for the compounds shown in Figure 2.10 and Figure 2.11. The selectivity was promising, as many synthesised compounds showed toxicity towards *T.brucei rhodesience* while not impinging the activity of

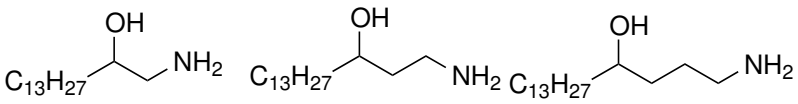

	112	SI	109	SI	114	SI
T.brucei IC_{50}:	0.27 ± 0.01 µM	83	0.27 ± 0.01 µM	83	2.77 ± 0.10 µM	>9
P.Falciparum TM4 IC_{50}:	18.6 ± 1.48 µM	1.2	20.2 ± 0.95 µM	1.1	19.5 ± 5.29 µM	1.1
P.Falciparum K1CB1 IC_{50}:	19.9 ± 1.36 µM	1.1	20.8 ± 2.38 µM	1.1	> 20 µM	-
VERO IC_{50}:	22.4 ± 1.23 µM	-	22.3 ± 1.09 µM	-	> 25 µM	-

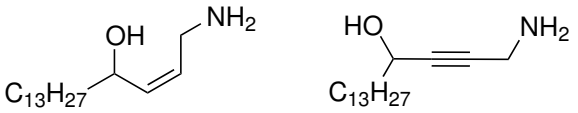

	159	SI	160	SI
T.brucei IC_{50}:	2.41 ± 0.13 µM	>10.4	0.7 ± 0.02 µM	>71
P.Falciparum TM4 IC_{50}:	14.6 ± 1.56 µM	>1.7	9.6 ± 1.80 µM	>5.2
P.Falciparum K1CB1 IC_{50}:	> 20 µM	-	30.5 ± 13.4µM	>1.6
VERO IC_{50}:	> 25 µM	-	>50 µM	-

Figure 2.11: *in vitro* activities of hydroxyl-amine linker length derivatives against *T. brucei rhodesience* and *P.falciparum*

a host cell. Two of the more potent hydroxyamines, compounds **109** and **112** showed over 80-fold selectivity towards *T.brucei rhodesience* compared to a model host cell line. Selectivity towards *P.falciparum* was, in general, not observed with the first two series of compounds shown in Figure 2.10 and Figure 2.11. The high selectivity towards *T.brucei rhodesience* is a promising start as to explore further compounds containing the myristoyl hydroxyamine motif of **109**.

A carbamate protection, discussed in section 2.1.1, led to the generation of the first substituted target **108**. The activity of several of the intermediates and **108** were assessed against *T.brucei rhodesience* and *P.falciparum* and are shown in Figure 2.13. The structure activity dependancy on the hydroxyl and amine functional groups is clearly shown by the cyclic carbamate **132** which shows little activity against both *T.brucei rhodesience* and *P.falciparum.* Compound **144** was assumed to have activity though a generalised toxicity mechanism and did not show any selectivity towards *T.brucei rhodesience* or *P.falciparum* over a human cell line. These results can be rationalised since the nitrogen in **132**, **133** and **144** are part of a amide bond, and therefore does not form a charged species at physiological pH. Introduction of the glycine as a substituted amine did not show any improved activity compared to **109**, however, the selectivity over the

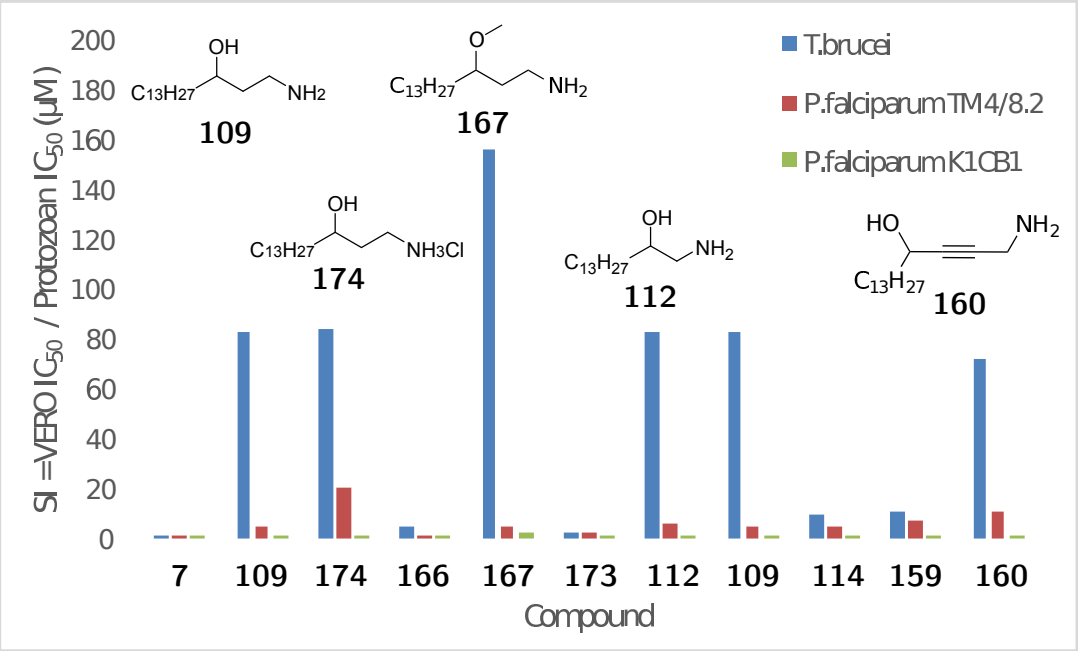

Figure 2.12: Selectivity of hydroxamines of *T. brucei rhodesience* compaired to VERO

VERO cell line increased to over 167. This adds to the evidence that this series of compounds may be working by NMT inhibition.

The synthesis of several substituted amine derivatives of the hydroxyamine **109** were developed in sections 2.1.3 and 2.2.2. The benzyl amine **149** showed a similar activity and selectivity profile towards *T.brucei rhodesience* compared with **109** (Figure 2.14). This demonstrated that the benzyl substituent was not hindering the binding mechanism of the hydroxyamine fragment of **149** at the active site or altering its transportation and bioavailability. Introduction of the benzyl amine substituent increased the selectivity of **149** towards *P.falciparum*. **149** showed sub micro-molar potency and 60 fold selectivity towards *P.falciparum* K1CB1, a multi drug resistant strain of malaria over the VERO cell line. Introduction of a 3-phenyl propyl amine substituent, shown in **161**, did not impact potency with **161** showing the same activity as **109** towards *T.brucei rhodesience.* Despite **161** having the same activity as **109**, the introduction of a 3-phenyl propyl amine substituent led to a 7 fold decrease in selectivity. No selectivity was observed towards *T.brucei rhodesience* or *P.falciparum* by introduction of a benzyl biphenyl substitution **162** indicating a generalised toxicity mechanism was present.

The hydroxyamine **109** is a novel myristic acid derivative that has been demon-

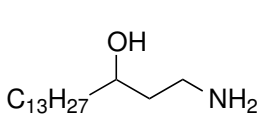

109

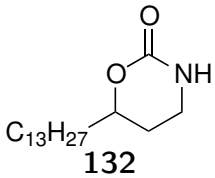

132

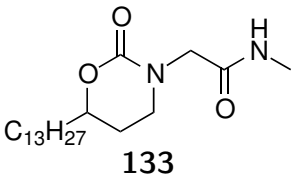

133

		SI		SI		SI
T.brucei IC_{50}:	0.27 ± 0.01 µM	83	>50 µM	-	33.9 ± 0.67 µM	>1.5
P.Falciparum TM4 IC_{50}:	20.2 ± 0.95 µM	1.1	>50 µM	-	>50 µM	-
P.Falciparum K1CB1 IC_{50}:	20.8 ± 2.38 µM	1.1	>50 µM	-	>50 µM	-
VERO IC_{50}:	22.3 ± 1.09 µM	-	>50 µM	-	>50 µM	-

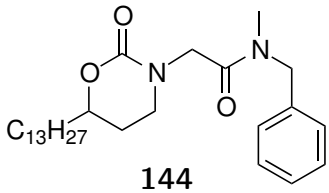

144

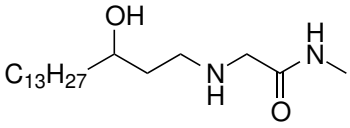

108

		SI		SI
T.brucei IC_{50}:	33.7 ± 3.67 µM	0.7	0.30 ± 0.01 µM	>167
P.Falciparum TM4 IC_{50}:	21.8 ± 2.98 µM	1.1	> 50 µM	-
P.Falciparum K1CB1 IC_{50}:	19.7 ± 1.27 µM	1.2	> 50 µM	-
VERO IC_{50}:	23.2 ± 0.4 µM	-	>50 µM	-

Figure 2.13: *in vitro* activities of carbamate and glycyl derivatives against *T. brucei rhodesience* and *P.falciparum*

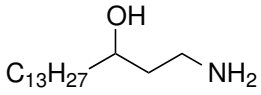

109

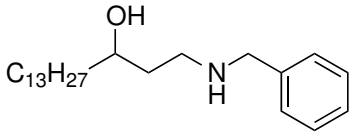

149

		SI		SI
T.brucei IC_{50}:	0.27 ± 0.01 µM	83	0.33 ± 0.02 µM	61
P.Falciparum TM4 IC_{50}:	20.2 ± 0.95 µM	1.1	2.58 ± 0.51 µM	7.8
P.Falciparum K1CB1 IC_{50}:	20.8 ± 2.38 µM	1.1	0.36 ± 0.05 µM	56
VERO IC_{50}:	22.3 ± 1.09 µM	-	20.1 ± 4.6 µM	-

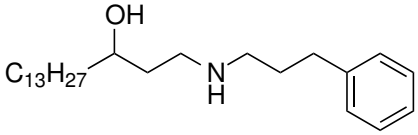

161

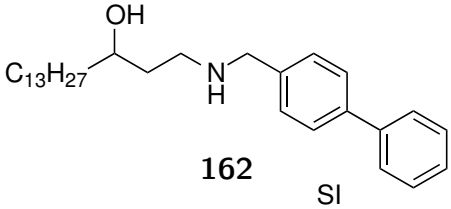

162

		SI		SI
T.brucei IC_{50}:	0.28 ± 0.01 µM	12	2.85 ± 0.12 µM	1.2
P.Falciparum TM4 IC_{50}:	1.49 ± 0.9 µM	2.3	3.00 ± 0.66 µM	1.1
P.Falciparum K1CB1 IC_{50}:	0.31 ± 0.05 µM	11	2.36 ± 0.62 µM	1.4
VERO IC_{50}:	3.43 ± 0.24 µM	-	3.36 ± 0.56 µM	-

Figure 2.14: *in vitro* activities of aromatic amine derivatives against *T. brucei rhodesience* and *P.falciparum*

strated to show an 80-fold selectivity and micro-molar activity towards *T.brucei rhodesience.* Although the specific mode of action of the compounds has not been implicitly described in this chapter, as *in vitro* assays with isolated NMT were not currently available, inhibition of NMT was considered likely. This chapter provides an excellent baseline to explore the introduction of statin fragments into **109**. The following chapter will explore the concept of piggybacking some activity from the HMG-CoA reductase inhibitors with the potential of applying them to NMT.

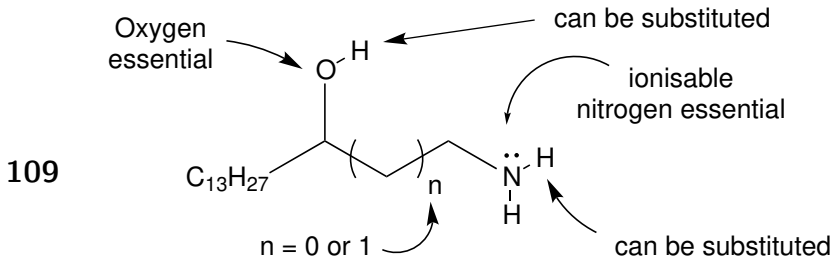

Figure 2.15: Results of structure-activity studies on the hydroxyamine **109**

Chapter 3

CoA-myristoyl mimetics

3.1 Introduction of early HMG-reductase inhibitor fragments

Having demonstrated activity of the hydroxyamine **109**, synthesis of more potent derivatives of **109** was explored. One aspect of the transition state that was not investigated in Chapter 2 was a Coenzyme A mimetic, which was successfully used in the development of the statins. Structures from the early development of the statins provided inspiration for new targets. In 1980, Sato reported the cholesterol biosynthesis inhibitor **73** with a micro-molar cholesterol biosynthesis inhibitory potency.[77] The lactone **73** contains a simple lipophilic CoA segment and the incorporation of this structure into the aminoalcohol **109** was explored. The hydroxyamine **175** has a similar structure to the early statin **73** and was envisioned to improve the efficacy of *N*-Myristoyltransferase inhibitors. Therefore, synthesis of the new target **175** was explored.

Scheme 3.1 shows two possible synthetic routes to the target hydroxyamine **175**. A linear route could be conceived by starting with a Grignard reaction between 3-phenylpropanal and tridecylmagnesium bromide to generate **176**. Oxidation of the resulting alcohol followed by addition of lithiated acetonitrile would give the hydroxynitrile **177**. Reduction of the nitrile in **177** would give the desired amine **175** in 3 steps. An alternative convergent approach was envisaged in which the acetylide anion **178** could be added to the ketonitrile **124**. This route

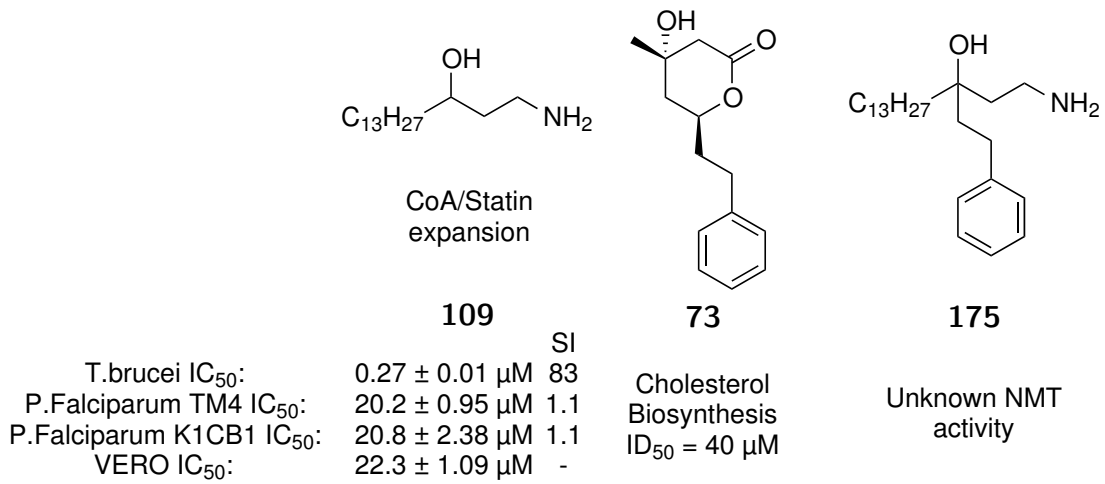

Figure 3.1: Introduction of the 2-ethylphenyl moiety to the hydroxyamine **109** as the tertiary alcohol **175**.[77]

would allow for a modular approach to expand the functionality of **109**. However, the addition of the phenylacetylide anion **178** to ketonitriles is uncommon, and challenges were expected.

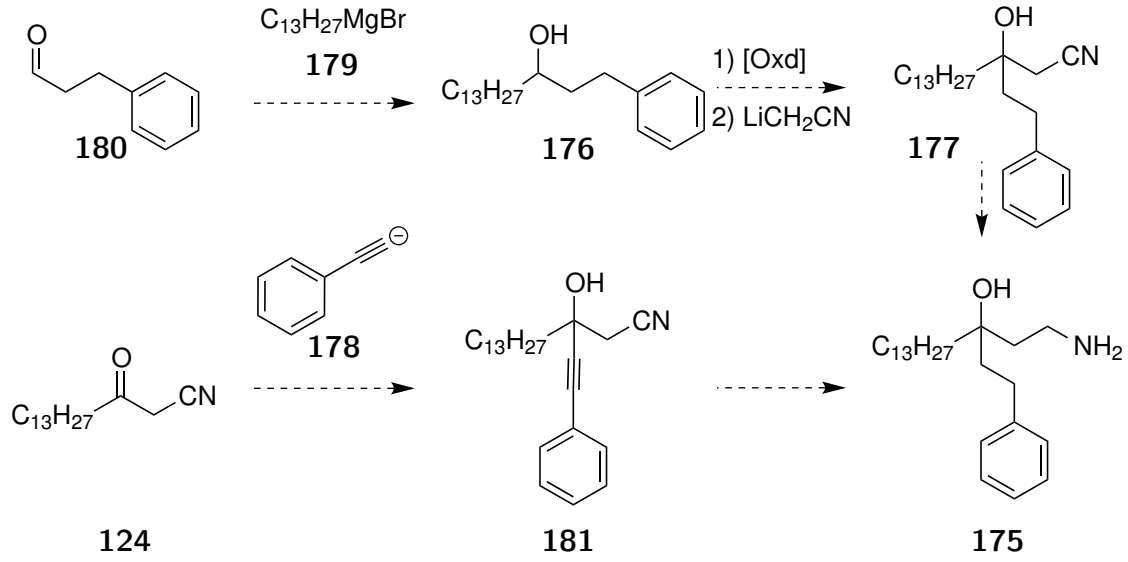

Scheme 3.1: Proposed linear and convergent synthesis of hydroxyamine **175**.

The key hurdle for the convergent synthesis of **175** was the addition the phenylacetylide **178** to the ketonitrile **124** as the competing deprotonation reaction was expected to be favoured. Organocerium reagents have been reported to improve addition reactions of easily enolisable systems.[112–114] Figure 3.2a shows the contrasting yields between organolithium and organocerium reagents in the addition of phenyl acetylide to cyclopent-3-en-1-one **182**. The lithium phenylacetylide

178 gave **183** in modest 30% yield whereas the cerium phenylacetylide **184** gave **183** in 89% yield. Lithium acetylides are inherently strong bases and are expected to easily deprotonate the protons alpha to both the carbonyl and nitrile and form the enolate **185** (Figure 3.2b). Organocerium acetylides are less basic and have been demonstrated to improve nucleophilicity.[112–114] The use of organocerium reagents was expected to favour ketonitrile addition and introduce new functionality shown in **186**.

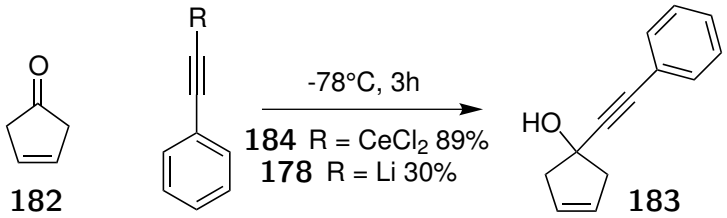

(a) Improvements to the addition reaction outcome using cerium reagents.[112]

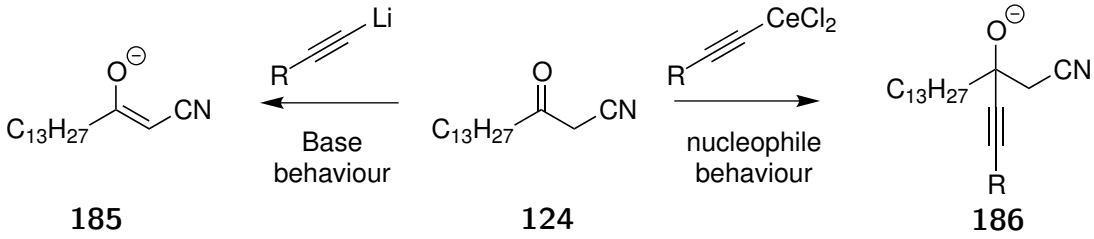

(b) Competing reaction outcomes of the addition reaction to the ketonitrile **124**

Figure 3.2: Convergent synthesis strategies towards **175** shown in Scheme 3.1

Addition reactions using simple Grignard reagents and lithiated acetylides were performed to determine if standard conditions generated the addition product **181**. When methylmagnesium bromide or lithium phenyl acetylide were added to the ketonitrile **124**, only starting material was recovered (Table 3.1.1). This result confirmed the acidic nature of the ketonitrile **124** and its preference to enolise in the presence of Grignard reagents and lithium acetylides. The cerium acetylide was made by transmetalation of lithium phenylacetylide using anhydrous cerium chloride and showed promising results. Anhydrous cerium chloride was obtained by progressively heating the heptahydrate up to 140°C overnight *in vacuo*. Phenylacetylene was deprotonated with *n*-butyllithium at -84°C and stirred with anhydrous cerium chloride before addition of **124**. The use of a large excess of the organocerium reagent nucleophile did not improve the yield. Per-

forming the reaction with a small excess of the cerium transmetalated nucleophile at -84°C for 5 hours gave **181** in modest yield.

Table 3.1.1: Addition optimisation using cerium chloride

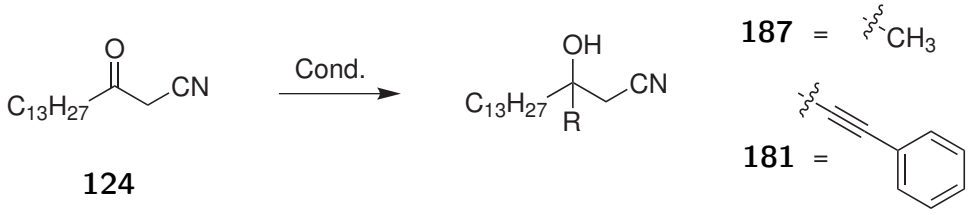

124

Conditions	**124**:**181**	Yield **181**
MeMgI (1.3 eq), **124**, 0°C, 1h.	Recovered **124**	-
PhC≡CH **188** (1.2 eq), *n*-BuLi (1.1 eq), THF, **124**, -84°C to RT, 15h.	Recovered **124**	-
PhC≡CH **188** (1.3 eq), *n*-BuLi (1.2 eqv), Anh. $CeCl_3$ (1.4 eqv), **124**, -84°C to -45°C, 2h.	71:29	13%
PhC≡CH **188** (2.4 eq), *n*-BuLi (2.2 eq), Anh. $CeCl_3$ (2.5 eqv), **124**, -84°C, 2h.	-	15%
PhC≡CH**188** (1.4 eq), *n*-BuLi (1.3 eq), Anh. $CeCl_3$ (1.5 eq), **124**, -84°C, 5h.	44:56	34%

The ^{1}H NMR spectrum of the product, the propargyl alcohol **181**, possessed signals at 7.46-7.30 ppm (m, 5H) associated with the phenyl group and a indicative AB pattern at 2.86 and 2.82 ppm due to non-equivalent protons adjacent to the nitrile. The ^{13}C NMR spectrum possessed two signals at 88.5 and 86.5 ppm that were assigned to the disubstituted alkyne. The carbonyl signal of the ketonitrile **124** at 197.7 ppm was replaced by a new signal at 69.0 ppm consistent with a hydroxyl substituent. The nitrile signal had shifted from 114.0 to 116.7 ppm confirming the nitrile was still intact and available for the subsequent reduction steps.

Exposure of the propargyl alcohol **181** to palladium on carbon under a hydrogen atmosphere reduced the alkyne to the alcohol **189** in 2.5 hours (Scheme 3.2). The ^{13}C NMR spectrum of **189** confirmed reduction as the two key alkyne signals were no longer present. The nitrile in **189** was then reduced to the primary amine **175** using lithium aluminium hydride in modest yield. Reduction was confirmed as **175** no longer showed a nitrile ^{13}C NMR signal of at 116.7 ppm. Overall the synthetic route to **175** is short and modular which allows for analogues to be made quickly.

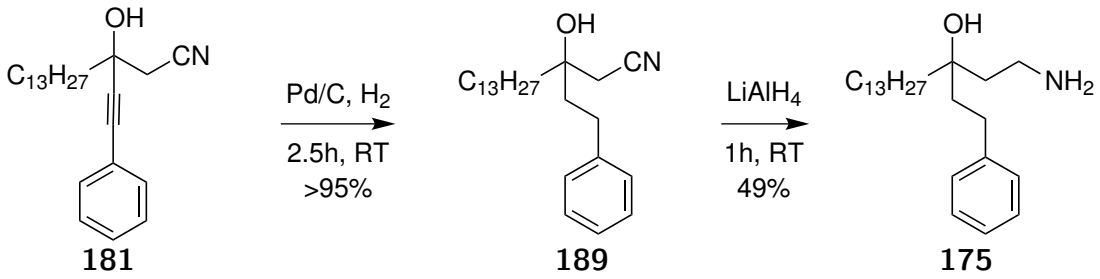

Scheme 3.2: Hydrogenation and reduction of addition product **181**.

Figure 3.3 shows compound **77** which was reported by Stokker[79,80] to be a HMG-reductase inhibitor. The hydrophobic 2,4-dichlorophenyl moiety was discovered to emulate the hydrophobic segment of Compactin. The 2,4-dichlorophenyl moiety was introduced into the new potential NMT inhibitor target **190** and its synthesis explored.

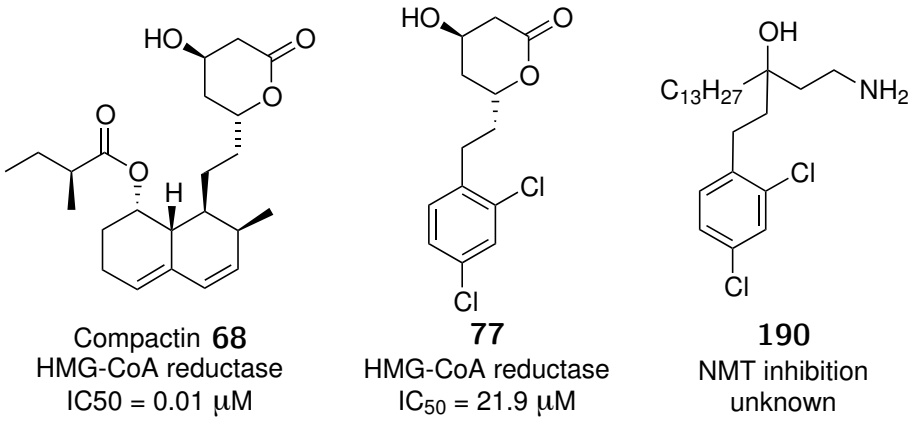

Figure 3.3: Introduction of the 2,4-dichlorophenyl fragment.

The new target **190** was made using a similar procedure to the phenylethyl derivative **175** (Table 3.1.1 and Scheme 3.2). 2,4-Dichlorophenylacetylene **191** was made using an adapted procedure described by Ghaffarzadeh who reacted 2,4-dichloroacetophenone **192** with phosphorous pentachloride in pyridine under microwave irradiation on the 1 mmol scale. (Scheme 3.3).[115] The reaction was scaled up to 40 mmol by placing the reagents in a preheated oil bath at 150°C for 12.5 min. The reaction gave the alkyne **191** in modest yield, however this material contained some minor chlorinated impurities. Despite these minor impurities the material showed NMR spectral data identical to that reported by Arioli[116] and was used in the following addition reaction.

With gram quantities of the alkyne **191** available, the reaction conditions used

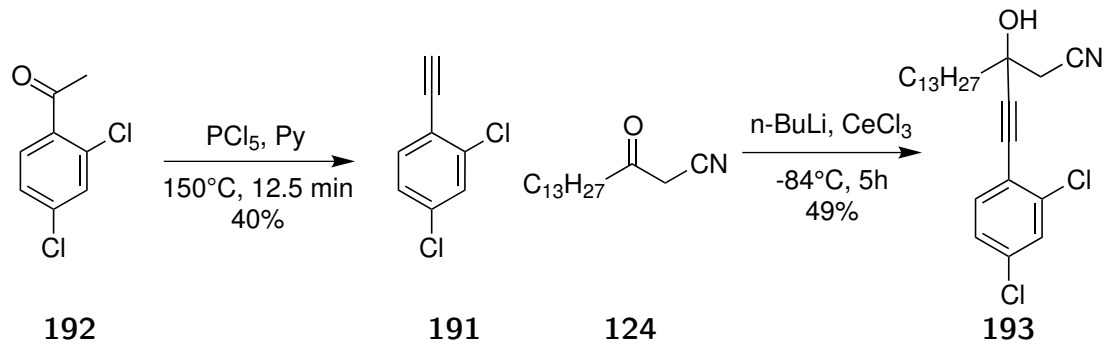

Scheme 3.3: Generation of aromatic terminal alkyne using PCl_5 and cerium transmetalated addition.

to add phenylacetylene to the ketonitrile **124** were applied. A sequential lithiation of the terminal alkyne **191** followed by transmetalation with anhydrous cerium chloride and addition to **124** at -84°C for 5 hours gave **193** in good yield (Scheme 3.3). The ^{1}H NMR spectrum of the propargyl alcohol **193** showed aromatic signals of the starting alkyne **191** and aliphatic signals from the myristoyl chain. Isolation of **193** was confirmed as the ^{13}C NMR spectrum no longer had a carbonyl signal at 197.7 ppm and no carbonyl IR signal at 1716 cm^{-1}. A new hydroxyl substituted carbon signal was present in the ^{13}C spectrum at 69.2 ppm with a new hydroxyl stretch at 3423 cm^{-1} in the IR spectrum. The carbon spectrum also showed signals at 94.6 and 82.3 ppm indicative of a disubstituted alkyne. Unreacted starting materials were easily recovered using column chromatography and scale up generated desired propargyl alcohol **193** in a modest yield.

Hydrogenation of the alkyne **193** proceeded using palladium on carbon under a hydrogen atmosphere at room temperature (Scheme 3.4). The material isolated after filtration though celite did not show ^{13}C alkyne signals at 94.6 and 82.3 ppm of the starting material. The nitrile on **194** had a ^{13}C signal at 117.4 ppm and a IR signal at 2254 cm^{-1}. Exposure of **194** to lithium aluminium hydride generated the target **190** in low yield due to isolation difficulties during chromatography. The infrared spectrum of the aminoalcohol **190** no longer showed a nitrile absorbance at 2254 cm^{-1}. The singlet at 2.61 ppm of **194** was transformed into a multiplet at 2.70 ppm indicative of a amine substituted methine. Sufficient quantities of hydroxyamine **190** were generated for biological assessment.

New targets were then envisioned by changing the location of the hydrophobic

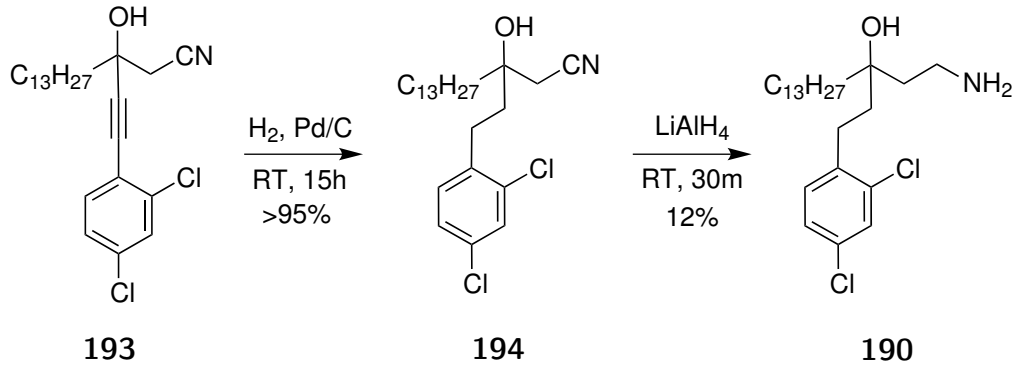

Scheme 3.4: Hydrogenation and reduction of **193**.

phenylethyl fragment (Figure 3.4). Benzyl amine substitutions may have better access to a hydrophobic pocket. This approach is analogous to the positioning these hydrophobic features in the HMG-CoA reductase inhibitors **77**[79,80] and **195**.[117] Synthesis of **196** and **197** was proposed by a reductive amination of **109** with their respective benzaldehydes.

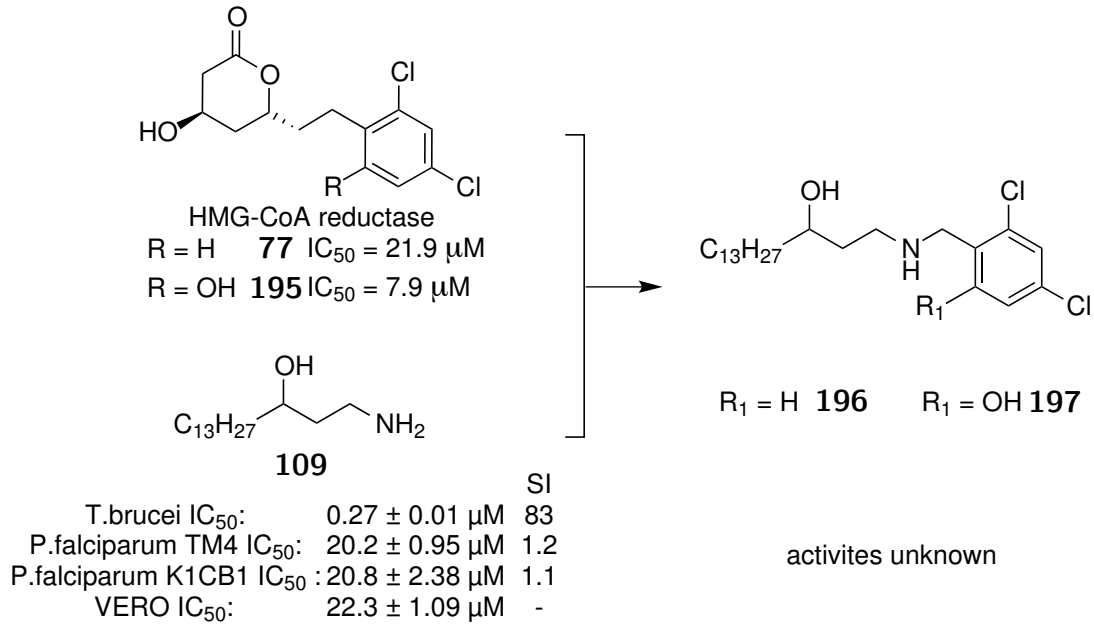

Figure 3.4: New targets that incorporate the 2,4-dichlorophenyl fragment.

The hydroxyamine **109** was stirred with 2,4-dichlorobenzaldehyde before addition of sodium borohydride (Scheme 3.5). A new polar and UV active spot was isolated in modest yield. The ^{13}C NMR showed 6 aromatic signals combined with two amine substituted methine signals at 50.4 and 48.1 ppm. The ^{1}H NMR spectrum showed the expected alkyl amine substituted methine at 2.99 and 2.79 ppm, with the benzyl protons seen as an AB pattern at 3.91 and 3.86 ppm. Focus was then

shifted to the synthesis of **197** using similar conditions.

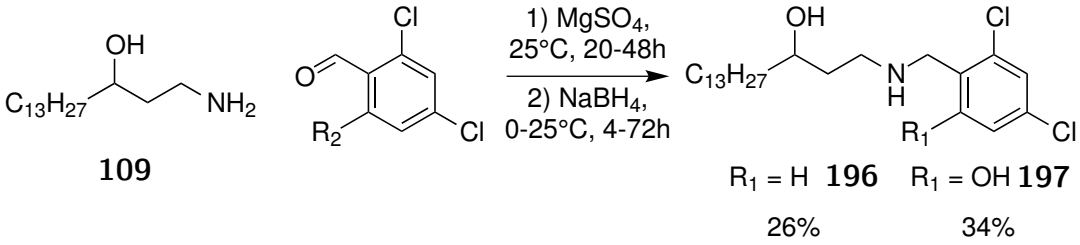

Scheme 3.5: Reductive amination of **109** to give **196** and **197**

A reductive amination using 2,4-dichlorosalicaldehyde gave **197** in modest yield (Scheme 3.5). The DEPT spectrum of **197** in DMSO-d_6 showed 4 substituted signals in the aromatic region and the ^{1}H NMR spectrum showed pair of doublets at 6.82 and 6.62 ppm with long range coupling of 2.1 Hz. The benzyl and alkyl amine substituted methylene signals were present as a singlet and multiplet at 3.99 and 2.64 ppm respectively. The hydroxy substituted methine signal at 3.44 ppm remained. Further targets based from HMG-reductase inhibitors were planned.

3.2 4'-Fluorobiphenyls

During the drug development of the synthetic statins, the addition of a 4'-fluorophenyl group greatly improved potency towards the inhibition of HMG-CoA reductase. The potency improvement can been seen by comparing **77** and **89** in Figure 3.5.[80] Introduction of the 4'-fluorophenyl group improved HMG-CoA reductase binding though polar interactions between the guanidinium group contained on Arg590 and the fluorophenyl substituent.[84] Consequently the 4'-fluorophenyl moiety is a feature all the synthetic Statins. Inclusion of the 4'-fluorophenyl moiety thus led to two new NMT inhibitor targets **199** and **200**, and their synthesis was planned by building on chemistry described in this chapter.

The synthesis of the targets **199** and **200** was envisaged using the organocerium addition reaction described previously. The first target was the unchlorinated biphenyl **199** which required the synthesis of its alkyne precursor **201**. A Suzuki cross-coupling reaction between the boronic acid **202** and 2-bromoacetophenone

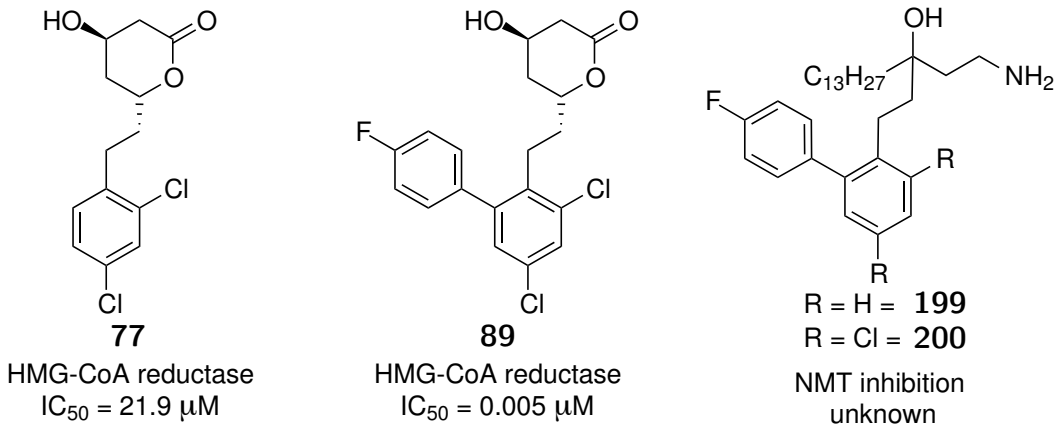

Figure 3.5: Incorporation of the 6-(4'-fluorophenyl)-2,4-dichlorobiphenyl system.

203 would generate the acetophenone **204**. Subjecting the acetophenone **204** to the same conditions used to make **191** in Scheme 3.3 would give the first target alkyne precursor **201** (Scheme 3.6). Conversion of **201** to the cerium acetylide and addition to the ketonitrile **124** would generate **205** and reduction of the alcohol would generate the first target **199**.

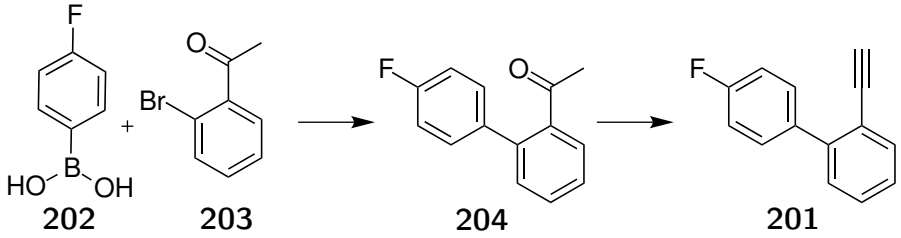

Scheme 3.6: Proposed synthesis of the key biphenyl precursor **201**

A similar biphenyl has been made by reacting 2,4-fluorophenylboronic acid with 2'-bromoacetophenone **203**.[118] Applying these conditions, an aqueous solution of the boronic acid **202** and the bromide **203** was stirred with TBAB and palladium acetate overnight at 70°C which gave the biphenyl **204** in good yield (Scheme 3.8). The ^{1}H and ^{13}C NMR spectra of **204** matched that described by Yoshikai.[119] Methods to convert the acetophenone system contained on **204** were then investigated.

An effective method for converting the acetophenone **204** to the alkyne **201** used phosphorous pentachloride.[115] The biphenyl acetophenone **204** was exposed to phosphorous pentachloride in pyridine and heated at 110°C using a microwave

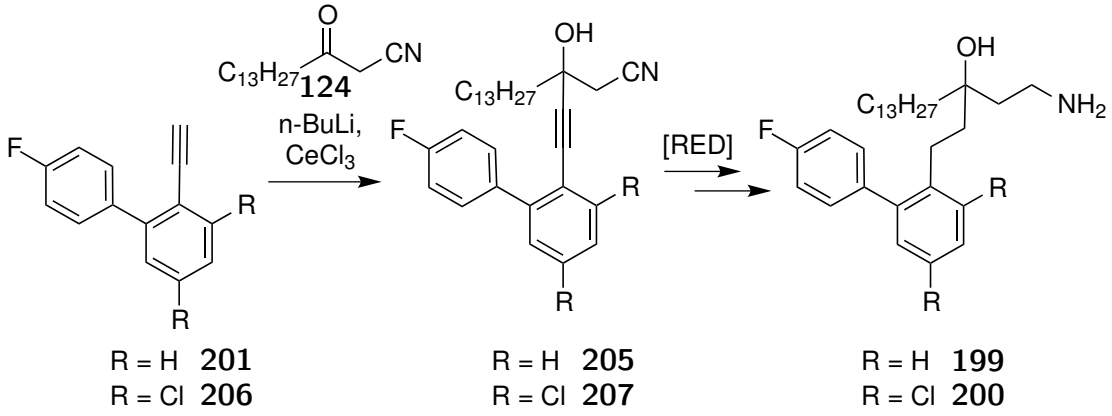

Scheme 3.7: Synthesis of new targets **199** and **200** via organocerium addition

reactor. The ^{1}H NMR methyl signal at 2.06 ppm of the starting acetophenone **204** was converted to the a terminal alkyne signal at 3.05 ppm. The presence the alkyne in **201** was confirmed by the disappearance of the respective ^{13}C NMR ketone and methyl signals at 204.6 and 30.6 ppm and conversion to new signals at 83.1 and 80.5 ppm. A sufficient amount of the terminal alkyne **201** was generated for the subsequent addition reaction.

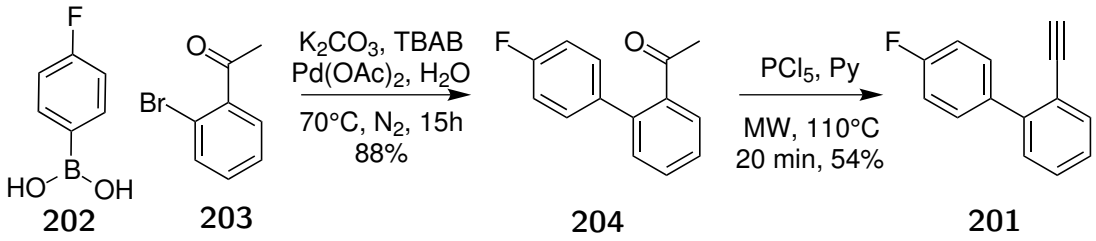

Scheme 3.8: Suzuki coupling of **203** prior to elimination to give **201**.

Using the chemistry described previously, the terminal alkyne **201** was converted to the propargyl alcohol **205** in modest yield (Scheme 3.9). The ^{1}H NMR signals showed both aromatic and aliphatic signals which included a distinctive AB pattern at 2.71 and 2.67 ppm attributed to the methylene alpha to the nitrile. The ^{13}C NMR spectrum of the isolated material was difficult to analyse due to ^{13}C-^{19}F coupling however a key signal at 69.0 ppm indicated the successful formation of the alcohol and this was confirmed by a IR stretch at 3432 cm^{-1}. The ^{13}C NMR spectrum showed alkyne signals of **201** shifted downfield to 91.4 and 86.0 ppm in **205** with the nitrile signal of **124** also showing a subtle shift from 114.0 to 116.6 ppm in **205**. The desired addition product was easily separable using column

chromatography recovering 62 % of the starting alkyne.

Hydrogenation of the alkyne of **205** using palladium on carbon under a hydrogen atmosphere proceeded smoothly (Scheme 3.9). The ^{1}H NMR showed new benzyl doublet of doublets at 2.62 ppm with the AB pattern of **205** collapsing into a singlet at 2.36 ppm. The isolated material had a distinct absence of alkyne and alkene signals in both the ^{1}H and ^{13}C NMR spectra. Sodium borohydride was added to a solution of the hydrogenation product **208** and cobalt chloride to give the hydroxyamine **199** in low yield (Scheme 3.9). The^{1}H NMR spectrum showed two distinct broad multiplets at 2.90 and 2.54 ppm which correlate with aryl and amine substituted methylenes.

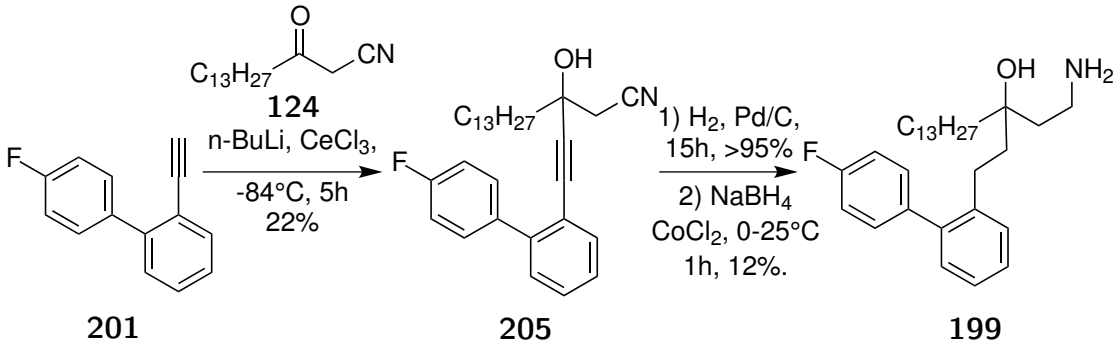

Scheme 3.9: Transmetative addition and subsquient reduction.

With the first 4-fluorobiphenyl target **199** generated, attention was focused onto the synthesis of the 6-(4'-fluorophenyl)-2,4-dichlorophenyl target **200**, which required the synthesis of the alkyne precursor **206** summarised in Scheme 3.10. The organopalladium species required for the Suzuki cross-coupling reaction is formed by a C-H activation at the *ortho* position of 2,4-dichlorobenzaldehyde **80**. Scheme 3.10 illustrates how C-H activation is directed at the ortho position by converting the aldehyde to the oxime **209** in a strategy described by Dubost.[120] Applying a Cory-Fuchs synthesis to **210** would generate the alkyne precursor **206** as input for the addition reaction with the ketonitrile **124**.

Scheme 3.11 shows two C-H activation pathways to functionalise the *ortho* position of the starting benzaldehyde **80** by conversion to its methyl oxime **209**. A shorter efficient cross coupling of **209** with 4-fluorophenylboronic acid **211** was based on conditions reported by Sun.[121] This pathway would generate the biaryl **212** directly from the methyl oxime **209** and hydrolysis would generate

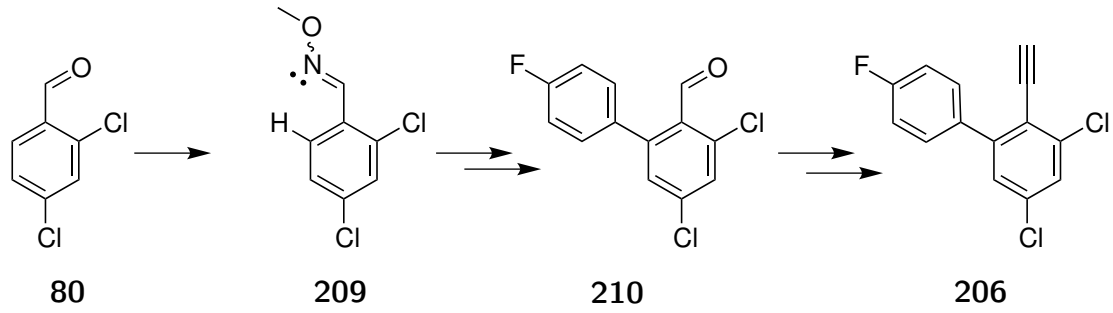

Scheme 3.10: Generation of the alkyne **206** through a bromination, Suzuki cross-coupling and Cory-Fuchs alkyne synthesis.

the biarylbenzaldehyde **210** in 3 steps from 2,4-dichorobenzaldehyde **80**. An alternative method by bromination of the methyl oxime **209** would generate **213** which, after hydrolysis, would be converted to 6-bromo-2,4-dichlorobenzaldehyde **214** using a procedure reported by Dubost.[120] A Suzuki cross-coupling reaction of **214** with 4-fluorophenylboronic acid **211** would give the biarylbenzaldehyde **210** in 4 steps from 2,4-dichlorobenzaldehyde **80**.

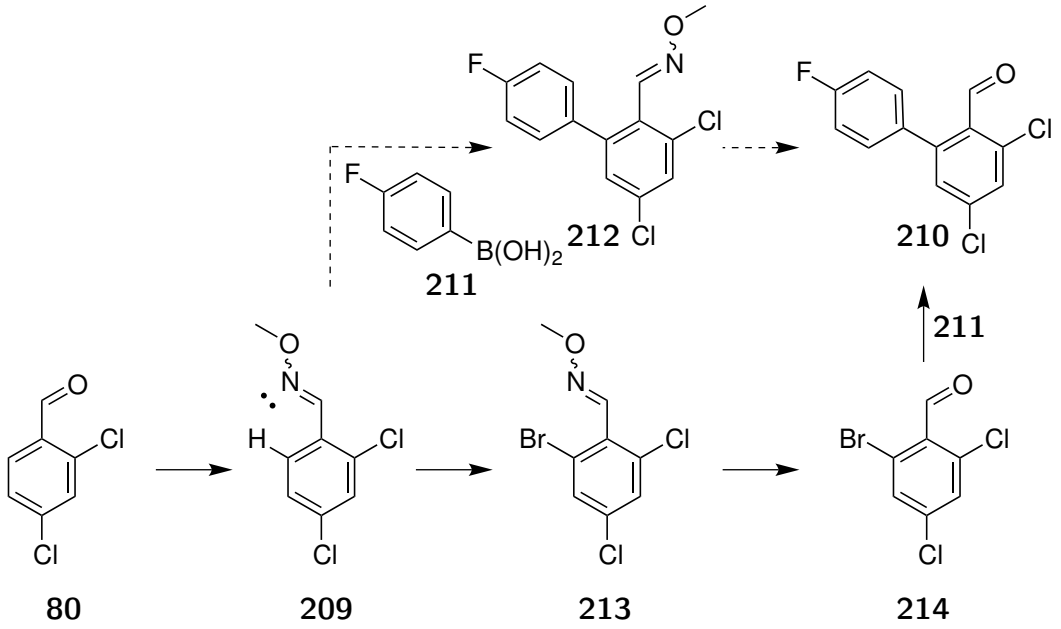

Scheme 3.11: ortho C-H activation by oxime functionalisation of **80** towards the synthesis of **210**

The first stage in the synthesis of the biaryl **210** was to generate the oxime **209**. The benzaldehyde **80** was stirred with methylhydroxyamine hydrochloride and pyridine at room temp for 2 hours (Scheme 3.12).[120] The method used a non-aqueous workup by filtering the reaction mixture though a plug of silica to

isolate **209** with a E:Z ratio of 95:5 in near quantitative yields and spectral data identical to the literature.[120] The mixture of isomers was used in the following steps without purification.

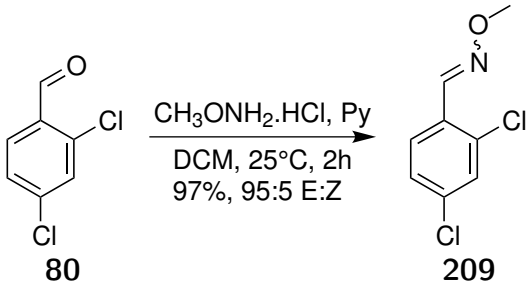

80 **209**

Scheme 3.12: Direct C-H activated suzuki

Introduction of the oxime functional group set the system up for *ortho*-substitution though C-H activation. Stokker *et al* used a benzyl imine to stabilise a palladium complex, which was isolated before a Grignard reaction generated the biaryl system (Reaction 1 Scheme 3.13[80]). Repetition of this pathway was avoided as it required an equivalent of expensive palladium acetate. A direct cross-coupling method using copper triflate and a catalytic amount of palladium acetate was reported by Sun *et al.* to couple *O*-methyl-(*E*)-2-methyl-benzaldoxime **215** with 4-fluoroboronic acid **211** in a 82% yield (Reaction 2 Scheme 3.13[121]). However, applying these to conditions to **209** returned starting materials (Reaction 3 Scheme 3.13). The result may be attributed to electron withdrawing effects present on the aromatic system on **209**. Consequently, synthesis of 2-bromo-4,6-dichlorobenzaldehyde **214** was explored (Scheme 3.11).

Bromination of the oxime **209** was reported by Dubost[120] using palladium acetate and *N*-bromosuccinimide (Scheme 3.14). The reaction proceeded via the oxime stabilised palladium intermediate **217**, and a mixture of geometric isomers was isolated with a ratio of E:Z 60:40 in good yield. These isomers were separated by column chromatography on a small scale but resolving the mixture on a large scale was not required.

With the brominated oxime **213** in hand, an assessment of whether to install the 4-fluorophenyl moiety before or after oxime deprotection was required. Scheme 3.15 shows both pathways. A Suzuki cross-coupling reaction on **213** would give the precursor **218** to the intermediate biaryl **210**. An alternative pathway would be

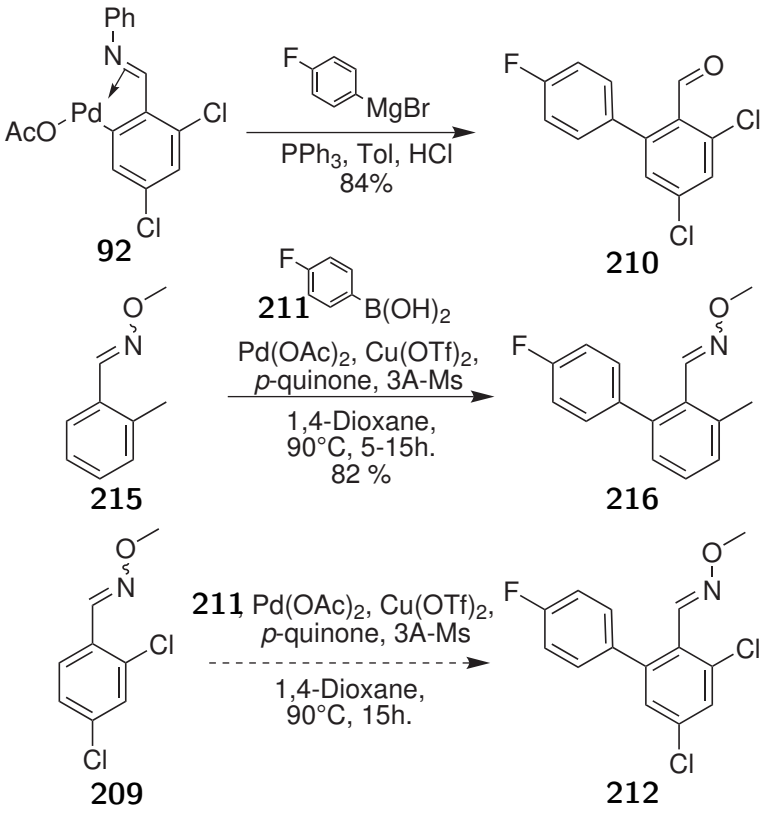

Scheme 3.13: 1) Addition of Grignard reagent to **92** reported by Stokker et al[80] 2) C-H activated Suzuki cross-coupling reported by Sun *et al.*[121] 3) Unsucsessful C-H activated Suzuki cross-coupling reaction on **209**

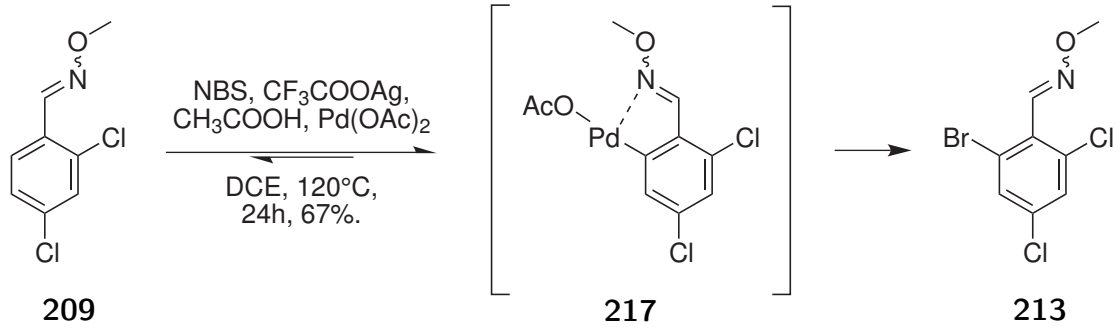

Scheme 3.14: *Ortho* C-H bromination via a oxime stabilised paladium intermediate reported by Dubost *et al.*[120]

to hydrolyses the oxime prior to coupling generating **210** with the same number of steps.

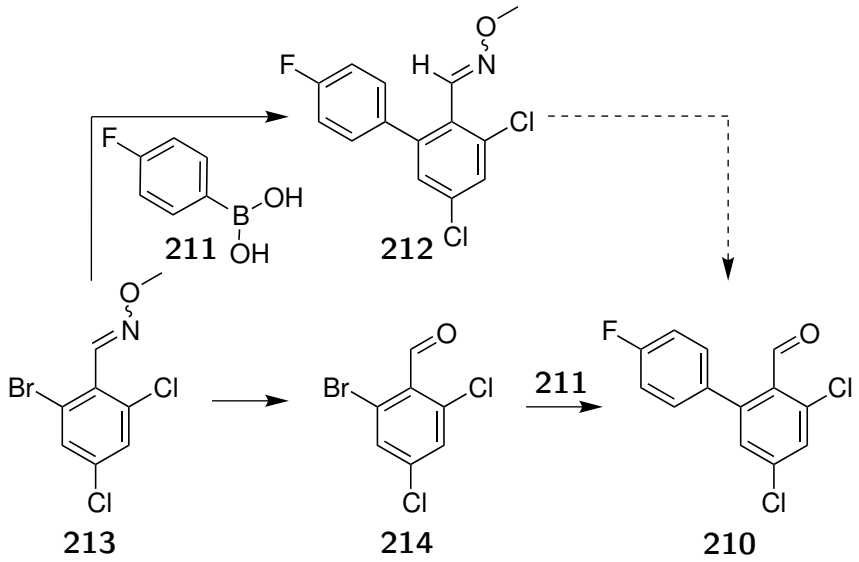

Scheme 3.15: Suzuki cross-coupling reaction of oxime **213**.

Scheme 3.16 illustrates the Suzuki cross-coupling reaction between **211** and **213** which was based on conditions used previously in Scheme 3.8. 4-Fluorophenylboronic acid and the oxime **213** were stirred with palladium acetate and TBAB at 70°C overnight to give **212** in low yield. The brominated oxime **213** was consumed in the reaction and gave a complex mixture. The major fraction of the mixture was isolated and assigned as the *E*-isomer **218**. **218** contained a benzyl-imine ^{1}H NMR signal at 8.02 ppm which correlated with the benzyl-imine signal of the *E*-isomer of **213** at 8.15 ppm. Two new aromatic ^{1}H NMR signals at 7.25 and 7.11 ppm indicated the formation of the biaryl system in **218**. The remaining fractions were isolated as complex mixtures. It was probable that the mixture to contained the mono and disubstituted products **219** and **220** respectively (Scheme 3.16). As a result, hydrolysis of the brominated oxime **213** prior to coupling was performed as per Scheme 3.15.

The oxime **213** was converted to its benzaldehyde **214** using a aqueous formaldehyde solution and a catalytic amount of *p*-toluenesulfonic acid at 100°C (Scheme 3.17).[120] The reaction gave excellent reproducible yields and gave multigram quantities of 2-bromo-4,6-dichlorobenzaldehyde **214**.[120] With the generation of the benzaldehyde **214**, Suzuki cross-coupling reaction with 4-fluorophenylboronic

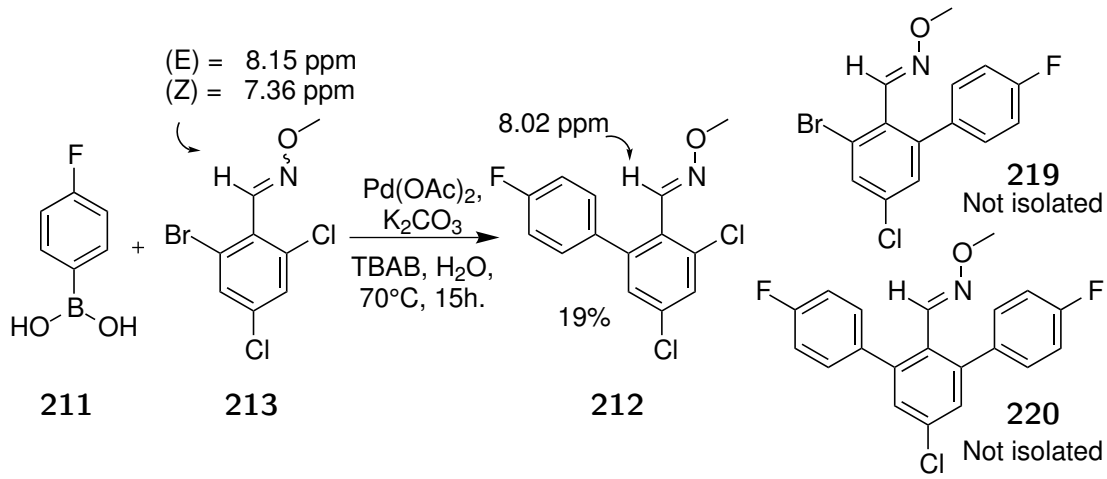

Scheme 3.16: Suzuki cross-coupling reaction using the oxime **213**.

acid **211** was explored.

The Suzuki cross-coupling reaction between the bromide **214** and 4-fluorophenylboronic acid **211** was performed using palladium acetate, tetrabutylammonium bromide and potassium carbonate in DMF at room temperature (Scheme 3.17). The conditions were based on a literature method, without supporting the palladium (II) on molecular sieves.[122] The reaction gave **210** in good yield. The ^{1}H NMR spectrum of **210** gave a benzaldehyde signal at 10.05 ppm within variance of the literature values of 10.2[80] and 10.13 ppm[123]. Two new fluorine coupled ^{1}H NMR multiplets at 7.25 and 7.13 ppm integrating for 2H indicated a successful biaryl coupling. A new ^{13}C NMR benzaldehyde signal at 189.8 ppm was present as was a large fluorine splitting (J = 249 Hz) present in the C-F substituted ^{13}C signal at 164.4 ppm. The conversion of the benzaldehyde **210** into the key terminal alkyne intermediate **206** continued.

Conversion of aldehydes to alkynes can be performed in a single step by Seyferth-Gilbert Homologation using the Ohira-Bestmann reagent, however a two step Cory-Fuchs synthesis was favoured. Preference for undertaking two step synthesis was primarily based on a patent published by Li[124] that utilised significantly cheaper and more readily available starting materials. The biaryl **210** was stirred with 2 equivalents of carbon tetrabromide and 4 equivalents of triethyl phosphite at -45°C for 90 min (Scheme 3.18).[124] The aldehyde signal in **210** at 10.05 ppm was replaced with a new singlet at 7.22 ppm in **221** in the ^{1}H NMR spectrum. A debromative elimination would generate the required alkyne **206**.

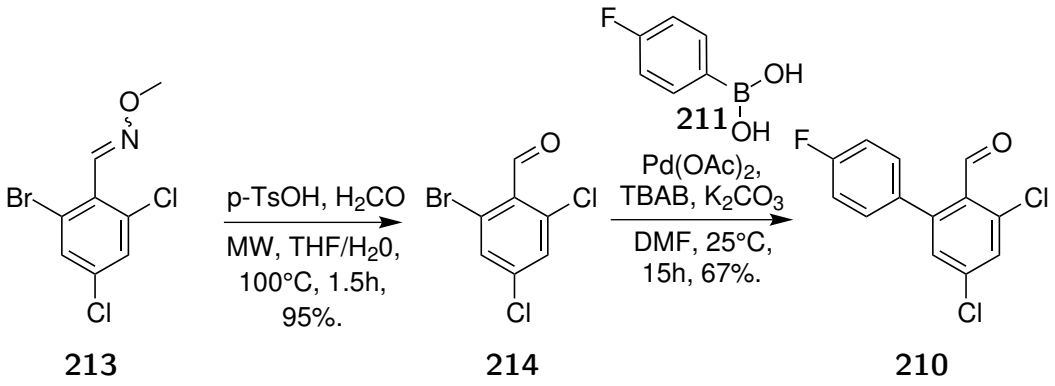

Scheme 3.17: Hydrolysis of the oxime **213** and subsequent Suzuki cross-couping reaction with 4-fluoroboronic acid **211**.

When the dibromide **221** was stirred in a solution of potassium *tert*-amylate (KTA) in toluene, the bromoalkyne **222** was isolated in good yield. The ^{1}H NMR of **222** showed a absence of the vinylic signal of the starting material **221** at 7.22 ppm and two new substituted alkyne ^{13}C NMR signals at 75.8 and 59.7 ppm. The reaction was repeated and the intermediate **222** was treated *in situ* with methanol, dimethylphosphite and KTA which gave **206** in excellent yield. The addition of methanol prior to addition of dimethyl phosphite and KTA was reported by Li to avoid byproducts.[124] The new terminal alkyne **206** had a singlet at 3.37 ppm in the ^{1}H NMR spectrum and two signals at 87.1 and 78.7 ppm in the^{13}C NMR spectrum. The addition reaction could now be investigated between the alkyne **206** and the ketonitrile **124**.

The addition reaction between the alkyne **206** and the ketonitrile **124** using the cerium chemistry described previously in Table 3.1.1 gave the desired propargyl alcohol **207** in good yield. (Scheme 3.19) The ^{13}C NMR spectrum showed characteristic substituted alkyne signals at 81.7 and 69.2 ppm which are typical for this type of propargyl alcohol. The ^{1}H NMR signal at 2.69 ppm was typical of the methylene alpha to the nitrile. Heterogeneous hydrogenation of the alkyne in **207** was explored.

Hydrogenation of the alkyne contained on **207** was attempted using palladium on carbon under a hydrogen atmosphere at room temperature (Table 3.2.1). Consumption of the starting material occurred, however the alkene **223** was isolated. The reaction stopped after the first alkyne hydrogenation indicating hydrogen-

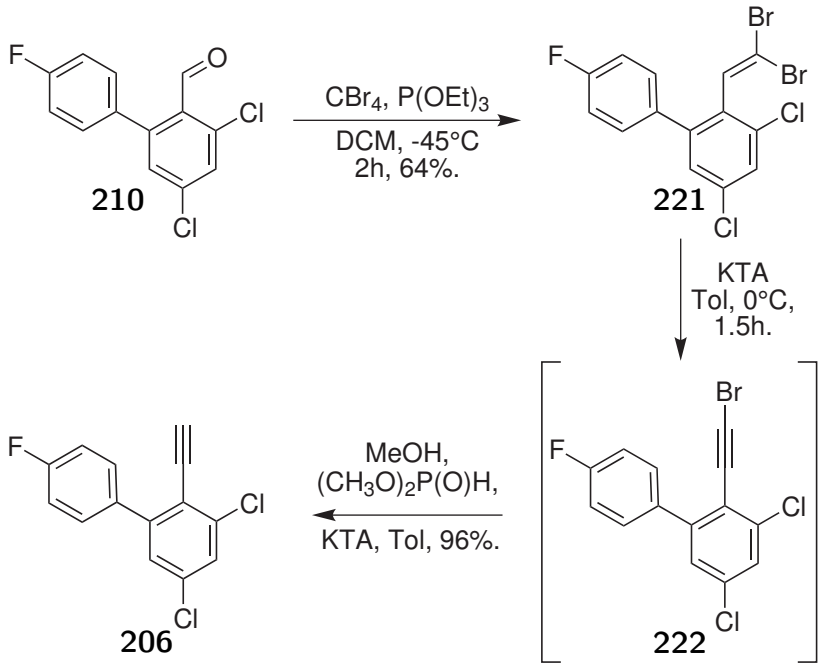

Scheme 3.18: Modified Cory-Fuch alkyne synthesis utilising triethyl phosphite and dimethyl phosphite.

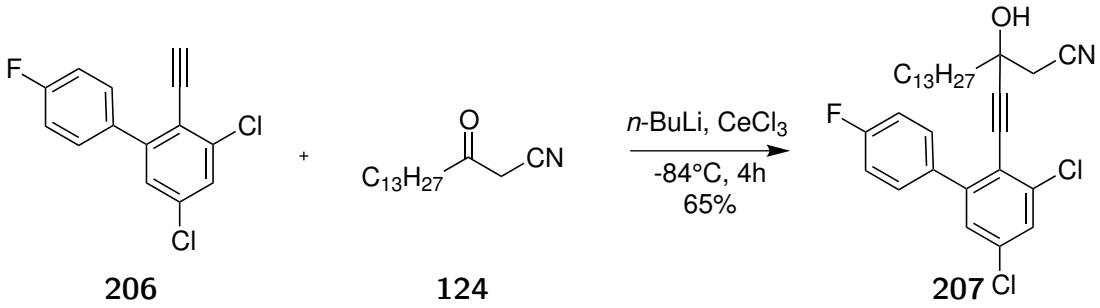

Scheme 3.19: Addition of alkyne **206** to the ketonitrile **124**.

ation of the *cis*-alkene **223** did not progress using these conditions. The NMR spectra were initially confusing but provided information as to why the second hydrogenation step did not proceed. New vinylic signals of **223** in the ^{1}H NMR spectrum were present at 6.47 and 5.53 ppm and are shown in Figure 3.7. The apparent pair of doublet of doublets can be assigned to a 1:1 mixture of diastereoisomers. Rotation is restricted between the single bond between the benzene ring and the alkene causing an axis of chirality. With two centres of asymmetry in the molecule, 4 diastereoisomers can be produced and are illustrated in Figure 3.6.

Table 3.2.1: Incomplete hydrogenation of **207**.

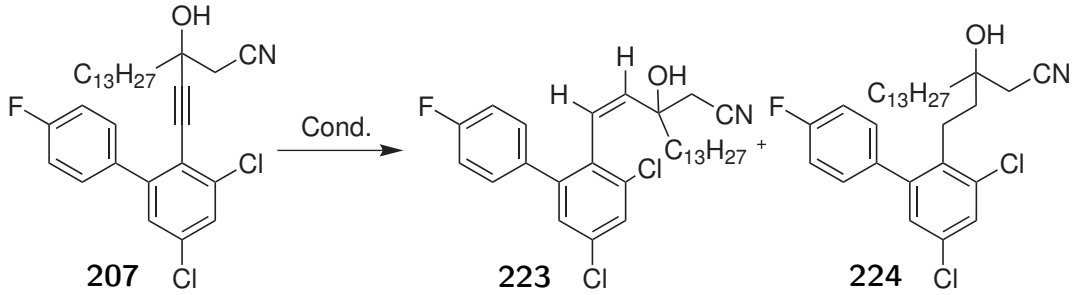

Conditions	**207**:**223**:**224**
Pd/C (25 %wt), H_2, EtOAc, 25°C, 15h.	0:100:0
Pd/C (25 %wt), H_2, EtOAc, 25°C, 96h.	0:100:0
Pd/C (25 %wt), H_2, EtOAc, 78°C, 15h.	complex mixture

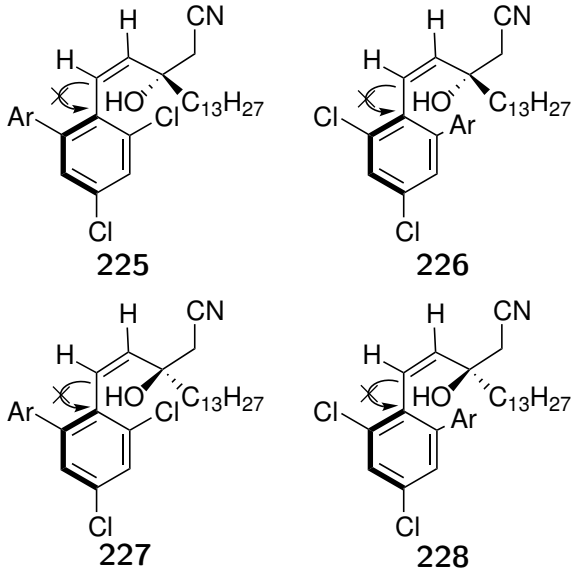

Figure 3.6: Possible diastereoisomers contained in **223**.

Each of the two pairs of diastereoisomers, **225**/**228** and **227**/**226** show two alkene signals. The vinylic benzyl proton (Ha) was identical for both pairs of diastereoi-

somers and appears as a doublet at 6.49 ppm. The neighbouring vinylic proton (Hb) showed different chemical shifts for each pair of diastereoisomers and consequently these vinylic signals at 5.53 ppm appear as two separate doublets at 5.57 and 5.50 ppm (Figure 3.7). The highly hindered and rotationally restricted system consequently showed a complicated ^{13}C NMR spectrum. Signals were further split independently from that caused by a ^{19}F substitution. Previous hydrogenations were performed successfully in Scheme 3.4 and Scheme 3.9. The hinderance induced from a 2-chloro-6-phenyl substitution of the vinylbenzyl system in **223** led to the incomplete hydrogenation and an alternative synthesis of the target **229** was investigated.

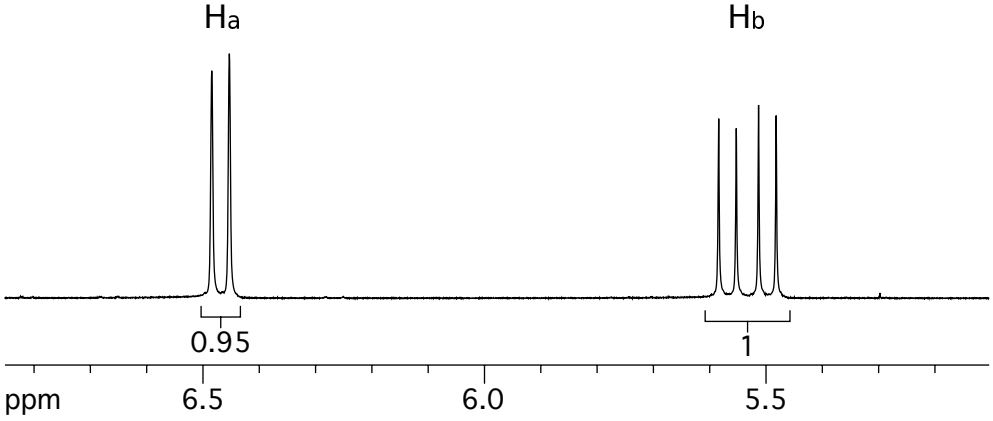

Figure 3.7: ^{1}H NMR of the mixture of isomers contained in **223**.

The first alternative to be trailled was the use of a chemical hydrogen donor, diimide. Diimide was prepared *in situ* from *p*-toluenesulfonyl hydrazide and sodium acetate in ethanol under reflux.[125] The ^{1}H NMR spectrum of the crude product showed the reaction did not occur.

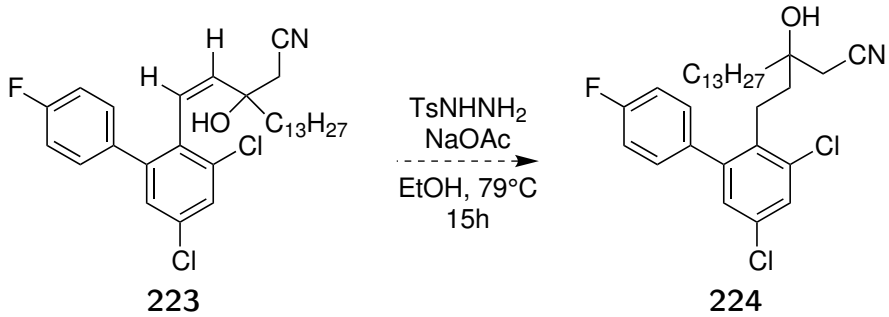

Scheme 3.20: Hydrogenation attempt using tosyl diimmide.

Isomerisation of the double bond to the *E* configuration may make the alkene

less hindered that the *Z*, making it more susceptible to hydrogenation. When the alkene **223** was exposed to iodine at room temperature no reaction occurred.

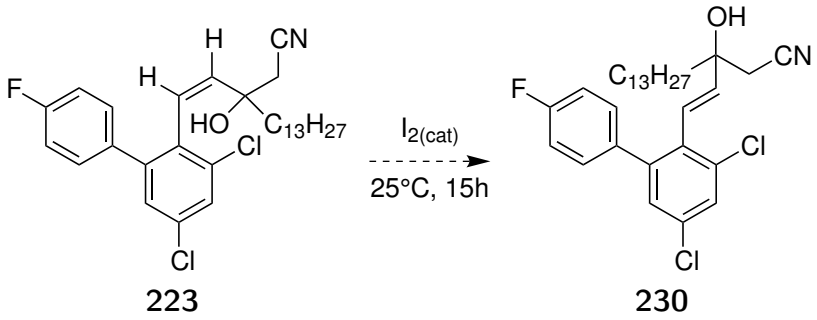

223 **230**

Scheme 3.21: Isomerisation attempt using Iodide.

With little evidence that isomerisation was proceeding an alternative reduction using lithium aluminium hydride was proposed. Literature provided evidence that allyl alcohols, specifically 3-phenyl propenol, are susceptible to 1,4-hydride addition.[126–128] Variable yields of 12 - 55% were obtained previously using lithium aluminium hydride for nitrile reduction of this type of hydroxynitrile and for the total reduction of the ketonitrile **124**. The alkene **223** was exposed to lithium aluminium hydride at room temperature in THF (Scheme 3.22). The starting material was consumed, indicating nitrile reduction, however ^{1}H NMR analysis of the crude showed a complex mixture. The mixture contained several new *Z*-alkene signals and resolving the mixture was not attempted as chromatographic separation was deemed unlikely. An attempt was made to reduce the nitrile to the free amine **231** prior to hydrogenation. Sodium borohydride was added to a solution of **223** and cobalt chloride (Scheme 3.22). The starting material was consumed and the ^{1}H signal at 2.44 ppm of the starting material was no longer present. A significantly cleaner crude was isolated using cobalt chloride and sodium borohydride compared to previous attempts lithium aluminium hydride. The crude amine **231** was exposed to palladium on carbon under a hydrogen atmosphere. No changes were seen to the alkene signals. With the alkene remaining intact methods to completely remove the alkene were abandoned.

A complex mixture was obtained in Table 3.2.1 when **223** was exposed to palladium on carbon under a hydrogen atmosphere at 78°C which was reexamined more closely. Two new singlets were present around 2.4 ppm in the ^{1}H NMR

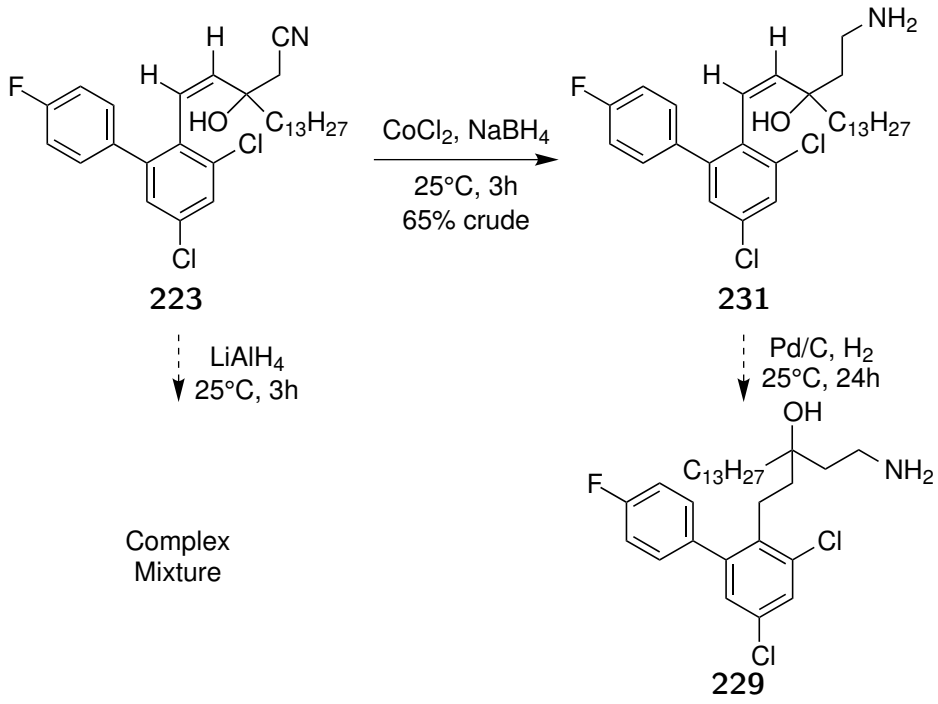

Scheme 3.22: Unsucsessful attempts to generate **229**.

spectrum indicating a full but incomplete hydrogenation occurred. When the alkyne **223** was exposed to a weight equivalent of palladium on carbon under a hydrogen atmosphere in refluxing ethyl acetate for 5 hours (Figure 3.8a), two difficult to separate products **208** and **224** were isolated in low yield. The structure of the reductive dechlorination biphenyl **208** was confirmed as it had a ^{13}C NMR spectra identical to that of an authentic sample obtained from a previous synthesis (Scheme 3.9). The elevated temperatures utilised in Scheme 3.8a are similar to a reported reductive dechlorination reaction.[129] Figure 3.8b shows the reductive dechlorination reaction on a similar system that uses palladium on carbon and tritium gas to convert **232** to ^{3}H-radiolabeled amphetamine **233**.[130] Careful spectral analysis was required to confirm that **224** was successfully separated from the other possible mono-chlorinated products. The DEPT spectrum of **224** offered critical information on the chlorine substitution pattern. Figure 3.9 shows the aromatic region overlays of the DEPT NMR spectra of the reductive dechlorination product **208**, the intact 3,5-dichloro-4'-fluorobiphenyl **206** and the desired 2,4-dichlorobiphenyl product **224**. These comparisons were required as fluorine coupling along the biphenyl system yields the absolute number of ^{13}C signals invalid. Introduction of new C-H bonds by reductive dechlorination leads

to extra positive DEPT signals in **208** when compared with the 3,5-dichloro-4'-fluorobiphenyl system precursor **206** and **224**. The 3,5-dichloro-4'-fluorobiphenyl system remained intact in **224** as it contained 6 positive DEPT signals expected. The ^{1}H NMR spectrum of **224** no longer showed signals at 6.47 and 5.53 ppm indicating the successful hydrogenation of *cis*-alkene in **223**. The aromatic region contained 4 distinct signals expected for the 3,5-dichloro-4'-fluorobiphenyl system (Figure 3.10). The pair of doublets at 7.10 and 7.40 with *meta*-coupling of 2.2 Hz provide concluding evidence that reductive dechlorination had not occurred and a mono dechlorination product was not isolated. The ^{13}C signal at 117.3 ppm in **224** confirmed the presence of a nitrile. Synthesis of **224** was not considered ideal, using large quantities of palladium on carbon and starting materials so as to generate **224** in low yield, but with milligram quantities of **224** isolated its reduction in the following step was explored.

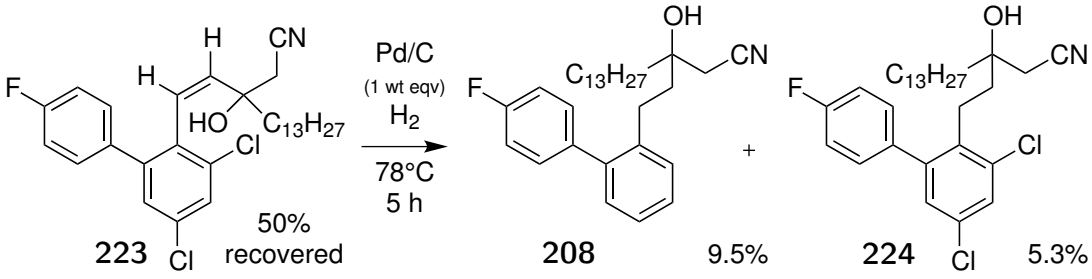

(a) Forcing conditions used to isolate **224**.

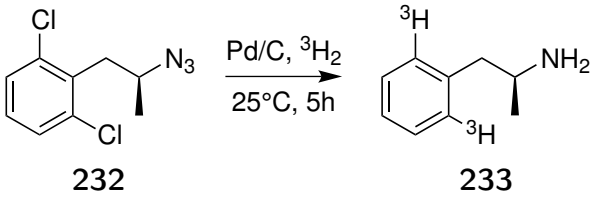

(b) Reductive dechlorination reported by Lamb *et al.*[130]

Figure 3.8: Reductive dechlorination using hydrogen and palladium on carbon.

The nitrile was reduced by adding sodium borohydride to a solution of **224** and cobalt chloride at 0°C (Figure 3.10). Purification gave the target in modest yield with the distinct absence of the nitrile signal of the starting material. The 3,5-dichloro-4'-fluorobiphenyl system remained intact with ^{1}H NMR signals and splitting equivalent to those in Figure 3.10. The amine substituted methylene ^{1}H signals were characteristic appearing with significant overlap as a pair of mul-

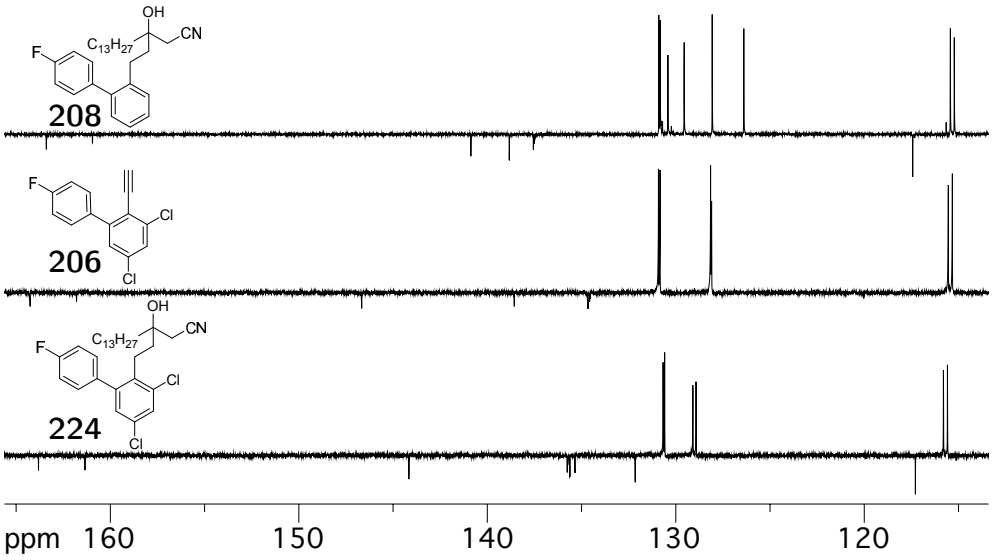

Figure 3.9: Expansion of the ^{13}C-DEPT aromatic region of **208**, **206** and **224**.

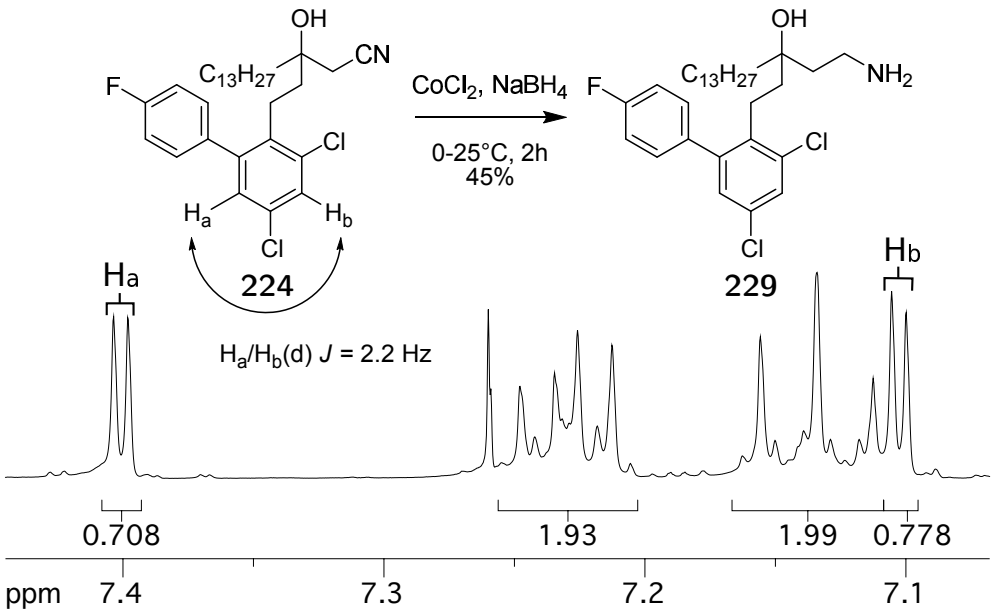

Figure 3.10: Expansion of the ^{1}H NMR aromatic region of **224** and subsquent reduction of the nitrile **224**.

tiplets at 2.6 ppm. With the synthesis of **229** complete, alternative targets were proposed.

The introduction of the 6-(4'fluoro)-2,4-dichloro functionality, derived from the potent HMG-reductase inhibitor **77**, was proposed as a amine substituent (Figure 3.11). Further structure-activity information about the 6-(4'fluoro)-2,4-dichloro moiety would be obtained by comparison of the target **234** to its precursor **109**. Generation of **234** by reductive amination would make use of 2-(4'-fluorophenyl)-4,6-dichlorobenzaldehyde **210** synthesised previously in Scheme 3.17.

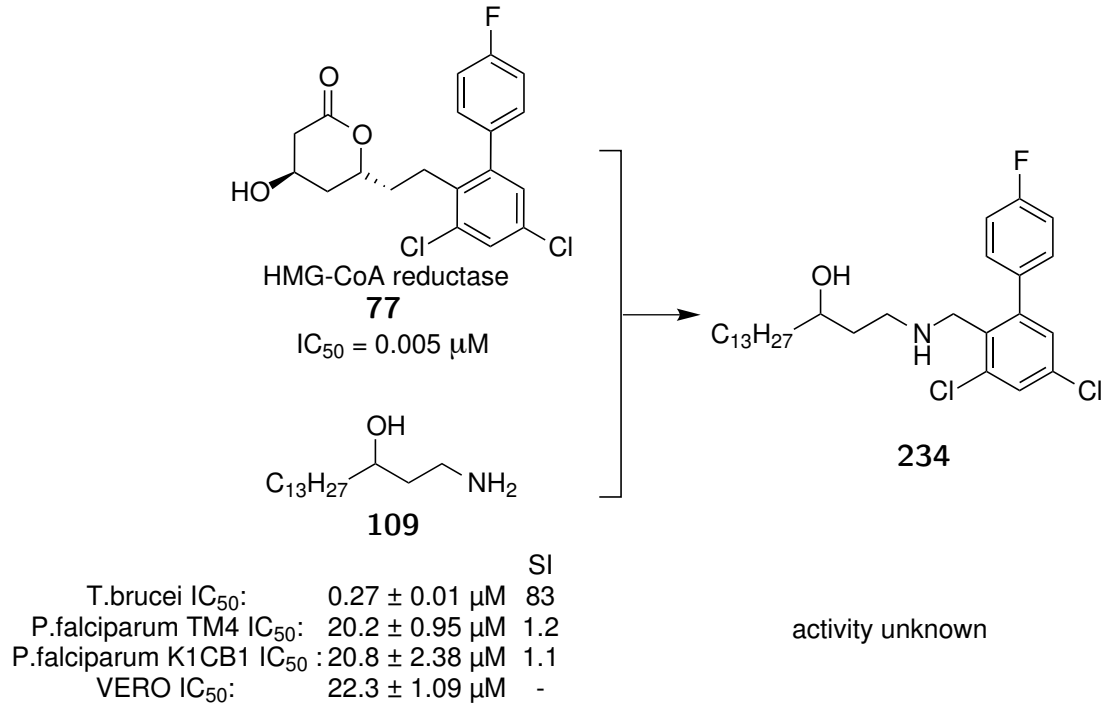

Figure 3.11: Introduction of the 6-(4'fluoro)-2,4-dichloro fragment as a amine substitution.

The benzaldehyde **210** was stirred with the amine **109** and anhydrous magnesium sulphate at 50°C for 48 hours before addition of sodium borohydride (Scheme 3.23). The ^{1}H NMR spectrum of the product showed a new benzylic AB pattern which overlapped with the hydroxy substituted methine and appeared as a multiplet at 3.71 ppm. Two ^{13}C NMR substituted amine signals at 48.4 and 47.9 ppm were present. The mixture of alkyl and aromatic signals in both the ^{1}H and ^{13}C spectra correlated with those obtained from previously synthesised compounds of this type.

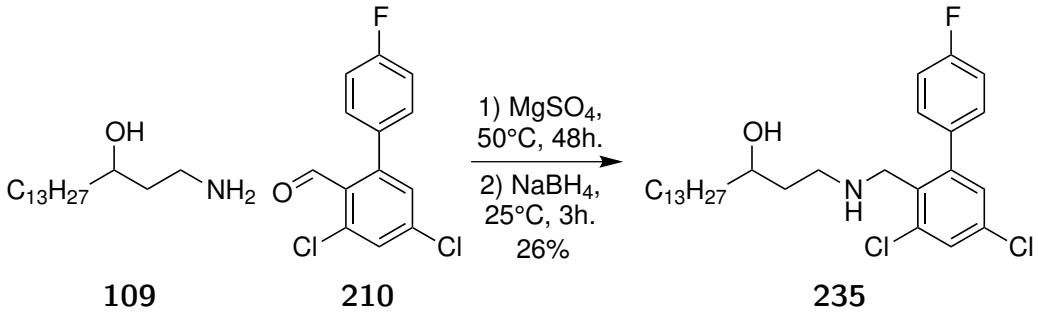

Scheme 3.23: Reductive amination to generate **235**.

3.3 Fluvastatin

With the introduction of the 2-(4'-fluorophenyl)-4,6-dichlorophenyl system complete, other means to introduce the established statin structural features to NMT inhibitors were explored. Scheme 3.24 shows fluvastatin **236**, a clinically available HMG-reductase inhibitor, which contains a indole core substituted with 4'-fluorophenyl and a isopropyl group. The isopropyl group, along with the 4'-fluorophenyl, are standard features of many of the synthetic statins and its inclusion was explored by incorporation into the new target **116**. Comparison with the previous targets will explore the structure-activity dependency of the isopropyl group towards NMT inhibition.

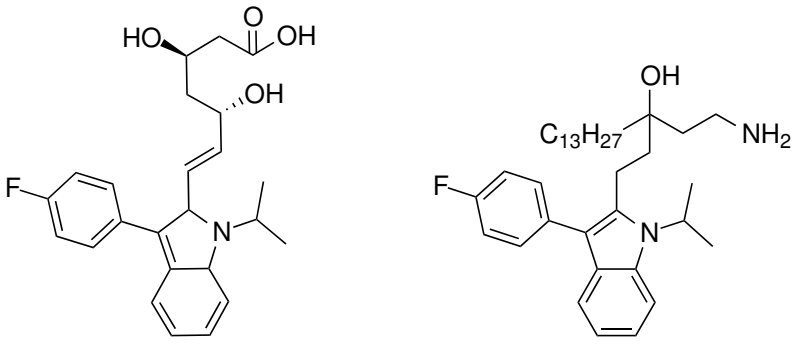

Scheme 3.24: Incorporation of fluvastatin features into NMT inhibitors.

Incorporation of the hydrophobic fluvastatin fragment into a potential NMT inhibitor required the synthesis of the key alkyne intermediate **237** (Scheme 3.25). The same addition reaction using the alkyne **237**, akin to Scheme 3.19, would

introduce this fluvastatin fragment as a tertiary alcohol. The first phase of the synthesis of the key alkyne intermediate **237** was to prepare the indole **96** via a Bischler-Möhlau indole synthesis.[131] The second phase was to formylate the indole to give **238** before performing a two step Corey-Fuchs[132] synthesis to generate **237**.

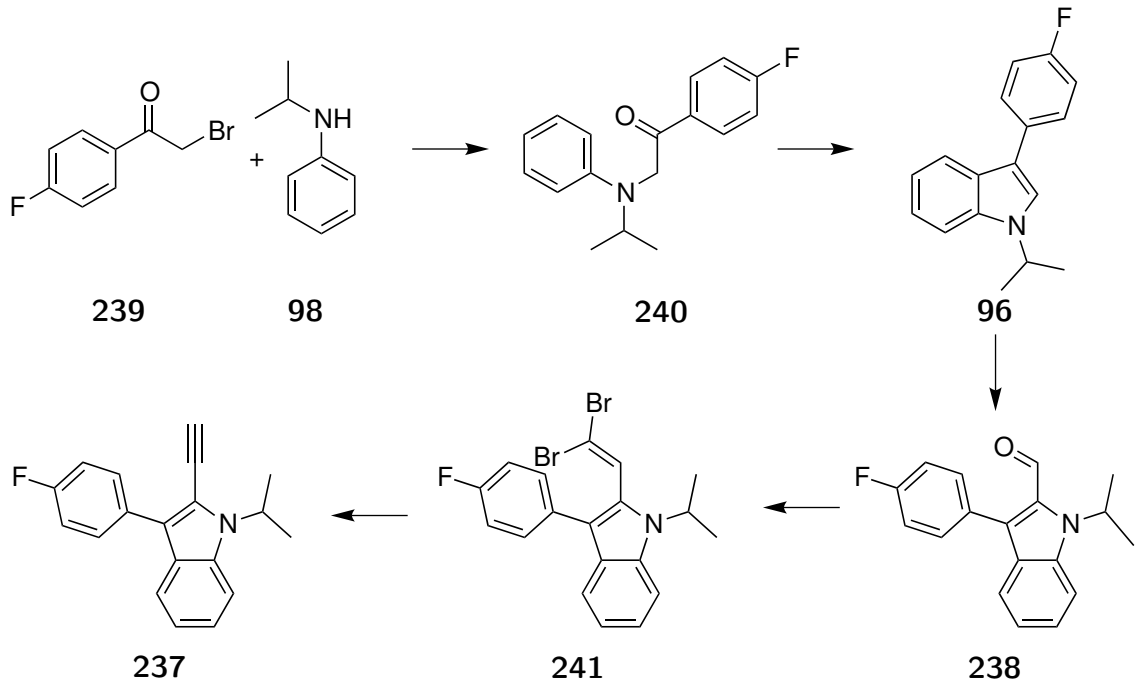

Scheme 3.25: Overview for the synthesis of propenal

One of the starting materials for the Bischler-Möhlau indole synthesis was the acetophenone **239**, which was obtained by bromination of 4'-fluoroacetophenone **242** (Table 3.3.1). When bromine was added to a solution of 4'-fluoroacetophenone **242** at room temperature **239** was isolated from a mixture containing the dibrominated **243** and the starting material. The ^{1}H NMR showed a downfield singlet at 4.41 ppm (2H) and a ^{13}C NMR signal at 30.5 ppm, both indicative of a monobromo substituted methylene. The ^{1}H and ^{13}C NMR spectra both showed splitting in the aromatic region due to fluoride substitution. The melting point and FT-IR of the 2-bromo-4´-fluoroacetophenone matched that reported in the literature.[133] Purification of multigram quantities of **239** by column chromatography was problematic and methods were explored that avoided the disproportionation reaction described by Kröhnke[134] in Scheme 3.26.

Table 3.3.1 shows the improved result by addition of the Lewis acid, aluminium

Table 3.3.1: Bromination of 4-fluoroacetophenone

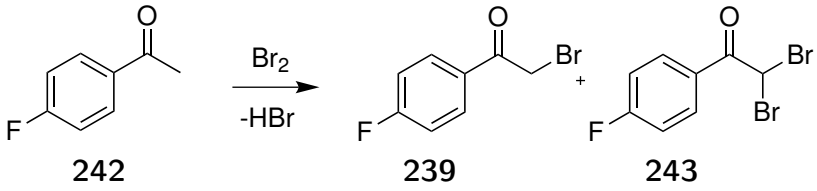

Conditions	**242**:**239**:**243**	Yield
0.9 eq Br_2, $CHCl_3$, 25°C, 1.5h	7:84:9	77%
1 eq Br_2, $AlCl_3$, Ether, 25°C, 15min	2:97:<1	79%

trichloride, which was used in the bromination of acetophenone.[135] The reaction rate was accelerated thus avoiding significant formation of the dibrominated product **243** from the competing disproportionation reaction. The method was implemented on 10 – 20 g scale without the need for purification by column chromatography.

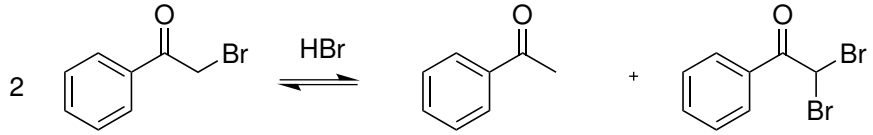

Scheme 3.26: Disproponation reaction of acetophenone proposed by Kröhnke *et al.*[134]

Although *N*-isopropylaniline is commercially available it was prepared in one step. The reductive amination of aniline and acetone exposed to zinc dust and acetic acid gave *N*-isopropylaniline in excellent yield (Scheme 3.27).[136] The ^{1}H NMR,[13] C NMR and IR spectra all possessed signals which matched those reported in the literature. A small impurity of *N,N*-diisopropylaniline **244** was present but it was deemed to be insignificant for the following step. The method was successful at the 20 - 40 g scale without the need for further purification.

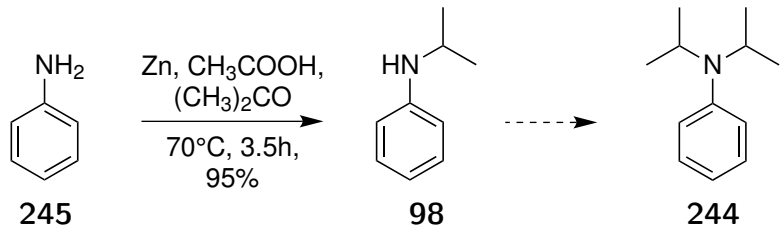

Scheme 3.27: Formaion of *N*-isopropylanaline by reducive amination

With 2-bromo-4'-fluoroacetophenone **239** and isopropyl aniline **98** in hand, a

Bischler-Möhlau synthesis of the indole **96** was attempted.[83,131,137] The reaction proceeds by a substitution reaction between the acetophenone **239** and *N*-isopropylaniline **98** to give **240** which can undergo an intramolecular electrophilic aromatic substitution to generate the indole **96**.

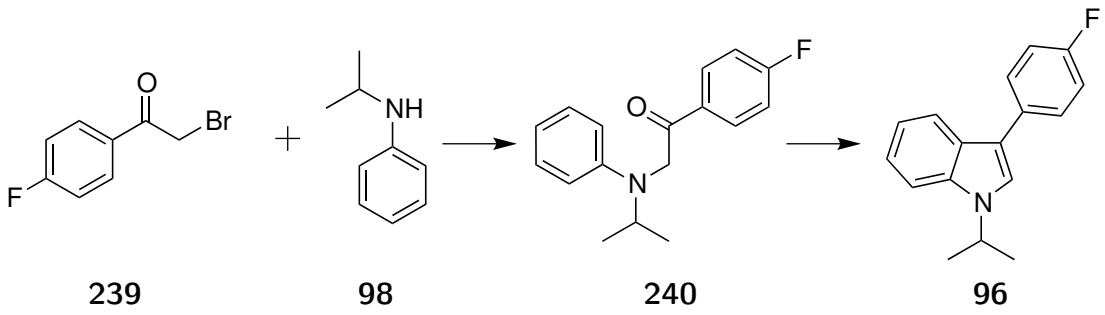

239 **98** **240** **96**

Scheme 3.28: Bischler-Möhlau indole synthesis of Fluvastatin segement

Initially **240** was isolated before proceeding with annulation. A mixture of the acetophenone **239** and 2 equivalents of *N*-isopropylaniline **98** was heated at reflux in ethanol for 20 hours. The^{1}H NMR spectrum of **240** showed a new singlet at 4.60 ppm, this combined with signals comparable to each starting material, provided evidence that substitution had occurred. The substitution reaction releases an equivalent of hydrobromic acid and the literature procedure used a second equivalent of *N*-isopropylaniline as a acid scavenger. Although purification of **240** was achieved by chromatography, recovery of *N*-isopropylaniline proved difficult.

The substitution reaction was optimised by testing a range of bases. Alternative bases were tested to avoid using a second equivalent of *N*-isopropyl aniline **98** and to provide a simple purification procedure. Table 3.3.2 summarises trials in which substitution product **240** was isolated before the annulation step. The use of a biphasic sodium carbonate system showed consumption of the bromide but gave a complex mixture without significant generation of the desired ketoamine **240**. The use of triethylamine showed full consumption of the bromide **239**, however a major proportion of *N*-isopropylaniline **98** was present after workup. Triethylamine, a competitive nucleophile, underwent alkylation and formed a quaternary ammonium salt that was removed during workup. *N,N*-Diisopropylethylamine (DIPEA, Hunigs base)[138], a non-nucleophilic base, gave promising results. The excess DIPEA was removed via acid workup and the crude material was of suffi-

cient purity for the next step. Attempts were then made to combine the substitution and annulation steps into a one pot procedure.

Table 3.3.2: Optimisation of the substitution reaction.

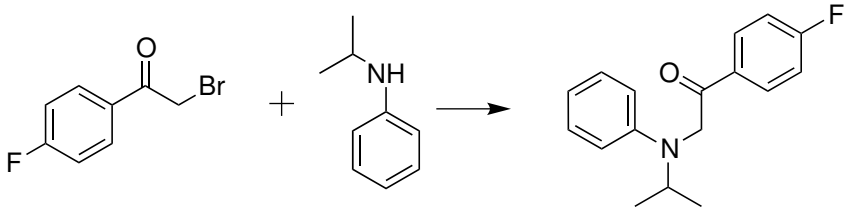

239 **98** **240**

Conditions	**239**:**240**	Yield
1:2 eq **239**:**98**, EtOH, 78°C 20h.	0:100	73%
1:1:1.5 eq **239**:**98**:Na_2CO_3, EtOH, 78°C 2h.	complex mixture	N/A
1:1:1.1 eq **239**:**98**: TEA, EtOH, 78°C 24h	0:100	N/A
1:1:1.5 eq **239**:**98**:DIPEA, EtOH, 78°C 6.5h.	0:100	>95% (crude)

A two stage, one pot alkylation followed by annulation was not formally reported in the literature (Scheme 3.29). Tang *et al.*[131] discussed yields greater than 90% using a non-radiolabeled system, but on hot runs only achieved 60% thus requiring purification of **240** before annulation. The final manufacturing process discussed a one pot substitution and annulation method however a detailed experimental was not presented.[83] Attempts using DIPEA or a second equivalent of *N*-isopropylaniline **98** followed by addition of zinc chloride (Scheme 3.29) gave only the acetophenone **240** without significant annulation to the indole **96**. The activity of the zinc chloride Lewis acid catalyst was neutralised by exposure to a Lewis base. Efforts were then focused towards isolating the ketoamine **240** before conversion to the indole **96**.

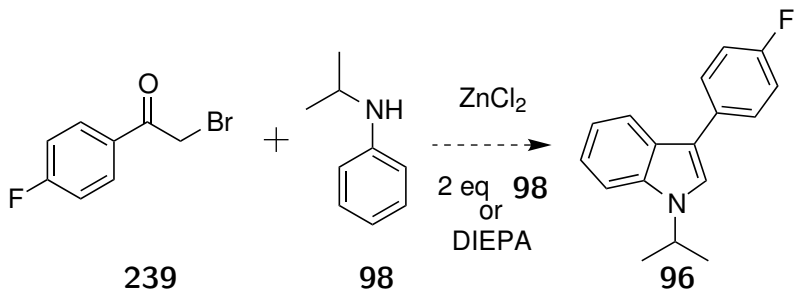

239 **98** **96**

Scheme 3.29: One pot indole synthesis of **96**.

The annulation of ketoamine **240** using zinc chloride to give the indole **96** is

reported.[131,137] In practice the reaction required a vast excess of the Lewis acid to promote internal electrophilic aromatic substitution despite vigorous drying. (Table 3.3.3). Reactions frequently would not initiate or conversion would be slow. Longer reaction times were coupled with low yields because the ketoamine **240** was thermally unstable. The reaction generates 1 mol equivalent of water which may deactivate zinc chloride as the reaction progresses, so the use of molecular sieves as a water scavenger was trailed. The use of molecular sieves did improve yields but mechanical problems (stirring and filtering) were encountered on scale up and thus their use avoided. The final conditions involved the use of a large excess of zinc chloride, more than that described in the literature. However a method was successfully applied at a 10 – 20 g scale requiring only simple purification. The formation of the desired indole **96** was confirmed by ^{1}H and ^{13}C NMR spectra and melting point which matched the literature. The subsequent formylation was explored.

Table 3.3.3: Optimisation of indole formation using zinc chloride as a catalyst.

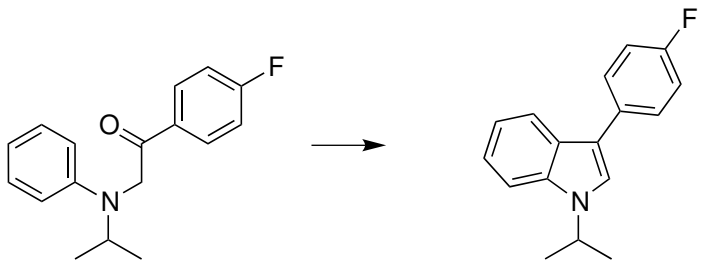

240 **96**

Conditions	**240**:**96**	Yield
2 eq $ZnCl_2$, EtOH, 78°C, 17h.	100:0	N/A
20 eq $ZnCl_2$, EtOH, 78°C, 72h.	0:100	42%
purified **240**, 30 eq $ZnCl_2$, 3 wt eq 4A mol sieve, 15h.	0:100	>98%
crude **240**, 30 eq $ZnCl_2$, 10 eq 4A mol sieve, 78°C, 24h.	<2:98	57%
crude **240**, 25 eq $ZnCl_2$, 78°C, 15h.	<2:98	70%

Conditions for formylation of the indole **96**, via a Vilsmeier-Haack reaction, were available.[137,139] When the indole **96** was exposed to two equivalents of (chloromethylene)dimethyliminium chloride generated *in situ* from phosphorous oxychloride and DMF (Scheme 3.30), **238** was isolated in good yield. Aldehyde signals could be seen in the ^{1}H and ^{13}C NMR spectra at 9.81 ppm and 183.7 ppm respectively.[137] Methods to perform a Corey-Fuchs alkyne synthesis on **238**,

towards **237**, were explored.

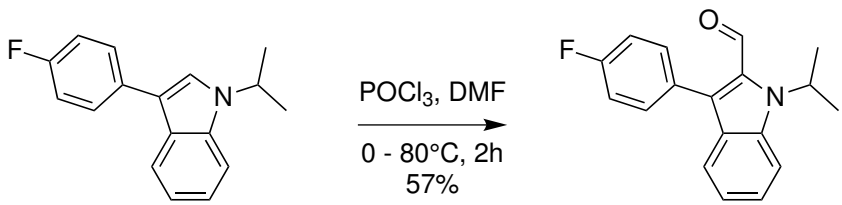

96 **238**

Scheme 3.30: Vilsmeier-Hack formylation of **96**.[137,139]

Scheme 3.31 illustrates the conversion of the formylindole **238** to the alkyne **237** using a procedure detailed by Thottathil.[132] The aldehyde **238** was reacted with two equivalents of triethyl phosphite and carbon tetrabromide at -45°C for 3.5 hours. The vinylic dibromide **241** no longer showed an aldehyde signal, replaced by a new vinylbenzyl ^{1}H signal at 7.57 ppm. The DEPT spectrum showed the correct number of CH signals taking into account fluorine splitting. Remaining carbon tetrabromide was removed during column chromatography and the vinylic dibromide **241** was isolated in excellent yield. The second step of the Corey-Fuchs synthesis was followed from the same literature procedure.

Conversion of the dibromide **241** to the alkyne **237** was distinct from a standard Corey-Fuchs procedure and did not undergo a Fritsch-Buttonberg-Wiechell rearrangement. Thottathil[132] detailed a procedure that used potassium *tert*-amylate, a mild base, instead of butyllithium to eliminate the vinylic benzyl proton on **241** to give the intermediate **246**. Potassium *tert*-amylate was added to a solution of the dibromide **241** in toluene at 0°C. The first elimination reaction showed consumption of **241** after 20 min and **246** was visible as a new spot. The second phase converted the bromide **246** to the alkyne **237** using mild conditions in a single pot. Methanol, dimethyl phosphite and a second equivalent of potassium *tert*-amylate was added to the solution of the bromoalkyne **246** at 0°C. The alkyne **237** was isolated in excellent yield with new singlet at 3.55 ppm in the ^{1}H NMR spectrum, indicative of a terminal alkyne. The presence of the alkyne system was visible in the ^{13}C NMR spectra with key signals at 85.9 and 76.4 ppm. With gram quantities of the alkyne **237** available, the synthesis of the target amine **116** continued via an addition reaction outlined in Scheme 3.32.

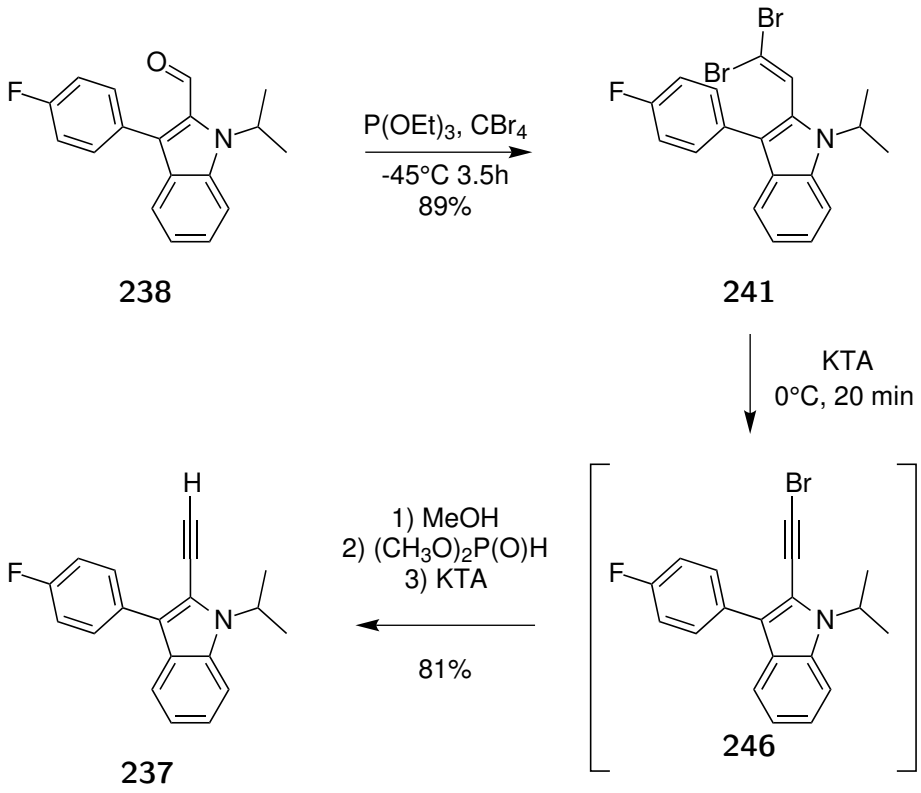

Scheme 3.31: Coversion to the alkyne using a modified Corey-Fuchs approach.

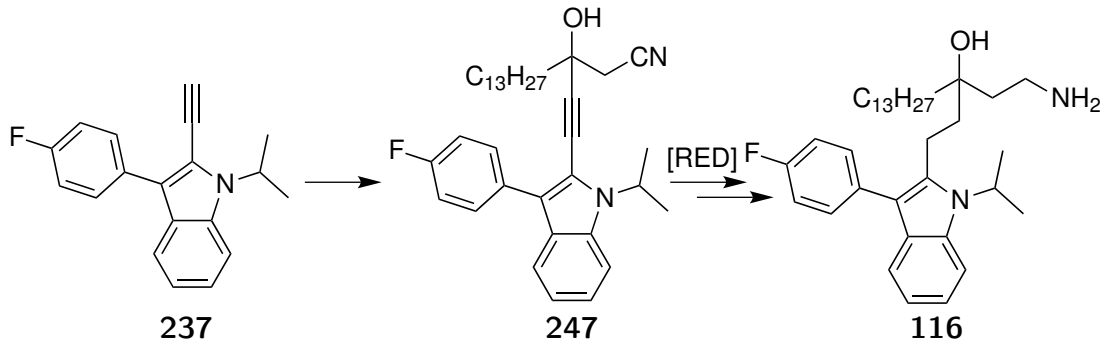

Scheme 3.32: Proposed synthesis of **116**.

The use of organocerium reagents to add alkynes to the ketonitrile **124**, used throughout this chapter, proceeded under the usual conditions to give **247** in excellent yield. The terminal alkyne ^{1}H NMR signal was no longer present and replaced with a new overlaid signal at 2.83 ppm indicative of the hydroxy nitrile system contained on **247**. The two terminal alkyne ^{13}C NMR signals were replaced by two new signals at 96.6 and 79.1 ppm. The fluvastatin fragment was stable under the addition conditions as aromatic region and isopropyl signals remained unchanged. Reduction of the alkyne contained in **247** was then explored.

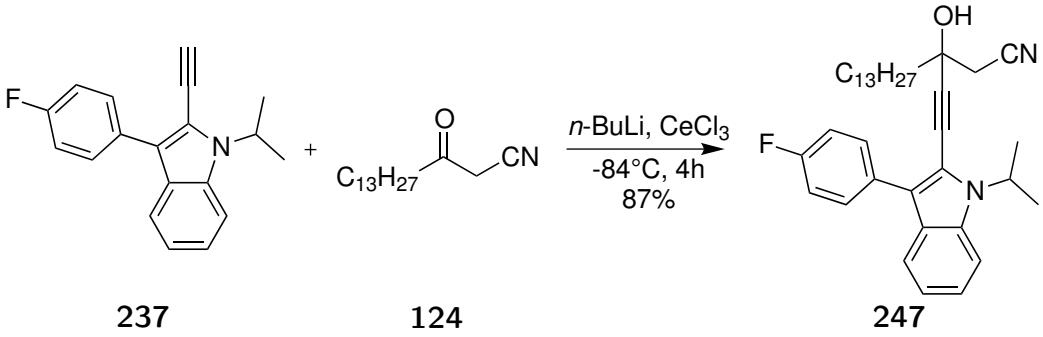

237 **124** **247**

Scheme 3.33: Cerium acetylide addition of **237** to **124**.

Hydrogenation of the indole **247** mirrored problems encountered previously with the hydrogenation of **207** (Table 3.2.1). When the alkyne **247** was exposed to palladium on carbon under a hydrogen atmosphere overnight at room temperature the alkene **248** was isolated (Scheme 3.34). Figure 3.12 shows the vinylic region of the ^{1}H NMR spectrum of **248**. The alkene signals of **248** appeared at a pair of doublets 6.68 and 5.95 ppm and the *cis*-isomer was assigned from the coupling constant of 12.2 Hz. The isopropyl indole substitution on **248** was less hindering compared to the previous 2-chloro substitution on the biphenyl **223** as no further splitting of the signal at 5.95 ppm originated from restricted rotation. The decrease in hindrance was attributed to the substitution bond angles of the 5 membered ring of the indole system compared to the 6 membered ring in the biphenyl **223**. Despite the indole **248** being less hindered than the 2-chlorobiphenyl **223** the second hydrogenation step did not proceed and consequently the reaction was repeated at higher temperature.

The alkene intermediate **248** was exposed to palladium on carbon in ethyl acetate

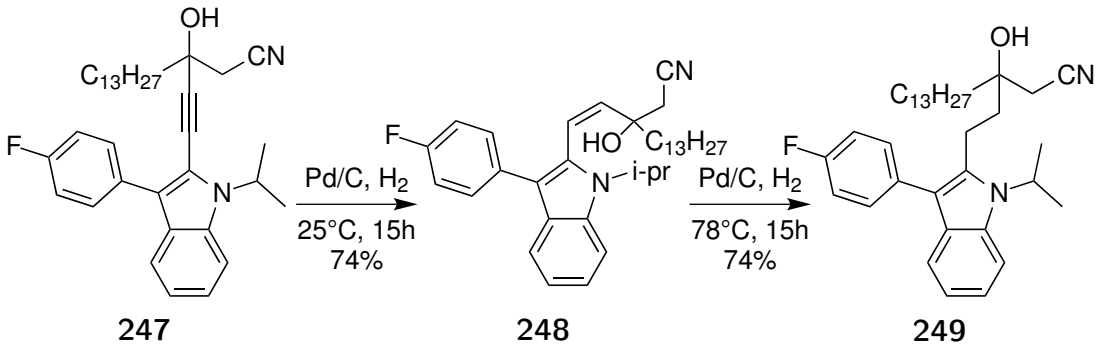

Scheme 3.34: Hydrogenation of **247**.

under reflux in a hydrogen atmosphere. The hydrogenation of the *cis*-alkene proceeded and the product **249** was isolated without the over-reduction problems encountered previously in Figure 3.8a when chlorine substituents were present. Neither the alkyne or alkene signals of the starting material and the intermediate were present. A new benzylic triplet was present at 2.89 ppm in the ^{1}H NMR spectrum and the hydroxynitrile methylene signal appeared at 2.47 ppm. A signal at 117.4 ppm in the ^{13}C spectrum confirmed the availability of the nitrile for the final reduction step.

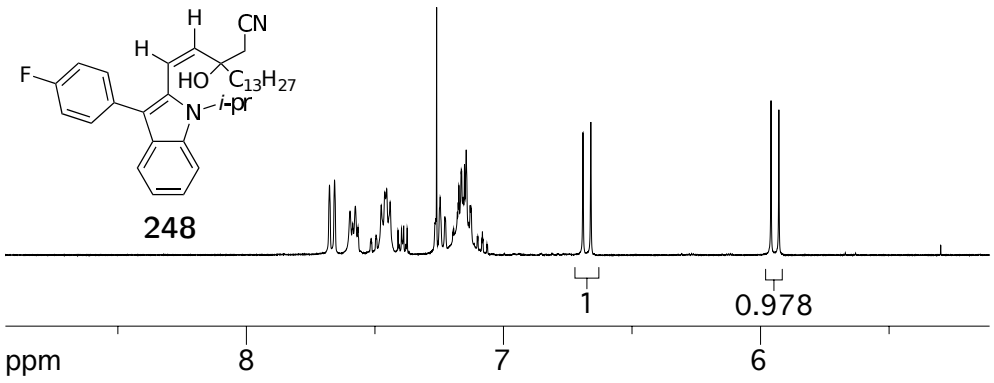

Figure 3.12: Expanded aromatic region of **248**.

When sodium borohydride was added to a solution of the nitrile **249** and cobalt chloride (Scheme 3.35), the nitrile was consumed and the amine formed in good yield. No signal was present at 117.4 ppm in the ^{13}C spectrum and nitrile reduction was confirmed with a absence of the nitrile absorbance at 2255 cm^{-1} in the IR spectrum. The ^{1}H signals of the amine **249** at 2.89 and 2.47 ppm collapsed into a multiplet at 2.90 ppm that fitted with other hydroxyamines of this type.

Alternative approaches as to incorporate the fluvastatin moiety were explored.

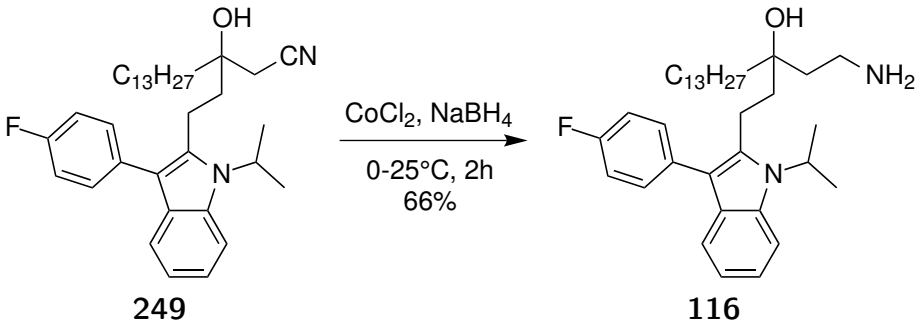

249 **116**

Scheme 3.35: Reduction of the nitrile on **249**.

Two new targets, **117** and **250**, were envisioned and incorporated the fluvastatin fragment though a reductive amination of the hydroxyamine **109**. These targets were designed to test if the incorporation of the fluvastatin moiety, though a amine linker, increased the potency of **109**. The first target **117** made use of the available formylated fluvaststin intermediate **238** isolated in Scheme 3.30.

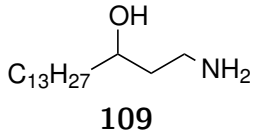

109

		SI
T.brucei IC_{50}:	0.27 ± 0.01 µM	83
P.Falciparum TM4 IC_{50}:	20.2 ± 0.95 µM	1.1
P.Falciparum K1CB1 IC_{50}:	20.8 ± 2.38 µM	1.1
VERO IC_{50}:	22.3 ± 1.09 µM	-

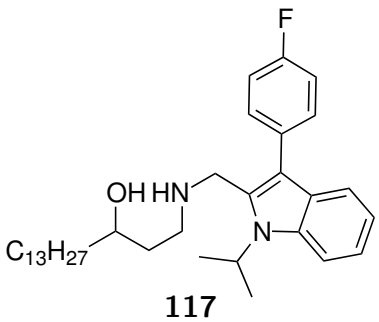

117

Activity unknown

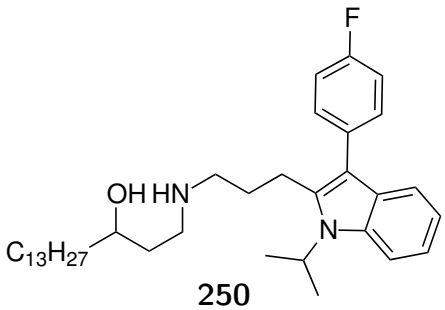

250

Activity unknown

Figure 3.13: New targets for synthesis **117** and **250**.

The reductive amination of the hydroxyamine **109** with the benzaldehyde **238** was performed as a two step procedure (Scheme 3.36). Sodium borohydride was added to the imine intermediate, formed by stirring **109** and benzaldehyde **238** at 50°C in a sealed vessel for 48 hours. The amine **117** was UV active and contained complex ^{1}H and ^{13}C NMR aromatic signals which were comparable to the starting aldehyde **238**. The myristoyl chain signal at 1.30 ppm was present in the ^{1}H NMR spectrum along with a key hydroxy substituted methine at 3.62

ppm. The amino benzyl methylene signal at 3.59 ppm was complimented by the adjacent amine substitution multiplets between 2.4 and 2.6 ppm confirming the presence of a secondary amine. With the first fluvastatin reductive amination target **117** isolated, different strategies were explored towards the synthesis of the longer linker length target **250** in Figure 3.12.

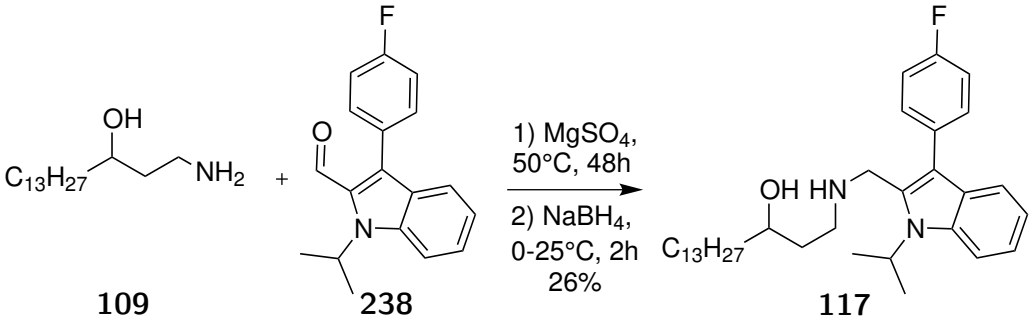

109 **238** **117**

Scheme 3.36: The reductive amination of **109** with **238**.

The synthesis of the target **250** is outlined in Scheme 3.37. Installing the propenal chain, to the indole **96** was proposed from methods developed for the manufacture of fluvastatin. Removal by reduction of the alkene in **100** was to ensure the mobility of the longer linker. The reductive amination of the aldehyde **251** with the hydroxyamine **109** was expected to give **250** in 3 steps from the indole **96**.

Acylation of the indole **96** in Scheme 3.37 required the synthesis of 3-(*N*-Methyl-*N*-phenylamino)acrolein (MPAA) **99** using methods reported by Lee *et al.*[140] *N*-methylformanilide **252** and butylvinyl ether **253** were added to a solution of oxalyl chloride at -10°C to give MPAA **99** in good yield (Scheme 3.38). The reaction proceeds via the imine intermediate **254** which is hydrolysed to **99** upon workup. The ^{1}H NMR spectrum showed a aldehyde signal 9.27 ppm (d, J = 8.1 Hz, 1H) coupled to a vinylic proton at 5.47 ppm (dd, J = 13.0, 8.1 Hz, 1H). ^{13}C NMR signals matched the literature.[140] The material was purified by vacuum distillation, to give multigram quantities of MPAA **99**.

The modified Vilsmier-Hack acylation using MPAA **99** was well reported in the literature.[83,131,140] The reaction, shown in Scheme 3.39, was designed specifically for the generation of the propenal **100**; a key intermediate in a process to generate fluvastatin **3**. The reaction proceeds as a 3 stage, single pot operation. The first stage is the generation electrophilic iminium salt **255** by reacting **99** with

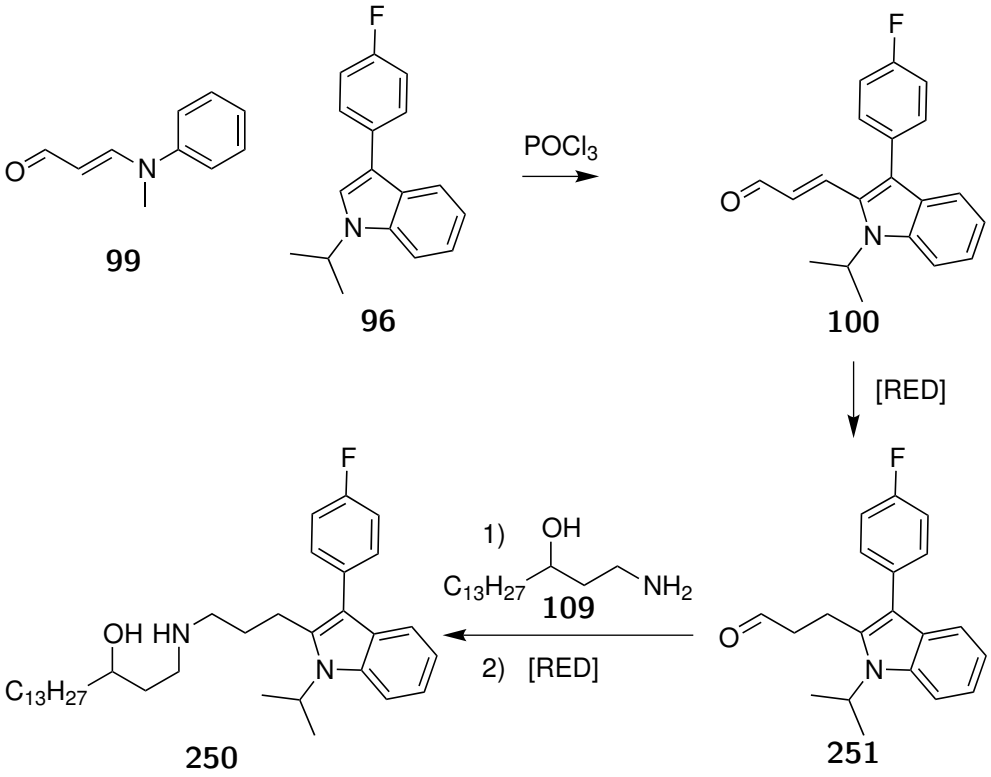

Scheme 3.37: Proposed synthesis of **250**.

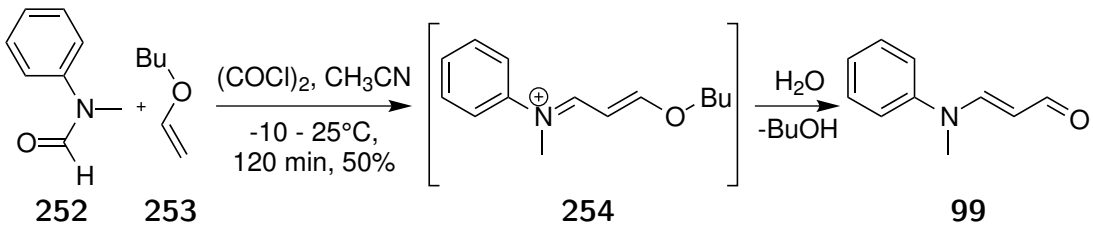

Scheme 3.38: Preparation of MPAA **99**.[140]

phosphorous oxychloride. The second step saw the introduction of the nucleophilic indole **96** which generated the resonance stabilised iminium salt **256** via a electrophilic aromatic substitution. Quenching converted the iminium salt **256** to the propenal **100** which was isolated in excellent yield. The new aldehyde signal at 9.59 ppm (d, J = 7.6 Hz, 1H) showed coupling to a new alkene signal at 6.34 ppm (dd, J = 16.2, 7.6 Hz, 1H). The ^{13}C NMR spectrum showed a new aldehyde signal at 193.4 ppm that confirmed the installation of the propenal chain. Hydrogenation of the alkene on **100** was explored.

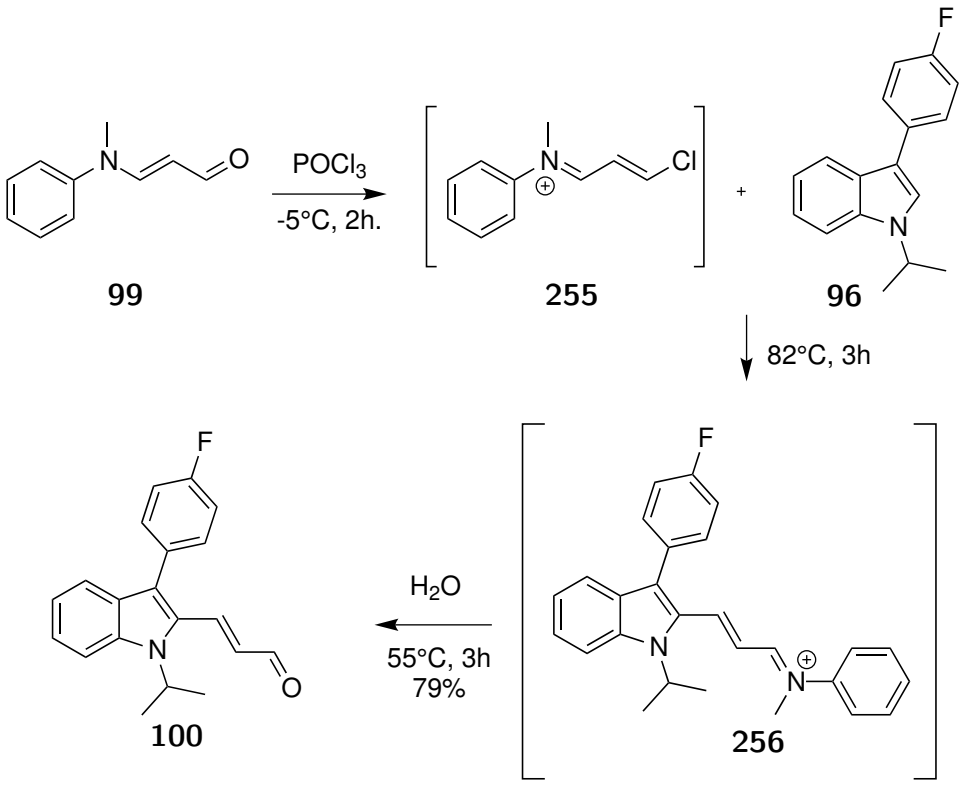

Scheme 3.39: The modified Vilsmeer-Hack on **96** using MPAA **99**

The penultimate step in Scheme 3.37 was the removal of the alkene in **100**, its position and purpose was specific to HMG-CoA reductase inhibition and not considered a structurally significant feature for the proposed NMT inhibitors. If the potency of the target **250** shows potential, the structure activity relationship for inclusion of the alkene could easily be explored. **100** was recovered when exposed to triethylsilane and palladium chloride in a selective hydrogenation procedure.[141] (Table 3.3.4). A total reduction to the saturated alcohol **257** followed by oxidation to the aldehyde **251** was pursued. The use of lithium aluminium hydride gave the allylic alcohol **258** as the major product. Exposure to sodium borohydride

also gave **258** as the sole product. Favourable results were obtained using sodium borohydride in pyridine[142,143] obtaining a 19:81 mix of **258**:**257**, however the mixture could not be separated by column chromatography. Standard alkene hydrogenation procedures, using palladium on carbon under a hydrogen atmosphere, led to a complex mix of products.

Table 3.3.4: Hydrogenation of propenal system.

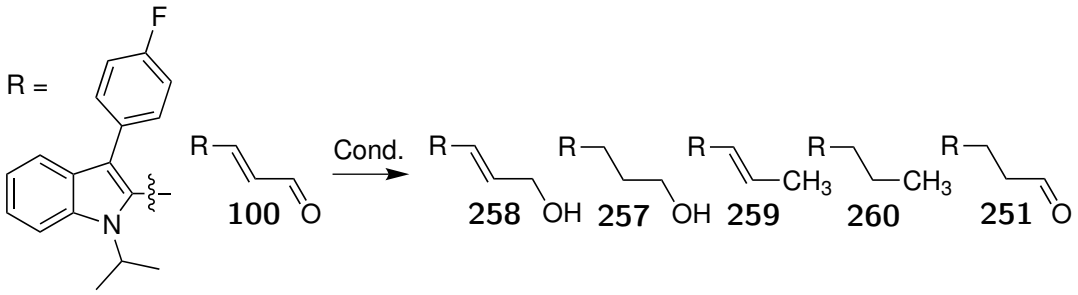

Conditions	**100**	**258**	**257**	**259**	**260**	**251**	Yield
EtOH, Et_3SiH, $PdCl_2$, rt, 48h.	100%	-	-	-	-	<1%	
THF, $LiAlH_4$, rt, 15h.	<1%	69%	31%	-	-	-	
EtOH, $NaBH_4$, rt, 15h.	<1%	100%	-	-	-	-	
Py, $NaBH_4$, -20°C, 72h.	<1%	19%	81%	-	-	-	
EtOAc, Pd/C, H_2 , rt, 68h.	2%	10%	34%	19%	5%	30%	
EtOAc, Pd/C, KOAc, H_2O, H_2, rt, 36h.	<1%	-	15%	-	-	85%	72%

Special hydrogenation conditions, based on the hydrogenation of cinnamaldehyde, were then applied to **100**.[144] Addition of potassium acetate and water increased the selectivity towards 3-phenylpropanal, avoiding the generation of significant quantities of either 3-phenylpropanol or cinnamic alcohol. These conditions were mirrored, using hydrogen at atmospheric pressure, and a 15:85 mixture of **257**:**251** was obtained. Critically, the separation of mixture was achieved by column chromatography and **251** was isolated in good yield. The product contained characteristic signals in the ^{1}H NMR spectrum at 9.73 (1H, t), 3.17 (2H, t) and 2.71 (2H, m); assigned to the saturated aldehyde chain of **251**. The ^{13}C NMR spectrum mirrored the change with new signals at 200.4, 44.4 and 17.7 ppm.

Reductive amination using the aldehyde **251** was explored to make the amine **250**. The hydroxyamine **109** was heated in the presence of the **251** before addition of sodium borohydride (Scheme 3.40). The ^{1}H NMR spectrum of the amine **250**

showed 4 distinct amine substituted methine multiplets between 2 and 2.5 ppm. The hydroxy multiplet and benzyl triplet signals were present at 3.77 and 2.64 ppm respectively. No aldehyde signal of the starting material was present in the ^{1}H NMR spectrum and **250** showed expected signals from both the fluvastatin and myristic fragments.

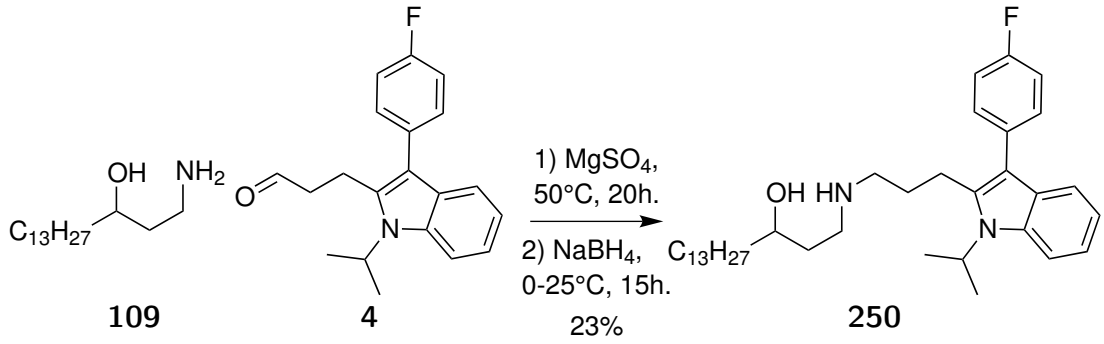

Scheme 3.40: reductive amination using **251**

A suite of new compounds have been synthesised that combine fragments inspired by HMG-CoA reductase inhibitors with the hydroxyamine **109**. Many of the compounds were synthesised using organocerium reagents or though a reductive aminations from aldehydes. The toxicity of these new derivatives of parent hydroxyamine **109** was assessed against *T. brucei rhodesience and P. falciparum.*

3.4 *in vitro* Protozoan toxicity

The synthesis of compounds throughout this chapter were designed to incorporate the fragments of HMG-reductase inhibitors that are associated with the binding site of the Coenzyme A substrate, and apply their binding potential towards NMT. It is assumed that increased potential towards NMT will result in a greater toxicity towards *T. brucei rhodesience and P. falciparum.* Compound **261** showed nano-molar potency as a cholesterol biosynthesis inhibitor[77] and the phenyl moiety was incorporated, at two sites, into the hydroxyamine **109** developed in Chapter 2 as to explore its application towards NMT. Introduction of a non-polar benzylamine substitution, discussed in chapter 2, improved selectivity towards *P.falciparum.* Figure 3.14 shows the tertiary alcohol **175** which has been demonstrated to offer no improvements to potency and selectivity towards

either *T.brucei rhodesience or P.falciparum* by incorporating a 3-phenyl fragment linked as a tertiary alcohol.

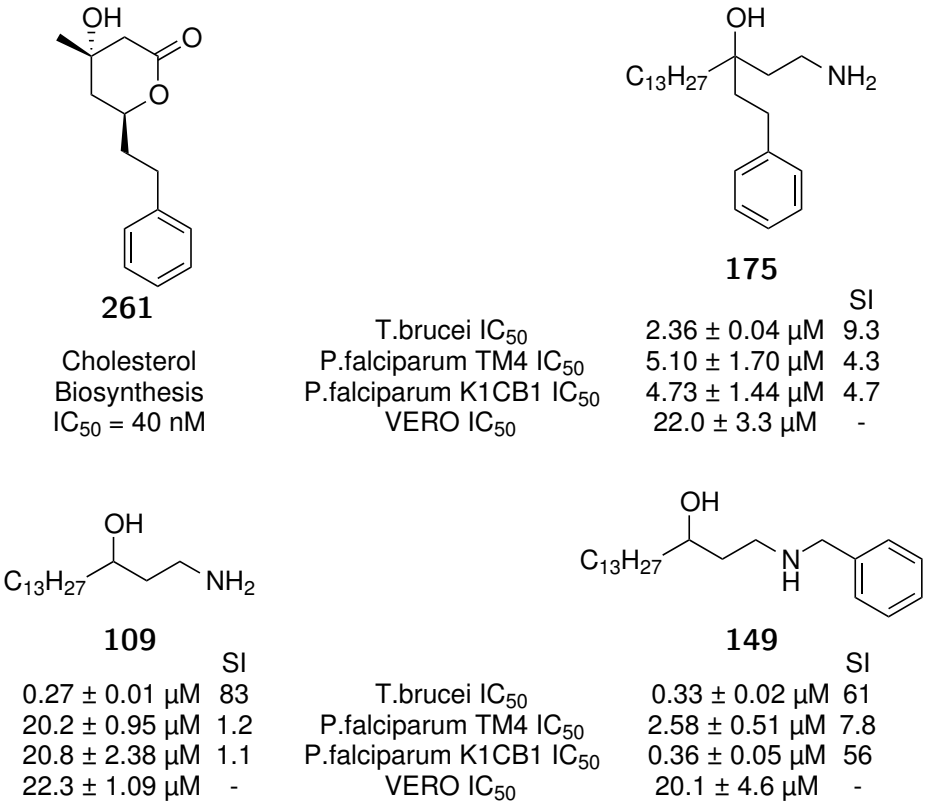

Figure 3.14: Structure-activity results against *T. brucei rhodesience* and *P. falciparum* though introduction of the phenyl fragment inspired from **261**

To further explore the potential for incorporation of statin fragments into potential NMT inhibitors, several tertiary alcohols were synthesised throughout this chapter and their activities against *T.brucei* and *P.falciparum* are shown in Figure 3.15. The inclusion of a 2,4-dichlorophenyl substitution in **190** slightly improved the selectivity towards *T.brucei* compared to unhalogenated **175**. This trend was not followed by introduction of the biphenyl system in **199**, for which the potency was about 10 times less than the unsubstituted **109**, with **199** showing a typical activity type associated with tertiary alcohol series. No notable changes in activity were observed though the combination of the 2,4-dichlorophenyl substitution in **190** with the biphenyl substitution contained on **199**. A slight drop in potency towards *P.falciparum* was observed by introduction of the fluvastatin fragment in compound **116**, which again did not improve the potency or selectivity compared to **109**. No changes were observed in the toxicity to VERO cells in any of the tertiary alcohols compared to the parent compound **109**.

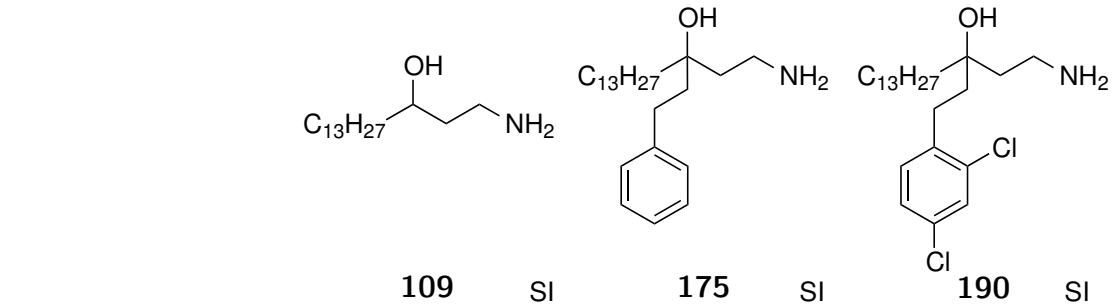

	109	SI	**175**	SI	**190**	SI
T.brucei IC_{50}:	0.27 ± 0.01 µM	83	2.36 ± 0.04 µM	9.3	2.69 ± 0.07 µM	12
P.falciparum TM4 IC_{50}:	20.2 ± 0.95 µM	1.2	5.10 ± 1.70 µM	4.3	23.7 ± 2.43 µM	1.4
P.falciparum K1CB1 IC_{50} :	20.8 ± 2.38 µM	1.1	4.73 ± 1.44 µM	4.7	20.51 ± 2.2 µM	1.6
VERO IC_{50}:	22.3 ± 1.09 µM	-	22.0 ± 3.3 µM	-	32.3 ± 15.6 µM	-

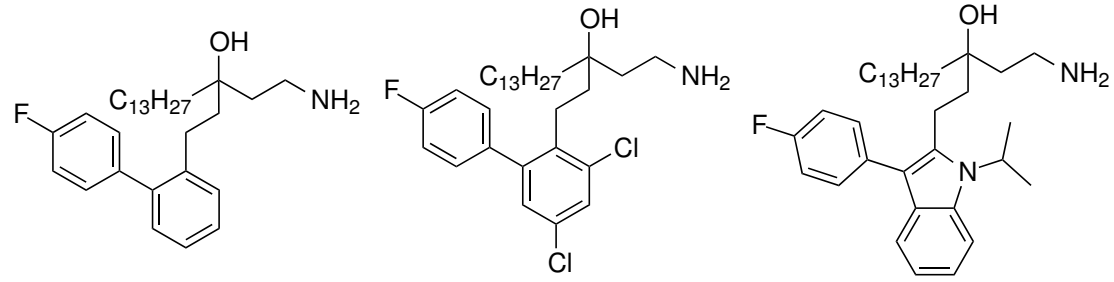

199	SI	**229**	SI	**116**	SI
2.28 ± 0.14 µM	9.9	3.29 ± 0.16 µM	8.0	2.75 ± 0.21 µM	8.8
3.95 ± 0.97 µM	5.7	4.95 ± 0.59 µM	5.3	24.2 ± 3.60 µM	1.0
3.62 ± 1.28 µM	6.2	3.45 ± 0.26 µM	7.7	14.4 ± 4.57 µM	1.7
22.6 ± 0.7 µM	-	26.4 ± 2.59 µM	-	24.3 ± 2.1 µM	-

Figure 3.15: Structure-activity results of statin inspired tertiary alcohols.

Throughout this chapter several of the statin-like fragments were incorporated into the hydroxyamine **109** as amine substituents. Some selectivity improvements were observed in the benzylamine **149**, generated in Chapter 2 and consequently other aromatic statin-like amine substitutions were synthesised and their toxicity assessed against *T.brucei rhodesience and P.falciparum* (Figure 3.16). No improvements to potency or selectivity were observed by introducing a 2,4-dichlorobenzyl amine substitution in **196**, a trend continued by adding a 2-(4'-fluorophenyl) substitution in **262**. **197** showed improved results compared to **196**, however its potency and selectivity profile did not improve on the profile of the unsubstituted benzylamine **149**. No improvements to potency or selectivity were demonstrated by incorporation of a fluvastatin fragment in compounds **117** and **250**.

The specific mode of action for the activity of the parent hydroxyamine **109** has not been implicitly demonstrated, but inhibition of NMT is likely. Genetic comparisons or specific homology studies have not been performed, so as to compare the active sites of NMT and HMG-reductase. If the active sites of NMT and HMG-reductase were structurally similar, antagonists, or fragments thereof, for HMG-reductase could potently be applied to NMT. Throughout this chapter a 'piggy-backing' concept was explored that incorporated statin fragments into the proposed NMT inhibitor **109**. An order of magnitude drop in potency was demonstrated by compounds shown in Figure 3.15 and Figure 3.16 compared to the parent hydroxyamine **109**. Since incorporation of statin fragments offered limited improvements to the potency of **109** towards *T.brucei rhodesience or P.falciparum* it can therefore be concluded that the structural features of the statins have a specific mechanism of action towards HMG-reductase which can not be easily exploited and applied to NMT. Further inclusion of the statins were abandoned and variations of the myristoyl chain contained in the parent hydroxyamine **109** were instead explored in Chapter 4 in a attempt to improve potency.

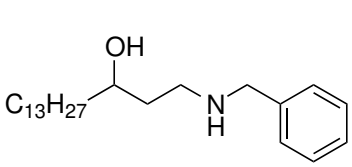

149

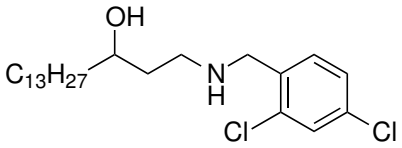

196

		SI		SI
T.brucei IC_{50}	0.33 ± 0.02 µM	61	20.5 ± 0.61 µM	>2.4
P.falciparum TM4 IC_{50}	2.58 ± 0.51 µM	7.8	27.7 ± 5.43 µM	>1.8
P.falciparum K1CB1 IC_{50}	0.36 ± 0.05 µM	56	2.83 ± 0.24 µM	>18
VERO IC_{50}	20.1 ± 4.6 µM	-	>50 µM	-

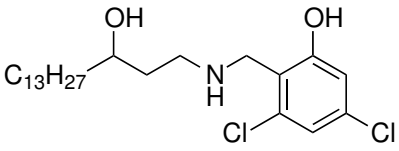

197

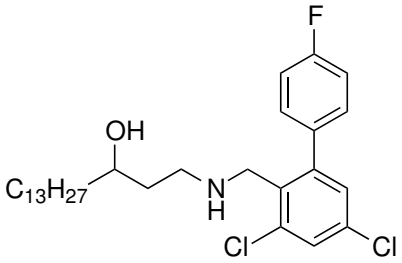

262

		SI		SI
T.brucei IC_{50}	4.89 ± 0.17 µM	5.1	>25 µM	-
P.falciparum TM4 IC_{50}	2.44 ± 0.40 µM	>10	>25 µM	-
P.falciparum K1CB1 IC_{50}	2.29 ± 0.49 µM	>10	16.1 ± 3.66 µM	>1.6
VERO IC_{50}	>25 µM	-	>25 µM	-

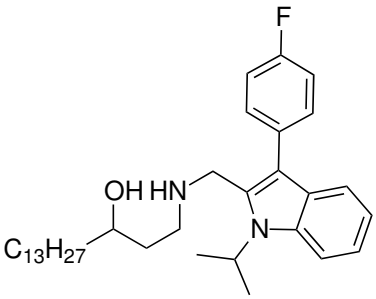

117

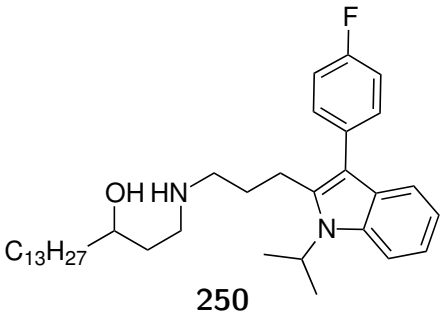

250

		SI		SI
T.brucei IC_{50}	20.4 ± 0.81 µM	>2.5	19.2 ± 1.33 µM	1.2
P.falciparum TM4 IC_{50}	>50 µM	-	8.42 ± 3.76 µM	2.8
P.falciparum K1CB1 IC_{50}	24.7 ± 11.8 µM	>0.5	3.49 ± 1.01 µM	6.7
VERO IC_{50}	>50 µM	-	23.5 ± 1.58 µM	-

Figure 3.16: Structure-activity results of statin inspired benzylamines.

Chapter 4

Myristic chain derivatives

In Chapter 2 the hydroxyamine **109** was demonstrated to have a selective toxicity towards *T.brucei* and the installation of a benzylamine substitution improved the selectivity towards *P.falciparum*. The importance of the oxygen and ionisable nitrogen was demonstrated, as was the importance of the linker length in the hydroxyamine system. In Chapter 3, HMG reductase inhibitors fragments were incorporated as alcohol and amine substitutions, which did not improve the potency or selectivity profiles of **109**. Variation of the myristoyl chain contained **109** is to be explored throughout this chapter as to introduce features that could improve the potency or selectivity of **109**.

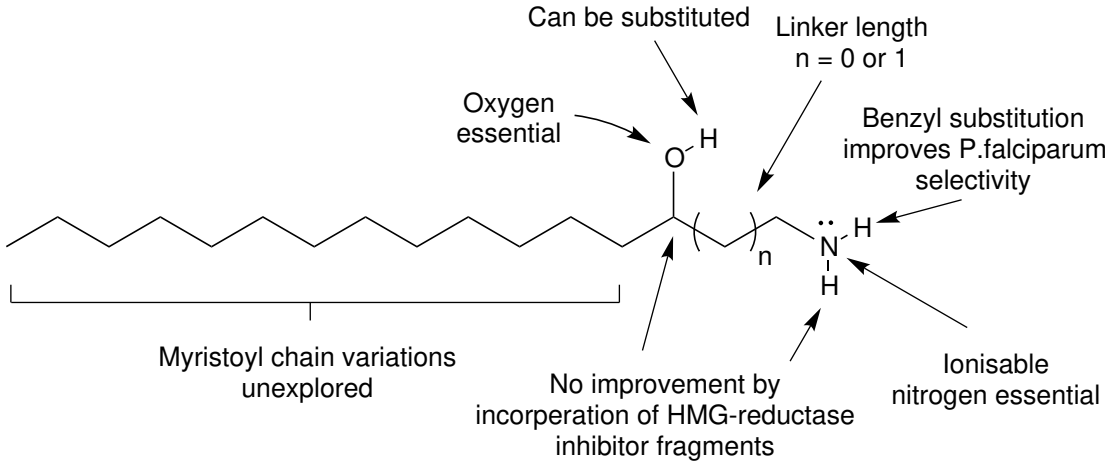

109

Figure 4.1: Structure activity relationship of **109**.

4.1 C5 *Cis*-alkene

The first myristoyl chain derivative introduces a *cis*-alkene to the myristoyl chain of the hydroxyamine **109**. The position of the alkene on C5 was based on a increased myristoylation rate when the Z5 myristic isomer of myristic acid was used to myristoylate peptides in a model system (Figure 4.2).[145] A series of alkyne myristic acid derivatives (Y2-Y13) were also tested in the same system. Interestingly, when the alkyne was installed on Y5 no myristoylated peptides were formed in the same assay. It was postulated that Z5 myristic acid could have a positive binding efficiency towards NMT due to the kink in the myristoyl pocket and the inactivity of the Y5 analog was caused from the rigidity introduced at position 5.

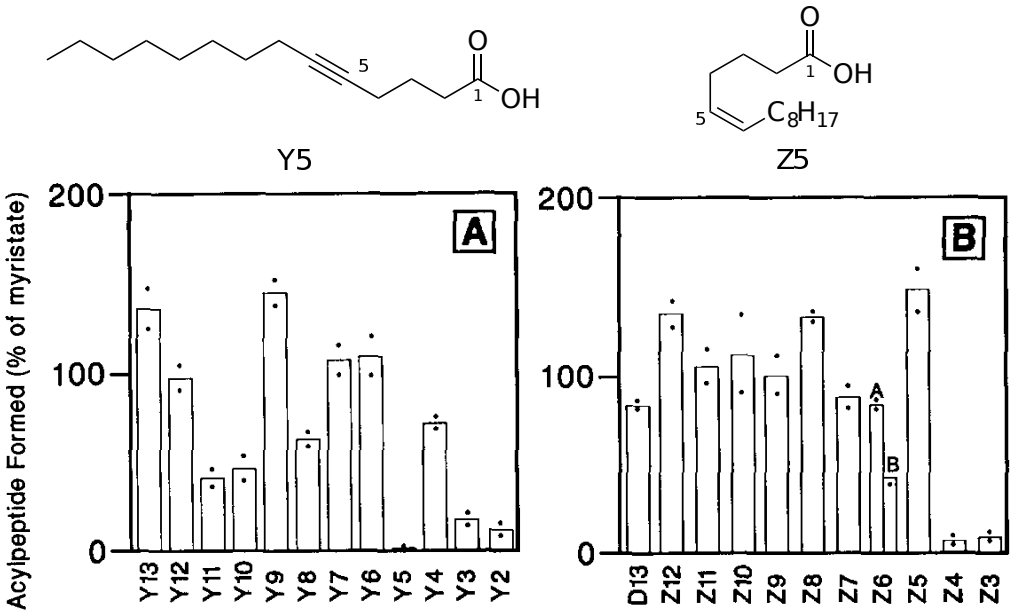

Figure 4.2: Myristoylation rates using alkyne (Y2-Y13) and *z*-alkene (Z3-Z12) derivatives of myristic acid. Figure reproduced from Kishore *et al.*[145]

The new target **263** embeds the alkene at the C5 position as to explore the antagonist properties of the alkene and merge it with hydroxyamine system in **109** developed in chapter 2 (Figure 4.3). The C5 *cis*-alkene could be introduced into the hydroxyamine **263** using alkyne chemistry. A substitution reaction between ethyl 4-bromobutrate **264** and 1-decyne **265** would give the alkyne **265** (Scheme 4.1). A stereospecific partial hydrogenation of the alkyne in **265** would give the *cis*-

alkene **266**. The hydroxyamine **263** would then be made following the procedure developed in Chapter 2 using lithiated acetonitrile followed by reduction.

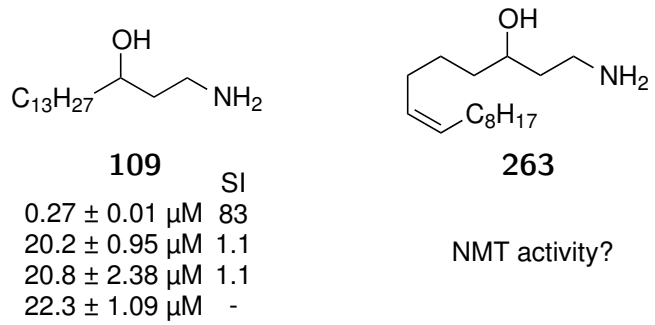

Figure 4.3: The new hydroxyamine target **263** based on Z5.

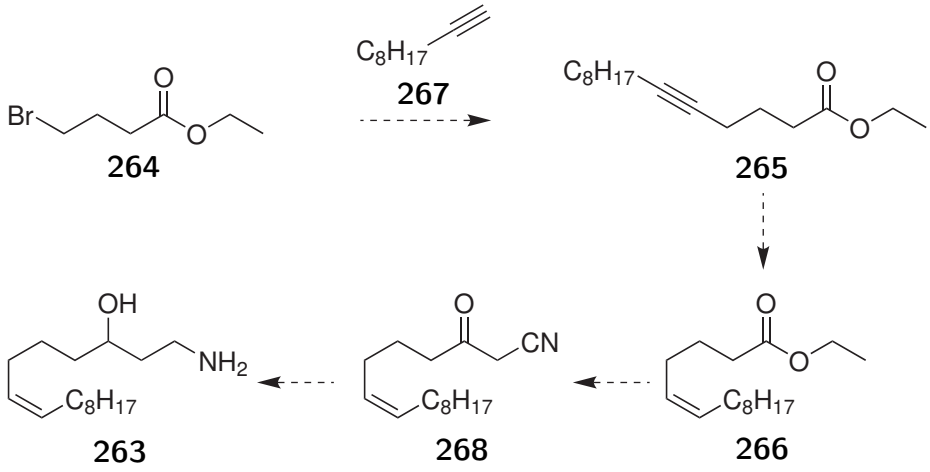

Scheme 4.1: Proposed synthesis of the alkene **263**

Although, 1-decyne **267** is commercially available, it was made in two steps from 1-decene **269**. The procedure used was adapted from a method for the generation of 1-pentadecyne reported by Mun.[146] Addition of bromine to 1-decene at room temperature proceeded in excellent yield (Scheme 4.2). The reaction gave rise to sufficiently pure **270** for the subsequent elimination reaction. The ^{1}H NMR spectrum of **270** showed 3 distinctive multiplet signals between 4.20 and 3.60 ppm indicative of 1,2-dibromo substitution. The ^{13}C NMR spectrum showed 10 signals and were identical to the literature.[147] As the boiling point of **267** is significantly lower than 1-pentadecyne[146] the elimination reaction was conducted in a distillation setup.[148] When the dibromide **270** and potassium hydroxide were reacted under phase transfer conditions as part of a reactive vacuum distillation, multigram quantities of 1-decyne **267** were isolated. A fractionation column was

used to avoid distillation of the intermediate bromoalkenes. The distillate had ^{1}H and ^{13}C NMR spectra that were identical to those found in the literature.[149]

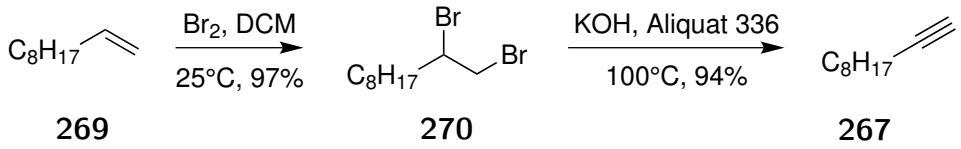

269 **270** **267**

Scheme 4.2: alkylation of cyclic carbamate

The next phase was to perform a substitution reaction between the alkyne **267** and the halo-ester **264**. The halo-ester **264** has two potential electrophiles in the molecule, the halide and the ester, so several reaction outcomes were possible. Surprisingly, this transformation did not proceed when either butyllithium[150] or sodium hydride[151] was used to deprotonate 1-decyne to form its acetylide. On reaction of the acetylide with the bromide **264** at room temperature, only starting materials were recovered. The same conditions were repeated under reflux and starting material was again recovered.

Table 4.1.1: Substitution of terminal alkyne

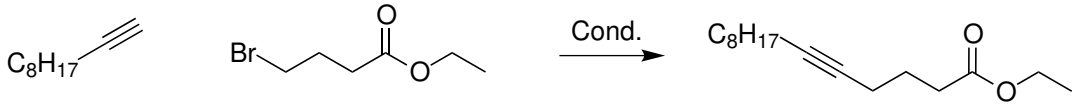

267 **264** **265**

Conditions	**264** : **265**
267, *n*-BuLi (0.9 eqv), THF, -84°C to RT, 5min, **264** (1.1 eqv), -84°C to RT, 15h.	100 : 0
267, **264** , NaH (1.5 eqv), THF, RT, 15h.	100 : 0
267, **264** , NaH (1.5 eqv), THF, 66°C, 15h.	100 : 0

An improved leaving group, iodide, was installed to give **271**. The use of **271** with butyllithium at room temperature returned starting materials (Table 4.1.2). When the reaction under the same conditions were heated under reflux a new product **272** was isolated. The same product was observed when HMPA was used as an additive. The new product was identified as the ether **272** from its NMR spectra and the mechanism grounds.

The loss of the ester group was visible by the disappearance of carbonyl signal in the ^{13}C NMR spectrum and lack of the ethyl ester signals in the ^{1}H NMR spectrum. The ether **272** contained 14 ^{13}C NMR signals including key substituted

Table 4.1.2: substitution of terminal alkyne

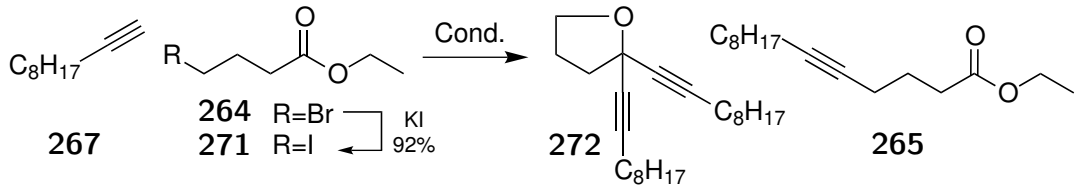

Conditions	**264** or **271** : **272** : **265**
267, *n*-BuLi (0.9 eqv), THF, -84°C to RT, 5min, **271** (1 eqv), -84°C to RT, 24h.	100 : 0 : 0
267, *n*-BuLi (0.9 eqv), THF, -84°C to RT, 20 min, **271** (0.8 eqv), 66°C, 15h.	0 : 100 : 0
267, *n*-BuLi (0.9 eqv), THF, -84°C to RT, 5 min, HMPA (1.1 eqv), **264** (1.1 eqv), -84°C to RT, 15h.	0 : 100 : 0 (TLC)

alkyne signals at 80.0 and 70.4 ppm. Symmetry was inferred as the terminal methyl ^{1}H NMR signal at 0.90 ppm integrated to 6H with respect to the down-field ether substituted methylene triplet at 4.00 ppm. The mechanism for the formation of the ether **272** is proposed in Scheme 4.3. The ester undergoes a two-fold addition reaction with alkyne anion **273** to generate the alkoxide **274**. The alkoxide **274** can cyclise via a intramolecular substitution reaction to give **272**. Formation of **272** provided evidence for the preferential nucleophilic affinity of the acetylide **273** towards the carbonyl over the halogen group. Consequently an alternative synthesis was envisaged without the use of a halo-ester starting material.

A new pathway was developed based on a reported substitution reaction between terminal alkynes and haloacids using sodium hydride in refluxing THF.[151] Applying these substitution conditions between 1-decyne **267** and 4-bromobutyric acid **276** would give 5-hexadecynoic acid **277**. The method uses two equivalents of sodium hydride to deprotonate the carboxylic acid the alkyne anion. The carboxylate would deter addition at the carbonyl favouring substitution. A Fisher esterification of **277** would then give **265** which intersects with Scheme 4.1 for conversion to the target **263**.

Preparation of 4-bromobutyric acid **276** was required. A method using a ring opening reaction on γ-butyllactone was available and applied on the large scale.[152] A mixture of γ-butyllactone, hydrobromic and sulphuric acid was held under reflux for 6 hours resulting in isolation of **276** in good yield and purity. ^{1}H NMR

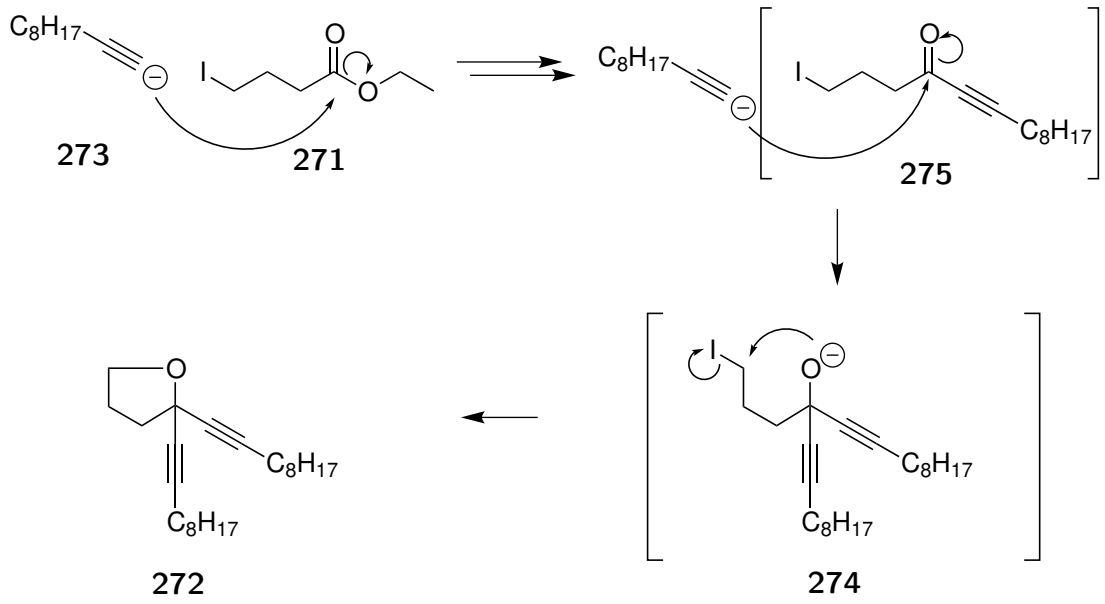

Scheme 4.3: Proposed mechanism for the generation of the undesired ether **272**.

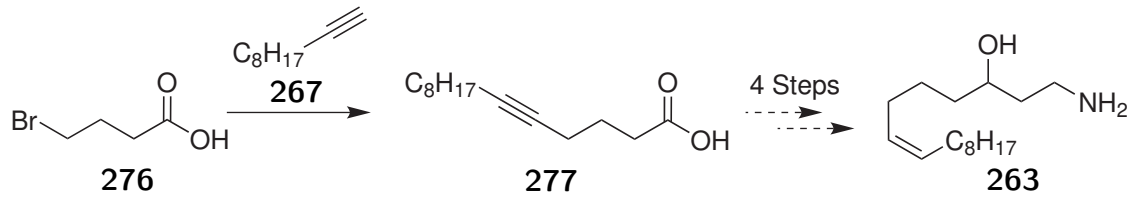

Scheme 4.4: Generation of **263** via the carboxilic acid **277**.

spectrum showed the distinctive triplet at 3.48 ppm from a bromine substituted methylene and all signals were identical to those found in the literature.[152] A Finkelstein reaction with potassium iodide gave **278** in excellent yield.[153,154]

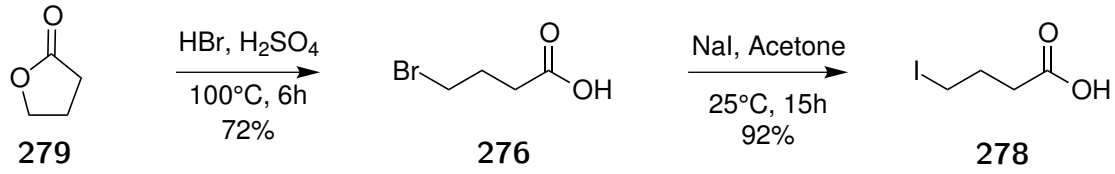

Scheme 4.5: Preparation of 4-bromobutyric acid and 4-iodobutyric acid.

A substitution reaction was tested between 1-decyne and the respective bromo and iodo acids **276** and **278**. No conversion was witnessed when exposing the halo-acids **276** and **278** to 1-decyne and sodium hydride in THF and DMF respectively at room temperature (Table 4.1.3). When butyllithium was used to deprotonate the alkyne and HMPA[155–157] was used as an additive at room temperature, a complex mixture was observed and the desired 5-hexadecynoic acid **277** was isolated in a 10% yield. The other major products were not characterised. The low yield, while employing carcinogenic HMPA, in the early phases of Scheme 4.4 was deemed a critical obstacle and a alternative procedure to generate 5-hexadecynoic acid **277** was explored.

Table 4.1.3: Substitution reaction of acids **276** and **278**

Conditions	Yield
276, **267** (1.3 eqv), NaH (5 eqv), THF, RT, 24 h.	0%
278, **267** (1.3 eqv), NaH (5 eqv), DMF, RT, 72 h.	0% conversion
267 (3.3 eqv), *n*-BuLi (3.2 eqv), THF, -84°C to RT, 5 min, HMPA (2.1 eqv), **276** (1 eqv), -84°C to RT, 15h.	10%

Attempts to generate the carboxylic acid **277** in a single step were abandoned. Alternative methods that masked the reactivity of the carboxylic acid functional group were investigated. A substitution reaction using a TBS protected 4-bromobutanol **280** was reported by Tasdemir (Scheme 4.6), however a alternative protection was investigated due to low yields reported by Tasdemir.[158] A

THP protected 4-bromobutanol, made using 3,4-dihydro-2*H*-pyran (DHP), and the subsequent acetylide substitution was reported in the literature[155,159,160] and is the basis of the protective pathway towards the target **263**.

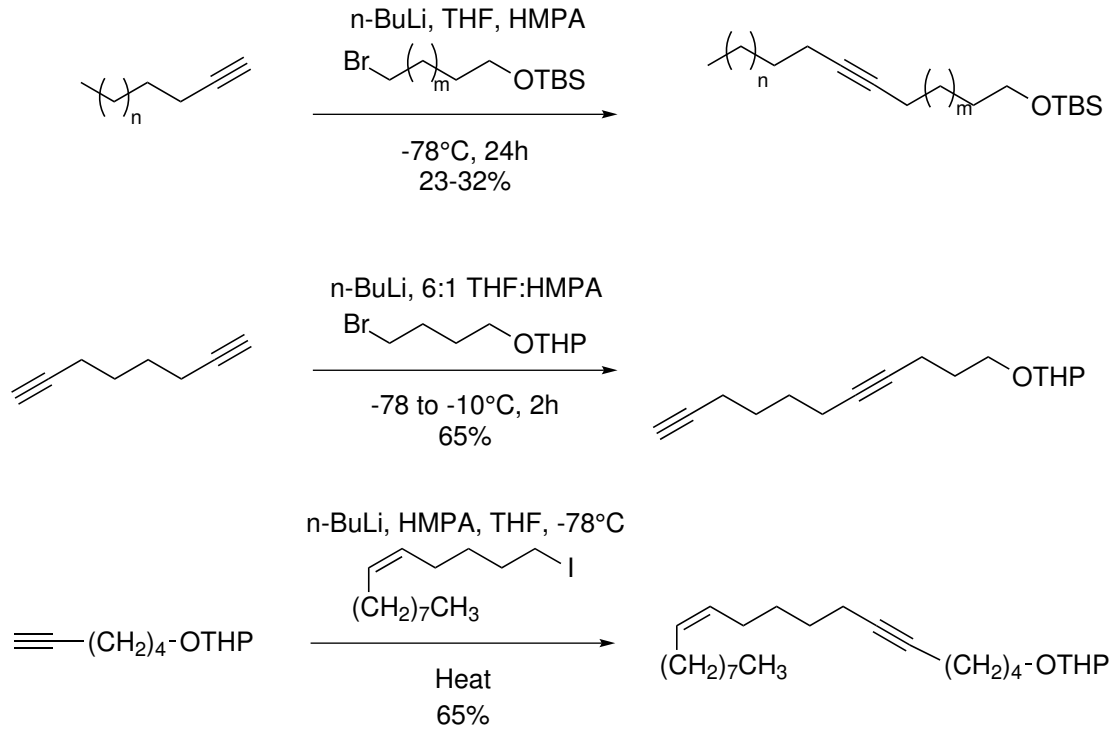

Scheme 4.6: The low yielding TBS protected acetylide substitution reported by Tasdemir (Top).[158] THP protected acetylide substitutions reported respectivly by Falck[155](middle) and (bottom).Albu[159]

Scheme 4.7 outlines the applied THP protection strategy that circumvents the problems observed earlier by masking the reactivity of the carboxylic acid functional group. A substitution reaction between 1-decyne and the protected alcohol **281** would generate the alkyne **282** for partial hydrogenation to the critical alkene intermediate **283**. A deprotective oxidation using Jones reagent would convert the *cis*-alkene **283** to the desired carboxylic acid **284**. The acid **284** would be available for conversion, over 3 steps, to the target hydroxyamine **263** using strategies previously discussed in Scheme 4.1.

The starting material for Scheme 4.7, 4-bromobutanol, is synthesised by a ring opening of THF with hydrobromic acid.[161] THF was heated under reflux with hydrobromic and sulphuric acid for 5 hours (Scheme 4.8). The excess acids were removed though a basic workup to give a product which had NMR spectra identical with the literature.[162] 4-Bromobutanol was isolated on multi-gram scale with suf-

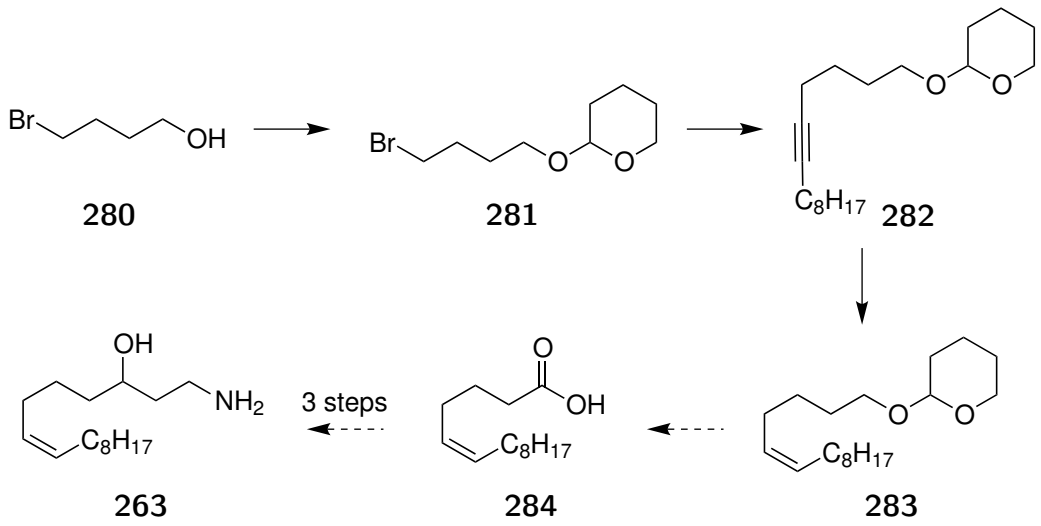

Scheme 4.7: THP protection strategy to generate the z alkene

ficient purity to be used in the following step without further purification.

The reaction of 4-bromobutanol with 3,4-dihydro-2*H*-pyran, using a catalytic amount of *p*-toluenesulfonic acid, was stirred overnight at room temperature and gave the protected alcohol **281**. The product from the reaction was purified by column chromatography to give **281** that had 9 ^{13}C NMR signals and matched those reported by Snider.[160] With the reactivity of the carboxylic functional group successfully masked the substitution reaction between **281** and 1-decyne was explored.

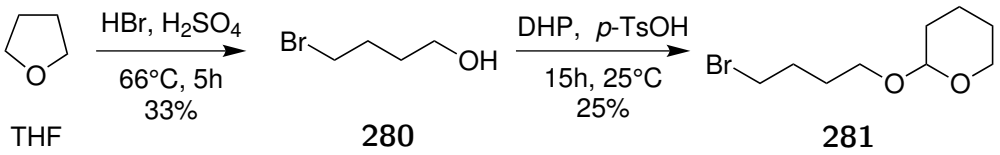

Scheme 4.8: Preparation of the bromide **281**.

The substitution of alkyl halides with acetylide anions was reported by Faulk[155] (Scheme 4.6). 1-Decyne was deprotonated using butyllithium and stirred with **281** overnight in THF with HMPA. No conversion was witnessed. A literature acetylide substitution (Reaction 3 Scheme 4.6) used butyllithium and HMPA at elevated temperatures.[159] No detailed conditions were reported by Albu[159] but promising results were obtained when using two equivalents of each HMPA and the alkyne anion at elevated temperatures overnight. The material isolated after column chromatography showed the theoretical 19 signals in the ^{13}C NMR spec-

trum with two key substituted alkyne signals at 80.6 and 79.9 ppm. A successful substitution reaction was confirmed in the ^{1}H NMR spectrum with signals at 2.17 and 2.11 ppm assigned to the proparglylic protons. When the reaction was scaled, a shorter reaction time gave excellent results with yields at 80 - 83 % on a multigram scale. With the substitution difficulties encountered now overcome by protection, methods for partial reduction of the alkyne were explored.

Table 4.1.4: Substitution of THP protected 4-bromobutanol with 1-decyne.

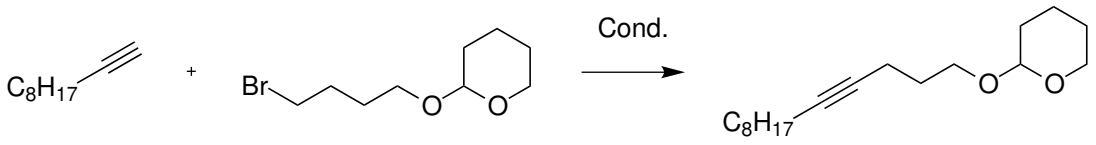

267 **281** **282**

Conditions	**281** : **282**
267, HMPA (1.1 eqv), *n*-BuLi (0.9 eqv), -84°C to RT, 5min, **281** (1.1 eqv), -84°C to RT, 15h.	100 : 0
267 (2.2 eqv), HMPA (2 eqv), *n*-BuLi (2 eqv), -84°C, 30min, **281** (1 eqv), -84°C to 66°C, 15h.	57%
267 (2.1 eqv), HMPA (2 eqv), *n*-BuLi (2 eqv), -84°C, 30min, **281** (1 eqv), -84°C to 66°C, 3h.	83%

Partial reduction of the alkyne on the substitution product **282** was envisioned as per Scheme 4.7. Lindlars catalyst is routinely used to hydrogenate alkynes to their *cis*-alkene counterparts.[163] The catalyst was not immediately available and its preparation[164] from palladium chloride was expensive and laborious. A trial using a Zn(Cu/Ag) amalgam[165] did not proceed with starting material recovered (Table 4.1.5). A hydrogenation trial using a catalytic amount of nickel boride, prepared *in situ* from nickel acetate and sodium borohydride and poisoned with ethylene diamine before addition of **282** showed promising results in line with the literature[166,167] with new ^{1}H NMR alkene signals at 5.37 ppm witnessed.

Further examination of the literature reported the partial alkyne reduction of a similar system using a equivalent of nickel boride under hydrogenation conditions.[155] A complete alkyne hydrogenation was witnessed when these conditions were applied to the alkyne **282** and the alkene **283** was isolated without the need for purification. The two alkyne signals in the ^{13}C NMR spectrum of the starting material were replaced with two new signals at 130.4 (CH) and 129.6 (CH) ppm. Unfortunately the individual ^{1}H NMR alkene signals overlapped and

Table 4.1.5: Partial hydrogenation of the alkyne **282**

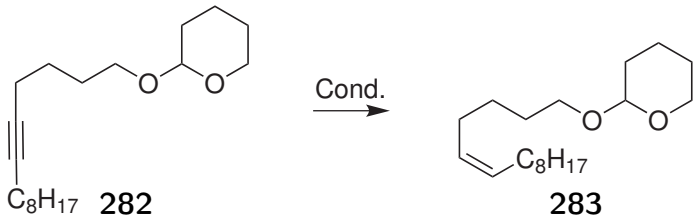

282 **283**

Conditions	Conversion
Zn(Cu/Ag), MeOH/H_2O, 25C, 15h.	0%
$Ni(OAc)_2$ (10 mol%), $NaBH_4$ (10 mol%), EDA (20 mol%), EtOH, H_2, 96h.	20%
$Ni(OAc)_2$ (1 eqv), $NaBH_4$ (1.3 eqv), EDA (4.4 eqv), EtOH, H_2, 90 min.	80% yield

the stereochemistry of the product was inferred from the results obtained in the literature.

Although the reduction of the alkyne to the alkene was successful, this step was postponed in the synthesis to avoid any risk of isomerism. Scheme 4.9 shows the generation of alkyne ester **285** prior to exposure of the alkyne to the hydrogenation conditions utilised in Table 4.1.5. Nitriles have been shown to be sensitive to reduction in the presence of cobalt boride[90,168] and thus it was considered advantageous to install the alkene, via hydrogenation, prior to the introduction of the ketonitrile system. The first step of Scheme 4.9 is the deprotective oxidation of **282**.

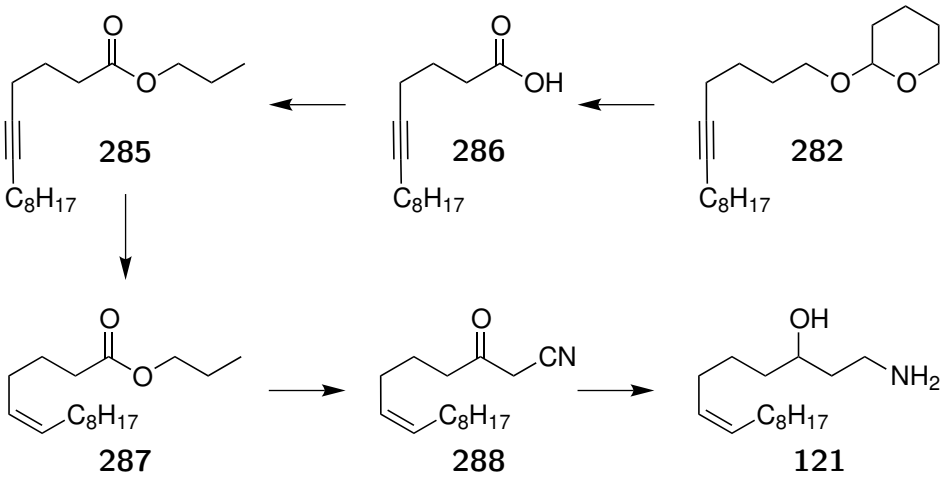

Scheme 4.9: Ester formation prior to partial hydrogenation

The conversion of the THP ether **282** to its acid **286** was performed in one step

by exploiting the THP groups sensitivity to acidic oxidative conditions. Jones reagent, which is inherently acidic, was reported[169] to act as both a deprotective and oxidative reagent towards a THP protected alcohol. When the THP ether **282** was stirred with Jones reagent overnight, the starting material was no longer visible to TLC and no alphatic ^{1}H NMR THP signals were present which confirmed deprotection. A new ^{13}C NMR signal at 180.1 ppm indicated the successful oxidation of the alcohol intermediate. A crude material was isolated in quantitive yield with sufficient purity to avoid column chromatography and proceed to the next esterification step.

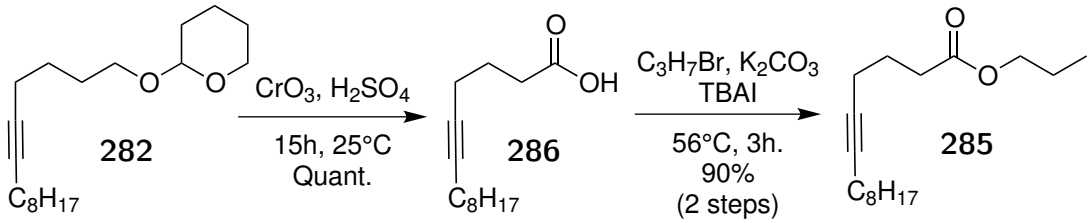

Scheme 4.10: Conversion to the alkyne ester

Conversion of the acid **286** to its propyl ester **285** used standard conditions.[170] The crude acid was stirred with excess 1-bromopropane and potassium carbonate in refluxing acetone for 3 hours using a catalytic amount of TBAI. The propyl ester was isolated in excellent yield and purity after column chromatography. 3 new signals were present in the ^{13}C NMR spectrum with the critical signals observed at 66.0 (CH_2) and 10.5 (CH_3) ppm. The ^{1}H NMR spectrum also showed 3 new signals at 4.01 (t, 2H), 1.62 (m, 2H) and 0.92 (t, 2H) ppm confirming the presence of the propyl ester **285**.

With multigram quantities of **285** isolated, the ketonitrile **288** was prepared via the alkene **287** (Scheme 4.11). The ester was converted to the alkene **287** using conditions developed in Table 4.1.5 in good yield with two new signals at 131.3 and 128.5 ppm in the ^{13}C NMR spectrum attributed to the alkene. The ^{1}H NMR spectrum also showed new alkene signals at 5.36 ppm confirming partial reduction had occurred. The penultimate step in the generation of the target hydroxyamine **121** was the introduction of the ketonitrile system to **287**.

The same conditions were used to convert the ester **287** to the ketonitrile **288** as in Chapter 2. The conditions were replicated in Scheme 4.11 by exposing the

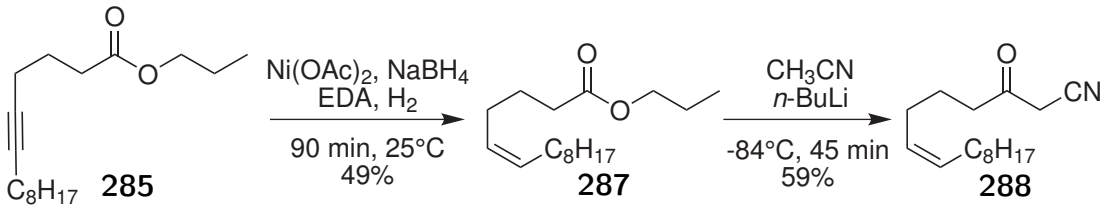

Scheme 4.11: introduction of the cis-alkene prior to conversion to the ketonitrile **288**

ester **287** to lithiated acetonitrile at -84°C for 45 min. The ketonitrile **288** was isolated in good yield after column chromatography. The new compound had representative signals for the ketonitrile, 197.5 and 113.9 ppm in the ^{13}C NMR spectrum and 3.43 ppm in the ^{1}H NMR spectrum. As a result of the introduction of the ketonitrile system enough polarity was introduced to resolve the individual alkene signals at 5.43 and 5.28 ppm. Analysis of the splitting pattern confirmed the isolation of the *cis*-isomer assigned from the coupling constant of 10.80 Hz (Figure 4.4). The reduction of the ketonitrile system contained on **288** would generate the target C5 *cis*-hydroxyamine **263**.

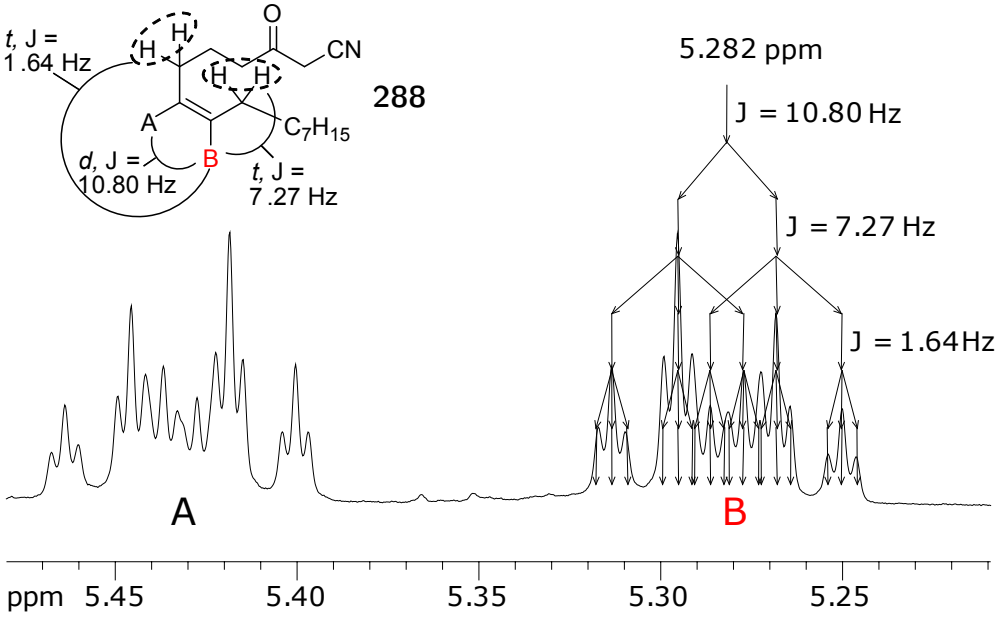

Figure 4.4: ^{1}H NMR spectrum of the ketonitrile **288** confirming the Z geometry.

The conditions were also replicated from Chapter 2 to reduce the ketonitrile **288** system. The hydroxyamine **263** was generated by exposing the ketonitrile **288** to lithium aluminium hydride at 0°C (Scheme 4.12). The carbonyl and nitrile ^{13}C

NMR signals were respectively replaced with new signals at 72.9 and 40.7 ppm indicative of hydroxy and amine substitutions. The ^{1}H NMR spectrum mirrored the introduction of the hydroxyamine system with 3 new multiplets at 3.80, 3.14 and 2.86 ppm. The alkene remained intact with ^{13}C NMR signals at 130.3 and 129.7 however its stereochemistry is inferred from its precursor as the alkenes individual ^{1}H NMR signals now appeared as a combined multiplet at 5.25 ppm.

The C5 hydroxy amine **263** was the first compound to introduce functionality to the myristoyl chain of the parent amine **109**. Unfortunately the biological activity of **263** did not improve on the potency demonstrated by the **109**. The selectivity of **263** towards *T.brucei rhodesience* was diminished compared to **109** but its toxicity towards the VERO cell was lowered. It could be inferred that the activity of Z5 myristic acid has a alternative mechanism for peptide enrichment in the biological system other than improved binding efficiency into the hydrophobic pocket of NMT. Since the introduction of an alkene at position 5 did not improve the potency or selectivity profile of **109** alternative strategies to functionalise the myristoyl chain were explored.

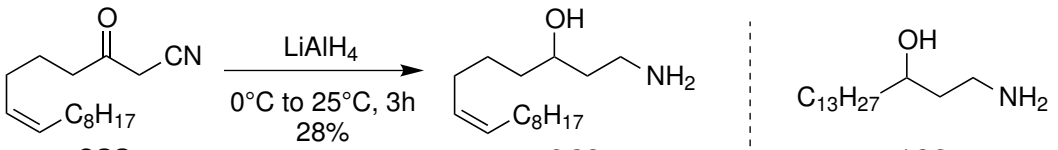

288 **263** **109**

	263	SI	109	SI
T.brucei IC_{50}:	3.12 ± 0.05 µM	>16	0.27 ± 0.01 µM	83
P.Falciparum TM4 IC_{50}:	21.0 ± 2.79 µM	>2.4	20.2 ± 0.95 µM	1.1
P.Falciparum K1CB1 IC_{50}:	17.5 ± 2.25 µM	>2.9	20.8 ± 2.38 µM	1.1
VERO IC_{50}:	>50 µM	-	22.3 ± 1.09 µM	-

Scheme 4.12: Reduction to give the hydroxyamine **263** and its biological comparison with **109**

4.2 C6 Phenoxy Ether

A screen of 244 commercial available myristic acid analogues against HAT revealed 20 with high toxicity (Figure 1.12[40,41]). The incorporation, through synthesis, of these features into the myristic chain of new NMT inhibitors is not practicable. Computational static docking experiments were performed using AutoDock Vina and designed to investigate the possibility that enzyme-ligand interactions were responsible for the activity of the report myristic analogues by competitive inhibition.

5-(4-Butoxyphenyl)pentanoic acid **289** was listed as having a high activity against HAT. A clear trend became visible when simulated docking a series of phenoxy ethers inspired from the structure of **289**. A single simulated docking experiment was performed on a series of myristic acid analogues using established protocols.[171,172] The series moved the phenoxy moiety from the C3 position in **290** though the myristic chain ending with C10 in **291** (Figure 4.5).

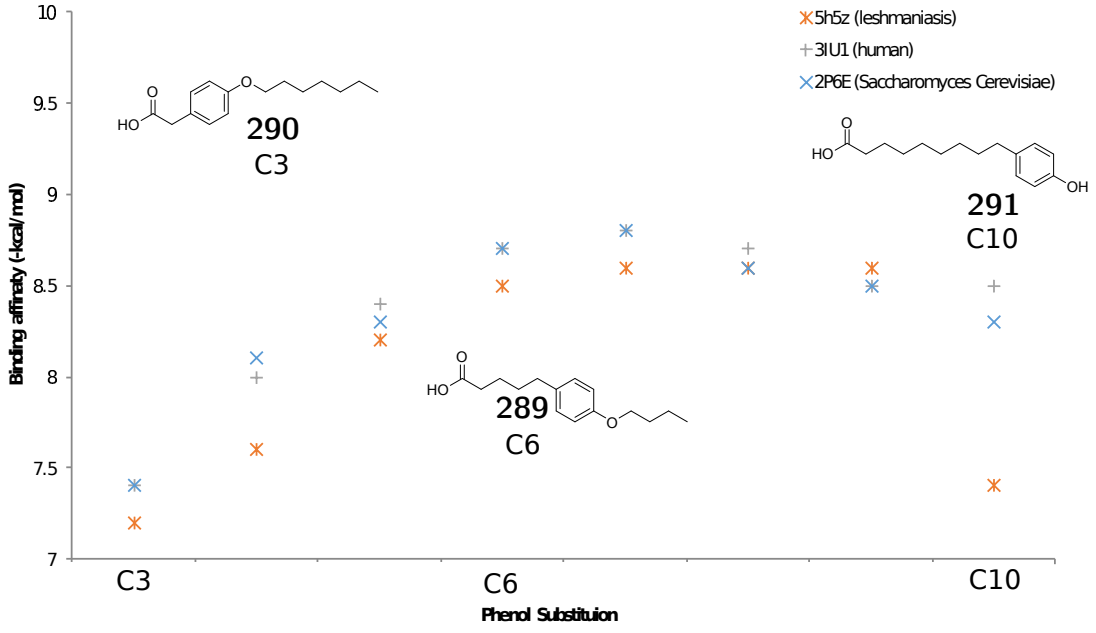

Figure 4.5: The binding efficiency of a series of myristic acid analogues computational static docked using AutoDock Vina.

The series of individual simulations showed a trend where binding affinity is maximised when the phenoxy moiety is situated in the central portion of the myristoyl chain. A similar trend was observed when docking the same series to enzyme crys-

tallography data from different species. The trend provided some evidence that the mechanism behind high HAT toxicity of **289**, reported by Doering as having a HAT activity, may be via competitive inhibition of NMT.[41]

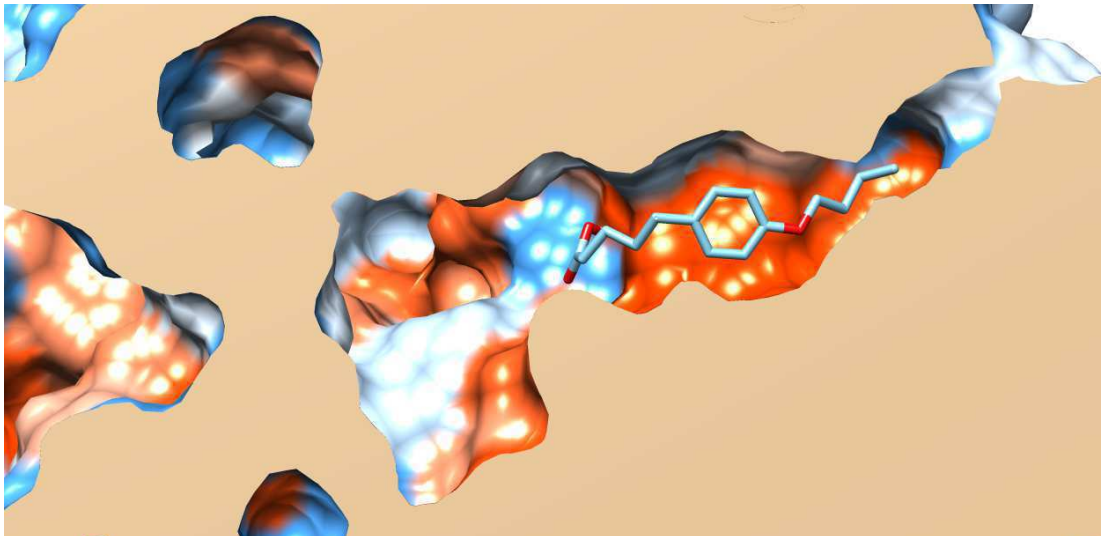

Figure 4.6: C6 phenoxy substituted **289** docked into the hydrophobic pocked of 2P6E (*Saccharomyces Cerevisiae*) using AutoDock Vina.

5-(4-Butoxyphenyl)pentanoicacid **289** featured a phenoxy moiety at the C6 position was reported to be active against HAT at 10 µM. The new target **120** incorporates the C6 phenoxy feature with the hydroxyamine features of **109** developed in Chapter 2 (Figure 4.7). The combination of the C6 phenoxy and hydroxyamine features in **120** may offer improvement to the potency compared with **109**. A synthetic pathway as to generate **120** was explored.

Scheme 4.13 outlines the synthesis of the target **120** utilising a Sonogashira cross-coupling reaction as the key carbon-carbon bond forming reaction. A hydrogenation of the alkyne in **292** followed by oxidation would give the aldehyde **293**. Using chemistry developed from Chapter 2, the addition of lithiated acetonitrile was expected to generate the hydroxynitrile **294** which could be reduced to give the target **120**.

1-Bromo-4-butoxybenzene **295** was made following a literature procedure.[173] 4-bromophenol was heated with excess 1-bromobutane and potassium carbonate isolating **295** by vacuum distillation in excellent yield (Scheme 4.14). ^{1}H and ^{13}C NMR spectra correlated with reported values.[173] With gram quantities of **295** in hand the Sonogashira cross-coupling reaction was explored.

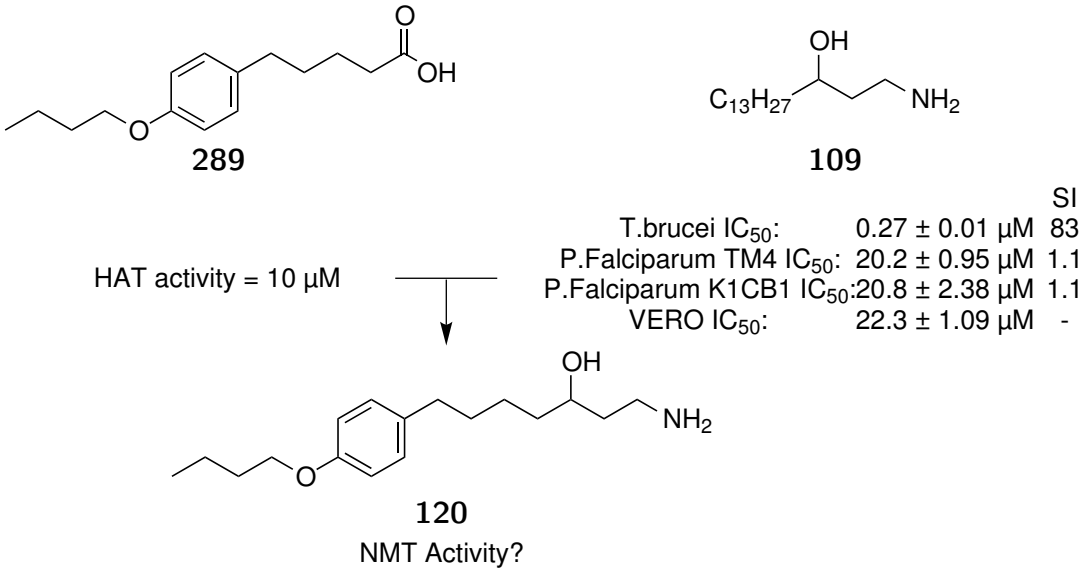

Figure 4.7: The new sythetic target **120**.

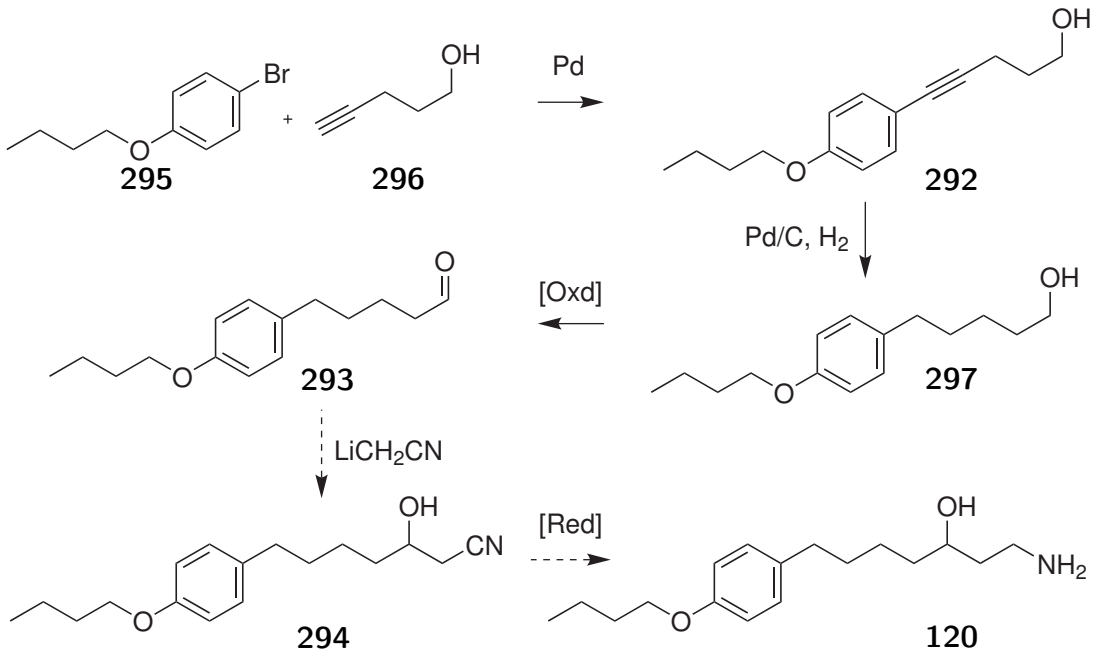

Scheme 4.13: The synthetic pathway towards the target **120**.

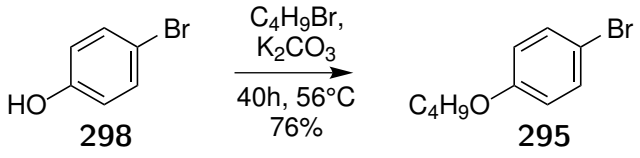

Scheme 4.14: Alkylation of **298**.

Gschneidtner[174] reported the Sonogashira cross-coupling of THP protected 4-bromophenol **299** and 2-methylbut-3-yn-2-ol **300** in near quantitative yield (reaction 1 Scheme 4.15). The conditions, using bis(triphenylphosphine)palladium dichloride and copper iodide, were replicated for the coupling of the alkyne **296** to the bromide **295** (reaction 2 Scheme 4.15) to give the alkyne in modest yield. The ^{1}H NMR spectrum of the purified material possessed 10 signals each with correct integration values and the ^{13}C NMR spectrum contained the expected 13 signals indicating coupling had occurred. The spectrum showed two ^{13}C-NMR signals 87.7 and 81.1 ppm indicative of a substituted alkyne system. It also had signals at 67.9 and 62.1 ppm that were assigned to the phenoxy and the alcohol substituted methylene.

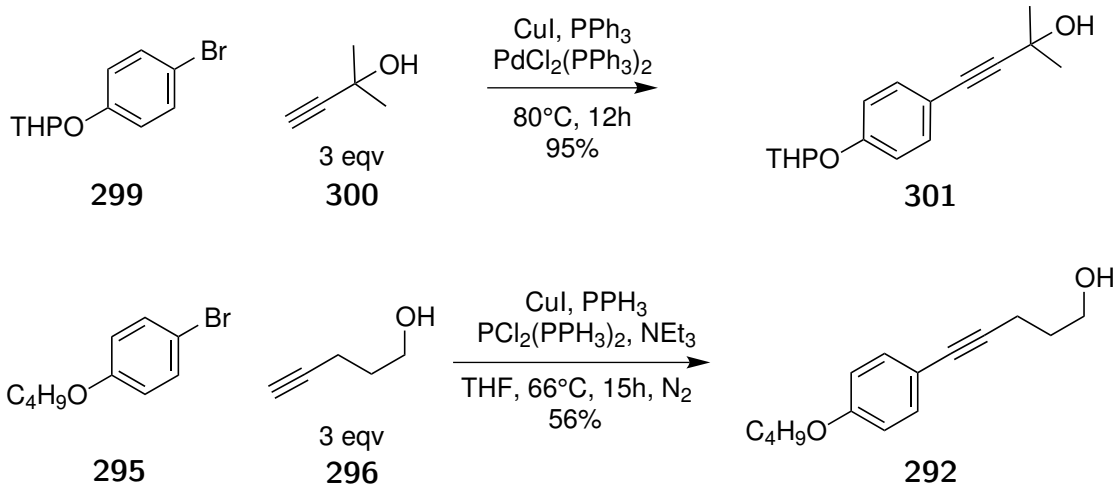

Scheme 4.15: Sonogashira reaction reported by Gschneidtner[174] (Top) modified conditions reported to produce the Sonogashira product **292**.

The alkyne was successfully hydrogenated to give **297** by exposure of the alkyne **292** to palladium on carbon under a hydrogen atmosphere for 15 hours (Scheme 4.16). The ^{13}C NMR spectrum no longer showed alkyne signals at 87.7 and 81.1 ppm which were replaced by two new alkyl signals at 35.1 ppm and 32.8 ppm. A new signal in the ^{1}H NMR spectrum at 3.66 ppm (*t*, 2H) confirmed the introduction of benzylic protons.

Oxidation of **297** was required to generate the aldehyde **293** as outlined in Scheme 4.13. Exposing **297** to IBX in DMSO at room temperature resulted in a complex mixture. A Swern oxidation was conducted, as it is a mild oxidation, utilising the dimethylchlorosulphonium ion generated *in situ* from DMSO

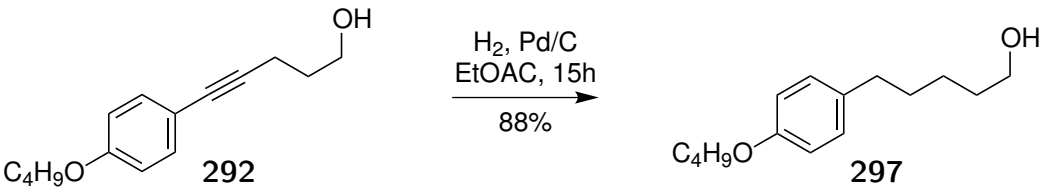

Scheme 4.16: Hydrogenation of **292**.

and oxalyl chloride at low temperatures (Scheme 4.17). Applying these conditions to the alcohol **297** gave the aldehyde **293** in good yield . The ^{1}H NMR spectrum showed a triplet at 9.75 ppm indicating the formation of the aldehyde. The ^{13}C NMR spectrum showed a signal at 202.6 ppm and a single oxo-substituted methylene signal at 67.8 ppm.

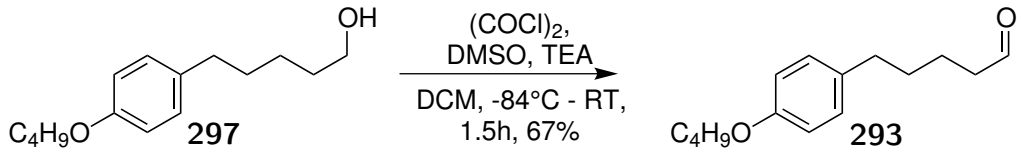

Scheme 4.17: Swern oxidation of **297**.

Using conditions from Chapter 2, addition of lithiated acetonitrile at -84°C returned a significant quantity of the staring material together with at least one other unknown (Scheme 4.18). The recovery of starting material confirmed that lithiated acetonitrile was undergoing a acid-base reaction with the aldehyde **293** and the enolate, when quenched with water, returned the starting material on workup. As a consequence the synthesis of **294** from its aldehyde **293** were abandoned and a alternative synthesis of **294** explored.

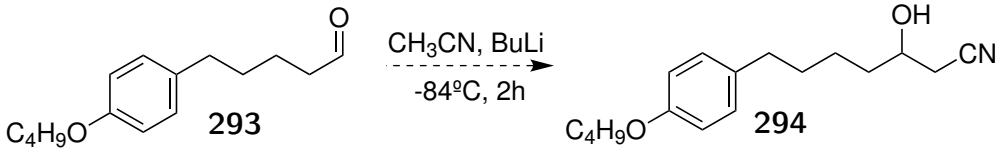

Scheme 4.18: Attempted lithiated acetonitrile addition to the aldehyde **293**.

An alternative synthesis of the target hydroxyamine **120**, via the ester **302**, was examined (Scheme 4.19). Oxidation of the aldehyde **293** to the carboxylic acid **303** followed by substitution would generate the ester **302**. An addition reaction with lithiated acetonitrile was expected to proceed as ester **302** is significantly

less acidic than its equivalent aldehyde **293**. The reduction of the ketonitrile **304** would give the target **120** for biological evaluation and circumvents problems encountered in the synthesis of **294** via Scheme 4.18.

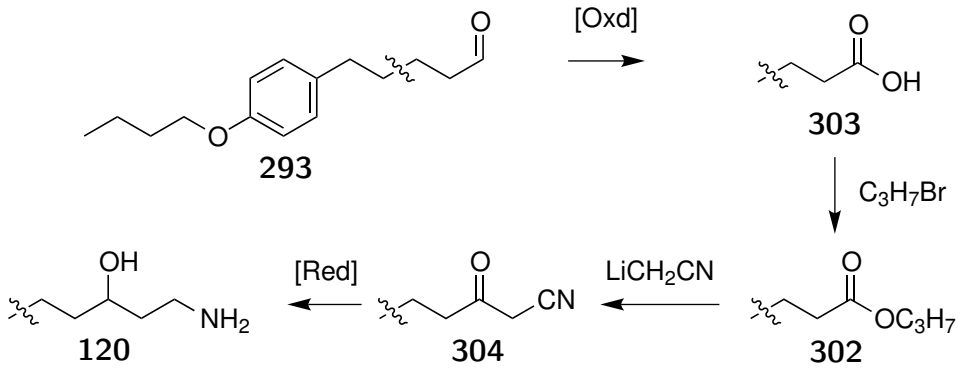

Scheme 4.19: Revised synthetic stratergy towards **120** via the ester **302**.

Pinnick oxidation conditions were used from a literature method which also contained a unreactive phenoxy ether system.[170] The aldehyde **293** was exposed to sodium chlorite in a buffered biphasic system (Scheme 4.20). 3 equivalents of 2-methyl-2-butene (2M2B) was used to scavenge the hypochlorous acid byproduct. The reaction proceeded with consumption of the starting material as observed by TLC. Both the ^{1}H and ^{13}C NMR spectra showed the disappearance of their respective aldehyde signals at 9.75 and 202.6 ppm and a new carboxylic acid carbonyl signal was present at 179.6 ppm in the ^{13}C NMR spectrum. The crude material was obtained with sufficient purity to be used for the following esterification reaction without purification.

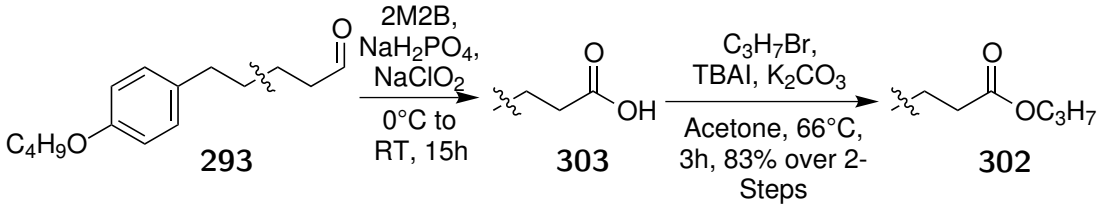

Scheme 4.20: Conversion of the aldehyde **293** to the ester **302**.

The crude acid was exposed to conditions also reported by Wright.[170] The acid **303** was stirred with excess bromopropane and sodium carbonate in acetone and heated under reflux for 3 hours using TBAI as a catalyst. After purification by column chromatography, the ^{1}H NMR spectrum showed new alkyl signals with the new key triplet at 4.03 ppm indicating ester substitution. The ^{13}C NMR

spectrum showed 3 new alkyl signals at 66.0, 22.1, 10.5 ppm indicative of the propyl ester chain. Ester formation was also confirmed by the ^{13}C NMR carbonyl signal shift from 179.9 to 173.9 ppm. The two step conversion of the aldehyde **293** to its propyl ester gave an excellent yield and gram scale quantities of **302** were available for the subsequent addition reaction.

The ester **302** was exposed to excess lithiated acetonitrile at -84°C and the ketonitrile **304** was isolated in good yield (Scheme 4.21). The ^{1}H NMR spectrum showed t a singlet at 3.40 ppm indicative the methine adjacent to the carbonyl and nitrile. The ^{13}C NMR spectrum also showed the disappearance of the propyl alkyl signals and generation of new signals at 113.9 and 197.5 from the ketonitrile system. The phenoxy moiety remained intact confirmed by the pair of aromatic signals and the oxygen substituted methylene at 3.94 ppm in the ^{1}H NMR spectrum. The reduction of the ketonitrile system was explored using lithium aluminium hydride.

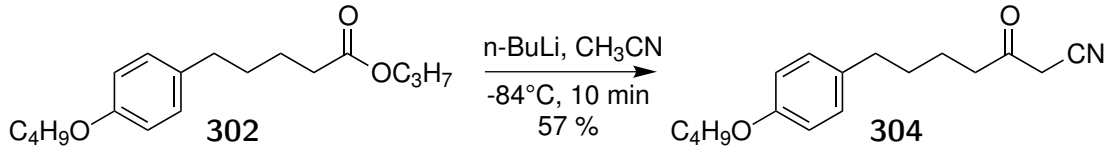

Scheme 4.21: Lithioacetonitrile addition to the ester **302**.

The C6 phenoxy ketonitrile **304** was exposed to a suspension of lithium aluminium hydride for 3 hours. The crude was purified by column chromatography and the ^{13}C NMR spectrum contained new hydroxy substituted signal at 73.5 ppm. Three new broad multiplets ^{1}H NMR spectrum were present at 3.80, 3.13 and 2.83 ppm respectively attributed to the hydroxy and amine substituted methine signals.

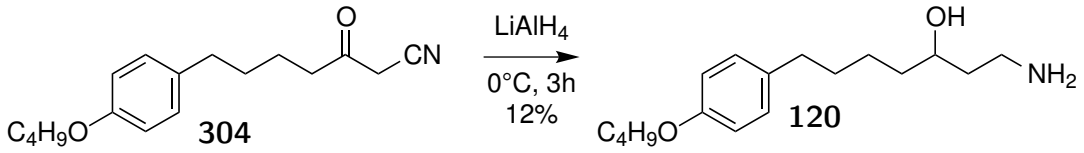

Scheme 4.22: Reduction of **304**

The hydroxyamine **120** is a myristoyl chain derivative inspired from the work of Doering *et al.*[41] Unfortunately **120** did not improve on the selectivity or potency

profile compared to **109**. The absolute mode of action of 5-(4-butoxyphenyl)pentanoic acid **289** was not demonstrated by Doering.[41] If competitive inhibition of NMT was the mechanism of toxicity of 5-(4-butoxyphenyl)pentanoic acid **289** it could be assumed that incorporation of the 4-butoxyphenyl fragment into the myristoyl chain of a NMT inhibitor would lead to greater toxicity towards *T.brucei rhodesience or P.falciparum.* As no improvements to the potency profile of **120** was observed it was considered unlikely that the mechanism of action of 5-(4-butoxyphenyl)pentanoicacid **289** was via competitive inhibition of NMT. Alternative strategies are to be proposed in the following chapter as to improve the potency and selectivity profile of **109**.

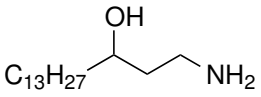

109

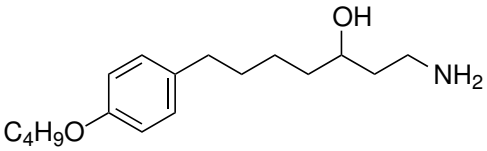

120

		SI		SI
T.brucei IC_{50}:	0.27 ± 0.01 µM	83	2.79 ± 0.21 µM	>18
P.Falciparum TM4 IC_{50}:	20.2 ± 0.95 µM	1.1	21.1 ± 3.42 µM	>2.4
P.Falciparum K1CB1 IC_{50}:	20.8 ± 2.38 µM	1.1	22.4 ± 3.06 µM	>2.2
VERO IC_{50}:	22.3 ± 1.09 µM	-	>50 µM	-

Scheme 4.23: Comparison of biological activies of **120** and ??.

Chapter 5

Conclusions

The aim of the study was to develop new leads for the treatment against the protozoa causing African sleeping sickness (*T. Brucei*) and Malaria (*P. Falciparum*). The compounds investigated were inspired by the transition state of *N*-myristoyl transferase. The synthesis of simplified transition state mimetics **305** provided structures that were active towards *T.brucei rhodesience* and *P.falciparum* (Figure 5.1).

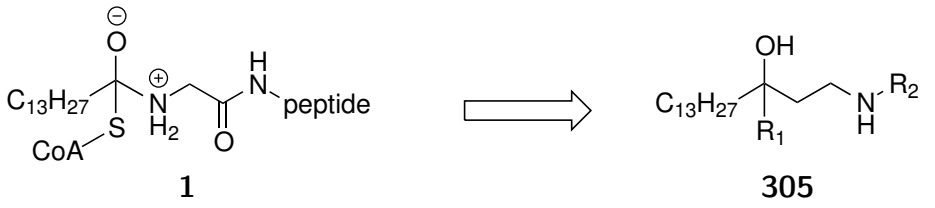

Figure 5.1: Using the NMT transition state as a source for 1-amino-3-hexadecanol based mimetics

The synthesis of transition state mimetics used ethyl myristate as a starting material. The addition of lithiated acetonitrile to ethyl myristate generated the ketonitrile **124** which was used as a key intermediate in Chapter 3. The ketonitrile **124** was reduced with lithium aluminum hydride to give the hydroxyamine **109**. The amine of the hydroxyamine **109** was substituted using a reductive amination. The reductive amination of hydroxyamine **109** with benzaldehyde generated **149**. The benzyl protecting group left the reactivity of the amine intact and an alkylation with 2-bromo-*N*-methyl acetamide followed by debenzylation using formic

acid over palladium gave the glycyl substituted product **108**.

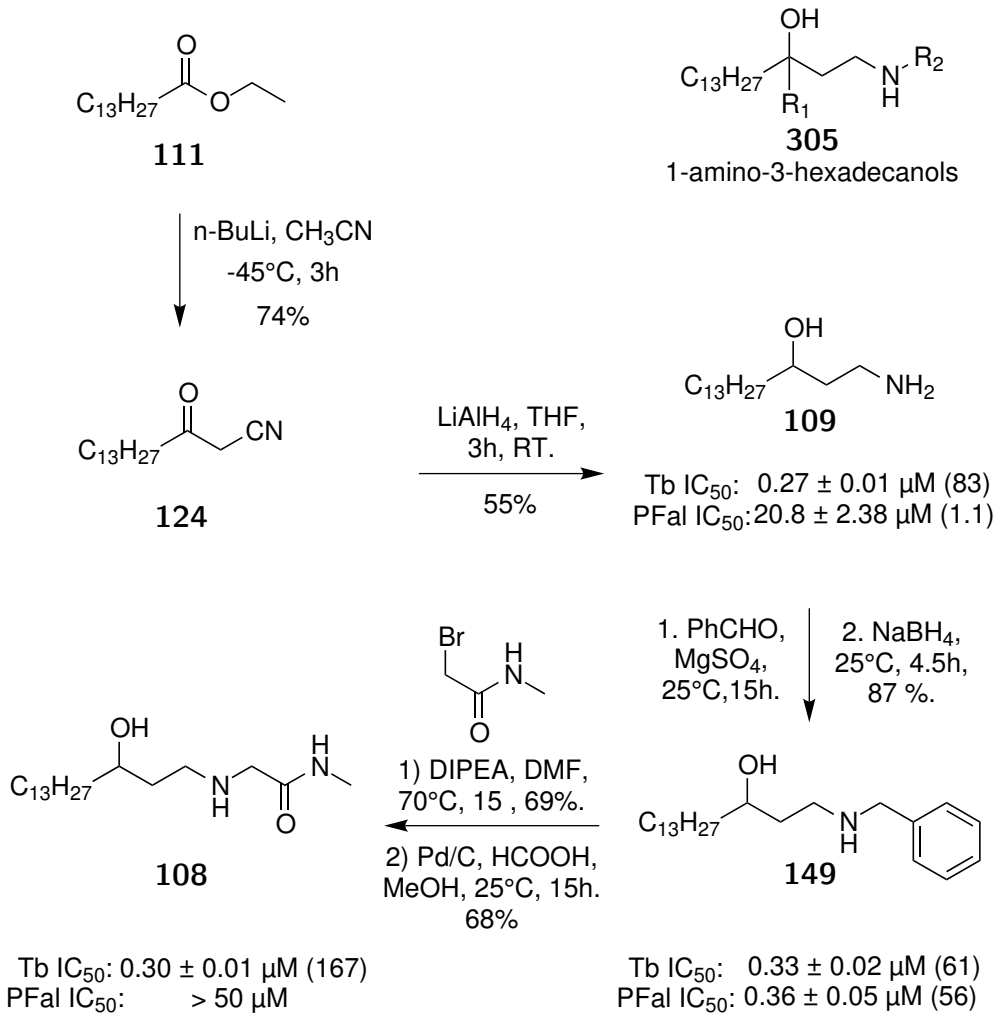

Scheme 5.1: Secondary hydroxyamines developed in Chapter 2 active against *T. brucei* and *P.falciparum* (SI)

The parent hydroxyamine **109** showed micro molar anti-protozoan activity. Structure-activity relationship studies of this compound demonstrated that the oxygen atom and an ionizable amine were essential. A linker length between the alcohol and the amine beyond 2 carbons was demonstrated to negatively impact protozoan activity and was consequently maintained at 2 carbons for subsequent derivatives. Substitution of the both the amine and hydroxy functional groups was tolerated and some species selectivity was also observed. A *N*-benzyl substitution of the parent hydroxyamine **109** improved the selectivity towards *P.falciparum.* Introduction of a glycyl amine substitution in **108** improved the selectivity towards *T.brucei.* Using the structure of the transition state of NMT as a guide gave compounds that successfully inhibited the growth of *T.brucei rhodesience* and

P.falciparum.

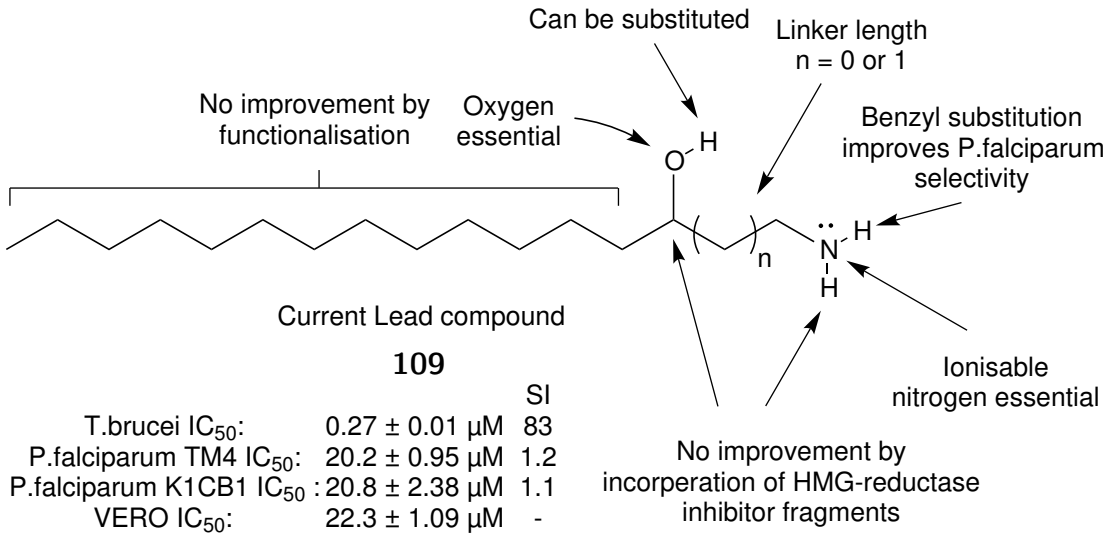

Figure 5.2: Structure activity relationships of the hydroxyamine **109**.

Further compounds were synthesised to investigate the application of statin fragments into the parent hydroxyamine **109**. The synthetic strategies developed in Chapter 2 were used as the basis to add complexity to the hydroxyamine **109** in Chapter 3. Reductive amination using the hydroxyamine **109** incorporated statin fragments as amine derivatives. Furthermore a cerium acetylide addition followed by hydrogenation provided access a range of tertiary alcohol derivatives by overcoming the inherent acidity of the ketonitrile **124**. This proof of concept study revealed that the hydrophobic fragments of the HMG-reductase inhibitors reduced the inhibition towards *T.brucei* and *P.falciparum*, but they did not hinder the activity entirely.

Two further inhibitors were synthesised in Chapter 4 which introduced functionality into the myristoyl chains. The first used a alkyne alkylation which required a HMPA additive and generated the alkyne **282** which was subsequently reduced to a C5 alkene on the myristoyl chain prior to deprotection (Figure 5.3). The chemistry developed in Chapter 2 was then applied to install the 3-hydroxyamine system to generate the hydroxyamine **263**. The second chain derivative used a Sonogashira cross-coupling reaction to install a C6 phenoxy fragment into the myristoyl chain. The key intermediate **292** was then hydrogenated, converted to its propyl ester before the same chemistry developed in Chapter 2 was applied and generated the hydroxyamine **120**. The added functionality of both inhibitors

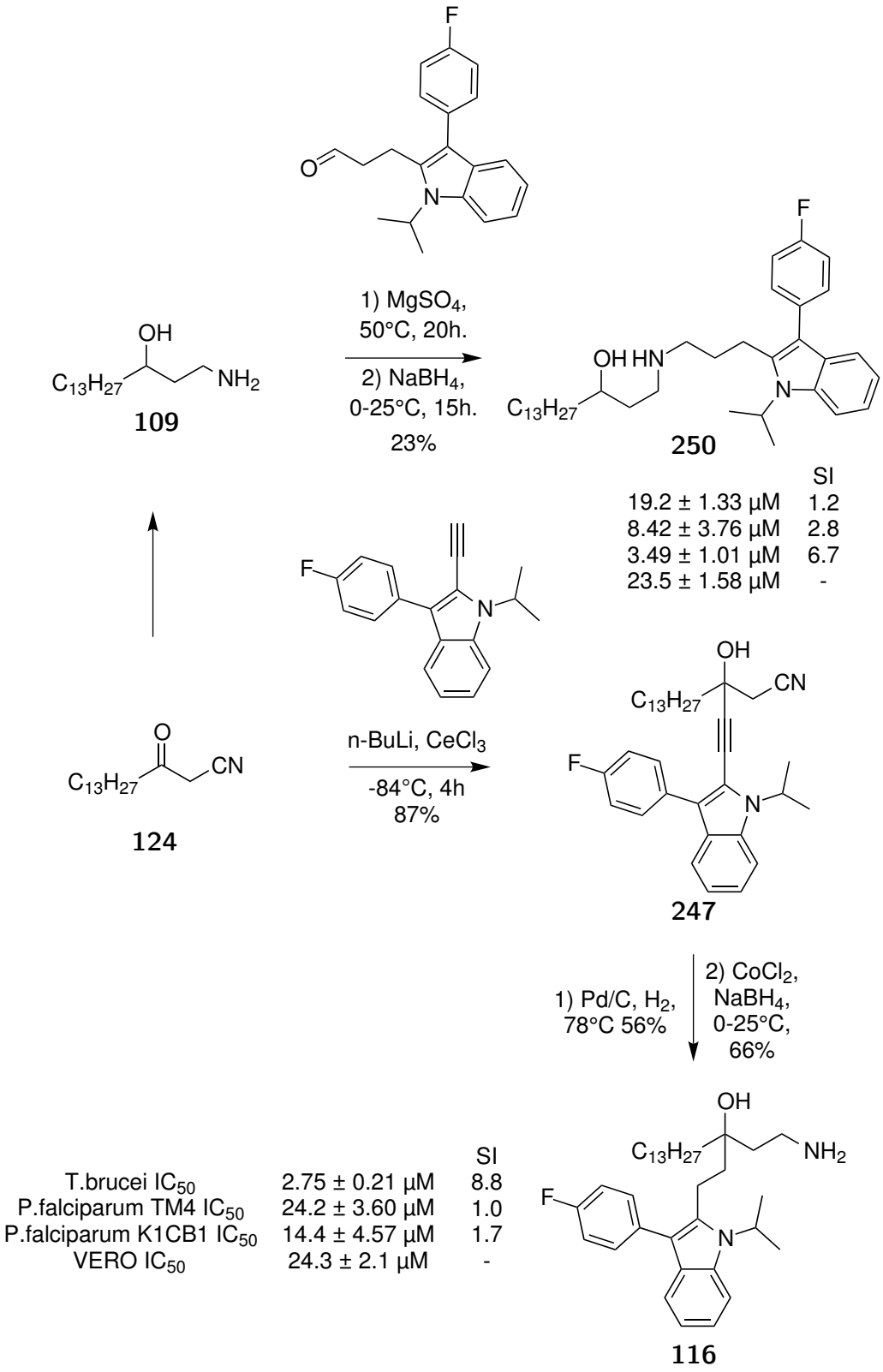

Scheme 5.2: Secondary hydroxyamines developed in Chapter 3 active against *T. brucei* and *P.falciparum*.

did not improve on the potency profile compared to the hydroxyamine **109** but a functionalised chain did not remove activity towards *T.brucei rhodesience* and *P.falciparum* completely.

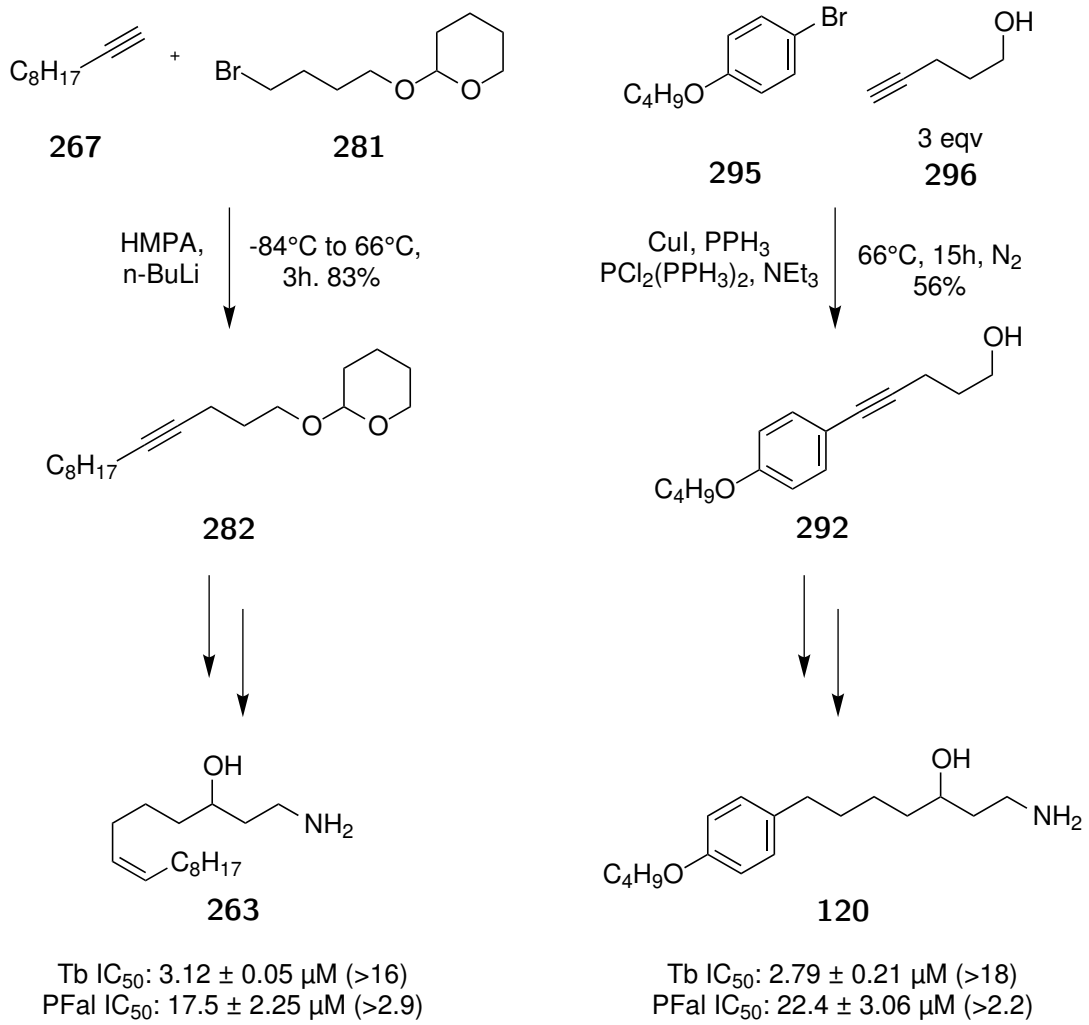

Figure 5.3: Chain derivatives developed in Chapter 4 active against *T. brucei* and *P.falciparum*.

The lead compound is the hydroxyamine **109** shown in Scheme 5.3. Several aspects of its structure-activity relationship were determined in Chapter 2, 3 and 4. The results warrant further investigation and could be the starting point for future research campaigns. Future work must conclusively determine if the activity of the hydroxyamine **109** towards *T.brucei rhodesience* and *P.falciparum* is a result of inhibition of NMT. An isolated protozoan NMT assay would provide critical information about the mode of action of the hydroxyamine **109**. A comparison of its potency towards protozoan NMT and a whole organism assay could also demonstrate if the transport of hydroxyamine **109** is hindered across

the cell membrane or it is readily degraded by the protozoa.

Whether or not these compounds are inhibitors of NMT, they could be used as leads for the inhibition of *T.brucei rhodesience* and *P.falciparum* and could be developed further using chemistry explored in this thesis and more traditional medicinal chemistry permutations which may yet improve potency profile of **109** (Scheme 5.3). Further structure-activity investigations could begin by isolation of each enantiomer of the hydroxyamine **109** and conclude if one is significantly more active than the other. Another strategy could use the acidity of the ketonitrile **124** to substitute between the ketone to the nitrile. A hydride reduction would generate derivatives of the hydroxyamine **109** yet to be explored. Further investigation is required to determine if and/or which polar substituents are tolerated when incorporated into the myristoyl chain. Decreasing the lipophilicity of the myristoyl chain may improve the physiochemical properties of **109**, however the impacts of such substituents on potency remain largely unexplored.

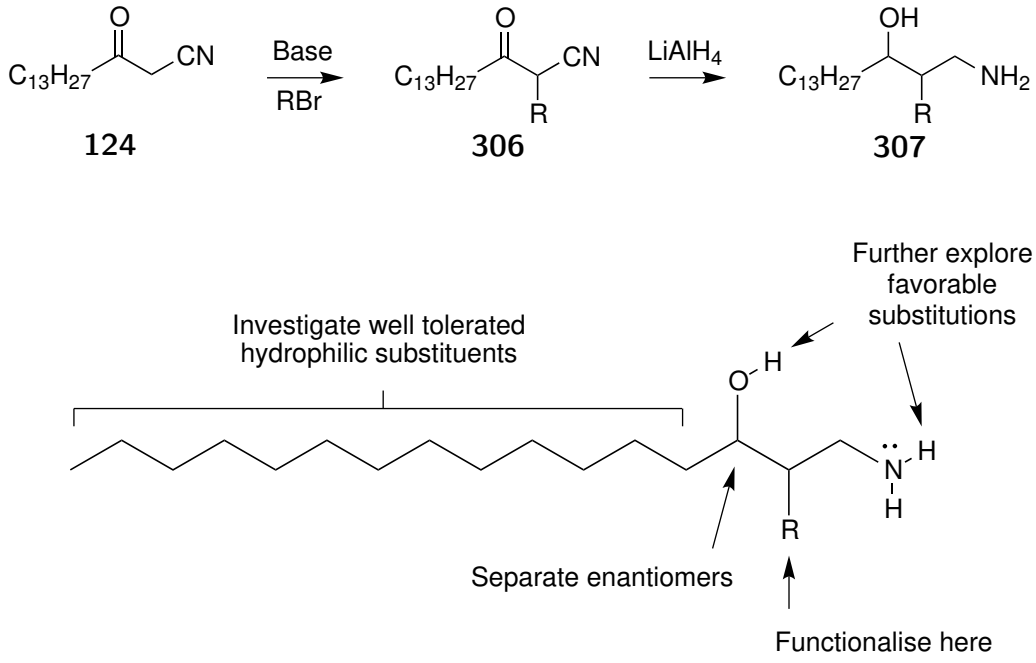

Scheme 5.3: Future work

If the activity of the hydroxyamine **109** is not demonstrated through NMT inhibition further attempts to optimise **109** based on the NMT transition state is unwarrented. NMT inhibition is a validated target and a strong contender towards clinical applications with novel modes of action towards protozoan diseases.

Several leads have been published and show a good prospect for development. For example, Bell *et al* reported several interesting novel scaffolds exemplified in Figure 1.21 which are yet to be derivatised and optimised as NMT inhibitors with anti-protozoan activity.[61] These structures were discovered from a HTS and are excellent starting points for research campaigns specifically targeting NMT as anti-*trypanosoma* compounds. The structures have been demonstrated to be inhibitors of *T. brucei* and *L. donovani* NMT however their structure-activity relationship in whole cell assays are yet to be investigated through derivatisation.

Chapter 6

Experimental

6.1 General procedures

Reactions were conducted under a nitrogen atmosphere at room temperature unless otherwise stated. Materials were obtained from commercial sources and used without further purification unless otherwise stated. Melting points were determined on a Crown Scientific Barnstead Electrothermal 9100 apparatus. NMR spectra were obtained on an Ultrashield Bruker 400 spectrometer and were conducted at 298 K. All ^{1}H NMR spectra were recorded at a frequency of 400 MHz while all ^{13}C NMR spectra were recorded at a frequency of 100MHz. $CDCl_3$ (^{1}H, 7.26 ppm; ^{13}C, 77.16 ppm). Multiplicity was assigned as follows: s = singlet, d = doublet, t = triplet, q = quarter, m = multiplet and br = broad. Infrared spectra were recorded on a Perkin Elmer Fourier Transform-IR spectrometer 100 equipped with a ZnSe-diamond crystal ATR accessory; spectra were acquired between 4000-650 cm^{-1}. High resolution ESI mass measurements were recorded in positive and negative ionisation mode on a LTQ Orbitrap XL instrument carried out at Curtin University. Solvents (tetrahydrofuran, dichloromethane and acetonitrile) were dried using methods described in Armarego and Chai.[175] Thin layer chromatography (TLC) was run on Merck aluminium backed silica gel 60 F254 sheets and visualised under ultraviolet light or permanganate stain. Compounds were purified by flash chromatography on Davisil silica gel 40—63 μm. Petroleum spirits (PS) refers to the fraction of alkanes that boils between 40-

60°C.

6.2 Chapter 2 experimental

6.2.1 Linear synthesis towards 108

Ethyl tetradecanoate 111

A solution of myristic acid (19.9 g, 87.3 mmol) and concentrated sulphuric acid (2.5 mL, 4.7 g, 47 mmol) in EtOH (120 mL) was heated under reflux for 24 h. The reaction mixture was allowed to cool and concentrated under reduced pressure. The pale yellow oil was dissolved in petroleum spirit (250 mL) and washed with water (100 mL), $NaHCO_3$ solution (5%, 100 mL) and brine (100 mL). The organic phase was dried over anhydrous $MgSO_4$ and concentrated under reduced pressure to give a crude light yellow oil (21.0 g) that was purified by fractional distillation under a reduced pressure (200°C / approx 4mm Hg) to give the ester **111** as a colourless oil (17.7 g, 79 %). The NMR spectra were identical to those reported.[176]

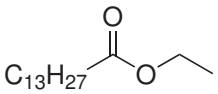

111

^{1}H NMR ($CDCl_3$): δ 4.12 (q, J = 7.1 Hz, 2H), 2.28 (t, J = 7.6 Hz, 2H), 1.61 (m, 2H), 1.30-1.23 (m, 23H), 0.88 (t, J = 6.9 Hz, 3H). ^{13}C NMR ($CDCl_3$): δ 174.1 (C), 60.3 (CH_2), 34.6 (CH_2), 32.1 (CH_2), 29.82 (CH_2), 29.79 (CH_2), 29.75 (CH_2), 29.61 (CH_2), 29.50 (CH_2), 29.42 (CH_2), 29.31 (CH_2), 25.2 (CH_2), 22.8 (CH_2), 14.40 (CH_3), 14.26 (CH_3).

3-Oxohexadecanenitrile 124

A solution of anhydrous acetonitrile (2.5 mL, 47.9 mmol, freshly distilled from P_2O_5) in anhydrous THF (20 mL) was added dropwise to a solution of *n*-BuLi (26.5 mL, 1.6 M in hexanes, 42.4 mmol) in anhydrous THF (40 mL) at -84°C. After 45 min a solution of ethyl tetradecanoate **111** (5.02 g, 19.6 mmol) in THF (20 mL) was added dropwise and the reaction mixture warmed to -45°C for 2 hours before addition of HCl (1M, 50 mL). The reaction mixture was allowed to warm to room temperature and concentrated under reduced pressure. The residue was

diluted with $CHCl_3$ (150 mL) and washed with $NaHCO_3$ solution (5%, 50 mL) and brine (50 mL). The organic phase was dried over anhydrous $MgSO_4$ and the filtrate concentrated under reduced pressure to give a light yellow solid (5.15 g). The crude material was triturated with cold (0°C) petroleum spirit (2 x 20 mL) and dried under reduced pressure to give **124** as a colourless fluffy solid (3.63 g, 74%) that did not require further purification.

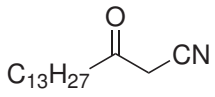

124

Melting range: 89 - 90°C. ^{1}H NMR($CDCl_3$): δ 3.43 (s, 2H), 2.61 (t, J = 7.4 Hz, 2H), 1.62 (m, 2H), 1.32-1.26 (m, 20H), 0.88 (t, J = 6.9 Hz, 3H). ^{13}C NMR ($CDCl_3$): δ 197.7 (C), 114.0 (C), 77.2 (CH_2), 42.3 (CH_2), 32.0 (CH_2), 29.77 (CH_2), 29.75 (CH_2), 29.74 (CH_2), 29.67 (CH_2), 29.51 (CH_2), 29.46 (CH_2), 29.38 (CH_2), 29.0 (CH_2), 23.5 (CH_2), 22.8 (CH_2), 14.2 (CH_3). IR (ATR, cm^{-1}) 2918, 2850, 2259, 1716, 1471, 1310, 1069, 931, 720. HRMS (ESI): Molecular ion not found.

1-Aminohexadecan-3-ol 109

A solution of the ketonitrile **124** (3.52 g, 14 mmol) in anhydrous THF (40 mL) was added dropwise to a suspension of $LiAlH_4$ (1.74 g, 46 mmol) in anhydrous THF (15 mL) at -10°C. The reaction mixture was allowed to warm to room temperature over 3.5 h and cooled to 0°C before sequential addition of water (1.7 mL) and sodium hydroxide (15 %w/v, 1.7 mL), anhydrous THF (50 mL) and water (5 mL). The reaction mixture was stirred for 30 min and filtered. The filtrate was concentrated to give a pale yellow material (3.14 g, 87%) that was purified by column chromatography (5-25% MeOH, 1% TEA in $CHCl_3$) to give **109** as a colourless solid (1.98 g, 55 %).

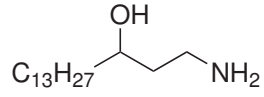

109

Melting range: 84 - 87°C. ^{1}H NMR ($CDCl_3$): δ 3.82-3.77 (m, 1H), 3.16-3.11 (m, 1H), 2.88-2.81 (m, 1H), 1.63-1.58 (m, 1H), 1.50-1.35 (m, 4H), 1.35-1.20 (m, 23H), 0.88 (t, J = 6.5 Hz, 3H). ^{13}C NMR ($CDCl_3$): δ 73.5 (CH), 41.1 (CH_2), 38.1 (CH_2), 37.6 (CH_2), 32.1 (CH_2), 29.93 (CH_2), 29.83 (CH_2), 29.81 (CH_2), 29.79 (CH_2), 29.5 (CH_2), 25.7 (CH_2), 22.8 (CH_2), 14.3 (CH_3). IR (ATR, cm^{-1}) 3358, 3294, 3124, 2918, 2849, 1597, 1463, 1352, 1076, 931, 723. HRMS

(ESI) m/z $C_{16}H_{35}NO$ $[M+H]^+$ = 258.2791, found = 258.2782.

2-Bromo-*N*-methylacetamide 125

Methylamine hydrochloride (4.45 g, 65.9 mmol) was added to a solution of NaOH (6.61 g, 165 mmol, 2.5 eqv) in a 1:1 H_2O:DCM mixture (40 mL) in a ice/salt bath. The mixture was stirred for 5 min before dropwise addition of a solution of 2-bromoacetyl bromide (6.0 mL, 68.9 mmol, 1.05 eq) in DCM (10 mL). After 30 min the aqueous phase was extracted with DCM (2 x 50 mL) and the organic combined extracts were dried with anhydrous $MgSO_4$, and concentrated under reduced pressure to give **125** as an off white solid (7.46 g, 75%) that did not require further purification. The NMR spectra were identical to those reported.[95]

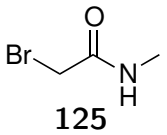

125

^{1}H NMR ($CDCl_3$): δ 6.54 (s, 1H), 3.88 (s, 2H), 2.86 (d, J = 4.9 Hz, 3H). ^{13}C NMR ($CDCl_3$): δ 166.0, 29.3, 27.1.

6.2.2 Protection via benzyl carbamate formation

Benzyl (3-hydroxyhexadecyl)carbamate 130

A solution of CBzCl (160 µl, 1.12 mmol in anhydrous DCM (1 mL) was added dropwise over 10 min to a solution of 3-hydroxylhexadec-1-amine **109** (247 mg, 0.96 mmol) and DIPEA (160 µl, 1.86 mmol) in anhydrous DCM (10 mL) at -10°C. The reaction mixture was left to warm to room temperature over 15 hours and diluted with DCM (100 mL). The solution was washed with hydrochloric acid (1 M, 2 x 100 mL), $NaHCO_3$ solution (5 %, 100 mL) and brine (100 mL). The organic phase was dried over anhydrous $MgSO_4$ and the filtrate concentrated under reduced pressure to give a pale yellow solid (329 mg) that was purified by column chromatography (20% EtOAc in PS) to give the carbamate **130** as a colourless powder (237 mg, 63%).

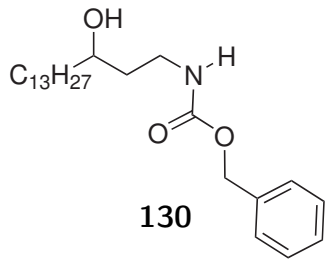

130

Melting range: 79 - 80°C. ^{1}H NMR ($CDCl_3$): δ 7.36-7.30 (m, 5H), 5.14-5.10 (m, 2H), 3.66-3.62 (m, 1H), 3.52-3.50 (m, 1H), 3.23-3.19 (m, 1H), 1.98-1.91 (bs, 2H), 1.70-1.61 (m, 1H), 1.55-1.37 (m, 3H), 1.35-1.20 (m, 22H), 0.90-0.86 (m, 3H). ^{13}C NMR ($CDCl_3$): δ 157.3 (C), 136.7 (C), 128.7 (CH), 128.27 (CH), 128.25 (CH), 69.6 (CH), 66.9 (CH_2), 38.3 (CH_2), 37.68 (CH_2), 37.48 (CH_2), 32.1 (CH_2), 29.84 (CH_2), 29.83 (CH_2), 29.81 (CH_2), 29.80 (CH_2), 29.76 (CH_2), 29.5 (CH_2), 25.9 (CH_2), 22.8 (CH_2), 14.3 (CH_3). HRMS (ESI): Molecular ion not found. IR (ATR, cm^{-1}): 3426, 3332, 2916, 2850, 1683, 1541, 1257, 1039, 698.

6.2.3 Protection via cyclic carbamate formation

Tetrahydro-6-tridecyl-2*H*-1,3-oxazine-2-one 132

A solution of CDI (207 mg, 1.25 mmol, 1.07 eqv) in anhydrous THF (3 mL) was added dropwise to a rapidly stirred solution of hydroxyamine **109** (302 mg, 1.17 mmol) in anhydrous THF (7 mL) under N_2 at room temperature. The mixture was heated under reflux for 6 hours. The reaction mixture was allowed to cool and concentrated under reduced pressure. The residue was dissolved in $CHCl_3$ (50 mL) and washed with HCl (1M, 3 x 10 mL). The combined aqueous washings were back extracted with $CHCl_3$ (10 mL). The combined organic extracts were washed with brine (15 mL), dried over anhydrous $MgSO_4$ and concentrated under reduced pressure to give **132** as a light yellow solid (297 mg, 90 %) that did not require further purification.

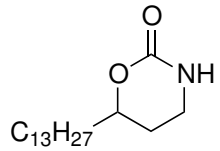

132

Melting range: 116 - 120 °C. ^{1}H NMR ($CDCl_3$): δ 5.80 (s, 1H), 4.24 (m, 1H), 3.35 (m, 2H), 1.93-1.92 (m, 1H), 1.77-1.71 (m, 2H), 1.58 (s, 1H), 1.25 (s, 22H), 0.88 (t, 3H). ^{13}C NMR ($CDCl_3$): δ 154.9 (C), 77.7 (CH), 39.3 (CH_2), 35.1 (CH_2), 32.1 (CH_2), 29.82 (CH_2), 29.79 (CH_2), 29.77 (CH_2), 29.69 (CH_2), 29.63 (CH_2), 29.53 (CH_2), 29.49 (CH_2), 26.4 (CH_2), 25.0 (CH_2), 22.8 (CH_2), 14.3 (CH_3). HRMS (ESI) m/z $C_{17}H_{33}NO_2[M+H]^+$ = 284.2584, found = 284.2575. IR (ATR, cm^{-1}): 3289, 2955, 2916, 2848, 1687, 1668, 1482, 1668, 1482, 1307, 1152,

1054, 767, 694.

N-Methyl-2-(2-oxo-6-tridecyl-1,3-oxazinan-3-yl)acetamide 133

A solution of carbamate **132** (97 mg, 0.34 mmol, 1 eqv) in anhydrous THF (1 mL) was added dropwise to a suspension of sodium hydride (22 mg, 57%, 0.52 mmol, 1.5 eqv) in anhydrous THF (1 mL) at 0°C. After 45 min, the solution changed colour from pale yellow to dark brown. The reaction mixture was cooled to 0°C before a solution of 2-bromo-*N*-methyl acetamide **125** (133 mg, 0.87 mmol, 2.6 eqv) in anhydrous THF (1 mL) was added rapidly. The reaction mixture was heated under reflux for 1 hour then allowed to cool to room temperature. The solution was concentrated under reduced pressure to give a oily semi-solid. The crude material was dissolved in EtOAc (25 mL), washed with sodium metabisulfite (1 %, 25 mL), HCl (1 M, 25 mL), brine (25 mL) and dried over anhydrous $MgSO_4$ before concentration under reduced pressure to give a yellow solid (114 mg). This material was purified by column chromatography (0-10% MeOH in EtOAc) to give the substituted carbamate **133** as a off white solid (39 mg, 32 %) and **138** as a off white solid (37 mg, 31%).

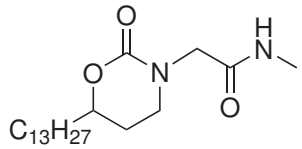

133

Melting range: 107 - 108°C. ^{1}H NMR ($CDCl_3$): δ 6.47-6.45 (m, 1H), 4.28-4.25 (m, 1H), 4.03 (d, J = 15.3 Hz, 1H), 3.80 (d, J = 15.3 Hz, 1H), 3.50-3.39 (m, 2H), 2.80 (d, J = 4.8 Hz, 3H), 2.04-1.99 (m, 1H), 1.91-1.69 (m, 3H), 1.61-1.54 (m, 1H), 1.49-1.21 (m, 21H), 0.89-0.86 (t, 3H). ^{13}C NMR ($CDCl_3$): δ 169.5 (C), 155.0 (C), 78.0 (CH), 53.5 (CH_2), 46.3 (CH_2), 34.9 (CH_2), 32.1 (CH_2), 29.83 (CH_2), 29.79 (CH_2), 29.77 (CH_2), 29.69 (CH_2), 29.61 (CH_2), 29.51 (CH_2), 29.50 (CH_2), 27.4 (CH_2), 26.3 (CH_3), 24.9 (CH_2), 22.8 (CH_2), 14.3 (CH_3). IR (ATR, cm^{-1}): 3326, 2918, 2851, 1659, 1495, 1287, 1135, 763. HRMS (ESI) m/z $C_{20}H_{38}N_2O_3$[M+H]$^+$ = 355.2955, found = 355.2957.

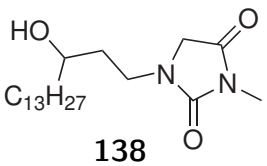

138

Melting range: 67 - 70 °C. ^{1}H NMR ($CDCl_3$): δ 3.91 (d, J = 17.5 Hz, 1H), 3.87 (d, J = 17.5 Hz, 1H), 3.77 (m, 1H), 3.59-3.54 (m, 1H), 3.34 (m, J = 4.7 Hz, 1H), 3.02 (s, 3H), 1.74-1.68 (m, 1H), 1.58-1.52 (m, 1H), 1.47-1.42 (m, 3H), 1.31-1.22 (m, 22H), 0.87 (t, J = 6.9 Hz, 3H).^{13}C NMR ($CDCl_3$): δ 170.2 (C), 157.7 (C), 68.8 (CH), 50.3 (CH_2), 40.0 (CH_2), 37.6 (CH_2), 35.3 (CH_2), 32.1 (CH_2), 29.83 (CH_2), 29.82 (CH_2), 29.80 (CH_2), 29.74 (CH_2), 29.5 (CH_2), 25.9 (CH_2), 25.1 (CH_3), 22.8 (CH_2), 14.3 (CH_3). IR (ATR, cm^{-1}): 3385, 2916, 2849, 1767, 1692, 1491, 1106, 762. HRMS (ESI) m/z $C_{20}H_{38}N_2O_3$ $[M+H]^+$ = 355.2955, found = 355.2962.

6.2.4 Synthesis via duel protected 2-bromo-*N*-methyl-*N*-benzyl acetamide

N-Benzylmethylamine 145

A mixture of benzyl bromide (5.13 g, 30.0 mmol) and methyl amine (8M in MeOH, 50 mL, 400 mmol, 13.3 eqv) in methanol (60 mL) was stirred rapidly overnight and concentrated under reduced pressure. The resulting mixture was diluted with $NaHCO_3$ (50 mL, 5%) and extracted with EtOAc (8 x 50 mL). The combined organic extracts were dried over anhydrous $MgSO_4$ and the filtrate concentrated under reduced pressure. The oil (3.38 g) was analysed by ^{1}H NMR and characterised as a 1:1 molar mixture of **145**:**147** and used in the following step without purification.

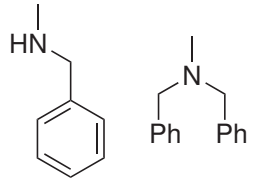

145 **147**

^{1}H NMR ($CDCl_3$, **145**): 3.76 (s, 2H), 2.46 (s, 3H). (The NMR spectra were identical to those reported.[177]) ^{1}H NMR ($CDCl_3$, **147**): 3.52 (s, 4H), 2.19 (s, 3H). (The NMR spectra were identical to those reported.[178])

2-Bromo-*N*-methyl-*N*-benzylacetamide 143

A solution of bromoacetyl bromide (2.6 mL, 29.85 mmol, 1.07 eq) in dry DCM (20 mL) was added dropwise over 15 min to a stirred solution of crude methyl benzylamine **145** (3.38 g, 27.87mmol, 1.00 eq) and TEA (3.8 mL, 2.76 g, 27.31 mmol, 0.98 eq) in dry DCM (50 mL) at 0°C. The reaction mixture was left to warm to room temperature and stirred for 20 min. The mixture was cooled to 0°C and HCl (1M, 50 mL) was added dropwise. The reaction mixture was extracted with DCM (2 x 40 mL) and the combined organic extracts were dried over anhydrous $MgSO_4$. The filtrate was concentrated under reduced pressure to give a viscous brown oil (6.80 g) that was purified by column chromatography (10 - 20% EtOAc in PS) to give **143** as a yellow semi solid (1.02 g, 14% over 2 steps).

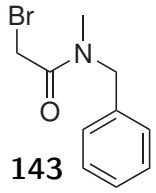

143

^{1}H NMR ($CDCl_3$): δ 7.34-7.25 (m, 5H), 4.60 (m, 2H), 4.14-3.93 (m, 2H), 2.99 (m, 3H). ^{13}C NMR ($CDCl_3$): δ 167.0 (C), 136.6 (C), 135.9 (C), 129.2 (CH), 128.8 (CH), 128.18 (CH), 128.11 (CH), 127.7 (CH), 126.5 (CH), 54.3 (CH_2), 51.4 (CH_2), 41.5 (CH_3), 35.7 (CH_3), 34.6 (CH_3), 26.5 (CH_2), 26.2 (CH_2). IR (ATR, cm^{-1}): 3030, 1644, 1452, 1402, 1078, 730, 697. HRMS (ESI) m/z $C_{10}H_{12}BrNO$ $[M+H]^+$ = 242.0175, found = 242.0175

***N*-Benzyl-*N*-methyl-2-(2-oxo-6-tridecyl-1,3-oxazinan-3-yl) acetamide 144**

A suspension of NaH (53 mg, 57%, 1.25 mmol, 1.4 eqv) and the above crude carbamate **132** (253 mg, 0.893 mmol, 1 eqv) in anhydrous THF (3 mL) was stirred for 30 min at room temperature. A solution of 2-bromo-*N*-methyl-*N*-benzyl acetamide **143** (326 mg, 1.346 mmol, 1.5 eqv) in anhydrous THF (3 mL) was added and the reaction mixture heated under reflux for 1.5h. The reaction mixture was cooled to 0°C before addition of saturated NH_4Cl (2 mL). The mixture was concentrated under reduced pressure. The resulting residue was dissolved in $CHCl_3$ (50 mL) and washed with water (50 mL), HCl (1M, 50 mL) and brine (50 mL).

The organic phase was dried over anhydrous $MgSO_4$ and the filtrate concentrated under reduced pressure. The resulting crude material (568 mg) was purified by column chromatography (50-100% EtOAc in PS) to give **144** as a colourless solid (332 mg, 84%).

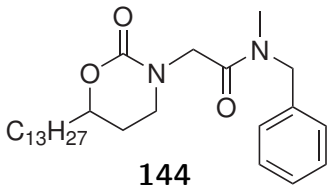

144

Melting range: 63 - 65°C. ^{1}H NMR ($CDCl_3$): δ 7.39-7.27 (m, 3H), 7.25-7.19 (m, 2H), 4.56 (d, J = 22.4 Hz, 2H), 4.35-4.08 (m, 3H), 3.57-3.44 (m, 1H), 3.37-3.27 (m, 1H), 2.93 (d, J = 27.1 Hz, 3H), 2.03-1.88 (m, 2H), 1.78-1.72 (m, 1H), 1.64 (s, 1H), 1.65-1.36 (m, 4H), 1.35-1.20 (m, 20H), 0.88 (t, J = 6.9 Hz, 3H). ^{13}C NMR ($CDCl_3$): δ 168.4 (C), 167.9 (C), 154.6 (C), 136.8 (C), 136.2 (C), 129.2 (CH), 128.8 (CH), 128.2 (CH), 127.9 (CH), 127.6 (CH), 126.5 (CH), 77.8 (CH), 52.8 (CH_2), 51.4 (CH_2), 50.37 (CH_2), 50.33 (CH_2), 46.08 (CH_2), 46.04 (CH_2), 35.06 (CH_2), 35.00 (CH_2), 34.4 (CH_3), 33.9 (CH_3), 32.1 (CH_2), 29.82 (CH_2), 29.79 (CH_2), 29.70 (CH_2), 29.64 (CH_2), 29.56 (CH_2), 29.54 (CH_2), 29.49 (CH_2), 27.4 (CH_2), 24.9 (CH_2), 22.8 (CH_2), 14.3 (CH_3). IR (ATR, cm^{-1}): 3547, 3479, 2919, 2851, 1688, 1672, 1643, 1491, 1284, 1129, 698. HRMS (ESI) m/z $C_{27}H_{44}N_2O_3$ $[M+H]^+$ = 445.3425, found = 445.3429.

N-Benzyl-2-((3-hydroxyhexadecyl)amino)-*N*-methylacetamide 148

A solution of cyclic carbamate **144** (180 mg, 0.4 mmol) and LiOH (90 mg, 2.15 mmol, 5 eq) in EtOH (4 mL) and water (1 mL) was heated under reflux overnight. The reaction mixture was allowed to cool to room temperature and concentrated to dryness *in vacuo*. The reaction mixture was triturated with small aliquots of $CHCl_3$, filtered and concentrated to give **148** as a colourless solid (126 mg, 74%) that did not require further purification.

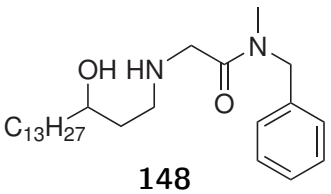

148

Melting range: 75 - 77°C. ^{1}H NMR ($CDCl_3$): δ 7.39-7.27 (m, 3H), 7.26-7.13 (m, 2H), 5.30 (d, J = 40.3 Hz, 1H), 4.53 (d, J = 53.1 Hz, 2H), 3.81-3.76 (m, 1H), 3.46 (d, J = 6.4 Hz, 2H), 3.03-2.68 (m, 5H), 2.25-2.23 (m, 1H), 1.62-1.35 (m, 5H), 1.35-1.15 (m, 25H), 0.88 (t, J = 6.9 Hz, 3H). ^{13}C NMR ($CDCl_3$): δ 171.3 (C), 170.9 (C), 137.0 (C), 136.2 (C), 129.2 (CH), 128.8 (CH), 128.2 (CH), 128.0 (CH), 127.7 (CH), 126.4 (CH), 73.2 (CH), 52.4 (CH_2), 51.3 (CH_2), 50.0 (CH_2), 49.7 (CH_2), 49.02 (CH_2), 48.89 (CH_2), 37.9 (CH_2), 35.1 (CH_2), 34.3 (CH_3), 33.7 (CH_3), 32.1 (CH_2), 29.92 (CH_2), 29.82 (CH_2), 29.80 (CH_2), 29.79 (CH_2), 29.5 (CH_2), 25.8 (CH_2), 22.8 (CH_2), 14.3 (CH_3). HRMS (ESI) m/z $C_{26}H_{46}N_2O_2$ $[M+H]^+$ = 419.3632, found = 419.3619.

IR (ATR, cm^{-1}): 3281, 3131, 2919, 2849, 1651, 1633, 1431, 1281, 1103, 725.

2-((3-Hydroxyhexadecyl)amino)-*N*-methylacetamide 108

Sodium metal (72 mg, 3.13 mmol, 22 eqv) was dissolved in condensed ammonia (approx 5 mL) at -84°C. The blue solution was stirred for 5 min before dropwise addition of a solution of **148** (60 mg, 0.143 mmol) and *tert*-butyl alcohol (100 μL) in anhydrous THF (1.5 mL). The solution was stirred for 20 min condensing ammonia gas into the reaction as required to ensure fluidity. Sat. NH_4Cl solution (2 mL) was added and the reaction mixture allowed to warm to room temperature over 30 min. The reaction mixture was absorbed onto silica and purified using column chromatography (2-4% $MeOH_{(sat.\ in\ NH_3)}$ in $CHCl_3$) to give **108** as a colourless solid (14 mg, 30%).

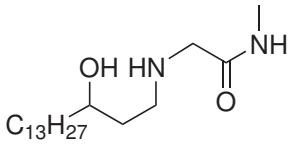

108

Melting point: 105°C. ^1H NMR ($CDCl_3$): δ 6.89 (s, 1H), 3.77 (s, 1H), 3.34-3.27 (m, 2H), 2.92-2.73 (m, 5H), 1.72-1.64 (m, 1H), 1.61-1.50 (m, 1H), 1.50-1.37 (m, 3H), 1.37-1.17 (m, 23H), 0.94-0.80 (m, 4H). ^{13}C NMR ($CDCl_3$): δ 171.7 (C), 72.2 (CH), 52.7 (CH_2), 48.3 (CH_2), 38.1 (CH_2), 36.2 (CH_2), 32.1 (CH_2), 29.82 (CH_2), 29.77 (CH_2), 29.5 (CH_2), 26.0 (CH_3), 25.7 (CH_2), 22.8 (CH_2), 14.3 (CH_3). HRMS (ESI) m/z $C_{19}H_{40}N_2O_2$ $[M+H]^+$ = 329.3163, found = 329.3151. IR (ATR, cm^{-1}): 3302, 3266, 3103, 2918, 2850, 1667, 1571, 1466, 1270, 1129, 914, 722.

6.2.5 Benzyl amine protection

1-(Benzylamino)hexadecan-3-ol 149

A mixture of the hydroxyamine **109** (463 mg, 1.80 mmol), benzaldehyde (209 mg, 1.97 mmol, 1.1 eqv) and anhydrous $MgSO_4$ (252 mg) in dry DCM:THF (5:1, 15 mL) was stirred overnight. The resulting mixture was filtered and the residue washed with a small amount of DCM. The combined filtrates were concentrated under reduced pressure to give a yellow crystalline solid (729 mg). The crystals were dissolved in MeOH (17 mL) and cooled in a ice bath before slow addition

of $NaBH_4$ (76 mg, 2.00 mmol, 1.12 eq). The mixture was stirred for 4.5 hours at 25°C and cooled to 0°C before addition of hydrochloric acid solution (1M, 5 mL). The reaction mixture was allowed to warm to room temperature before the pH was adjusted to > 7 using $NaHCO_3$ solution (5%) and concentrated to dryness under reduced pressure. The residue was triturated with $CHCl_3$ (2 x 30 mL) and the filtrate concentrated under reduced pressure to give **149** as a colourless crystalline solid (537 mg, 87 %) that did not require further purification.

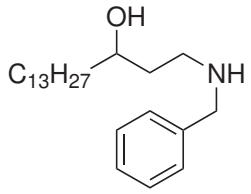

149

Melting range: 45 - 47°C. ^{1}H NMR ($CDCl_3$): δ 7.33-7.23 (m, 5H), 3.83-3.72 (m, 3H), 3.02 (m, J = 3.6 Hz, 1H), 2.78 (m, J = 3.3 Hz, 1H), 1.66-1.60 (m, 1H), 1.55-1.37 (m, 4H), 1.36-1.32 (m, 23H), 0.88 (t, J = 6.9 Hz, 3H). ^{13}C NMR ($CDCl_3$): δ 139.6 (C), 128.6 (CH), 128.3 (CH), 127.3 (CH), 73.9 (CH), 54.0 (CH_2), 48.6 (CH_2), 38.0 (CH_2), 35.2 (CH_2), 29.94 (CH_2), 29.84 (CH_2), 29.82 (CH_2), 29.80 (CH_2), 29.5 (CH_2), 25.8 (CH_2), 22.8 (CH_2), 14.3 (CH_3). IR (ATR, cm^{-1}) 3290, 3166, 2919, 2846, 1463, 1452, 1357, 1111, 1072, 880, 796, 745, 695. HRMS (ESI) m/z $C_{23}H_{41}NO$ $[M+H]^+$ = 348.3261, found = 348.3264.

2-(Benzyl(3-hydroxyhexadecyl)amino)-*N*-methylacetamide 150

A solution of the benzyl amine **149** (47 mg, 0.135 mmol), 2-bromo-*N*-methylacetamide (27 mg, 0.177 mmol, 1.31 eq) and DIPEA (25 mg, 0.248 mmol) in DMF (1 mL) was stirred overnight at 70°C under N_2. The reaction mixture was concentrated under reduced pressure and the residue dissolved in toluene (5 mL). The solution was washed with K_2CO_3 solution (5%, 3 x 1 mL) and the aqueous washings were back extracted with toluene (2 mL). The combined organic phases were dried over anhydrous $MgSO_4$ and concentrated under reduced pressure. The residue (54 mg) was purified by column chromatography (5% MeOH in $CHCl_3$) to yield **150** as a brown oil (39 mg, 69%).

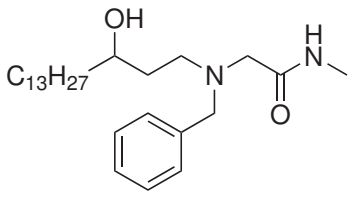

150

^{1}H NMR ($CDCl_3$): δ 7.36-7.26 (m, 5H), 7.12-7.11 (m, 1H), 3.73-3.60 (m, 3H), 3.17-3.08 (m, 2H), 2.79 (d, J = 4.9 Hz, 3H), 2.71 (td, J = 6.6, 2.4 Hz, 2H), 1.71-1.60 (m, 2H), 1.45-1.40 (m, 2H), 1.32 (m, 23H), 0.89 (t, J = 6.8 Hz, 3H). ^{13}C NMR ($CDCl_3$): δ 171.5 (C), 137.5 (C), 129.1 (CH), 128.7 (CH), 127.7 CH), 71.2 (CH), 59.2 (CH_2), 58.1 (CH_2), 52.7 (CH_2), 37.9 (CH_2), 33.8 (CH_2), 32.0 (CH_2), 29.79 (CH_2), 29.77 (CH_2), 29.72 (CH_2), 29.5 (CH_2), 25.9 (CH_3), 25.7 (CH_2), 22.8 (CH_2), 14.2 (CH_3). IR (ATR, cm^{-1}): 3383, 3306, 2922, 2851, 1652, 1537, 1144, 908, 731. HRMS (ESI) m/z $C_{26}H_{46}N_2O_2$ $[M+H]^+$ = 419.3632 , found = 419.3628.

2-((3-Hydroxyhexadecyl)amino)-N-methylacetamide 108

A solution of the benzyl amine **150** (32 mg, 0.076 mmol) in formic acid solution (3 mL, 5% in MeOH) was degassed with nitrogen (x 3). Pd/C (10 mg, 5 wt%) was added and the reaction mixture stirred for 15h. The reaction mixture was filtered and concentrated under reduced pressure. The residue was redissolved in a small quantity of MeOH and the pH adjusted to > 7 with Na_2CO_3 solution (5%). The mixture was concentrated to dryness under reduced pressure and triturated with $CHCl_3$. The filtrate was concentrated under reduced pressure to give a colourless solid (22 mg) that was purified by column chromatography (3:1:96 MeOH:TEA:$CHCl_3$) to give **108** as a colourless solid (17 mg, 68%). The spectra data obtained matched that obtained in experiment 6.2.4

6.2.6 Amine linker length variation

2-Hydroxypentadecanenitrile 113[107]

Tetradecanal (1.0 g, 4.71 mmol) was added to a vigorously stirred solution of sodium bisulfite (1.0 mL, 40%, 9.42 mmol, 2 eq) in water (5 mL). A white chunky precipitate formed instantaneously. NaCN (940 mg, 18.85 mmol, 4 eq) was added and stirred overnight in a sealed tube. The chunks remained unchanged and were broken up with a glass rod before methanol (2 mL) was added and sonicated and

regularly shaken vigorously for 1 hour. A yellow colour progressively developed and a subtle change of appearance to the precipitate was observed. The reaction mixture was extracted with $CHCl_3$ (3 x 50 mL) and concentrated under a stream of nitrogen. The aqueous portions of the work up were added to household bleach to destroy the remaining cyanide. The crude reaction mixture was purified by column chromatography (DCM, Short column) to give **113** as a colourless power (557 mg, 49%).

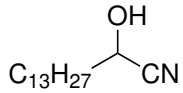

113

Melting range: 52 - 54°C. ^{1}H NMR ($CDCl_3$): δ 4.47 (t, J = 6.7 Hz, 1H), 2.66-2.50 (m, 1H), 1.84 (dt, J = 9.5, 6.7 Hz, 2H), 1.56-1.43 (m, 2H), 1.42-1.18 (m, 20H), 0.96-0.82 (m, 3H). ^{13}C NMR ($CDCl_3$): δ 120.1 (C), 61.6 (CH), 35.4 (CH_2), 32.1 (CH_2), 29.81 (CH_2), 29.78 (CH_2), 29.77 (CH_2), 29.72 (CH_2), 29.60 (CH_2), 29.49 (CH_2), 29.48 (CH_2), 29.1 (CH_2), 24.7 (CH_2), 22.8 (CH_2), 14.3 (CH_3). IR (ATR, cm^{-1}) 3395, 2913, 2849, 2253, 147, 1323, 1074, 939, 716, 563. HRMS (ESI): Molecular ion not found.

1-Aminopentadecan-2-ol 112

$LiAlH_4$ (40 mg, 1.05 mmol) was added to a stirred solution of the cyanohydrin **113** (202 mg, 0.844 mmol) in anhydrous THF (5 mL) at 0°C. The reaction mixture was allowed to warm to room temperature for 3 hours and cooled in a ice bath. HCl solution (1M) was added and the reaction mixture allowed to warm to room temperature. The pH of the solution was adjusted > 7 with a solution of K_2CO_3 (5 %) and the mixture concentrated to dryness under reduced pressure. The solid was triturated with portions of $CHCl_3$, filtered and the filtrate concentrated under reduced pressure. The resulting solid was purified by column chromatography (10:1:89 MeOH:$NH_{3(aq)}$:$CHCl_3$) to give **112** as a colourless solid (60 mg, 29%).

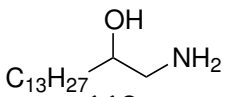

112

Melting range: 66-71°C. ^{1}H NMR (MeOD): δ 3.54-3.48 (m, 1H), 2.66 (dd, J = 13.0, 3.6 Hz, 1H), 2.51 (dd, J = 13.0, 8.0 Hz, 1H), 1.50-1.23 (m, 26H), 0.90 (t, J = 6.9 Hz, 3H). ^{13}C NMR (MeOD): δ 73.4 (CH), 36.0 (CH_2), 33.1 (CH_2), 30.82 (CH_2), 30.80 (CH_2), 30.78 (CH_2), 30.76 (CH_2), 30.5 (CH_2), 26.8 (CH_2), 23.7

(CH_2), 14.4 (CH_3). IR (ATR, cm^{-1}) 3320, 2955, 2915, 2849, 1593, 1490, 1471, 1071, 718. HRMS (ESI) m/z $C_{15}H_{33}NO$ $[M+H]^+$ = 244.2635, found = 244.2625.

N,N-Bis(trimethylsilyl)propargylamine 155[109]

Hexamethyldisilazane**157** (17.0 mL, 13.1 g, 2.2 eq) was added to a solution of *n*-BuLi (48.0 mL, 1.6M, 76.8 mmol, 2.1 eq) in Et_2O (40 mL) at -84°C and allowed to warm to room temperature for 1 hour. The solution was cooled in a ice bath and propargyl bromide **156** (4.1 mL, 80 %wt in toluene, 37.1 mmol) in Et_2O (10 mL) was added and stirred overnight. A sample (9.0 mL, utilised in following experiment) of the reaction mixture was removed and the remaining reaction mixture quenched on a ice cold buffer solution (3.8g KH_2PO_4: 4.5 g Na_2HPO_4 in 50 mL H_2O) and filtered. The organic phase was washed with cold brine and dried over sodium carbonate and concentrated. The crude material was distilled and the first fraction was discarded before collecting **155** as a clear liquid (3.38 g, 49 %, 86 % pure) that decomposed during storage at -20°C within 3 days. The NMR spectra were identical to those reported.[109]

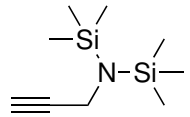

155

^{1}H NMR ($CDCl_3$): δ 3.53 (d, J = 2.4 Hz, 2H), 2.13 (t, J = 2.4 Hz, 1H), 0.15 (s, 18H). ^{13}C NMR ($CDCl_3$): δ 86.3, 69.8, 34.0, 1.8.

Tris(trimethylsilyl)-1-aminoheptadec-2-yn-4-ol 153

A solution of lithiated **155** (9.0 mL, preparation detailed above) was added to a solution of tetradecanal (495 mg, 2.33 mmol) in ether (1 mL) at -84°C and warmed to room temperature over 20 hours. Et_2O (5 mL) and TMSCl (0.45 mL, 3.54 mmol) was added to the reaction mixture at -84°C and allowed to warm to room temperature for 5 hours. The reaction mixture added to a ice cold buffer solution (0.38 g KH_2PO_4: 0.45 g Na_2HPO_4 in 5 mL H_2O) with Et_2O (10 mL) and quickly filtered. The organic phase quickly washed with ice cold brine, dried over Na_2CO_3 and concentrated under reduced pressure for 3 hours to give **153** as a unstable yellow oil (838 mg, 75%) that was used in the following steps without further purification.

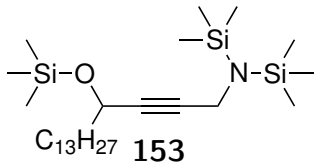

153

^{1}H NMR (C_6H_6): δ 4.46 (tt, J = 6.4, 1.7 Hz, 1H), 3.55 (d, J = 1.7 Hz, 2H), 1.88-1.82 (m, 3H), 1.62-1.55 (m, 2H), 1.40-1.20 (m, 19H), 0.96-0.86 (m, 3H), 0.26 (s, 9H), 0.24 (s, 18H). ^{13}C NMR (C_6H_6): δ 86.2 (C), 84.0 (C), 63.3 (CH), 39.5 (CH_2), 34.5 (CH_2), 32.4 (CH_2), 30.19 (CH_2), 30.16 (CH_2), 30.12 (CH_2), 29.9 (CH_2), 25.8 (CH_2), 23.1 (CH_2), 14.4 (CH_3), 2.0 (CH_3), 0.5(CH_3).

Z-Tris(trimethylsilyl)-1-aminoheptadec-2-en-4-ol 158

The forgoing crude TMS ether **153** (745 mg, 1.54 mmol) was dissolved in EtOAc (3 mL, K_2CO_3 pretreated). The atmosphere was evacuated and replaced with nitrogen (x 3) before addition of Pd/C (10%, 125 mg, 17 wt%). A hydrogen atmosphere was introduced (x 3) and left stirring overnight at room temperature. The reaction mixture was filtered though celite and concentrated under reduced pressure to give **158** as a yellow oil (593 mg, 79%) that was used in the following step without purification.

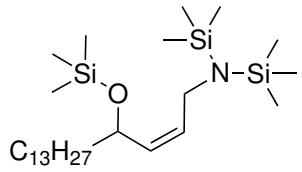

158

^{1}H NMR (C_6H_6): δ 5.46 (dt, J = 11.6, 4.8 Hz, 1H), 5.37-5.31 (m, 1H), 4.49-4.44 (m, 1H), 3.74 (ddd, J = 17.7, 5.5, 2.2 Hz, 1H), 3.62 (ddd, J = 17.7, 4.6, 2.3 Hz, 1H), 1.73-1.65 (m, 2H), 1.61-1.24 (m, 20H), 0.94-0.90 (m, 5H), 0.21 (d, J = 0.3 Hz, 9H), 0.20 (d, J = 0.3 Hz, 18H). ^{13}C NMR (C_6H_6): δ 134.8 (CH), 132.9 (CH), 69.4 (CH), 43.0 (CH_2), 38.9 (CH_2), 32.4 (CH_2), 30.20 (CH_2), 30.15 (CH_2), 30.14 (CH_2), 29.9 (CH_2), 25.9 (CH_2), 23.2 (CH_2), 14.4 (CH_3), 2.3 (CH_3), 0.7 (CH_3). IR (ATR, cm^{-1}) 2955, 2923, 2854, 1458, 1249, 1065, 1027, 875, 836, 753, 680.

Z-1-Aminoheptadec-2-en-4-ol 159

The forgoing crude TMS ether **158** (593 mg, 1.22 mmol) was stirred in a solution of TBAF (4.4 mL, 1M in THF) overnight at room temperature. The reaction mixture was concentrated under reduced pressure, dissolved in $CHCl_3$ (200 mL) and washed with water (3 x 100 mL). The combined aqueous phases were back

extracted with $CHCl_3$ (3 x 75 mL) and the combined organic extracts dried over anhydrous $MgSO_4$. The filtrate was concentrated under reduced pressure and the residue (231 mg) was purified by column chromatography (6% in $MeOH_{(Sat.\ NH_3)}$ in $CHCl_3$) to give **159** as a colourless power (131 mg, 40 %).

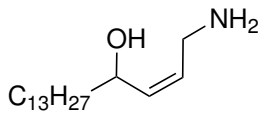

159

Melting range: 84 - 90°C. ^{1}H NMR (C_6H_6): δ 5.57 (dd, J = 11.3, 6.9 Hz, 1H), 5.42 (dt, J = 11.3, 6.0 Hz, 1H), 4.39 (q, J = 5.9 Hz, 1H), 3.08 (dd, J = 13.4, 7.0 Hz, 1H), 2.91 (dd, J = 13.4, 5.6 Hz, 1H), 1.79-1.67 (m, 4H), 1.56-1.22 (m, 23H), 0.92 (t, J = 6.7 Hz, 3H).^{13}C NMR (C_6H_6): δ 136.9 (CH), 130.5 (CH), 67.6 (CH), 39.0 (CH_2), 38.2 (CH_2), 32.4 (CH_2), 30.30 (CH_2), 30.27 (CH_2), 30.23 (CH_2), 30.17 (CH_2), 29.9 (CH_2), 26.1 (CH_2), 23.2 (CH_2), 14.4 (CH_3). IR (ATR, cm^{-1}): 3416, 3340, 2917, 2850, 1594, 1466, 1378, 1067, 720. HRMS (ESI) m/z $C_{17}H_{35}NO$ $[M+H]^+$ = 270.2791, found = 270.2782.

1-Aminoheptadec-2-yn-4-ol 160

The crude alkyne **153** (972 mg) was stirred in a solution of TBAF (6.5 mL, 1M in THF) overnight at room temperature. The reaction mixture was concentrated under reduced pressure, diluted with $CHCl_3$ (200 mL) and washed with water (3 x 100 mL). The combined aqueous phases were back extracted with $CHCl_3$ (3 x 75 mL). The combined organic phases were dried over $MgSO_4$, filtered and concentrated to give a yellow semi solid (548 mg). The crude material was purified by column chromatography [6% in $MeOH_{(Sat.\ NH_3)}$ in $CHCl_3$] to yield **160** as an off white solid (334 mg, 62%).

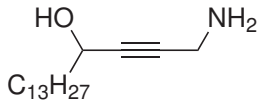

160

Melting range: 53 - 56°C. ^{1}H NMR (C_6H_6): δ 4.41 (t, J = 6.4 Hz, 1H), 3.18 (s, 2H), 1.83-1.76 (m, 5H), 1.58-1.55 (m, 2H), 1.31 (m, 20H), 0.93-0.90 (m, 3H). ^{13}C NMR (C_6H_6): δ 85.05 (C), 84.99 (C), 62.3 (CH), 38.7 (CH_2), 32.4 (CH_2), 31.7 (CH_2), 30.22 (CH_2), 30.17 (CH_2), 29.95 (CH_2), 29.87 (CH_2), 25.9 (CH_2), 23.2 (CH_2), 14.4 (CH_3). HRMS (ESI) m/z $C_{17}H_{34}NO$ $[M+H]^+$ = 268.2635, found = 268.2625. IR (ATR, cm^{-1}): 3359, 3285, 3088, 2920, 2848, 1466, 1319, 1067, 1005, 723.

1-Aminoheptadecan-4-ol 114

The propargyl alcohol **160** was dissolved in EtOAc (4 mL) and degassed with nitrogen (x 3). Pd/C (10%, 22 mg) was added and a hydrogen atmosphere introduced (x 3). The reaction mixture was stirred overnight and filtered though celite. The clear solution was concentrated under reduced pressure to give **114** as colourless solid (95 mg, 74%) that did not require further purification.

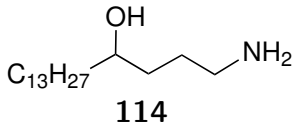

114

Melting range: 90 - 95°C. ^{1}H NMR (C_6H_6): δ 3.58-3.52 (m, 1H), 2.42-2.37 (m, 1H), 2.27-2.21 (m, 1H), 1.73-1.12 (m, 28H), 0.96-0.87 (m, 3H). ^{13}C NMR (C_6H_6): δ 71.3 (CH), 42.2 (CH_2), 38.6 (CH_2), 37.4 (CH_2), 32.4 (CH_2), 30.47 (CH_2), 30.34 (CH_2), 30.25 (CH_2), 30.23 (CH_2), 30.17 (CH_2), 29.9 (CH_2), 26.7 (CH_2), 23.2 (CH_2), 14.4 (CH_3). HRMS (ESI) m/z $C_{17}H_{37}NO$ $[M+H]^+$ = 272.2948, found = 272.2937. IR (ATR, cm^{-1}): 3354, 3281, 3175, 2916, 2850, 1560, 1471, 1074, 719.

6.2.7 Amine substitutions from cyclic carbamate 132

3-([1,1'-Biphenyl]-4-ylmethyl)-6-tridecyl-1,3-oxazinan-2-one 164

A suspension of the cyclic carbamate **132** (98 mg, 0.346 mmol), 4-(chloromethyl)-1,1'-biphenyl **165** (78 mg, 0.384 mmol, 1.1 eq), sodium hydride (20 mg, 60%, 0.500 mmol, 1.44 eqv) and a single crystal of NaI was stirred in THF (2 mL) for 90 hours at 25°C under N_2. Saturated ammonium chloride solution (approx 0.25 mL) was added and the reaction mixture was concentrated under reduced pressure. The resulting solid was triturated with $CHCl_3$ (50 mL) and the filtrate concentrated under reduced pressure to give a yellow solid (157 mg) that was purified by column chromatography to give **164** as a colourless solid (53 mg, 33%).

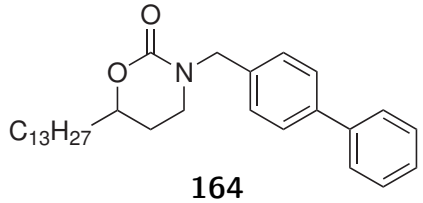

164

Melting range: 127 - 130°C. ^{1}H NMR ($CDCl_3$): δ 7.61-7.55 (m, 4H), 7.46-7.32 (m, 5H), 4.65 (d, J = 14.9 Hz, 1H), 4.56 (d, J = 14.9 Hz, 1H), 4.26-4.20 (m, 1H), 3.31-3.23 (m, 1H), 3.23-3.17

(m, 1H), 1.99-1.93 (m, 1H), 1.84-1.70 (m, 2H), 1.61-1.44 (m, 2H), 1.43-1.19 (m, 21H), 0.88 (t, J = 6.9 Hz, 3H). ^{13}C NMR ($CDCl_3$): 154.4 (C), 140.82 (C), 140.73 (C), 136.0 (C), 128.9 (CH), 128.7 (CH), 127.53 (CH), 127.47 (CH), 127.2 (CH), 77.4 (CH), 52.3 (CH_2), 44.0 (CH_2), 35.1 (CH_2), 32.1 (CH_2), 29.82 (CH_2), 29.79 (CH_2), 29.78 (CH_2), 29.69 (CH_2), 29.62 (CH_2), 29.56 (CH_2), 29.49 (CH_2), 27.4 (CH_2), 24.9 (CH_2), 22.8 (CH_2), 14.3 (CH_3). IR (ATR, cm^{-1}) 2918, 2850, 1685, 1664, 1488, 1272, 1159, 1128, 1006, 757, 699. HRMS (ESI) m/z $C_{30}H_{43}NO_2$ $[M+H]^+$ = 450.3367, found = 450.3344.

1-(([1,1'-Biphenyl]-4-ylmethyl)amino)hexadecan-3-ol 162

A mixture of the carbamate **164** (25 mg, 0.055 mmol) and $LiOH.H_2O$ (106 mg, 2.53 mmol, 45 eqv) in a H_2O:EtOH mixture (1:10, 2 mL) was heated in a sealed vessel at 150°C by microwave irradiation (0 - 400W) for 2 hours. The resulting reaction mixture was concentrated to dryness under reduced pressure. The white solid was stirred overnight in $CHCl_3$ (50 mL) and filtered. The filtrate was concentrated under reduced pressure to give a white solid (24 mg) that was purified by column chromatography [5% MeOH (saturated with NH_3) in $CHCl_3$] to give **162** as a colourless solid (20 mg, 85 %).

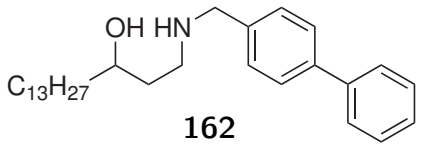

162

Melting range: 55 - 60°C. ^{1}H NMR ($CDCl_3$): δ 7.64-7.56 (m, 4H), 7.51-7.42 (m, 4H), 7.42-7.34 (m, 1H), 3.94 (d, J = 13.1 Hz, 1H), 3.87 (d, J = 13.1 Hz, 1H), 3.84-3.79 (m, 1H), 3.14-3.06 (m, 1H), 2.96-2.87 (m, 1H), 1.78-1.59 (m, 2H), 1.57-1.38 (m, 3H), 1.38-1.18 (m, 22H), 0.95-0.83 (m, 3H). ^{13}C NMR ($CDCl_3$): δ 141.0 (C), 140.7 (C), 135.4 (C), 129.4 (CH), 128.9 (CH), 127.56 (CH), 127.55 (CH), 127.2 (CH), 72.8 (CH), 52.7 (CH_2), 47.4 (CH_2), 37.9 (CH_2), 34.15 (CH_2), 34.14 (CH_2), 32.1 (CH_2), 29.83 (CH_2), 29.80 (CH_2), 29.78 (CH_2), 29.5 (CH_2), 25.8 (CH_2), 22.8 (CH_2), 14.3 (CH_3). IR (ATR, cm^{-1}) 3290, 2919, 2847, 1489, 1464, 1356, 1110, 1094, 1073, 888, 834, 762, 726, 689. HRMS (ESI) m/z $C_{29}H_{45}NO$ $[M+H]^+$ = 424.3574, found = 424.3554.

6.2.8 Amine derivatives via reductive amination

1-((3-Phenylpropyl)amino)hexadecan-3-ol 161

A mixture of 1-aminohexadecan-3-ol **109** (103 mg, 0.400 mmol), 3-phenylpropanal **163** (59 mg, 0.440 mmol, 1.10 eq) and anhydrous $MgSO_4$ (112 mg) in anhydrous DCM:THF(5:1, 5 mL) was stirred for 15 hours under N_2. The mixture was filtered and concentrated under reduced pressure. The resulting material was dissolved in EtOH (3 mL) and $NaBH_4$ (20 mg, 0.529 mmol, 1.3 eq) added and stirred under N_2 at room temperature for 24 hours. The reaction mixture was cooled to 0°C and hydrochloric acid (1 mL, 1M) added. The mixture was stirred briefly at room temperature before adjusting the pH > 7 by addition of NaOH solution (2M) and concentrated to dryness *in vacuo*. The resulting solid was triturated with $CHCl_3$ (4 x 5 mL) and concentrated under reduced pressure to give a white crystalline solid (118 mg) that was purified by column chromatography (10% $MeOH_{(Sat.\ NH_3)}$ in $CHCl_3$) to give **161** as a colourless oil (38 mg, 25%).

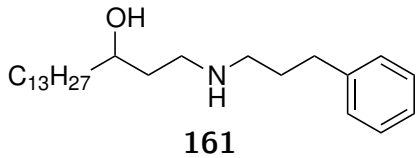

161

^{1}H NMR ($CDCl_3$): δ 7.30-7.24 (m, 2H), 7.21-7.15 (m, 3H), 3.81-3.75 (m, 1H), 3.03-2.94 (m, 1H), 2.79-2.53 (m, 5H), 1.85-1.75 (m, 2H), 1.64-1.56 (m, 1H), 1.54-1.18 (m, 26H), 0.93-0.84 (m, 3H). ^{13}C NMR ($CDCl_3$): δ 142.0 (C), 128.50 (CH), 128.49 (CH), 126.0 (CH), 73.9 (CH), 49.26 (CH_2), 49.18 (CH_2), 38.1 (CH_2), 35.1 (CH_2), 33.7 (CH_2), 32.1 (CH_2), 31.6 (CH_2), 29.93 (CH_2), 29.84 (CH_2), 29.83 (CH_2), 29.80 (CH_2), 29.79 (CH_2), 29.5 (CH_2), 25.8 (CH_2), 22.8 (CH_2), 14.3 (CH_3) IR (ATR, cm^{-1}) 3264.82, 2918.99, 2849.97, 1467.23, 1453.07, 1112.23, 1074.18, 910.37, 898.54, 742.04, 713.65, 696.87. HRMS (ESI) m/z $C_{25}H_{45}NO$ $[M+H]^+$ = 376.3574, found = 376.3557.

6.2.9 Hydroxyl methylation

(*R*/*S*)-3-Hydroxyhexadecanenitrile 166

$NaBH_4$ (70 mg, 1.85 mmol, 1.4 eq) was added to a suspension of the ketonitrile **124** (324 mg, 1.29 mmol) in EtOH (10 mL) and petroleum spirit (2 mL) at 0°C. The reaction mixture left to warm to room temperature for 15 hours, then cooled to 0°C. Saturated NH_4Cl solution (1 mL) was added and the reaction mixture was concentrated under reduced pressure. The residue was diluted in $CHCl_3$ (25 mL) and washed with hydrochloric acid (1 M, 25 mL). The aqueous phase was extracted with $CHCl_3$ (25 mL). The combined organic extracts were washed with brine (25 mL) and dried over a mixture of K_2CO_3 and $MgSO_4$. The filtrate was concentrated under reduced pressure to give a light yellow semi solid that was purified by column chromatography (DCM) to give **166** as colourless wax (231 mg, 71 %).

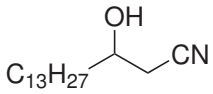

166

Melting range: 44 - 47°C. ^{1}H NMR ($CDCl_3$): δ 3.94-3.93 (m, 1H), 2.52 (dd, J = 17.1, 5.5 Hz, 2H), 2.13 (d, J = 5.2 Hz, 1H), 1.60-1.25 (m, 24H), 0.87 (t, J = 6.5 Hz, 3H). ^{13}C NMR ($CDCl_3$): δ 117.8 (C), 68.0 (CH), 36.7 (CH_2), 32.1 (CH_2), 29.81 (CH_2), 29.78 (CH_2), 29.75 (CH_2), 29.66 (CH_2), 29.61 (CH_2), 29.48 (CH_2), 29.45 (CH_2), 26.2 (CH_2), 25.5 (CH_2), 22.8 (CH_2), 14.2 (CH_3). IR (ATR, cm^{-1}): 3372, 2912, 2848, 2265, 1471, 1100, 1079, 717. HRMS (ESI) m/z $C_{16}H_{31}NO$ $[M+H]^+$ = 254.2478, found = 254.2475.

3-Methoxyhexadecanenitrile 168

Ag_2O (500 mg, 2.16 mmol) was added to a solution of **166** (198 mg, 0.781 mmol) in MeI (5 mL) and stirred in a sealed vessel for 5 days at room temperature. The reaction mixture was concentrated under a stream of nitrogen and dispersed in DCM (25 mL) and filtered. The filtrate was washed with water (25 mL), dried over magnesium sulphate and concentrated under reduced pressure to give **168** as a light yellow oil (199 mg, 95%) that was used in the following step

without further purification. An analytically pure sample was obtained by column chromatography (5% EtOAc in PS).

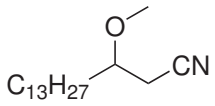

168

^{1}H NMR ($CDCl_3$): δ 3.45-3.40 (m, 4H), 2.51 (t, J = 5.3 Hz, 2H), 1.40-1.26 (m, 24H), 0.88 (t, J = 6.9 Hz, 3H). ^{13}C NMR ($CDCl_3$): δ 117.7 (C), 77.0 (CH), 57.5 (CH_3), 34.0 (CH_2), 32.1 (CH_2), 29.81 (CH_2), 29.78 (CH_2), 29.75 (CH_2), 29.68 (CH_2), 29.63 (CH_2), 29.60 (CH_2), 29.49 (CH_2), 25.1 (CH_2), 22.8 (CH_2), 22.5 (CH_2), 14.2 (CH_3). IR (ATR, cm^{-1}): 2922, 2853, 2250, 1465, 1105, 722. HRMS (ESI) m/z $C_{17}H_{33}NO$ $[M+H]^+$ = 268.2635, found = 268.2623.

3-Methoxyhexadecan-1-amine 167

$NaBH_4$(230 mg, 6.08 mmol) was added to a solution of crude **168** (153 mg, 0.572 mmol) and $CoCl_2.6H_2O$ (320 mg, 1.17 mmol) in EtOH (2 mL) at 0°C. The solution was left to stir at this temperature for 2 hours and allowed to warm to room temperature for 1 hour. Hydrochloric acid (3M, 10 mL) was added dropwise and stirred until the black precipitate dissolved. Ammonia solution (30%) was added to the reaction mixture until pH > 7 and extracted with $CHCl_3$ (3 x 25 mL). The combined extracts were washed with brine (3 x 25 mL), dried over anhydrous $MgSO_4$ and concentrated under reduced pressure to give a pink oil (146 mg) that was purified by column chromatography (10:1:89 MeOH:$NH_{3(aq)}$:$CHCl_3$) to give **167** as a yellow oil (50 mg, 32%).

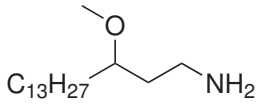

167

^{1}H NMR ($CDCl_3$): δ 3.30 (s, 3H), 3.23 (quintet, J = 5.9 Hz, 1H), 2.78 (t, J = 7.02 Hz, 2H), 1.69 (s, 3H), 1.61 (td, J = 7.0, 6.1 Hz, 2H), 1.51-1.39 (m, 3H), 1.29 (dd, J = 14.8, 7.2 Hz, 20H), 0.86 (t, J = 6.9 Hz, 3H). ^{13}C NMR ($CDCl_3$): δ 79.6 (CH), 56.5 (CH_3), 39.0 (CH_2), 37.4 (CH_2), 33.6 (CH_2), 32.1 (CH_2), 29.99 (CH_2), 29.82 (CH_2), 29.80 (CH_2), 29.78 (CH_2), 29.77 (CH_2), 29.75 (CH_2), 29.5 (CH_2), 25.3 (CH_2), 22.8 (CH_2), 14.2 (CH_3). IR (ATR, cm^{-1}) 2921.2, 2852.1, 1570.8, 1465.6, 1316.1, 819.0, 720.8. HRMS (ESI) m/z $C_{17}H_{37}NO$ $[M+H]^+$ = 272.2948, found = 272.2948.

6.3 Chapter 3 experimental

6.3.1 Phenyl analogues

3-Hydroxy-3-(phenylethynyl)hexadecanenitrile 181

A solution of *n*-BuLi (1.5 mL, 2.4 mmol, 1.3 eq) was added dropwise to a stirred solution of phenyl acetylene (270 mg, 1.54 mmol, 1.4 eq) in anhydrous THF (3.5 mL) at -84°C. The mixture was allowed to warm to room temperature before it was added dropwise to a suspension (previously stirred for 2 hours) of anhydrous cerium chloride (1.02 g $CeCl_3.7H_2O$ progressively heated to 140°C under Hi-Vac overnight, 2.74 mmol, 1.5 eqv) in THF (8 mL) at -84°C. After 30 min, a solution of the ketonitrile **124** (454 mg, 1.81 mmol, 1 eq) in anhydrous THF (5 mL) was added dropwise. The reaction mixture was held at -84°C for 5 hours before addition of sat. NH_4Cl (5 mL) and stirred overnight. The reaction mixture was concentrated under reduced pressure and hydrochloric acid (1M, 50 mL) added. The mixture was extracted with $CHCl_3$ (3 x 50 mL). The combined extracts were washed with brine (50 mL) and dried over a mixture of anhydrous K_2CO_3 and $MgSO_4$. The filtrate was concentrated under reduced pressure to give a crude yellow semi solid (803 mg) which was purified by column chromatography (75-100 % DCM in PS) to give **181** as a light yellow oil (217 mg, 34 %).

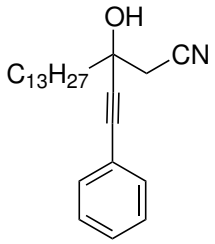

181

^{1}H NMR ($CDCl_3$): δ 7.46-7.30 (m, 5H), 2.86 (d, J = 16.4 Hz, 1H), 2.82 (d, J = 16.4 Hz, 1H), 2.59 (s, 1H), 1.89-1.85 (m, 2H), 1.64-1.57 (m, 3H), 1.40-1.26 (m, 19H), 0.88 (t, J = 6.9 Hz, 3H).^{13}C NMR ($CDCl_3$): δ 132.0 (CH), 129.1 (CH), 128.5 (CH), 121.7 (C), 116.7 (C), 88.5 (C), 86.5 (C), 69.0 (C), 41.6 (CH_2), 32.5 (CH_2), 32.1 (CH_2), 29.82 (CH_2), 29.79 (CH_2), 29.76 (CH_2), 29.67 (CH_2), 29.59 (CH_2), 29.57 (CH_2), 29.49 (CH_2), 24.5 (CH_2), 22.8 (CH_2), 14.3 (CH_3). HRMS (ESI): Molecular ion not found. IR (ATR, cm^{-1}): 3423, 2922, 2853, 2258, 1490, 1465, 1378, 1071, 756, 691.

3-Hydroxy-3-phenethylhexadecanenitrile 189

A solution of the propargyl alcohol **181** (53 mg, 0.15 mmol) in EtOAc (1.5 mL) was degassed before the addition of Pd/C (22 mg, 41 wt%). The stirred reaction mixture was exposed to a hydrogen atmosphere for 2.5 hours. The reaction was filtered though celite and concentrated under reduced pressure to give **189** as a clear oil (51 mg, 96%) that did not require further purification.

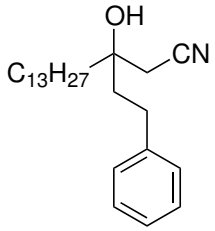

189

^{1}H NMR ($CDCl_3$): δ 7.32-7.28 (m, 2H), 7.23-7.19 (m, 3H), 2.69 (dd, J = 9.8, 7.2 Hz, 2H), 2.56 (s, 2H), 1.93 (td, J = 8.6, 4.2 Hz, 2H), 1.77 (s, 1H), 1.71-1.67 (m, 2H), 1.34-1.24 (m, 22H), 0.89 (t, J = 6.9 Hz, 3H). ^{13}C NMR ($CDCl_3$): δ 141.3 (C), 128.7 (CH), 128.4 (CH), 126.3 (CH), 117.6 (C), 73.1 (C), 41.0 (CH_2), 39.4 (CH_2), 32.1 (CH_2), 29.99 (CH_2), 29.82 (CH_2), 29.79 (CH_2), 29.75 (CH_2), 29.68 (CH_2), 29.63 (CH_2), 29.50 (CH_2), 29.49 (CH_2), 29.39 (CH_2), 23.7 (CH_2), 22.8 (CH_2), 14.3 (CH_3). IR (ATR, cm^{-1}): 3444, 2917, 2848, 2256, 1468, 1460, 751, 698. HRMS (ESI): Molecular ion not found.

1-Amino-3-(phenethyl)hexadecan-3-ol 175

A solution of the nitrile **189** (65 mg, 0.182 mmol) in anhydrous THF (1 mL) was added dropwise to a cooled suspension of $LiAlH_4$ (11 mg, 0.448 mmol) in THF (0.5 mL) at -10°C. The reaction mixture was warmed to room temperature for 1 hour and cooled on a ice bath. Water (100 µl), potassium hydroxide (10%, 100 µl) and water (100 µl) were added and stirred for 30 min. The reaction mixture was diluted with $CHCl_3$, dried over magnesium sulphate and filtered. The filtrate was concentrated under reduced pressure and purified by column chromatography (10:2:88 MeOH:TEA:$CHCl_3$) to give **175** as a yellow oil (32 mg, 49%).

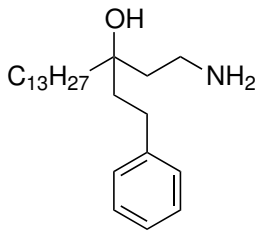

175

^{1}H NMR ($CDCl_3$): δ 7.29-7.15 (m, 5H), 3.03 (t, J = 6.1 Hz, 2H), 2.86-2.56 (m, 6H), 1.85-1.70 (m, 2H), 1.66-1.60 (m, 2H), 1.60-1.49 (m, 2H), 1.37-1.14 (m, 21H), 0.90-0.84 (m, 3H). ^{13}C NMR ($CDCl_3$): δ 143.1 (C), 128.5 (CH), 125.8 (CH), 74.8 (C), 41.5 (CH_2), 39.4 (CH_2), 32.1 (CH_2), 30.5 (CH_2), 30.2 (CH_2), 29.84 (CH_2), 29.82 (CH_2), 29.81 (CH_2), 29.5 (CH_2), 24.1 (CH_2), 22.8 (CH_2), 14.3 (CH_3). IR (ATR, cm^{-1}) 2922, 2852, 1603, 1496, 1455, 743, 697. HRMS (ESI) m/z $C_{24}H_{43}NO$ $[M+H]^+$ = 362.3417, found = 362.3418.

6.3.2 2,4-Dichlorophenyl analogues

2,4-Dichlorophenylacetelyene 191

Pyridine (28 mL, 34.6 mmol) was added dropwise to PCl_5 (8.11 g, 38.9 mmol) in an ice bath under N_2 and the mixture was allowed to warm to room temperature. 2,4-Dichloroacetophenone (7.25 g, 38.4 mmol) was added and immediately placed on a preheated oil bath at 150°C for 12.5 min and cooled to 0°C. HCl (150 mL, 3M) was added and the reaction mixture was extracted with DCM (3 x 100 mL). The extracts were washed with brine (100 mL) and dried over anhydrous $MgSO_4$. Silica was added and filtered though celite. The clear yellow solution was concentrated to give a yellow solid (4.37 g). This was recrystallised from petroleum spirit (25 mL) at -40°C and washed with ice cold petroleum spirit (5 x 5 mL) and dried under reduced pressure to give **191** as small brown crystals (2.65 g, 40%, 90% pure).

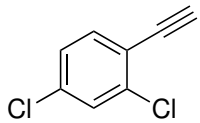

191

^{1}H NMR ($CDCl_3$): δ 7.45 (dd, J = 8.3, 0.3 Hz, 1H), 7.43 (dd, J = 2.1, 0.3 Hz, 1H), 7.21 (dd, J = 8.3, 2.1 Hz, 1H), 3.40 (s, 1H). ^{13}C NMR ($CDCl_3$): δ 137.2 (C), 135.4 (C), 134.7 (CH), 129.5 (CH), 127.1 (C), 120.8 (C), 83.5 (CH), 79.4 (C). (Matches[116])

3-((2,4-Dichlorophenyl)ethynyl)-3-hydroxyhexadecanenitrile 193

A solution of *n*-BuLi (1.45 mL, 1.6M) was added dropwise to a stirred solution of **191** (422 mg, 2.47 mmol) in anhydrous THF (4 mL) at -84°C. The solution was allowed to warm to room temperature and added dropwise to a suspension (previously stirred for 2 hours at room temp) of anhydrous cerium chloride (1.264 g $CeCl_3.7H_2O$ progressively heated to 140°C under high vacuum overnight, 3.39 mmol) in anhydrous THF (10 mL) at -84°C. After 40 min at this temperature, a solution of the ketonitrile **124** (510 mg, 2.03 mmol) in anhydrous THF (5 mL) was added and the reaction mixture stirred for 4 hours before addition of sat. NH_4Cl (10 mL). The reaction mixture was allowed to warm to room temperature and concentrated under reduced pressure. Water (50 mL) was added and extracted with DCM (3 x 75 mL). The combined extracts were washed with brine (50 mL) and dried over $MgSO_4$. The filtrate was concentrated under reduced pressure to give a crude light yellow semisolid (761 mg) which was purified by column chromatography (75-100% DCM in PS) to give **193** as a yellow oil (423 mg, 49 %).

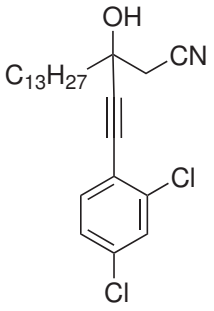

193

^{1}H NMR ($CDCl_3$): δ 7.43-7.40 (m, 2H), 7.22 (dd, J = 8.4, 2.1 Hz, 1H), 2.91-2.81 (m, 2H), 2.61 (s, 1H), 1.91-1.87 (m, 2H), 1.64-1.60 (m, 3H), 1.40-1.26 (m, 19H), 0.88 (t, J = 6.9 Hz, 3H). ^{13}C NMR ($CDCl_3$): δ 137.2 (C), 135.7 (C), 134.3 (CH), 129.5 (CH), 127.2 (CH), 120.3 (C), 116.5 (C), 94.6 (C), 82.3 (C), 69.2 (C), 41.6 (CH_2), 32.3 (CH_2), 32.1 (CH_2), 29.82 (CH_2), 29.80 (CH_2), 29.75 (CH_2), 29.64 (CH_2), 29.58 (CH_2), 29.53 (CH_2), 29.50 (CH_2), 24.5 (CH_2), 22.8 (CH_2), 14.3 (CH_3). IR (ATR, cm^{-1}) 3423, 2923, 2853, 2259, 1584, 1547, 1474, 1379, 1101, 1059, 868, 820, 772, 721. HRMS (ESI): Molecular ion not found.

3-(2,4-Dichlorophenethyl)-3-hydroxyhexadecanenitrile 194

A solution of the propargyl alcohol **193** (256 mg, 0.606 mmol) in EtOAc (2.5 mL) was degassed under reduced pressure before addition of 10% Pd/C (32 mg, 12.5% wt). The reaction mixture was stirred under a hydrogen atmosphere for 15h at

room temperature. A nitrogen atmosphere was introduced and the suspension was filtered though celite. The filtrate was concentrated under reduced pressure to give **194** as a yellow oil (256 mg, 99%) that did not require further purification.

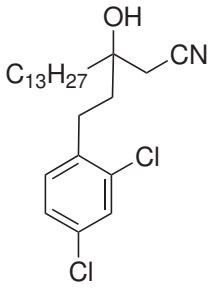

194

^{1}H NMR ($CDCl_3$): δ 7.37 (m, 1H), 7.20-7.17 (m, 2H), 2.79-2.75 (m, 2H), 2.58 (s, 2H), 1.87-1.83 (m, 2H), 1.81 (s, 1H), 1.34-1.24 (m, 24H), 0.88 (t, J = 6.9 Hz, 3H). ^{13}C NMR ($CDCl_3$): δ 137.5 (C), 134.5 (C), 132.8 (C), 131.3 (CH), 129.5 (CH), 127.5 (CH), 117.4 (C), 73.0 (C), 39.3 (CH_2), 39.1 (CH_2), 32.1 (CH_2), 29.97 (CH_2), 29.82 (CH_2), 29.79 (CH_2), 29.75 (CH_2), 29.67 (CH_2), 29.62 (CH_2), 29.50 (CH_2), 29.36 (CH_2), 27.5 (CH_2), 23.8 (CH_2), 22.8 (CH_2), 14.3 (CH_3). IR (ATR, cm^{-1}) 3466, 2920, 2851, 2254, 1470, 1455, 1049, 864, 827, 567. HRMS (ESI): Molecular ion not found.

1-Amino-3-(2,4-dichlorophenethyl)hexadecan-3-ol 190

A solution of **194** (154 mg, 0.361 mmol) in anhydrous THF (1 mL) was added dropwise to a suspension of $LiAlH_4$ (16 mg, 0.421 mmol) in anhydrous THF (1 mL) in a salt/ice bath. After 5 min, the solution was allowed to warm to room temperature for 30 min before being quenched with water (5 drops), KOH (10%, 5 drops) and water (5 drops). The mixture was stirred for 20 min before addition of DCM (70 mL) and then filtered. The filtrate was dried over $MgSO_4$ and concentrated under reduced pressure to give a yellow oil (119 mg) which was purified by column chromatography (10:2.5:87.5 MeOH:TEA:$CHCl_3$) to give the amine **190** as a yellow oil (19 mg, 12 %).

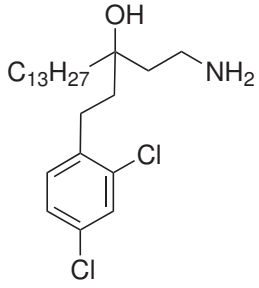

190

^{1}H NMR ($CDCl_3$): δ 7.34-7.32 (m, 1H), 7.19-7.12 (m, 2H), 3.09 (m, 1H), 2.70 (m, 2H), 1.74-1.68 (m, 4H), 1.57-1.56 (m, 2H), 1.28 (m, 23H), 0.88 (t, J = 6.9 Hz, 3H). ^{13}C NMR ($CDCl_3$): δ 139.0 (C), 134.5 (C), 132.2 (C), 131.3 (CH), 129.3 (CH), 127.3 (CH), 74.9 (C), 39.29 (CH_2), 39.14 (CH_2), 37.7 (CH_2), 37.4 (CH_2), 32.1 (CH_2), 31.1 (CH_2), 30.5 (CH_2), 29.87 (CH_2), 29.85 (CH_2), 29.84 (CH_2), 29.82

(CH_2), 29.5 (CH_2), 27.7 (CH_2), 24.1 (CH_2), 22.8 (CH_2), 14.3 (CH_3). IR (ATR, cm^{-1}) 3325, 2923, 2852, 1652, 1587, 1561, 1472, 1382, 1102, 1050, 865, 817, 721. HRMS (ESI) m/z $C_{25}H_{41}Cl_2NO$ $[M+H]^+$ = 430.2638 , found = 430.2654.

1-((2,4-Dichlorobenzyl)amino)hexadecan-3-ol 196

A mixture of 1-aminohexadecan-3-ol **109** (98 mg, 0.381 mmol), 2,4-dichlorobenzaldehyde (71 mg, 0.405 mmol, 1.06 eq) and anhydrous $MgSO_4$ (103 mg) in anhydrous DCM:THF (5:1, 5 mL) was stirred for 20 hours under nitrogen at room temperature. The reaction mixture was filtered and the filtrate concentrated under reduced pressure. The residue was dissolved in dry EtOH (6 mL) and $NaBH_4$ (21 mg, 0.555 mmol, 1.45 eq) added and stirred for 72 hours under N_2 at room temperature. HCl (1M) was added and the reaction mixture was stirred briefly at room temperature before adjusting the pH > 7 by addition of NaOH (2M) and concentration to dryness under reduced pressure. The resulting material was triturated with $CHCl_3$, filtered and the filtrate concentrated under reduced pressure to give a mixture of a clear oil and white crystalline solid (129 mg). The mixture was triturated with petroleum spirit (4 x 2 mL) and remaining solid (71 mg) was further purified by column chromatography (4% $MeOH_{(Sat.\ NH_3)}$ in $CHCl_3$) to give **196** as a colourless powder (41 mg, 26%).

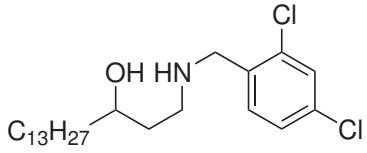

196

Melting range: 59 - 60°C. ^1H NMR ($CDCl_3$): δ 7.38 (d, J = 2.1 Hz, 1H), 7.33 (d, J = 8.2 Hz, 1H), 7.22 (dd, J = 8.2, 2.1 Hz, 1H), 3.91 (d, J = 13.9 Hz, 1H), 3.86 (d, J = 13.8 Hz, 1H), 2.99 (d, J = 1.4 Hz, 1H), 2.79 (d, J = 3.5 Hz, 1H), 1.40-1.37 (m, 5H), 1.31-1.25 (m, 24H), 0.88 (t, J = 6.8 Hz, 3H). ^{13}C NMR ($CDCl_3$): δ 134.74 (C), 134.67 (C), 134.0 (C), 131.4 (CH), 129.6 (CH), 127.4 (CH), 73.4 (CH), 50.4 (CH_2), 48.1 (CH_2), 37.9 (CH_2), 34.9 (CH_2), 32.1 (CH_2), 29.88 (CH_2), 29.84 (CH_2), 29.83 (CH_2), 29.80 (CH_2), 29.77 (CH_2), 29.5 (CH_2), 25.7 (CH_2), 22.8 (CH_2), 14.3 (CH_3). IR (ATR, cm^{-1}) 3266, 2957, 2917, 2848, 1594, 1565, 1468, 1095, 1042, 1020, 867, 836, 723. HRMS (ESI) m/z $C_{23}H_{39}Cl_2NO$ $[M+H]^+$ = 416.2481, found = 416.2669.

3,5-Dichloro-2-(((3-hydroxyhexadecyl)amino)methyl)phenol 197

A mixture of 1-aminohexadecan-3-ol **109** (102 mg, 0.397 mmol), 2,4-dichlorosalicaldehyde (76 mg, 0.398 mmol) and anhydrous $MgSO_4$ (144 mg) in anhydrous DCM:THF (5:1, 2.2 mL) was stirred for 48 hours in a sealed vessel at room temperature. The reaction mixture was filtered and the filtrate concentrated under reduced pressure. The residue was dissolved in dry EtOH (4 mL) and $NaBH_4$ added (16 mg, 0.422 mmol) added and stirred for 4 hours under N_2 at room temperature. HCl (1M) was added and the reaction mixture was stirred briefly at room temperature before adjusting the pH > 7 by addition of NaOH (2M) and concentration to dryness under reduced pressure. The resulting material was triturated with $CHCl_3$, filtered and the filtrate concentrated under reduced pressure to give a clear oil (129 mg). The oil was purified by column chromatography (6-8% $MeOH_{(Sat.\ NH_3)}$ in $CHCl_3$) to give **197** as a white powder (59 mg, 34%).

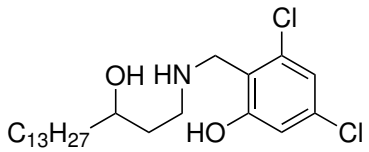

197

Melting range: 117 - 119°C. ^{1}H NMR (DMSO-d_6): δ 6.82 (d, J = 2.1 Hz, 1H), 6.62 (d, J = 2.1 Hz, 1H), 3.99 (s, 2H), 3.46-3.43 (m, 1H), 2.64 (m, 2H), 1.54-1.44 (m, 2H), 1.31-1.18 (m, 24H), 0.87-0.83 (m, 3H). ^{13}C NMR (DMSO-d_6): δ 162.2 (C), 133.0 (C), 132.4 (C), 119.1 (C), 117.0 (CH), 115.0 (CH), 68.0 (CH), 47.4 (CH_2), 45.0 (CH_2), 37.3 (CH_2), 35.8 (CH_2), 31.3 (CH_2), 29.10 (CH_2), 29.01 (CH_2), 28.98 (CH_2), 28.7 (CH_2), 25.1 (CH_2), 22.1 (CH_3). IR (ATR, cm^{-1}): 3089, 2916, 2851, 1571, 1536, 1411, 1267, 966, 816. HRMS (ESI) m/z $C_{23}H_{40}Cl_2NO_2$ $[M+H]^+$ = 432.2431, found = 432.2411.

6.3.3 4'-Fluorobiphenyl analogues

1-(4'-Fluorobiphenyl-2-yl)ethanone 204

$Pd(OAc)_2$ (113 mg, 0.503 mmol, 8.5 mol%) was added to a stirred mixture of 2-bromoacetophenone (802 µl, 5.91 mmol), 4-fluorophenylboronic acid (1.02 g, 7.31 mmol, 1.23 eqv), K_2CO_3 (2.04 g, 14.8 mmol, 2.50 eqv) and TBAB (1.97 g, 6.11 mmol, 1.03 eqv) in water (10 mL) and heated at 70°C under N_2 for 15

h. The reaction mixture was allowed to cool, diluted with water (50 mL) and extracted with EtOAc (1 x 50 mL). The extract was washed with water (3 x 10 mL) before back extracting the combined washings with EtOAc (1 x 50 mL). The combined extracts were dried over anhydrous $MgSO_4$ and concentrated under reduced pressure to give a black residue (1.48 g) that was purified by column chromatography (50 - 100% DCM in petroleum spirt) to yield **204** as a yellow oil (1.12 g, 88%). The NMR spectra match those reported.[119]

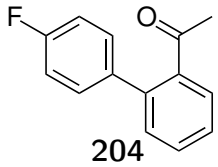

204

^{1}H NMR ($CDCl_3$): δ 7.55 (ddd, J = 7.6, 1.5, 0.5 Hz, 1H), 7.51 (td, J = 7.5, 1.5 Hz, 1H), 7.43 (dd, J = 7.5, 1.3 Hz, 1H), 7.35 (ddd, J = 7.6, 1.3, 0.5 Hz, 1H), 7.32-7.29 (m, 2H), 7.14-7.10 (m, 2H), 2.06 (s, 3H). ^{13}C NMR ($CDCl_3$): δ 204.6 (C), 164.0 (C), 161.6 (C), 140.9 (C), 139.5 (C), 136.9 (C), 130.9 (CH), 130.62 (CH), 130.54 (CH), 130.44 (CH), 128.1 (CH), 127.7 (CH), 115.9 (CH), 115.7 (CH), 30.6 (CH_3) IR (ATR, cm^{-1}) 1685, 1606, 1597, 1512, 1474, 1443, 1355, 1268, 1222, 1159, 837.5, 820, 763.

2-Ethynyl-4'-fluoro-1,1'-biphenyl 201

The acetophenone **204** (1.10 g, 5.12 mmol) was added to a mixture of PCl_5 (1.07 g, 5.13 mmol, 1.00 eq) in pyridine (10mL, 124 mmol, 24 eq). The mixture was heated using microwave irritation (0 - 400 W) for 20 min at 110°C. The dark red to brown solution was poured into a ice cold HCl solution (3M, 150 mL) and extracted with petroleum spirit (3 x 80 mL). The combined extracts were washed with brine (100 mL), dried over anhydrous $MgSO_4$. The filtrate was concentrated to give a golden oil (622 mg) that was purified by column chromatography (petroleum spirits) to give **201** as a colourless oil (503 mg, 54%).

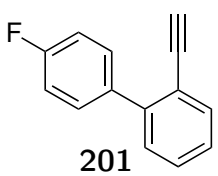

201

^{1}H NMR ($CDCl_3$): δ 7.62 (d, J = 7.7 Hz, 1H), 7.58-7.53 (m, 2H), 7.43-7.29 (m, 3H), 7.15-7.09 (m, 2H), 3.05 (s, 1H). ^{13}C NMR ($CDCl_3$): δ 163.8 (C), 161.4 (C), 143.5 (C), 136.37 (C), 136.34 (C), 134.0 (CH), 131.08 (CH), 131.00 (CH), 129.6 (CH), 129.2 (CH), 127.3 (CH), 120.6 (C), 115.2 (CH), 115.0 (CH), 83.1 (CH), 80.5 (C). IR (ATR, cm^{-1}) 3287, 3060, 2105, 1607, 1511, 1476 1442, 1220,

1158, 835, 757, 650, 618, 562.

3-((4'-Fluoro-[1,1'-biphenyl]-2-yl)ethynyl)-3-hydroxy hexadecanenitrile 205

A solution of *n*-BuLi (1.4 mL, 1.6M, 2.24 mmol, 1.11 eq) was added dropwise to a solution of the alkyne **201** (463 mg, 2.36 mmol) in anhydrous THF (3 mL) at -84°C. The solution was warmed to room temperature and added dropwise to a suspension (previously stirred for 2 hours at room temperature) of anhydrous cerium chloride (962 mg $CeCl_3.7H_2O$ progressively heated to 140°C under Hi-Vac overnight, 2.58 mmol) in anhydrous THF (8 mL) at -84°C and held at this temperature for 30 min. A solution of the ketonitrile **124** (508 mg, 2.02 mmol) in anhydrous THF (5 mL) was added and the reaction mixture was held at -84°C for 4 hours before addition of sat. NH_4Cl (10 mL). The reaction mixture was left to warm to room temperature and concentrated under reduced pressure. The reaction mixture was dissolved in HCl (1 M, 75 mL) and extracted with DCM (3 x 50 mL). The combined extracts were washed with brine (150 mL) and dried over a combination of anhydrous K_2CO_3 and $MgSO_4$. The filtrate was concentrated under reduced pressure to give a light yellow semi solid (932 mg) that was purified using column chromatography (DCM) to give **205** as a light yellow oil (198 mg, 22%).

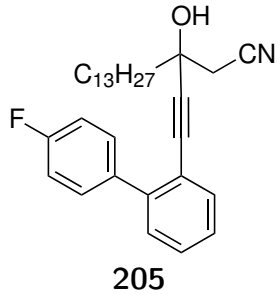

205

^{1}H NMR ($CDCl_3$): δ 7.56 (m, 1H), 7.53-7.48 (m, 2H), 7.43-7.30 (m, 3H), 7.15-7.09 (m, 2H), 2.71 (d, J = 16.4 Hz, 1H), 2.67 (d, J = 16.4 Hz, 1H), 1.75-1.67 (m, 2H), 1.40-1.19 (m, 23H), 0.90-0.86 (m, 3H). ^{13}C NMR ($CDCl_3$): δ 163.8 (C), 161.4 (C), 143.5 (C), 136.46 (C), 136.43 (C), 133.4 (CH), 131.08 (CH), 131.00 (CH), 129.55 (CH), 129.42 (CH), 127.4 (CH), 120.2 (C), 116.6 (C), 115.2 (CH), 115.0 (CH), 91.4 (C), 86.0 (C), 69.0 (C), 41.6 (CH_2), 32.3 (CH_2), 32.1 (CH_2), 29.84 (CH_2), 29.80 (CH_2), 29.77 (CH_2), 29.70 (CH_2), 29.61 (CH_2), 29.58 (CH_2), 29.51 (CH_2), 24.4 (CH_2), 22.8 (CH_2), 14.3 (CH_3). IR (ATR, cm^{-1}) 3432, 2923, 2853, 2258, 1606, 1514, 1479, 1223, 1159, 1094, 837, 759. HRMS (ESI): Molecular ion not found.

3-(2-(4'-Fluoro-[1,1'-biphenyl]-2-yl)ethyl)-3-hydroxy hexadecanenitrile 208

A stirred solution of the alkyne **205** (176 mg, 0.394 mmol) was dissolved in EtOAc (3 mL) and degassed prior to addition of Pd/C (5%w/w, 20 mg). The mixture was stirred under a hydrogen atmosphere (x 3) for 15 hours at room temperature and filtered though celite. The filtrate was concentrated under reduced pressure to give **208** as a white waxy solid (172 mg, 96 %) that did not require further purification.

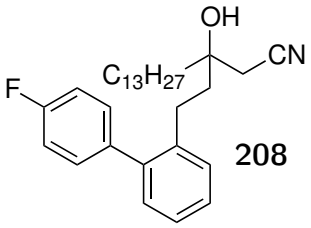

208

^{1}H NMR ($CDCl_3$): δ 7.32-7.23 (m, 5H), 7.18 (d, J = 7.4, 1H), 7.14-7.09 (m, 2H), 2.62 (dd, J = 10.2, 7.0 Hz, 2H), 2.36 (s, 2H), 1.69 (m, 2H), 1.48-1.43 (m, 2H), 1.31-1.18 (m, 21H), 1.09-1.07 (m, 2H), 0.90-0.87 (m, 3H). ^{13}C NMR ($CDCl_3$): δ 163.4 (C), 161.0 (C), 140.9 (C), 138.8 (C), 137.57 (C), 137.53 (C), 130.92 (CH), 130.84 (CH), 130.4 (CH), 129.6 (CH), 128.1 (CH), 126.4 (CH), 117.4 (C), 115.5 (CH), 115.2 (CH), 72.9 (C), 40.7 (CH_2), 38.9 (CH_2), 32.1 (CH_2), 29.97 (CH_2), 29.84 (CH_2), 29.81 (CH_2), 29.76 (CH_2), 29.73 (CH_2), 29.59 (CH_2), 29.51 (CH_2), 29.3 (CH_2), 27.3 (CH_2), 23.5 (CH_2), 22.8 (CH_2), 14.3 (CH_3). IR (ATR, cm^{-1}) 3476, 2922, 2852, 2252, 1512, 1482, 1469, 1220, 1159, 837, 766, 724. HRMS (ESI): Molecular ion not found.

1-Amino-3-(2-(4'-fluoro-[1,1'-biphenyl]-2-yl)ethyl)hexadecan-3-ol 199

$NaBH_4$ (127 mg, 3.36 mmol) was added to a solution of crude nitrile **208** (153 mg, mmol) and $CoCl_2.6H_2O$ (179 mg, 0.653 mmol) in EtOH (3 mL) at 0°C. The reaction mixture was stirred for 1 hour at room temperature before addition of HCl solution (1M, 10mL). The mixture was made alkaline by addition of concentrated ammonia solution (5 mL) and concentrated to dryness under reduced pressure. The residue was triturated with chloroform (5 x 20 mL) and the filtrate concentrated to give a crude brown oil (107 mg) that was purified by column chromatography (5-10% MeOH, 1% TEA in $CHCl_3$) to give **199** as a waxy white solid (19 mg, 12%).

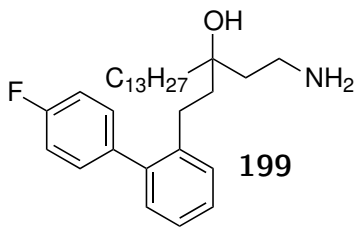

199

^{1}H NMR ($CDCl_3$): δ 7.32-7.03 (m, 8H), 2.97-2.83 (m, 2H), 2.63-2.46 (m, 2H), 1.66-1.41 (m, 4H), 1.39-1.08 (m, 23H), 1.01-0.91 (m, 2H), 0.92-0.84 (m, 3H). ^{13}C NMR ($CDCl_3$): 163.3 (C), 160.9 (C), 140.9 (C), 140.3 (C), 137.90 (C), 137.86 (C), 130.97 (CH), 130.89 (CH), 130.2 (CH), 129.7 (CH), 127.9 (CH), 125.9 (CH), 115.2 (CH), 115.0 (CH), 74.9 (C), 40.9 (CH_2), 38.9 (CH_2), 37.5 (CH_2), 37.1 (CH_2), 32.1 (CH_2), 30.4 (CH_2), 29.92 (CH_2), 29.87 (CH_2), 29.85 (CH_2), 29.83 (CH_2), 29.82 (CH_2), 29.5 (CH_2), 27.6 (CH_2), 23.7 (CH_2), 22.8 (CH_2), 14.3 (CH_3). HRMS (ESI) m/z $C_{30}H_{46}FNO$ $[M+H]^+$ = 456.3636, found = 456.3633. IR (ATR, cm^{-1}): 3150.0, 3140, 2923, 2853, 1512, 1221, 1157, 1091, 1091, 1008, 837. 759.

6.3.4 4'-Fluoro-2,4-dichlorobiphenyl analogues

2,4-Dichlorobenzaldehyde *O*-methyl oxime 209[120]

2,4-Dichlorobenzaldehyde (1.31 g, 7.49 mmol) was added to a solution of methoxy amine hydrochloride (0.75 g, 8.98 mmol, 1.2 eq) and pyridine (2.4 mL, 2.35 g, 29.8 mmol, 4.0 eq) in dry DCM (15 mL). The solution was stirred at room temperature for 2 hours and concentrated to dryness. The reaction mixture was filtered though a plug of silica and the residue washed with DCM until the filtrate was no longer active under UV to TLC. The filtrate was concentrated under reduced pressure to give 2,4-dichlorobenzaldehyde-*O*-methyloxime **209** as a colourless crystalline solid (1.48 g, 97 %, 96:4 E:Z). The NMR spectra were identical to those reported.[120]

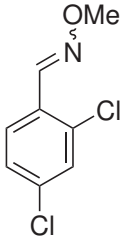

209

^{1}H NMR ($CDCl_3$): δ 8.41 (s, 1H), 7.83 (d, J = 8.5 Hz, 1H), 7.39 (d, J = 2.1 Hz, 1H), 7.24 (ddd, J = 8.5, 2.1, 0.7 Hz, 1H), 4.00 (s, 3H). ^{13}C NMR ($CDCl_3$): δ 144.8, 136.2, 134.4, 129.8, 128.8, 128.0, 127.6, 62.5.

2-Bromo-4,6-dichlorobenzaldehyde *O*-methyl oxime[120]

2,4-Dichlorobenzaldehyde *O*-methyloxime **209** (5.95 g, 29.2 mmol), NBS (10.57 g, 59.4 mmol, 2.0 eq), acetic acid (1.68 mL, 29.37, 1.0 eq), silver trifluoroacetate (657 mg, 2.97 mmol, 0.10 eq) and palladium acetate (660 mg, 2.94 mmol, 0.10 eq) were suspended in DCE (60 mL) and heated in a sealed vessel at 120°C for 24 hours. The reaction mixture was allowed to cool and filtered. The residue was washed with DCM (200 mL). The combined filtrates were washed with water (2 x 100 mL). The aqueous phase was back extracted with DCM (50 mL). The combined extracts were washed with brine (1 x 50mL), dried over anhydrous $MgSO_4$ and concentrated under reduced pressure onto silica. The crude/silica mixture was subjected to column chromatography (10 - 25% DCM in PS) to give 2-bromo-4,6-dichlorobenzaldehyde *O*-methyl oxime as colourless crystalline solid (5.56 g, 67 %, **308**:**309**, E:Z, 2:1). he NMR spectra were identical to those reported.[120]

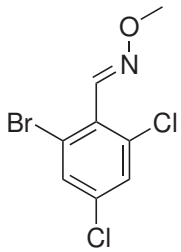

308 *E*

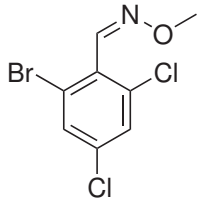

309 *Z*

^{1}H NMR ($CDCl_3$) (*E*): δ 8.15 (s, 1H), 7.56 (d, J = 2.0 Hz, 1H), 7.41 (d, J = 2.0 Hz, 1H), 4.02 (s, 3H). ^{13}C NMR ($CDCl_3$): δ 145.1 (CH), 135.55 (C), 135.47 (C), 131.8 (CH), 129.43 (CH), 129.30 (C), 124.6 (C), 62.7, (CH_3).^{1}H NMR ($CDCl_3$): (*Z*) δ 7.52 (d, J = 1.9 Hz, 1H), 7.39 (d, J = 1.9 Hz, 1H), 7.36 (s, 1H), 3.94 (s, 3H). ^{13}C NMR ($CDCl_3$): δ 142.4 (CH), 135.7 (C), 134.3 (C), 130.95 (CH), 130.91 (C), 128.6 (CH), 122.8 (C), 62.6 (CH_3). (Matches[120])

3,5-Dichloro-4'-fluoro-[1,1'-biphenyl]-2-carbaldehyde *O*-methyl oxime 212

A mixture of 2-bromo-4,6-dichlorobenzaldehyde *O*-methyl oxime (141 mg, 0.5 mmol, 2:1 **308**:**309**), 4-fluorophenylboronic acid (85 mg, 0.607 mmol, 1.2 eqv), K_2CO_3 (211 mg, 1.526 mmol, 3.1 eqv), TBAB (155 mg, 0.481 mmol, 1 eqv), $Pd(OAc)_2$ (16 mg, 14 mol%) in water (2.5 mL) was stirred at 70°C for 15 hours. The reaction mixture was allowed to cool, diluted with EtOAc (10 mL) and

washed with water (3 x 10 mL). The aqueous phase was back extracted with EtOAc (5 mL) and the combined extracts were dried over anhydrous $MgSO_4$. The filtrate was concentrated under reduced pressure to give a brown solid (160 mg) that was purified by column chromatography (10% DCM in PS) to give **212** as a colourless oil (29 mg, 19 %).

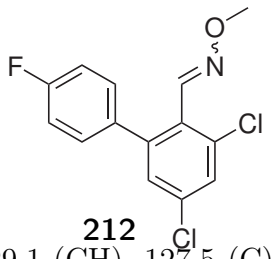

212

^{1}H NMR ($CDCl_3$): δ 8.02 (s, 1H), 7.48 (d, J = 2.1 Hz, 1H), 7.28-7.23 (m, 3H), 7.13-7.09 (m, 2H), 3.79 (s, 3H). ^{13}C NMR ($CDCl_3$): δ 163.9 (C), 161.4 (C), 145.1 (CH), 144.3 (C), 135.18 (C), 135.12 (C), 135.08 (C), 134.97 (C), 131.36 (CH), 131.28 (CH), 129.3 (CH), 129.1 (CH), 127.5 (C), 115.4 (CH), 115.2 (CH), 62.2 (CH_3). HRMS (ESI) m/z $C_{14}H_{10}Cl_2FNO$ $[M+H]^+$ = 298.0196, found = 298.0190.

2-Bromo-4,6-dichlorobenzaldehyde 214[120]

A solution the 2-bromo-4,6-dichlorobenzaldehyde *O*-methyl oxime (298 mg, 1.06 mmol), *p*-toluenesulfonic acid (385 mg, 2.24 mmol, 2.1 eq) and formaldehyde (1.2 mL, 35% in water, 420 mg, 14 mmol) in THF:H_2O (10:1, 4.1 mL) was heated under microwave irradiation (0 - 400 W) at 100°C for 1h. The crude reaction mixture was concentrated on to a small amount of silica and purified using column chromatography (35 % DCM in PS) to give **214** as yellow crystals (273 mg, 100%).

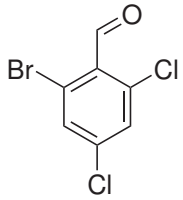

214

^{1}H NMR ($CDCl_3$): δ 10.32 (t, J = 0.3 Hz, 1H), 7.63 (dd, J = 1.9, 0.3 Hz, 1H), 7.47 (dd, J = 2.0, 0.3 Hz, 1H).^{13}C NMR ($CDCl_3$): δ 189.0, 139.5, 137.6, 133.1, 130.6, 130.0, 125.6.

2-(4'-Fluorophenyl)-4,6-dichlorobenzaldehyde 210

A mixture of 6-bromo-2,4-dichlorobenzaldehyde **214** (4.45 g, 17.69 mmol), 4-fluorophenylboronic acid (2.72 g, 19.44 mmol, 1.10), TBAB (0.379 g, 1.798 mmol,

0.102 eq), K_2CO_3 (3.01 g, 21.81 mmol, 1.232 eq) and $Pd(OAc)_2$ (226 mg, 1.518 mmol, 8.6 mol%) was stirred under N_2 at room temperature. After 16 hours, a second addition of $Pd(OAc)_2$ (115 mg) was required after monitoring the reaction by NMR showed a incomplete reaction. The reaction mixture was left to stir at room temperature for a total of 130 hours before concentrating under a stream of nitrogen. The residues were dissolved in toluene (150 mL) and washed with water (75 mL). The aqueous phase was extracted with toluene (50 mL) and the combined organic phases washed with HCl (1M, 100 mL), $NaHCO_3$ (5%, 100 mL) and brine (100 mL) before being dried with anhydrous $MgSO_4$. The filtrate was concentrated under a stream of nitrogen overnight to give a yellow/brown solid (4.64 g) that was purified by column chromatography (20-35% DCM in PS) to yield **210** as a yellow solid (3.38 g, 67%).

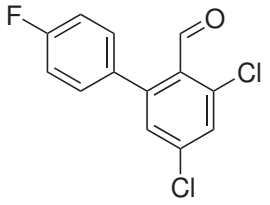

210

^{1}H NMR ($CDCl_3$): δ 10.05 (s, 1H), 7.51 (d, J = 2.0 Hz, 1H), 7.28 (d, J = 2.0 Hz, 1H), 7.28-7.23 (m, 2H), 7.16-7.12 (m, 2H). Matches[80] ^{13}C NMR ($CDCl_3$): δ 189.8 (CH), 164.4 (C), 161.9 (C), 146.5 (C), 138.6 (C), 136.3 (C), 133.04 (C), 133.01 (C), 131.25 (CH), 131.17 (CH), 130.30 (C), 130.17 (CH), 130.02 (CH), 115.9 (CH), 115.7 (CH).

3,5-Dichloro-2-(2,2-dibromovinyl)-4'-fluoro-1,1'-biphenyl 221

A solution of the aldehyde **210** (3.63 g, 13.45 mmol) and CBr_4 (9.41 g, 28.37 mmol, 2.1 eq) in anhydrous DCM (30 mL) was added dropwise to a stirred solution of triethyl phosphite (9.6 mL, 56.0 mmol, 4.2 eq) in anhydrous DCM (3.5 mL) at -45°C. The temperature was maintained for 90 min and TLC showed consumption of **210**. The reaction mixture was poured onto an iced saturated $NaHCO_3$ solution and extracted with DCM (2 x 50 mL). The combined extracts were washed with $NaHCO_3$ (Sat. 1 x 60 mL, 5% 1 x 60 mL) and brine (1 x 60 mL) before being concentrated under reduced pressure. The resulting material was purified using column chromatography (PS) to give **221** as a colourless oil (3.78 g, 64%).

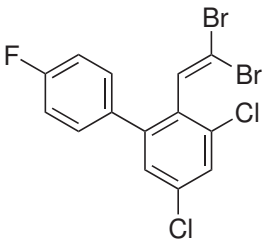

221

^{1}H NMR ($CDCl_3$): δ 7.44 (d, J = 2.1 Hz, 1H), 7.30-7.26 (m, 2H), 7.24 (d, J = 2.1 Hz, 1H), 7.22 (s, 1H), 7.14-7.09 (m, 2H). ^{13}C NMR ($CDCl_3$): δ 164.1 (C), 161.6 (C), 143.4 (C), 134.91 (C), 134.88 (C), 134.6 (C), 134.0 (CH), 132.5 (C), 130.81 (CH), 130.73 (CH), 128.8 (CH), 128.5 (CH), 115.7 (CH), 115.5 (CH), 96.4 (C). HRMS (ESI): Molecular ion not found. IR (ATR, cm^{-1}): 1603, 1576, 1546, 1508, 1435, 1380, 1224, 1158, 1096, 1055, 886, 824.

3,5-Dichloro-2-ethynyl-4'-fluoro-1,1'-biphenyl 206

A solution of **221** (3.73 g, 8.79 mmol) in dry toluene (25 mL) was added dropwise to a solution of potassium *tert*-amylate (5 mL, 25 % in Tol.) at 0°C over 25 min. The reaction mixture was stirred at 0°C for 90 min before addition of methanol (1.8 mL). A sample was removed and a aqueous workup isolated the intermediate **222**. Dimethyl phosphite (1.1 mL, 12.0 mmol, 1.4 eqv) and potassium *tert*-amylate (4.9 mL, 8.44 mmol, 1.0 eqv) were sequentially added and the reaction mixture held at 0°C for 45 min before being poured onto saturated NH_4Cl solution (35 mL). The reaction mixture was diluted with toluene (60 mL) and washed with water (2 x 30 mL), $NaHCO_3$ solution (saturated 2 x 30 mL, 5% 2 x 30 mL) and brine (2 x 30 mL). The organic phase was dried over $MgSO_4$ and concentrated under reduced pressure to give a light blue solid (2.31 g) that was purified by column chromatography (PS) to give **206** as a colourless solid (2.23 g, 96%).

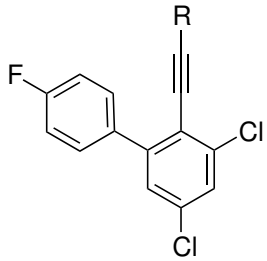

R= H **206**

R= Br **222**

206: Melting range: 105 - 106 °C. ^{1}H NMR ($CDCl_3$): δ 7.53-7.48 (m, 2H), 7.44 (d, J = 2.1 Hz, 1H), 7.24 (d, J = 2.1 Hz, 1H), 7.15-7.09 (m, 2H), 3.37 (s, 1H). ^{13}C NMR ($CDCl_3$): δ 164.2 (C), 161.8 (C), 146.7 (C), 138.5 (C), 134.85 (C), 134.66 (C), 134.62 (C), 131.03 (CH), 130.95 (CH), 128.2 (CH), 119.5 (C), 115.4 (CH), 115.2 (CH), 87.1 (C), 78.7 (CH). HRMS (ESI): Molecular ion not found. IR (ATR, cm^{-1}): 3285, 1601, 1577, 1543, 1507, 1431, 1410, 1382, 1220, 1159, 1101, 1054, 847, 828, 695.

222: ^{1}H NMR ($CDCl_3$): δ 7.55-7.48 (m, 2H), 7.47-7.43 (m, 1H), 7.26-7.25 (m, 1H), 7.22-7.12 (m, 2H). ^{13}C NMR ($CDCl_3$): δ 164.3 (C), 161.8 (C), 146.7 (C), 138.6 (C), 134.66 (C), 134.57 (C), 134.54 (C), 130.92 (CH), 130.84 (CH), 128.15 (CH), 128.10 (CH), 120.0 (C), 115.5 (CH), 115.3 (CH), 75.8 (C), 59.7 (C).

3-((3,5-Dichloro-4'-fluoro-[1,1'-biphenyl]-2-yl)ethynyl)-3-hydroxyhexadecanenitrile 207

n-BuLi (3.55 mL, 1.6M, 5.70 mmol) was added to a solution of **206** (1.51 g, 5.70 mmol) in THF (12 mL) at -84°C and allowed to warm to room temperature. After 5 min, the solution was added dropwise to a suspension (previously stirred for 2 hours at room temp) of anhydrous cerium chloride (2.30 g $CeCl_3.7H_2O$ progressively heated to 140°C for 2 hours, 6.18 mmol) in anhydrous THF (18 mL) at -84°C under N_2. After 30 min, a solution of the ketonitrile **124** (1.21 g, 4.75 mmol) in THF (5 mL) was added and reaction mixture was held at -84°C for 4 hours before dropwise addition of saturated NH_4Cl solution (10 mL). The reaction mixture was allowed to warm to room temperature and concentrated under a stream of nitrogen. The residue was dissolved in DCM (100 mL) and washed with hydrochloric acid (1M, 100 mL). The washings were back extracted with DCM (2 x 50 mL). The combined extracts were washed with brine (200 mL) before being dried over anhydrous $MgSO_4$ and concentrated under reduced pressure. The resulting residue was purified by column chromatography (75 - 100% DCM in PS) to give **207** as a light blue oil (1.33 g, 65%).

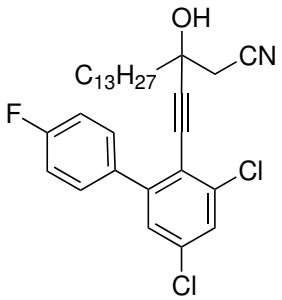

207

^{1}H NMR ($CDCl_3$): δ 7.50-7.45 (m, 2H), 7.44 (d, J = 2.1 Hz, 1H), 7.25 (d, J = 2.1 Hz, 1H), 7.17-7.12 (m, 2H), 2.69 (d, J = 0.7 Hz, 2H), 1.75-1.71 (m, 2H), 1.39-1.26 (m, 23H), 0.88 (t, J = 6.9 Hz, 3H).^{13}C NMR ($CDCl_3$): δ 164.3 (C), 161.8 (C), 146.5 (C), 138.2 (C), 135.2 (C), 134.69 (C), 134.66 (C), 131.02 (CH), 130.94 (CH), 128.26 (CH), 128.14 (CH), 119.2 (C), 116.3 (C), 115.6 (CH), 115.4 (CH), 97.7 (C), 81.7 (C), 69.2 (C), 41.4 (CH_2), 32.1 (CH_2), 29.83 (CH_2), 29.80 (CH_2), 29.75 (CH_2), 29.66 (CH_2), 29.58 (CH_2), 29.53 (CH_2), 29.50 (CH_2), 24.3 (CH_2), 22.8 (CH_2),

14.3 (CH_3). IR (ATR, cm^{-1}): 3432, 2923, 2853, 2261, 1605, 1510, 1226, 1159, 1059, 836, 786. HRMS (ESI): Molecular ion not found.

Z-3-(2-(3,5-Dichloro-4'-fluoro-[1,1'-biphenyl]-2-yl)vinyl)-3-hydroxyhexadecanenitrile 223

A solution of **207** (460 mg, 0.891 mmol) in EtOAc (3 mL) was degassed under reduced pressure and placed under N_2 (x 3). Pd/C (97 mg, 10%) was added and a hydrogen atmosphere introduced (x 3). The reaction mixture was rapidly stirred for 4 days and placed under a nitrogen atmosphere. The reaction mixture was filtered though celite and the filtrate concentrated under reduced pressure to give **223** as a golden oil (458 mg, 99%) that did not require further purification.

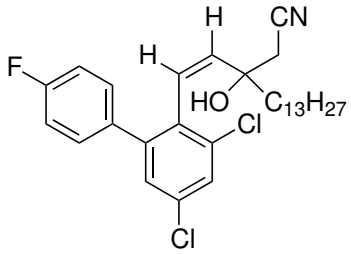

223

^{1}H NMR ($CDCl_3$): δ 7.41 (dd, J = 9.6, 2.1 Hz, 1H), 7.34-7.29 (m, 2H), 7.22 (apparent t, J = 2.2 Hz, 1H), 7.15-7.07 (m, 2H), 6.47 (d, J = 12.5 Hz, 1H), 5.53 (apparent d, J = 28.2, 12.5 Hz, 1H), 2.48-2.39 (m, 1H), 1.69 (s, 1H), 1.61-1.02 (m, 26H), 0.89 (td, J = 6.8, 2.4 Hz, 3H), 0.78-0.72 (m, 1H). ^{13}C NMR ($CDCl_3$): δ 163.9 (C), 161.42 (C), 161.40 (C), 143.2 (C), 142.7 (C), 136.02 (C), 135.98 (C), 135.77 (C), 135.74 (C), 135.3 (CH), 135.0 (CH), 134.08 (C), 134.04 (C), 133.87 (C), 133.77 (C), 133.4 (C), 131.56 (CH), 131.48 (CH), 131.32 (CH), 131.23 (CH), 128.48 (CH), 128.44 (CH), 128.2 (CH), 128.0 (CH), 126.6 (CH), 126.3 (CH), 116.90 (C), 116.78 (C), 115.78 (CH), 115.59 (CH), 115.56 (CH), 115.38 (CH), 74.6 (C), 40.7 (CH_2), 40.0 (CH_2), 32.1 (CH_2), 29.88 (CH_2), 29.83 (CH_2), 29.79 (CH_2), 29.78 (CH_2), 29.70 (CH_2), 29.60 (CH_2), 29.56 (CH_2), 29.50 (CH_2), 28.5 (CH_2), 23.5 (CH_2), 23.1 (CH_2), 22.8 (CH_2), 14.3 (CH_3). IR (ATR, cm^{-1}): 3467, 2923, 2852, 2252, 1605, 1510, 1378, 1225, 1159, 1102, 1053, 840, 816. HRMS (ESI): Molecular ion not found.

3-(2-(3,5-Dichloro-4'-fluoro-[1,1'-biphenyl]-2-yl)ethyl)-3-hydroxyhexadecanenitrile 224

A solution of **223** (884 mg, 1.71 mmol) in EtOAc (8 mL) was degassed under reduced pressure and placed under N_2 (x 3). 10% Pd/C (1.02 g) was added. The reaction mixture was heated at reflux under H_2 for 3 hours and allowed to cool. A N_2 atmosphere was introduced and the reaction mixture filtered though celite. The filtrate was concentrated under reduced pressure to give an oil (717 mg) that was purified by column chromatography (Column 1: 10% EtOAc in PS, Column 2: 75 - 100% DCM in PS) to give the starting material (515 mg) and **224** as a colourless oil (44 mg, 5%).

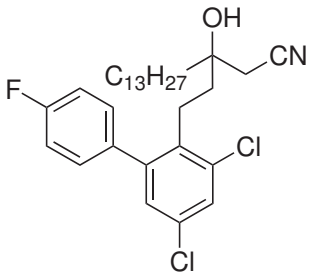

224

^{1}H NMR ($CDCl_3$): δ 7.40 (d, J = 2.2 Hz, 1H), 7.25-7.21 (m, 2H), 7.16-7.11 (m, 2H), 7.10 (d, J = 2.2 Hz, 1H), 2.67 (td, J = 8.7, 6.9 Hz, 2H), 2.37 (d, J = 3.7 Hz, 2H), 1.67-1.63 (m, 2H), 1.55 (s, 2H), 1.49-1.43 (m, 2H), 1.32-1.21 (m, 19H), 1.11-1.06 (m, 2H), 0.88 (t, J = 6.9 Hz, 3H). ^{13}C NMR ($CDCl_3$): δ 163.8 (C), 161.3 (C), 144.2 (C), 135.76 (C), 135.73 (C), 135.62 (C), 135.4 (C), 132.2 (C), 130.67 (CH), 130.59 (CH), 129.10 (CH), 128.92 (CH), 117.3 (C), 115.8 (CH), 115.6 (CH), 72.8 (C), 38.6 (CH_2), 38.1 (CH_2), 32.1 (CH_2), 29.95 (CH_2), 29.83 (CH_2), 29.79 (CH_2), 29.74 (CH_2), 29.71 (CH_2), 29.57 (CH_2), 29.50 (CH_2), 29.3 (CH_2), 24.7 (CH_2), 23.5 (CH_2), 22.8 (CH_2), 14.3 (CH_3). IR (ATR, cm^{-1}): 3485, 2923, 2852, 2251, 1605, 1552, 1508, 1390, 1222, 1158, 862, 839. HRMS (ESI): Molecular ion not found.

1-Amino-3-(2-(3,5-dichloro-4'-fluoro-[1,1'-biphenyl]-2-yl)ethyl) hexadecan-3-ol 229

$NaBH_4$ (20 mg, 0.528 mmol) was added to a solution of **224** (20 mg, 0.038 mmol) and $CoCl_2.6H_2O$ (22 mg, 0.080 mmol) in EtOH (0.5 mL) at 0°C. The reaction mixture was held at this temperature for 1 hour and then allowed to warm to room temperature for 1 hour. HCl (1M, 0.5 mL) was added and stirred at room temperature until the reaction mixture became clear. Concentrated NH_3

solution (1 mL) and water (4 mL) were added and the mixture extracted with $CHCl_3$ (5 x 3 mL). The combined extracts were dried over anhydrous $MgSO_4$ and concentrated under reduced pressure to give an oil (18 mg) that was purified by column chromatography (3 - 5 % MeOH, 1% $NH_{3(aq)}$ in $CHCl_3$) to afford **229** as a colourless oil (9 mg, 45%).

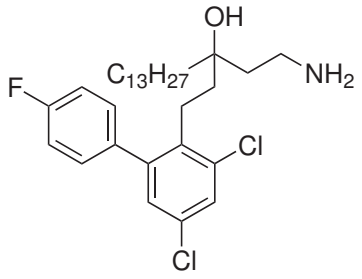

229

^{1}H NMR ($CDCl_3$): δ 7.37 (d, J = 2.2 Hz, 1H), 7.26-7.20 (m, 2H), 7.10 (m, 2H), 7.07 (d, J = 2.2 Hz, 1H), 2.92-2.77 (m, 4H), 2.73-2.52 (m, 3H), 1.57-1.38 (m, 5H), 1.38-1.08 (m, 24H), 1.08-0.92 (m, 3H), 0.93-0.85 (m, 3H). ^{13}C NMR ($CDCl_3$): δ 163.7 (C), 161.3 (C), 144.1 (C), 137.2 (C), 136.14 (C), 136.11 (C), 135.4 (C), 131.5 (C), 130.82, 130.74, 128.96, 128.78, 115.63, 115.54, 115.3, 74.7 (C), 39.1 (CH_2), 38.19 (CH_2), 38.12 (CH_2), 37.6 (CH_2), 32.1 (CH_2), 30.5 (CH_2), 29.87 (CH_2), 29.85 (CH_2), 29.84 (CH_2), 29.82 (CH_2), 29.78 (CH_2), 29.5 (CH_2), 25.2 (CH_2), 23.5 (CH_2), 22.9 (CH_2), 14.3 (CH_3). IR (ATR, cm^{-1}): 3349, 2922, 2851, 1605, 1508, 1390, 1221, 1159, 838. HRMS (ESI) m/z $C_{30}H_{44}Cl_2FNO$ $[M+H]^+$ = 524.2857, found = 524.2860.

1-(((3,5-Dichloro-4'-fluoro-[1,1'-biphenyl]-2-yl)methyl)amino) hexadecan-3-ol 235

A mixture of the amine **109** (98 mg, 0.381 mmol), benzaldehyde **210** (110 mg, 0.409 mmol, 1.1 eq) and $MgSO_4$ (126 mg) was suspended in anhydrous DCM (2 mL) and stirred for 48 hours in a sealed vessel at 50 °C. The filtrate was concentrated under reduced pressure and dissolved in EtOH (4 mL). $NaBH_4$ (15 mg) was added and stirred for 3 hours before addition of saturated NH_4Cl solution. K_2CO_3 solution (5%) was added until pH > 7 and extracted with $CHCl_3$ (3 x 25 mL). The extracts were dried with anhydrous $MgSO_4$ and concentrated under reduced pressure to give a crude colourless oil (148 mg) that was purified by column chromatography (1% MeOH $_{(Sat.\ NH_3)}$ in $CHCl_3$) to give **235** as a colourless oil (50 mg, 26%).

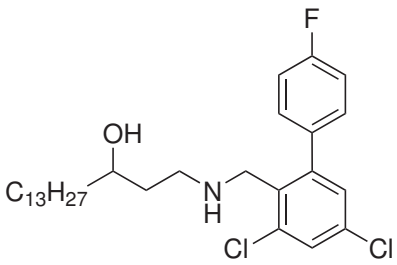

235

^{1}H NMR ($CDCl_3$): δ 7.41 (ad, J = 2.0 Hz, 1H), 7.34-7.29 (m, 2H), 7.17-7.11 (m, 3H), 3.77-3.66 (m, 3H), 2.82 (m, 1H), 2.58 (m, 1H), 1.60-1.53 (m, 1H), 1.47-1.15 (m, 27H), 0.91-0.83 (m, 3H). ^{13}C NMR ($CDCl_3$): δ 164.0 (C), 161.5 (C), 145.0 (C), 136.2 (C), 135.3 (C), 133.6 (C), 133.1 (C), 130.88 (CH), 130.80 (CH), 129.2 (CH), 128.9 (CH), 115.8 (CH), 115.5 (CH), 73.3 (CH), 48.4 (CH_2), 47.9 (CH_2), 37.8 (CH_2), 35.0 (CH_2), 32.1 (CH_2), 29.90 (CH_2), 29.83 (CH_2), 29.80 (CH_2), 29.79 (CH_2), 29.5 (CH_2), 25.7 (CH_2), 22.8 (CH_2), 14.3 (CH_3). IR (ATR, cm^{-1}): 3239, 3341, 2915, 2849, 1606, 1509, 1471, 1225, 1090, 836. HRMS (ESI) m/z $C_{29}H_{42}FNO$ $[M+H]^+$ = 510.2700, found = 510.2683.

6.3.5 Fluvastatin analogues

2-Bromo-4´-fluoroacetophenone 239

Method A

Bromine (17.5 g, 109.5 mmol) was added to a solution of 4'-fluoroacetophenone (15.01 g, 108 mmol) in $CHCl_3$ (150 mL) and stirred for 1.5h at room temperature. The reaction mixture was washed with 2% sodium metabisulphite solution (150 mL), sat. $NaHCO_3$ solution (150 mL) and water (100 mL). The organic phase was dried with anhydrous $MgSO_4$ and concentrated under reduced pressure to give a semi solid (23.1 g). ^{1}H NMR analysis on the crude showed a mixture of mono-brominated product, di-brominated product and the starting material (84:9:7). The crude material was purified by column chromatography in batches (20-50 % DCM in PS) to give a colourless solid (18.1 g, 77 %). The NMR spectra were identical to those reported.[179]

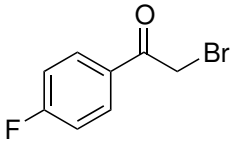

239

Melting point: 48.9°C (Lit. 48-49[133]). ^{1}H NMR (400HMz, $CDCl_3$) 8.05 – 8.00 (2 H, m), 7.2 – 7.14 (2 H, m), 4.41 (2 H, s). ^{13}C NMR ($CDCl_3$): δ 190.0, 166.3, 131.8, 130.5, 116.2, 30.5. IR (ATR, cm^{-1}) 2954, 1693, 1593, 1503, 1411, 1392, 1300, 1281, 1235, 1194, 1156, 1100, 995, 820.

Method B[135]

A solution of bromine (11.74 g, 73.4 mmol) in anhydrous Et_2O (5 mL) was added to a mixture of 4'-fluoroacetophenone (9.95 g, 72.0 mmol) and $AlCl_3$ (200 mg, 1.5 mmol, 2 mol%) in anhydrous Et_2O (15 mL) in an ice bath. The light yellow reaction mixture was concentrated under reduced pressure which formed crude yellow solid on cooling. The solid was triturated with portions of water and petroleum spirit yielding a off white solid (12.96 g, 79%, mp 46.0 – 47.0°C) that did not require further purification and had spectral data identical to the material isolated above.

N-Isopropylanaline 98[136]

Zinc powder (65.2 g, 0.997 mol) was slowly added to a solution of aniline (23.5 mL, 24.0 g, 0.257 mol) and acetone (20.5 mL, 16.1 g, 0.277 mol) in acetic acid (200 mL). The reaction mixture was heated at 70°C for 3.5h and allowed to cool. Methanol (100 mL) was added and the reaction mixture was filtered though celite. The residue was washed with methanol and the filtrate concentrated under reduced pressure. The residue was dissolved in $CHCl_3$ (150 mL) and neutralised by addition of ammonia solution (25%, approx. 100 mL). The aqueous phase was extracted with $CHCl_3$ (150 mL). The combined organic phases were washed with water (150 mL), dried over anhydrous $MgSO_4$ and concentrated under reduced pressure to give **98** as a yellow oil (33.06 g, 95%, 97% pure) that did not require further purification.

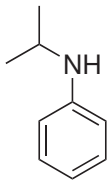

98

^{1}H NMR ($CDCl_3$): δ 7.30-7.23 (m, 2H), 6.81-6.76 (m, 1H), 6.70-6.67 (m, 2H), 3.72 (*septet*, J = 6.3 Hz, 1H), 3.50 (bs, 1H), 1.30 (d, J = 6.3 Hz, 6H). ^{13}C NMR ($CDCl_3$): δ 147.5 (C), 129.3 (CH), 117.0 (CH), 113.3 (CH), 44.2 (CH), 23.0 (CH_3).

1-(4-Fluorophenyl)-2-(isopropyl(phenyl)amino)ethanone 240

Method A[131]

A solution of 2-bromo-4'-fluoroacetophenone **239** (4.72 g, 21 mmol) and *N*-isopropyl aniline **98** (5.89 g, 43.5 mmol) in absolute EtOH (140 mL) was heated under at reflux for 20 hours, cooled and concentrated under reduced pressure. The residue was dissolved in $CHCl_3$ (80 mL) and washed with saturated Na_2CO_3 solution (2 x 50 mL) and water (50 mL). The aqueous washings were combined and extracted with $CHCl_3$ (3 x 100 mL). The combined organic extracts were dried over anhydrous $MgSO_4$ and concentrated under reduced pressure to give a brown crude material (8.9 g) that was purified by column chromatography (5% EtOAc in PS) to give **240** a yellow solid (5.52 g, 73 %). The NMR spectra matched those reported.[137]

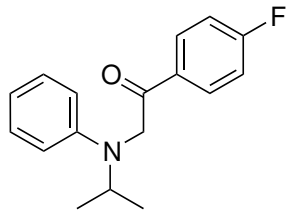

240

^{1}H NMR ($CDCl_3$): 8.11 – 8.07 (m, 2H), 7.22 – 7.15 (m, 4H), 6.72 (t, J = 7.3, 1H), 6.64 (d, J = 8.0, 1H), 4.60 (s, 2H), 4.24 (septet, 1H), 1.21 (d, J = 6.6 Hz, 6H). ^{13}C NMR ($CDCl_3$): δ 195.7, 167.3, 164.8, 148.7, 131.99, 131.96, 130.76, 130.66, 129.4, 117.3, 116.1, 115.9, 113.2, 51.5, 48.5, 20.2.

Method B

A solution of *N*-isopropylaniline **98** (6.22 g, 46.0 mmol), DIPEA (8.86 g, 68.55 mmol) and 2-bromo-4'-fluoroacetophenone **239** (10.0 g, 46.11 mmol) in dry EtOH (80 mL) was heated under reflux for 6.5h and allowed to cooled. The reaction mixture was concentrated under reduced pressure and the residue dissolved in DCM (300 mL) and washed with saturated Na_2CO_3 solution (2 x 300 mL). The combined washings were extracted with DCM (40 mL) and the combined extracts were dried over anhydrous $MgSO_4$ and concentrated under reduced pressure. **240** was isolated as a brown semi crystalline solid (13.1g, >100%) that was used in the following step without further purification.

3-(4-Fluorophenyl)-1-isopropyl-1*H*-indole 96

Method A

Zinc chloride (110 g, 807 mmol, 27 eq) was dried by carefully heating with a heatgun under reduced pressure directly before addition to a mixture of crushed

molecular sieves (4A, approx. 25g) and purified **240** (8.15 g, 30 mmol) in anhydrous EtOH (280mL). The reaction mixture was heated under reflux for 15h and allowed to cooled before being filtered through celite. The filtrate was concentrated under reduced pressure, dissolved in DCM (200 mL) and washed with water (700 mL). The aqueous washing was extracted with DCM (3 x 100 mL) and filtered though celite. The organic phase was dried over anhydrous $MgSO_4$ and concentrated under reduced pressure to give a **96** as white solid (7.7 g, Quant.) that did not require further purification.

Method B

Zinc chloride (165 g, 1.21 mol) was dried by carefully heating with a heatgun under reduced pressure then added to a solution of crude **240** (13.1g, 48 mmol) in anhydrous EtOH (350 mL). The mixture was heated for 13 hours, allowed to cool and concentrated under reduced pressure. The resulting residue was poured onto HCl (700 mL, 1M) and extracted with DCM (2 x 300 mL). The combined organic extracts were washed with HCl (500 mL, 1M) and brine (250 mL). The organic phase was dried over $MgSO_4$ and absorbed onto silica under reduced pressure. The material was filtered though silica and washed with 25% DCM in PS until the filtrate was free from UV activity to TLC. The filtrate was concentrated under reduced pressure to give **96** as pale yellow solid (8.06 g, 68%) which did not require further purification.

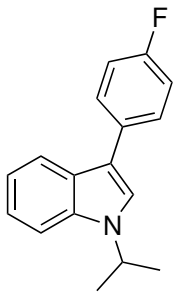

96

Melting Point: 93.9 – 96°C (lit: 94.5 – 95.50°C[137]) ^{1}H NMR ($CDCl_3$): δ 7.91 (m, 1H), 7.66-7.62 (m, 2H), 7.46 (d, J = 8.3 Hz, 1H), 7.38 (s, 1H), 7.32 – 7.28 (m, 1H), 7.24 - 7.20 (m, 1H), 7.19-7.14 (m, 2H), 4.75 (septet, J = 6.7 Hz, 1H), 1.60 (d, J = 6.7 Hz, 6H). ^{13}C NMR ($CDCl_3$): δ 162.7 (C), 160.2 (C), 136.4 (C), 132.1 (C), 128.92 (CH), 128.84 (CH), 126.3 (C), 121.9 (CH), 121.4 (CH), 120.1 (CH), 119.8 (CH), 116.1 (C), 115.8 (CH), 115.6 (CH), 109.9 (CH), 47.2 (CH), 23.0 (CH_3). IR (ATR, cm^{-1}) 2973, 1600, 1552, 1498, 1459, 1415, 1402, 1370, 1203, 1149, 1131, 1093, 1014, 845, 834, 806, 750.

3-(4-Fluorophenyl)-1-isopropyl-1*H*-indole-2-carbaldehyde 238[139]

Phosphorous oxychloride (4.4 mL, 47.0 mmol, 2.0 eqv) was added dropwise to DMF (4.0 mL, 51.6 mmol, 2.2 eqv) in an ice bath. The reaction mixture was warmed to 80°C before addition of the indole **96** (6.02 g, 23.8 mmol) in DMF (6 mL) over 10 min. After 2h, DMF (10 mL) was added, cooled to room temperature, and transferred to a dropping funnel. The reaction mixture added dropwise to a solution of sodium hydroxide (6 g) in water (120 mL) at 40°C. The reaction mixture stirred overnight at room temperature. The aqueous phase was extracted with toluene (4 x 30 mL). The combined extracts were washed with water (6 x 60 mL), brine (1 x 60 mL) and dried over anhydrous $MgSO_4$. The filtrate was concentrated under reduced pressure to give a golden oil (6.80 g) that was purified by column chromatography (25-50 % DCM in PS) to give **238** as a white solid (3.81 g, 57%).

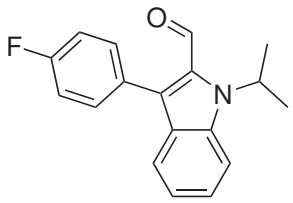

238

Melting range: 95 - 97°C. ^{1}H NMR ($CDCl_3$): δ 9.81 (s, 1H), 7.67-7.64 (m, 2H), 7.50-7.45 (m, 2H), 7.41 (m, 1H), 7.23-7.15 (m, 3H), 5.95-5.90 (m, 1H), 1.70 (d, J = 7.0 Hz, 6H). ^{13}C NMR ($CDCl_3$): δ 183.7 (CH), 163.9 (C), 161.5 (C), 138.0 (C), 132.77 (CH), 132.69 (CH), 132.1 (C), 130.7 (C), 128.27 (C), 128.24 (C), 127.07 (CH), 126.93 (C), 122.2 (CH), 120.9 (CH), 115.8 (CH), 115.5 (CH), 113.3 (CH), 48.1 (CH), 21.5 (CH_3). (Matches[137]) IR (ATR, cm^{-1}) 2966, 1661, 1603, 1529, 1495, 1458, 1379, 1352, 1339, 1321, 1217, 1150, 1119, 903, 841, 752.

2-(2,2-Dibromovinyl)-3-(4-fluorophenyl)-1-isopropyl-1H-indole 241 [124]

A solution of **238** (1.27 g, 4.5 mmol) and carbon tetrabromide (3.12 g, 9.4 mmol, 2.1 eqv) in DCM (10 mL) was added dropwise over a period of 20 min to a solution of triethyl phosphite (3.2 mL, 18.7 mmol, 4.2 eqv) in DCM (3 mL) at -45°C and held at this temperature for 3.5 hours. The reaction mixture was poured onto saturated $NaHCO_3$ solution (30 mL). The resulting mixture was extracted with DCM (2 x 20 mL). The combined organic extracts were washed with $NaHCO_3$ solution (5%, 3 x 50 mL) and brine (1 x 50 mL) and dried over anhydrous $MgSO_4$.

The filtrate was concentrated under reduced pressure to give a yellow oil and solid (4.78 g) that was purified by column chromatography (0 - 15% DCM in PS) to give **241** as a white solid (1.36 g, 89%).

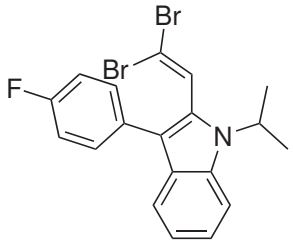

241

^{1}H NMR ($CDCl_3$): δ 7.75 (d, J = 8.0 Hz, 1H), 7.60 (d, J = 8.4 Hz, 1H), 7.57 (s, 1H), 7.50-7.46 (m, 2H), 7.30 (ddd, J = 8.5, 7.2, 1.1 Hz, 1H), 7.21-7.16 (m, 3H), 4.72 (sept, J = 7.0 Hz, 1H), 1.71 (d, J = 7.0 Hz, 6H). ^{13}C NMR ($CDCl_3$): δ 162.9 (C), 160.4 (C), 135.4 (C), 131.10 (C), 131.07 (C), 130.79 (CH), 130.71 (CH), 129.5 (CH), 127.6 (C), 122.6 (CH), 120.11 (CH), 119.99 (CH), 116.0 (C), 115.7 (CH), 115.5 (CH), 111.8 (CH), 98.8 (C), 48.8 (CH), 22.1 (CH_3).

2-Ethynyl-3-(4-fluorophenyl)-1-isopropyl-1*H*-indole 237 [124]

A solution of potassium *tert*-amylate (5.8 mL, 11.4 mmol, 1.08 eqv, 25% in toluene) was added over 20 mins to a solution of **241** (4.61 g, 10.6 mmol) in toluene (50 mL) at 0°C. After TLC showed consumption of the starting material, methanol (2.1 mL, 51.1 mmol) and dimethyl phosphite (1.26 mL, 13.7 mmol, 1.30 eqv) were respectively added followed by dropwise addition of potassium *tert*-amylate (5.6 mL, 11.0 mmol, 1.04 eqv, 25% in toluene) over 20 min. Cold saturated NH_4Cl solution (15 mL) was added after 20 min and the reaction mixture was concentrated under reduced pressure. The residue was dissolved in petroleum spirit and filtered though silica. The silica was washed with petroleum spirit until the eluent no longer show UV activity to TLC plates. The filtrate was concentrated under reduced pressure and recrystallised from petroleum spirit overnight at -20°C. The crystals were washed with cold petroleum spirit (2 x 5 mL) and dried under high vacuum to give **237** (2.36 g, 81%) as grey/light violet needles.

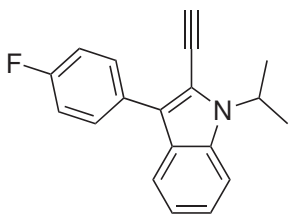

237

^{1}H NMR ($CDCl_3$): δ 7.75-7.69 (m, 3H), 7.52 (dt, J = 8.5, 0.8 Hz, 1H), 7.29 (ddd, J = 8.4, 7.0, 1.3 Hz, 1H), 7.19-7.13 (m, 3H), 5.08 (septet, J = 7.0 Hz, 1H), 3.55 (s, 1H), 1.72 (d, J = 7.0 Hz, 6H). ^{13}C NMR ($CDCl_3$): δ 163.1 (C), 160.6 (C), 135.4 (C), 130.91 (CH), 130.83 (CH), 130.24 (C), 130.21 (C), 126.4 (C), 123.6 (CH), 122.6 (C), 120.40 (CH), 120.33 (CH), 117.1 (C), 115.6 (CH), 115.3 (CH), 111.3 (CH), 85.9 (C), 76.4 (CH), 48.9 (CH), 21.8 (CH_3). IR (ATR, cm^{-1}): 3303, 2979, 2935, 2109, 1538, 1496, 1451, 1371, 1337, 1220, 1156, 838, 744, 665, 602. HRMS (ESI) m/z $C_{19}H_{16}FN$ $[M+H]^+$ = 277.1340, found = 278.1340.

3-((3-(4-Fluorophenyl)-1-isopropyl-1*H*-indol-2-yl)ethynyl)-3-hydroxyhexadecanenitrile 247

A solution of *n*-BuLi (2.8 mL, 1.6M, 4.09 mmol, 2.0 eqv) was added dropwise to a solution of the alkyne **237** (1.24 g, 4.46 mmol, 2.2 eqv) in anhydrous THF (20 mL) at -84°C. The solution was allowed to warm to room temperature and added dropwise to a suspension (previously stirred for 2 hours at room temp) of anhydrous cerium chloride (1.8 g $CeCl_3.7H_2O$ progressively heated to 140°C under Hi-Vac for at least 2 hours, 4.84 mmol, 2.4 eqv) in anhydrous THF (15 mL) at -84°C and held at this temperature for 40 min. A solution of the ketonitrile **124** (935 mg, 2.02 mmol) in anhydrous THF (15 mL) was added and the reaction mixture was held at -84°C for 4 hours before addition of saturated NH_4Cl solution (10 mL). The reaction mixture was left to warm to room temperature and concentrated under reduced pressure. HCl (1 M, 75 mL) was added and extracted with DCM (3 x 75 mL). The combined organic extracts were washed with brine (200 mL) and dried over a combination of K_2CO_3 and $MgSO_4$. The filtrate was concentrated under reduced pressure to give a residue that was purified using column chromatography (DCM) to give **247** as a colourless oil (1.40 g, 87 %).

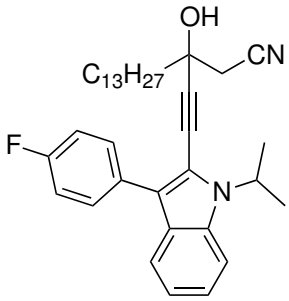

247

^{1}H NMR ($CDCl_3$): δ 7.76-7.74 (m, 1H), 7.72-7.68 (m, 2H), 7.54 (d, J = 8.5 Hz, 1H), 7.31 (ddd, J = 8.4, 7.1, 1.3 Hz, 1H), 7.21-7.15 (m, 3H), 5.09 (septet, J = 7.0 Hz, 1H), 2.84-2.82 (m, 3H), 1.86 (dd, J = 9.0, 7.6 Hz, 2H), 1.76 (d, J = 7.0 Hz, 6H), 1.37-1.31 (m, 22H), 0.94-0.91 (m, 3H). ^{13}C NMR ($CDCl_3$): δ 163.1 (C), 160.6 (C), 135.6 (C), 130.88 (CH), 130.80 (CH), 130.16 (C), 130.13 (C), 126.3 (C), 123.7 (CH), 122.7 (C), 120.47 (CH), 120.29 (CH), 116.60 (C), 116.40 (C), 115.6 (CH), 115.4 (CH), 111.3 (CH), 96.6 (C), 79.1 (C), 69.4 (C), 48.9 (CH), 41.7 (CH_2), 32.2 (CH_2), 32.0 (CH_2), 29.80 (CH_2), 29.75 (CH_2), 29.74 (CH_2), 29.65 (CH_2), 29.59 (CH_2), 29.46 (CH_2), 24.6 (CH_2), 22.8 (CH_2), 21.8 (CH_3), 14.2 (CH_3). IR (ATR, cm^{-1}): 3439, 2923, 2853, 2256, 2218, 1607, 1540, 1502, 1454, 1347, 1336, 1224, 1156, 1096, 837, 742. HRMS (ESI) m/z $C_{35}H_{45}FN_2O$ $[M+H]^+$ = 529.3589, found = 529.3590.

3-(2-(3-(4-Fluorophenyl)-1-isopropyl-1*H*-indol-2-yl)ethyl)-3-hydroxyhexadecanenitrile 249

A solution of **247** (1.18 g, 2.22 mmol) in EtOAc (10 mL) was degassed under reduced pressure and placed under N_2 (x 3). 10 %w/w Pd/C (130 mg, 11 %wt) was added, a H_2 atmosphere introduced and heated under reflux overnight. The reaction mixture was allowed to cool, placed under a N_2 atmosphere and filtered though celite. The filtrate concentrated under reduced pressure and the resulting residue purified by column chromatography (DCM) to give **249** as a colourless oil (881 mg, 74%).

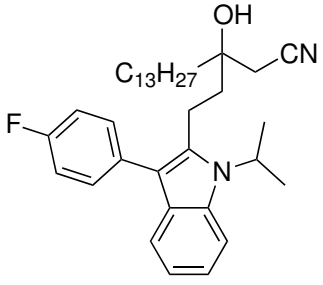

249

^{1}H NMR ($CDCl_3$): δ 7.59-7.57 (m, 1H), 7.52-7.50 (m, 1H), 7.42-7.37 (m, 2H), 7.15 (s, 3H), 7.10-7.06 (m, 1H), 4.73-4.66 (m, 1H), 2.93-2.87 (m, 2H), 2.47 (s, 2H), 1.91-1.80 (m, 2H), 1.78-1.70 (m, 6H), 1.61-1.51 (m, 2H), 1.38-1.12 (m, 23H), 0.92-0.86 (m, 3H). ^{13}C NMR ($CDCl_3$): δ 162.9 (C), 160.4 (C), 135.5 (C), 134.3 (C), 131.61 (CH), 131.54 (CH), 128.5 (C), 121.1 (CH), 119.5 (CH), 119.1 (CH), 117.4 (C), 115.7 (CH), 115.5 (CH), 113.6 (C), 112.0 (CH), 72.9

(C), 47.4 (CH), 39.06 (CH_2), 38.94 (CH_2), 32.0 (CH_2), 29.92 (CH_2), 29.79 (CH_2), 29.75 (CH_2), 29.72 (CH_2), 29.67 (CH_2), 29.60 (CH_2), 29.46 (CH_2), 29.2 (CH_2), 23.7 (CH_2), 22.8 (CH_2), 21.6 (CH_3), 19.4 (CH_2), 14.2 (CH_3). IR (ATR, cm^{-1}): 3485, 2925, 2854, 2255, 1558, 1505, 1462, 1350, 1221, 1155, 1093, 839, 817, 740, 727. HRMS (ESI) m/z $C_{35}H_{49}FN_2O$ $[M+H]^+$ = 533.3902, found = 533.3905.

1-Amino-3-(2-(3-(4-fluorophenyl)-1-isopropyl-1*H*-indol-2-yl)ethyl) hexadecan-3-ol 116

$NaBH_4$ (243 mg, 6.42 mmol) was added to a solution of **249** (320 mg, 0.601 mmol) and $CoCl_2.6H_2O$ (335 mg, 1.22 mmol) in EtOH (5 mL) at 0°C. After 1 hour at 0°C, the reaction mixture was allowed to warm to room temperature for 1 hour before addition of HCl (3M, 6 mL). Conc $NH_{3(aq)}$ (10 mL) and water (10 mL) were added and the resulting mixture extracted with $CHCl_3$ (3 x 30 mL). The combined organic extracts were dried over anhydrous $MgSO_4$ and concentrated under a stream of nitrogen to give an oil that was purified by column chromatography (2-4% MeOH, 1% $NH_{3(aq)}$ in $CHCl_3$) to give **116** as a colourless oil (214 mg, 66%).

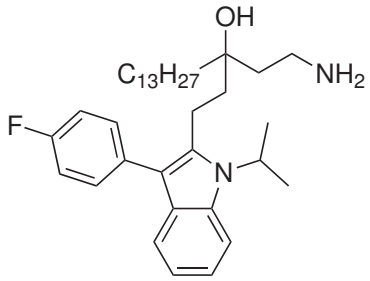

116

^{1}H NMR ($CDCl_3$): δ 7.58 (d, J = 8.2 Hz, 1H), 7.53 (dd, J = 7.9, 0.5 Hz, 1H), 7.45-7.41 (m, 2H), 7.19-7.06 (m, 4H), 4.80 (septet, J = 7.0 Hz, 1H), 3.00-2.80 (m, 7H), 1.80-1.65 (m, 9H), 1.57-1.44 (m, 5H), 1.37-1.15 (m, 20H), 0.91 (t, J = 6.8 Hz, 3H).^{13}C NMR ($CDCl_3$): δ 162.8 (C), 160.3 (C), 137.6 (C), 134.2 (C), 132.04 (C), 132.01 (C), 131.64 (CH), 131.57 (CH), 128.7 (C), 120.7 (CH), 119.3 (CH), 118.9 (CH), 115.5 (CH), 115.3 (CH), 113.1 (C), 111.9 (CH), 74.8 (C), 47.2 (CH), 40.0 (CH_2), 39.1 (CH_2), 38.1 (CH_2), 37.8 (CH_2), 32.1 (CH_2), 30.5 (CH_2), 29.86 (CH_2), 29.83 (CH_2), 29.81 (CH_2), 29.5 (CH_2), 24.3 (CH_2), 22.8 (CH_2), 21.68 (CH_3), 21.64 (CH_3), 19.4 (CH_2), 14.3 (CH_3). HRMS (ESI) m/z $C_{35}H_{53}FN_2O$ $[M+H]^+$ = 537.4215, found = 537.4213. IR (ATR, cm^{-1}): 3272, 3053, 2922, 2852, 1608, 1557, 1505, 1461, 1349, 1215, 1155, 940, 838, 815, 740.

3-(*N*-Methyl-*N*-phenylamino)acrolein 99[140]

A solution of *N*-methylformanilide (9.1 mL, 9.96 g, 73.7 mmol) and butyl vinyl ether (10.3 mL, 8.01 g, 80.0 mmol) in acetonitrile (10 mL) was added dropwise to a stirred solution of oxalyl chloride (10.1 g, 79.6 mmol) in acetonitrile (5 mL) at -10°C. The solution was allowed to warm to room temperature over 80 min. The reaction mixture was cooled in a ice bath before dropwise addition of Na_2CO_3 solution (20 %, approx 50 mL) until the pH > 7. The reaction mixture was diluted with water (100 mL) and extracted with toluene (3 x 70 mL). The combined organic extracts were washed with water (2 x 50 mL). The organic phase was dried with $MgSO_4$ and concentrated under reduced pressure to give a black viscous crude (10.9 g) that was distilled under reduced pressure to give **99** as a brown oil (5.4 g, 50 %). The NMR spectra matched reported values.[140]

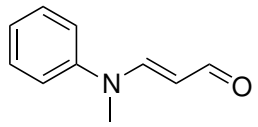

99

^{1}H NMR ($CDCl_3$): δ 9.27 (d, J = 8.1 Hz, 1H), 7.55 (d, J = 13.1 Hz, 1H), 7.43-7.38 (m, 2H), 7.25-7.22 (m, 1H), 7.20-7.16 (m, 3H), 5.47 (dd, J = 13.0, 8.1 Hz, 1H), 3.33 (s, 3H).^{13}C NMR ($CDCl_3$): δ 190.3, 156.4, 146.1, 129.7, 125.5, 120.6, 105.6, 37.4

3-(3-(4-Fluorophenyl)-1-isopropyl-1*H*-indol-2-yl) acrylaldehyde 100[131,140]

A solution of freshly distilled 3-(*N*-Methyl-*N*-phenylamino)acrolein **99** (10.5 g, 65.1 mmol) in dry acetonitrile (15 mL) was added over 45 min to a solution of freshly distilled phosphorus oxychloride (10.38 g, 67.7 mmol) in acetonitrile (25 mL) at -5°C. After 75 min at this temperature a solution of 1-(isopropyl)-3-(4'-fluorophenyl)-indole **100** (6.33 g, 25.0 mmol) in dry acetonitrile (50 mL) was added rapidly and the reaction mixture was heated under reflux for 3 h. The reaction mixture was allowed to cool to room temperature before addition of water (50 mL). The reaction mixture was heated to 55°C for 3 h. The reaction mixture was cooled, diluted with water (500 mL) and extracted with toluene (2 x 150 mL). The combined organic phases were washed with water (2 x 200 mL) and dried over anhydrous $MgSO_4$. The filtrate was concentrated under reduced

pressure and the residue purified by column chromatography (15% EtOAc in PS) to give **100** as yellow solid (6.05 g, 79%).

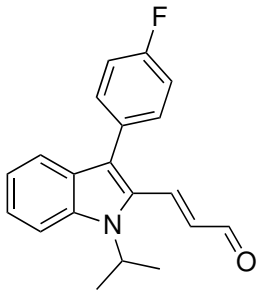

100

Melting point: 132°C (lit:129 - 130°C[140])^{1}H NMR ($CDCl_3$): δ 9.59 (d, J = 7.6 Hz, 1H), 7.64-7.54 (m, 3H), 7.43-7.39 (m, 2H), 7.34 (m, 1H), 7.23-7.19 (m, 2H), 7.15 (m, 1H), 6.34 (dd, J = 16.2, 7.6 Hz, 1H), 5.00 (septet, J = 7.0 Hz, 1H), 1.76 (d, J = 7.0 Hz, 6H). ^{13}C NMR ($CDCl_3$): δ 193.4 (CH), 163.6 (C), 161.1 (C), 141.1 (CH), 137.6 , 132.05 (CH), 131.97 (CH), 130.5 (C), 130.06 (C), 130.03 (C), 129.7 (CH), 128.4 (C), 124.7 (CH), 122.8 (C), 121.1 (CH), 120.7 (CH), 116.1 (CH), 115.9 (CH), 112.6 (CH), 48.3 (CH), 21.9 (CH_3). IR (ATR, cm-1) 2975, 1658, 1613, 1602, 1541, 1492, 1450, 1371, 1340, 1209, 1120, 1104, 1089, 1012, 1004, 956, 839, 739, 604.

3-(3-(4-Fluorophenyl)-1-isopropyl-1*H*-indol-2-yl)propanal 251

A mixture of the propenal **100** (1250 mg, 4.0 mmol), KOAc (approx. 5 mg) and water (25 µl) in EtOAc (12.5 mL) was degassed under reduced pressure and a replaced with a N_2 atmosphere (x 3). Pd/C (38 mg, 3 %wt, 10 %Pd) was added and a H_2 atmosphere introduced. After 36 hours at room temperature, a N_2 atmosphere was introduced and the reaction mixture was filtered though celite. The filtrate was concentrated under reduced pressure and the residue was purified by column chromatography (50% DCM in PS) to give **251** as a yellow solid (906 mg, 72 %).

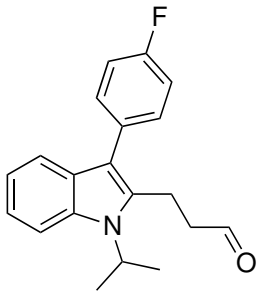

251

Melting range: 86 - 87°C. ^{1}H NMR (400 MHz; $CDCl_3$): δ 9.73 (s, 1H), 7.58 (d, J = 8.3 Hz, 1H), 7.51 (dt, J = 7.9, 0.6 Hz, 1H), 7.39-7.35 (m, 2H), 7.22-7.08 (m, 4H), 4.62 (septet, J = 7.0 Hz, 1H), 3.17 (t, J = 7.9 Hz, 2H), 2.71 (t, J = 7.9 Hz, 2H), 1.73 (d, J = 7.0 Hz, 6H). ^{13}C NMR ($CDCl_3$): δ 200.4 (CH), 163.0 (C), 160.5 (C), 134.6 (C), 134.4 (C), 131.66 (CH), 131.58 (CH), 131.45 (C), 131.42 (C), 128.6 (C), 121.3 (CH), 119.6 (CH), 119.2 (CH), 115.8 (CH), 115.6 (CH), 114.2 (C),

111.9 (CH), 47.5 (CH), 44.4 (CH_2), 21.7 (CH_3), 17.7(CH_2). IR (ATR, cm^{-1}): 2964, 2934, 1717, 1602, 1558, 1503, 1462, 1340, 1216, 1154, 1103, 1067, 836, 814, 749. HRMS (ESI) m/z $C_{20}H_{20}FNO$ $[M+H]^+$ = 310.1602, found = 310.1608.

1-((3-(3-(4-Fluorophenyl)-1-isopropyl-1H-indol-2-yl) propyl)amino)hexadecan-3-ol 250

A mixture of 1-aminohexadecan-3-ol **109** (99 mg, 0.389 mmol), the aldehyde **251** (126 mg, 0.409 mmol) and $MgSO_4$ (114 mg) in a dry DCM/THF mixture (5:1, 3 mL) was stirred at 50°C for 20 hours. The reaction mixture was filtered and concentrated under reduced pressure. $NaBH_4$ (20 mg, 0.528 mmol, 1.35 eq) was added to a solution of the residue in EtOH (4 mL) at 0°C. The reaction mixture was stirred overnight at room temperature before addition of with saturated NH_4Cl (1 mL). The reaction mixture was stirred for 1 hour and diluted with $NaHCO_3$ solution (5%, 20 mL). The resulting mixture was extracted with $CHCl_3$ (3 x 15 mL). The organic extracts were washed with water (30 mL) and brine (30 mL) before drying over K_2CO_3. The colourless oil (218 mg) was purified by column chromatography (2% $MeOH_{(Sat.\ NH_3)}$ in $CHCl_3$) to give **250** as a colourless oil (36 mg, 23%).

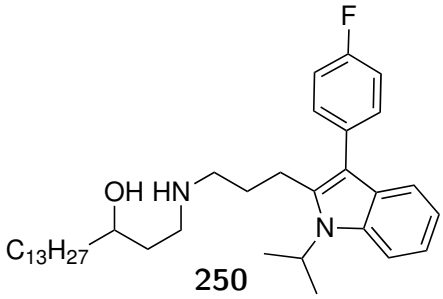

250

^1H NMR (C_6H_6): δ 7.69-7.66 (m, 1H), 7.44 (m, 1H), 7.33-7.30 (m, 2H), 7.24-7.17 (m, 2H), 7.03-6.99 (m, 2H), 4.33 (septet, J = 7.0 Hz, 1H), 3.77 (bs, 1H), 2.64 (s, 2H), 2.48 (dt, J = 11.8, 4.4 Hz, 1H), 2.37-2.31 (m, 1H), 2.24-2.19 (m, 1H), 2.12 (m, 1H), 1.67-1.59 (m, 2H), 1.54-1.25 (m, 35H), 0.91 (m, 3H). ^{13}C NMR (C_6D_6): δ 163.2 (C), 160.8 (C), 136.1 (C), 134.9 (C), 132.57 (C), 132.54 (C), 132.03 (CH), 131.96 (CH), 129.3 (C), 121.5 (CH), 119.9 (CH), 119.7 (CH), 115.9 (CH), 115.7 (CH), 114.0 (C), 112.2 (CH), 73.2 (CH), 49.1 (CH_2), 48.9 (CH_2), 47.4 (CH), 38.7 (CH_2), 35.9 (CH_2), 32.4 (CH_2), 30.8 (CH_2), 30.41 (CH_2), 30.31 (CH_2), 30.25 (CH_2), 30.23 (CH_2), 30.17 (CH_2), 29.9 (CH_2), 26.3 (CH_2), 23.2 (CH_2), 22.9 (CH_2), 21.38 (CH_3), 21.36 (CH_3), 14.4 (CH_3). IR (ATR, cm^{-1}): 3292, 2922, 2852, 1557, 1505, 1460, 1350, 1220, 1155, 1102, 835, 815, 741. HRMS (ESI) m/z $C_{36}H_{55}FN_2O$ $[M+H]^+$ =

551.4371, found = 551.4347.

1-(((3-(4-Fluorophenyl)-1-isopropyl-1H-indol-2-yl)methyl) amino)hexadecan-3-ol 117

A mixture of 1-aminohexadecan-3-ol **109** (102 mg, 0.396 mmol), the aldehyde **238** (113 mg, 0.402 mmol, 1.0 eq) and $MgSO_4$ (150 mg) were suspended in anhydrous DCM (2 mL) and stirred for 48h at 50°C in a sealed vessel. The reaction mixture was filtered and concentrated under reduced pressure. $NaBH_4$ (15 mg, 0.389 mmol) was added to a solution of the residue in anhydrous EtOH (4 mL) at 0°C. The reaction mixture was allowed to warm to room temperature over 2 hours before addition of saturated NH_4Cl (1 mL). The reaction mixture was diluted with K_2CO_3 solution (5 %) and extracted with $CHCl_3$ (3 x 25 mL). The combined organic extracts were dried over anhydrous $MgSO_4$ and the filtrate concentrated under reduced pressure to give a clear oil (196 mg). The oil was purified by column chromatography (1% $MeOH_{(Sat.\ NH_3)}$ in $CHCl_3$) to give **117** as a colourless oil (54 mg, 26%).

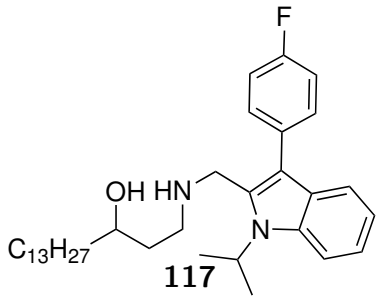

117

^{1}H NMR (Toluene-d_8): δ 7.64 (d, J = 7.8, 1H), 7.42 (d, J = 8.1 Hz, 1H), 7.22-7.17 (m, 3H), 7.16-7.08 (m, 2H), 7.01-6.92 (m, 3H), 4.71 (7, J = 7.0 Hz, 1H), 3.66-3.60 (m, 2H), 3.55 (ad, J = 13.0 Hz, 1H), 2.56 (m, J = 4.0 Hz, 1H), 2.43 (m, J = 3.9 Hz, 1H), 1.54-1.41 (m, 8H), 1.39-1.19 (m, 24H), 0.93-0.89 (t, J = 6.9 Hz, 3H). ^{13}C NMR (Toluene-d_8): δ 163.3 (C), 160.9 (C), 137.4 (C), 135.1 (C), 133.4 (C), 131.91 (CH), 131.84 (CH), 122.1 (CH), 120.1 (CH), 119.9 (CH), 115.71 (CH), 115.55 (C), 115.50 (CH), 112.4 (CH), 72.9 (CH), 48.9 (CH_2), 47.8 (CH), 44.4 (CH_2), 38.6 (CH_2), 36.3 (CH_2), 32.4 (CH_2), 30.42 (CH_2), 30.33 (CH_2), 30.29 (CH_2), 30.22 (CH_2), 29.9 (CH_2), 26.2 (CH_2), 23.2 (CH_2), 21.42 (CH_3), 21.39 (CH_3), 14.4 (CH_3). HRMS (ESI) m/z $C_{34}H_{51}FN_2O$ $[M+H]^+$ = 523.4058, found = 523.4040. IR (ATR, cm^{-1}): 3423, 2915, 2848, 1559, 1506, 1457, 1356, 1223, 1156, 837, 733.

6.4 Chapter 4 experimental

6.4.1 Chain analogues; position 5 alkene

1,2-Dibromodecane 270

A solution of bromine (5.5 mL, 17.1 g, 107 mmol) in dry DCM (75 mL) was added dropwise over 90 min to a solution of 1-decene (15.05 g, 107 mmol) in anhydrous DCM (125 mL) at 0 °C under N_2. The reaction mixture was allowed to warm to room temperature for 45 min. Bromine (approx 1-2 mL) was added to the colourless reaction mixture dropwise until an orange colour was sustained for > 10 min. Sodium metabisulfite solution (5%) was added dropwise to the reaction mixture until colourless. Anhydrous $MgSO_4$ was added and the reaction mixture was filtered. The filtrate was concentrated to give **270** as a light yellow oil (31.2 g, 97 %). The NMR spectra matched those reported.[147]

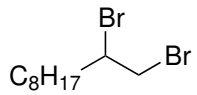

270

^{1}H NMR ($CDCl_3$): δ 4.20-4.14 (m, 1H), 3.85 (dd, J = 10.2, 4.5 Hz, 1H), 3.63 (dd, J = 10.1, 9.8 Hz, 1H), 2.13 (m, 1H), 1.83-1.74 (m, 1H), 1.59-1.24 (m, 12H), 0.89 (t, J = 6.9 Hz, 3H).^{13}C NMR ($CDCl_3$): δ 53.3, 36.5, 36.2, 32.0, 29.50, 29.34, 29.0, 26.9, 22.8, 14.2.

1-Decyne 267

1,2-dibromodecane (15.86 g, 52.8 mmol) and Aliquot 336 (0.3 mL, 0.265 g, 0.656 mmol) were placed in a round bottom flask (50 mL). Powdered KOH (12 g, 210 mmol) was added. The flask was set up for a vacuum distillation with a 10 cm fractionation column under reduced pressure (approx 40- 60 mm Hg) and the flask placed in a preheated oil bath (150°C) to obtain a biphasic distillate. Water was pipetted from biphasic colourless distillate obtained. The remaining distillate was diluted with DCM (approx 25 mL) and dried over anhydrous $MgSO_4$. The solution was carefully concentrated to give **267** as a colourless liquid (6.84 g, 94%) with a distinctive odour. The NMR spectra matched those reported.[149]

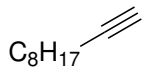

267

^{1}H NMR ($CDCl_3$): δ 2.18 (td, J = 7.1, 2.7 Hz, 2H), 1.93 (t, J = 2.7 Hz, 1H), 1.56-1.49 (m, 2H), 1.42-1.35 (m, 2H), 1.32-1.24 (m, 8H), 0.90-0.86 (m, 3H). ^{13}C NMR ($CDCl_3$): δ 84.9 (CH), 68.2 (C), 32.0 (CH_2), 29.33 (CH_2), 29.23 (CH_2), 28.9 (CH_2), 28.7 (CH_2), 22.8 (CH_2), 18.6 (CH_2), 14.2 (CH_3). IR (ATR, cm^{-1}) 3314, 2925, 2856, 2120, 1466, 624.

Ethyl 4-iodobutyrate 271

A suspension of ethyl 4-bromobutyrate (5.07 g, 26.0 mmol) in acetone (20 mL) was stirred with NaI (9.54 g, 63.6 mmol, 2.4 eqv) for 84h before being concentrated under reduced pressure. The material was triturated with 10% EtOAc in petroleum spirit (4 x 50 mL) and the filtrate was concentrated under reduced pressure to give **271** as a colourless oil (1.53 g, 62 %) that did not require further purification. The NMR spectra matched those reported.[153]

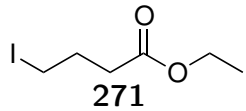

271

^{1}H NMR ($CDCl_3$): δ 4.16 (q, J = 7.1 Hz, 2H), 3.26 (t, J = 6.8 Hz, 2H), 2.46 (t, J = 7.2 Hz, 2H), 2.15 (tt, J = 7.2, 6.8 Hz, 2H), 1.28 (t, J = 7.1 Hz, 3H). ^{13}C NMR ($CDCl_3$): δ 172.5, 60.7, 35.0, 28.6, 14.4, 5.6.

4-Bromobutyric acid 276[152]

A solution of γ-butyrolactone (4.87 g, 56.6 mmol), HBr (32 mL, 48%) and conc. H_2SO_4 (7.6 mL) was slowly heated to reflux for 6 hours. The reaction mixture was poured onto water (150 mL) and extracted with Et_2O (3 x 50 mL). The combined organic extracts were washed with brine (50 mL), dried over anhydrous $MgSO_4$ and concentrated under reduced pressure to give 4-bromobutyric acid **276** as a light yellow oil (6.80 g, 72%) that did not require further purification.

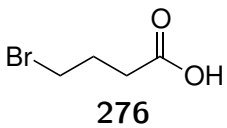

276

^{1}H NMR ($CDCl_3$): δ 3.48 (t, J = 6.4 Hz, 2H), 2.58 (t, J = 7.2 Hz, 2H), 2.18 (m, 2H). ^{13}C NMR ($CDCl_3$): δ 178.8, 32.50, 32.31, 27.5.

4-Iodobutyric acid 310

A suspension of 4-bromobutyric acid (1.98 g, 11.9 mmol) and NaI (4.61 g, 30.9 mmol) in acetone (8 mL) was stirred overnight. The resulting mixture was concentrated under reduced pressure and the residue was dissolved in Et_2O (50 mL) and washed with water (20 mL). The aqueous phase was back extracted with Et_2O (2 x 25 mL) and the combined organic extracts were washed with sodium metabisulfite solution (5%, 10 mL) and brine (10 mL). The organic phase was dried over anhydrous $MgSO_4$ and concentrated under reduced pressure to give **310** as a colourless semi-solid (2.35 g, 92%) that did not require further purification. The NMR spectra matched those reported.[154]

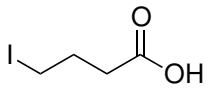

310

^{1}H NMR ($CDCl_3$): δ 3.25 (t, J = 6.7 Hz, 2H), 2.52 (t, J = 7.1 Hz, 2H), 2.14 (tt, J = 6.7, 7.1 Hz, 2H). ^{13}C NMR ($CDCl_3$): δ 178.6, 34.6, 28.3, 5.2.

4-Bromobutan-1-ol 280

HBr (16 mL, 48 %, 141 mmol) was added dropwise to a stirred solution of conc. H_2SO_4 (1 mL) in THF (14 mL, 172 mmol) at 0°C. The reaction mixture was heated under reflux for 5h and cooled in a ice bath. The pH of the reaction mixture was adjusted to > 7 by dropwise addition of a $NaHCO_3$ solution (5%). The reaction mixture was extracted with Et_2O (3 x 75 mL). The combined organic extracts were dried over anhydrous $MgSO_4$ and concentrated under reduced pressure to give **280** as a colourless oil (6.72 g, 31%) that did not require further purification. The NMR spectra matched those reported.[162]

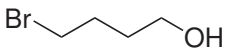

280

^{1}H NMR ($CDCl_3$): δ 3.61 (t, J = 6.4 Hz, 2H), 3.41 (t, J = 6.7 Hz, 2H), 1.93-1.87 (m, 2H), 1.69-1.64 (m, 2H). ^{13}C NMR ($CDCl_3$): δ 61.7, 33.8, 31.1, 29.2.

2-(4-Bromobutoxy)tetrahydro-2*H*-pyran 281

A solution of 4-bromobutanol **280** (2.02 g, 13.2 mmol), 3,4-dihydro-*2H*-pyran (1.30 mL, 1.20 g, 14.2 mmol) and *p*-TsOH (14 mg, 0.081 mmol, 3 mol%) in DCM

(15 mL) was stirred overnight at room temperature. The reaction mixture was concentrated under reduced pressure and purified by column chromatography (0 - 20% EtOAc in PS) to give **281** as a colourless oil (795 mg, 25 %). The NMR spectra matched those reported.[160]

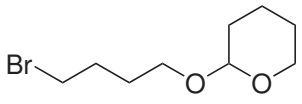

281

^{1}H NMR ($CDCl_3$): δ 4.55 (m, 1H), 3.83 (m, 1H), 3.75 (m, 1H), 3.51-3.37 (m, 4H), 1.99-1.92 (m, 2H), 1.83-1.66 (m, 5H), 1.58-1.47 (m, 5H).^{13}C NMR ($CDCl_3$): δ 98.9, 66.6, 62.4, 33.8, 30.8, 29.9, 28.5, 25.6, 19.7. IR (ATR, cm^{-1}) 2940, 2869, 1440, 1352, 1246, 1201, 1134, 1118, 1075, 1032, 986, 904, 868, 813.

2-(Tetradec-5-yn-1-yloxy)tetrahydro-2*H*-pyran 311

A solution of *n*-BuLi (6.5 mL, 1.3M in hexane) was added dropwise to a stirred solution of 1-decyne (1.26 g, 9.11 mmol, 2.12 eqv) and HMPA (1.5 mL, 8.60 mmol, 2.0 eqv) in THF (15 mL) at -84°C. After 30 min at this temperature, a solution of the bromide **281** (1.02 g, 4.28 mmol, 1.0 eqv) in THF (5 mL) was added. The reaction mixture was heated under reflux for 3 h before cooling in a ice bath. Water (5 mL) was added and the reaction mixture was concentrated under a stream of nitrogen overnight. The reaction mixture was dissolved in toluene (100 mL) and washed with brine (2 x 100 mL), water (2 x 100 mL) and brine (2 x 100 mL) before drying over anhydrous $MgSO_4$ and concentrated under reduced pressure. The crude residue was purified by column chromatography (2:1:97 EtOAc:TEA:PS) to give **311** as a colourless oil (1.05 g, 83%).

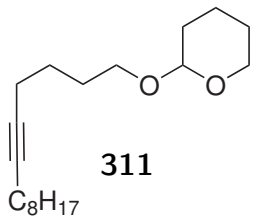

311

^{1}H NMR (400 MHz; $CDCl_3$): δ 4.56 (dd, J = 4.1, 2.8 Hz, 1H), 3.84 (td, J = 7.5, 3.6 Hz, 1H), 3.73 (dt, J = 9.7, 6.6 Hz, 1H), 3.51-3.46 (m, 1H), 3.39 (dt, J = 9.7, 6.4 Hz, 1H), 2.17 (s, 2H), 2.11 (s, 2H), 1.82 (dd, J = 8.8, 3.5 Hz, 1H), 1.73-1.65 (m, 3H), 1.60-1.42 (m, 8H), 1.38-1.26 (m, 10H), 0.87 (t, J = 6.9 Hz, 3H).^{13}C NMR ($CDCl_3$): δ 98.9 (CH), 80.6 (C), 79.9 (C), 67.2 (CH_2), 62.4 (CH_2), 32.0 (CH_2), 30.9 (CH_2), 29.34 (CH_2), 29.28 (CH_2), 29.26 (CH_2), 29.07 (CH_2), 29.02 (CH_2), 26.1 (CH_2), 25.6 (CH_2),

22.8 (CH_2), 19.8 (CH_2), 18.89 (CH_2), 18.75 (CH_2), 14.2 (CH_3). IR (ATR, cm^{-1}) 2925, 2855, 1455, 1440, 1352, 1201, 1076, 1110, 1034, 1021, 906, 869, 815. HRMS (ESI) m/z $C_{19}H_{34}O_2$ $[M+H]^+$ = 295.2632, found = 295.2632.

2-(*Z*-Tetradec-5-en-1-yloxy)tetrahydro-2*H*-pyran 283

$NaBH_4$ (218 mg, 0.741 mmol) was added to a stirred solution of $Ni(OAc)_2.4H_2O$ (189 mg, 0.759 mmol) in EtOH (5 mL) under a H_2 atmosphere. The stirred solution was left for 15 min at room temperature before addition of freshly distilled ethylenediamine (220 μl, 0.951 mmol) followed by a solution of the alkyne **311** in EtOH (5 mL). The reaction mixture was stirred for 90 min before addition of Et_2O (50 mL). The reaction mixture was filtered though a plug of silica and the residue was washed with Et_2O (2 x 20 mL). The combined filtrates were dried over anhydrous $MgSO_4$ and concentrated under reduced pressure to give **283** as a colourless oil (179 mg, 80%) that did not require further purification.

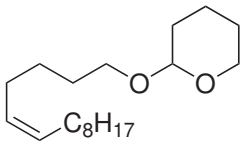

283

^{1}H NMR ($CDCl_3$): δ 5.35 (s, 2H), 4.57 (dd, J = 4.1, 2.9 Hz, 1H), 3.89-3.83 (m, 1H), 3.73 (dt, J = 9.6, 6.8 Hz, 1H), 3.51-3.46 (m, 1H), 3.38 (dt, J = 9.6, 6.6 Hz, 1H), 2.06-2.00 (m, 4H), 1.70 (d, J = 3.0 Hz, 1H), 1.62-1.49 (m, 6H), 1.44-1.39 (m, 2H), 1.34-1.26 (m, 13H), 0.87 (dt, J = 4.3, 2.5 Hz, 3H). ^{13}C NMR ($CDCl_3$): δ 130.4 (CH), 129.6 (CH), 98.9 (CH), 67.6 (CH_2), 62.4 (CH_2), 32.0 (CH_2), 30.9 (CH_2), 29.9 (CH_2), 29.66 (CH_2), 29.53 (CH_2), 29.47 (CH_2), 29.45 (CH_2), 27.4 (CH_2), 27.1 (CH_2), 26.6 (CH_2), 25.7 (CH_2), 22.8 (CH_2), 19.8 (CH_2), 14.2 (CH_3). IR (ATR, cm^{-1}): 2923, 2854, 1455, 1201, 1137, 1119, 1034, 1021, 869, 815, 721. HRMS (ESI) m/z $C_{19}H_{36}O_2$ $[M+H]^+$ = 297.2788, found = 297.2788.

Tetradec-5-ynoic acid 286

*J*ones reagent (1.3M, 50 mL, 65 mmol) was added dropwise to a solution of the protected alcohol **311** (3.05 g 10.37 mmol) in acetone (50 mL) at 0°C. The reaction was left to warm to room temperature overnight and concentrated under reduced pressure. The residue was diluted with H_2O (250 mL) and extracted

with EtOAc (3 x 100 mL). The extracts were washed with sodium bisulfide (1 x 100 mL, 1%), HCl (150 mL, 1M) and brine (150 mL) to give crude **286** as a light green oil (2.38 g, quant.) that was used in the next step without purification.

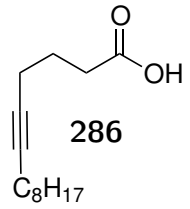

^{1}H NMR ($CDCl_3$): δ 2.52-2.44 (m, 2H), 2.27-2.20 (m, 2H), 2.17-2.10 (m, 2H), 1.85-1.77 (m, 2H), 1.51-1.41 (m, 2H), 1.41-1.21 (m, 10H), 0.91-0.85 (m, 3H). ^{13}C NMR ($CDCl_3$): δ 180.1 (C), 81.6 (C), 78.6 (C), 33.0 (CH_2), 32.0 (CH_2), 29.32 (CH_2), 29.23 (CH_2), 29.16 (CH_2), 29.00 (CH_2), 24.1 (CH_2), 22.8 (CH_2), 18.8 (CH_2), 18.3 (CH_2), 14.2 (CH_3). IR (ATR, cm^{-1}): 2926, 2955, 1708, 1414, 1242, 935. HRMS (ESI) m/z $C_{14}H_{24}O_2$ $[M+H]^+$ = 225.1849, found = 225.1848.

Propyl tetradec-5-ynoate 285

A mixture of crude **286** (2.38 g, 10.6 mmol), 1-bromopropane (5.20 g, 42.2 mmol, 4.0 eqv), TBAI (390 mg, 1.06 mmol, 0.1 eqv), K_2CO_3 (6.70 g, 48.48 mmol, 4.5 eqv) in acetone (25 mL) was heated under reflux for 3 hours and allowed to cool to room temperature and diluted with water (500 mL). The mixture was acidified with HCl solution (1M) and extracted with DCM (3 x 100 mL). The extracts were washed with brine (150 mL), dried over anhydrous $MgSO_4$ and concentrated under reduced pressure to give a crude brown oil with white crystals (2.53 g). The crude material was purified by column chromatography (4% EtOAc in PS) to give **285** as a light yellow oil (2.45 g, 90% over two steps).

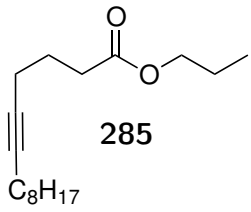

^{1}H NMR ($CDCl_3$): δ 4.01 (t, J = 6.7 Hz, 2H), 2.40 (dd, J = 8.5, 6.5 Hz, 2H), 2.19 (tt, J = 6.9, 2.4 Hz, 2H), 2.10 (tt, J = 7.0, 2.4 Hz, 2H), 1.81-1.74 (m, 2H), 1.67-1.58 (m, 2H), 1.46-1.41 (m, 2H), 1.35-1.21 (m, 11H), 0.92 (t, J = 7.4 Hz, 3H), 0.87-0.84 (m, 3H). ^{13}C NMR ($CDCl_3$): δ 173.5 (C), 81.3 (C), 78.9 (C), 66.0 (CH_2), 33.3 (CH_2), 32.0 (CH_2), 29.33 (CH_2), 29.24 (CH_2), 29.20 (CH_2), 29.0 (CH_2), 24.5 (CH_2), 22.8 (CH_2), 22.1 (CH_2), 18.8 (CH_2), 18.4 (CH_2), 14.2 (CH_3), 10.5 (CH_3). IR (ATR, cm^{-1}) 2926, 2855, 1736, 1457, 1205, 1157, 1062, 723. HRMS (ESI) m/z $C_{17}H_{30}O_2$ $[M+H]^+$ =

267.2319, found = 267.2320.

Propyl *Z*-tetradec-5-enoate 287

$NaBH_4$ (157 mg, 4.15 mmol, 1.1eqv) was added to a stirred solution of $Ni(OAc)_2.4H_2O$ (931 mg, 3.74 mmol, 1.0 eqv) in EtOH (25 mL) under a hydrogen atmosphere at room temperature. After 20 min, freshly distilled ethylenediamine (1.08 mL, 16.2 mmol, 4.3 eqv) was added directly before the addition of the alkyne **285** (1.00 g, 3.78 mmol) in EtOH (5 mL). The hydrogen atmosphere was maintained for 90 min before the reaction mixture was diluted with Et_2O (200 mL) and filtered though a plug of silica. The residue was washed with Et_2O (5 x 50 mL) and the filtrate concentrated under reduced pressure to give a crude clear oil (1.02 g) that was purified by column chromatography (30 - 50% DCM in PS) to yield **287** as a colourless oil (495 mg, 49%).

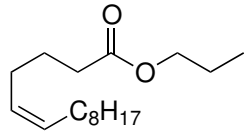

287

^{1}H NMR ($CDCl_3$): δ 5.43-5.37 (m, 1H), 5.35-5.29 (m, 1H), 4.03 (t, J = 6.7 Hz, 2H), 2.35-2.29 (m, 2H), 2.10-2.04 (m, 2H), 2.01 (m, 2H), 1.72-1.59 (m, 4H), 1.34-1.22 (m, 12H), 0.96-0.91 (m, 3H), 0.88 (t, J = 6.9 Hz, 3H). ^{13}C NMR ($CDCl_3$): δ 174.0 (C), 131.3 (CH), 128.5 (CH), 66.0 (CH_2), 33.9 (CH_2), 32.0 (CH_2), 29.86 (CH_2), 29.67 (CH_2), 29.48 (CH_2), 29.45 (CH_2), 27.4 (CH_2), 26.7 (CH_2), 25.1 (CH_2), 22.8 (CH_2), 22.2 (CH_2), 14.2 (CH_3), 10.5 (CH_3). IR (ATR, cm^{-1}) 3006, 2956, 2924, 1737, 1458, 1458, 1238, 1156, 1063, 722. HRMS (ESI) m/z $C_{17}H_{32}O_2$ $[M+H]^+$ = 269.2475, found = 269.2479.

Z-3-Oxohexadec-7-enenitrile

A solution of anhydrous acetonitrile (200 μl, 3.83 mmol, 2.6 eqv) in THF (0.3 mL) was added dropwise to a solution of *n*-BuLi (2.2 mL, 3.52 mmol, 2.4 eqv) in THF (2 mL) at -84°C and stirred for 30 min. A solution of the ester **287** (400 mg, 1.49 mmol) in THF (1 mL) was added dropwise and stirred for 45 min before addition of sat. NH_4Cl (3 mL). The reaction mixture was allowed to warm to room temperature and diluted with EtOAc (50 mL). The mixture was washed

with water (50 mL), HCl (1M, 50 mL) and brine (50 mL). The solution was dried over anhydrous $MgSO_4$ and concentrated under reduced pressure to give a yellow solid (525 mg) that was purified by column chromatography (15 - 20 % EtOAc in PS) to give **288** as a yellow oil (220 mg, 59%).

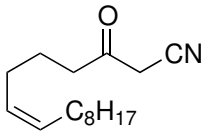

288

^{1}H NMR ($CDCl_3$): δ 5.43 (dtt, J = 10.8, 7.3, 1.6 Hz, 1H), 5.28 (dtt, J = 10.8, 7.3, 1.6 Hz, 1H), 3.43 (s, 2H), 2.64 (t, J = 7.3 Hz, 2H), 2.10 (m, 2H), 2.04-1.99 (m, 2H), 1.72 (m, 2H), 1.37-1.26 (m, 12H), 0.92-0.89 (m, 3H). ^{13}C NMR ($CDCl_3$): δ 197.5 (C), 131.9 (CH), 127.9 (CH), 113.9 (C), 41.6 (CH_2), 32.11 (CH_2), 32.03 (CH_2), 29.82 (CH_2), 29.65 (CH_2), 29.46 (CH_2), 29.44 (CH_2), 27.4 (CH_2), 26.3 (CH_2), 23.4 (CH_2), 22.8 (CH_2), 14.2 (CH_3). IR (ATR, cm^{-1}) 3007, 2923, 2853, 2263, 1730, 1457, 1403, 1374, 1306, 1087, 722. HRMS (ESI) m/z $C_{16}H_{27}NO$ $[M+H]^+$ = 250.2165, found = 250.2166.

Z-1-Aminohexadec-7-en-3-ol

A solution of the ketonitrile **288** (124 mg, 0.497 mmol) in THF (2 mL) was added to a stirred suspension of $LiAlH_4$ (65 mg, 1.73, 3.5 eqv) in THF (1 mL) at 0°C. The solution was allowed to warm to room temperature for 3 hours. The reaction mixture was cooled in a ice bath and Sat. NH_4Cl (1 mL) added dropwise. The pH was adjusted to > 7 with Sat. Na_2CO_3 solution and the reaction mixture was concentrated to dryness under reduced pressure. The reaction mixture was triturated with $CHCl_3$, filtered though celite and the filtrate concentrated under reduced pressure to give a crude yellow oil (85 mg) that was purified by column chromatography (10:1:89 MeOH:$NH_{3(aq)}$:$CHCl_3$) to give **263** as a yellow oil (35 mg, 28%).

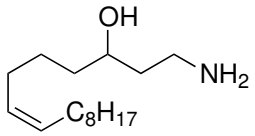

263

^{1}H NMR ($CDCl_3$): δ 5.39-5.31 (m, 2H), 3.83-3.77 (m, 1H), 3.16-3.11 (m, 1H), 2.91-2.82 (m, 1H), 2.91-2.64 (m, 4H), 2.09-1.96 (m, 4H), 1.65-1.17 (m, 17H), 0.91-0.83 (m, 3H). ^{13}C NMR ($CDCl_3$): δ 130.3 (CH), 129.7 (CH), 72.9 (CH), 40.7 (CH_2), 37.6 (CH_2), 37.3 (CH_2),

32.0 (CH_2), 29.9 (CH_2), 29.67 (CH_2), 29.48 (CH_2), 29.45 (CH_2), 27.40 (CH_2), 27.36 (CH_2), 25.9 (CH_2), 22.8 (CH_2), 14.2 (CH_3). IR (ATR, cm^{-1}) 3352, 3329, 3290, 3005, 2922, 2853, 1567, 1458, 1320, 1077, 940, 821, 721. HRMS (ESI) m/z $C_{16}H_{33}NO$ $[M+H]^+$ = 256.2635, found = 256.2633.

6.4.2 Chain analogues; C6 Phenoxy chain

1-Bromo-4-butoxybenzene 295

A suspension of 1-bromobutane (10 mL, 93.1 mmol), *p*-bromophenol (11.43 g, 66.06 mmol) and K_2CO_3 (10.82 g, 78.4 mmol) in acetone (125 mL) was heated under reflux for 40 hours. The reaction mixture was allowed to cool to room temperature, filtered and the filtrate concentrated under reduced pressure. The resulting residue was purified by vacuum distillation (approx 25 mm Hg) to give **295** as a light yellow oil (11.5 g, 76 %). The NMR spectra match those reported.[173]

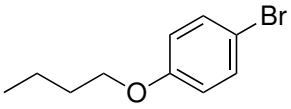

295

^{1}H NMR ($CDCl_3$): δ 7.36 (ad, J = 9.1 Hz, 2H), 6.78 (ad, J = 9.1 Hz, 2H), 3.92 (t, J = 6.5 Hz, 2H), 1.76 (m, 2H), 1.49 (m, 2H), 0.98 (t, J = 7.4 Hz, 3H). ^{13}C NMR ($CDCl_3$): δ 158.4, 132.3, 116.4, 112.7, 68.1, 31.4, 19.3, 14.0. IR (ATR, cm^{-1}): 2958, 2933, 2872, 1590, 1577, 1487, 1473, 1284, 1240, 1170, 1070, 1001, 971, 818.

5-(4-Butoxyphenyl)pent-4-yn-1-ol 292

A mixture of the bromide **295** (2.504 g, 10.9 mmol), pent-4-yn-1-ol (2.808 g, 33.3 mmol, 3.1 eq), $PdCl_2(PPh_3)_2$(383 mg, 0.539 mmol, 4.9 mol%), CuI (208 mg, 1.09 mmol, 10 mol%) and PPh_3 (290 mg, 1.105 mmol, 10 mol%) in 1:4 NEt_3:THF (70 mL) was heated under reflux for 15 hours under N_2. The black reaction mixture was allowed to cool and concentrated under reduced pressure. The residue was dispersed in DCM (150 mL), filtered and the filtrate washed with hydrochloric acid (1M, 4 x 100 mL) and brine (1 x 100 mL). The organic phase was dried over anhydrous K_2CO_3 and concentrated under reduced pressure to give a crude

yellow oil (3.3 g) which was purified by column chromatography (20% EtOAc in PS) to give **292** as a golden oil (1.41 g, 56%) that contained a small PPh_3 impurity.

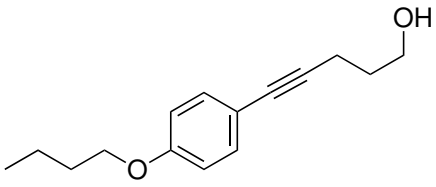

292

^{1}H NMR ($CDCl_3$): δ 7.32-7.29 (m, 2H), 6.81-6.78 (m, 2H), 3.94 (t, J = 6.5 Hz, 2H), 3.83-3.80 (m, 2H), 2.52 (m, 2H), 1.88-1.81 (m, 2H), 1.79-1.72 (m, 2H), 1.64 (s, 1H), 1.48 (m, 2H), 0.97 (t, J = 7.4 Hz, 3H). ^{13}C NMR ($CDCl_3$): δ 158.9 (C), 133.0 (CH), 115.7 (C), 114.5 (CH), 87.7 (C), 81.1 (C), 67.8 (CH_2), 62.1 (CH_2), 31.6 (CH_2), 31.4 (CH_2), 19.4 (CH_2), 16.2 (CH_2), 14.0 (CH_3). IR (ATR, cm^{-1})3441, 3387, 2960, 2907, 2873, 2932, 1604, 1508, 1472, 1285, 1242, 1174, 1041, 1008, 922, 828. HRMS (ESI) m/z $C_{15}H_{20}O_2$ $[M+H]^+$ = 233.1536, found 233.1527.

5-(4-Butoxyphenyl)pentan-1-ol 297

The alkyne **292** (1.39 g, 0.598 mmol) was dissolved in EtOAc (3 mL) and a nitrogen atmosphere introduced (x 3). Pd/C (150 mg, 5%) was added and a hydrogen atmosphere was introduced (x 3) stirred overnight at room temperature. A nitrogen atmosphere was introduced and the reaction mixture filtered. The filtrate was concentrated under reduced pressure to give **297** as a golden oil (1.25 g, 88%) that did not require further purification.

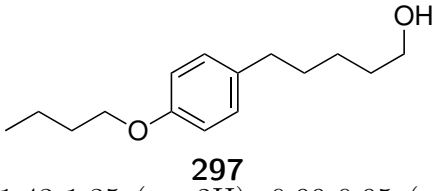

297

^{1}H NMR ($CDCl_3$): δ 7.09-7.05 (m, 2H), 6.87-6.80 (m, 2H), 3.95-3.92 (m, 2H), 3.65-3.62 (m, 2H), 2.56 (t, J = 7.6 Hz, 2H), 1.79-1.70 (m, 3H), 1.66-1.56 (m, 4H), 1.53-1.44 (m, 2H), 1.43-1.35 (m, 2H), 0.99-0.95 (m, 3H). ^{13}C NMR ($CDCl_3$): δ 157.4 (C), 134.6 (C), 129.3 (CH), 114.5 (CH), 67.8 (C), 63.1 (C), 35.1 (C), 32.8 (CH_2), 31.62 (CH_2), 31.56 (CH_2), 25.5 (CH_2), 19.4 (CH_2), 14.0 (CH_3). IR (ATR, cm^{-1}) 3326, 2931, 2859, 1611, 1510, 1464, 1241, 1175, 1068, 1042, 974, 827, 699. HRMS (ESI) m/z $C_{15}H_{24}O_2$ $[M+H]^+$ = 237.1849, found = 237.1839.

5-(4-Butoxyphenyl)pentanal 293

A solution of anhydrous DMSO (800 µl) in DCM (2 mL) was added dropwise to a stirred solution of oxalyl chloride (450 µl, 5.35 mmol) in anhydrous DCM (4 mL) at -84°C. The reaction mixture was held at this temperature for 20 min before the dropwise addition of a solution of the alcohol **297** (1.01 g, 4.28 mmol) in anhydrous DCM (2 mL). The reaction mixture required addition of anhydrous DCM (5 mL) to ensure fluidity. The reaction mixture was stirred for a further 20 min at -84°C before the addition of triethylamine (3 mL). The reaction mixture was left to progressively warm to room temperature and left for 30 min before dilution with DCM (100 mL). The reaction mixture was washed with water (100 mL), hydrochloric acid (2 x 100 mL, 1M) and brine (1 x 100 mL) and dried over anhydrous K_2CO_3. The filtrate was concentrated under reduced pressure and the resulting yellow oil (933 mg) was subjected to column chromatography (5% EtOAc in PS) to give the aldehyde **293** as a golden oil (668 mg, 67%).

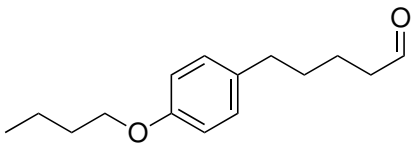

293

^{1}H NMR ($CDCl_3$): δ 9.75 (t, J = 1.8 Hz, 1H), 7.08-7.05 (m, 2H), 6.84-6.80 (m, 2H), 3.94 (t, J = 6.5 Hz, 2H), 2.58 (t, J = 7.1 Hz, 2H), 2.44 (m, 2H), 1.79-1.72 (m, 2H), 1.69-1.61 (m, 4H), 1.54-1.45 (m, 2H), 0.98 (t, J = 7.4 Hz, 3H). ^{13}C NMR ($CDCl_3$): δ 202.6 (CH), 157.5 (C), 133.9 (C), 129.3 (CH), 114.5 (CH), 67.8 (CH_2), 43.9 (CH_2), 34.8 (CH_2), 31.5 (CH_2), 31.2 (CH_2), 21.7 (CH_2), 19.4 (CH_2), 14.0 (CH_3). IR (ATR, cm^{-1})2932, 2867, 1724, 1611, 1510, 1390, 1241, 1176, 827. HRMS (ESI) m/z $C_{15}H_{22}O_2$ $[M\text{-}H]^+$ = 233.1547, found 233.1526.

5-(4-Butoxyphenyl)pentanoic acid 303

A solution of the aldehyde **293** (1.24 g, 5.29 mmol) and 2-methyl-2-butene (7.51 g, 107 mmol, 20 eqv) in 1:1 t-BuOH:THF (30 mL) was stirred with a solution of sodium dihydrogen phosphate (7.07 g, 58.9 mmol, 11 eqv) and sodium chlorite (1.47 g, 16.2 mmol, 3 eqv) in water (40 mL) overnight in a ice bath. The reaction mixture was diluted with hydrochloric acid (250 mL, 1M) and extracted with EtOAc (5 x 50 mL). The extracts were washed with sodium metabisulfite solution

(50 mL, 1%) and brine (50 mL) and dried over anhydrous $MgSO_4$. The filtrate was concentrated under reduced pressure to give **303** as brown crystalline solid (1.40 g, >100%) that was used in the following step without purification.

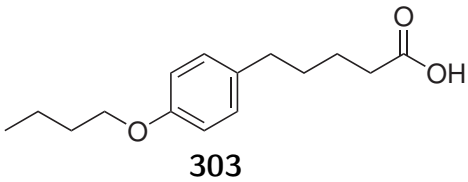

303

^{1}H NMR ($CDCl_3$): δ 7.12-7.08 (m, 2H), 6.87-6.83 (m, 2H), 3.97 (t, J = 6.5 Hz, 2H), 2.60 (t, J = 7.1 Hz, 2H), 2.39 (t, J = 7.1 Hz, 2H), 1.82-1.75 (m, 2H), 1.73-1.65 (m, 4H), 1.52-1.47 (m, 1H), 1.35-1.30 (m, 2H), 1.03-0.99 (m, 3H). ^{13}C NMR: δ 179.6 (C), 157.4 (C), 134.0 (C), 129.3 (CH), 114.5 (CH), 67.8 (CH_2), 34.7 (CH_2), 34.0 (CH_2), 31.5 (CH_2), 31.1 (CH_2), 24.4 (CH_2), 19.4 (CH_2), 14.0 (CH_3).

Propyl 5-(4-butoxyphenyl)pentanoate 302

A mixture of crude acid **303** (1.40 g, 5.59 mmol), 1-bromopropane (1.1 mL, 1.5 g, 12.1 mmol, 2 eqv), TBAI (215 mg, 0.582 mmol, 10 mol%) and K_2CO_3 (3.88 g, 28.0 mmol) in acetone (10 mL) was heated at reflux for 3 hours and then allowed to cool to room temperature. The reaction mixture was concentrated under reduced pressure and diluted with HCl (1M, until pH < 1) and extracted with EtOAc (4 x 25 mL). The organic phase was washed with brine (50 mL), dried over anhydrous $MgSO_4$ and concentrated. The crude yellow oil (1.64 g) was purified by column chromatography (5% EtOAc in PS) to give **302** as a clear oil (1.23 g, 83% over 2-Steps)

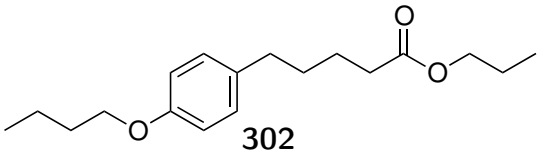

302

^{1}H NMR ($CDCl_3$): δ 7.08-7.06 (m, 2H), 6.83-6.81 (m, 2H), 4.03 (m, 2H), 3.94 (t, J = 6.5 Hz, 2H), 2.57 (t, J = 7.2 Hz, 2H), 2.33 (dd, J = 9.3, 5.1 Hz, 2H), 1.79-1.72 (m, 2H), 1.69-1.60 (m, 6H), 1.52-1.46 (m, 2H), 0.98 (t, J = 7.2 Hz, 3H), 0.94 (t, J = 7.2 Hz, 3H). ^{13}C NMR ($CDCl_3$): δ 173.9 (C), 157.4 (C), 134.1 (C), 129.3 (CH), 114.5 (CH), 67.8 (CH_2), 66.0 (CH_2), 34.8 (CH_2), 34.3 (CH_2), 31.5 (CH_2), 31.3 (CH_2), 24.7 (CH_2), 22.1 (CH_2), 19.4 (CH_2), 14.0 (CH_3), 10.5 (CH_3). IR (ATR, cm^{-1}) 2960, 2934, 2873, 1733, 1612, 1511, 1463, 1511, 1463, 1241, 1175, 1067, 826. HRMS (ESI) m/z $C_{18}H_{28}O_3[M+H]^+$ = 293.2111, found

= 293.2110.

7-(4-Butoxyphenyl)-3-oxoheptanenitrile 304

A solution of freshly distilled acetonitrile (270 µl, 212 mg, 5.17 mmol, 2.5 eqv) in THF (3 mL) was added dropwise to a stirred solution of *n*-BuLi (3.0 mL, 1.6 M, 4.8 mmol, 2.3 eqv) in THF (5 mL) at -84°C. The reaction mixture was stirred at this temperature for 30 min before dropwise addition of a solution of the ester **302** (604 mg, 2.06 mmol) in THF (3 mL). The reaction mixture was stirred at -84°C for 10 min before addition of sat. NH_4Cl solution. The reaction mixture was allowed to warm to room temperature and diluted with HCl (1M, 30 mL). The reaction mixture was extracted with DCM (3 x 30 mL) and the combined extracts were washed with brine and dried over anhydrous $MgSO_4$. The filtrate was concentrated under reduced pressure to give a crude yellow oil (557 mg) that was purified by column chromatography (15 - 20 % EtOAc in PS) to give **304** as a white waxy solid (321 mg, 57%).

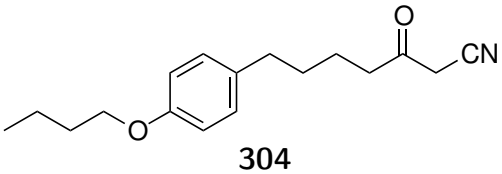

304

Melting point: 63°C. ^{1}H NMR ($CDCl_3$): δ 7.08-7.04 (m, 2H), 6.84-6.80 (m, 2H), 3.94 (t, J = 6.5 Hz, 2H), 3.40 (s, 2H), 2.63-2.55 (m, 4H), 1.79-1.72 (m, 2H), 1.68-1.58 (m, 4H), 1.49 (m, 2H), 0.99-0.96 (m, 3H). ^{13}C NMR ($CDCl_3$): δ 197.5 (C), 157.5 (C), 133.7 (C), 129.3 (CH), 114.5 (CH), 113.9 (C) 67.8 (CH_2), 42.1 (CH_2), 34.7 (CH_2), 32.0 (CH_2), 31.5 (CH_2), 30.8 (CH_2), 22.9 (CH_2), 19.3 (CH_2), 13.9 (CH_3). IR (ATR, cm^{-1}) 2936, 2871, 2261, 1711, 1611, 1510, 1239, 1176, 1037, 1007, 824, 817. HRMS (ESI) m/z $C_{17}H_{23}NO_2$ $[M+H]^+$ = 274.1802, found = 274.1797.

1-Amino-7-(4-butoxyphenyl)heptan-3-ol 120

A solution of the ketonitrile **304** (266 mg, 0.972 mmol) in THF (2 mL) was added dropwise to a suspension of $LiAlH_4$ (100 mg, 2.66 mmol) in THF (2 mL) in a ice bath. The reaction mixture was left in the ice bath to warm to room temperature over 3 hours. The reaction mixture was cooled to 0°C before addition of sat NH_4Cl solution, followed by 1M HCl. A solution of sat. Na_2CO_3 was added until pH >7

and extracted with EtOAc (4 x 25 mL). The extracts were washed with brine, dried over anhydrous $MgSO_4$ and concentrated to give a yellow crude (252 mg) that was purified by column chromatography (10:1:89 MeOH:$NH_{3(aq)}$:$CHCl_3$) to give **120** as a colourless power (20 mg, 12%).

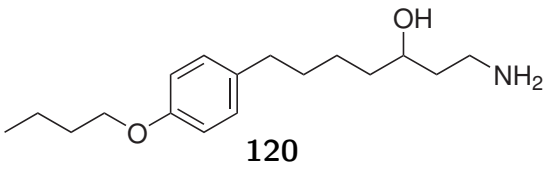

120

Melting point: 81°C. ^{1}H NMR ($CDCl_3$): δ 7.07 (d, J = 8.4 Hz, 2H), 6.80 (d, J = 8.5 Hz, 2H), 3.93 (t, J = 6.5 Hz, 2H), 3.83-3.77 (m, 1H), 3.16-3.10 (m, 1H), 2.87-2.80 (m, 1H), 2.55 (t, J = 7.7 Hz, 2H), 1.75 (m, 2H), 1.69-1.55 (m, 5H), 1.54-1.32 (m, 8H), 0.97 (t, J = 7.4 Hz, 3H). ^{13}C NMR ($CDCl_3$): δ 157.3 (C), 134.8 (C), 129.3 (CH), 114.4 (CH), 73.5 (CH), 67.8 (CH_2), 41.2 (CH_2), 37.9 (CH_2), 37.7 (CH_2), 35.2 (CH_2), 32.0 (CH_2), 31.6 (CH_2), 25.4 (CH_2), 19.4 (CH_2), 14.0 (CH_3). IR (ATR, cm^{-1}) 3361, 3276, 2956, 2923, 2871, 1612, 1510, 1475, 1243, 1177, 1069, 1026, 970, 809. HRMS (ESI) m/z $C_{17}H_{29}NO_2$ $[M+H]^+$ = 280.2271, found = 280.2275.

6.5 Biology

The assays were conducted by Prof. Sumalee Kamchonwongpaisan at the National Centre for Genetic Engineering and Biotechnology, Thailand.

Trypanosome culture and testing compounds in vitro

Trypanosome brucei rhodesiense (STB900) was maintained continuously in MEM/EBSS medium supplemented with 3 g/l Sodium bicarbonate, 4.5 g/l glucose, 25 mM HEPES, pH 7.3, 0.05 mM bathocuproinedisulphonic acid disodium salt, 1.5 mM L-cysteine, 1 mM hypoxanthine, 0.16 mM thymidine, 1 mM sodium pyruvate, 0.2 mM 2-mercaptoethanol, 1% MEM non-essential amino acid, and 15% heated fetal bovine serum, in a 5% CO_2 incubator. To assay anti-Tbr activity, a modified reported protocol was used.[180] Briefly, 2 x 10^4 Trypanasome cells in 175 µl culture media /well were incubated with 25 μl of varying concentrations of each compound in a 96-well plate under the same culture condition. The compounds

were dissolved in DMSO and the final concentration of DMSO in each well was 0.1% which causes no effect on parasite viability. Following 72-hour incubation, 20 µl Alamar Blue (a resazurin solution) was added in each well. The reaction was further incubated at 37°C, 5% CO_2 for 3 hours to allow irreversible reduction of resazurin (violet colour) to resorufin (pink color) by viable trypanosome cells. The fluorescence signals were measured by spectrofluorometer at ex530/em585 nm. The results were read as concentration of each compound that exhibit 50% growth inhibition (IC_{50}) from the dose-response curve established from the fluorescence signals at each concentration of compounds.

Parasite Culture and Antimalarial Testing in Vitro.

Two *P. falciparum* strains, TM4/8.2 (wild-type drug sensitive strain) and K1CB1 (multidrug resistant strain) were used in this study, these were generous gifts from S. Thaithong, Department of Biology, Faculty of Science, Chulalongkorn University. The parasites were maintained continuously in human erythrocytes at 37°C under 3% CO_2 in RPMI 1640 culture media (Gibco, USA) supplemented with 25 mM HEPES (Sigma), pH 7.4, 2 g/L NaHCO3 and 10% human serum. In vitro antimalarial activity was determined by using the [3H] hypoxanthine incorporation method. 1.5% cell suspension of parasitized erythrocytes with 1% parasitemia (200 µL) in each well was incubated with varying concentration of compound (25 µL) under the same culture conditions for 24 h. Parasite survival was determined by [3H] hypoxanthine incorporation assay. Briefly, 25 µL of 0.5 µCi [3H] hypoxanthine was added to each well, and the mixture was further incubated for 18-20 h. Then the cells were lysed with water and the parasite DNA was harvested onto 96-well microplates with built-in glass fiber filters (Unifilter TM plates, Packard, USA). The filters in the plates were air-dried, and then 22 µL of liquid scintillation fluid (Microscint, Packard) was added. The radioactivity on the filters was then measured using microplate scintillation counter (TopCount, Packard, USA). The IC50 of each compound was determined from dose-response curve.[181]

Cytotoxicity testing by sulforhodamine B (SRB) colorimetric assay.

African green monkey kidney fibroblast (VERO cells) and human epidermoid carcinoma (KB) cells were obtained from the bioassay laboratory, BIOTEC, NSTDA. Vero cells were maintained continuously in MEM/EBSS medium supplemented with 10% heated fetal bovine serum, 2.2 g/l Sodium bicarbonate, and 100 mM sodium pyruvate. KB cells were maintained continuously in DMEM/low glucose medium supplemented with 10% heated fetal bovine serum, 3.7 g/l Sodium bicarbonate, and 1%. Non-essential amino acid. Cytotoxicity was determined by sulforhodamine B (SRB) assay. Briefly, 1.9 x 104 cells were incubated with test compounds at 37°C, 5% CO_2 for 72 hours. Then, the cells were fixed with 10% trichloroacetic acid at 4∘C for 45 minute, washed with water and dried at room temperature overnight. Then the plate was stained with 0.057% (W/V) sulforhodamine B, washed 4 times with 1% (V/V) acetic acid, and left dry at room temperature overnight. Finally, 10X Tris-base was added to each well to dissolve protein-bound dye. The optical density was determined by spectrophotometer at wavelength 510 nm. The IC_{50} value of each compound was determined from the dose-response curve.[182]

Bibliography

[1] Gordon, J. I.; Duronio, R. J.; Rudnick, D. A.; Adams, S. P.; Gokel, G. W. *The Journal of biological chemistry* **1991**, *266*, 8647.

[2] Vetting, M. W.; Luiz, L. P.; Yu, M.; Hegde, S. S.; Magnet, S.; Roderick, S. L.; Blanchard, J. S.; Carvalho, L. P. S. D.; Yu, M.; Hegde, S. S.; Magnet, S.; Roderick, S. L.; Blanchard, J. S. *Archives of Biochemistry and Biophysics* **2005**, *433*, 212–226.

[3] Dyda, F.; Klein, D. C.; Hickman, A. B. *Annu. Rev. Biophys. Biomol. Struct* **2000**, *29*, 81–103.

[4] Rudnick, D. a.; McWherter, C. a.; Rocque, W. J.; Lennon, P. J.; Getman, D. P.; Gordon, J. I. *Journal of Biological Chemistry* **1991**, *266*, 9732–9739.

[5] Weston, S. A.; Camble, R.; Colls, J.; Rosenbrock, G.; Taylor, I.; Egerton, M.; Tucker, A. D.; Tunnicliffe, A.; Mistry, A.; Mancia, F.; de la Fortelle, E.; Irwin, J.; Bricogne, G.; Pauptit, R. A. *Nat Struct Mol Biol* **1998**, *5*, 213–221.

[6] Bhatnagar, R. S.; et al. *Nat Struct Mol Biol* **1998**, *5*, 1091–1097.

[7] Zheng, G. Q.; Hu, X.; Cassady, J. M.; Paige, L. A.; Geahlen, R. L. *Journal of pharmaceutical sciences* **1994**, *83*, 233–238.

[8] Tate, E. W.; Bell, A. S.; Rackham, M. D.; Wright, M. H. *Parasitology* **2014**, *141*, 37–49.

[9] Farazi, T. A.; Waksman, G.; Gordon, J. I. *Biochemistry* **2001**, *40*, 6335–6343.

[10] Wu, J.; Tao, Y.; Zhang, M.; Howard, M. H.; Gutteridge, S.; Ding, J. *Journal of Biological Chemistry* **2007**, *282*, 22185–22194.

[11] Towler, D. A.; Eubanks, S. R.; Towery, D. S.; Adams, S. P.; Glaser, L. *Journal of Biological Chemistry* **1987**, *262*, 1030–1036.

[12] Maurer-Stroh, S.; Eisenhaber, B.; Eisenhaber, F. *Journal of Molecular Biology* **2002**, *317*, 523–540.

[13] Hawksworth, D. L. *Mycol. Res.* **2001**, *105*, 1422–1432.

[14] Taylor, L. H.; Latham, S. M.; Woolhouse, M. E. J.; Taylor, L. H.; Lathamt, S. M.; Woolhouse, M. E. J.; Bush, E. *Philosophical Transactions of the Royal Society B: Biological Sciences* **2001**, *356*, 983–989.

[15] Garcia-Solache, M. A.; Casadevall, A. *mBio* **2010**, *1*, e00061–10.

[16] Center for Disease Control and Prevention; *Preventing Deaths from Cryptococcal Meningitis*; 2016. `http://www.cdc.gov/fungal/global/cryptococcal-meningitis.html`.

[17] Park, B. J.; Wannemuehler, K. A.; Marston, B. J.; Govender, N.; Pappas, P. G.; Chiller, T. M. *Aids* **2009**, *23*, 525–530.

[18] Center for Disease Control; *Preventing Deaths from Histoplasmosis*; 2016. `http://www.cdc.gov/fungal/global/histoplasmosis.html`.

[19] *Public Health Image Library*; 2006. `http://www.cdc.gov/`.

[20] Lemke, T. L.; Williams, D. A. *Foye's Principles of Medicinal Chemistry*, 2007.

[21] Langner, C. A.; Lodge, J. K.; Travis, S. J.; Caldwell, J. E.; Lu, T.; Li, Q.; Bryant, M. L.; Devadas, B.; Gokel, G. W.; Kobayashi, G. S.; Gordon, J. I. *Journal of Biological Chemistry* **1992**, *267*, 17159–17169.

[22] Parang, K.; Knaus, E. E.; Wiebe, L. I.; Sardari, S.; Daneshtalab, M.; Csizmadia, F. *Archiv der Pharmazie* **1996**, *329*, 475–482.

[23] Carballeira, M.; Neill, R. O.; Parang, K. *Chemistry and Physics of Lipids* **2007**, *150*, 82–88.

[24] Ortiz, D.; Parang, K.; Sardari, S. *Arch. Pharm. Pharm. Med. Chem.* **2004**, 152–155.

[25] Devadas, B.; Zupec, M. *Journal of medicinal ...* **1995**, *38*, 1837–1840.

[26] Sikorski, J. a.; Devadas, B.; Zupec, M. E.; Freeman, S. K.; Brown, D. L.; Lu, H. F.; Nagarajan, S.; Mehta, P. P.; Wade, a. C.; Kishore, N. S.; Bryant, M. L.; Getman, D. P.; McWherter, C. a.; Gordon, J. I. *Biopolymers* **1997**, *43*, 43–71.

[27] Lodge, J. K.; Jackson-machelski, E.; Devadas, B.; Zupec, M. E.; Getman, D. P.; Kishore, N.; Freeman, S. K.; Mcwherter, C. A.; Sikorski, J. A.; Gordon, J. I. *Microbiology* **1997**, 357–366.

[28] Devadas, B.; Freeman, S. K.; Mcwherter, C. A.; Kishore, N. S.; Lodge, J. K.; Jackson-machelski, E.; Gordon, J. I.; Sikorski, J. A. *Journal of medicinal chemistry* **1998**, *2623*, 996–1000.

[29] Masubuchi, M.; et al. *Bioorganic and Medicinal Chemistry Letters* **2001**, *11*, 1833–1837.

[30] Sogabe, S.; Masubuchi, M.; Sakata, K.; Fukami, T. A.; Morikami, K.; Shiratori, Y.; Ebiike, H.; Kawasaki, K.; Aoki, Y.; Shimma, N.; D'Arcy, A.; Winkler, F. K.; Banner, D. W.; Ohtsuka, T.; Sogabe, S. *Chemistry & Biology* **2002**, *9*, 1119–1128.

[31] Ebiike, H.; Masubuchi, M.; Liu, P.; Kawasaki, K.; Sogabe, S.; Hayase, M.; Fujii, T.; Sakata, K.; Shindoh, H.; Shiratori, Y.; Aoki, Y.; Ohtsuka, T.; Shimma, N. *Bioorganic and Medicinal Chemistry Letters* **2002**, *12*, 607 – 610.

[32] Masubuchi, M.; Hirosato, E.; Ken-ichi, K.; Satoshi, S.; Kenji, M.; Yasuhiko, S. *Bioorganic & Medicinal Chemistry* **2003**, *11*, 4463–4478.

[33] Kawasaki, K.-i.; Masubuchi, M.; Morikami, K.; Sogabe, S.; Fujii, T.; Sakata, K.; Shindoh, H.; Shiratori, Y.; Aoki, Y. *Bioorganic & medicinal chemistry letters* **2003**, *13*, 87–91.

[34] World Health Organisation; *Human African Trypanosomiasis (sleeping sickness)*; Tech. Rep. May; 2015. http://www.who.int/mediacentre/factsheets/fs259/en/#.

[35] Center for disease control and Prevention; *African Trypanosomiasis Disease Summary*; 2015. http://www.cdc.gov/parasites/sleepingsickness/disease.html.

[36] Center for Disease Control and Prevention; *Human African Trypanosomiasis (Sleeping Sickness)*; 2012. http://www.cdc.gov/parasites/sleepingsickness/.

[37] Gill, J.; Hobday, K.; Winderbank, A.; Windebank, A. *Experimental Neurology* **1995**, *133*, 113 – 123.

[38] World Health Organization; *Second WHO report on neglected tropical diseases: Sustaining the drive to overcome the global impact of neglected tropical diseases*; 2013.

[39] DNDi; *DNDi update: Sleeping Sickness. The last steps towards innovative oral therapies.*; Tech. Rep.; DNDi; 2017. https://www.dndi.org/wp-content/uploads/2017/10/DNDi_Sleeping_Sickness_Bro

[40] Doering, T. L.; Raper, J.; Buxbaum, L. U.; Adams, S. P.; Gordon, J. I.; Hart, G. W.; Englund, P. T. *Science* **1991**, *252*, 1851–1854.

[41] Doering, T. L.; Lu, T.; Werbovetz, K. A.; Gokel, G. W.; Hart, G. W.; Gordon, J. I.; Englund, P. T. *Proceedings of the National Academy of Sciences of the United States* **1994**, *91*, 9735.

[42] Berriman, M.; et al. *Science* **2005**, *309*, 416–422.

[43] Panethymitaki, C.; Bowyer, P. W.; Price, H. P.; Leatherbarrow, R. J.; Brown, K. a.; Smith, D. F. *The Biochemical journal* **2006**, *396*, 277–285.

[44] Price, H. P.; Menon, M. R.; Panethymitaki, C.; Goulding, D.; McKean, P. G.; Smith, D. F. *J. Biol. Chem.* **2003**, *278*, 7206–7214.

[45] Brenk, R.; Schipani, A.; James, D.; Krasowski, A.; Gilbert, I. H.; Frearson, J.; Wyatt, P. G. *ChemMedChem* **2008**, *3*, 435–444.

[46] Frearson, J. A.; et al. *Nature* **2010**, *464*, 728–32.

[47] Brand, S.; et al. *Journal of Medicinal Chemistry* **2012**, *55*, 1–29.

[48] Brand, S.; et al. *Journal of Medicinal Chemistry* **2014**, *57*, 9855–9869.

[49] World Health Organization; *Malaria Factsheet #94*; Tech. Rep.; 2015. `http://www.who.int/mediacentre/factsheets/fs094/en/`.

[50] World Health Organization; *Status report on artemisinin resistance*; Tech. Rep. September; 2014. `http://www.who.int/malaria/publications/atoz/status_rep_artemisinin_resist`

[51] Ashley, E. a.; et al. *New England Journal of Medicine* **2014**, *371*, 411–423.

[52] Raju, R. V. S.; Sharma, R. K. *Methods in Molecular Biology: Protein Lipidation Protocols. Preparation and Assay of Myristoyl-CoA:Protein N-Myristoyltransferase*; SpringerLink, Ed.; Totowa, NJ : Humana Press Inc.: Totowa, NJ, 1999; Vol. 116.

[53] Bowyer, P. W.; Tate, E. W.; Leatherbarrow, R. J.; Holder, A. A.; Smith, D. F.; Brown, K. A. *ChemMedChem* **2008**, *3*, 402.

[54] Bowyer, P. W.; Gunaratne, R. S.; Grainger, M.; Withers-Martinez, C.; Wickramsinghe, S. R.; Tate, E. W.; Leatherbarrow, R. J.; Brown, K. a.; Holder, A. A.; Smith, D. F. *The Biochemical journal* **2007**, *408*, 173–180.

[55] Yu, Z. Y.; Brannigan, J. a.; Moss, D. K.; Brzozowski, a. M.; Wilkinson, a. J.; Holder, a. a.; Tate, E. W.; Leatherbarrow, R. J. *Journal of Medicinal Chemistry* **2012**, *55*, 8879–8890.

[56] Yu, Z.; Brannigan, J. A.; Rangachari, K.; Heal, W. P.; Wilkinson, A. J.; Holder, A. A.; Leatherbarrow, R. J.; Tate, E. W. *Med. Chem. Commun.* **2015**, *6*, 1767–1772.

[57] Rackham, M. D.; Brannigan, J. A.; Moss, D. K.; Yu, Z.; Wilkinson, A. J.; Holder, A. A.; Tate, E. W.; Leatherbarrow, R. J. *Journal of Medicinal Chemistry* **2013**, 371–375.

[58] Rackham, M. D.; Brannigan, J. A.; Rangachari, K.; Meister, S.; Wilkinson, A. J.; Holder, A. A.; Leatherbarrow, R. J.; Tate, E. W. *Journal of Medicinal Chemistry* **2014**, *57*, 2773–2788.

[59] Goncalves, V.; Brannigan, J. A.; Whalley, D.; Ansell, K. H.; Saxty, B.; Holder, A. A.; Wilkinson, A. J.; Tate, E. W.; Leatherbarrow, R. J. *Journal of Medicinal Chemistry* **2012**, *55*, 3578–3582.

[60] Goncalves, V.; Brannigan, J. A.; Laporte, A.; Bell, A. S.; Roberts, S. M.; Wilkinson, A. J.; Leatherbarrow, R. J.; Tate, E. W.; Leatherbarrow, J.; Tate, E. W. *MedChemComm* **2017**, *8*, 191–197.

[61] Bell, A. S.; Mills, J. E.; Williams, G. P.; Brannigan, J. A.; Wilkinson, A. J.; Parkinson, T.; Leatherbarrow, R. J.; Tate, E. W.; Holder, A. A.; Smith, D. F. *PLoS Negl Trop Dis* **2012**, *6*, e1625.

[62] *US department of health and human service, What Is Coronary Heart Disease?*; 2013. `http://www.nhlbi.nih.gov/health/health-topics/topics/cad/`.

[63] NHS; *Coronary heart disease*; 2013. `http://www.nhs.uk/Conditions/Coronary-heart-disease/Pages/Introduction.aspx`.

[64] Heart Foundation; *Australian Heart disease factsheet*; 2013. `https://www.heartfoundation.org.au/SiteCollectionDocuments/Factsheet-Heart-disease.pdf`.

[65] Fauci., A. In *Harrisons manual of medicine*, 17th ed.; McGraw hill, 2009.

[66] Roth, B. D. *Progress in Medicinal Chemistry* **2002**, *40*, 1–22.

[67] Roitelman, J.; Olender, E. H.; Bar-Nun, S.; Dunn, W. A.; Simoni, R. D. *The Journal of Cell Biology* **1992**, *117*, 959–973.

[68] Stauffacher, C. V.; Haines, B. E.; Wiest, O.; Stauffacher, C. V. *Accounts of Chemical Research* **2013**, *46*, 2416–2426.

[69] Tabernero, L.; Bochar, D. a.; Rodwell, V. W.; Stauffacher, C. V. *Proceedings of the National Academy of Sciences of the United States of America* **1999**, *96*, 7167–71.

[70] Istvan, E. S.; Palnitkar, M.; Buchanan, S. K.; Deisenhofer, J. *The EMBO journal* **2000**, *19*, 819–830.

[71] Laughlin R, C. T. F. *JAMA* **1962**, *181*, 339–340.

[72] Brown, A. G.; Smale, T. C.; King, T. J.; Hasenkamp, R.; Thompson, R. H. *Journal of the Chemical Society, Perkin Transactions 1* **1976**, *0*, 1165–1170.

[73] Endo, A.; Tsujita, Y.; Kuroda, M.; Tanzawa, K. *European Journal of Biochemistry* **1977**, *77*, 31–36.

[74] Endo, A. *Atherosclerosis Supplements* **2004**, *5*, 125–130.

[75] Maggon, K. *Drug Discovery Today* **2005**, *10*, 739–742.

[76] News-medical; *Matrix Laboratories receives FDA approval for generic version Zocor Tablets: Mylan.* `http://www.news-medical.net/news/20100618/Matrix-Laboratories-receives-FDA`

[77] Sato, A.; Ogiso, A.; Noguchi, H.; Mitsui, S.; Kaneko, I.; Shimada, Y. *Chem. Pharm. Bull.* **1980**, *28*, 1509–1525.

[78] Nakamura, C. E.; Abeles, R. H. *Biochemistry* **1985**, *24*, 1364–1376.

[79] Stokker, G. E.; Hoffman, W. F.; Alberts, A. W.; Cragoe, E. J.; Deana, A. A.; Gilfillan, J. L.; Huff, J. W.; Novello, F. C.; Prugh, J. D.; Cragoe Jr, E. J.; Deana, A. A.; Gilfillan, J. L. *Journal of Medicinal Chemistry* **1985**, *28*, 347–358.

[80] Stokker, G. E.; et al. *Journal of Medicinal Chemistry* **1986**, *29*, 170–181.

[81] Hoffman, W.; Anderson, A.; Smith, P.; Willard, J.; Alberts, R.; Chen, A.; Willard, A. *Journal of Medicinal Chemistry* **1986**, *29*, 849–852.

[82] Roth, B. D.; Ortwine, D. F.; Hoefle, M. L.; Stratton, C. D.; Sliskovic, D. R.; Wilson, M. W.; Newton, R. S. *J.Med.Chem.* **1990**, *33*, 21–31.

[83] Repic, O.; Prasad, K.; Lee, G. T. *Organic Process Research and Development* **2001**, *5*, 519–527.

[84] Istvan, E. S.; Deisenhofer, J. *Science* **2001**, *292*, 1160–1164.

[85] Pedersen, T. R.; Kjekshus, J.; Berg, K.; Haghfelt, T.; Faeligrgeman, O.; G Thorgeirsson, K.; Miettinen, T.; Wilhelmsen, L.; Olsson, A. G.; Wedel, H. *Lancet* **1994**, *344*, 1383–1389.

[86] Monteiro, C. M.; Lourenço, N. M. T.; Afonso, C. A. M. *Tetrahedron Asymmetry* **2010**, *21*, 952–956.

[87] Kundig, E. P.; Ripa, A.; Liu, R. G.; Amurrio, D.; Bernardinelli, G. *Organometallics* **1993**, *12*, 3724–3737.

[88] Dimitrov, V.; Panev, S. *Tetrahedron: Asymmetry* **2000**, *11*, 1513–1516.

[89] Fleming, F. F.; Huang, A.; Sharief, V. A.; Pu, Y. *The Journal of Organic Chemistry* **1999**, *64*, 2830–2834.

[90] Satoh, T.; Suzuki, S.; Suzuki, Y.; Miyaji, Y.; Imai, Z. *Tetrahedron Letters* **1969**, *52*, 4555–4558.

[91] Midland, M. M.; Lee, P. E. *The Journal of Organic Chemistry* **1985**, *50*, 3237–3239.

[92] Anderson, K.; Chen, Y.; Chen, Z.; Luk, K.-C.; Rossman, P. L.; *US patent US2012/0184542: pyrido pyrimidines*; 2012.

[93] Cahiez, G. G.; Chaboche, C.; Duplais, C.; Giulliani, A.; Moyeux, A. *Advanced Synthesis and Catalysis* **2008**, *350*, 1484–1488.

[94] Weaver, W. E.; Whaley, W. M. *Journal of the American Chemical Society* **1947**, *69*, 515–516.

[95] Vasalatiy, O.; Zhao, P.; Woods, M.; Marconescu, A.; Castillo-Muzquiz, A.; Thorpe, P.; Kiefer, G. E.; Dean Sherry, A. *Bioorganic and Medicinal Chemistry* **2011**, *19*, 1106–1114.

[96] Salvatore, R. N.; Schmidt, S. E.; Shin, S. I.; Nagle, A. S.; Worrell, J. H.; Jung, K. W. *Tetrahedron Letters* **2000**, *41*, 9705–9708.

[97] Salvatore, R. N.; Yoon, C. H.; Jung, K. W. *Tetrahedron* **2001**, *57*, 7785–7811.

[98] Wuts, P. G. M. *Protective groups in organic synthesis* .; Greene 1931-, T. W.; Sons, J. W. &.; Service), W. I. O., Eds.; Hoboken, N.J. : WILEY: Hoboken, N.J., 2006.

[99] Salvatore, R. N.; Shin, S. I.; Flanders, V. L.; Jung, K. W. *Tetrahedron Letters* **2001**, *42*, 1799–1801.

[100] michael Ross, J.; Hirsh, A.; Boucher, R.; Zhang, J.; *International Patent WO2007/146: Phenyl substituted pyrazinoylguanidine sodium channel blockers possessing beta agonist activity.*; 2007.

[101] Millet, R.; Träff, A. M.; Petrus, M. L.; Bäckvall, J.-E. *Journal of the American Chemical Society* **2010**, *132*, 15182–15184.

[102] Se Hun Kwak and Kee-In Leea, J. M. S. *ARKIVOC* **2010**, *2010*, 55–61.

[103] Cappelli, A.; et al. *Journal of medicinal chemistry* **2011**, *54*, 7165–75.

[104] Hong, S.; Yang, J.; Weinreb, S. M. *The Journal of organic chemistry* **2006**, *71*, 2078–2089.

[105] Sun, C.; Bittman, R. *The Journal of organic chemistry* **2004**, *69*, 7694–9.

[106] ElAmin, B.; Anantharamaiah, G. M.; Royer, G. P.; Means, G. E. *journal of organic chemistry* **1979**, *44*, 3442–3444.

[107] Chandia, N. P.; Canales, J. C.; Azocar, I.; Vanlaer, S.; Pawar, V. G.; De Borggraeve, W. M.; Costamagna, J.; Dehaen, W. *Synthetic Communications* **2009**, *39*, 927–939.

[108] Corriu, R. J.; Huynh, V.; Moreau, J. J. *Tetrahedron Letters* **1984**, *25*, 1887–1890.

[109] Corriu, R. J. P.; Huynh, V.; Iqbal, J.; Moreau, J. J.; Vernhet, C. *Tetrahedron* **1992**, *48*, 6231–6244.

[110] Bai, C.-X.; Zhang, W.-z.; He, R.; Lu, X.-b.; Zhang, Z.-Q. *Tetrahedron Letters* **2005**, *46*, 7225–7228.

[111] Paz, N. R.; Santana, G.; Francisco, C. G.; Su, E.; Francisco, S. *Organic Letters* **2012**, *14*, 3388 – 3391.

[112] Imamoto, T.; Sugiura, Y.; Takiyama, N. *Tetrahedron Letters* **1984**, *25*, 4233–4236.

[113] Imamoto, T.; Takiyama, N.; Nakamura, K.; Hatajima, T.; Kamiya, Y. *Journal of the American Chemical Society* **1989**, *111*, 4392–4398.

[114] Liu, H.-j.; Liu, H.-J.; Shia, K.-S.; Shang, X.; Zhu, B.-Y. *Tetrahedron* **1999**, *55*, 3803–3830.

[115] Ghaffarzadeh, M.; Bolourtchian, M.; Fard, Z. H.; Halvagar, M. R.; Mohsenzadeh, F. *Synthetic Communications* **2006**, *36*, 1973–1981.

[116] Arioli, F.; Borrelli, S.; Colombo, F.; Falchi, F.; Filippi, I.; Crespan, E.; Naldini, A.; Scalia, G.; Silvani, A.; Maga, G.; Carraro, F.; Botta, M.; Passarella, D. *ChemMedChem* **2011**, *6*, 2009–2018.

[117] Hoffman, W.F. ; Cragoe Jr., A.W. ; Deana, E.J. ; Evans, A.A. ; Gould, B.E. ; Novello, J.L. ; Prugh, N.P. ; Rittle, J.W. ; Smith, F.C. ; Stokker, J.D. ; Willard, K. *J Med Chem* **1986**, *29*, 159 – 169.

[118] Molinari, A. J.; *International patent 2004050631. Preparation of substituted dihydrophenanthridine sulfonamides as estrogen receptor (ER) ligands for treatment of inflammatory diseases*; 2004.

[119] Yoshikai, N.; Matsumoto, A.; Norinder, J.; Nakamura, E.; Yoshikai, N.; Matsumoto, A.; Norinder, J.; Nakamura, E. *Synlett* **2010**, *2010*, 313–316.

[120] Dubost, E.; Fossey, C.; Cailly, T.; Rault, S.; Fabis, F. *journal of organic chemistry* **2011**, *76*, 6414–6420.

[121] Sun, C.-l.; Liu, N.; Li, B.-j.; Yu, D.-g.; Wang, Y.; Shi, Z.-j. *Organic Letters* **2010**, *12*, 184–197.

[122] Dey, R.; Ranu, B. C. *Tetrahedron Letters* **2012**, *53*, 1558–1560.

[123] Willard, A. K.; Novello, F. C.; Hoffman, W. F.; Cragoe Jr., E. J.; *U.S.patent: US4567289A. Substituted pyranone inhibitors of cholesterol synthesis.*; 1986.

[124] Li, W.; Thottathil, J.; *US Patent 5,298,625: 4-phosphinyl-3-keto-carboxylate and 4-phosphonyl-3-keto-carboxylate intermediates useful in the preparation of phosphorus containing HMG-CoA reductase inhibitors*; 1994. `http://www.google.com/patents/US5298625`.

[125] Du, K.; Guo, P.; Chen, Y.; Cao, Z.; Wang, Z.; Tang, W. *Angewandte Chemie - International Edition* **2015**, *54*, 3033 – 3080.

[126] Hochstein, F. a.; Brown, W. G. *Journal of the American Chemical Society* **1948**, *70*, 3484–6.

[127] Mayer, M.; Welther, A.; Jacobi von Wangelin, A.; Jacobi, A.; Wangelin, V. *ChemCatChem* **2011**, *3*, 1567–1571.

[128] Hendrix, W. T.; Rosenberg, J. L. *Journal of the American Chemical Society* **1976**, *98*, 4850–4852.

[129] Jimenez S, L.; Ramanathan, A. *Synthesis* **2010**, 217–220.

[130] Lamb, P. B.; McElhinny, C. J.; Sninski, T.; Purdom, H.; Carroll, F. I.; Lewin, A. H. *Journal of Labelled Compounds and Radiopharmaceuticals* **2009**, *52*, 457–462.

[131] Y.S.Tang; Jones, L.; Sunay, U. B. *Journal of labelled compounds and radiopharmaceuticals* **1997**, *41*.

[132] Thottathil, J.; Wen S, L.; *Process for the preparation of 4-phosphinyl-3-keto-carboxylate and 4-phosphonyl-3-keto-carboxylate useful in the preparation of phosphorus containing HMG-COA reductase inhibitors*; 1994.

[133] Lutz, R. E.; et al. *The Journal of Organic Chemistry* **1947**, *12*, 617–703.

[134] Kröhnke, F. *Berichte der deutschen chemischen Gesellschaft (A and B Series)* **1936**, *69*, 921–935.

[135] Cowper, R. M.; Davidson, L. H. *Organic Syntheses* **1939**, *19*, 24.

[136] V., M. I.; Ivanovi; D., M.; Piatak, D. M.; Boji; Dj, V. *Synthesis* **1991**, *1991*, 1043–1045.

[137] Walkup, R. E.; Linder, J. *Tetrahedron Letters* **1985**, *26*, 2155–2158.

[138] Hünig, S.; Kiessel, M. *Chemische Berichte* **1958**, *91*, 380–392.

[139] Wolleb, A.; Wolleb, H.; *J0222, wolleb, 2001.pdf*; 2001.

[140] Lee, G. T.; Amedio, J. C.; Underwood, R.; Prasad, K.; Repic, O. *The Journal of Organic Chemistry* **1992**, *57*, 3250–3252.

[141] Mirza-Aghayan, M.; Boukherroub, R.; Bolourtchian, M.; Rahimifard, M. *Journal of Organometallic Chemistry* **2007**, *692*, 5113–5116.

[142] Jackson, W. R.; Zurqiyah, A. *Journal of the Chemical Society (Resumed)* **1965**, 5280–5287.

[143] Raucher, S.; Hwang, K.-J. *Synthetic Communications* **1980**, *10*, 133–137.

[144] Castelijns, A. M. C.; Hogeweg, J. M.; Van, N. S. P. J. **1996**, 14 pp.

[145] Kishore, N. S.; Lu, T. B.; Knoll, L. J.; Katoh, A.; Rudnick, D. A.; Mehta, P. P.; Devadas, B.; Huhn, M.; Atwood, J. L.; Adams, S. P.; Gokel, G. W.; Gordon, J. I. *Journal of Biological Chemistry* **1991**, *266*, 8835–8855.

[146] Mun, J.; Onorato, A.; Nichols, F. C.; Morton, M. D.; Saleh, A. I.; Welzel, M.; Smith, M. B. *Organic & Biomolecular Chemistry* **2007**, *5*, 3826–3833.

[147] Kikushima, K.; Moriuchi, T.; Hirao, T. *Tetrahedron Letters* **2010**, *51*, 340–342.

[148] Vinczer, P.; Kovacd, T.; Novak, L.; Szantay, C. *Organic Preparations and Procedures International* **1989**, *21*, 232–237.

[149] Kabalka, G. W.; Wang, L.; Pagni, R. M. *ARKAK* **2001**, *2001*, 5–11.

[150] Buck, M.; Chong, J. M. *Tetrahedron Lett.* **2001**, *42*, 5825–5827.

[151] Patil, S.; Bukiya, A. N.; Li, W.; Dopico, A. M.; Miller, D. *Bioorganic & medicinal chemistry letters* **2008**, *18*, 3427–30.

[152] Wube, A. A.; Hüfner, A.; Thomaschitz, C.; Blunder, M.; Kollroser, M.; Bauer, R.; Bucar, F. *Bioorganic and Medicinal Chemistry* **2011**, *19*, 567–579.

[153] Thompson, C. M.; Frick, J. A. *Journal of Organic chemisty* **1989**, *54*, 890–896.

[154] Wolfe, S.; Akuche, C.; Ro, S.; Wilson, M.-C.; Kim, C.-K.; Shi, Z. *Canadian Journal of Chemistry* **2003**, *81*, 915–936.

[155] Falck, J. R.; Wallukat, G.; Puli, N.; Goli, M.; Arnold, C.; Konkel, A.; Rothe, M.; Fischer, R.; Müller, D. N.; Schunck, W.-H. *Journal of medicinal chemistry* **2011**, *54*, 4109–18.

[156] Bheemashankaa, K. *Journal of natural products* **1994**, *57*, 537–538.

[157] Kandula, M.; *WO2013175376A2.pdf*; 2013.

[158] Tasdemir, D.; Sanabria, D.; Lauinger, I. L.; Tarun, A.; Herman, R.; Perozzo, R.; Zloh, M.; Kappe, S. H.; Brun, R.; Carballeira, N. M. *Bioorganic & medicinal chemistry* **2010**, *18*, 7475–85.

[159] Albu, S.; Sverko, E.; Arts, M. T.; Capretta, A. *Tetrahedron Letters* **2011**, *52*, 787–788.

[160] Snider, B. B.; Lu, Q. *The Journal of organic chemistry* **1996**, *61*, 2839–2844.

[161] Vedejs, E.; Arnost, M. J.; Hagen, J. P. *Journal of Organic chemisty* **1979**, *44*, 3230–3238.

[162] Dickschat, J. S.; Bode, H. B.; Kroppenstedt, R. M.; Müller, R.; Schulz, S. *Organic & biomolecular chemistry* **2005**, *3*, 2824–2831.

[163] Lindlar, H. *Helvetica Chimica Acta* **1952**, *35*, 446–450.

[164] Publication, A.; Lindlar, H.; Dubuis, R. *Organic Syntheses* **1966**, *46*, 89.

[165] Boland, W.; Schroer, N.; Sieler, C.; Bottmuhle, A. D.; Feigel, M. *Helvetica Chemica Acta* **1987**, *70*, 1025 – 1040.

[166] Brown, H.; Brown, C. *Journal of the American Chemical Society* **1963**, *85*, 1005–1006.

[167] Brown, C. A.; Ahuja, V. K. *Journal of the Chemical Society, Chemical Communications* **1973**, 553.

[168] Ganem, B.; Osby, J. O. *Chemical Reviews* **1986**, *86*, 763–780.

[169] Santangelo, E. M.; Zarbin, P. H. G.; Cass, Q. B.; Ferreira, J. T. B.; Corrêa, A. G. *Synthetic Communications* **2001**, *31*, 3685–3698.

[170] Wright, N. E.; Snyder, S. A. *Angewandte Chemie - International Edition* **2014**, *53*, 3409–3413.

[171] Morris, G. M.; Huey, R.; Olson, A. J. *Current Protocols in Bioinformatics* **2008**, 1–40.

[172] Morris, G. G. M.; Huey, R.; Lindstrom, W.; Sanner, M. F.; Belew, R. K.; Goodsell, D. S.; Olson, A. J. *Journal of ...* **2009**, *30*, 2785–2791.

[173] Yao, Y.; Zhang, Q. T.; Tour, J. M. *Macromolecules* **1998**, *31*, 8600–8606.

[174] Gschneidtner, T. a.; Moth-Poulsen, K. *Tetrahedron Letters* **2013**, *54*, 5426–5429.

[175] Armarego, W. L.; Chai, C. L. L. *Purification of Laboratory Chemicals: Fifth Edition*, 2003.

[176] Monteiro, C. M.; Afonso, C. A. M.; Lourenc, N. M. T.; Lourenço, N. M. T. *Journal of Chemical Education* **2010**, *87*, 423–425.

[177] Adima, A.; Bied, C.; Moreau, J. J. E.; Man, M. W. C. *European Journal of Organic Chemistry* **2004**, 2582–2588.

[178] Hanada, S.; Ishida, T.; Motoyama, Y.; Nagashima, H. *Journal of Organic Chemistry* **2007**, *72*, 7551–7559.

[179] Ghorpade, A. K.; Huddar, S. N.; Akamanchi, K. G. *Tetrahedron Letters* **2016**, *57*, In Press.

[180] Gros, L.; Castillo-Acosta, V. M.; Jiménez, C. J.; Sealey-Cardona, M.; Vargas, S.; Estévez, A. M.; Yardley, V.; Rattray, L.; Croft, S. L.; Ruiz-Perez, L. M.; Urbina, J. A.; Gilbert, I. H.; González-Pacanowska, D. *Antimicrobial Agents and Chemotherapy* **2006**, *50*, 2595–2601.

[181] Yuthavong, Y.; Vilaivan, T.; Chareonsethakul, N.; Kamchonwongpaisan, S.; Sirawaraporn, W.; Quarrell, R.; Lowe, G. *Journal of Medicinal Chemistry* **2000**, *43*, 2738–2744.

[182] Vichai, V.; Kirtikara, K. *Nature Protocols* **2006**, *1*, 1112–1116.

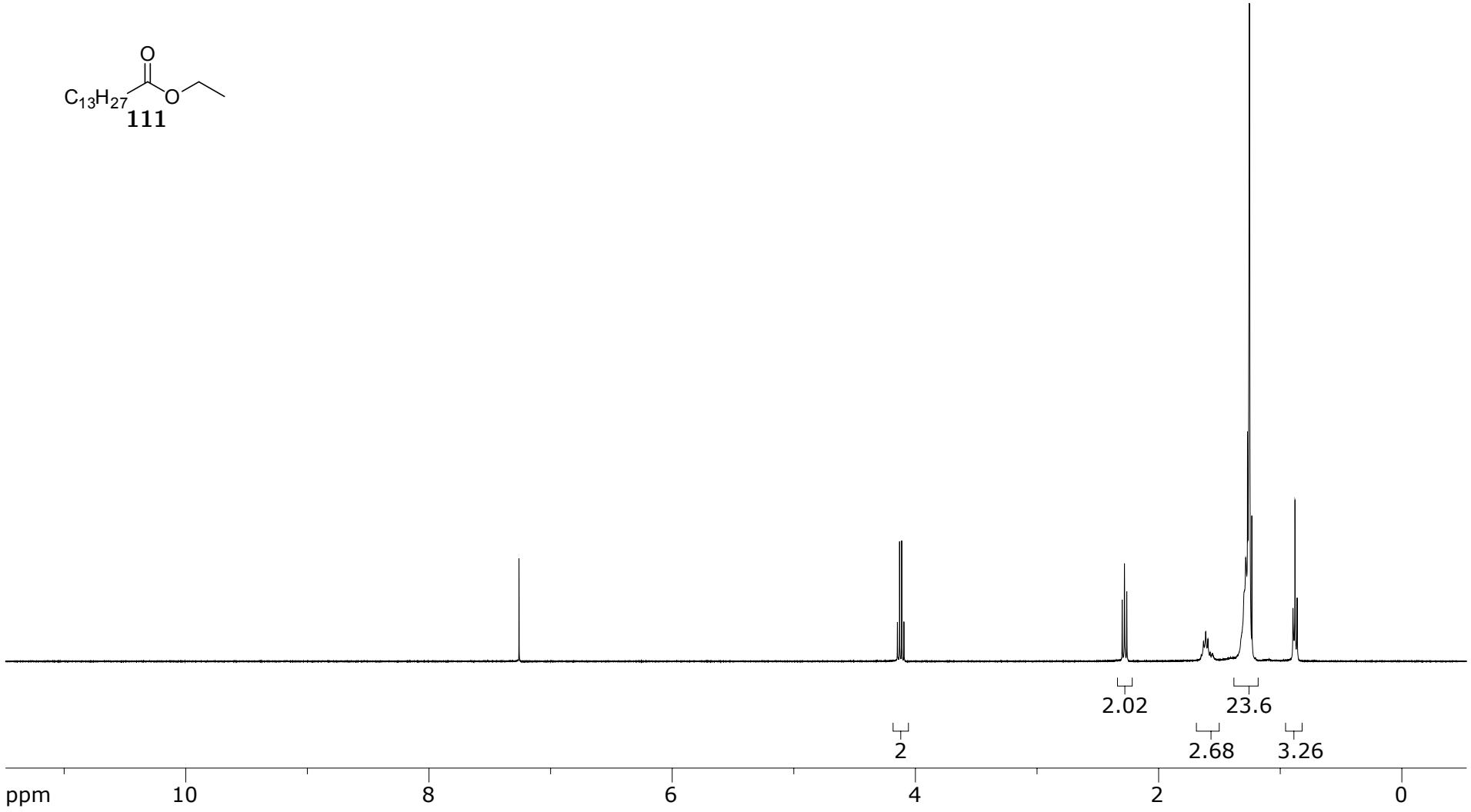

Figure A.1: 400 MHz ^{1}H NMR of **111** in $CDCl_3$

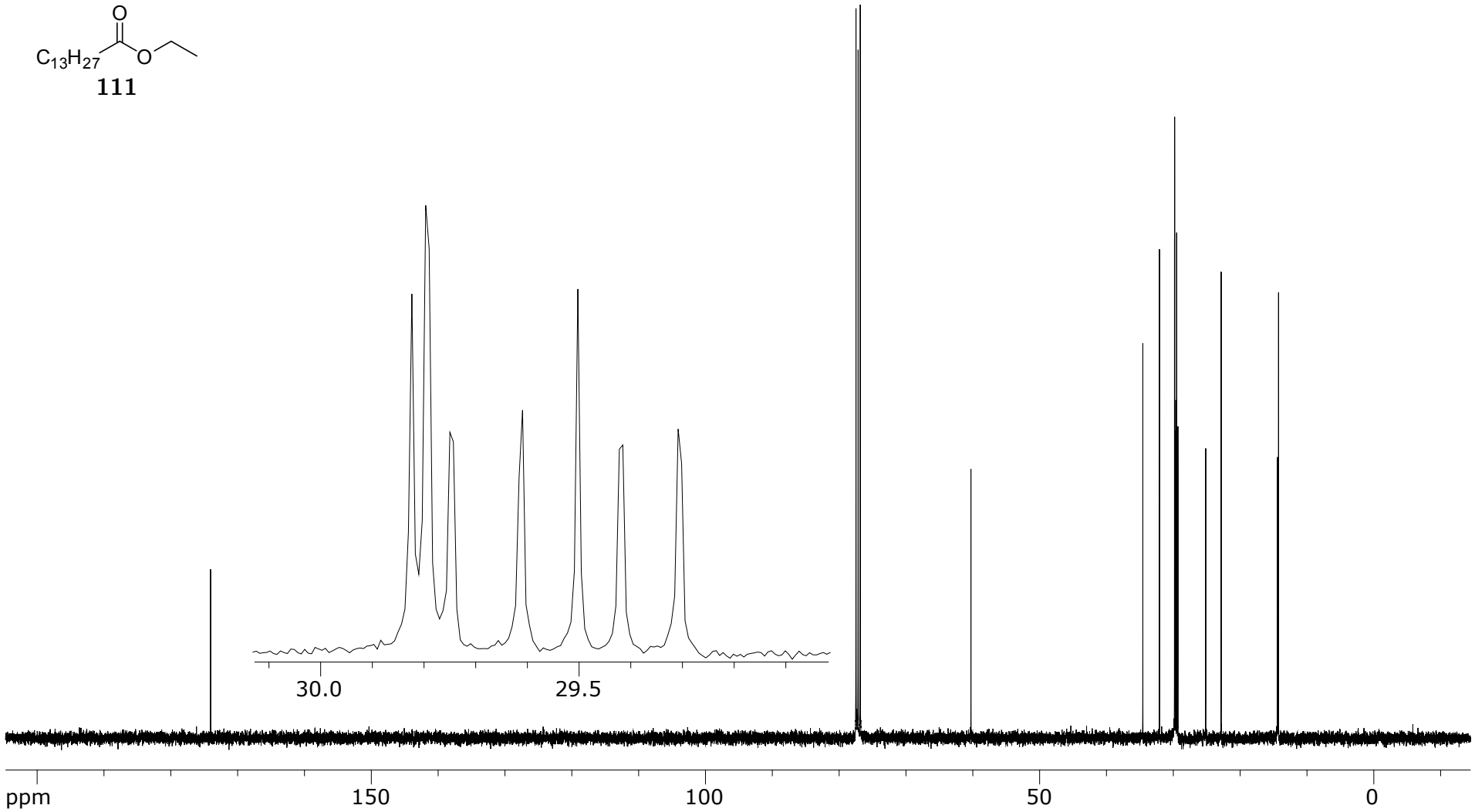

Figure A.2: 100 MHz ^{13}C NMR **111** in $CDCl_3$

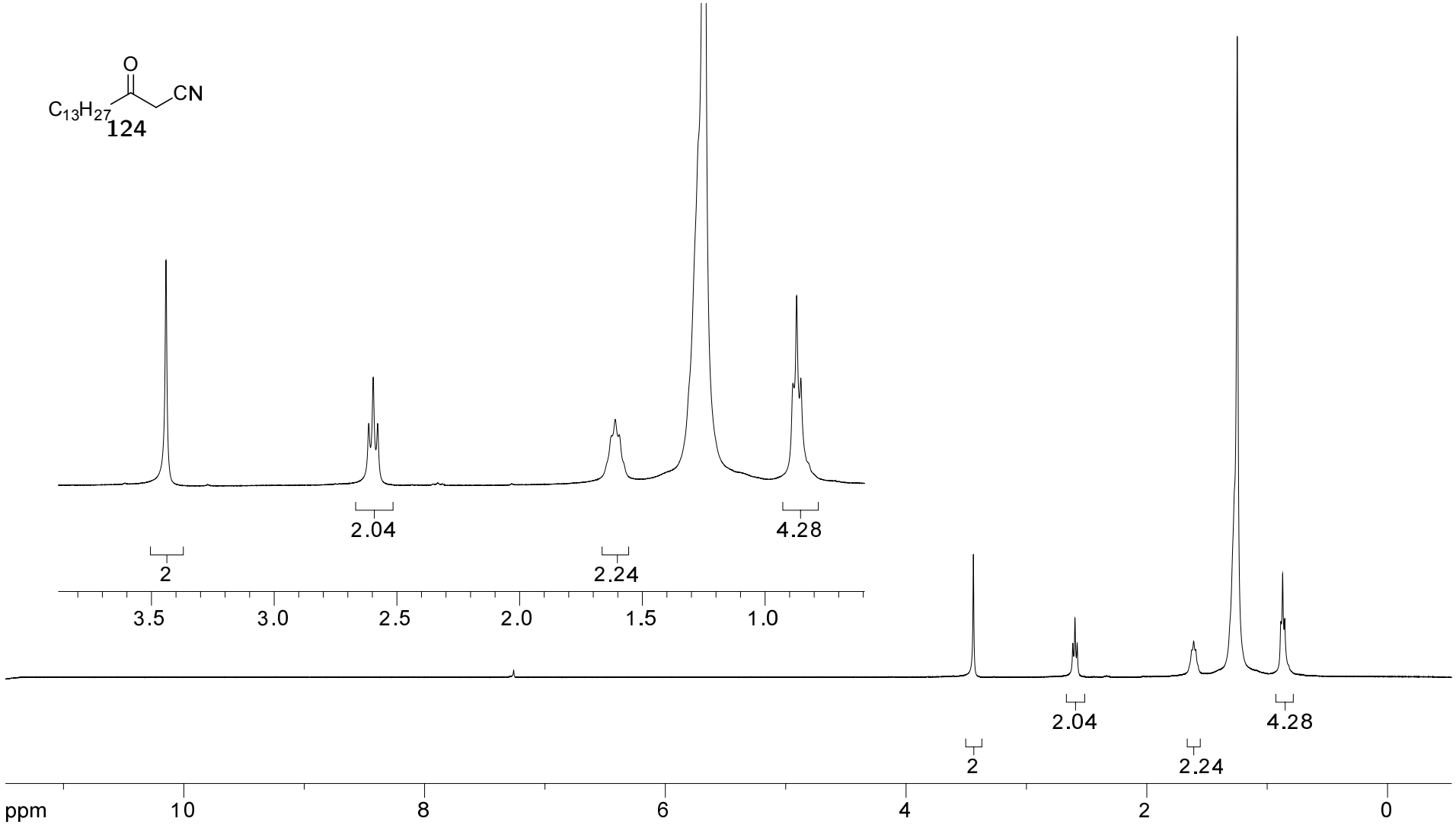

Figure A.3: 400 MHz ^{1}H NMR of **124** in $CDCl_3$

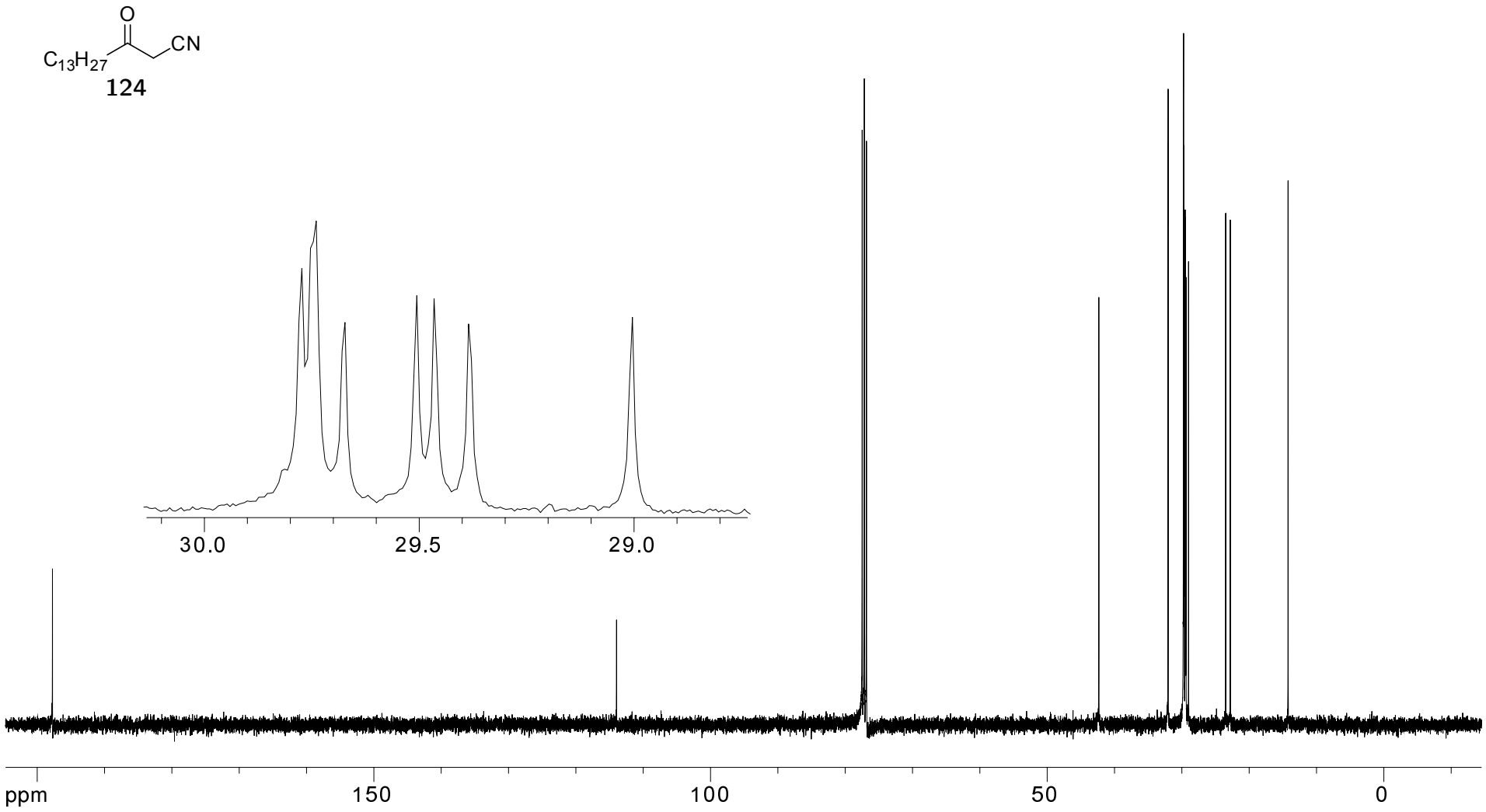

Figure A.4: 100 MHz ^{13}C NMR of **124** in $CDCl_3$

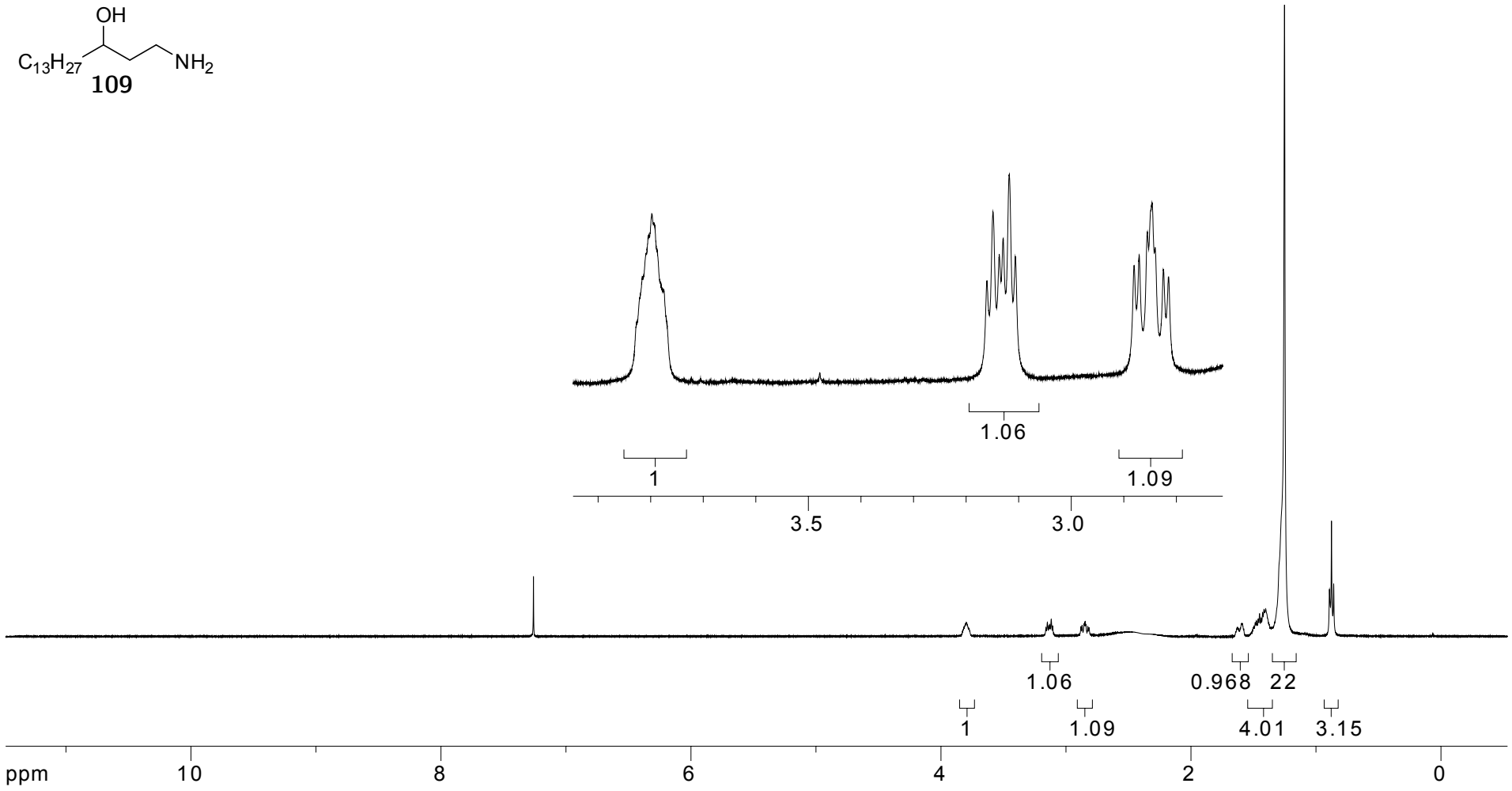

Figure A.5: 400 MHz ^{1}H NMR of **312** in $CDCl_3$

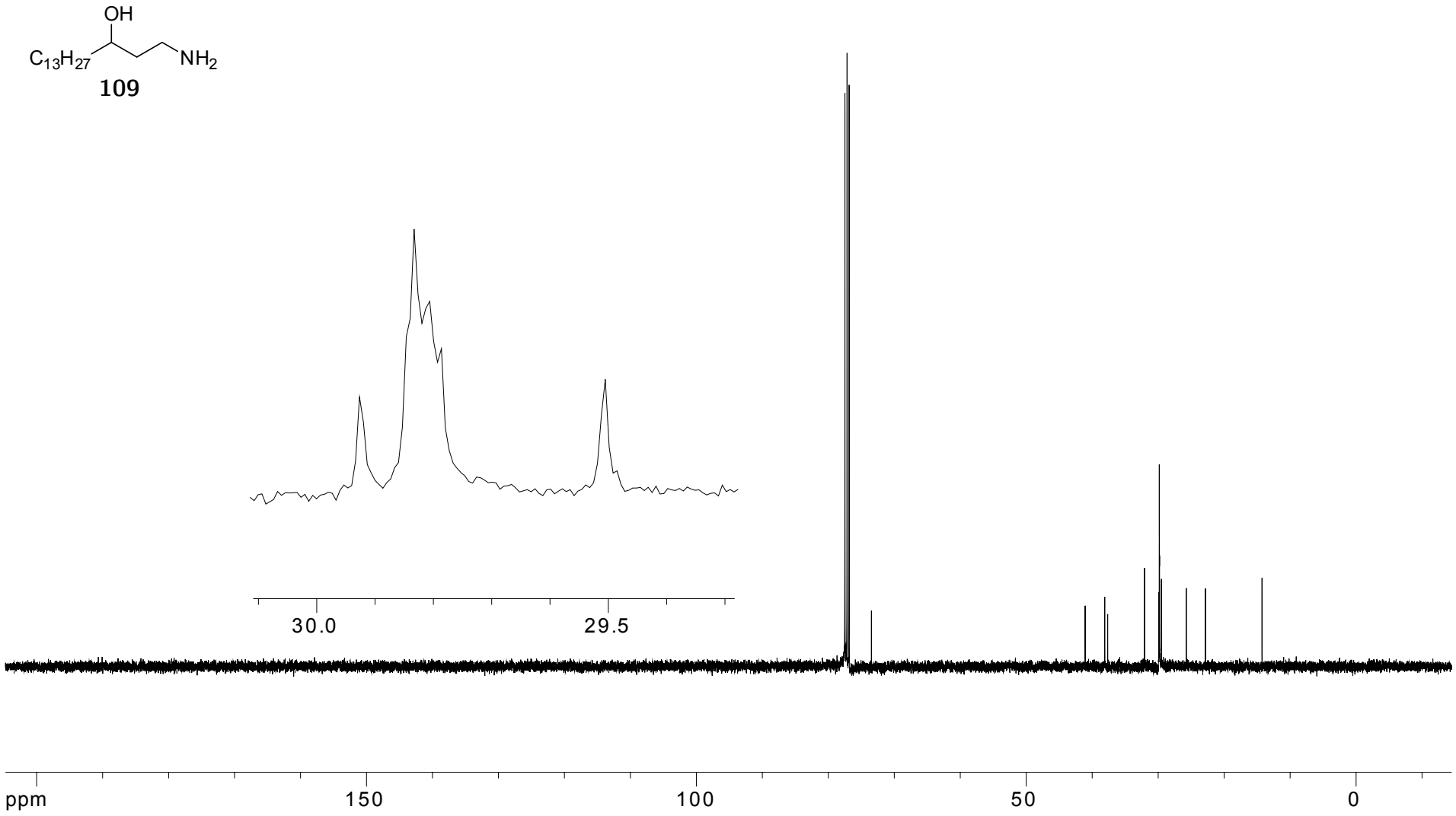

Figure A.6: 100 MHz ^{13}C NMR of **312** in $CDCl_3$

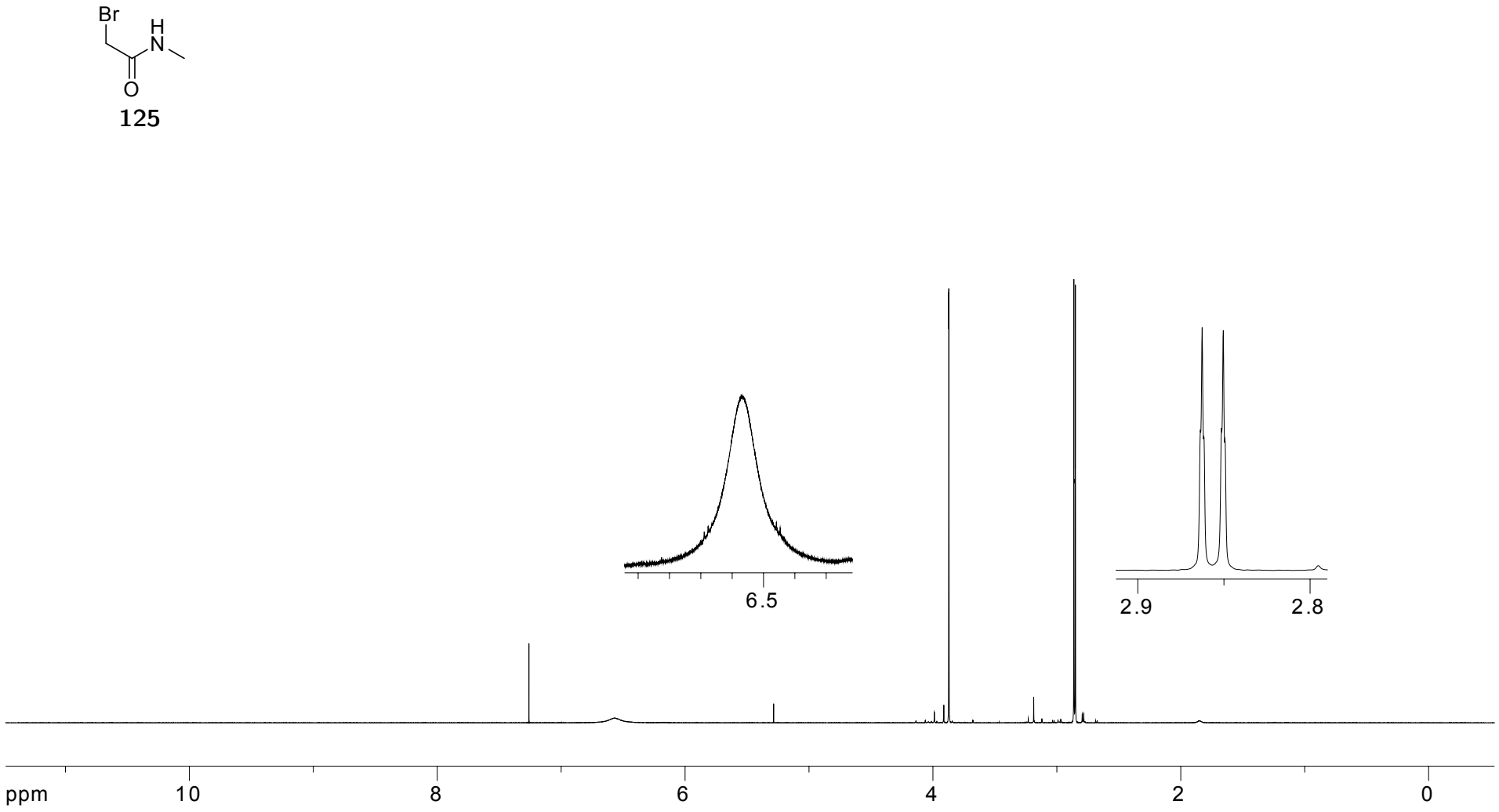

Figure A.7: 400 MHz ^{1}H NMR of **125** in $CDCl_3$

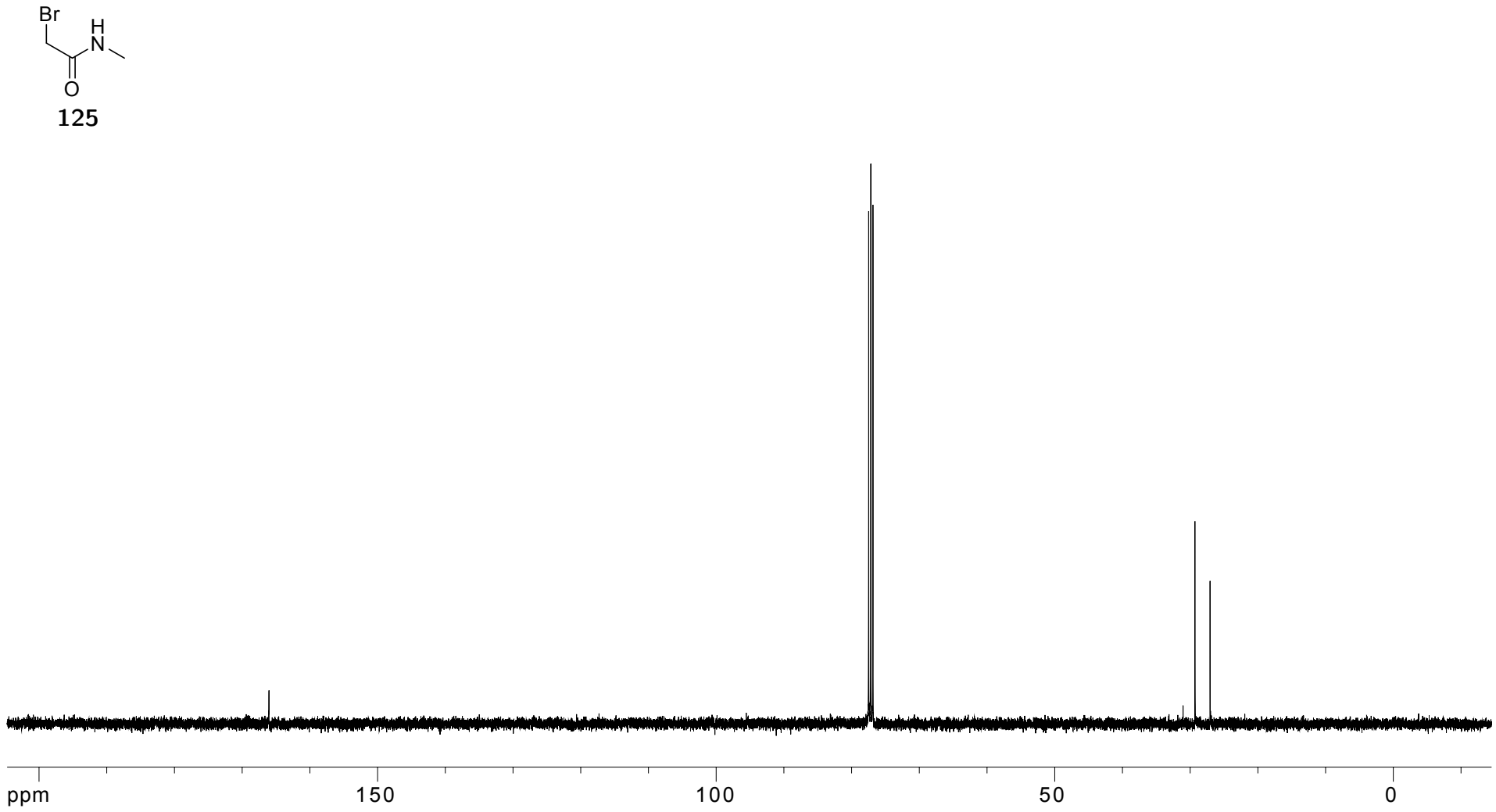

Figure A.8: 100 MHz ^{13}C NMR of **125** in $CDCl_3$

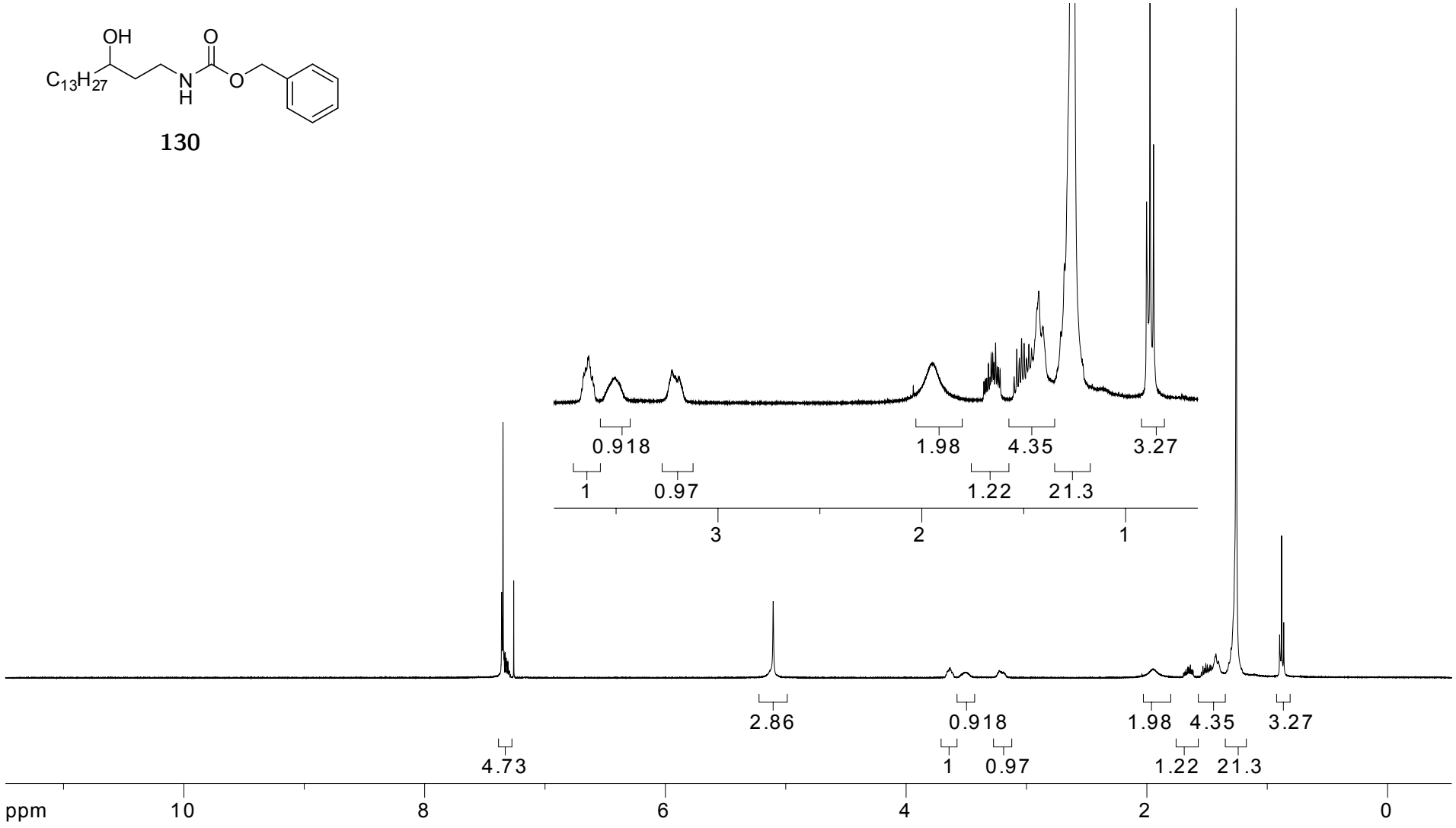

Figure A.9: 400 MHz ^{1}H NMR of **130** in $CDCl_3$

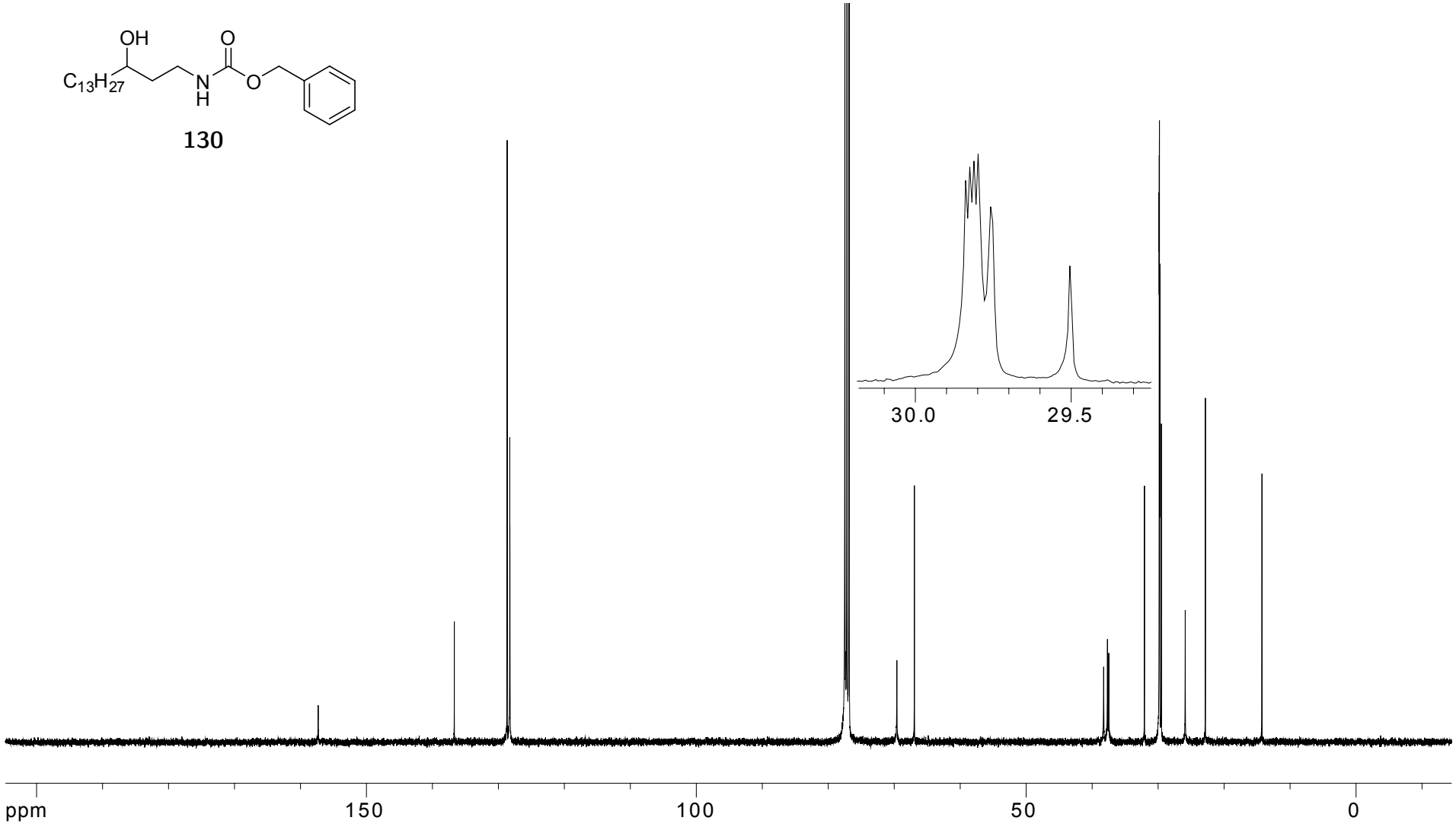

Figure A.10: 100 MHz ^{13}C NMR of **130** in $CDCl_3$

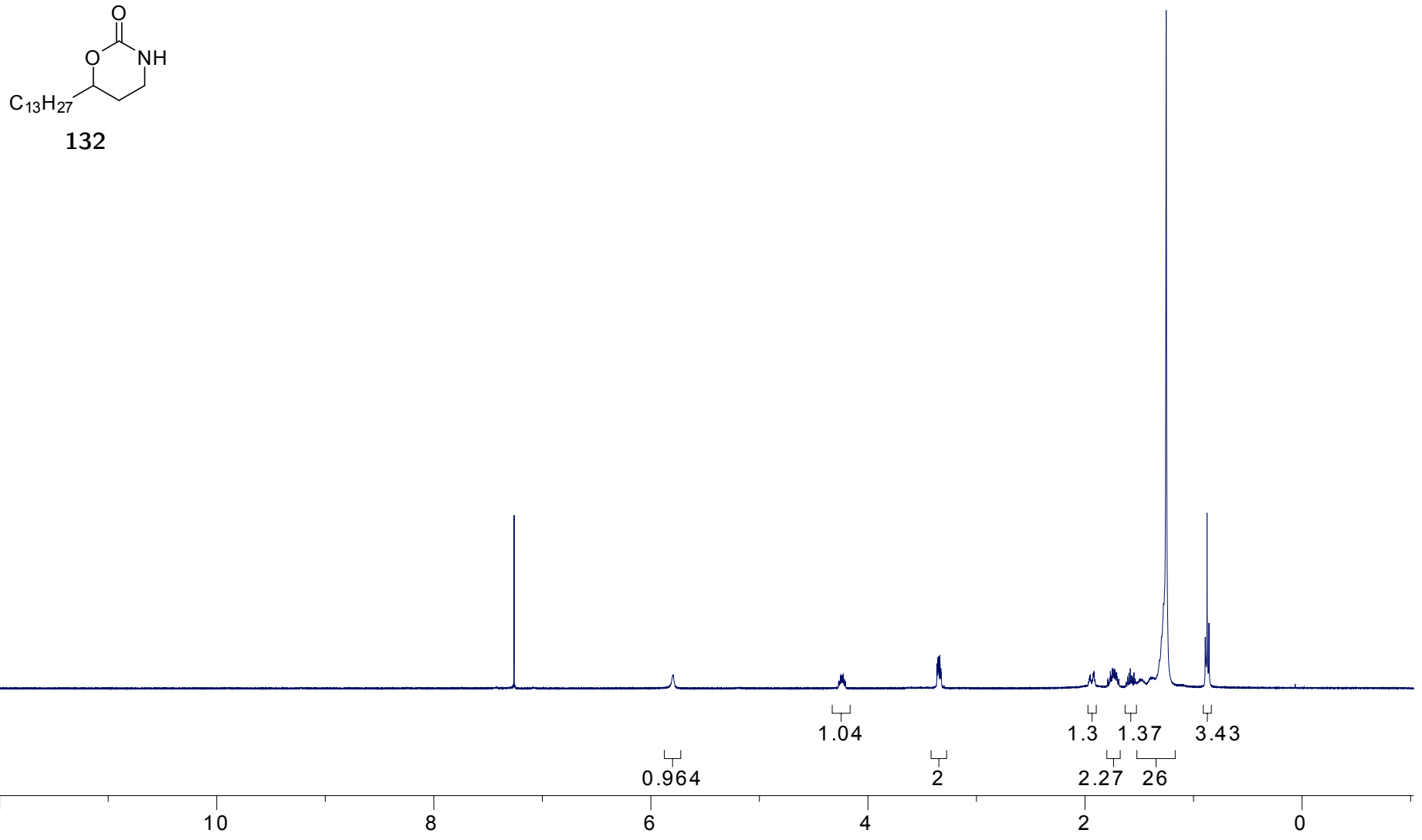

Figure A.11: 400 MHz ^{1}H NMR of **132** in $CDCl_3$

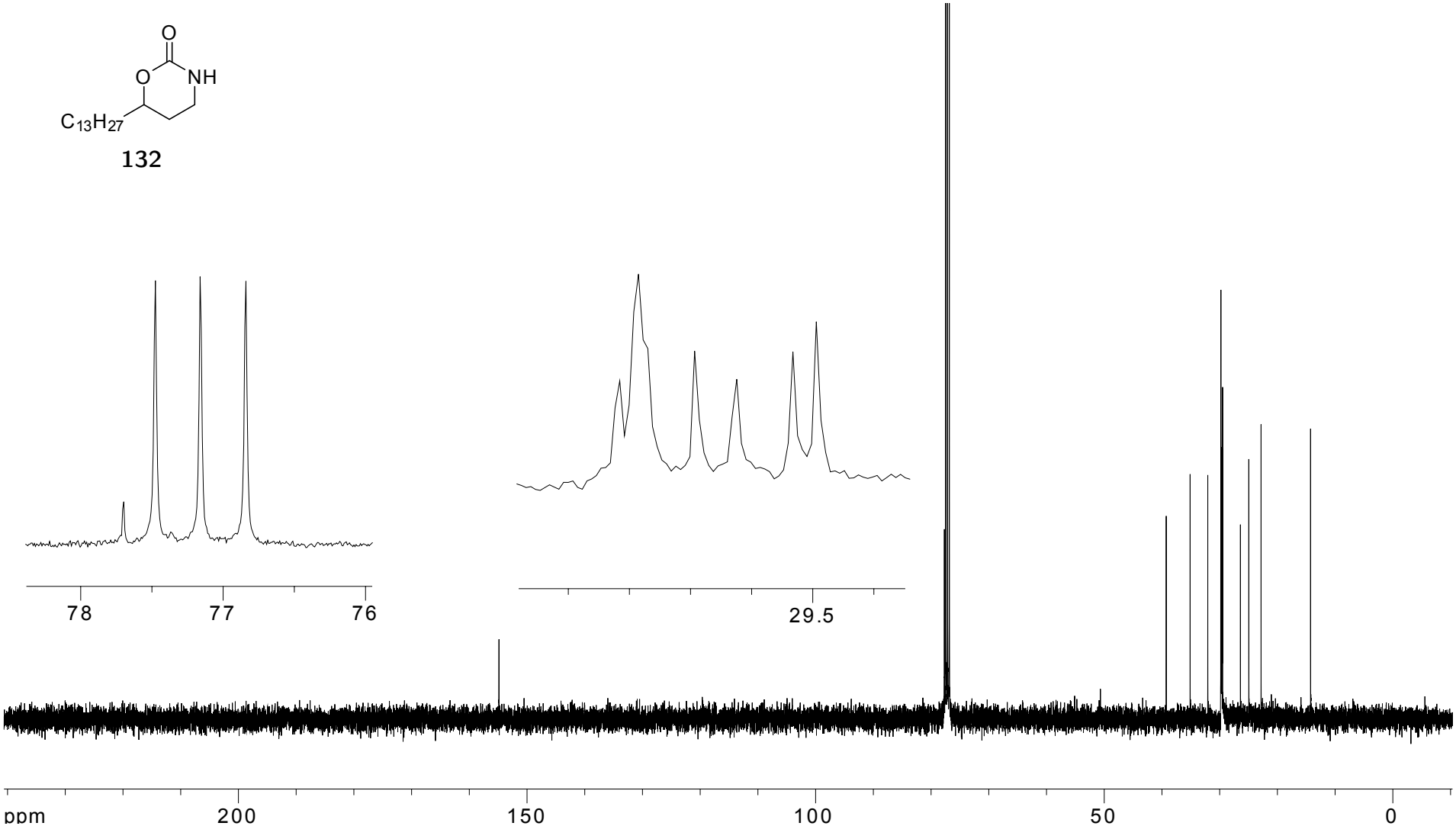

Figure A.12: 100 MHz ^{13}C NMR of **132** in $CDCl_3$

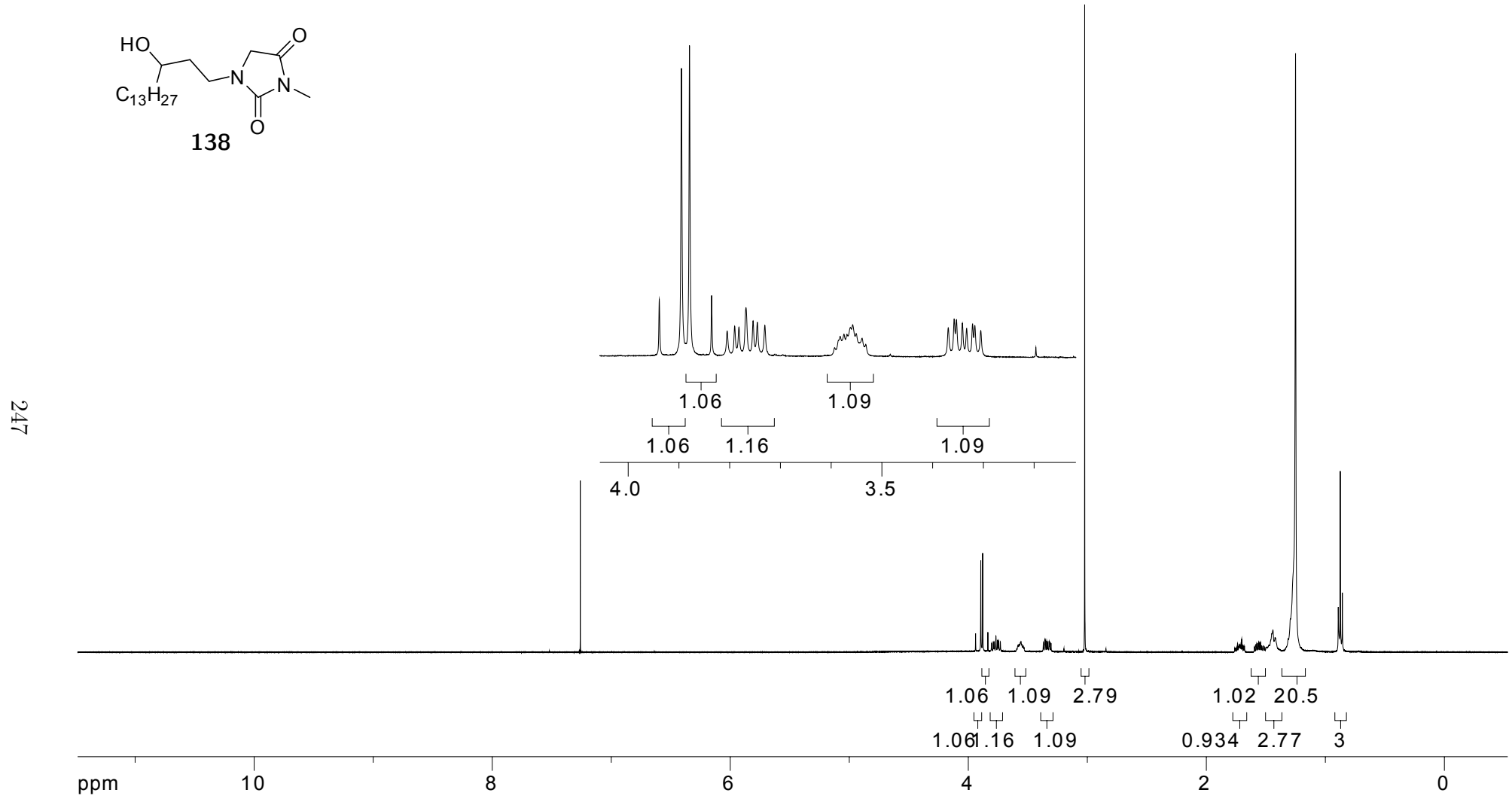

Figure A.13: 400 MHz ^{1}H NMR of **138** in $CDCl_3$

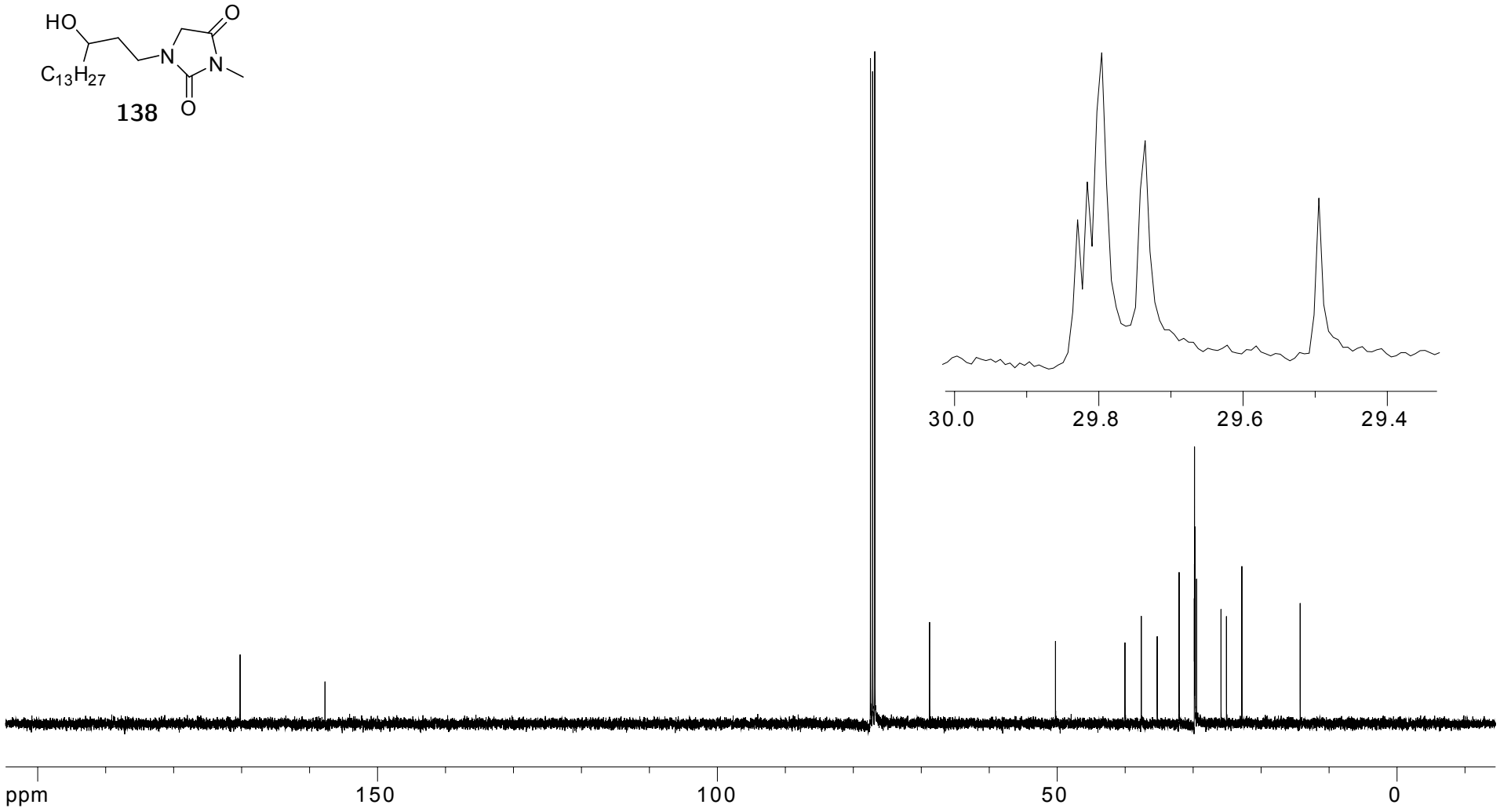

Figure A.14: 100 MHz ^{13}C NMR **138** in $CDCl_3$

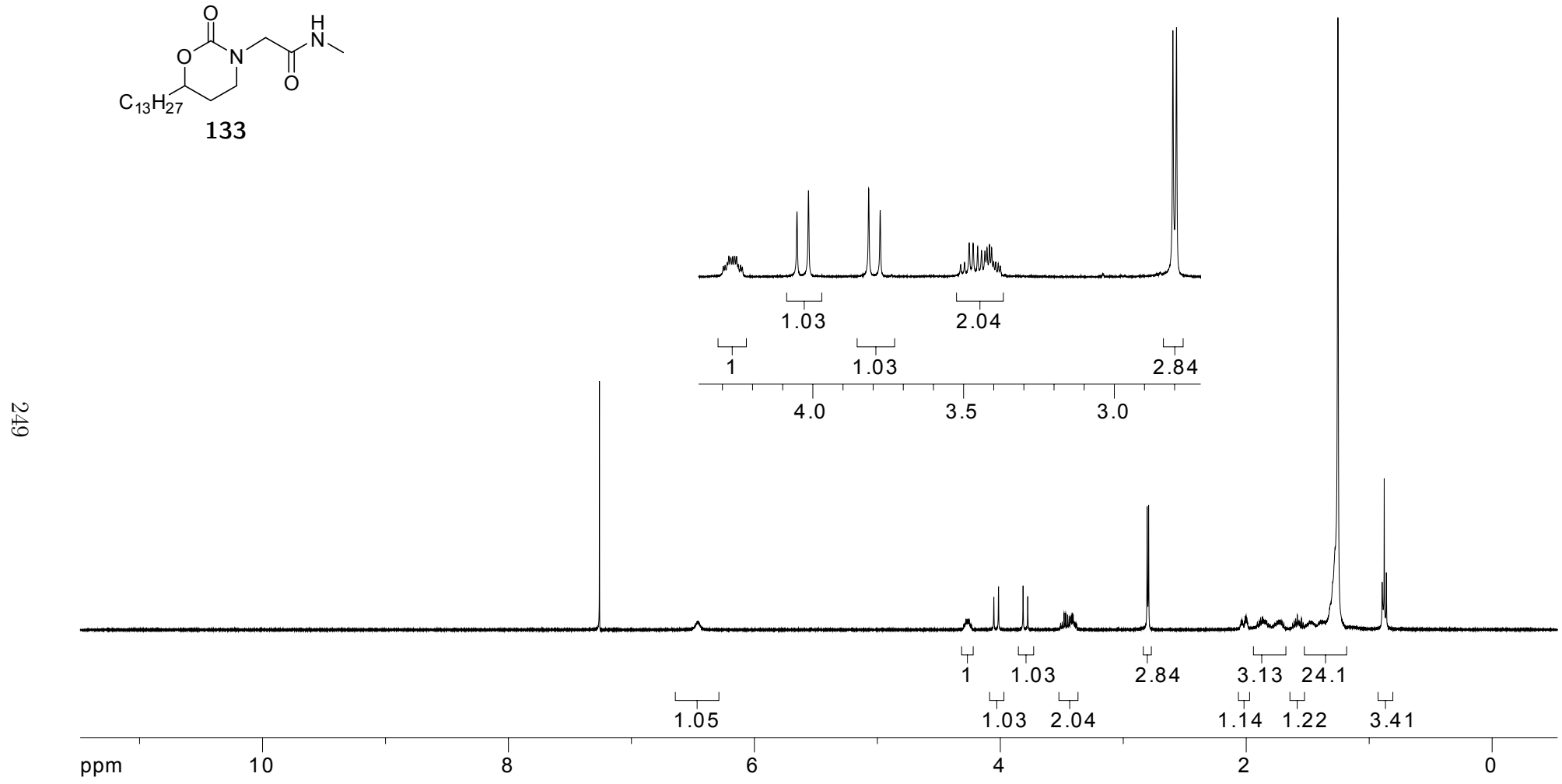

Figure A.15: 400 MHz ^{1}H NMR of **133** in $CDCl_3$

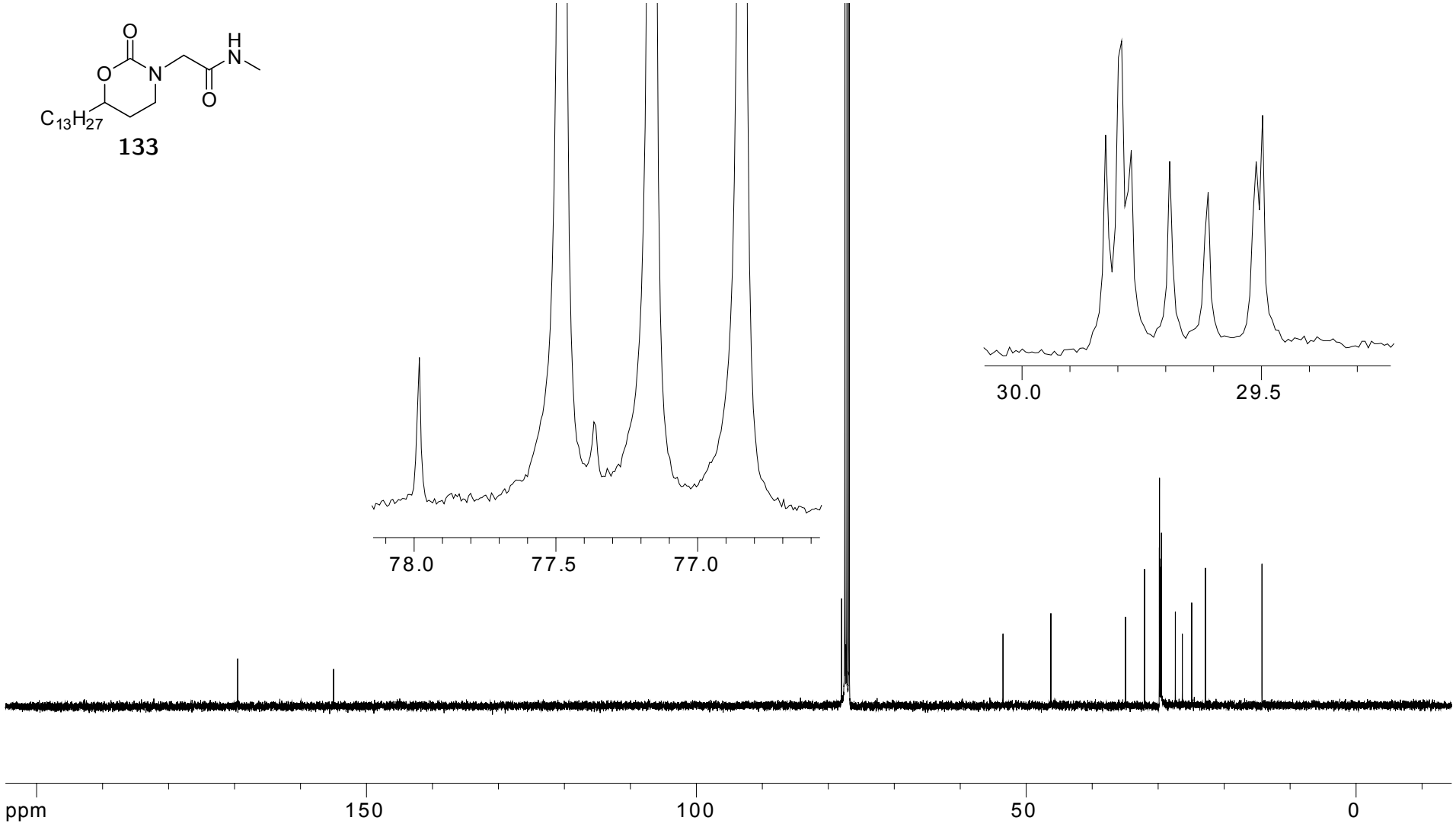

Figure A.16: 100 MHz ^{13}C NMR of **133** in $CDCl_3$

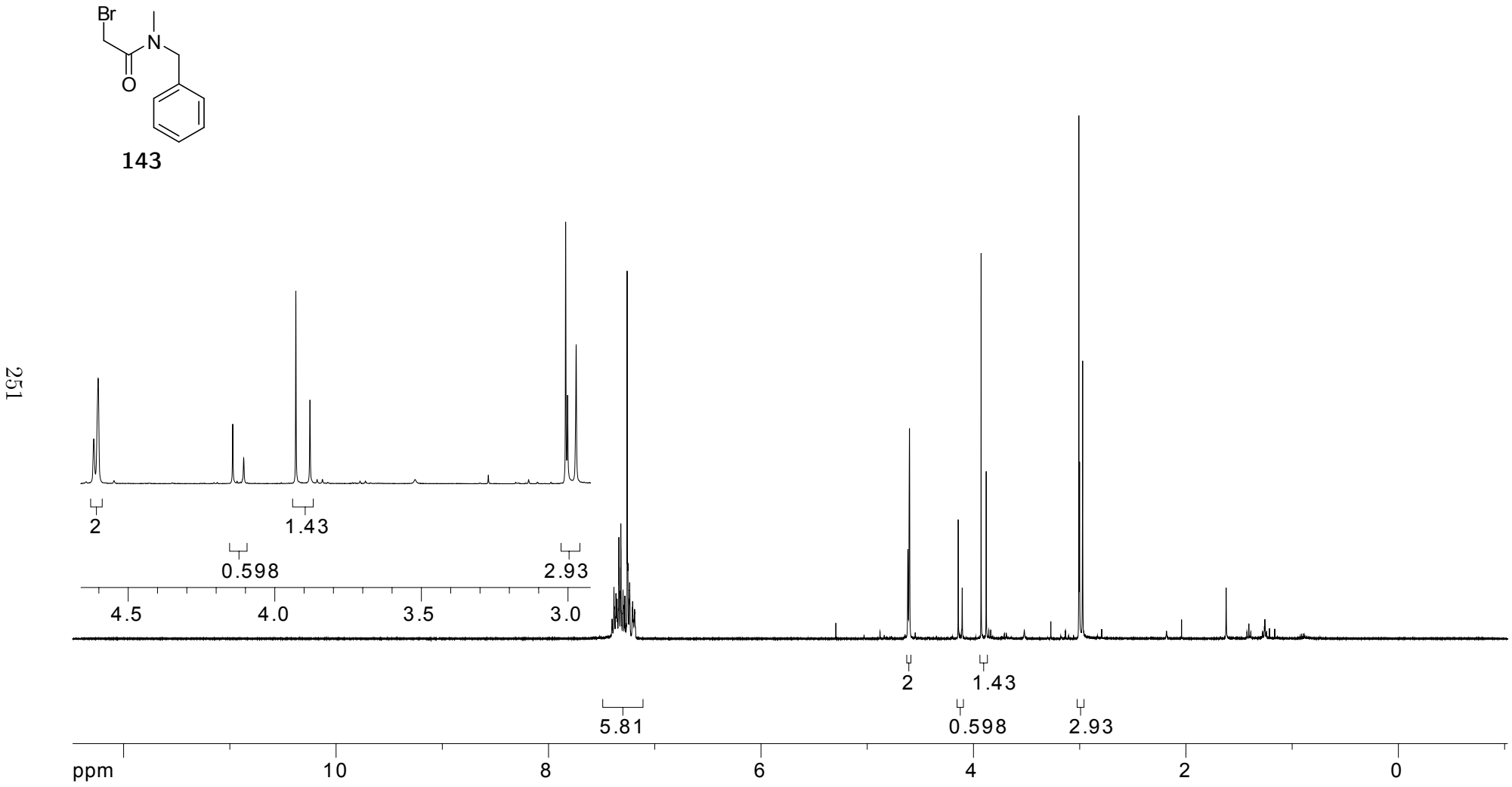

Figure A.17: 400 MHz ^{1}H NMR of **143** in $CDCl_3$

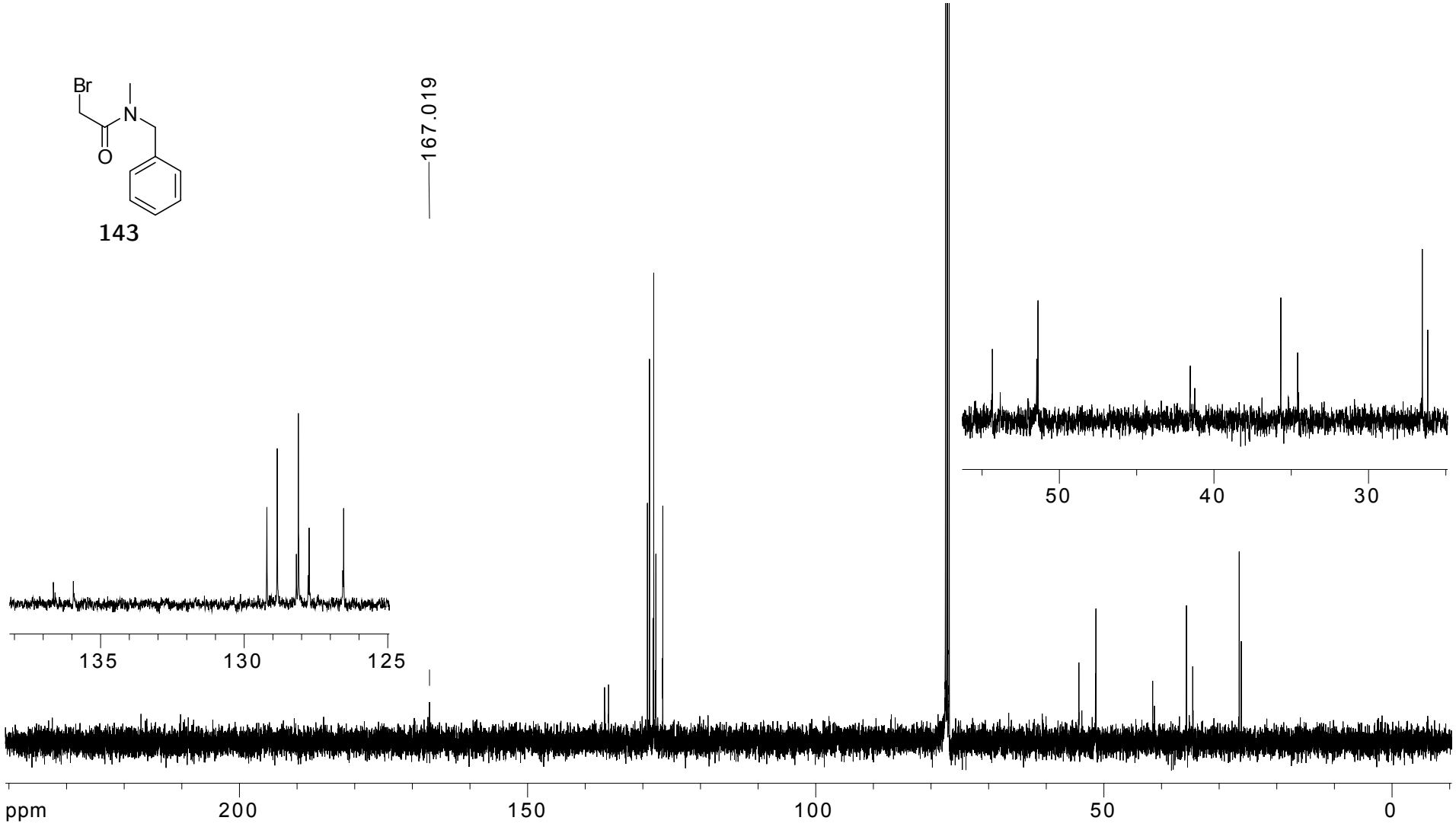

Figure A.18: 100 MHz ^{13}C NMR of **143** in $CDCl_3$

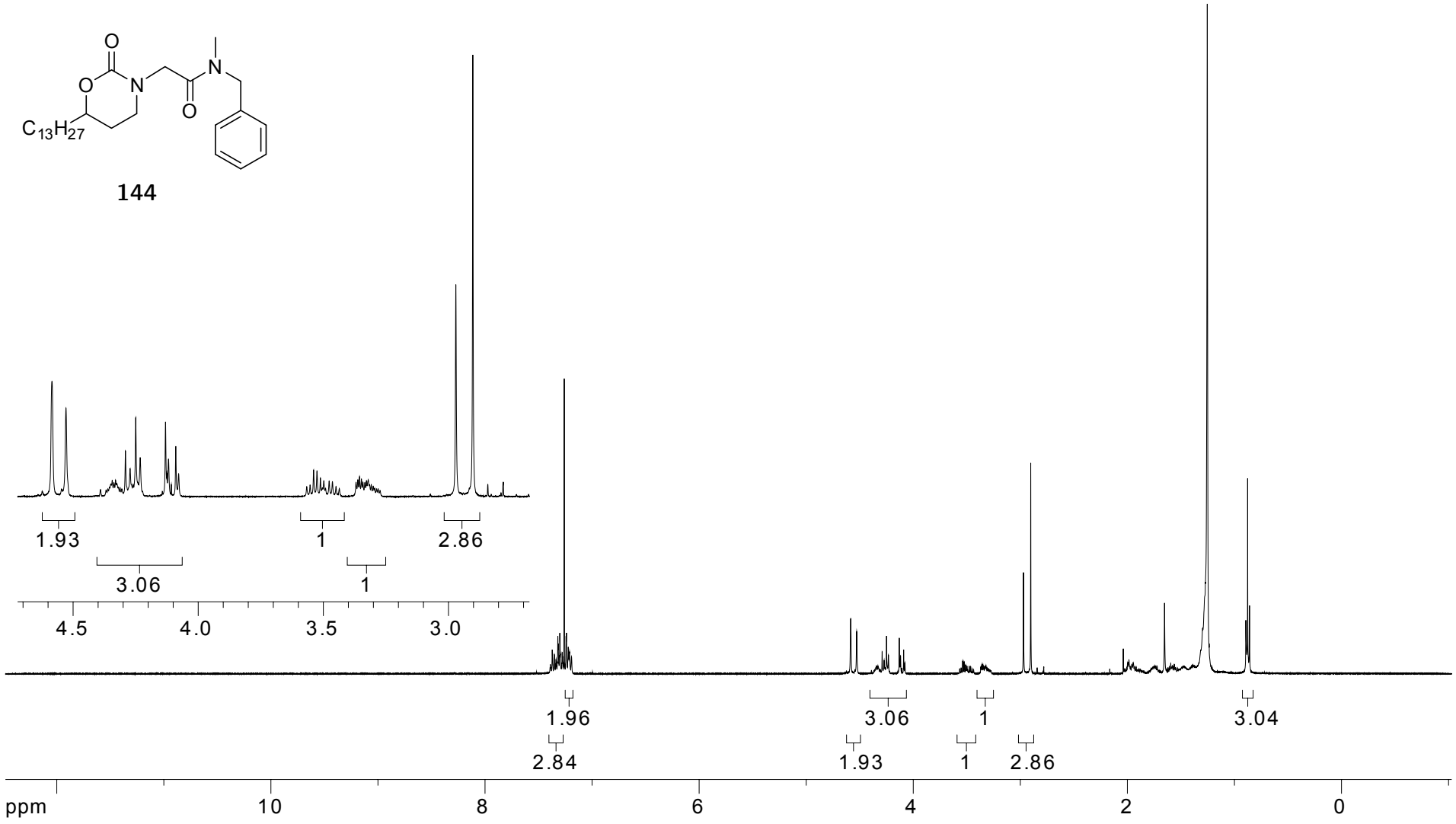

Figure A.19: 400 MHz ^{1}H NMR of **144** in $CDCl_3$

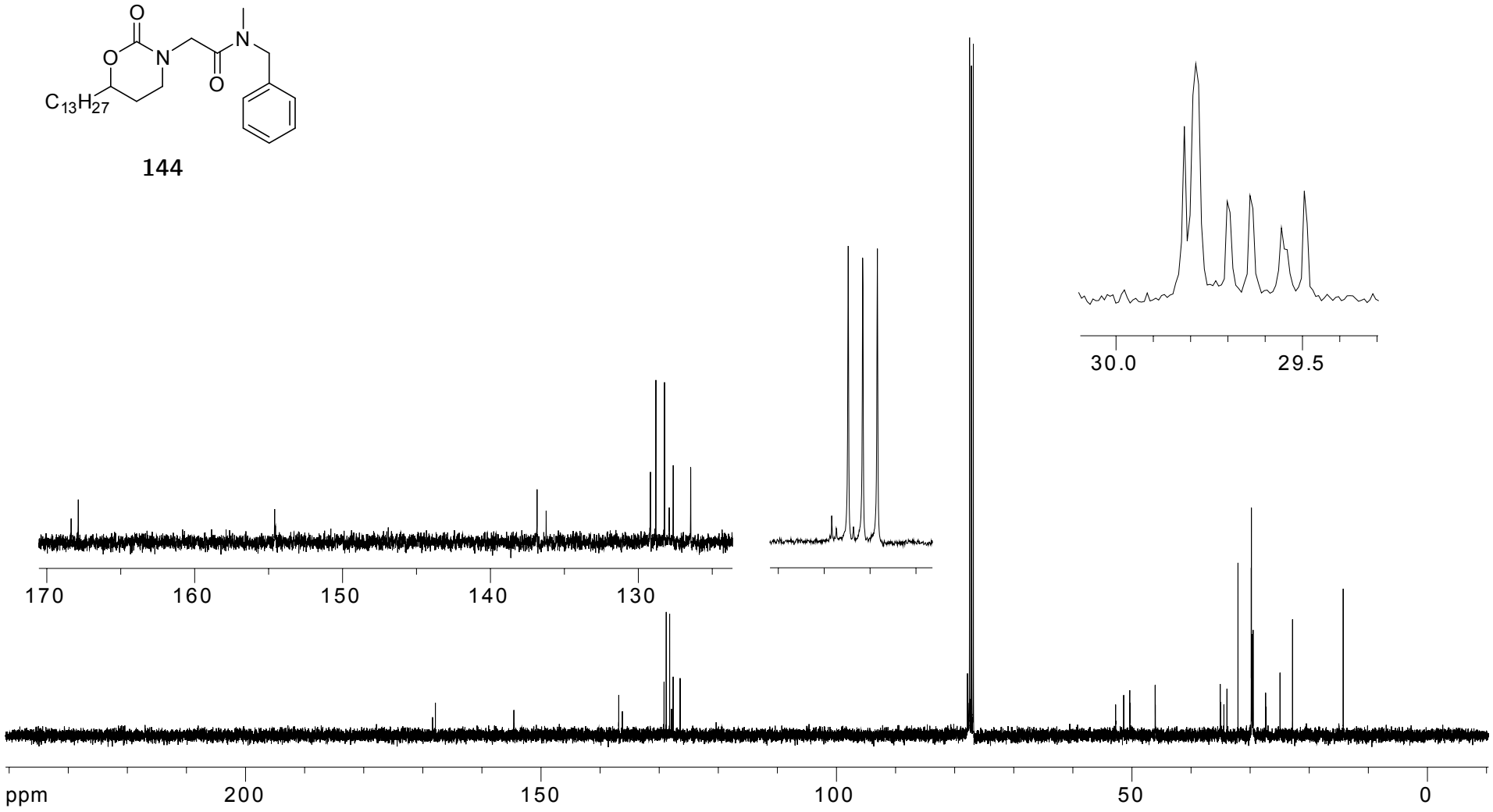

Figure A.20: 100 MHz ^{13}C NMR of **144** in $CDCl_3$

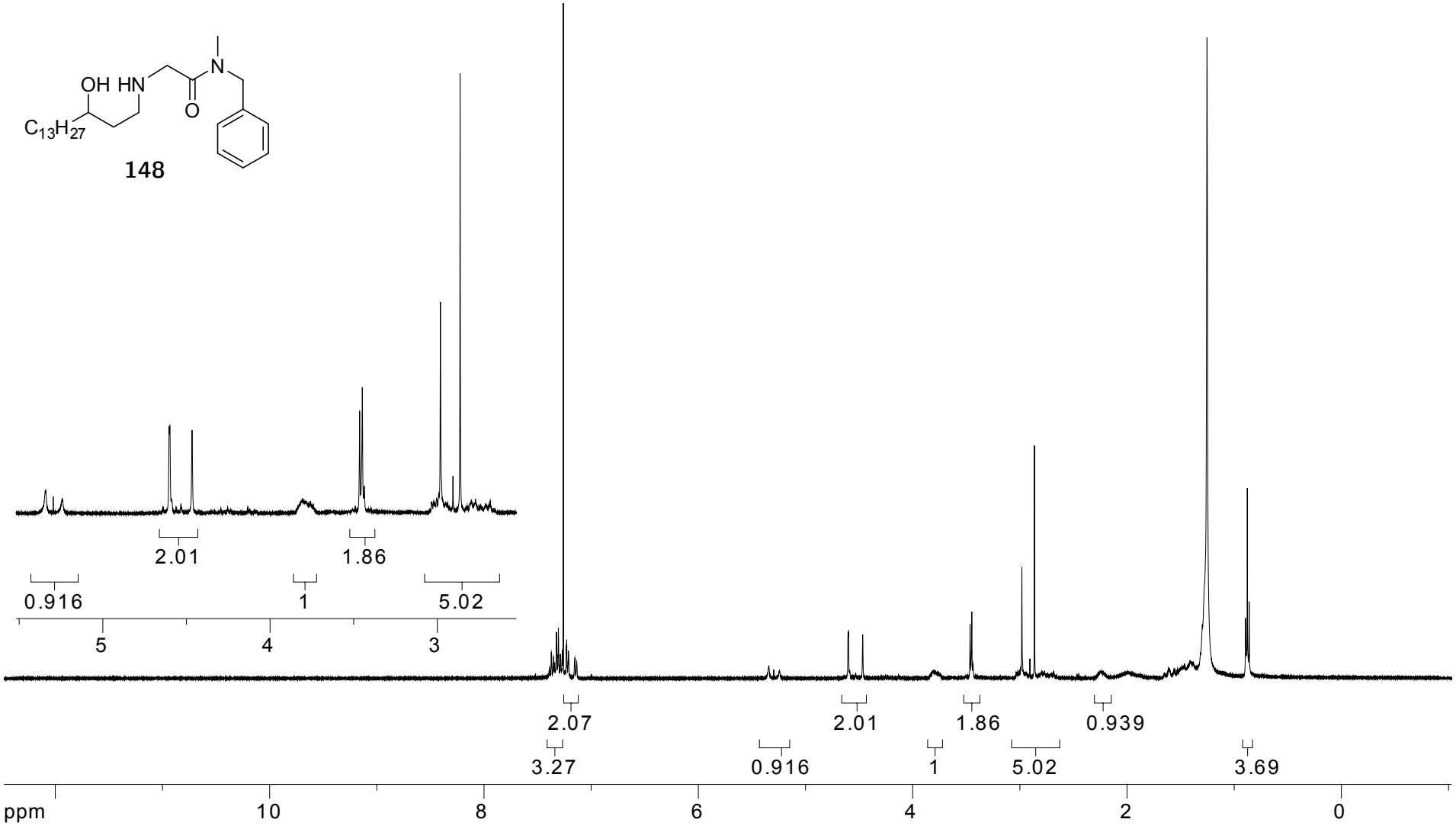

Figure A.21: 400 MHz ^{1}H NMR of **148** in $CDCl_3$

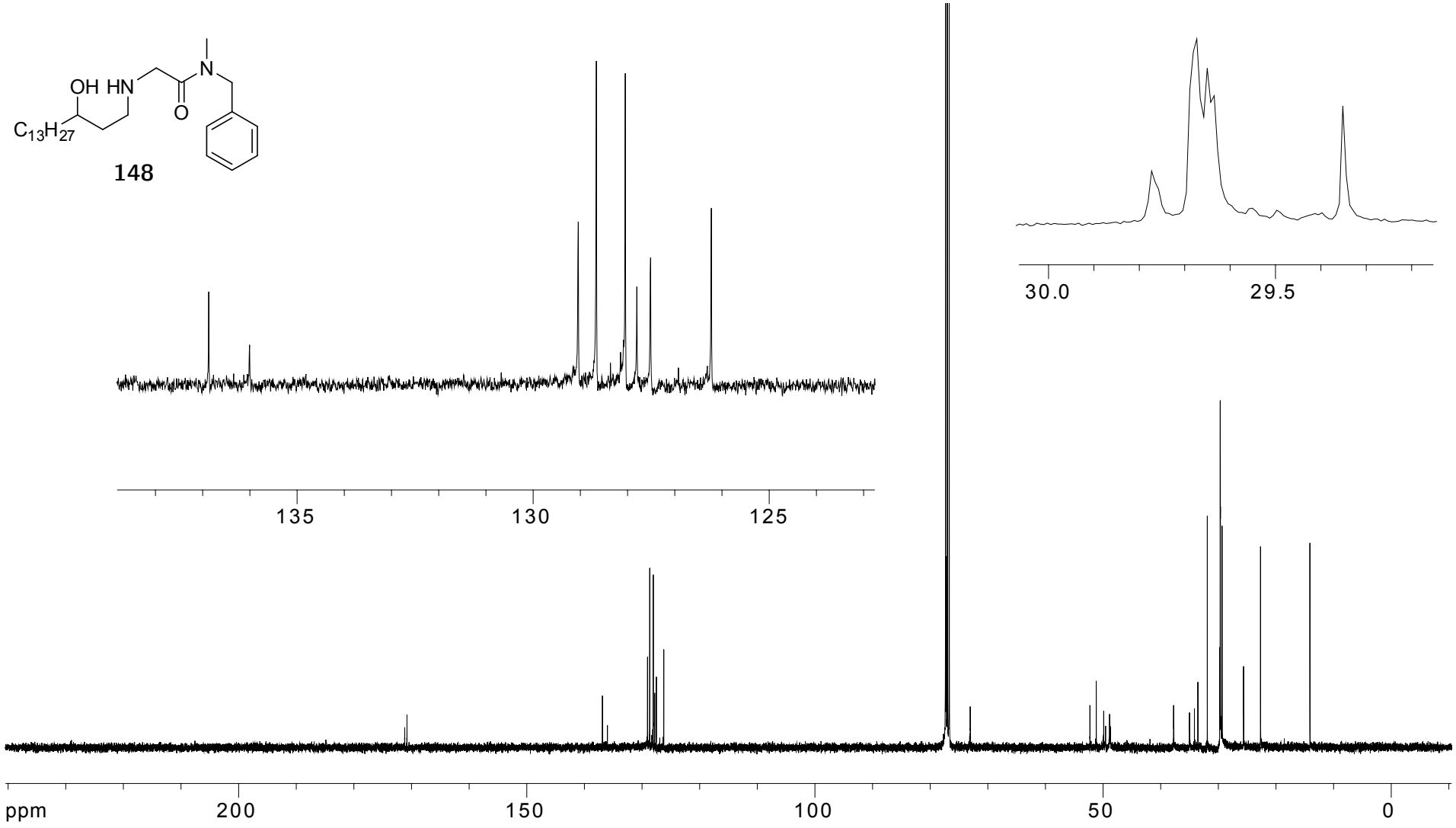

Figure A.22: 100 MHz ^{13}C NMR of **148** in $CDCl_3$

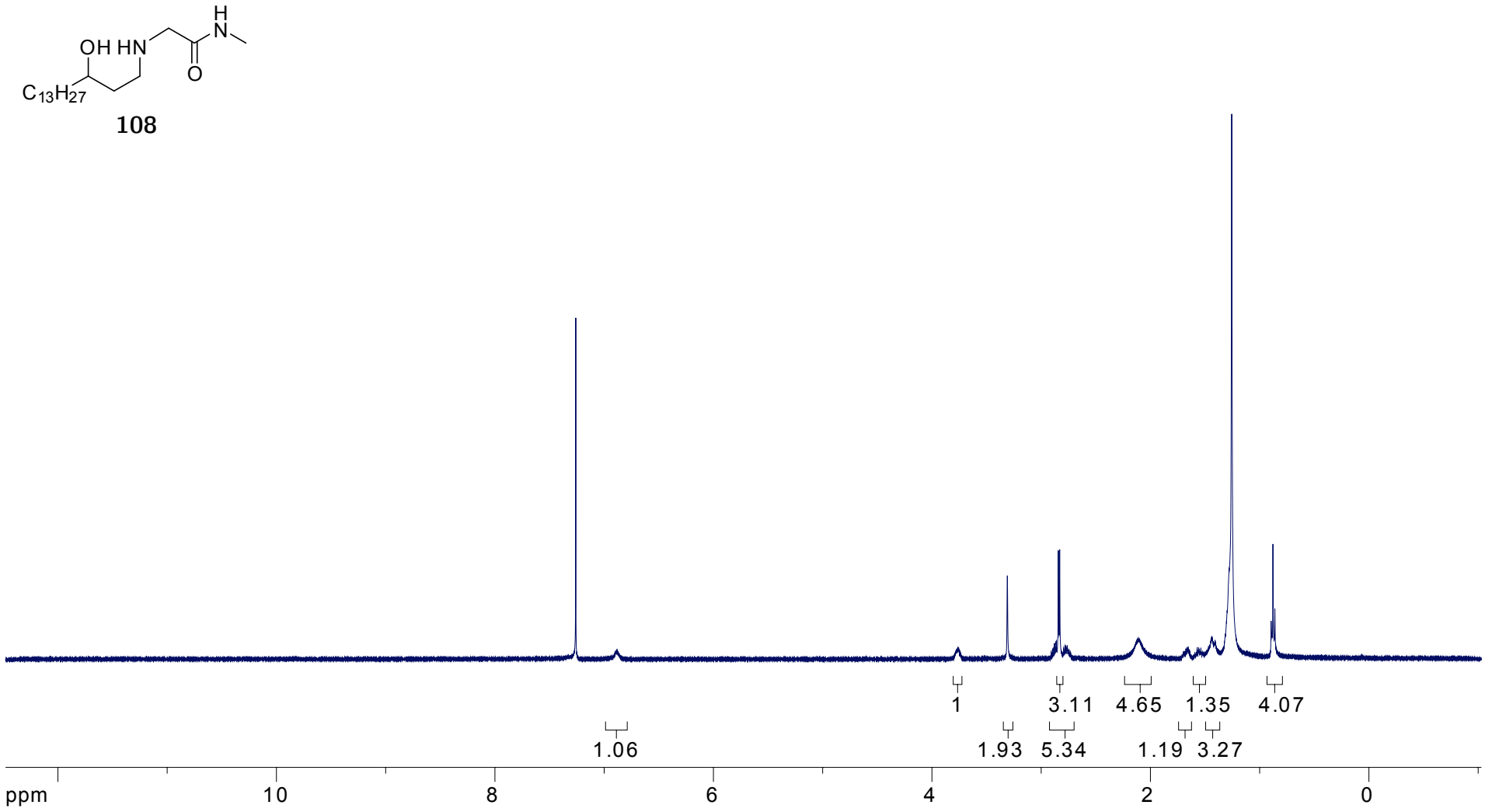

Figure A.23: 400 MHz ^{1}H NMR of **108** in $CDCl_3$

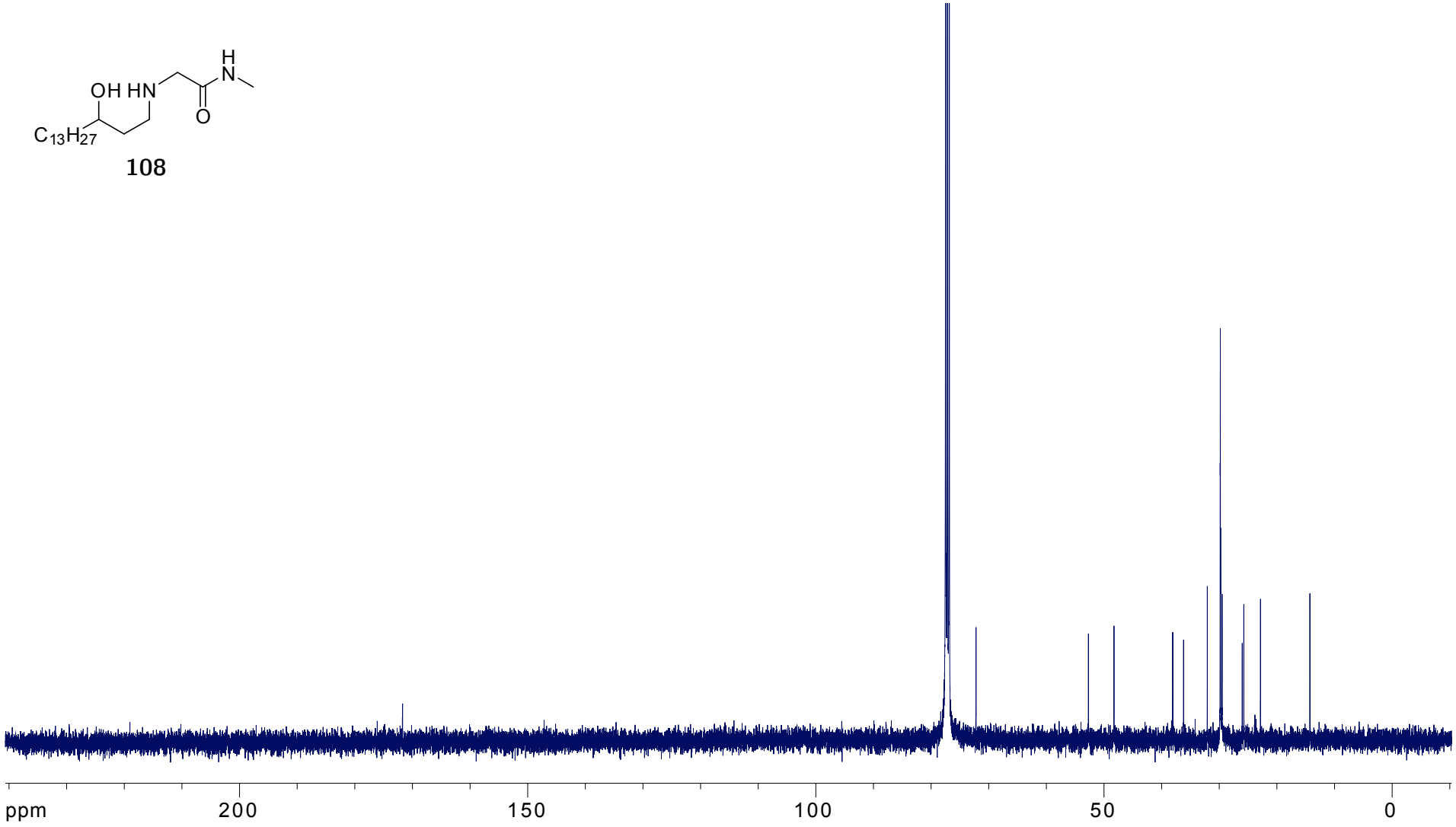

Figure A.24: 100 MHz ^{13}C NMR of **108** in $CDCl_3$

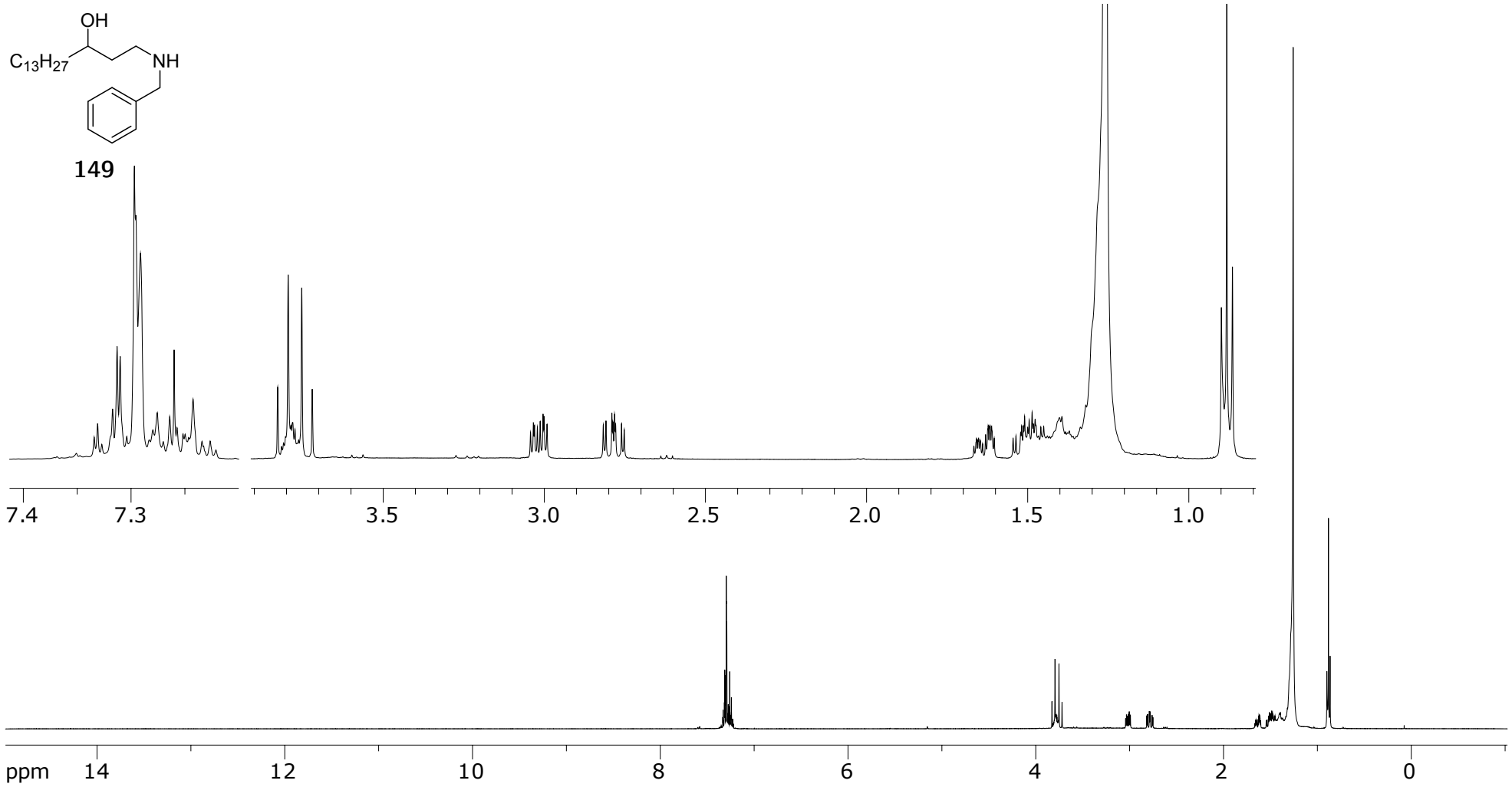

Figure A.25: 400 MHz ^{1}H NMR of **149** in $CDCl_3$

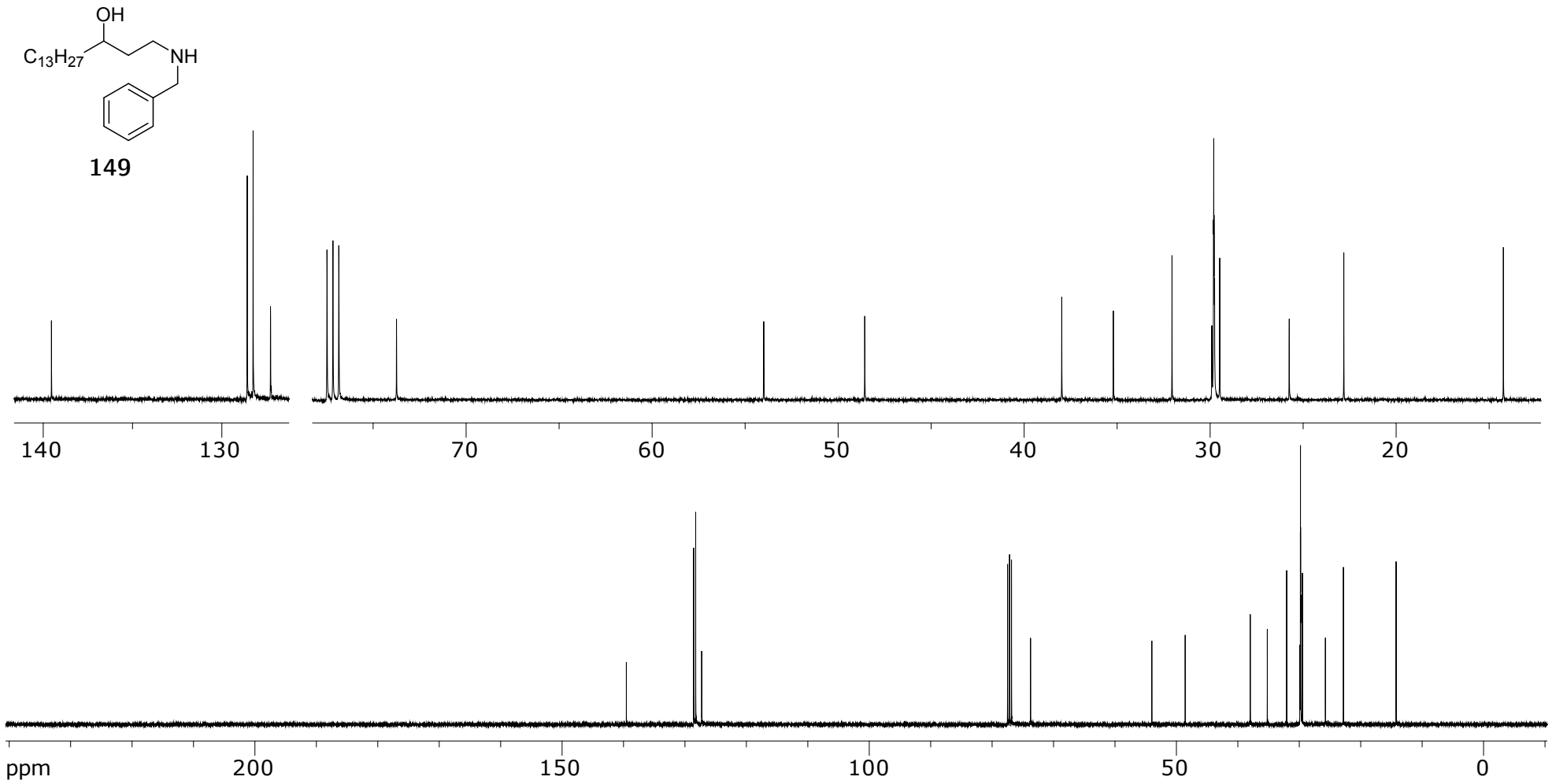

Figure A.26: 100 MHz ^{13}C NMR of **149** in $CDCl_3$

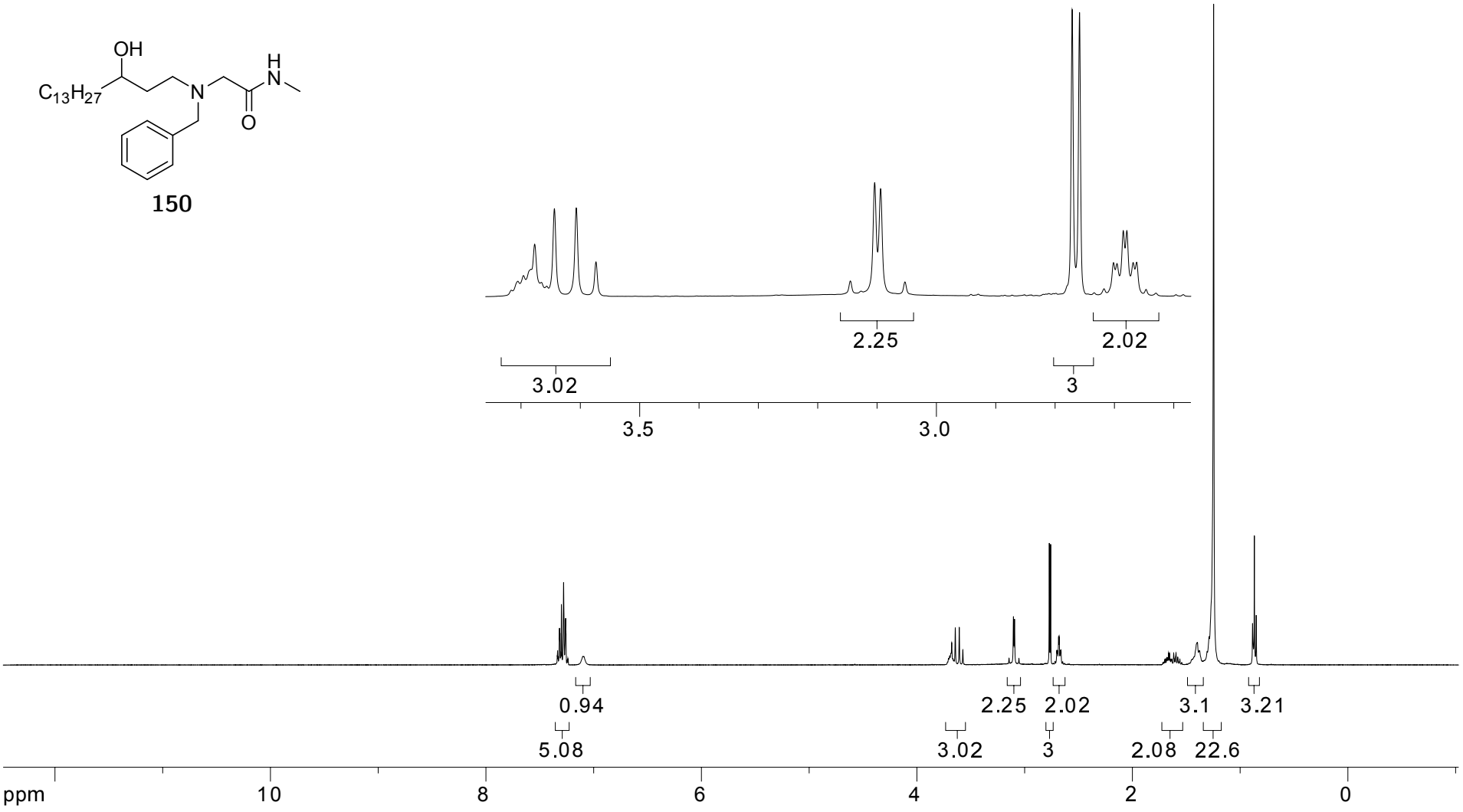

Figure A.27: 400 MHz ^{1}H NMR of **150** in $CDCl_3$

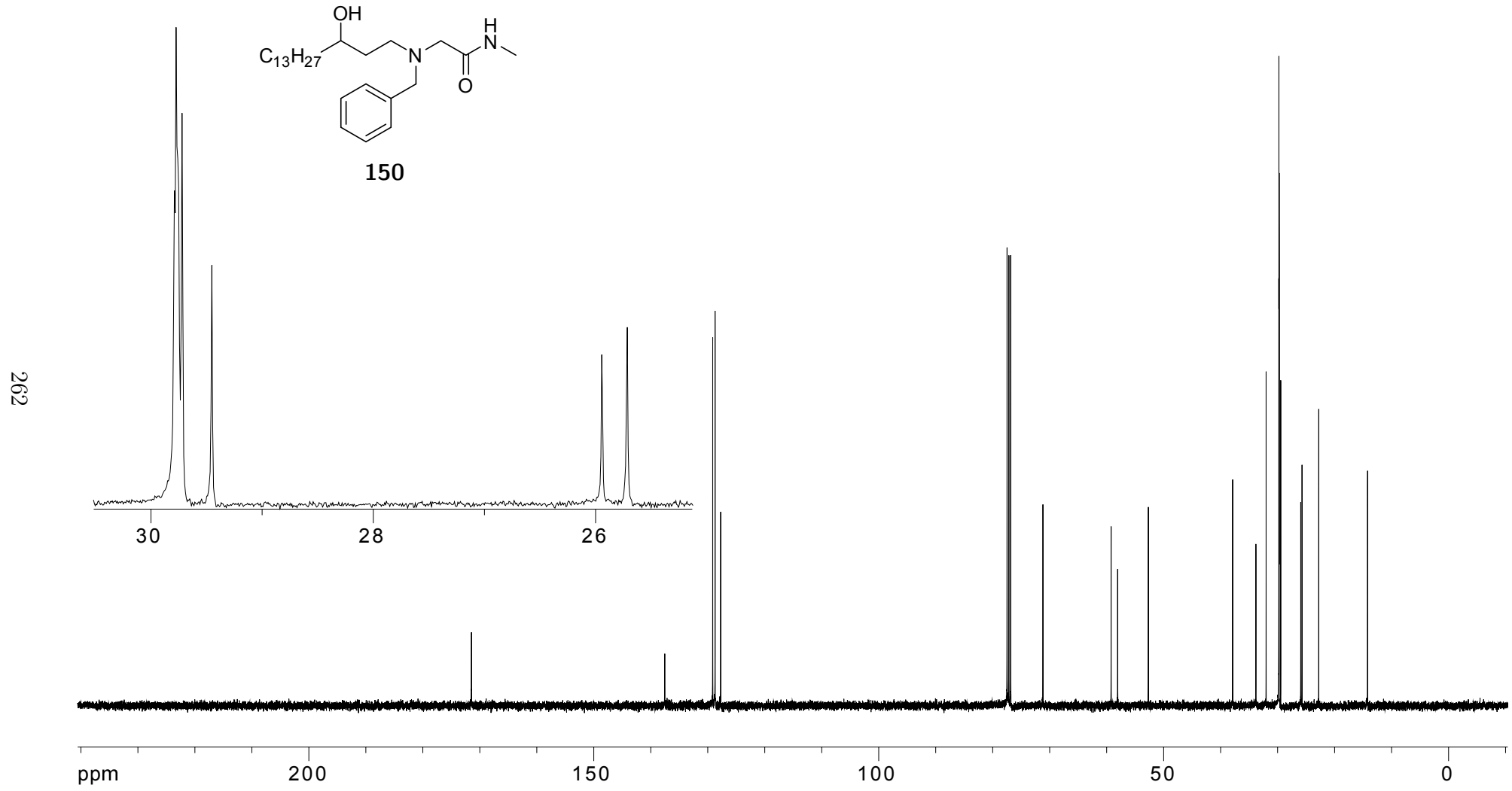

Figure A.28: 100 MHz ^{13}C NMR of **150** in $CDCl_3$

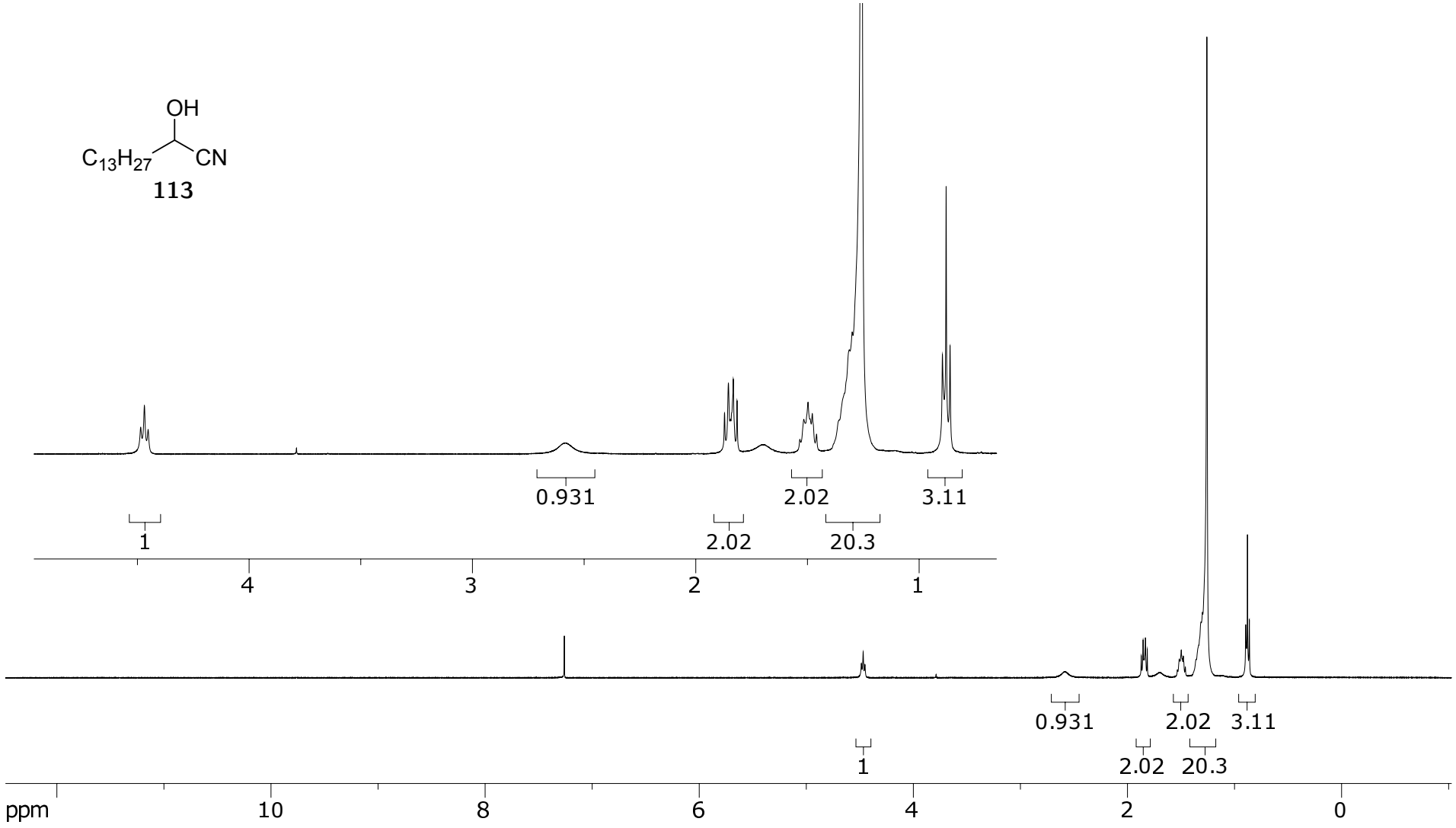

Figure A.29: 400 MHz ^{1}H NMR of **113** in $CDCl_3$

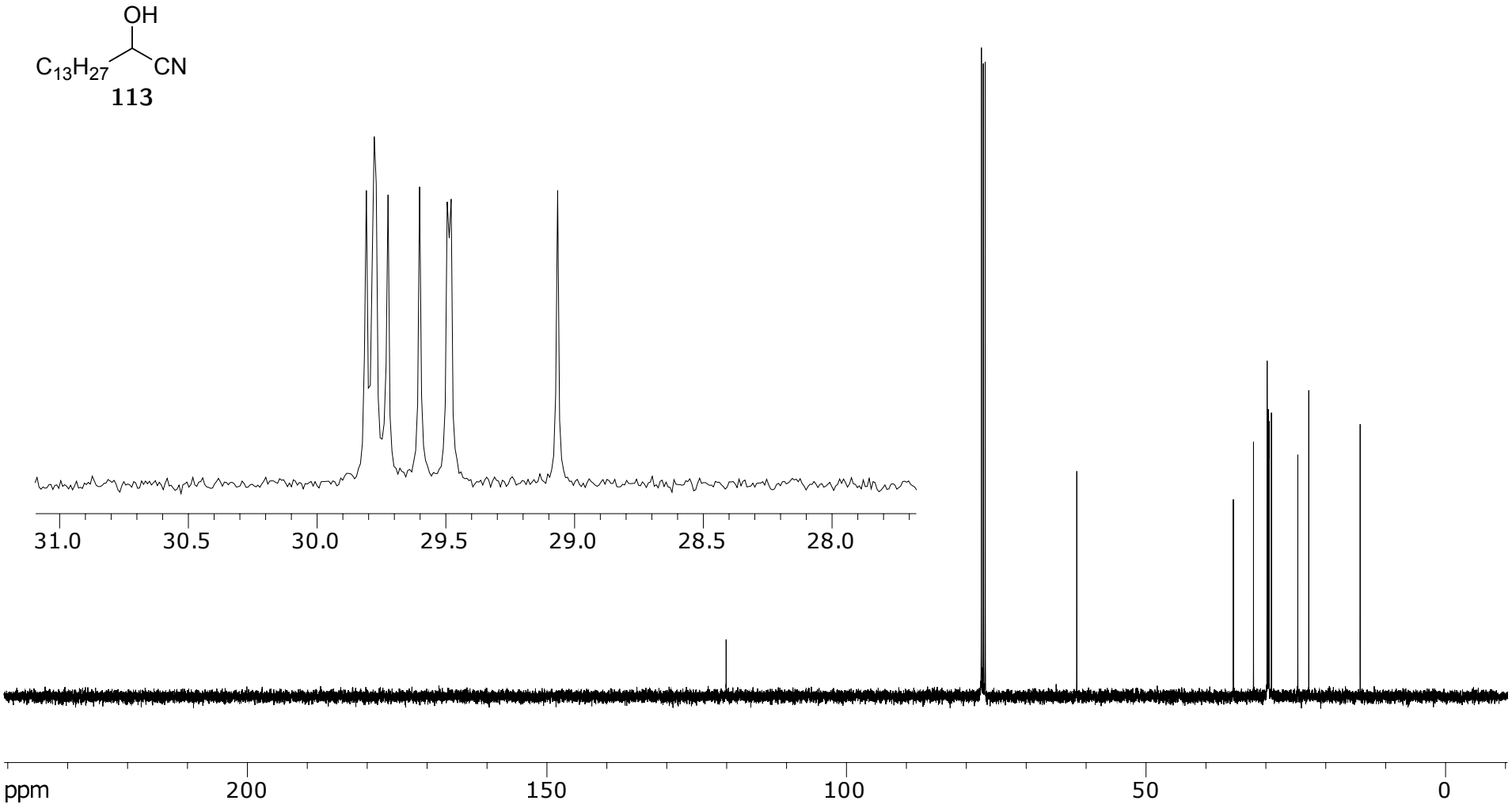

Figure A.30: 100 MHz ^{13}C NMR of **113** in $CDCl_3$

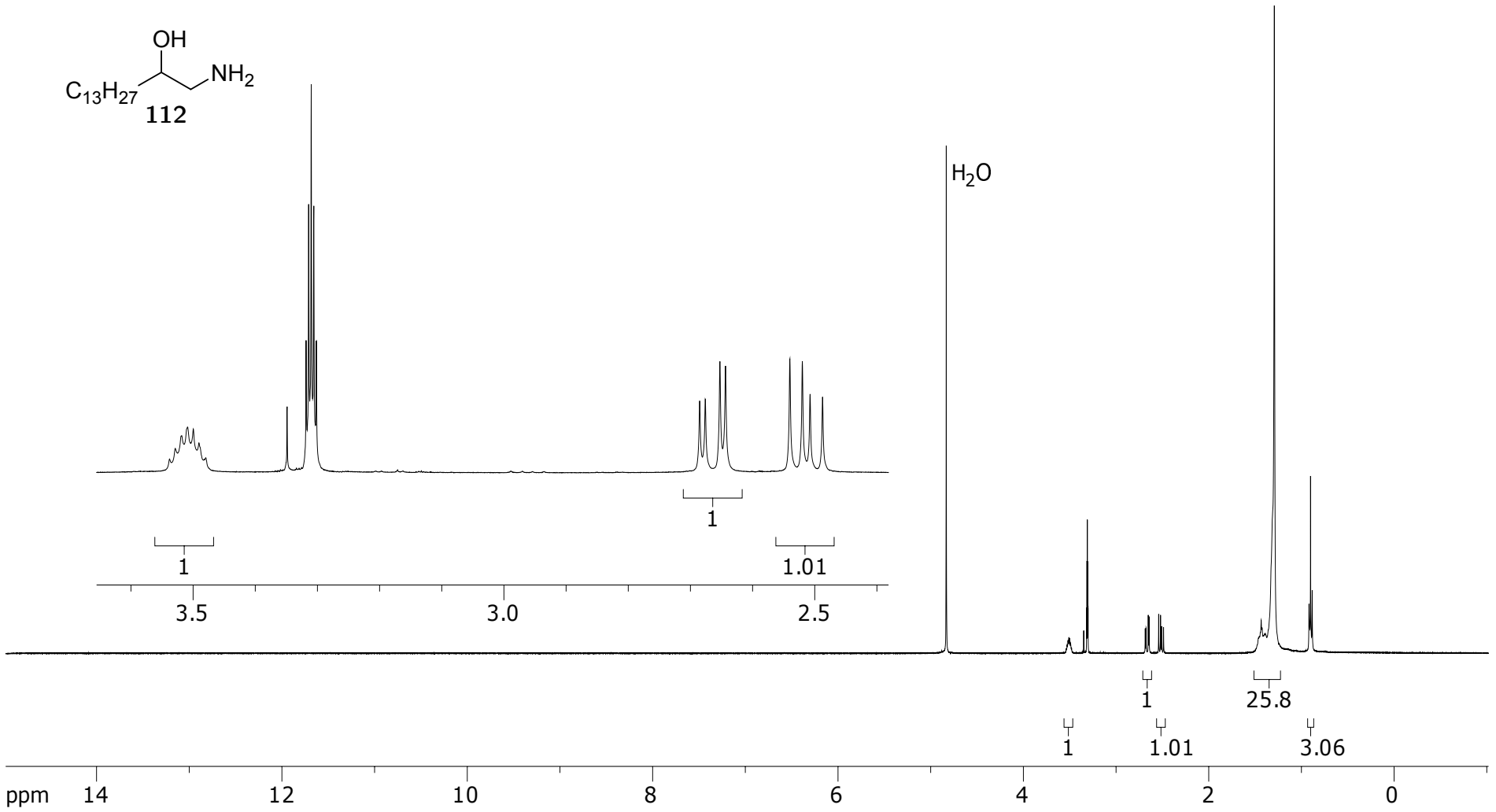

Figure A.31: 400 MHz ^{1}H NMR of **112** in $CDCl_3$

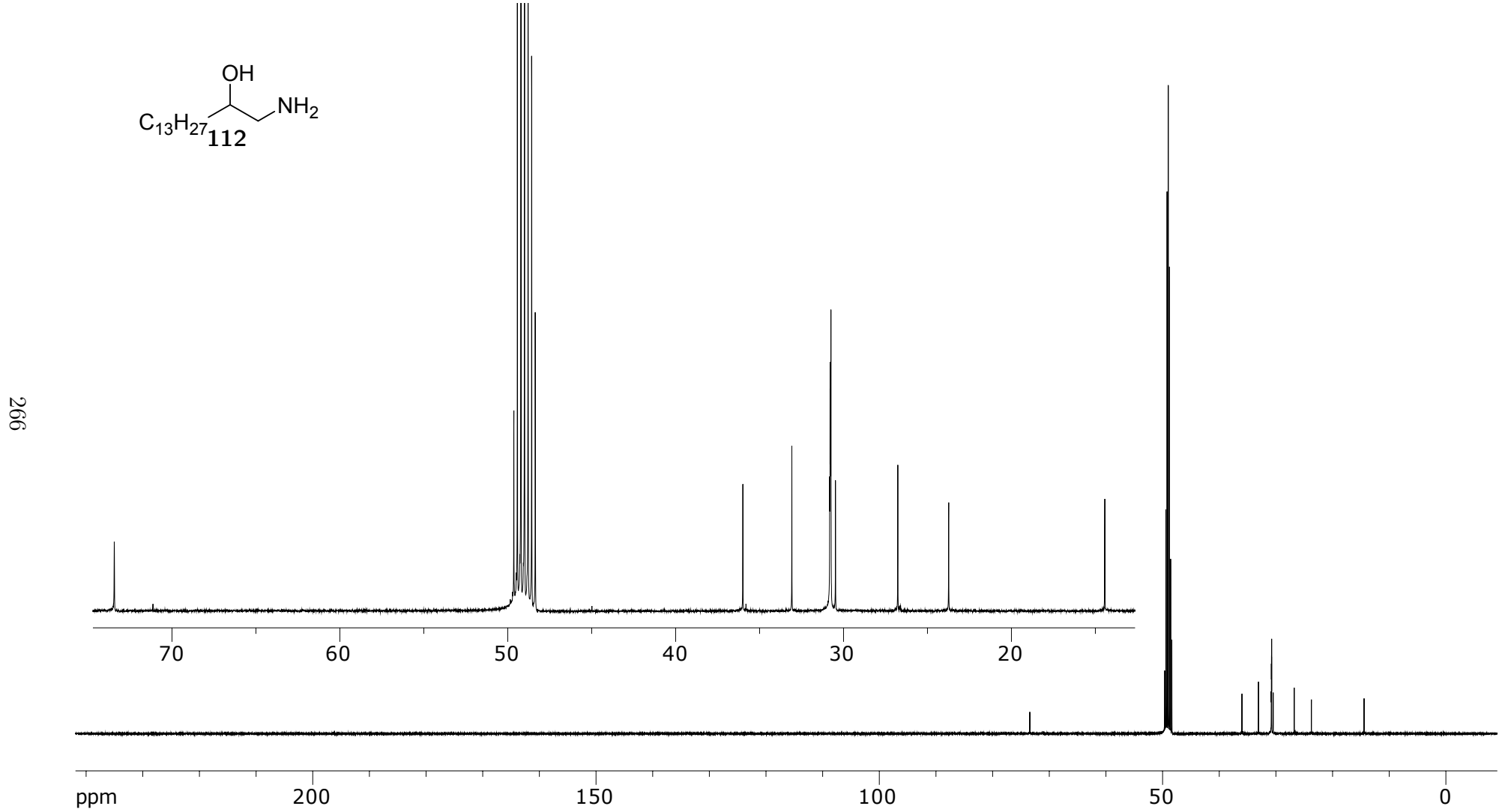

Figure A.32: 100 MHz ^{13}C NMR of **112** in $CDCl_3$

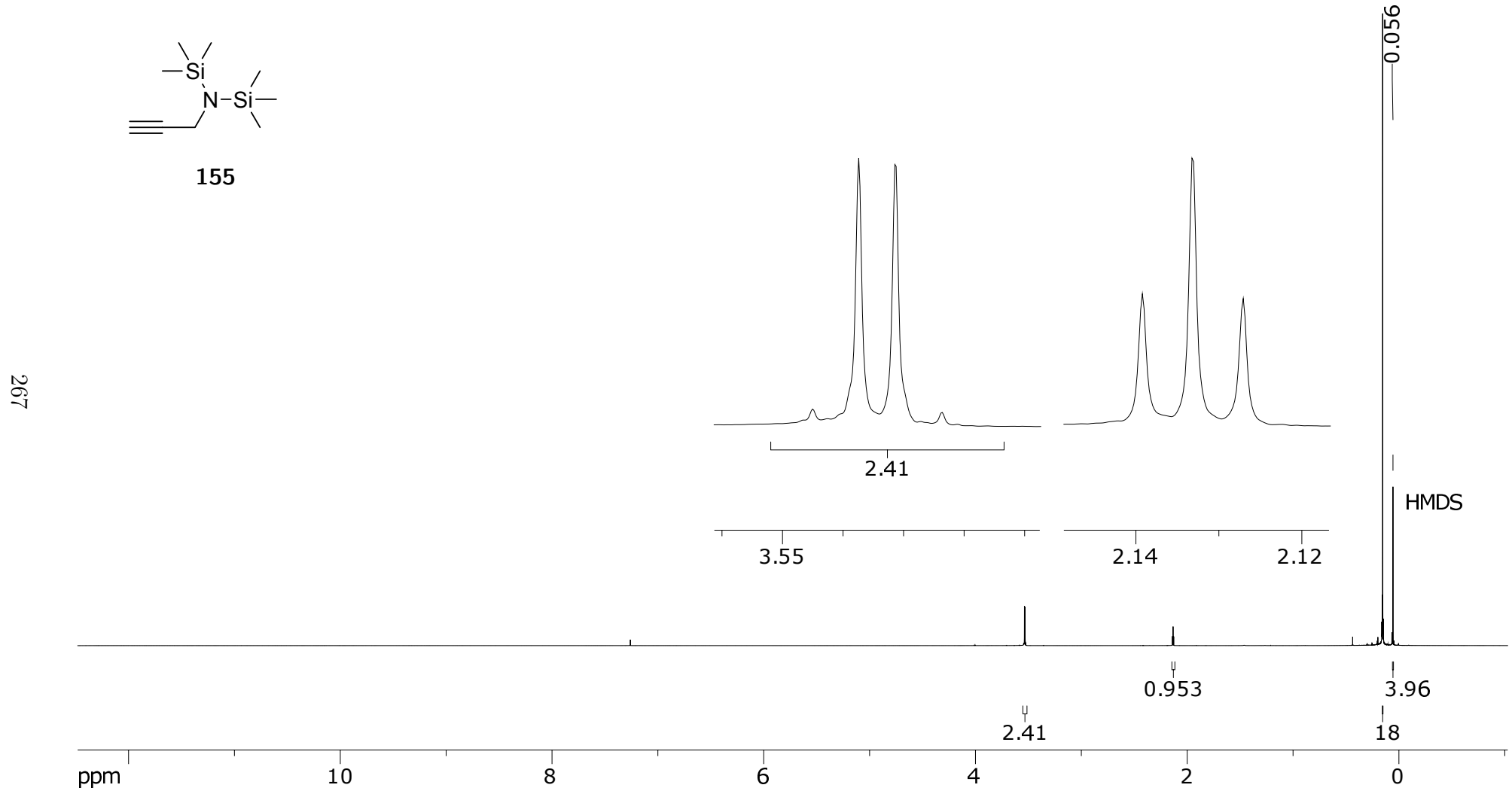

Figure A.33: 400 MHz ^{1}H NMR of **155** in $CDCl_3$

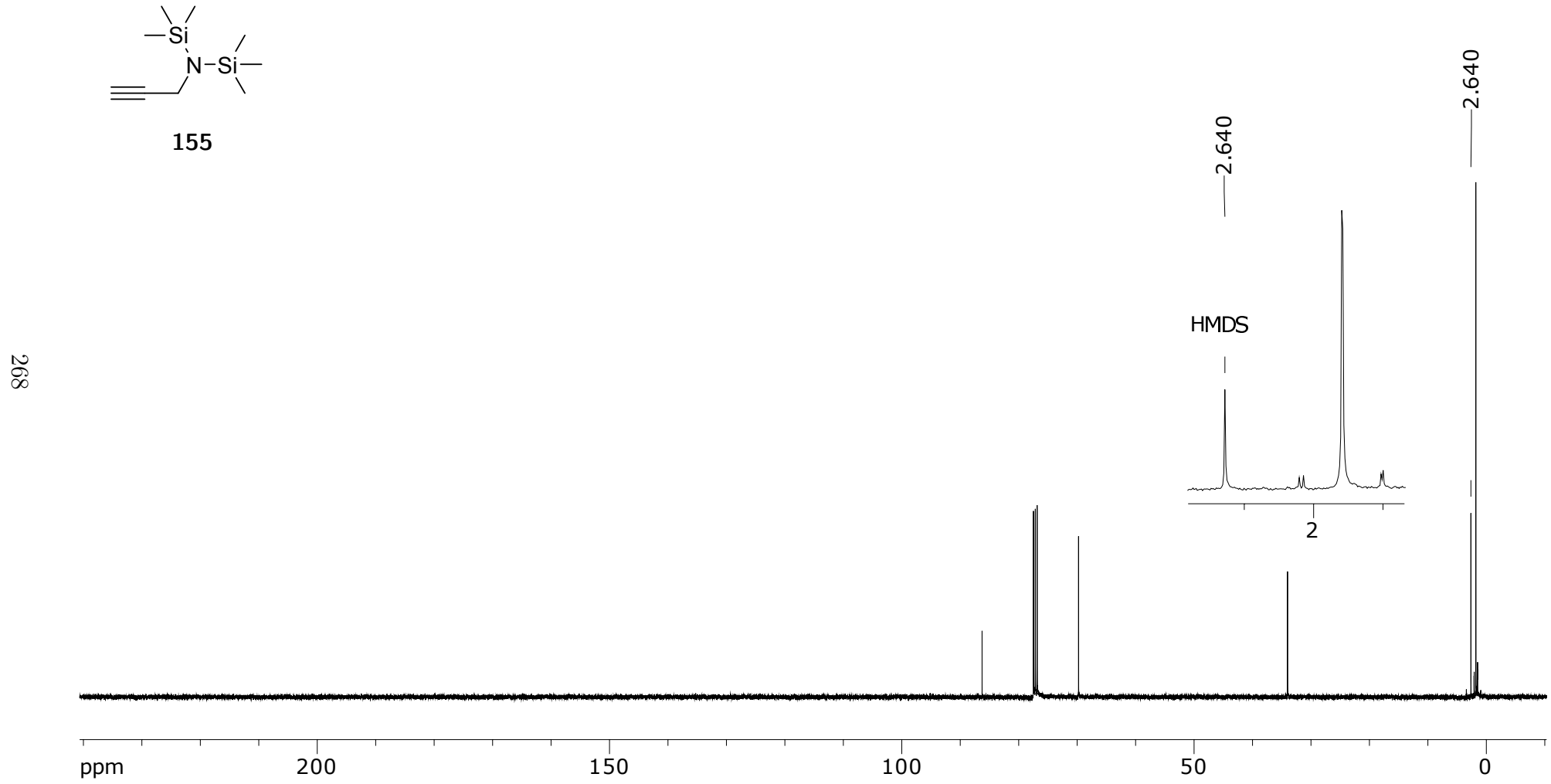

Figure A.34: 100 MHz ^{13}C NMR of **155** in $CDCl_3$

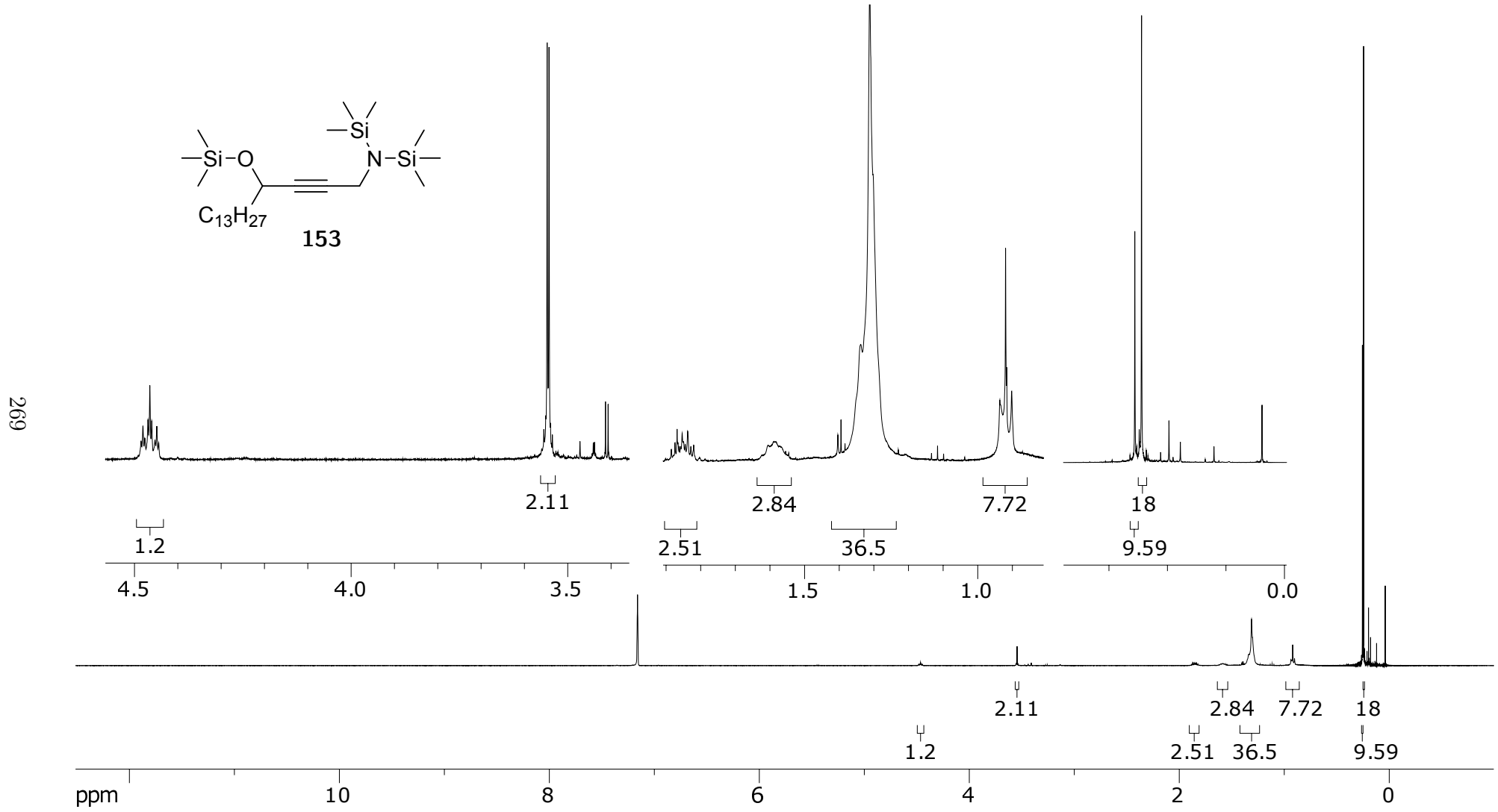

Figure A.35: 400 MHz ^{1}H NMR of **153** in C_6D_6

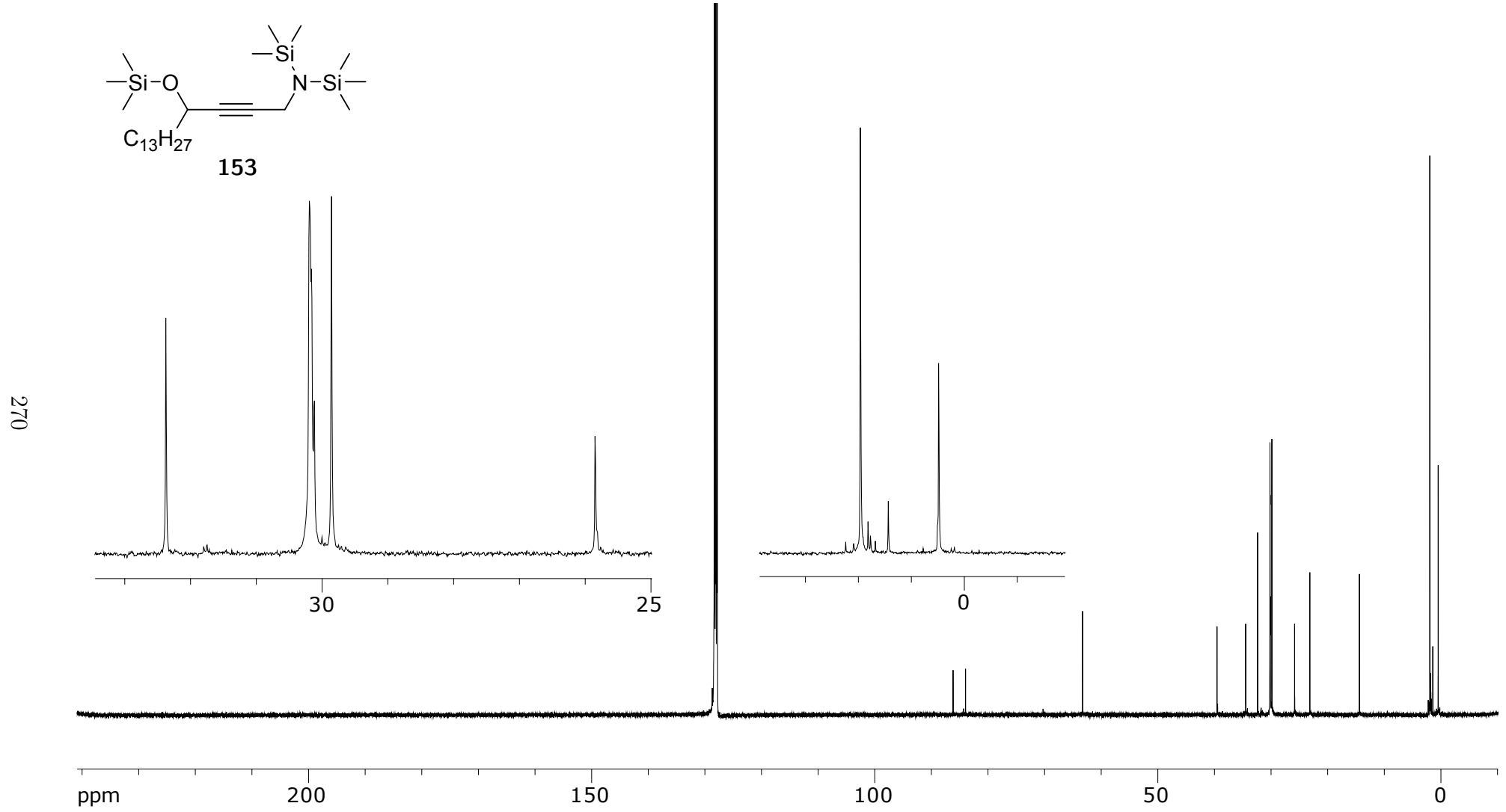

Figure A.36: 100 MHz ^{13}C NMR of **153** in C_6D_6

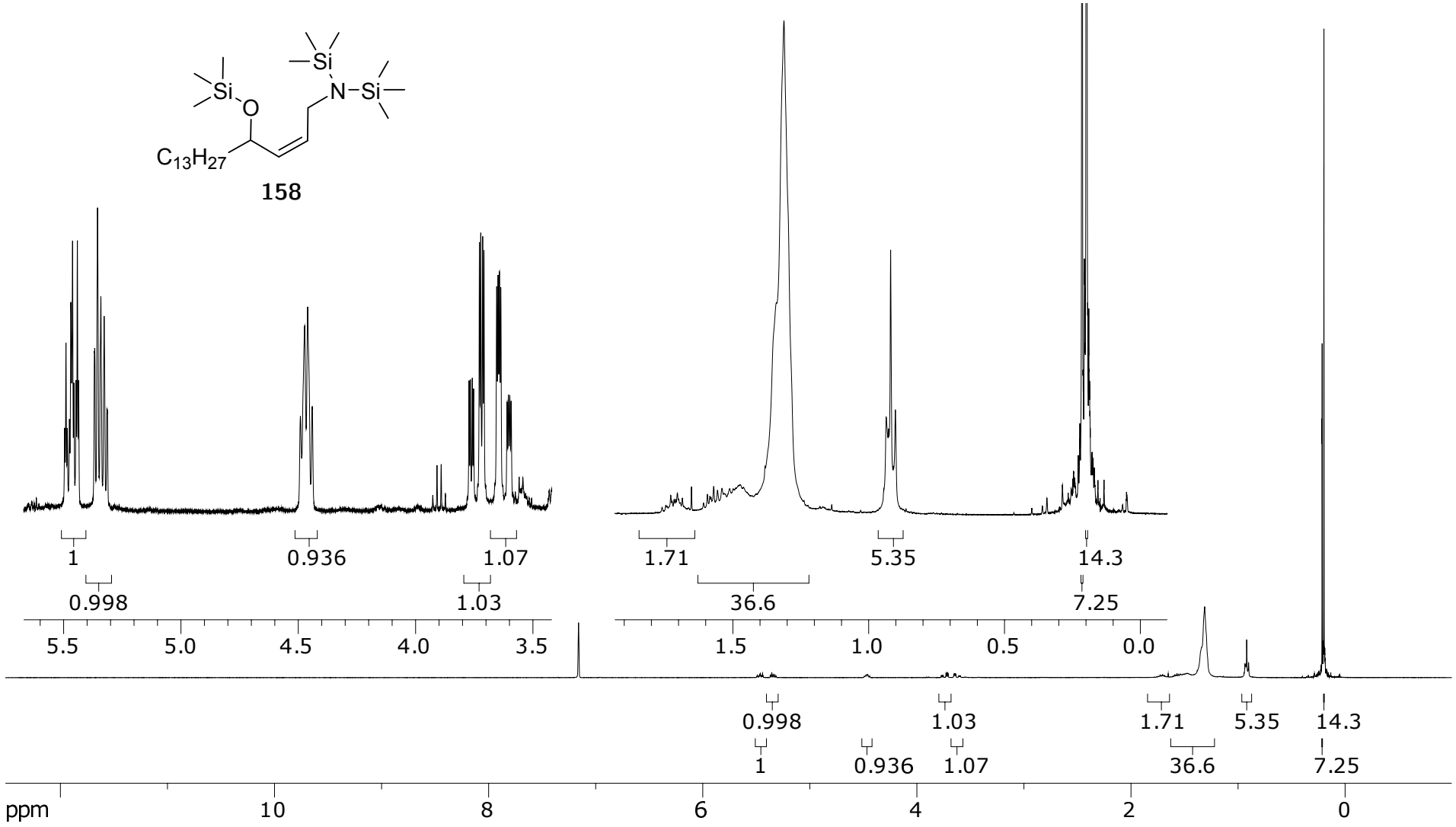

Figure A.37: 400 MHz ^{1}H NMR of **158** in C_6D_6

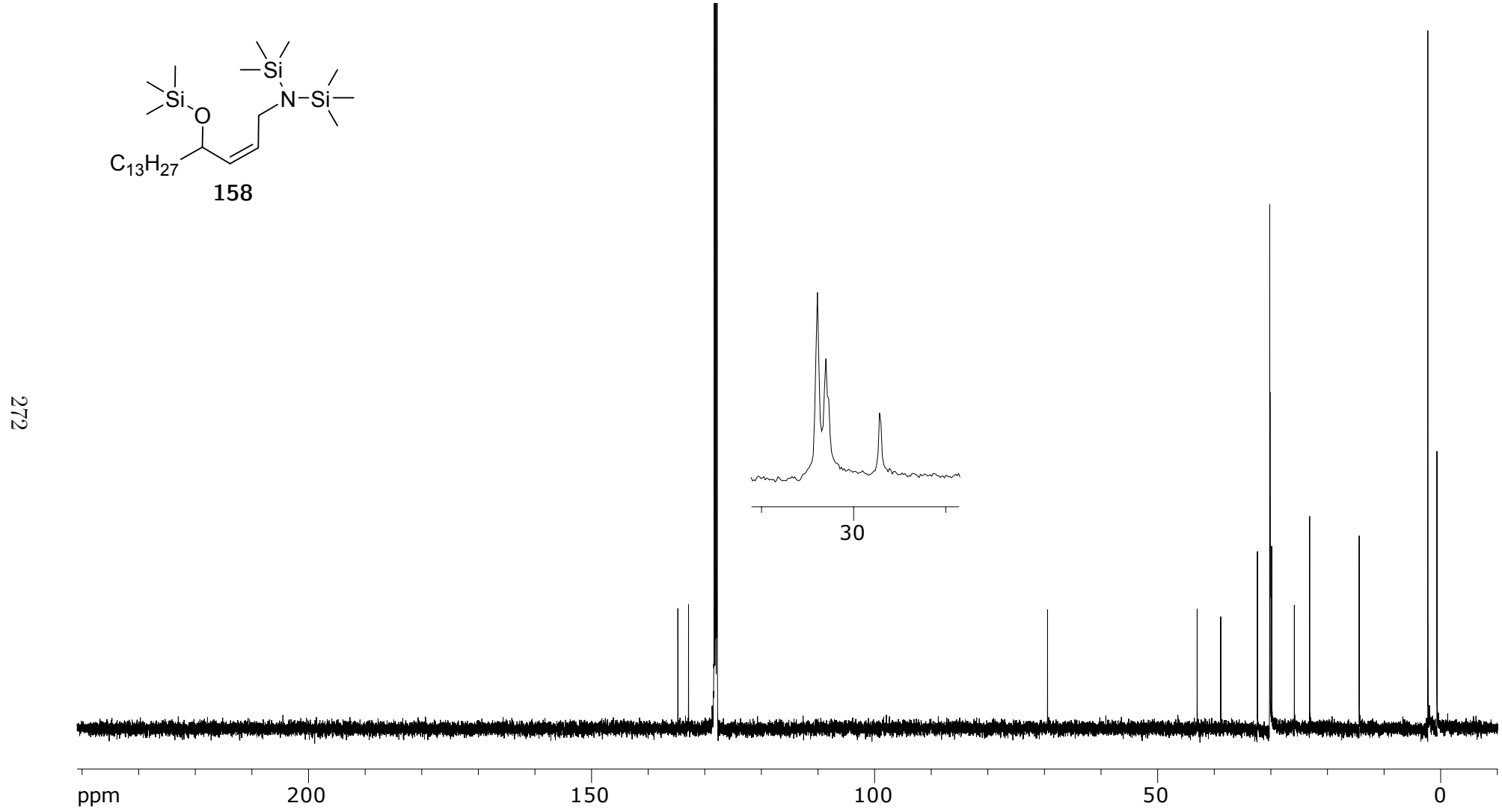

Figure A.38: 100 MHz ^{13}C NMR of **158** in C_6D_6

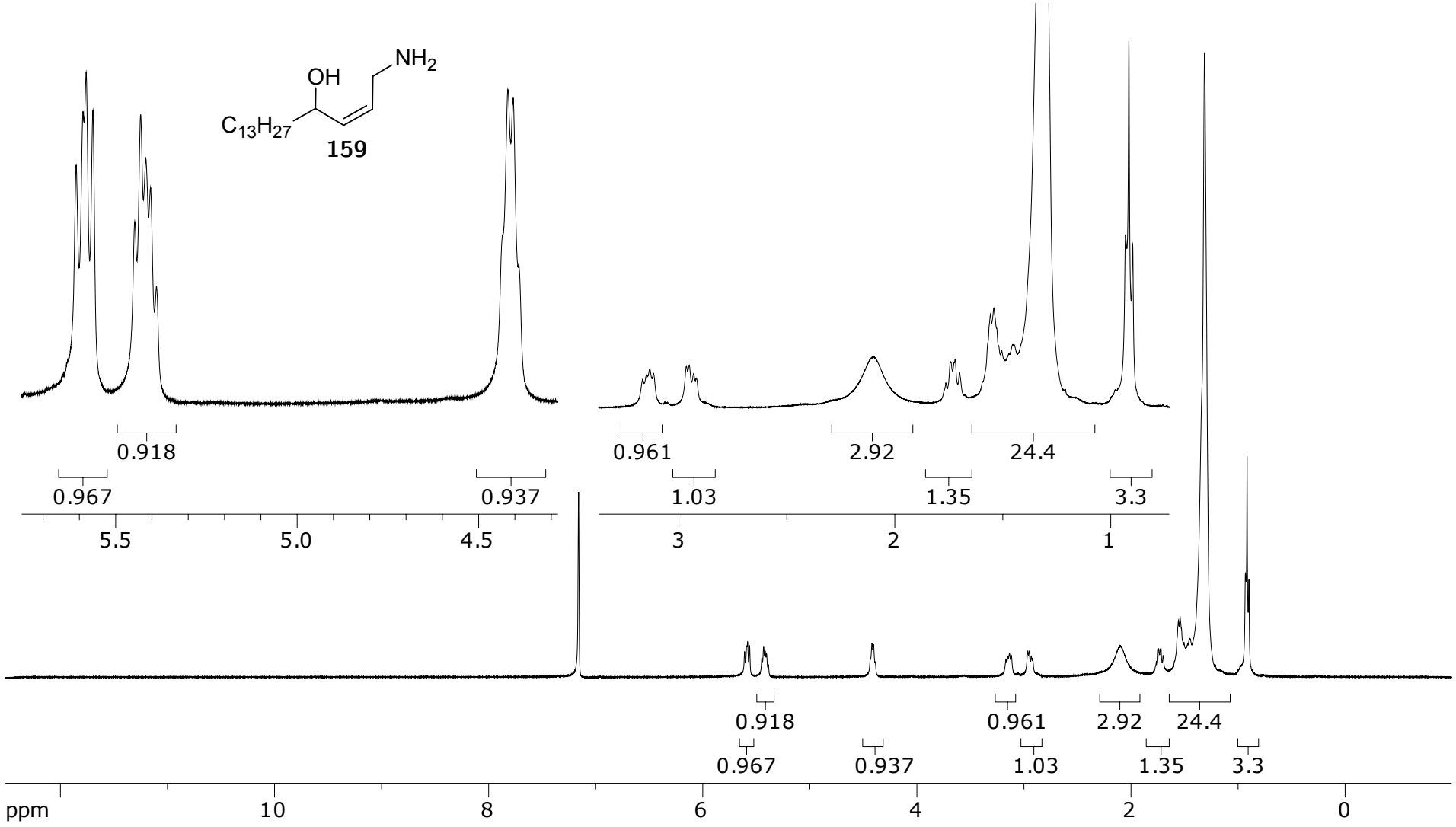

Figure A.39: 400 MHz ^{1}H NMR of **159** in C_6D_6

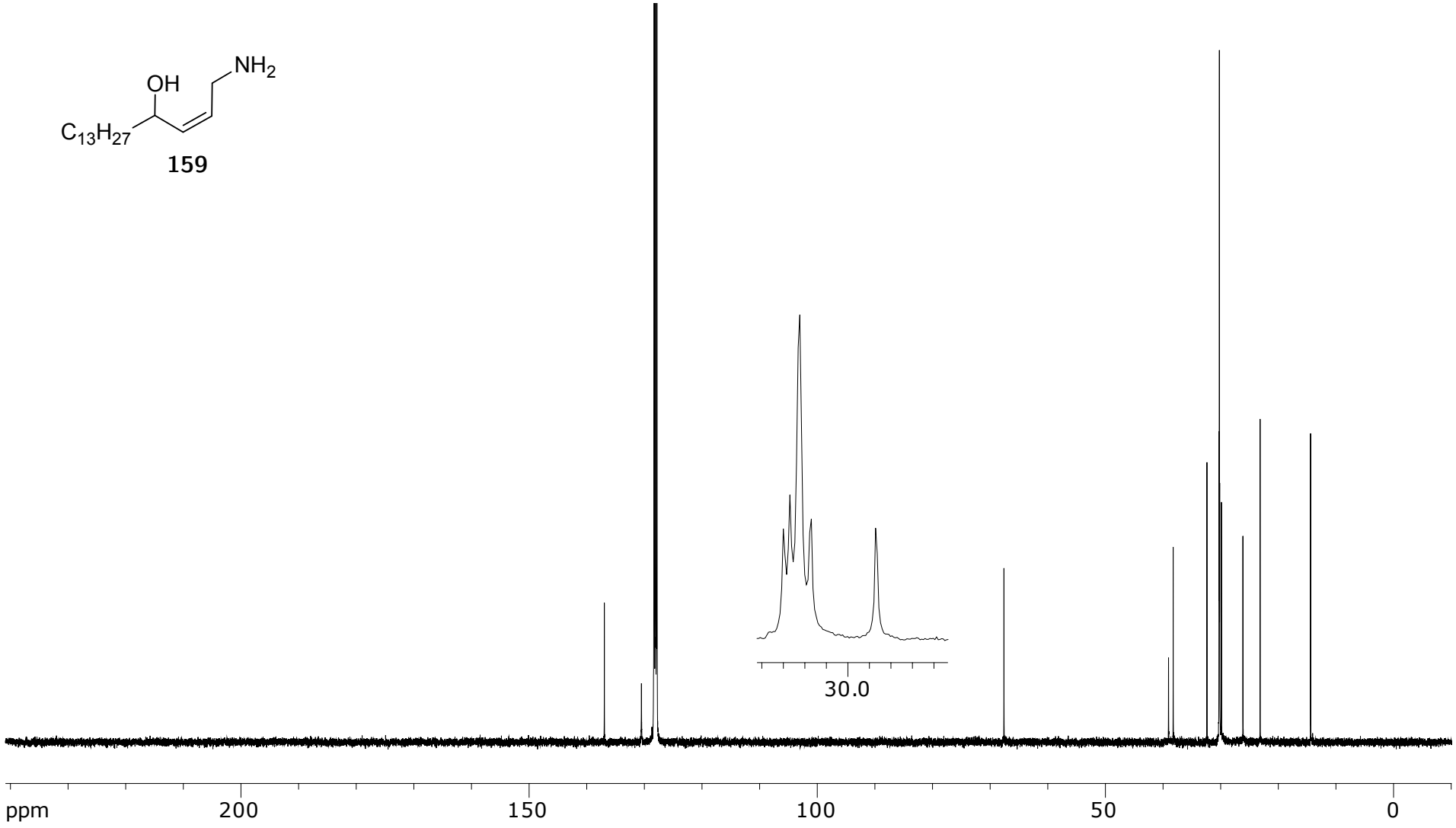

Figure A.40: 100 MHz ^{13}C NMR of **159** in C_6D_6

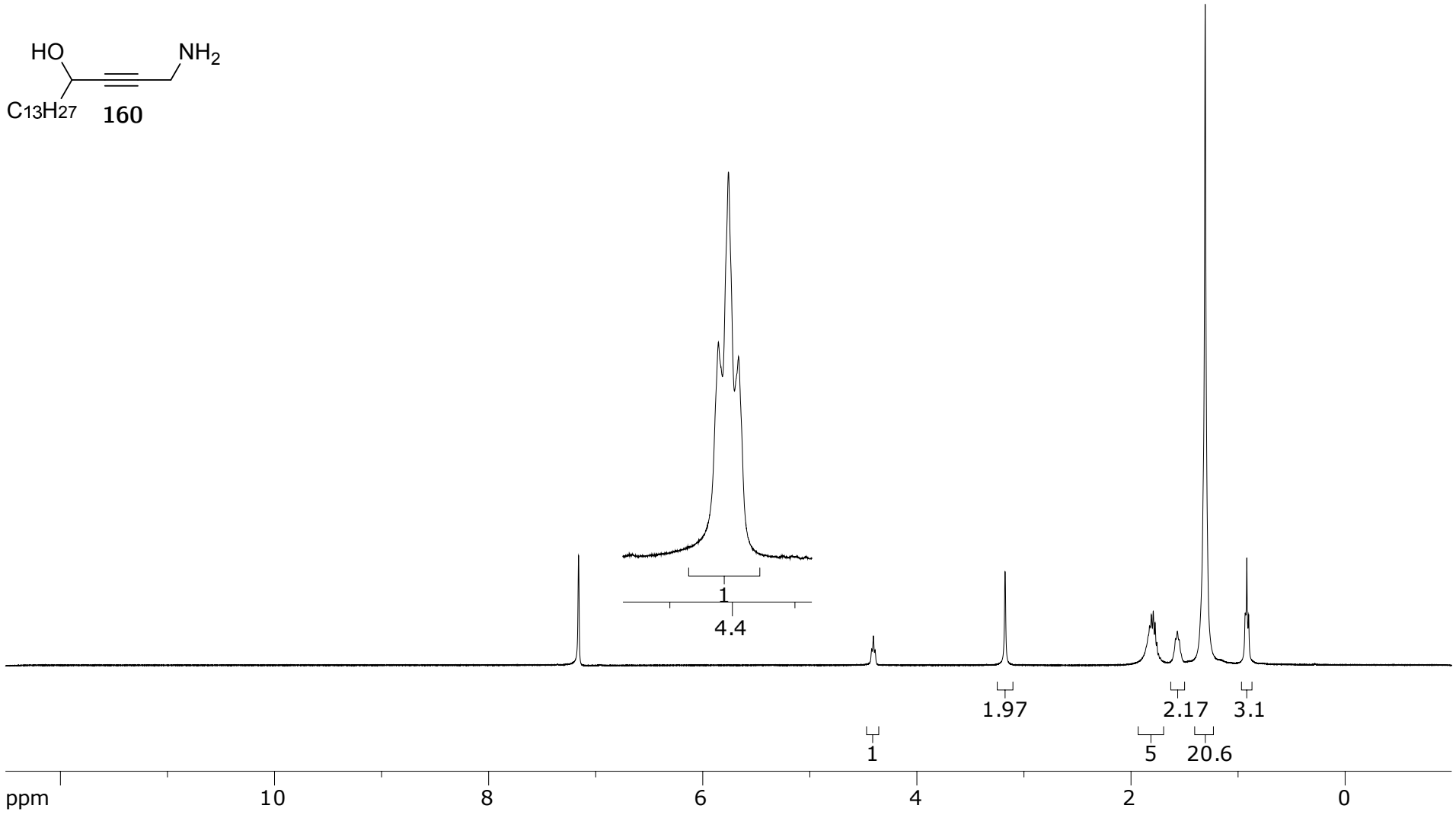

Figure A.41: 400 MHz ^{1}H NMR of **159** in C_6D_6

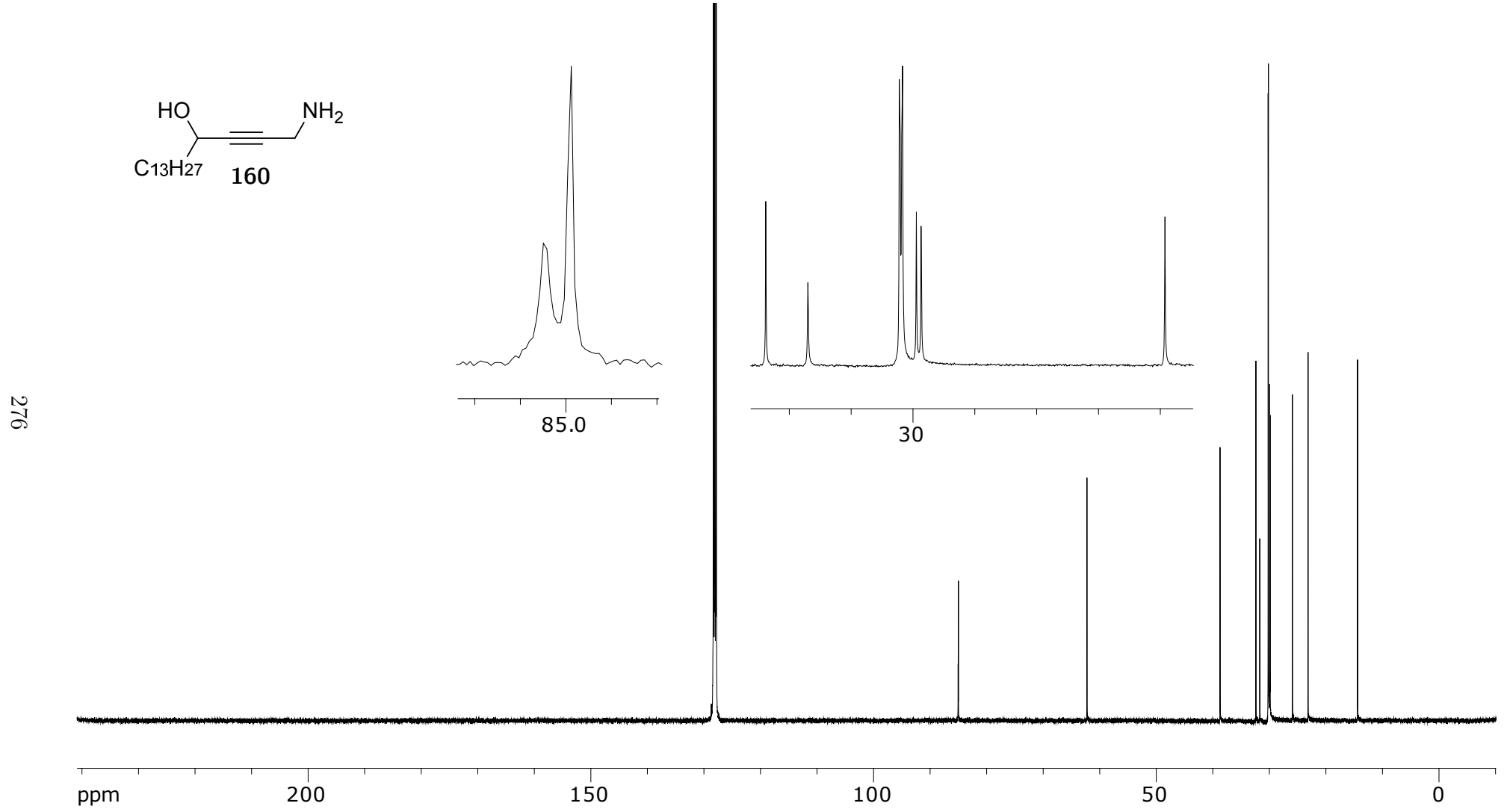

Figure A.42: 100 MHz ^{13}C NMR of **159** in C_6D_6

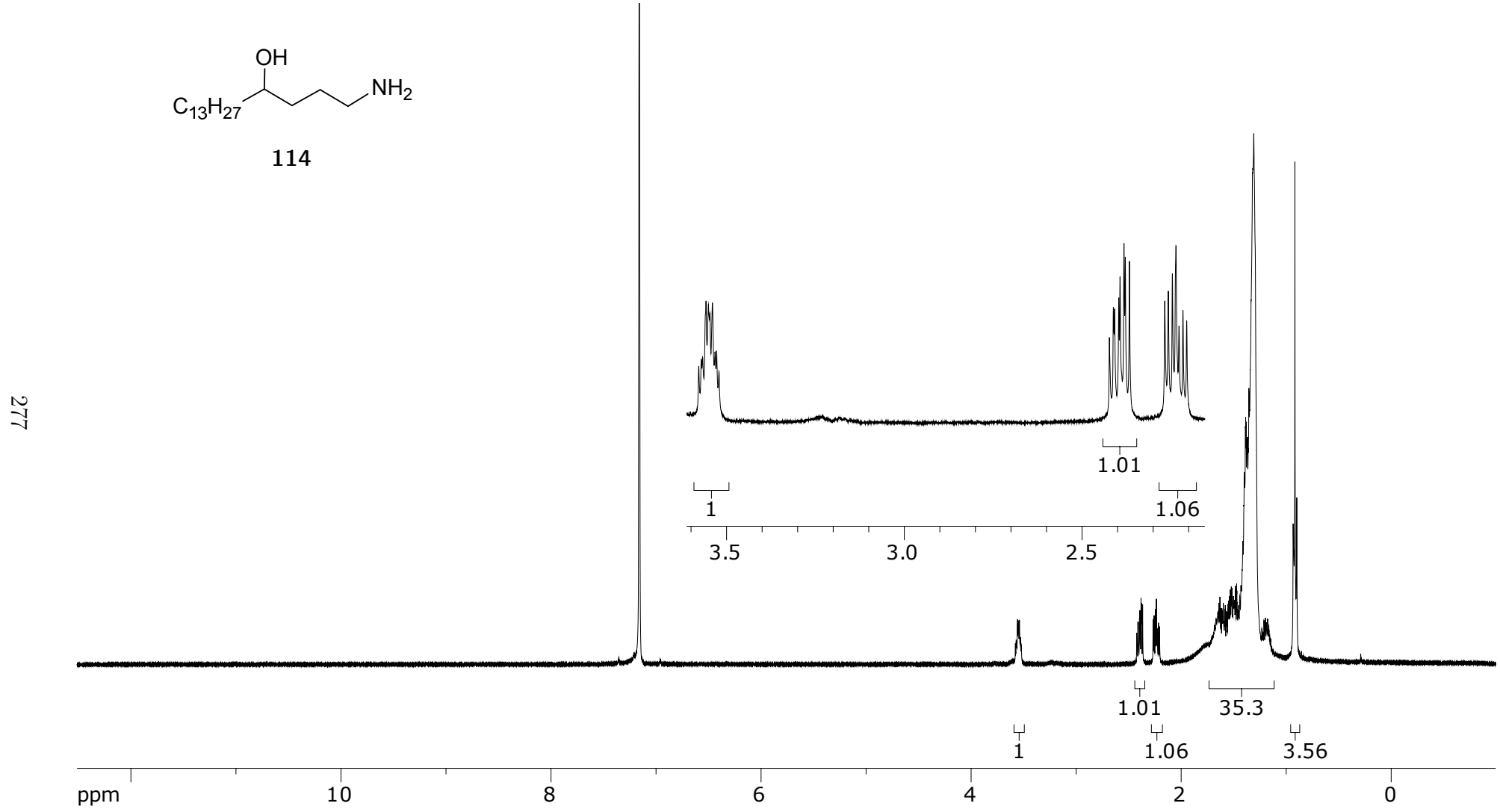

Figure A.43: 400 MHz ^{1}H NMR of **114** in C_6D_6

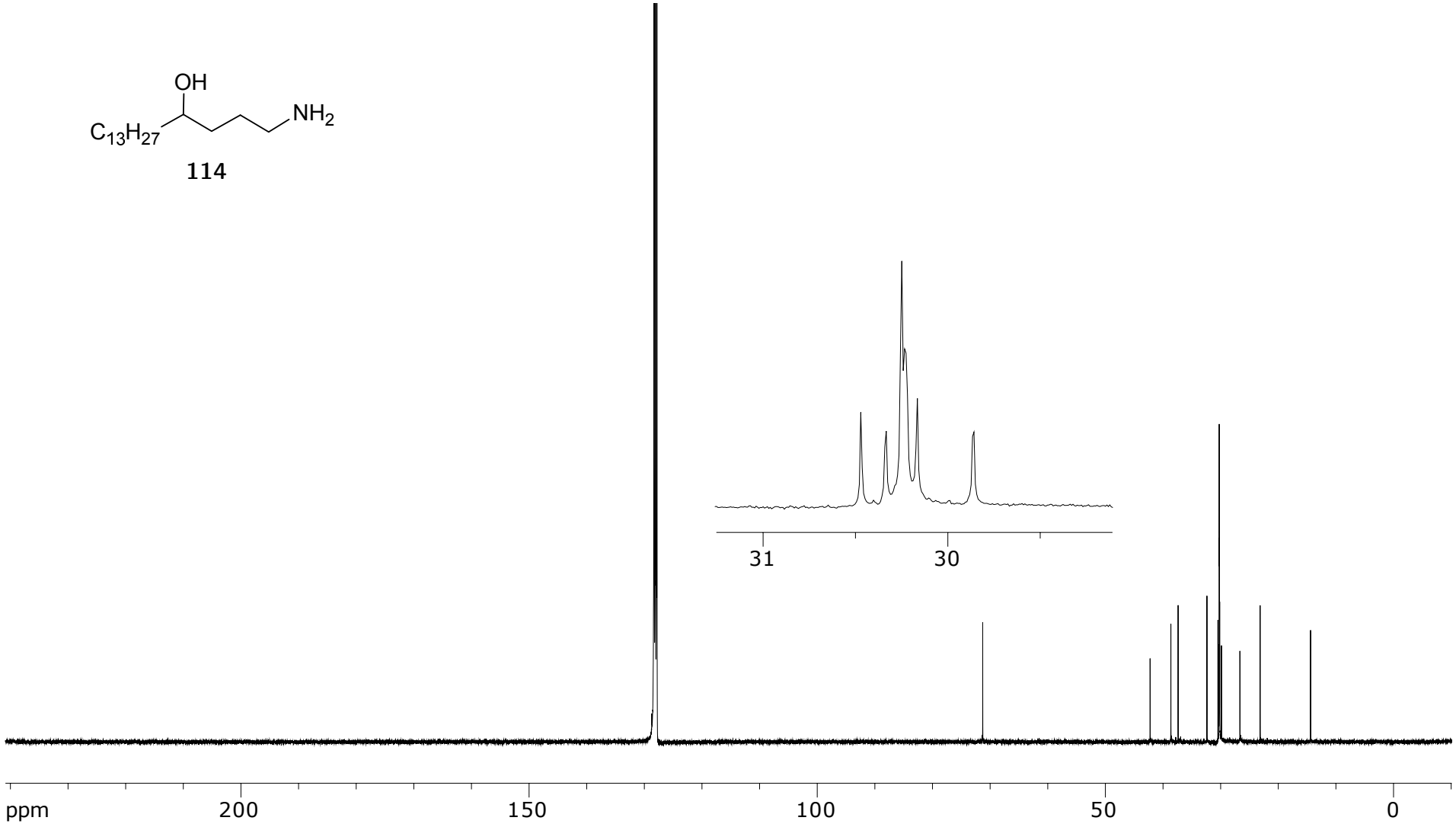

Figure A.44: 100 MHz ^{13}C of **114** NMR in C_6D_6

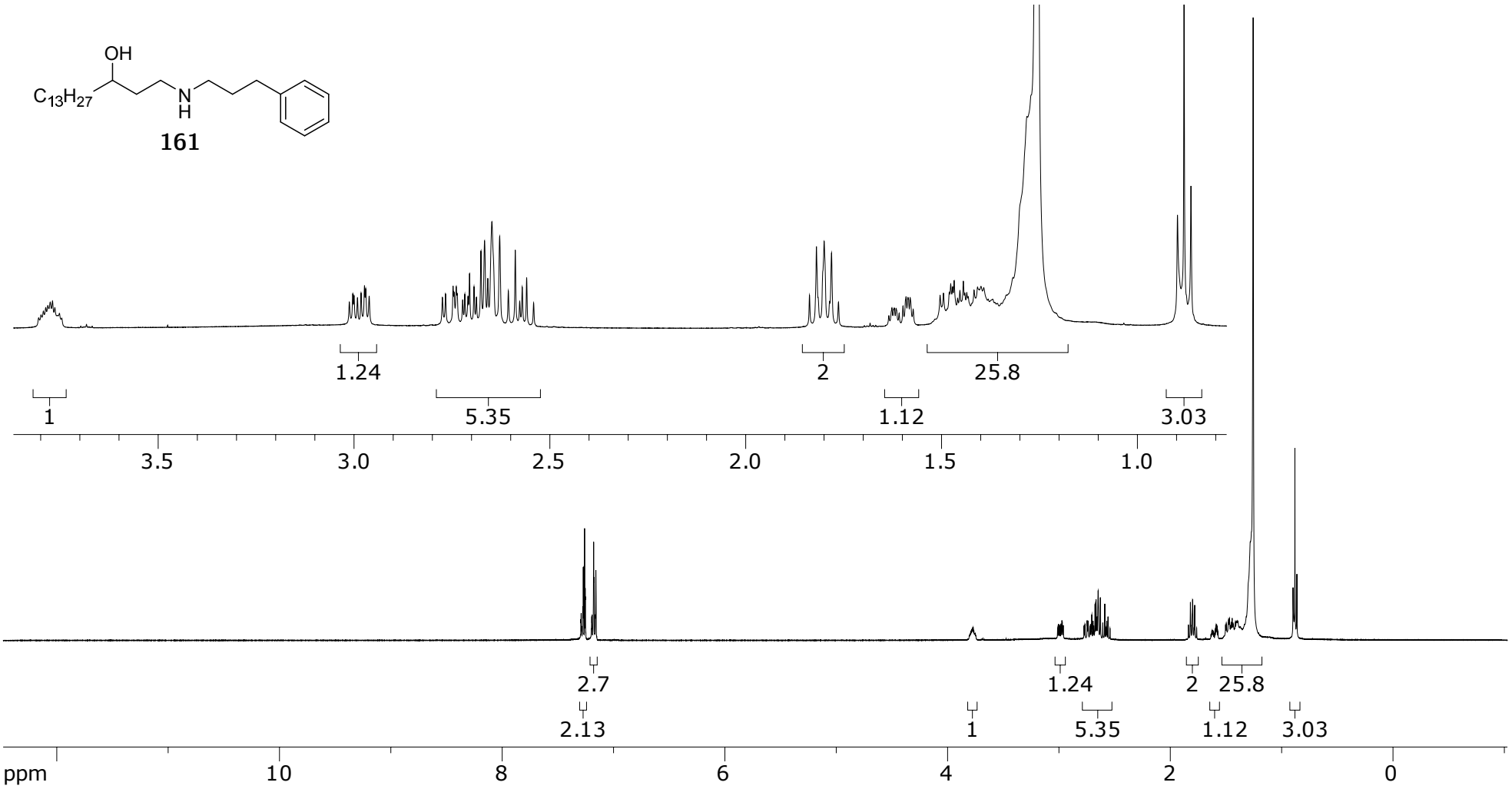

Figure A.45: 400 MHz ^{1}H NMR of **161** in $CDCl_3$

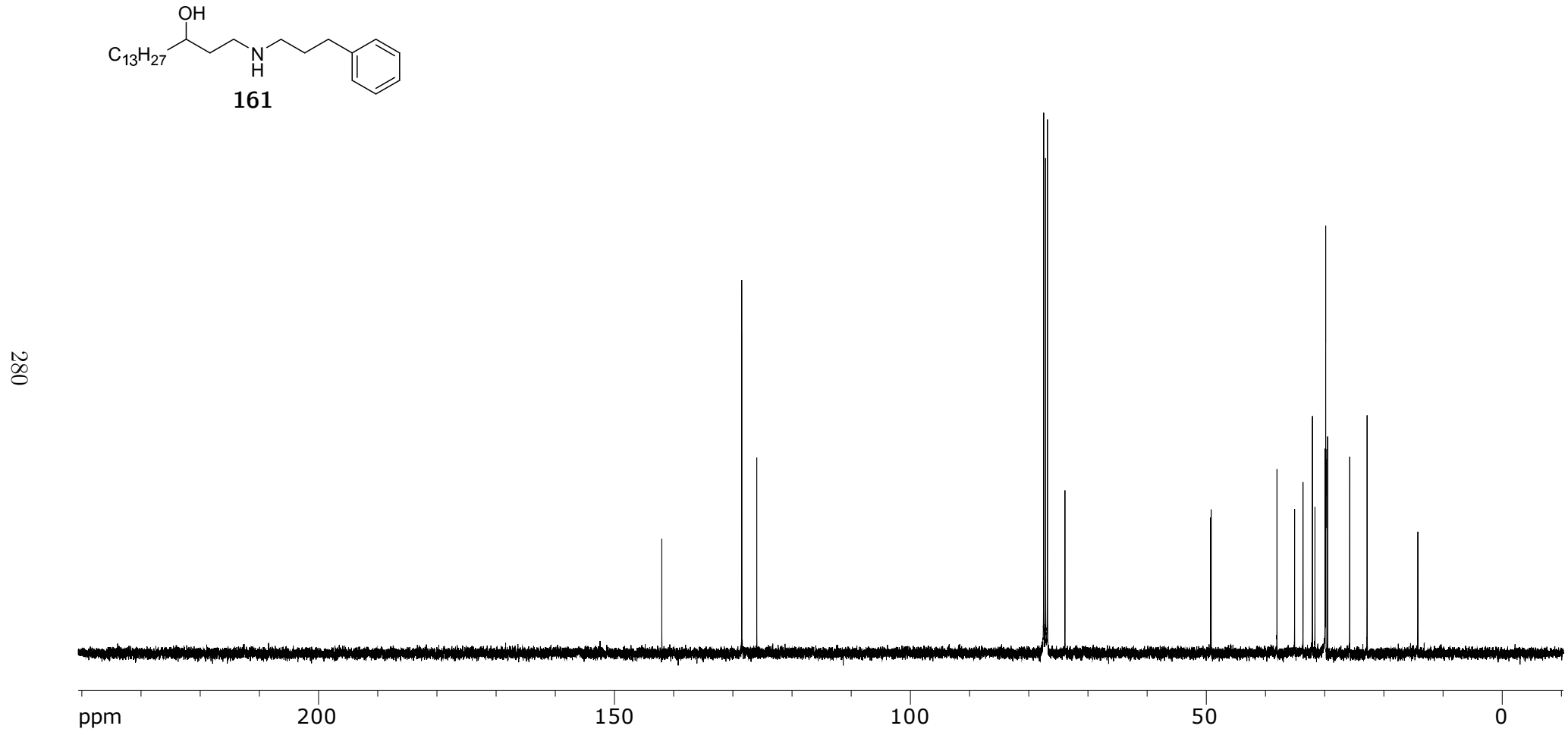

Figure A.46: 100 MHz ^{13}C NMR of **161** in $CDCl_3$

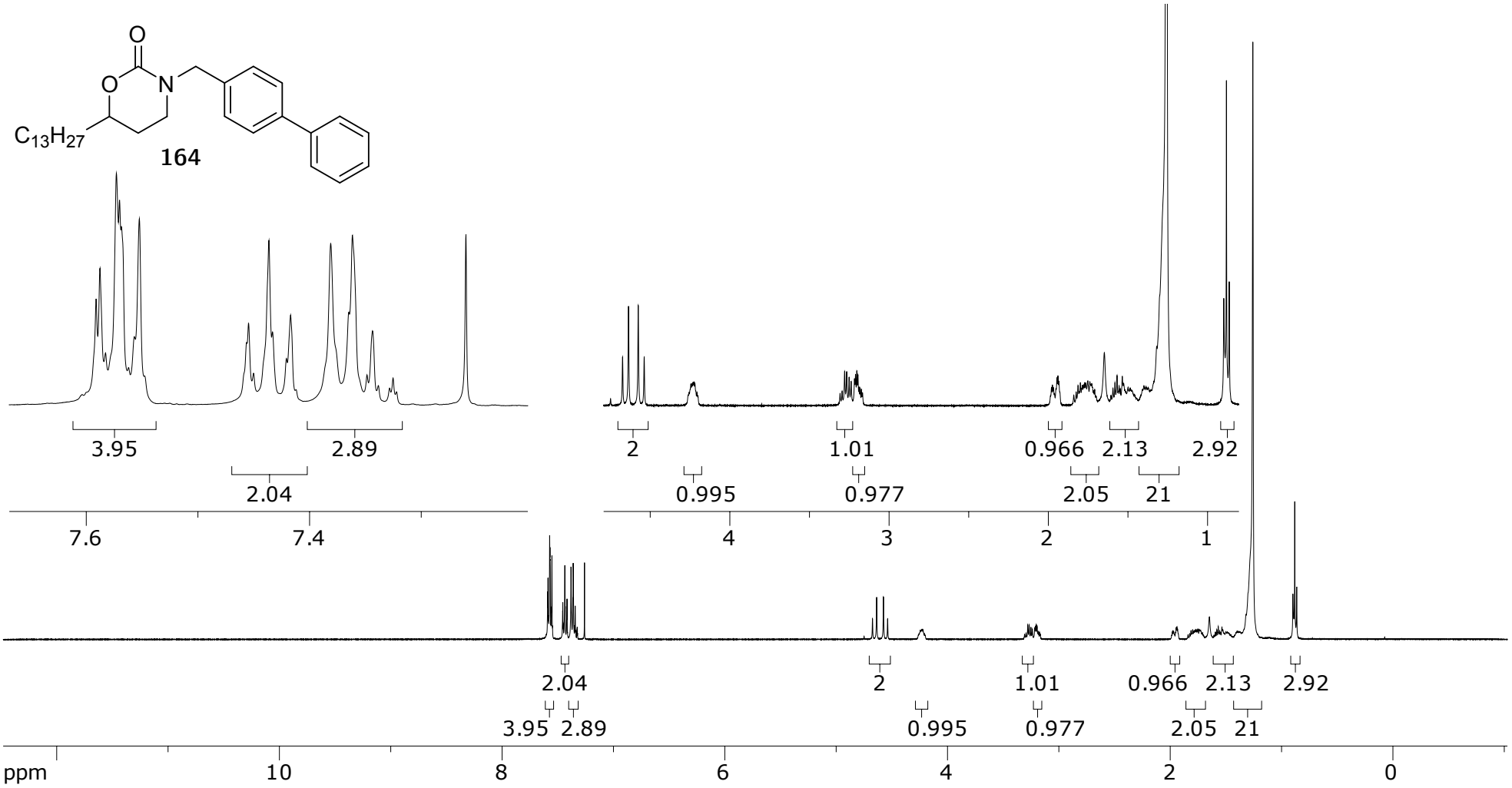

Figure A.47: 400 MHz ^{1}H NMR of **164** in

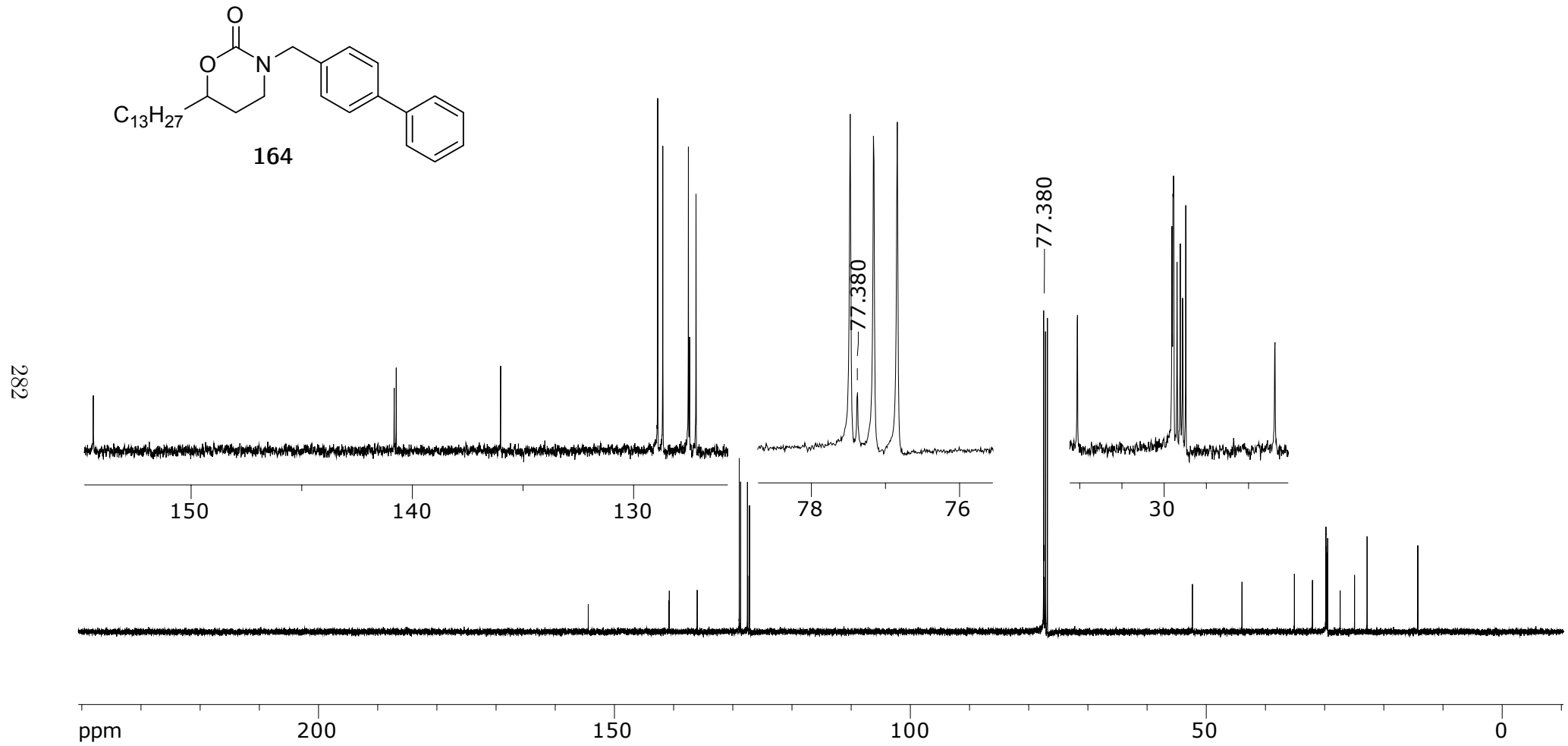

Figure A.48: 100 MHz ^{13}C of **164** NMR in

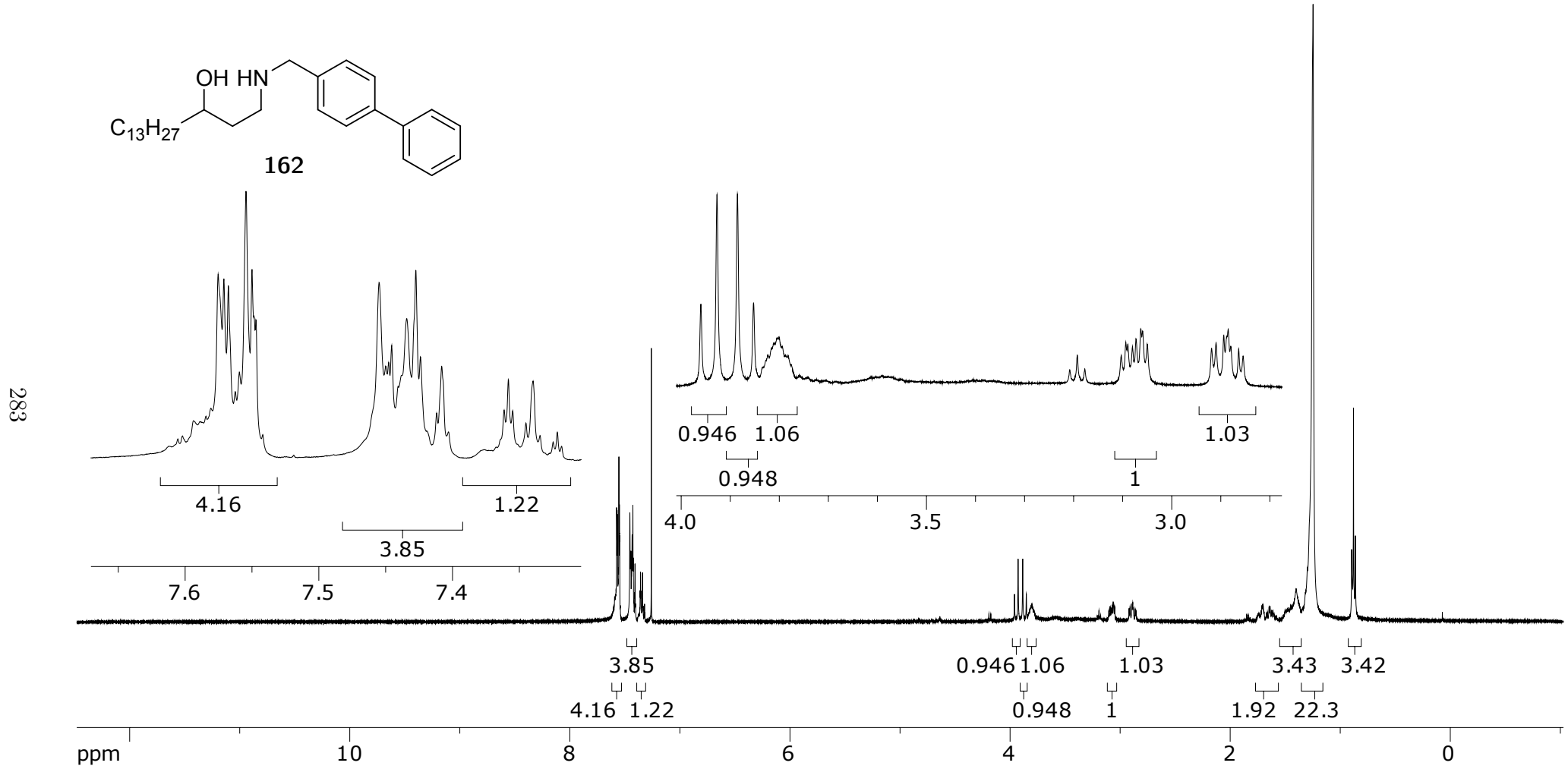

Figure A.49: 400 MHz ^{1}H NMR of **162** in

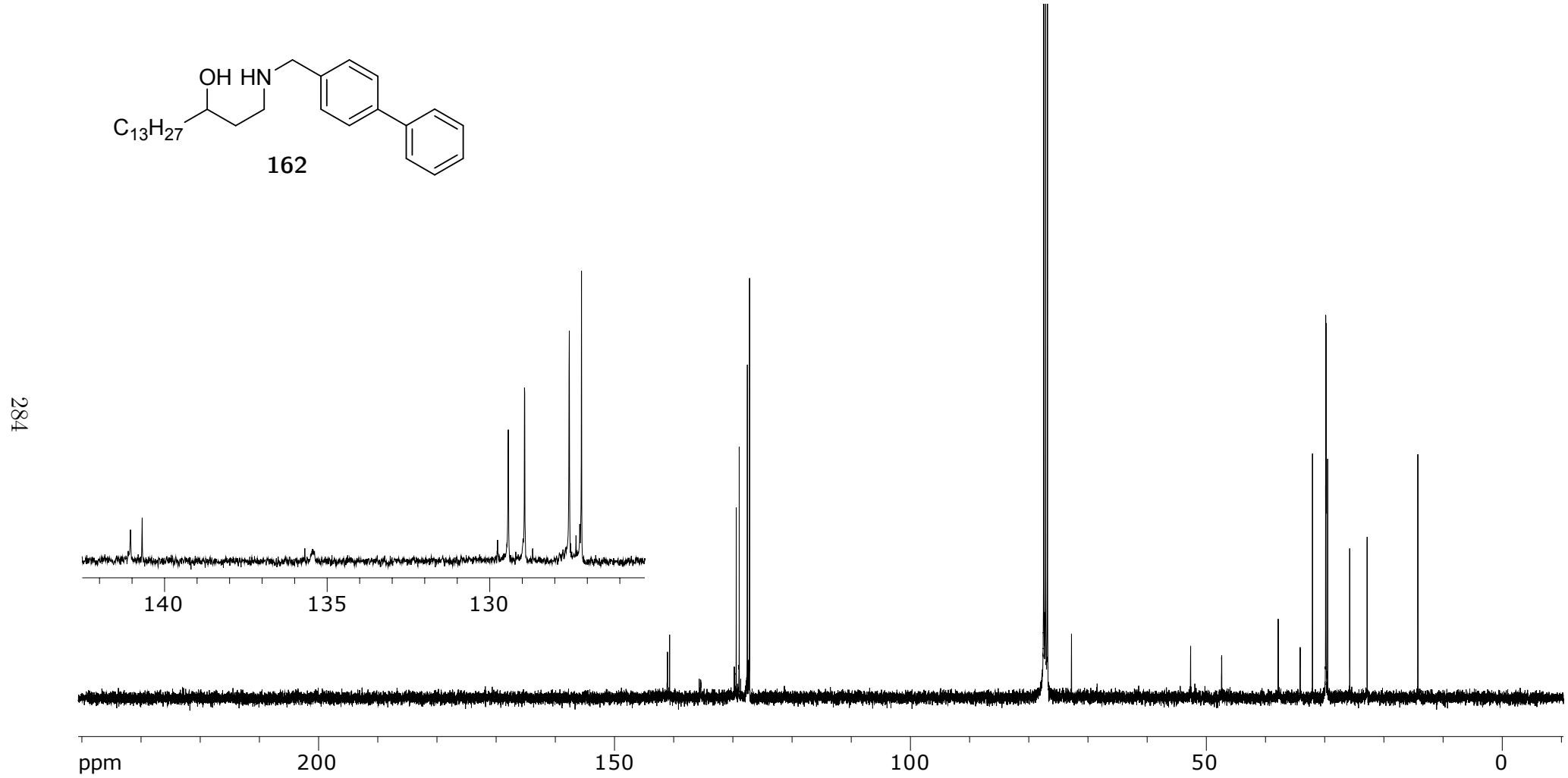

Figure A.50: 100 MHz ^{13}C of **162** NMR in

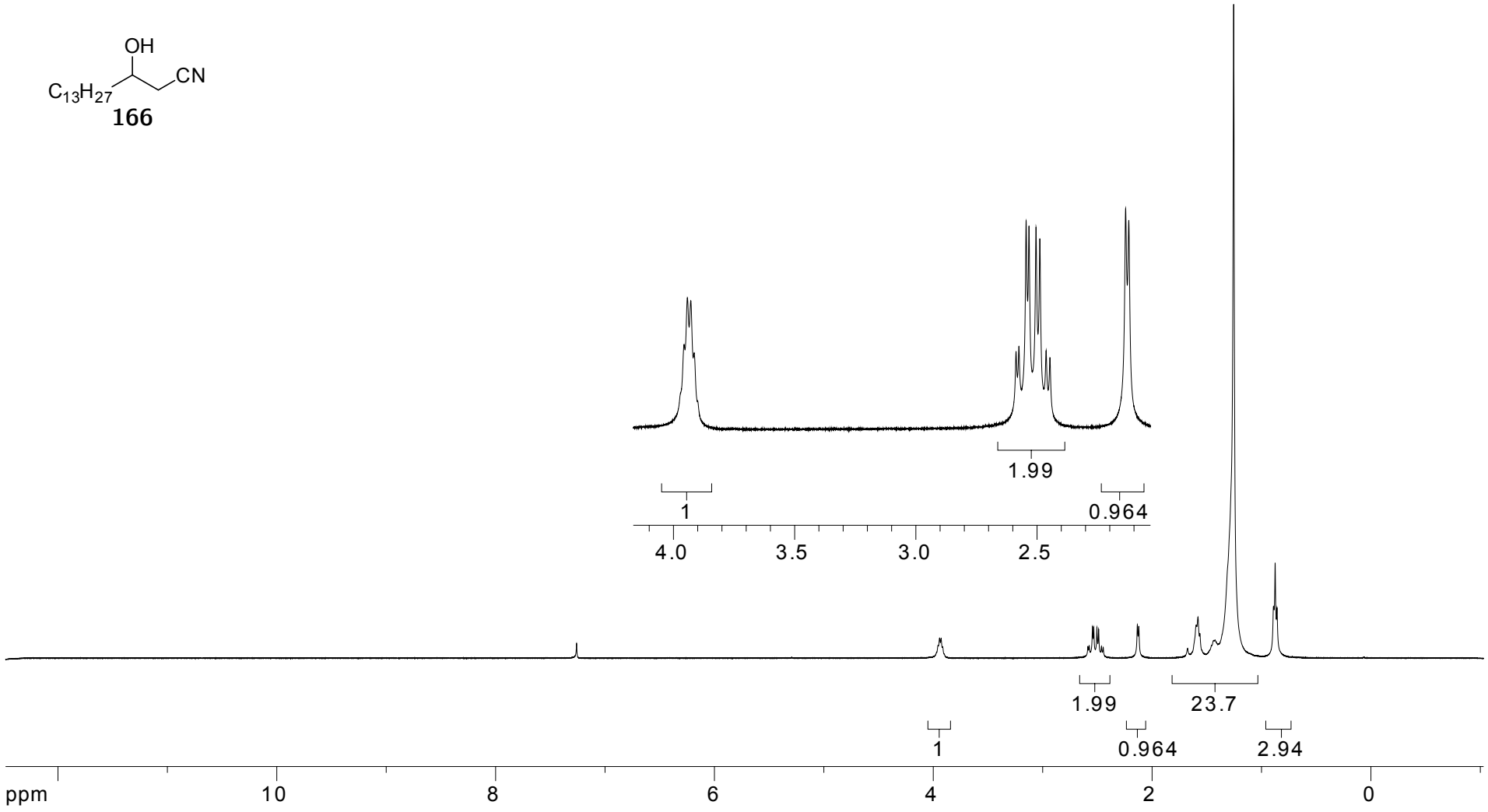

Figure A.51: 400 MHz ^{1}H NMR of **166** in $CDCl_3$

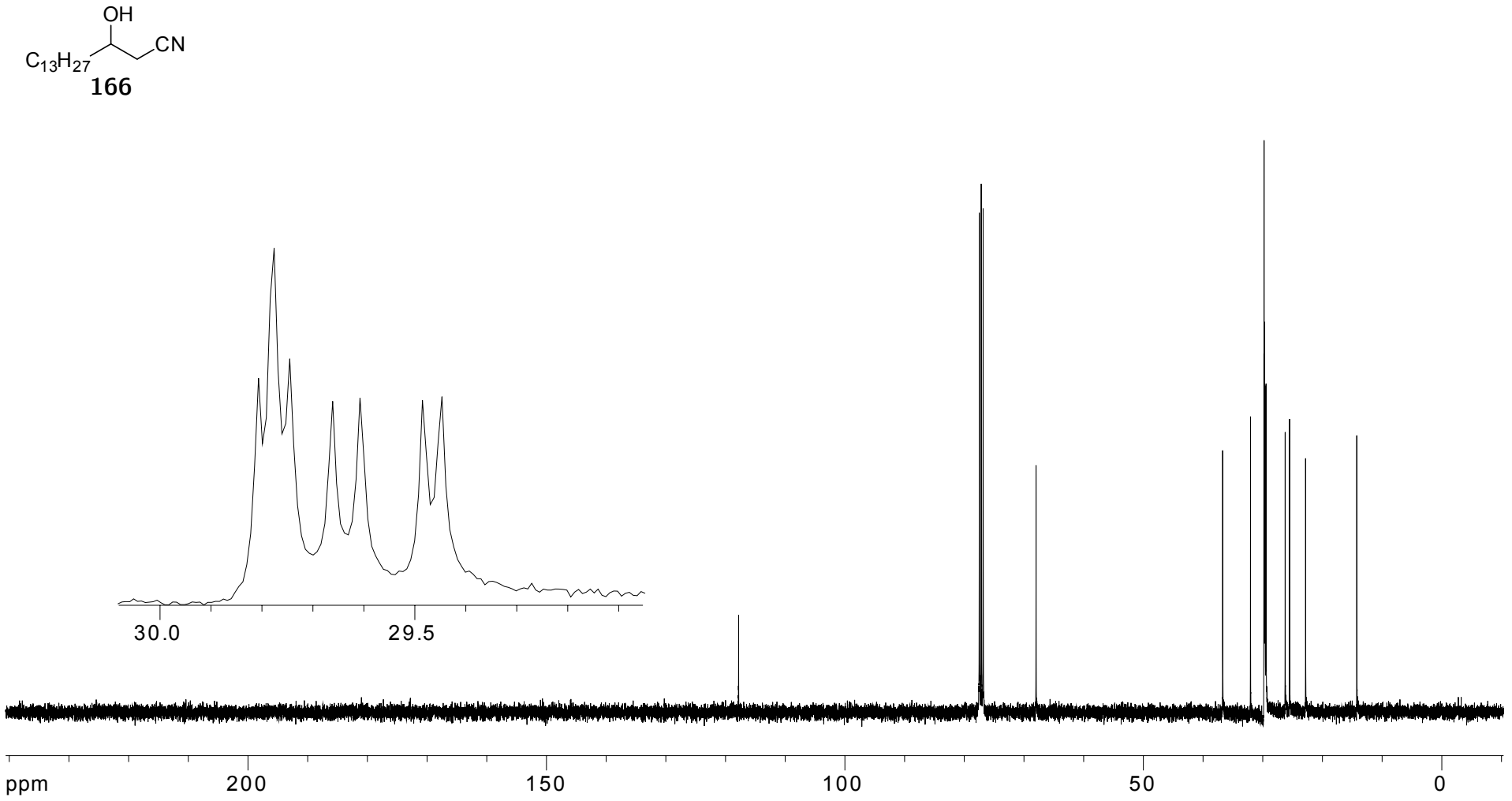

Figure A.52: 100 MHz ^{13}C NMR of **166** in $CDCl_3$

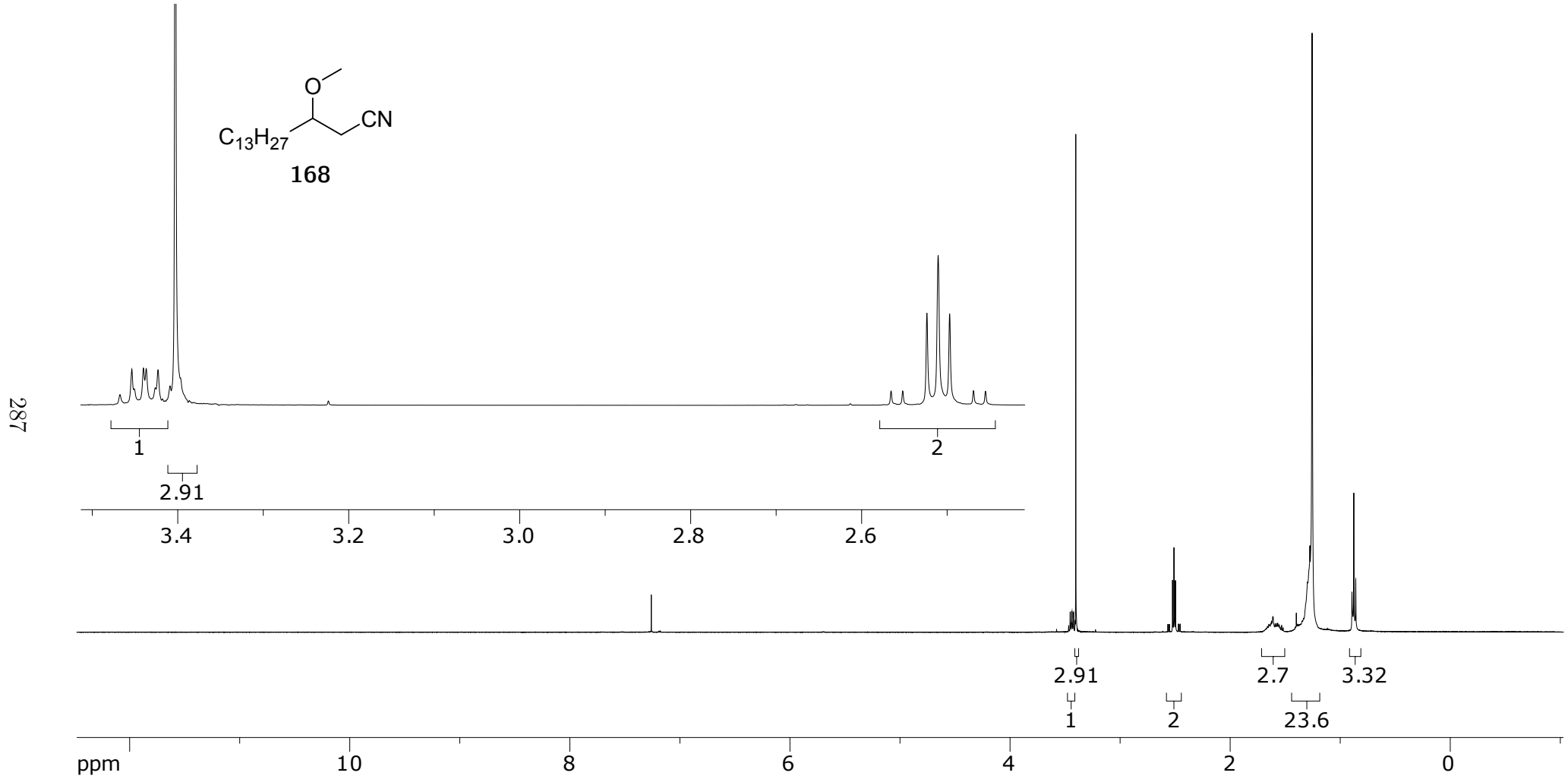

Figure A.53: 400 MHz ^{1}H NMR of **168** in $CDCl_3$

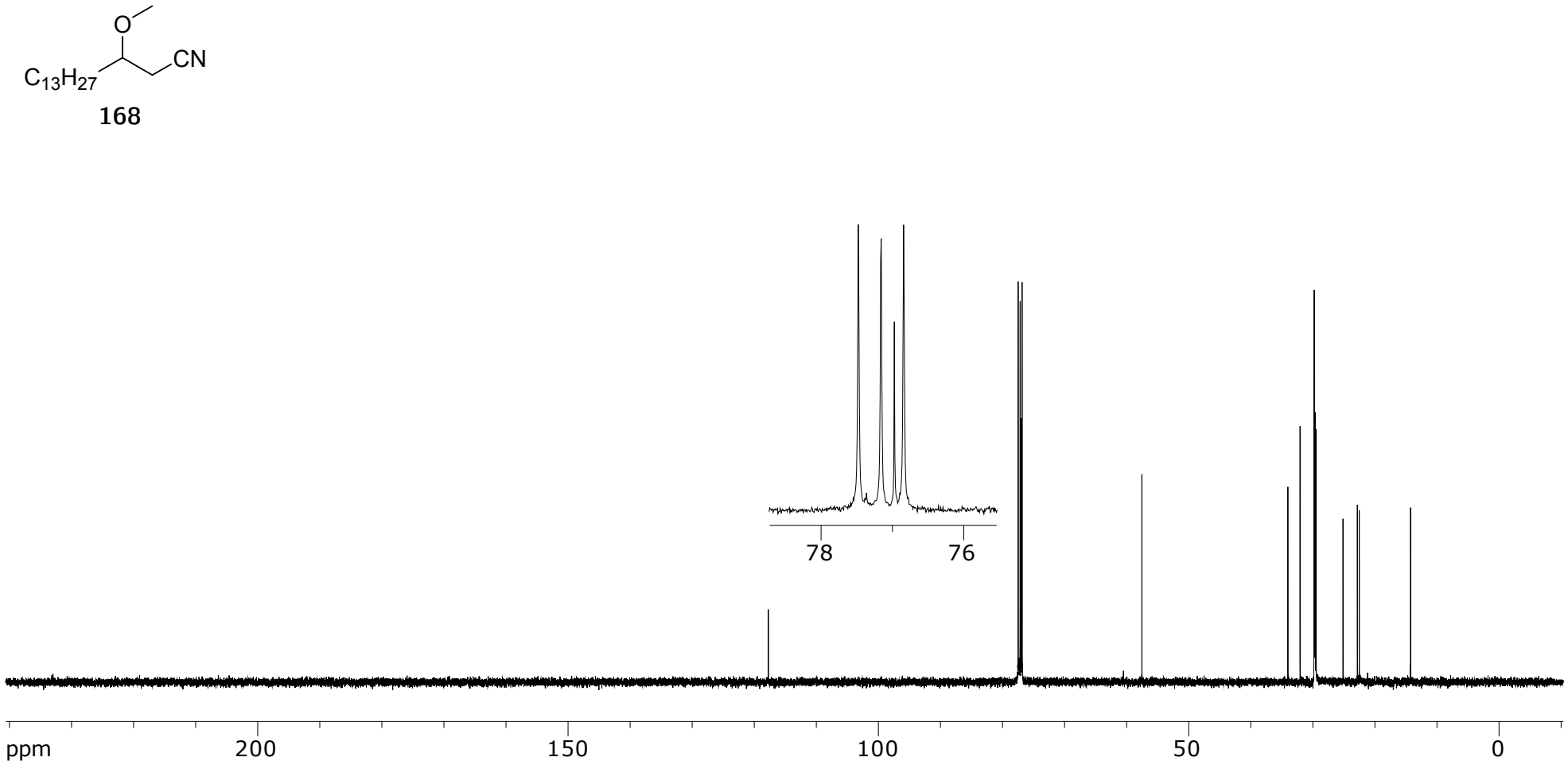

Figure A.54: 100 MHz ^{13}C NMR of **168** in $CDCl_3$

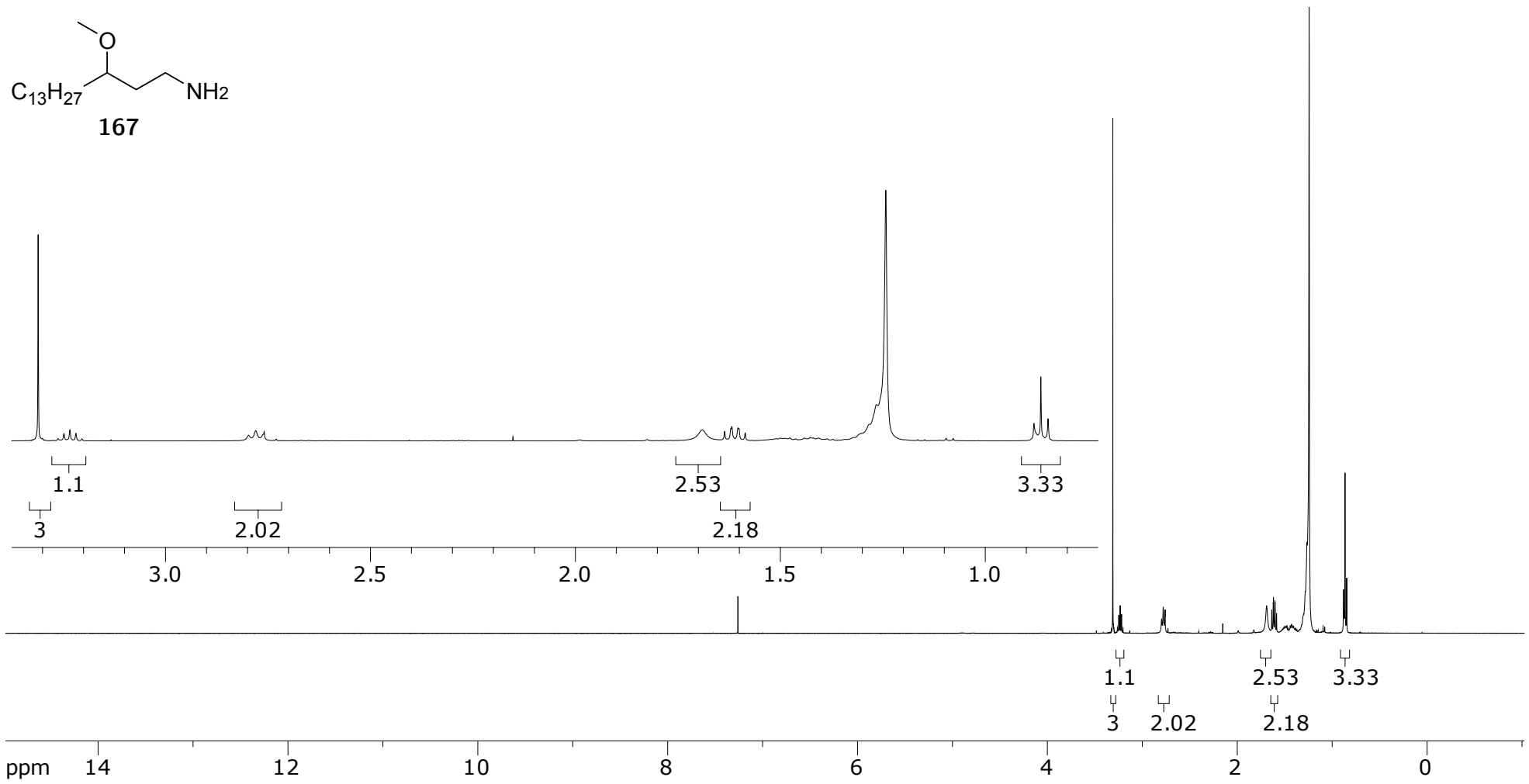

Figure A.55: 400 MHz ^{1}H NMR of **167** in $CDCl_3$

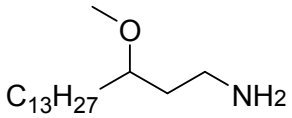

167

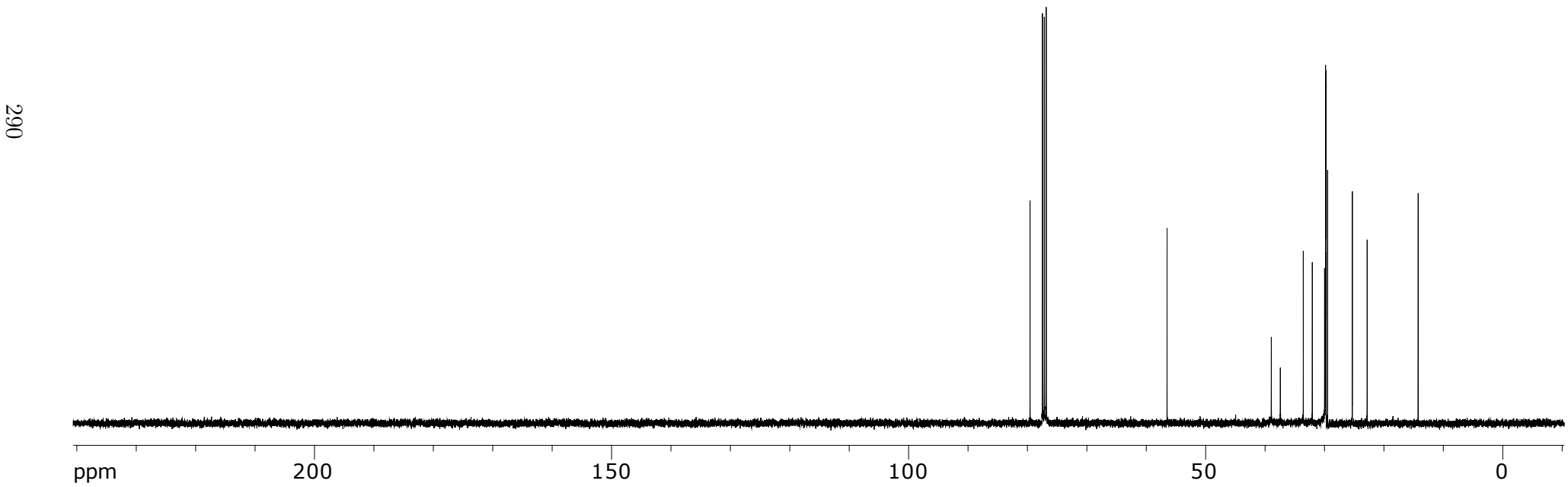

Figure A.56: 100 MHz ^{13}C NMR of **167** in $CDCl_3$

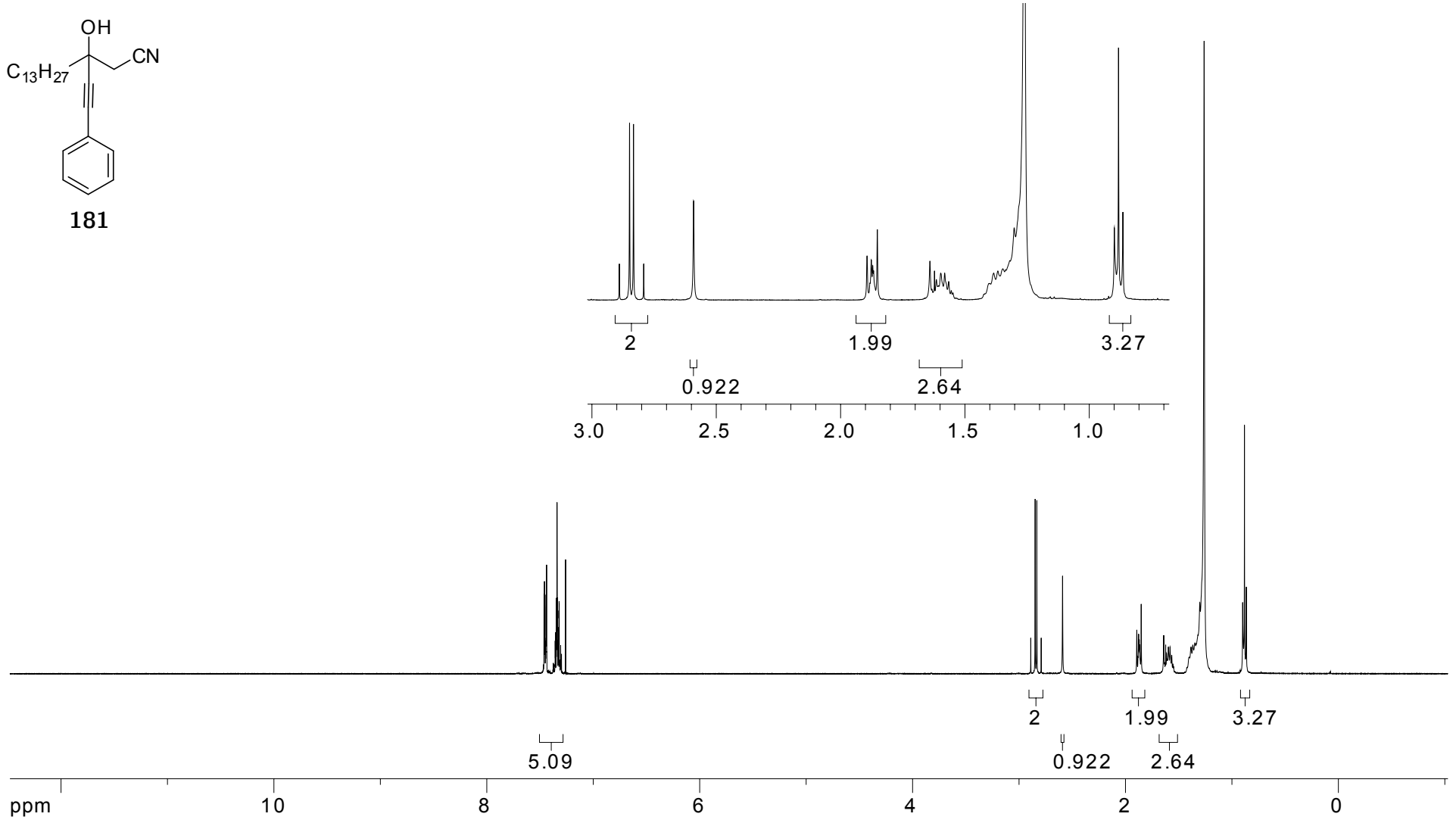

Figure A.57: 400 MHz ^{1}H NMR of **181** in $CDCl_3$

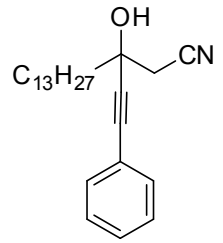

181

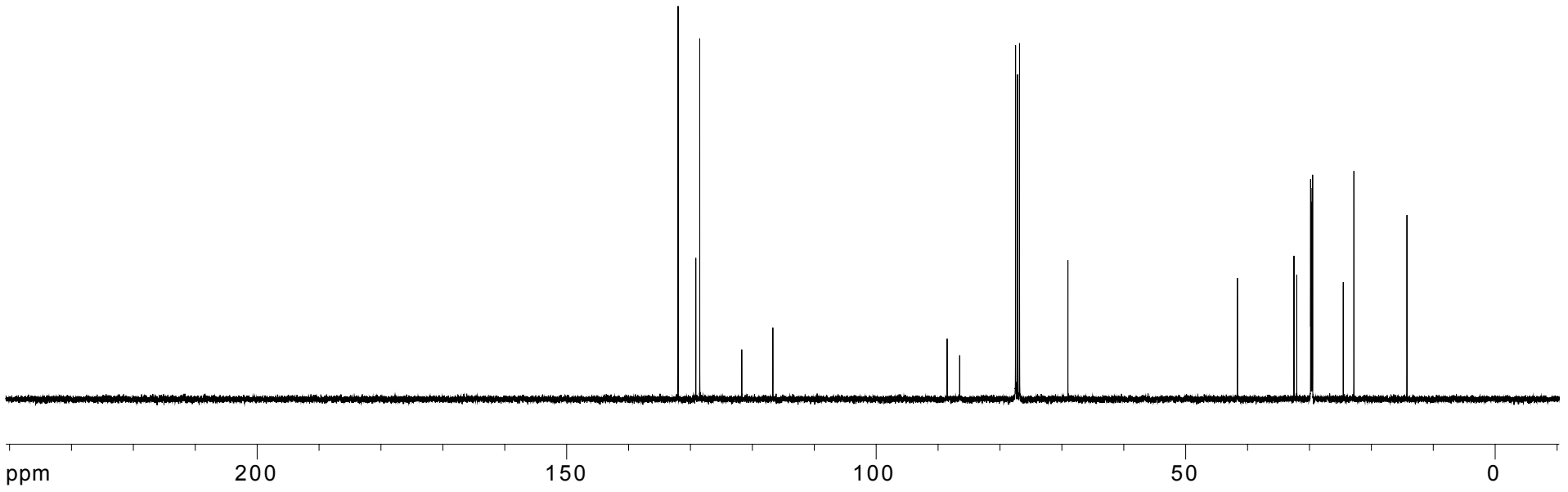

Figure A.58: 100 MHz ^{13}C NMR of **181** in $CDCl_3$

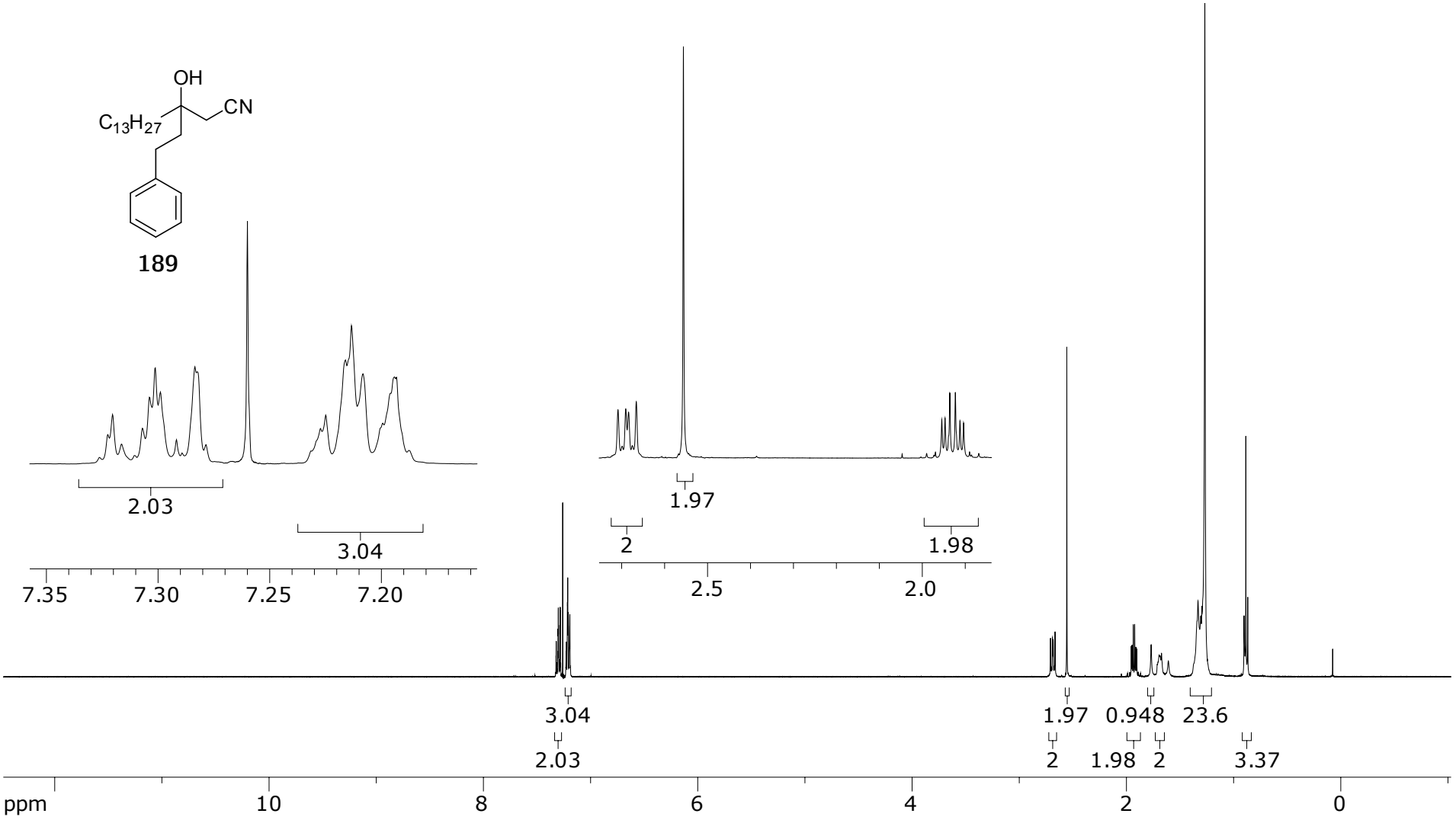

Figure A.59: 400 MHz ^{1}H NMR of **189** in $CDCl_3$

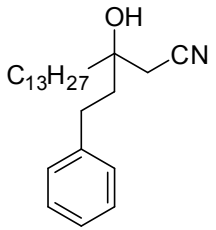

189

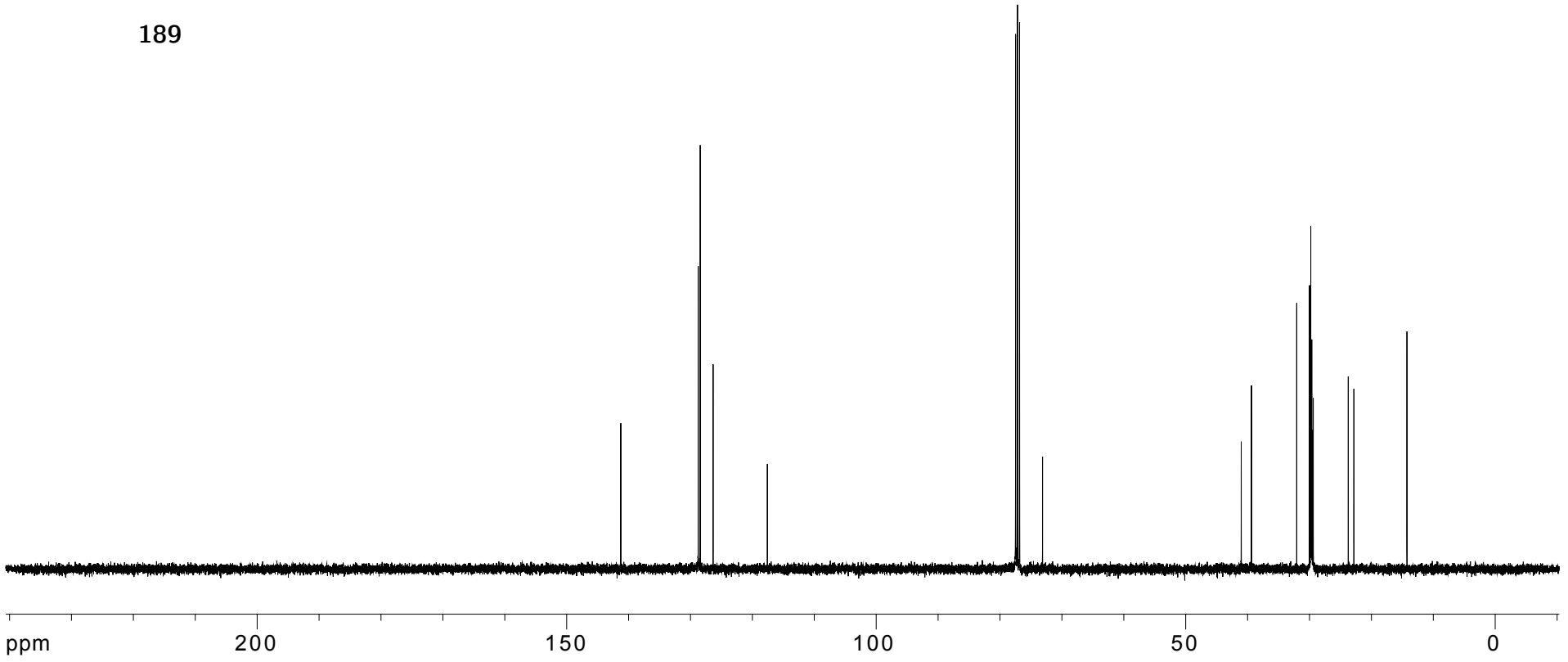

Figure A.60: 100 MHz ^{13}C NMR of **189** in $CDCl_3$

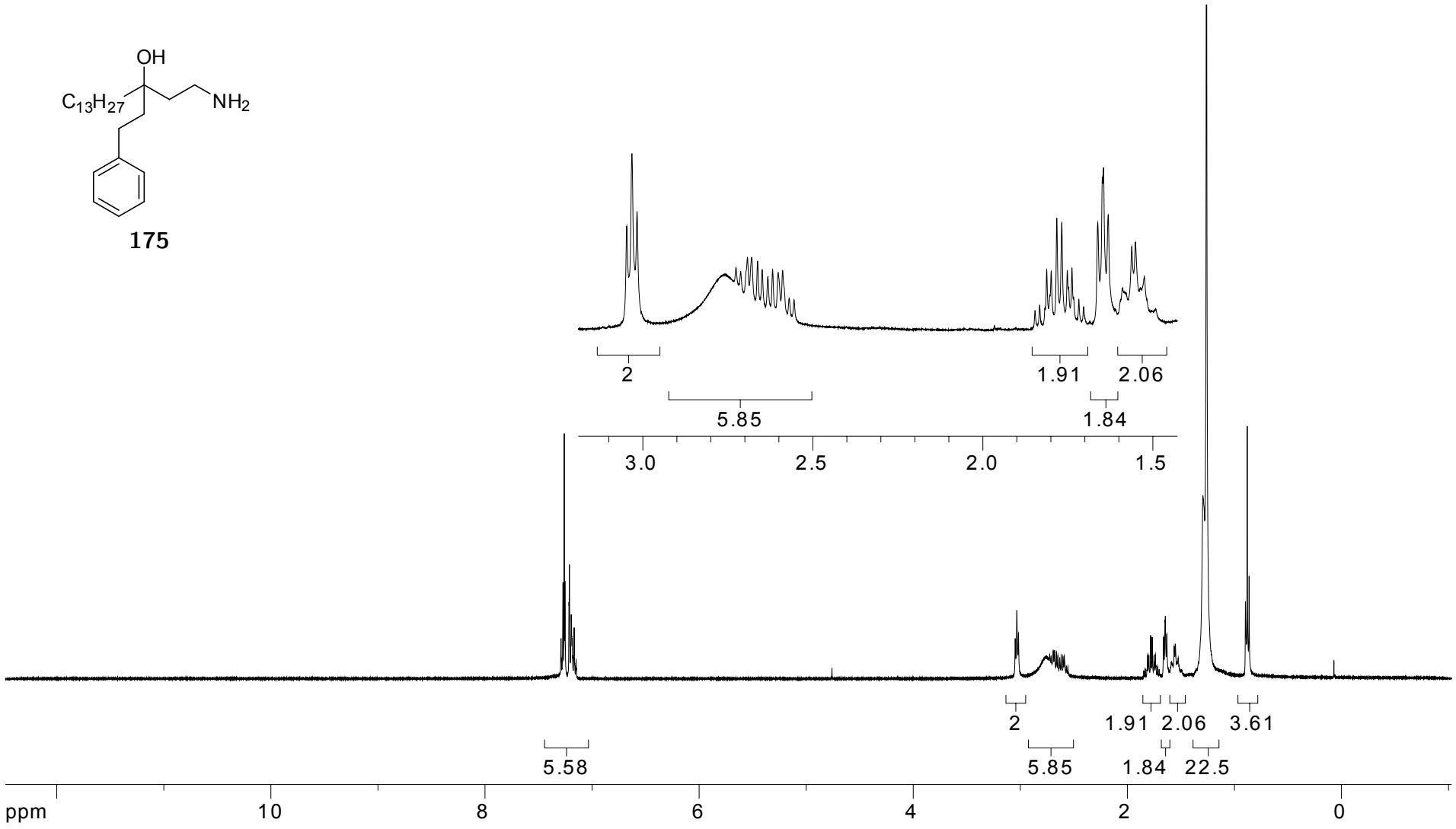

Figure A.61: 400 MHz ^{1}H NMR of **175** in $CDCl_3$

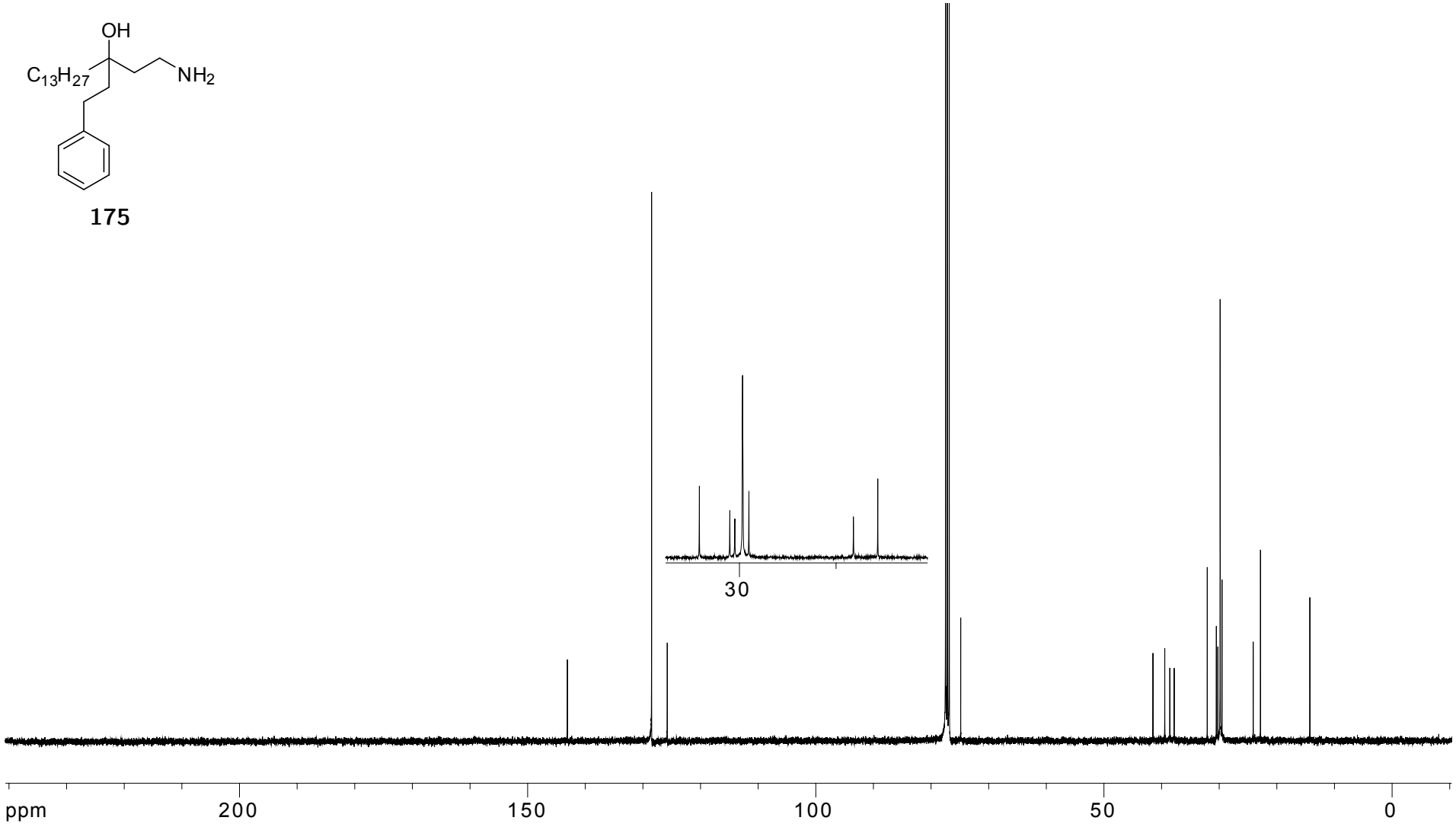

Figure A.62: 100 MHz ^{13}C NMR **175** in $CDCl_3$

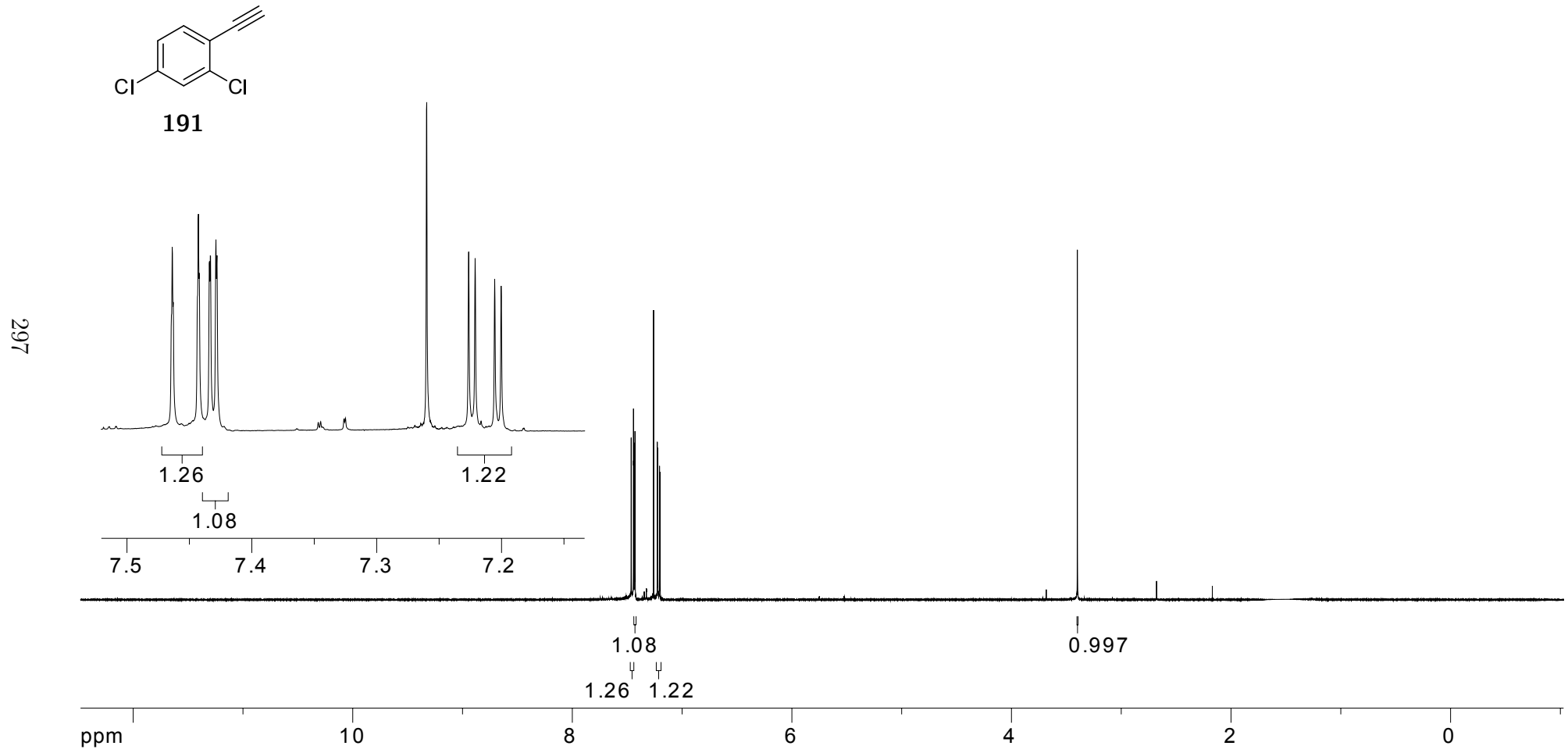

Figure A.63: 400 MHz ^{1}H NMR of **191** in $CDCl_3$

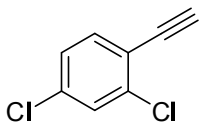

191

Figure A.64: 100 MHz ^{13}C NMR of **191** in $CDCl_3$

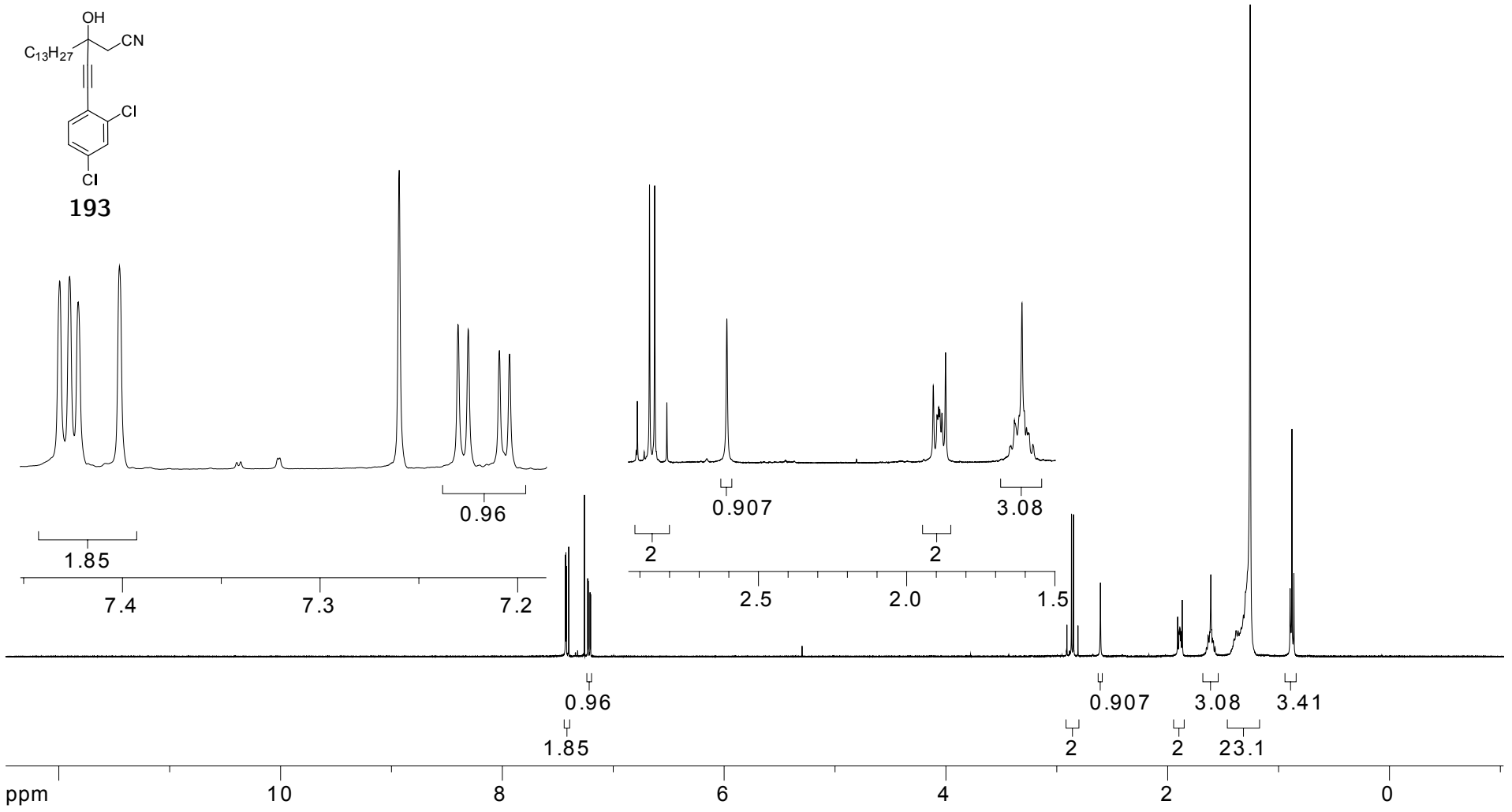

Figure A.65: 400 MHz ^{1}H NMR of **193** in $CDCl_3$

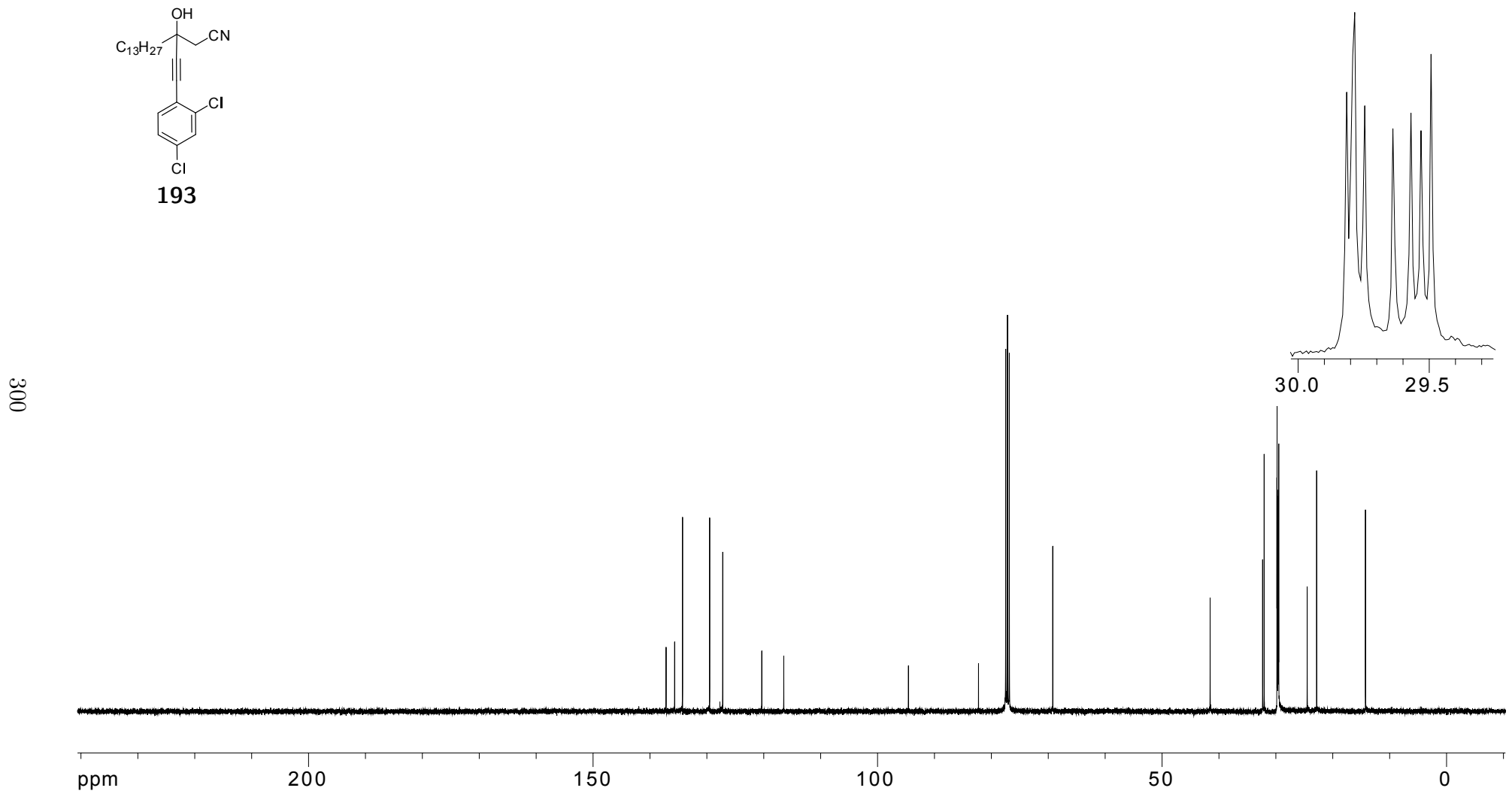

Figure A.66: 100 MHz ^{13}C NMR of **193** in $CDCl_3$

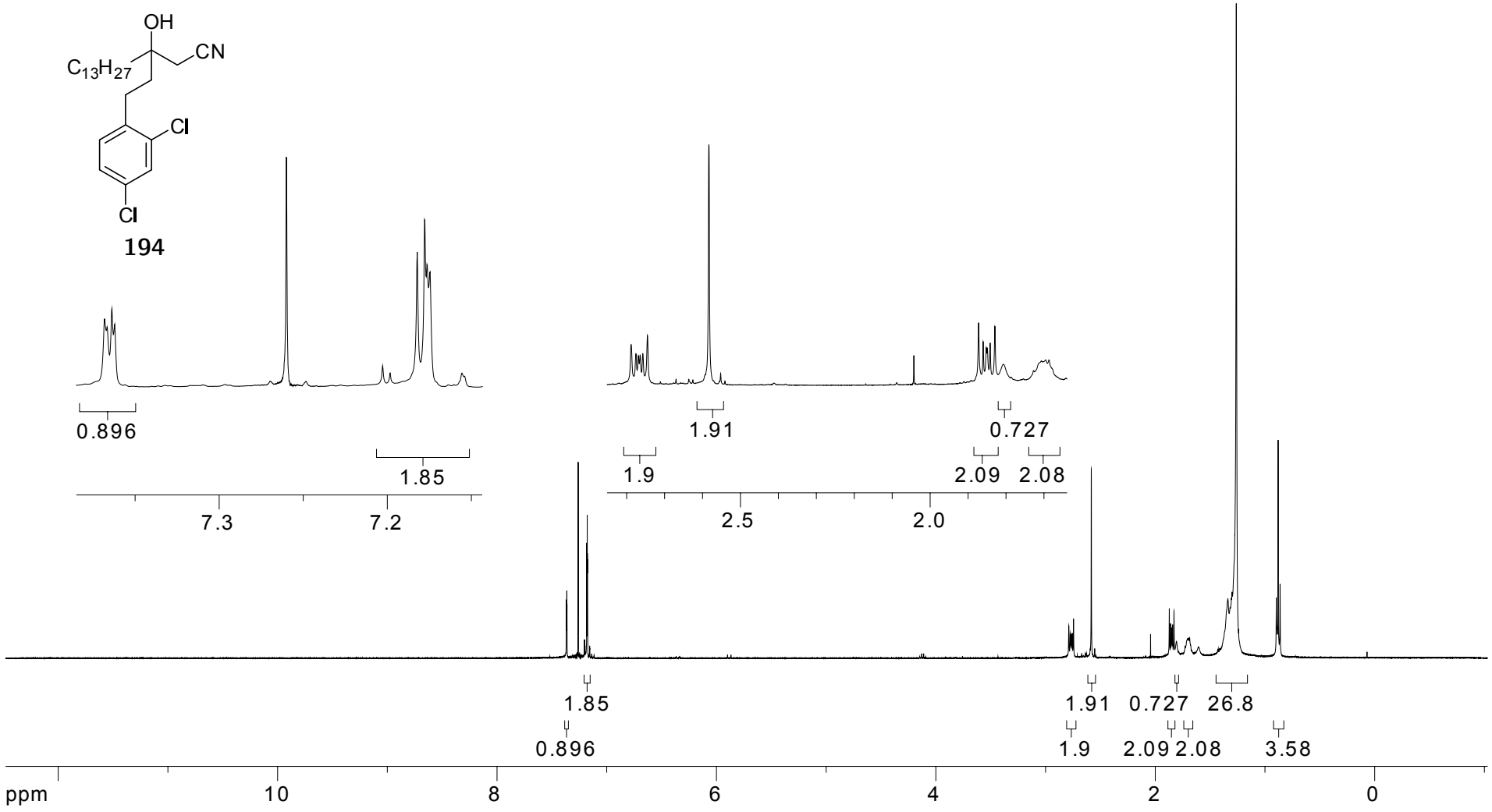

Figure A.67: 400 MHz ^{1}H NMR of **194** in $CDCl_3$

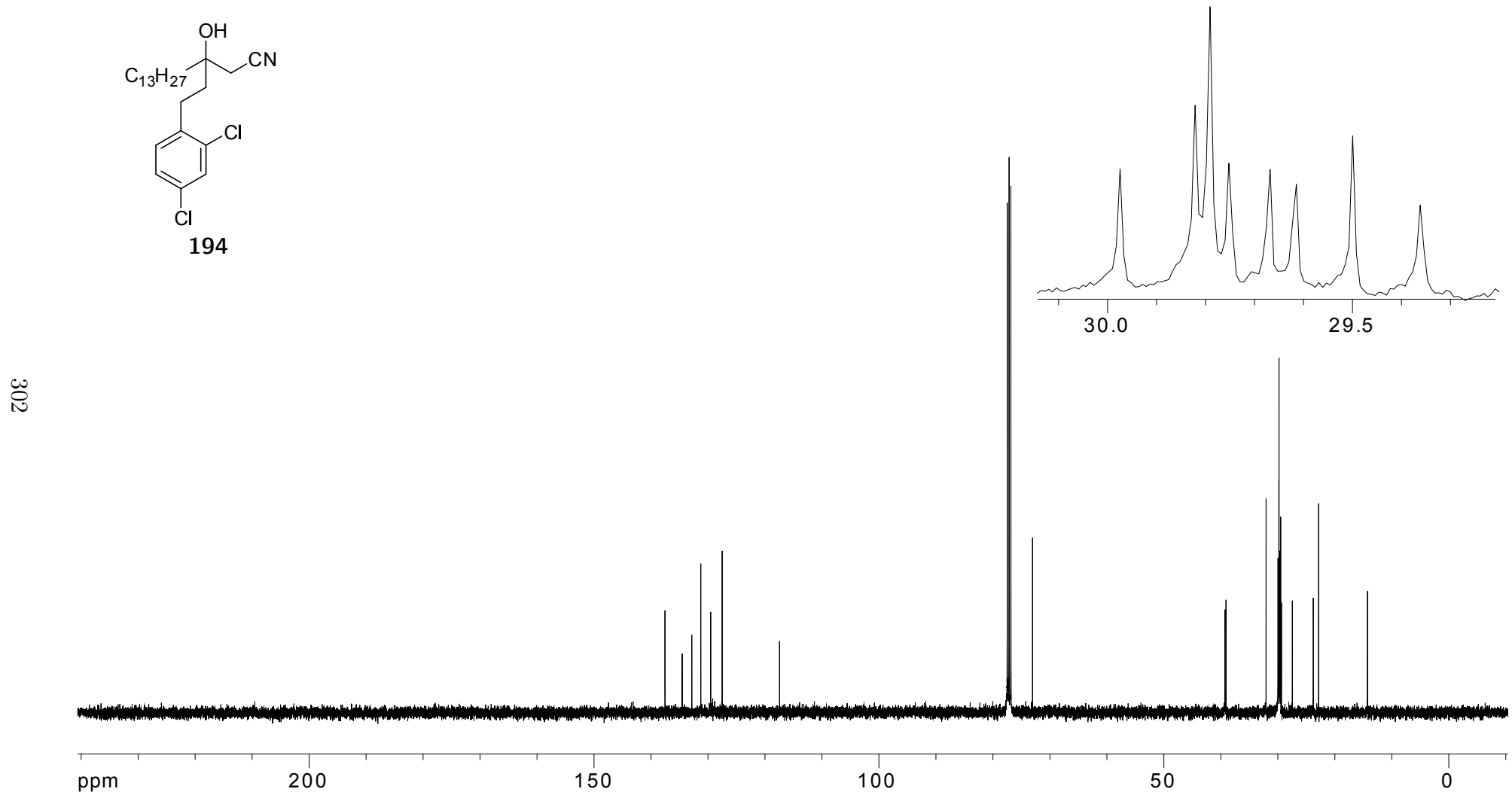

Figure A.68: 100 MHz ^{13}C NMR of **194** in $CDCl_3$

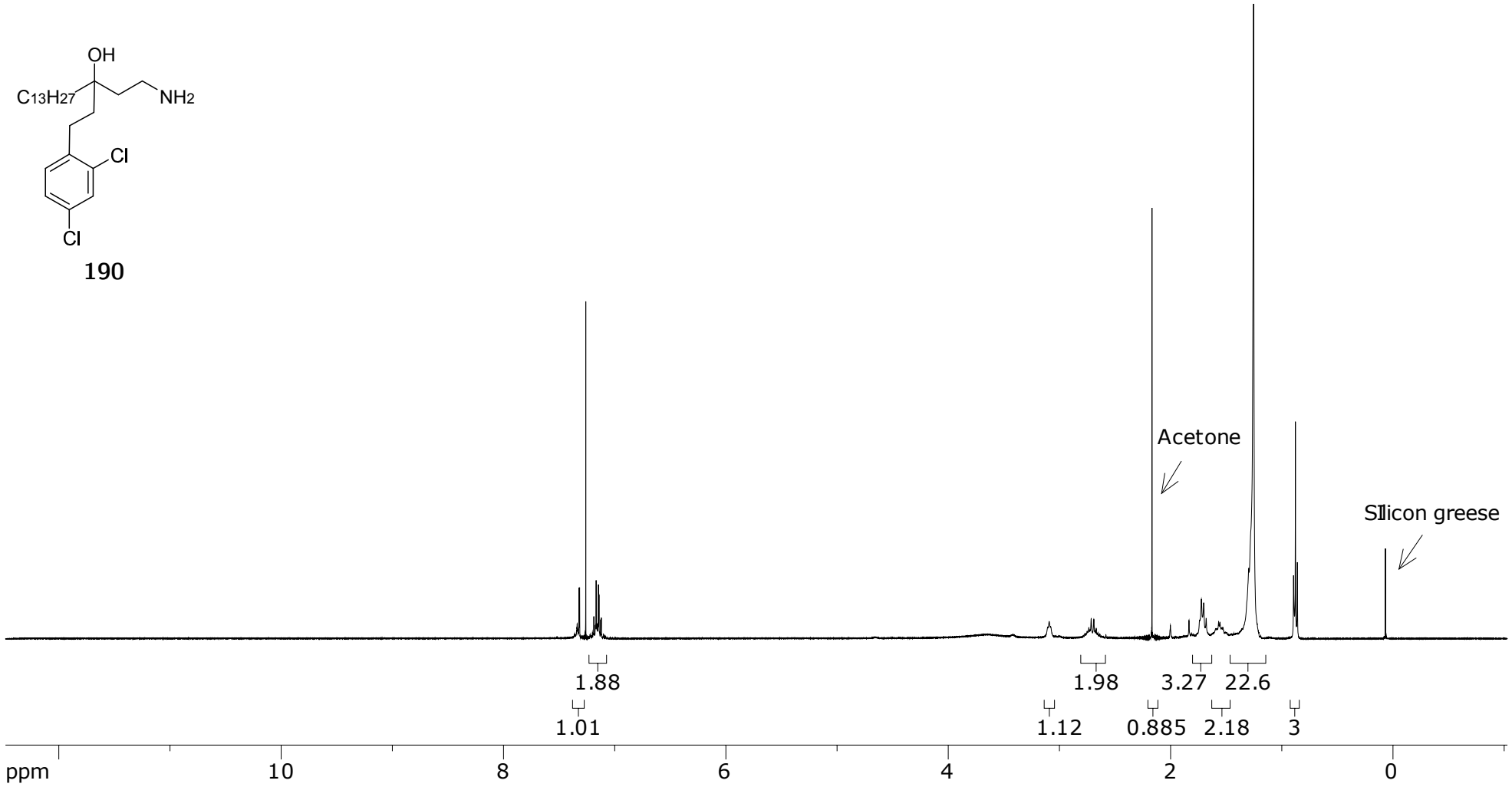

Figure A.69: 400 MHz ^{1}H NMR of **190** in $CDCl_3$

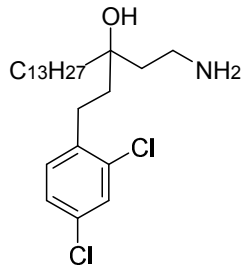

190

Figure A.70: 100 MHz ^{13}C NMR of **190** in $CDCl_3$

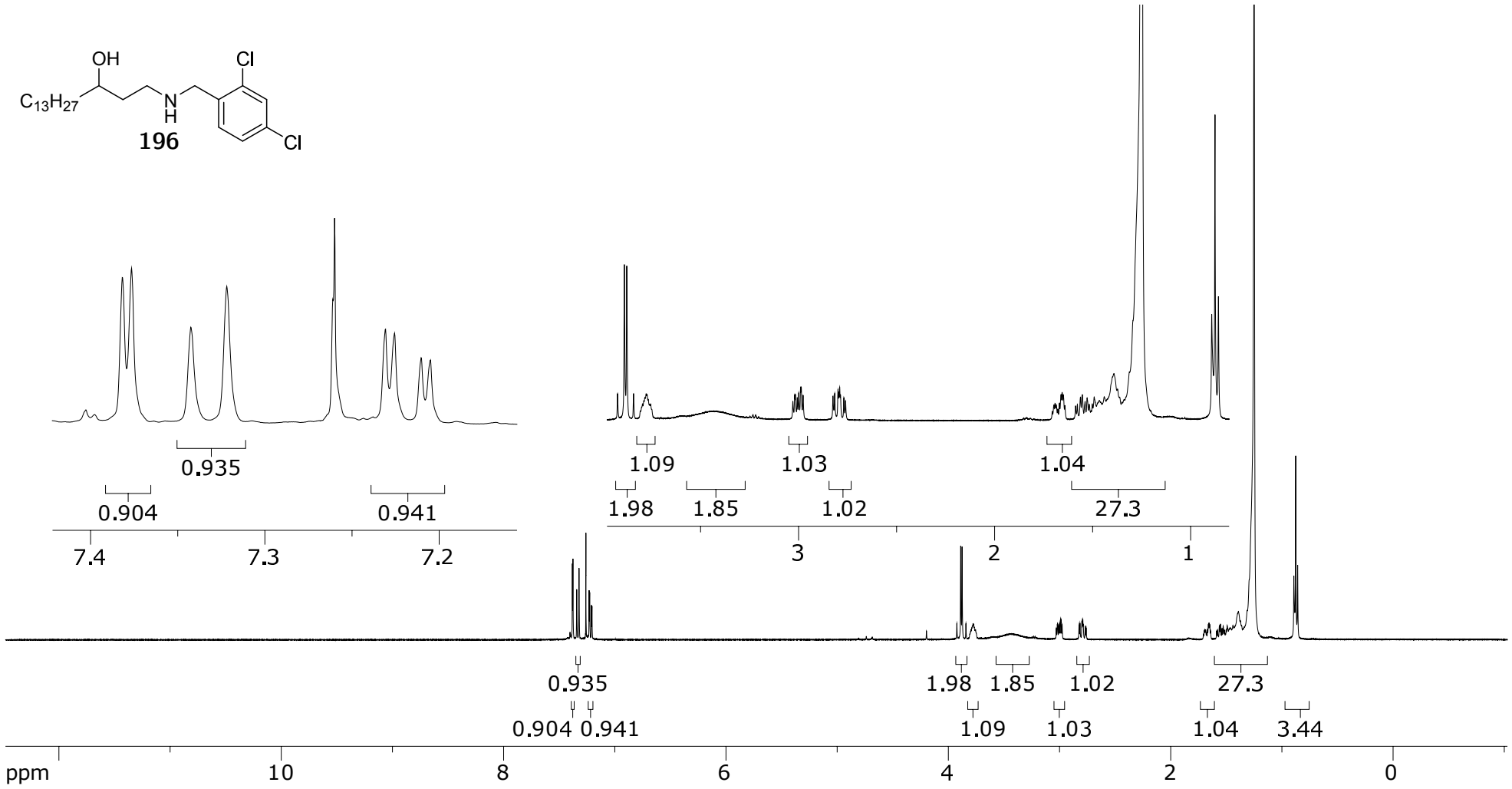

Figure A.71: 400 MHz ^{1}H NMR of **196** in $CDCl_3$

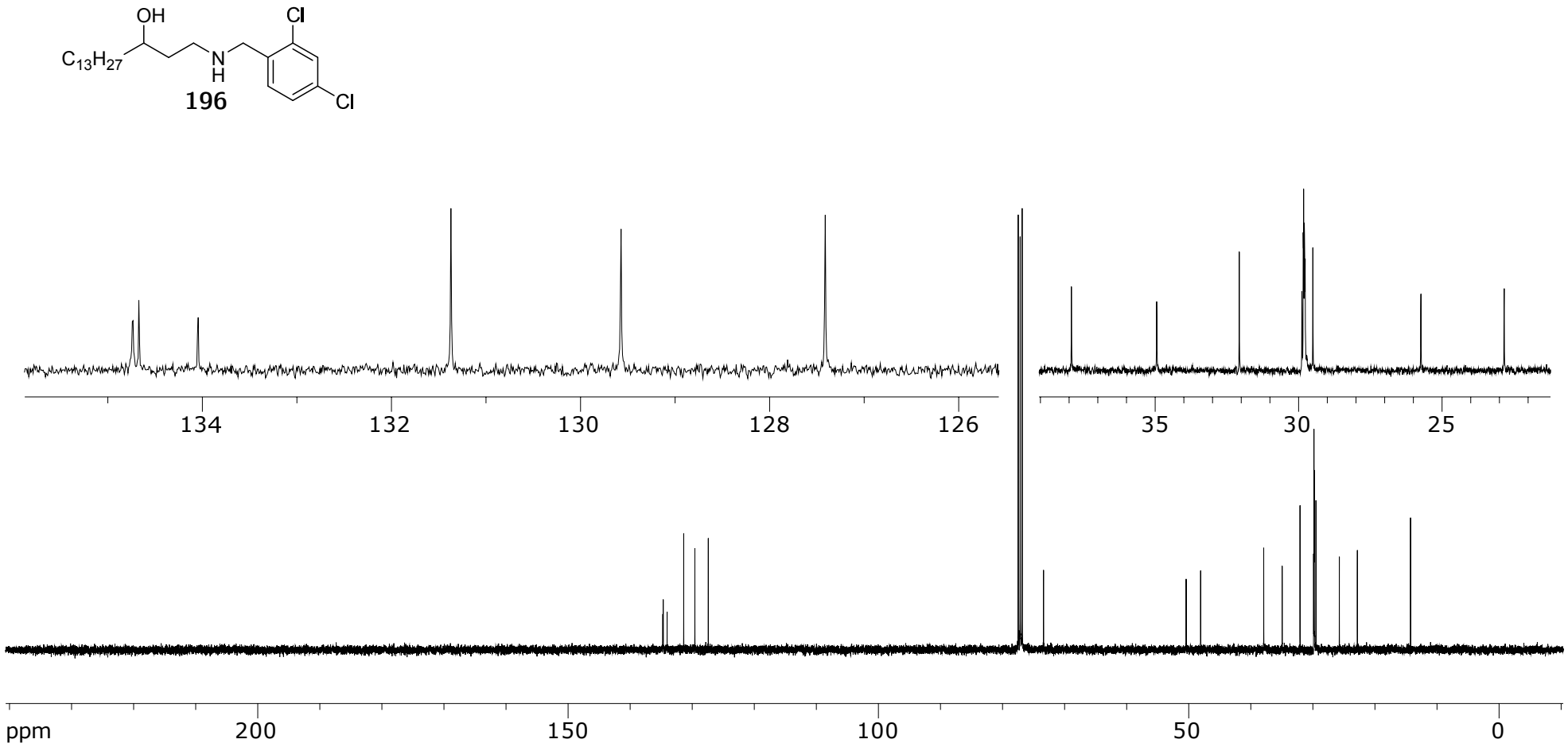

Figure A.72: 100 MHz ^{13}C NMR of **196** in $CDCl_3$

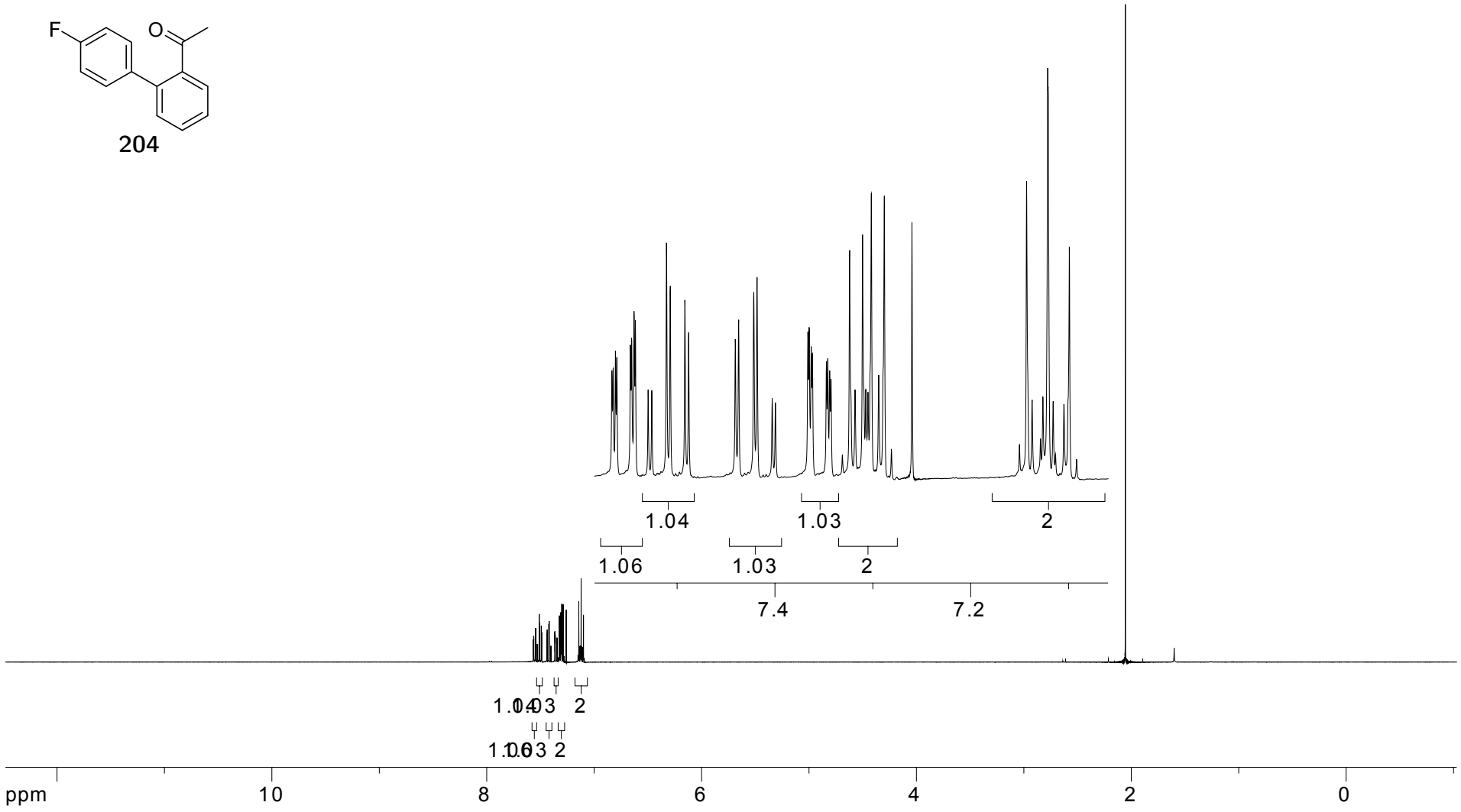

Figure A.73: 400 MHz ^{1}H NMR of **204** in $CDCl_3$

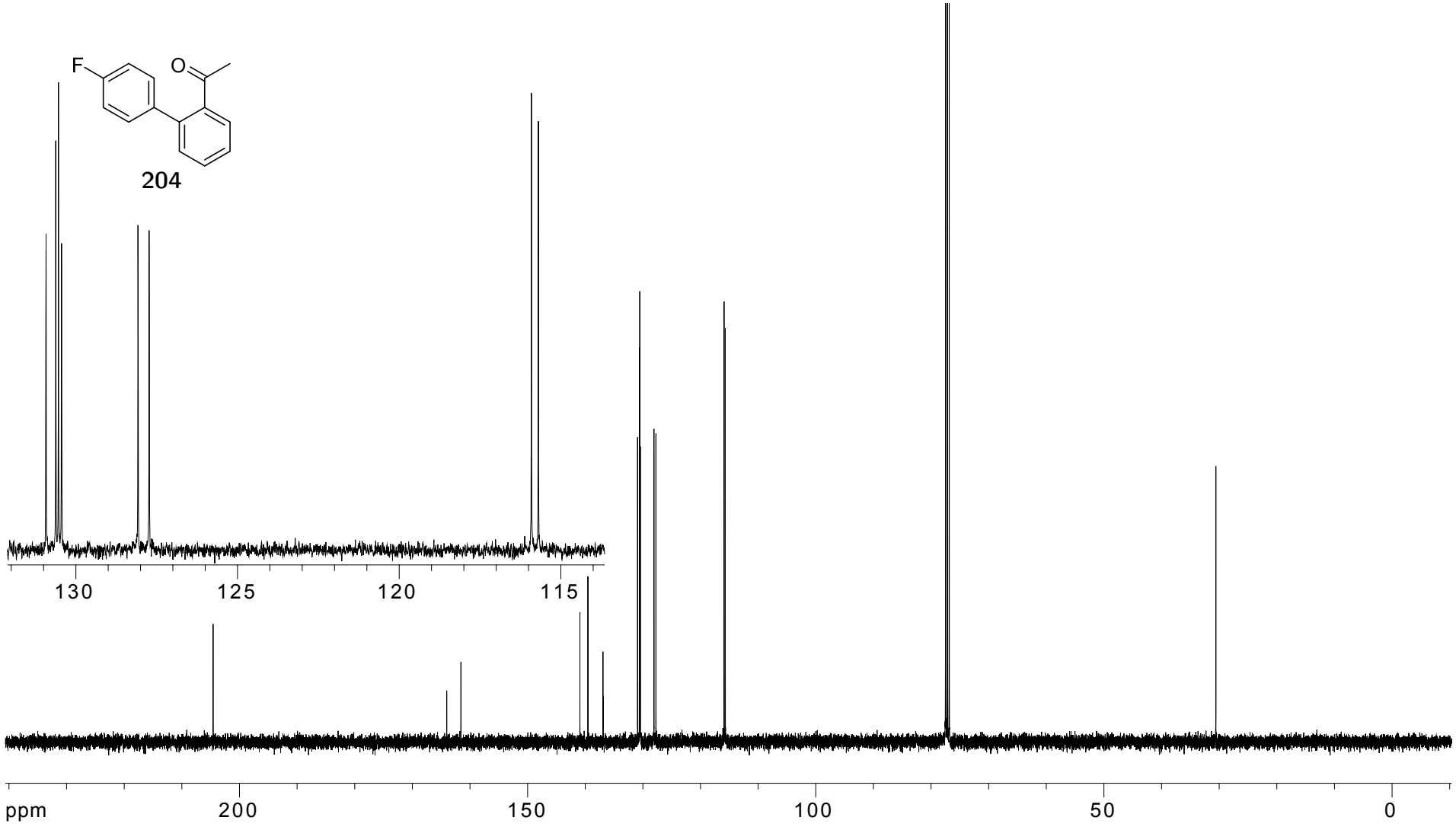

Figure A.74: 100 MHz ^{13}C NMR of **204** in $CDCl_3$

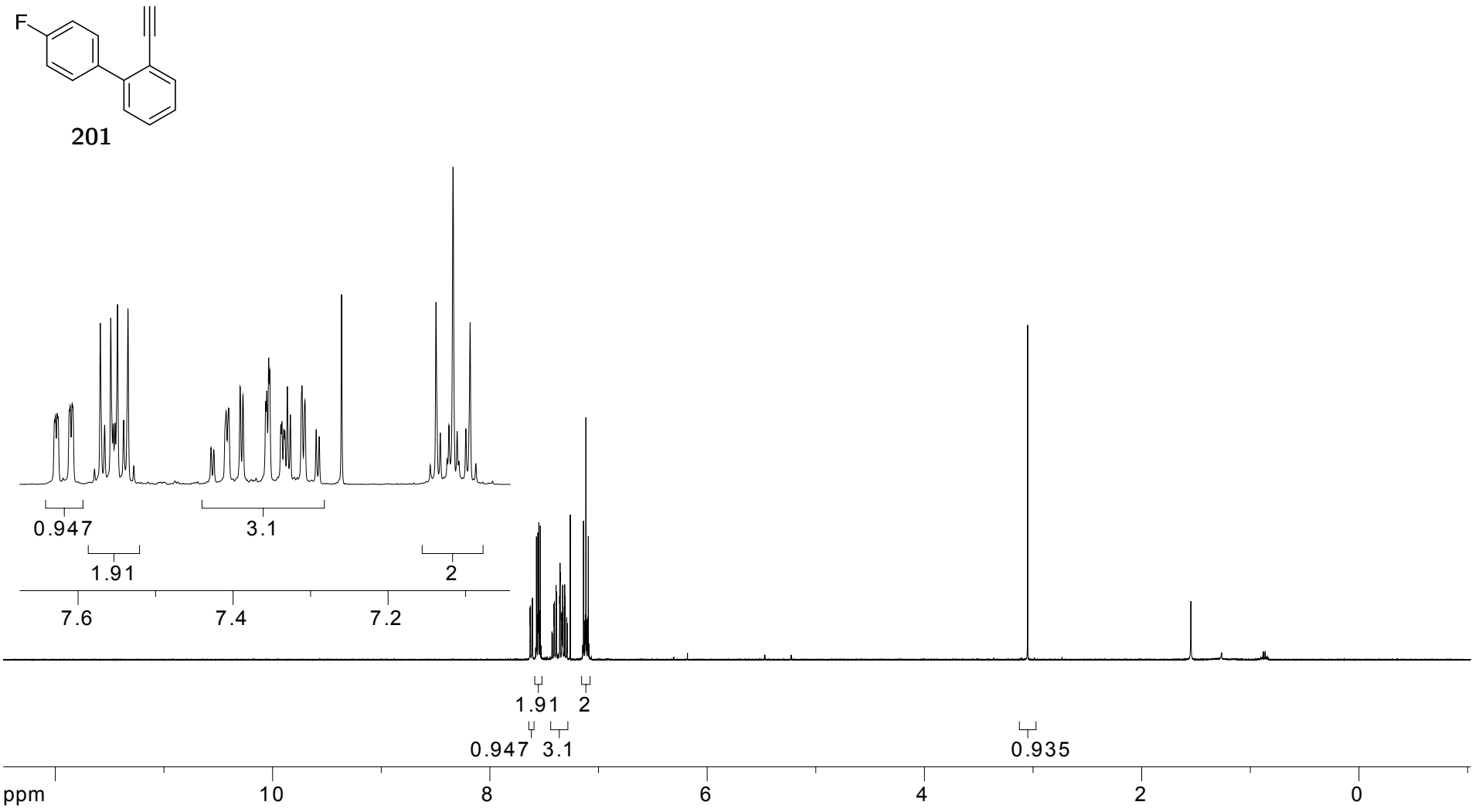

Figure A.75: 400 MHz ^{1}H NMR of **201** in $CDCl_3$

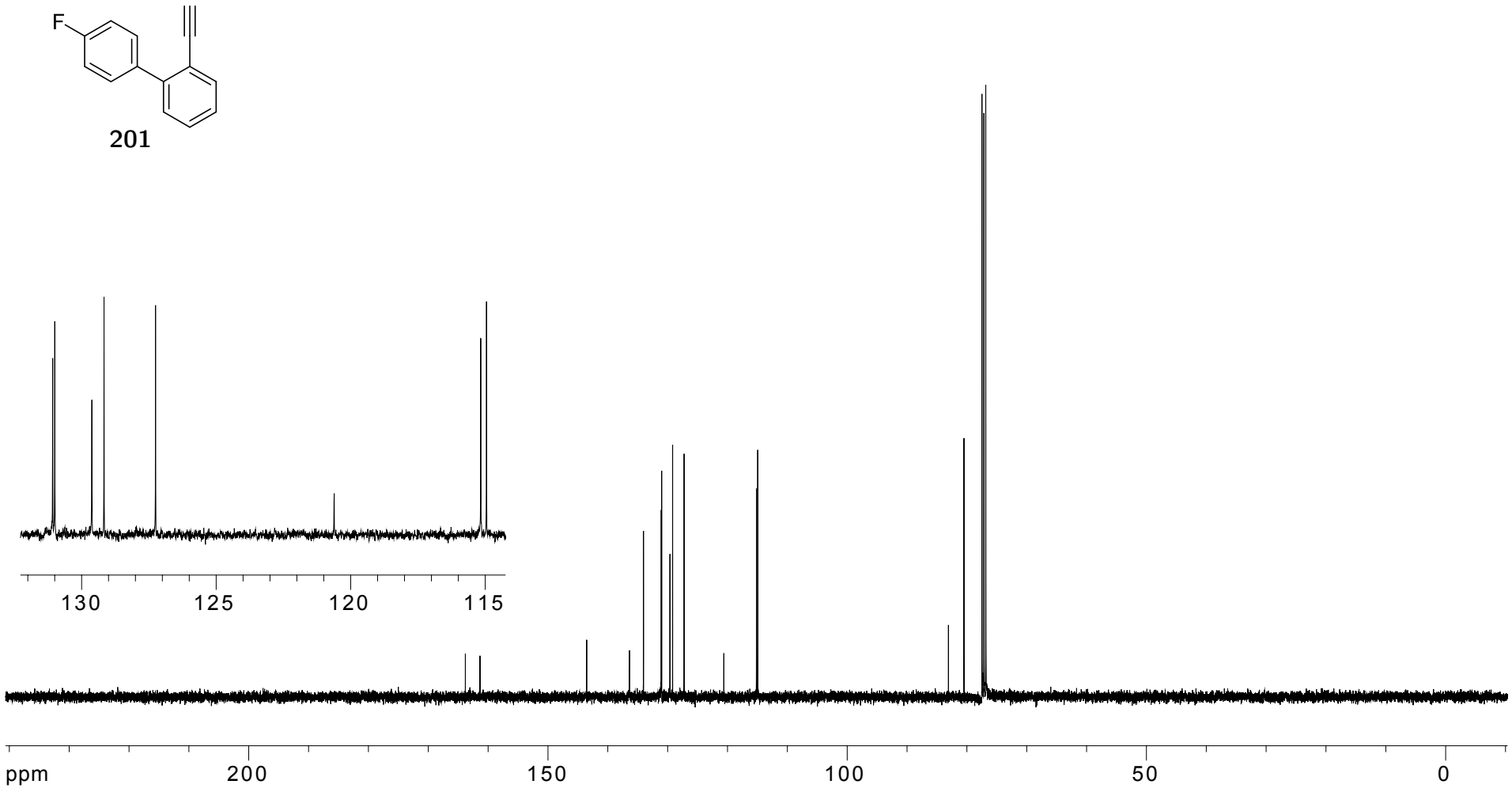

Figure A.76: 100 MHz ^{13}C NMR **201** in $CDCl_3$

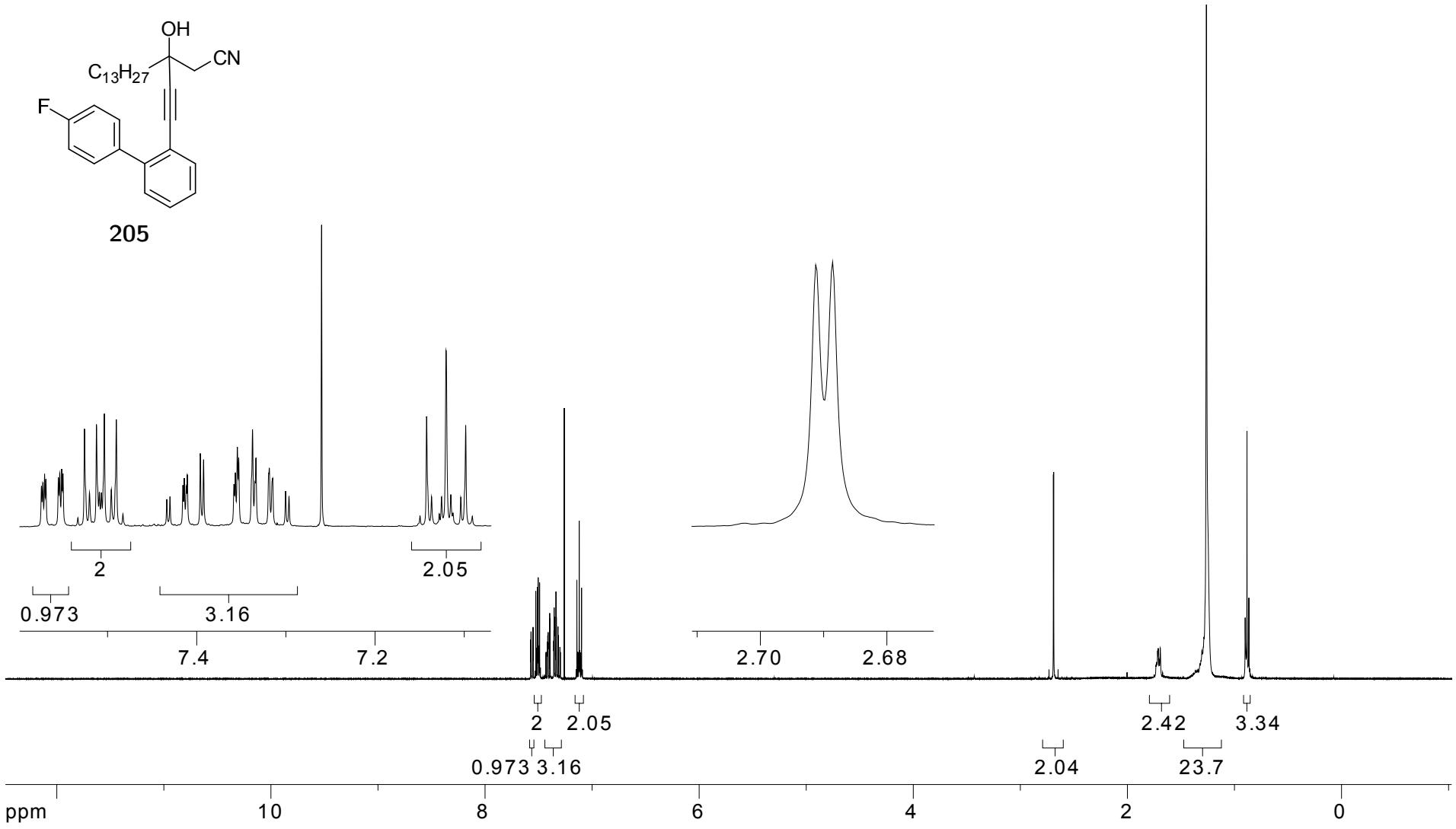

Figure A.77: 400 MHz ^{1}H NMR of **205** in $CDCl_3$

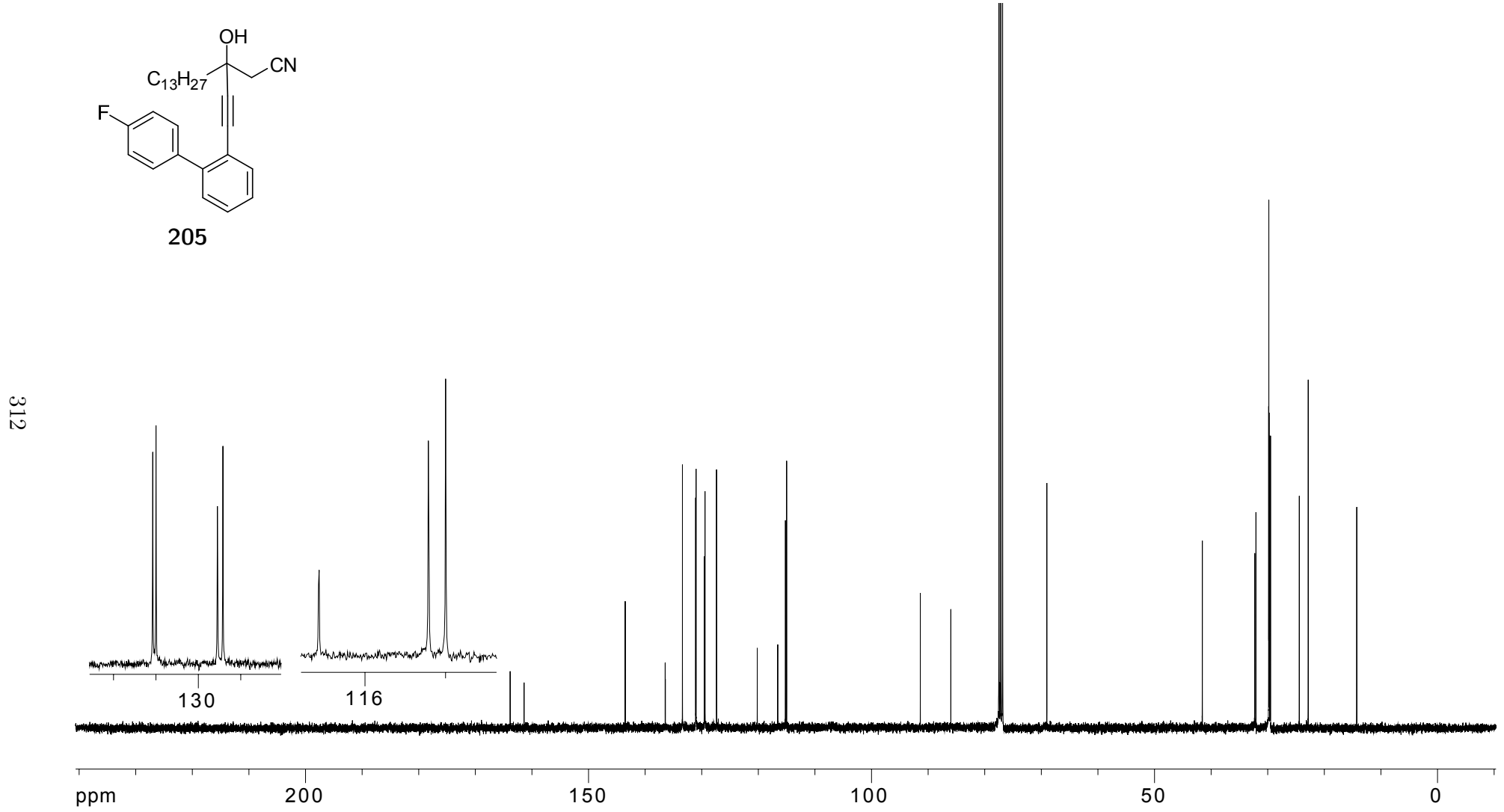

Figure A.78: 100 MHz ^{13}C NMR of **205** in $CDCl_3$

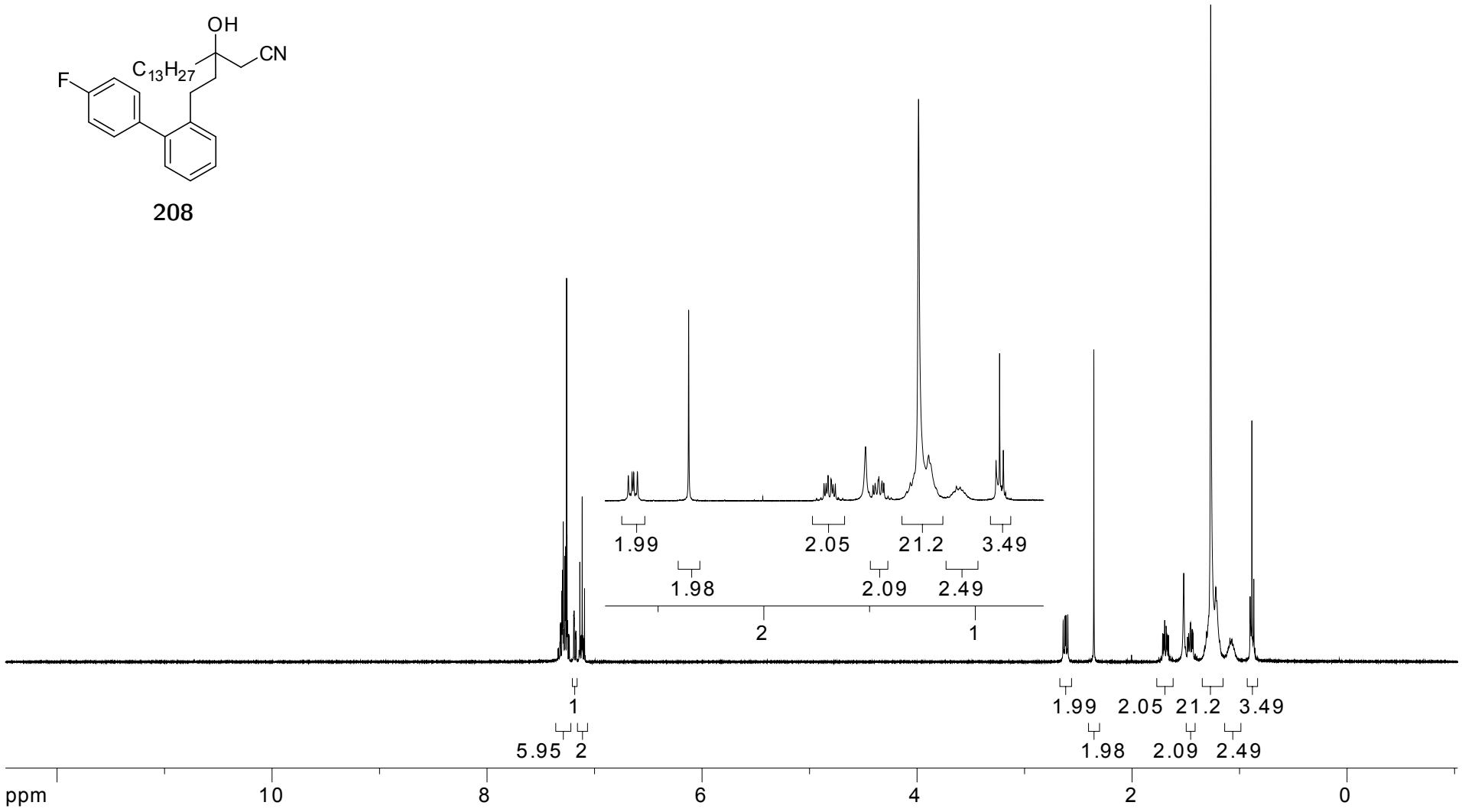

Figure A.79: 400 MHz ^{1}H NMR of **208** in $CDCl_3$

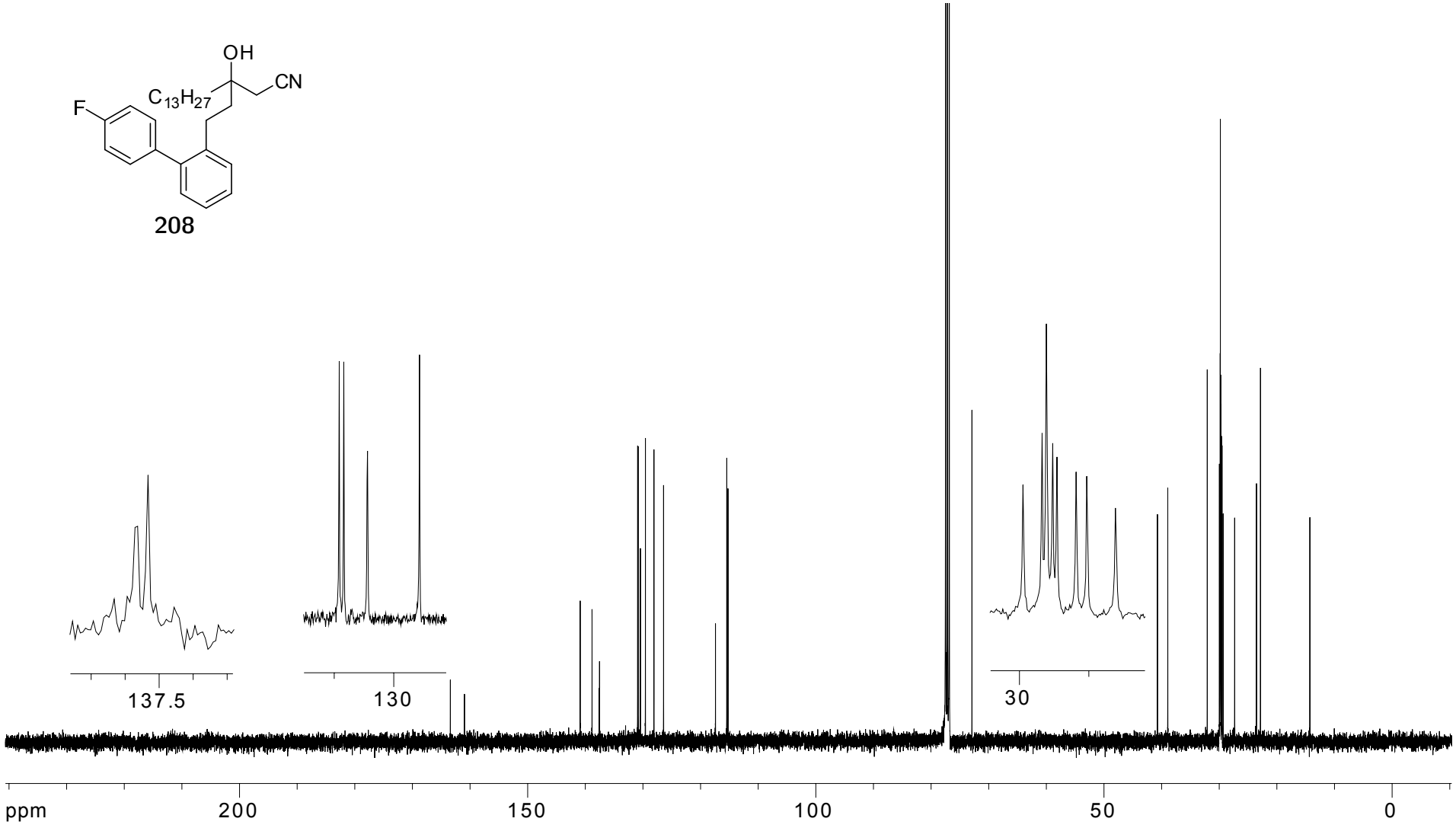

Figure A.80: 100 MHz ^{13}C NMR of **208** in $CDCl_3$

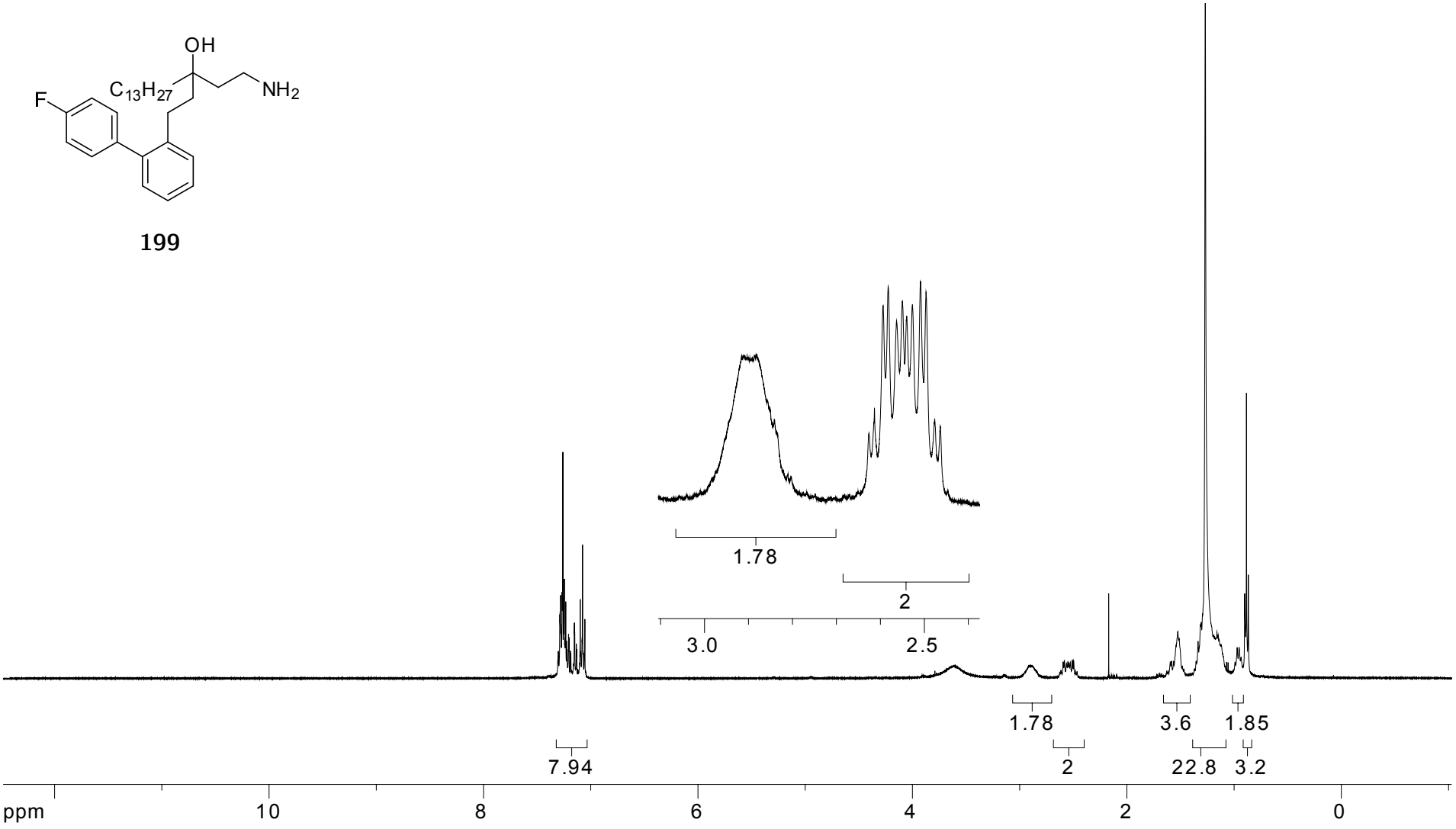

Figure A.81: 400 MHz ^{1}H NMR of **199** in $CDCl_3$

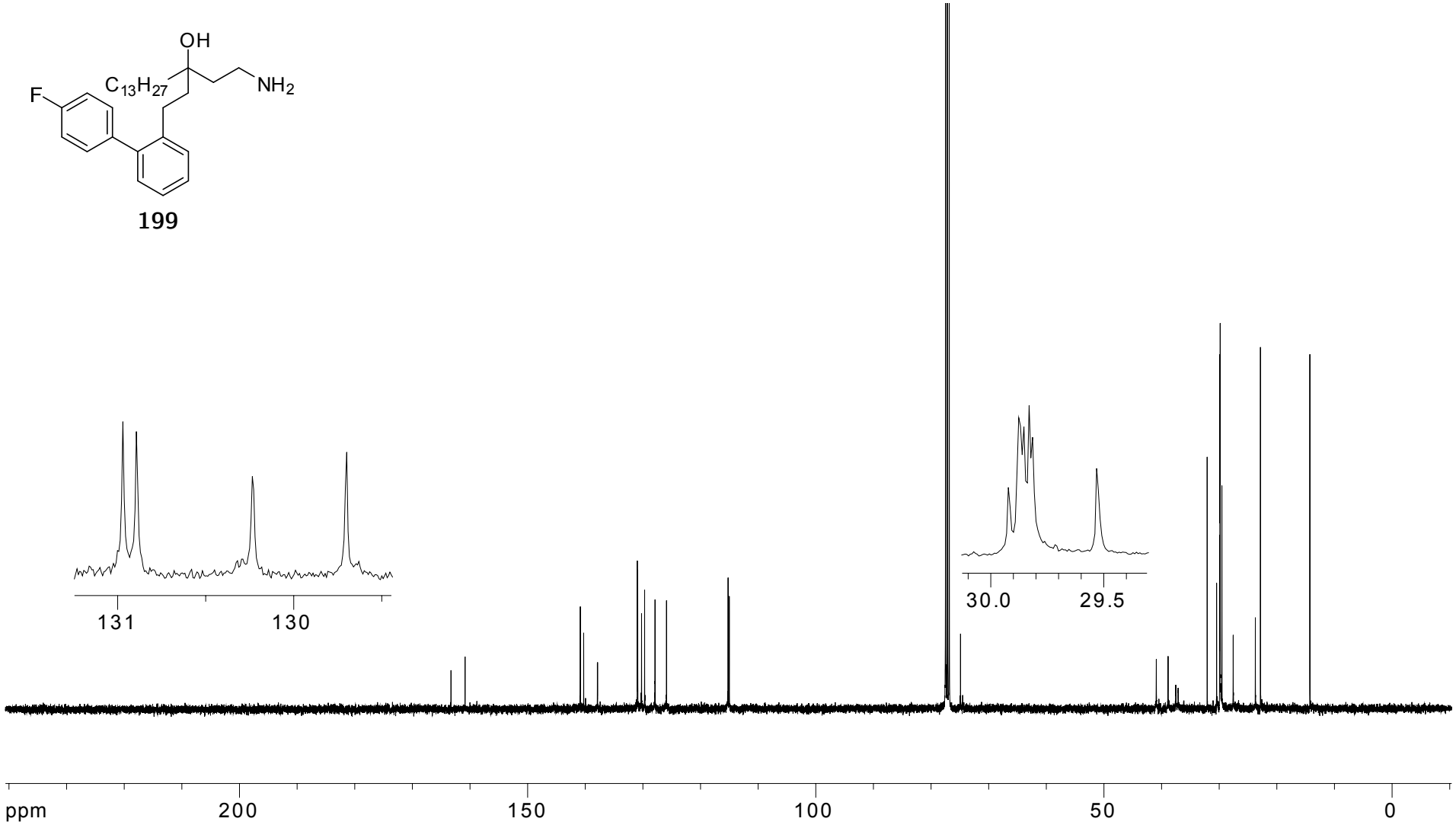

Figure A.82: 100 MHz ^{13}C NMR of **199** in $CDCl_3$

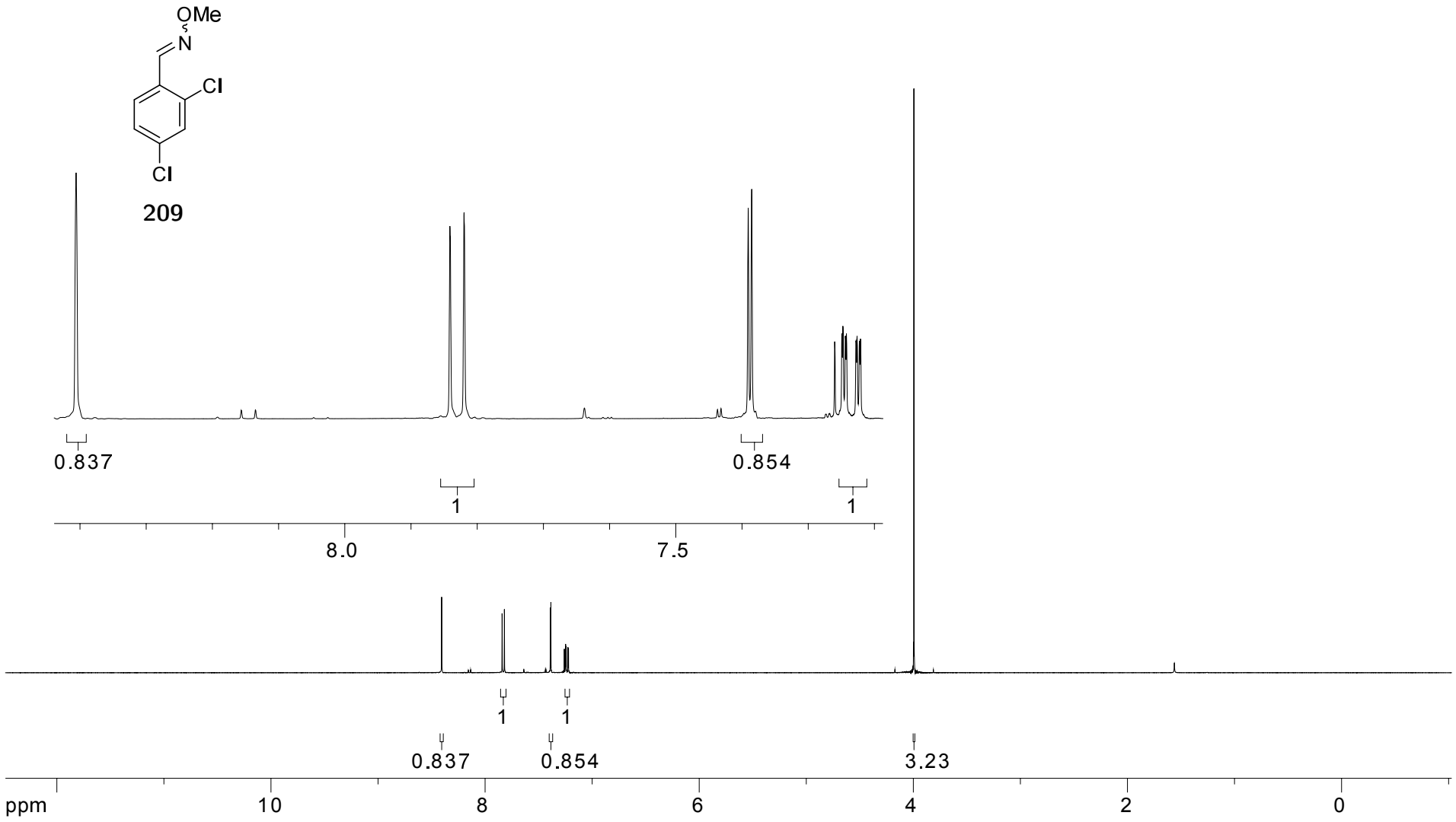

Figure A.83: 400 MHz ^{1}H NMR of **209** in $CDCl_3$

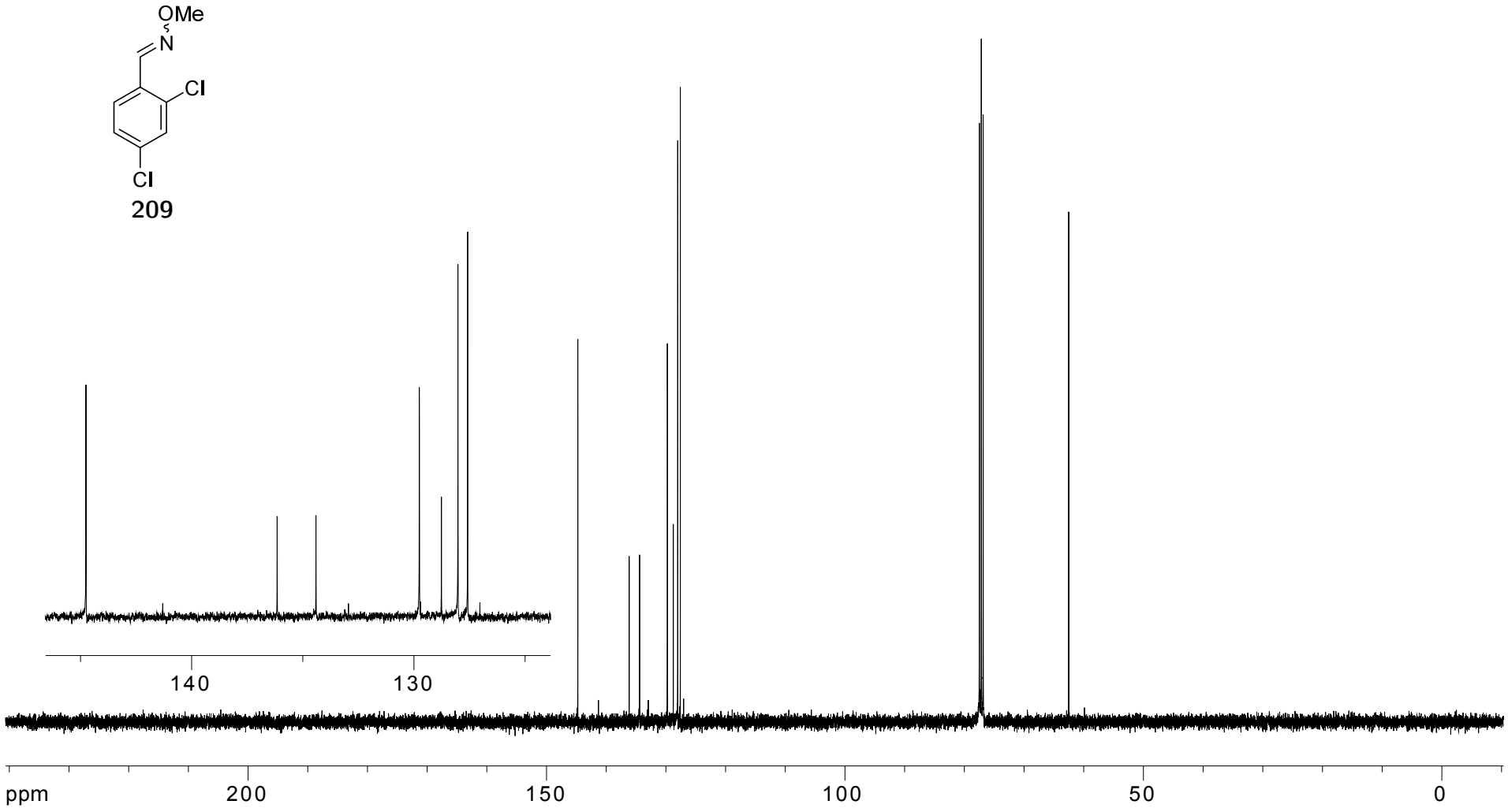

Figure A.84: 100 MHz ^{13}C NMR **209** in $CDCl_3$

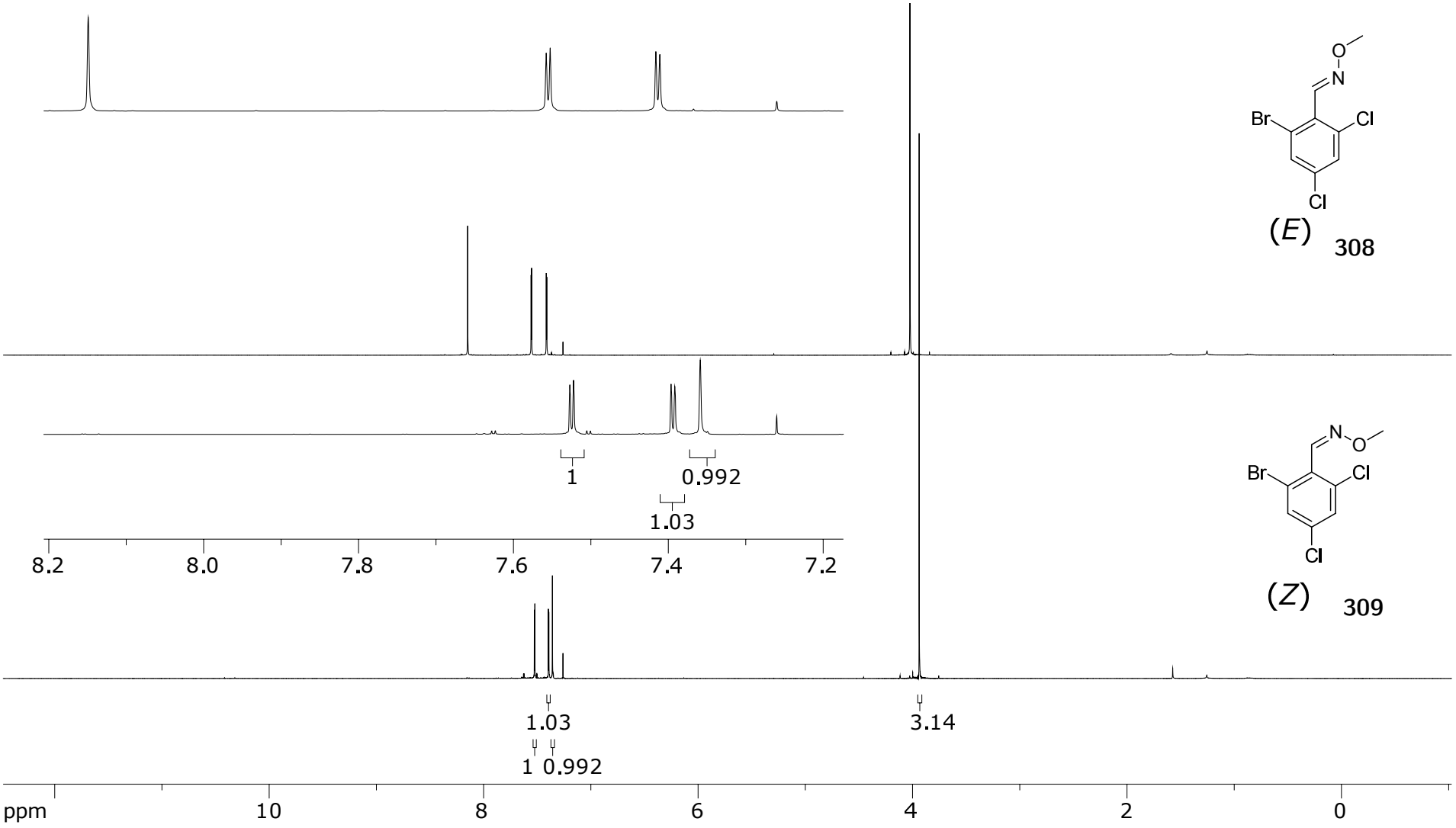

Figure A.85: 400 MHz ^{1}H NMR of **308** and **309** in $CDCl_3$

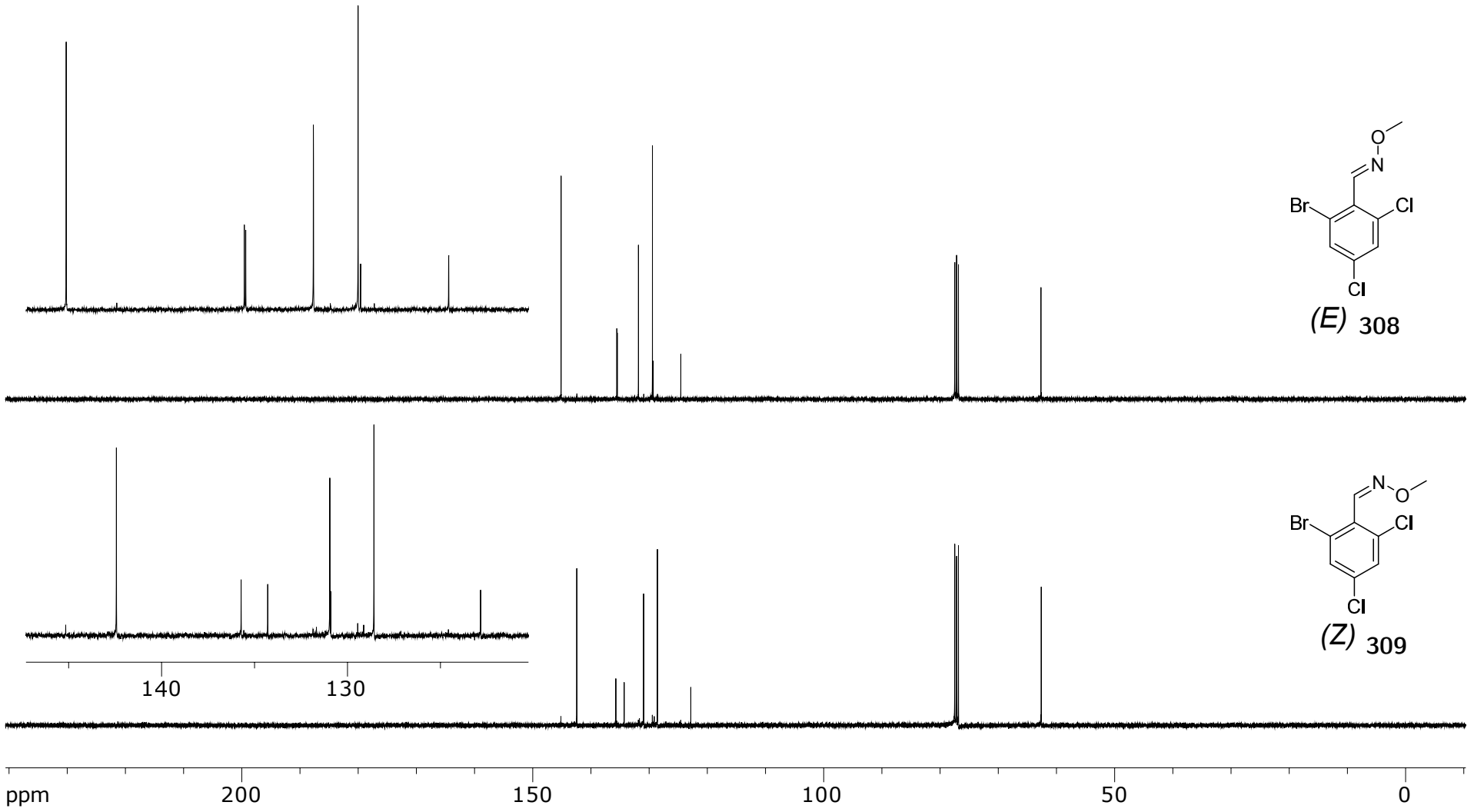

Figure A.86: 100 MHz ^{13}C NMR of **308** and **309** in $CDCl_3$

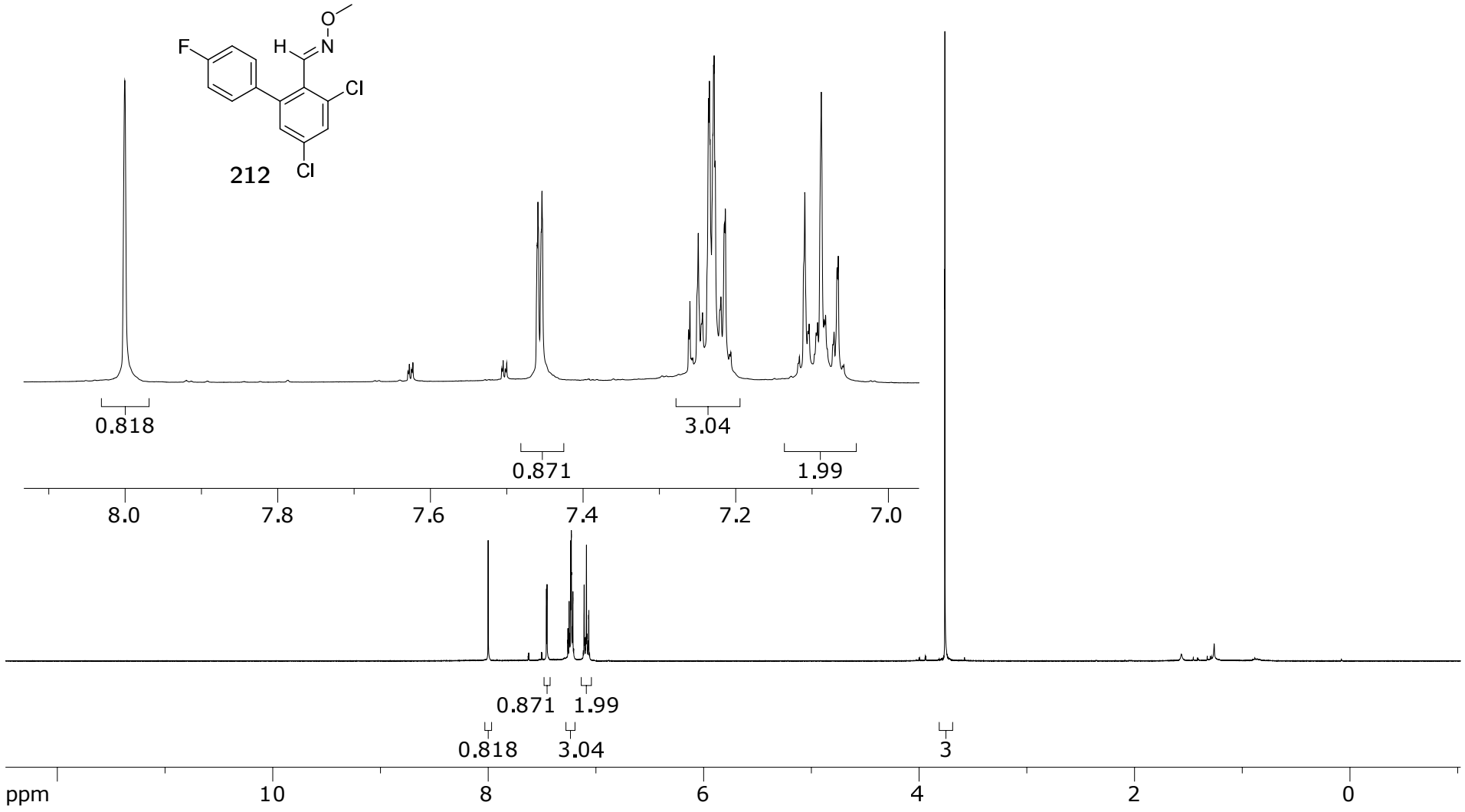

Figure A.87: 400 MHz ^{1}H NMR of **212** in $CDCl_3$

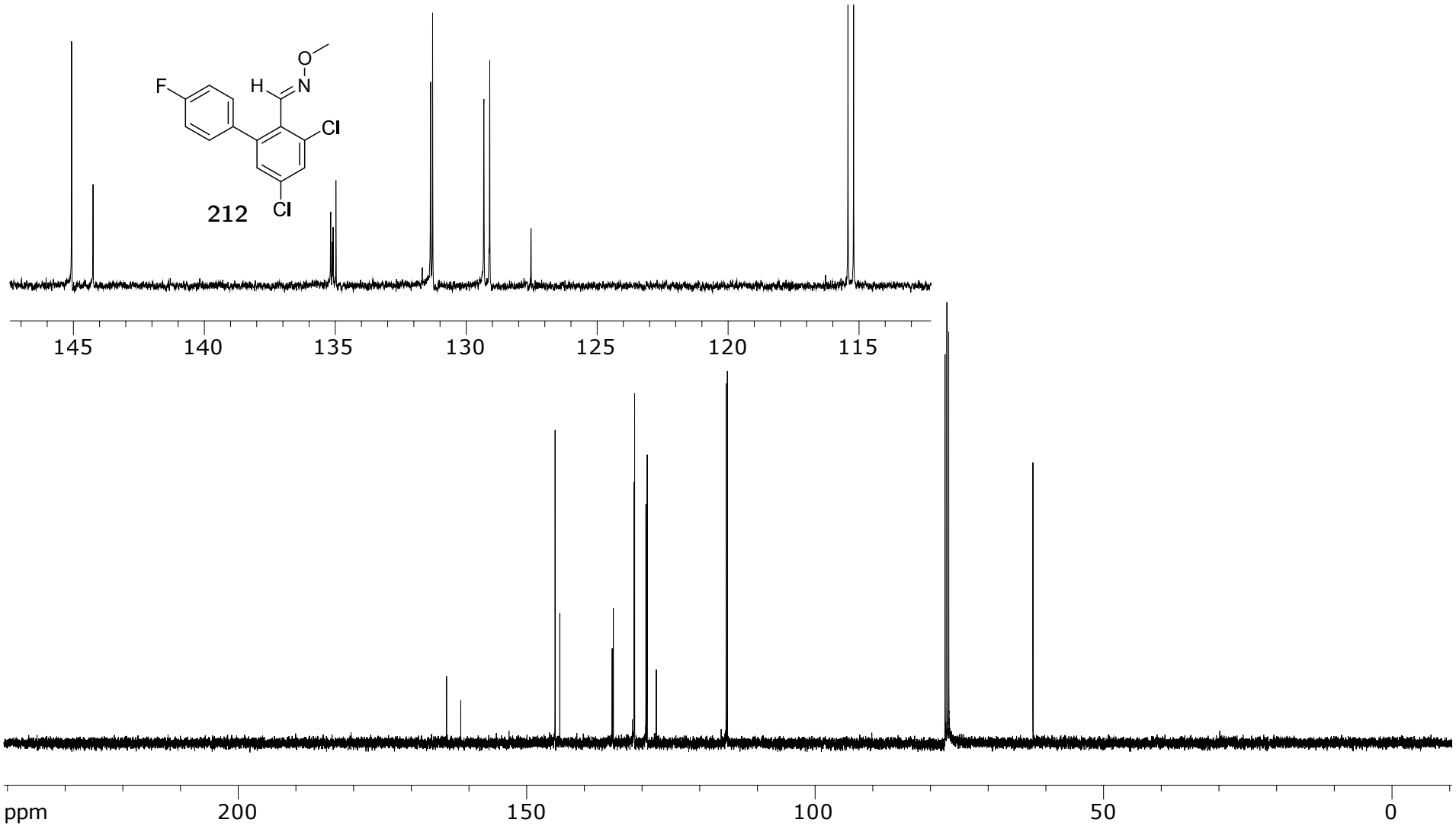

Figure A.88: 100 MHz ^{13}C NMR of **212** in $CDCl_3$

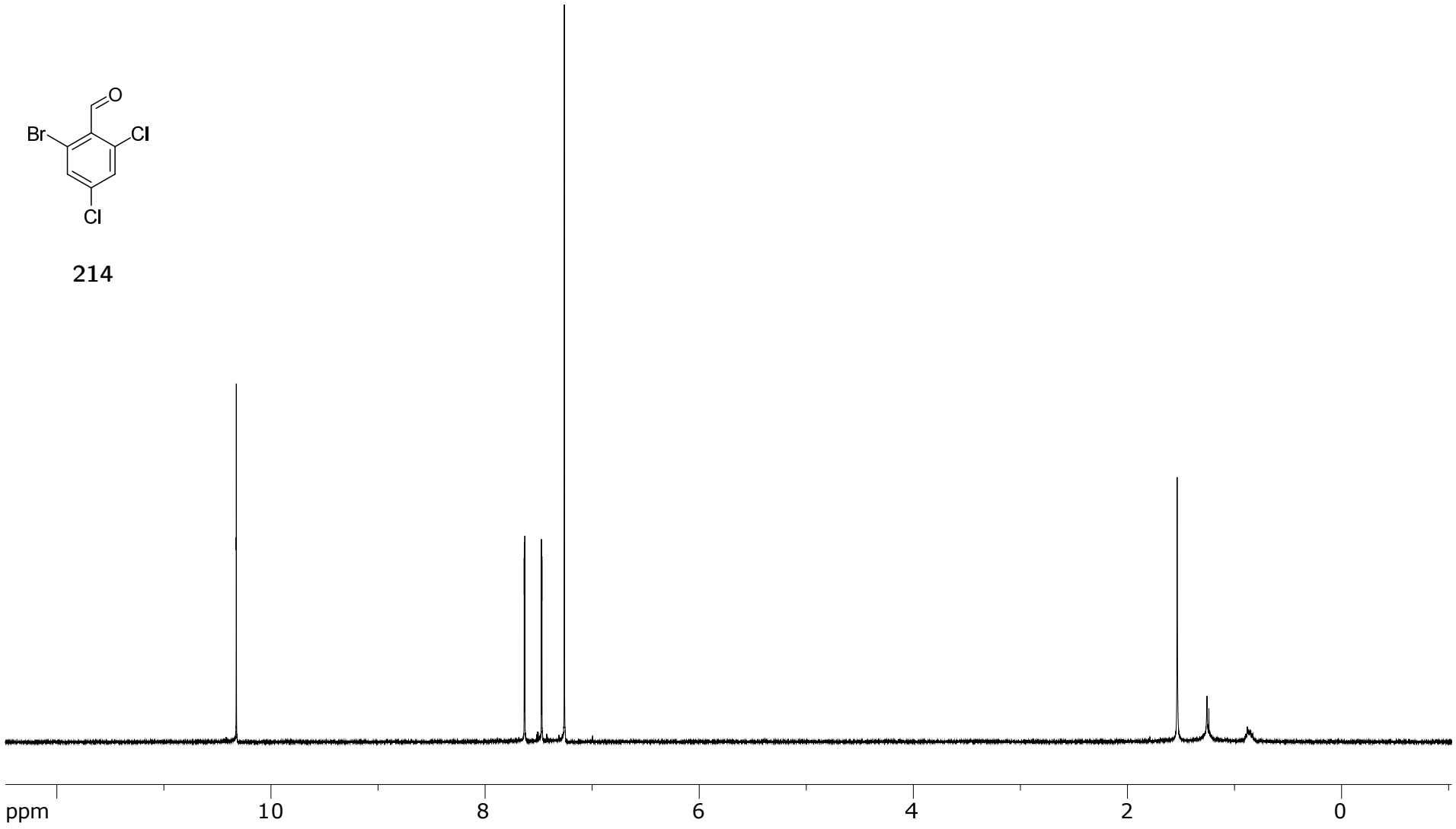

Figure A.89: 400 MHz ^{1}H NMR of **214** in $CDCl_3$

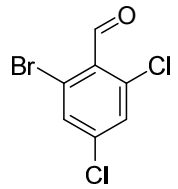

214

Figure A.90: 100 MHz ^{13}C NMR of **214** in $CDCl_3$

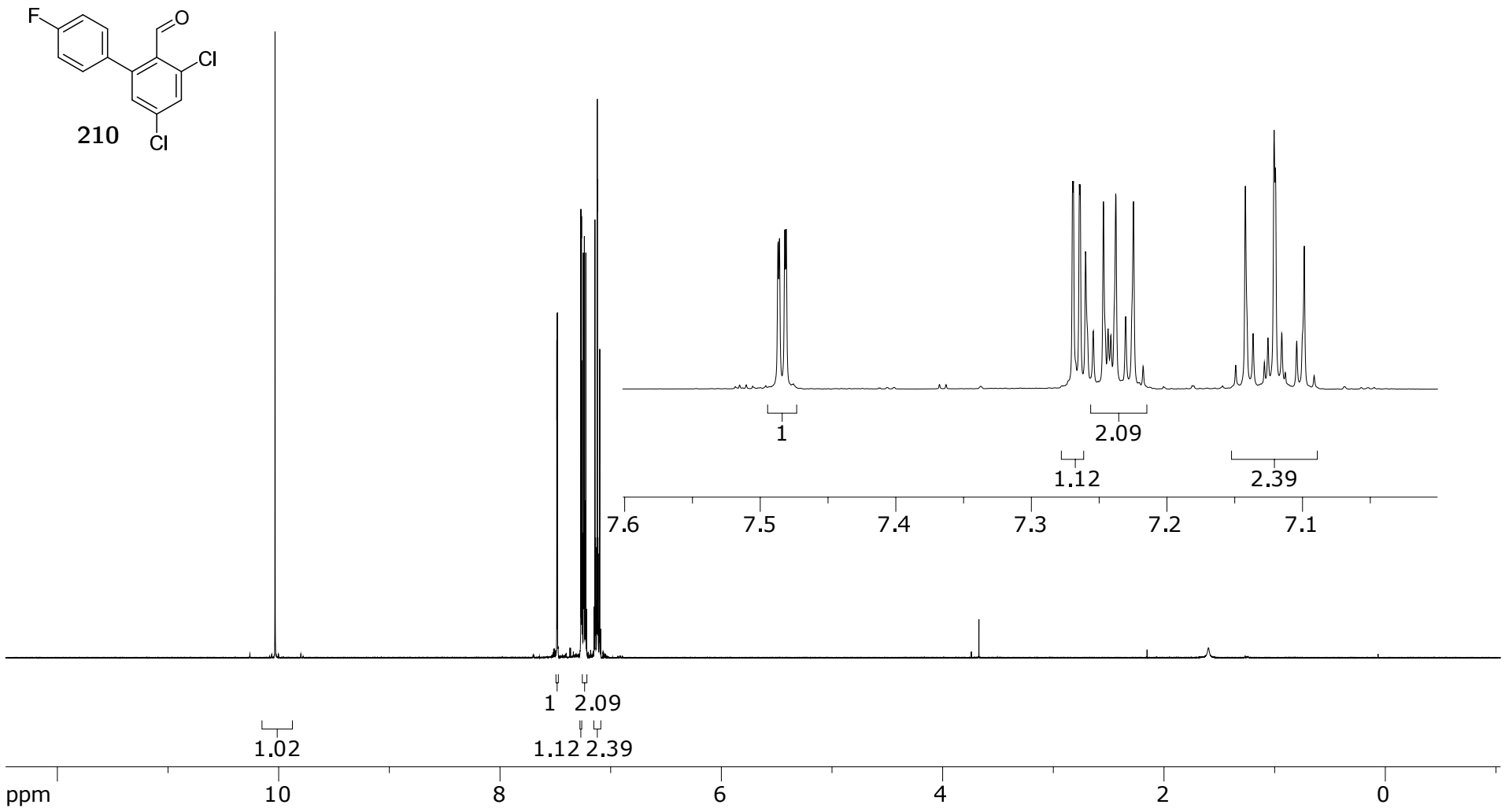

Figure A.91: 400 MHz ^{1}H NMR of **210** in $CDCl_3$

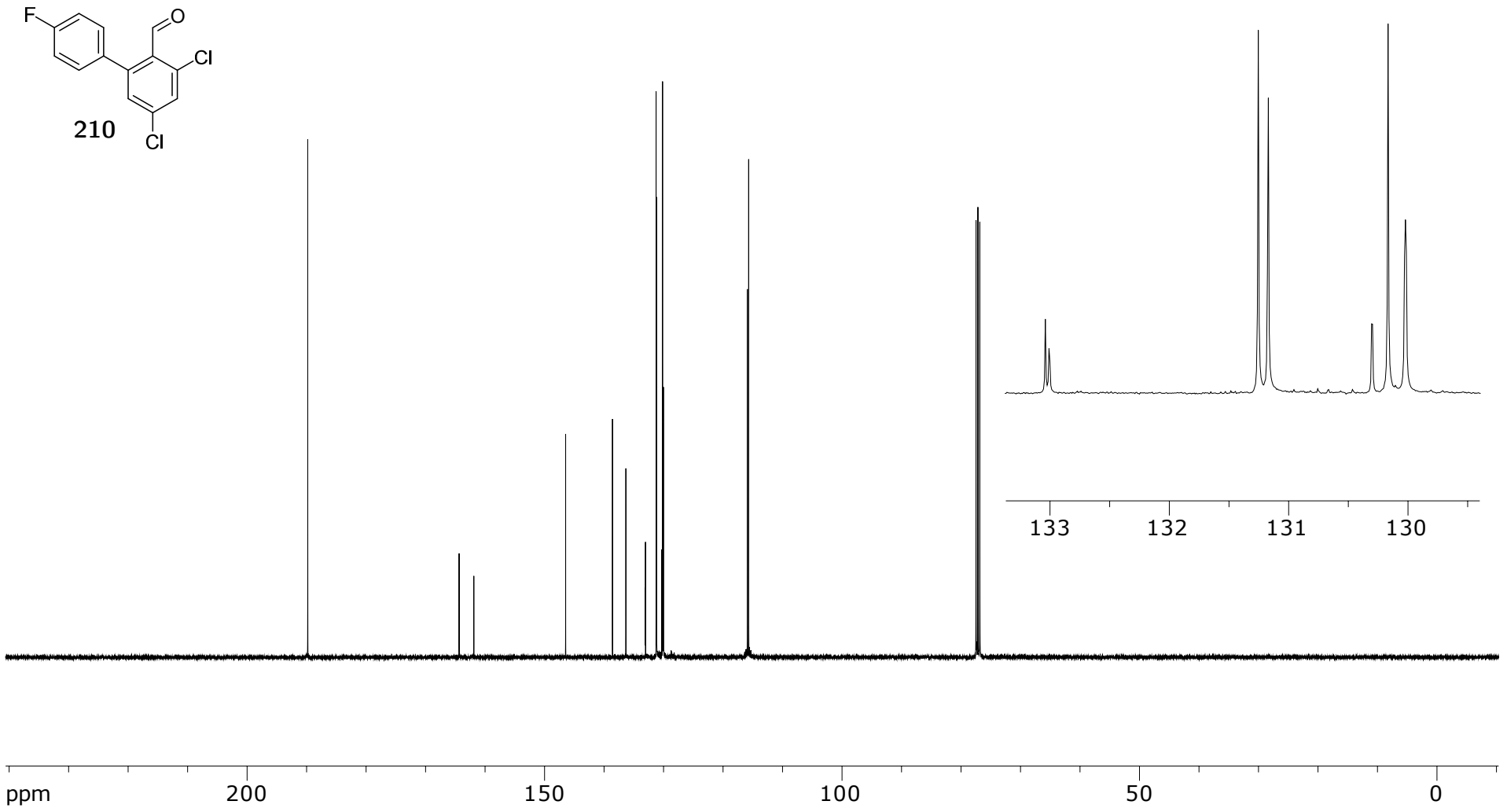

Figure A.92: 100 MHz ^{13}C NMR of **210** in $CDCl_3$

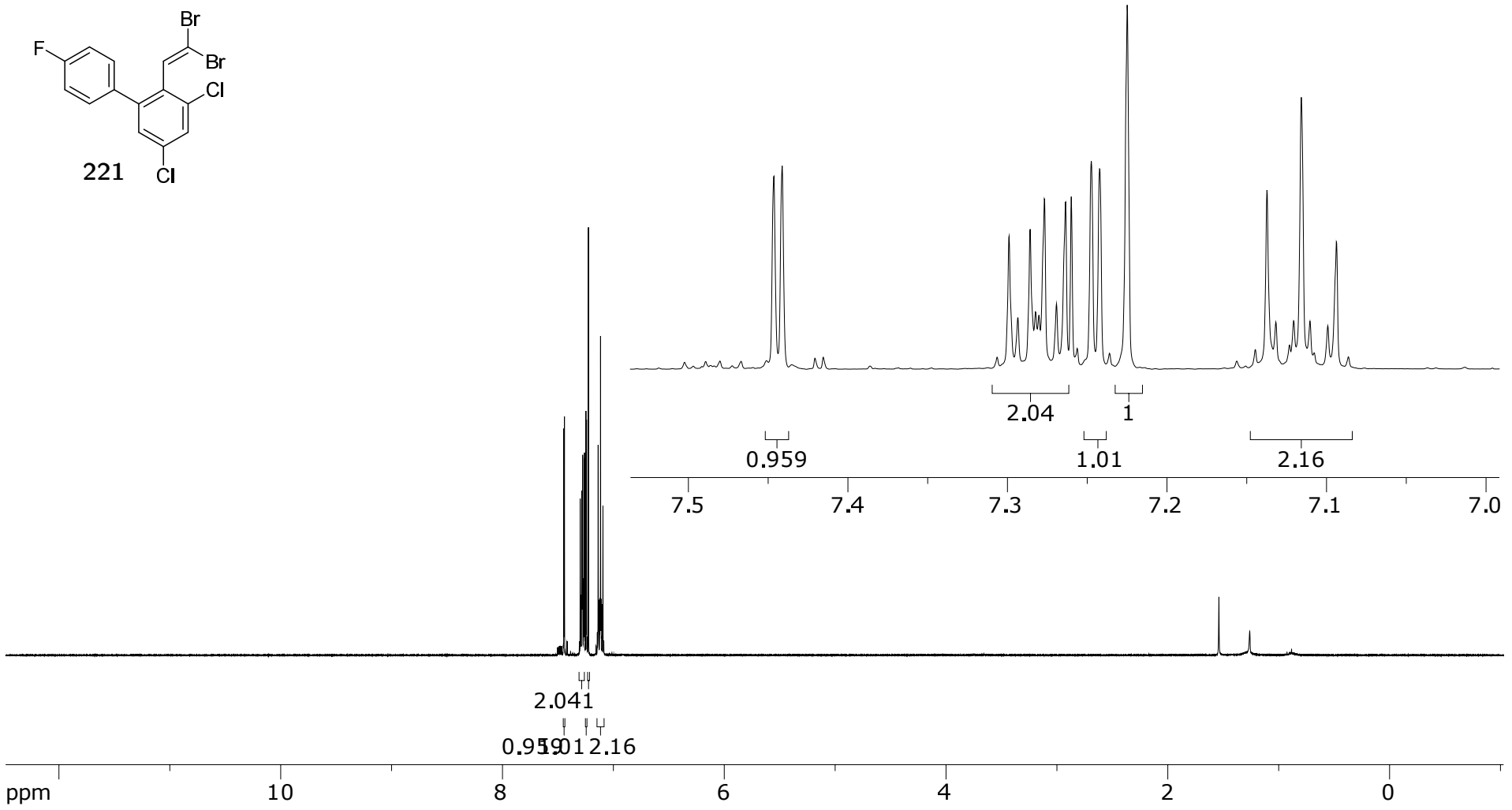

Figure A.93: 400 MHz ^{1}H NMR of **221** in $CDCl_3$

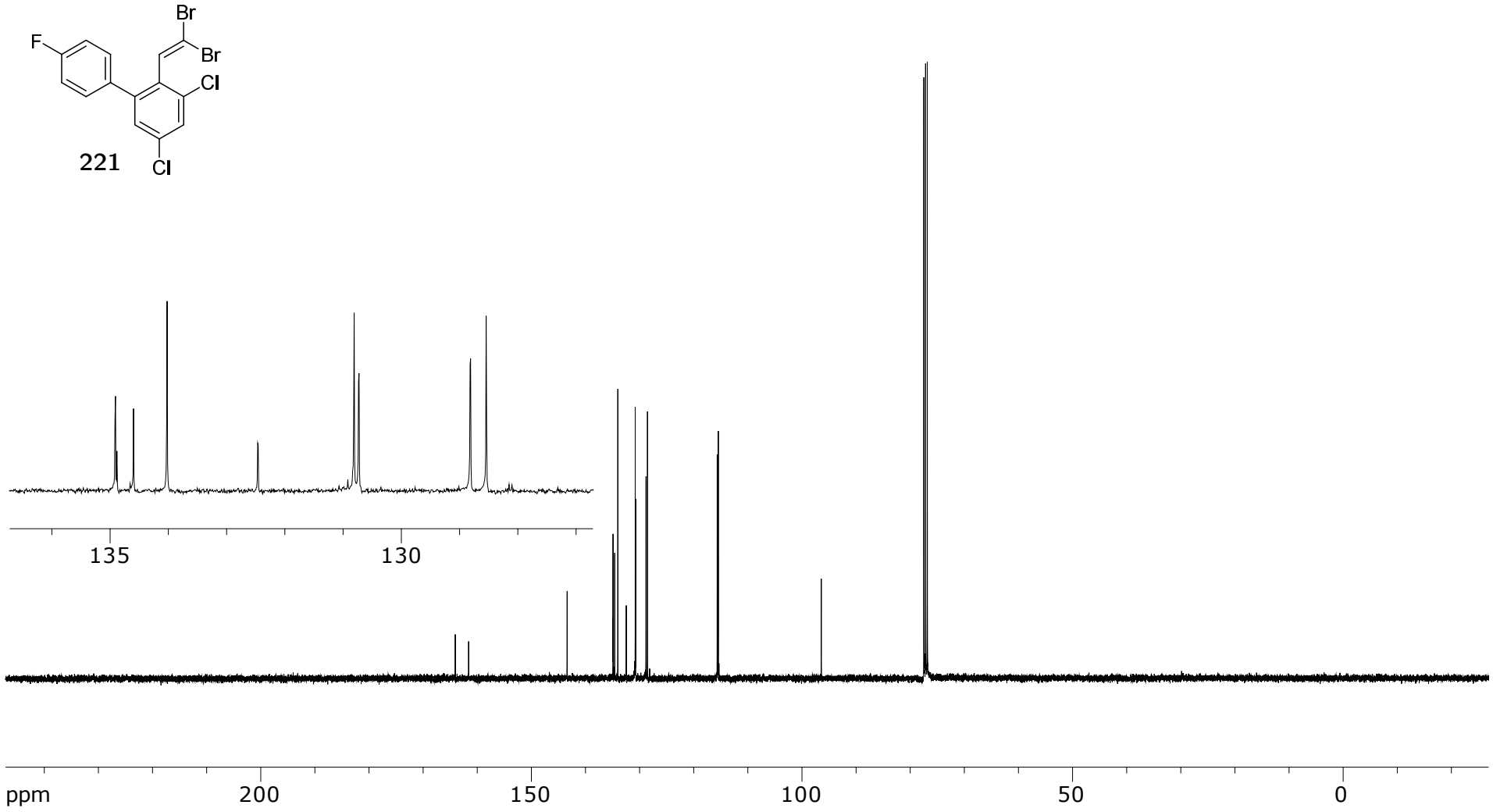

Figure A.94: 100 MHz ^{13}C NMR **221** in $CDCl_3$

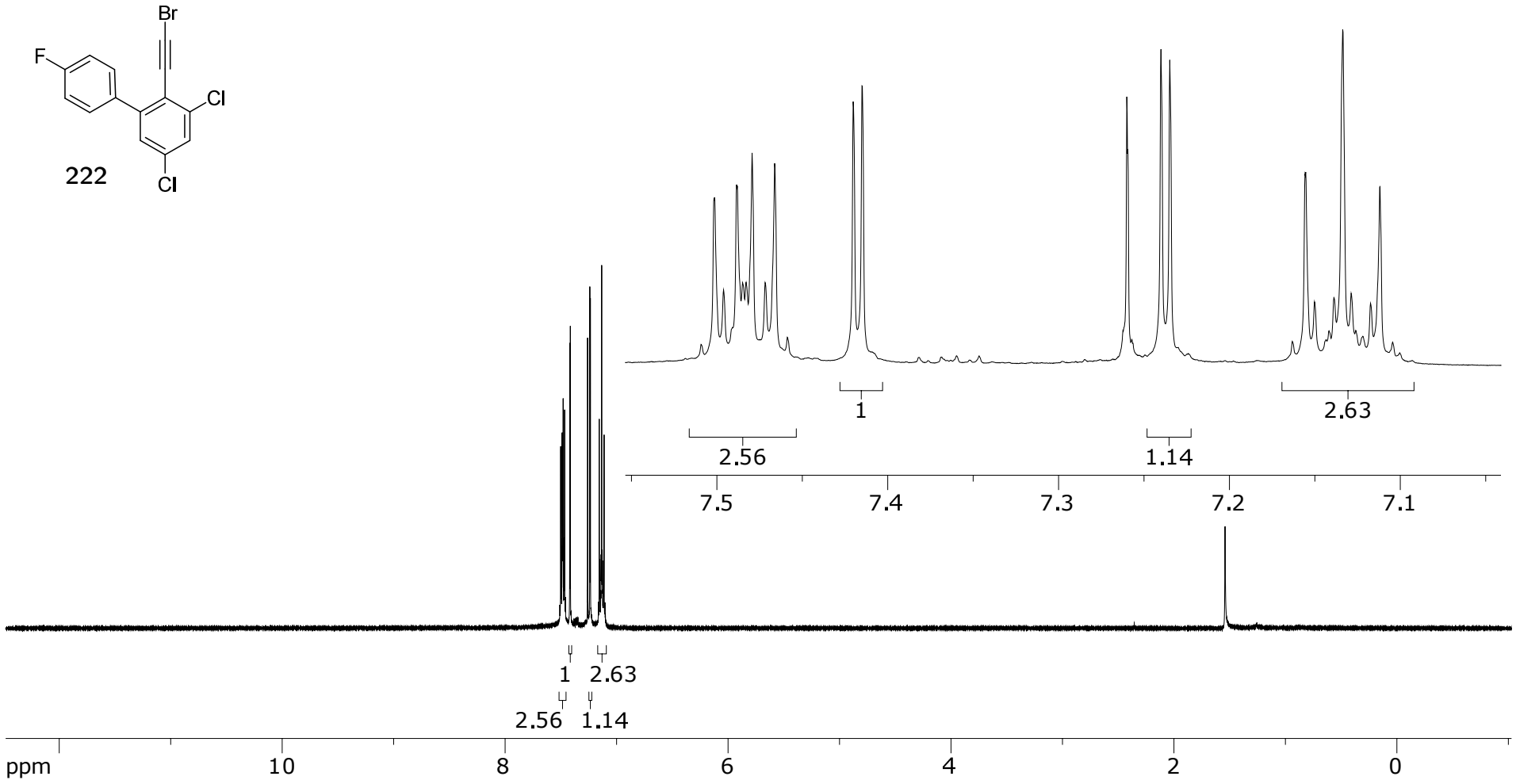

Figure A.95: 400 MHz ^{1}H NMR of **222** in $CDCl_3$

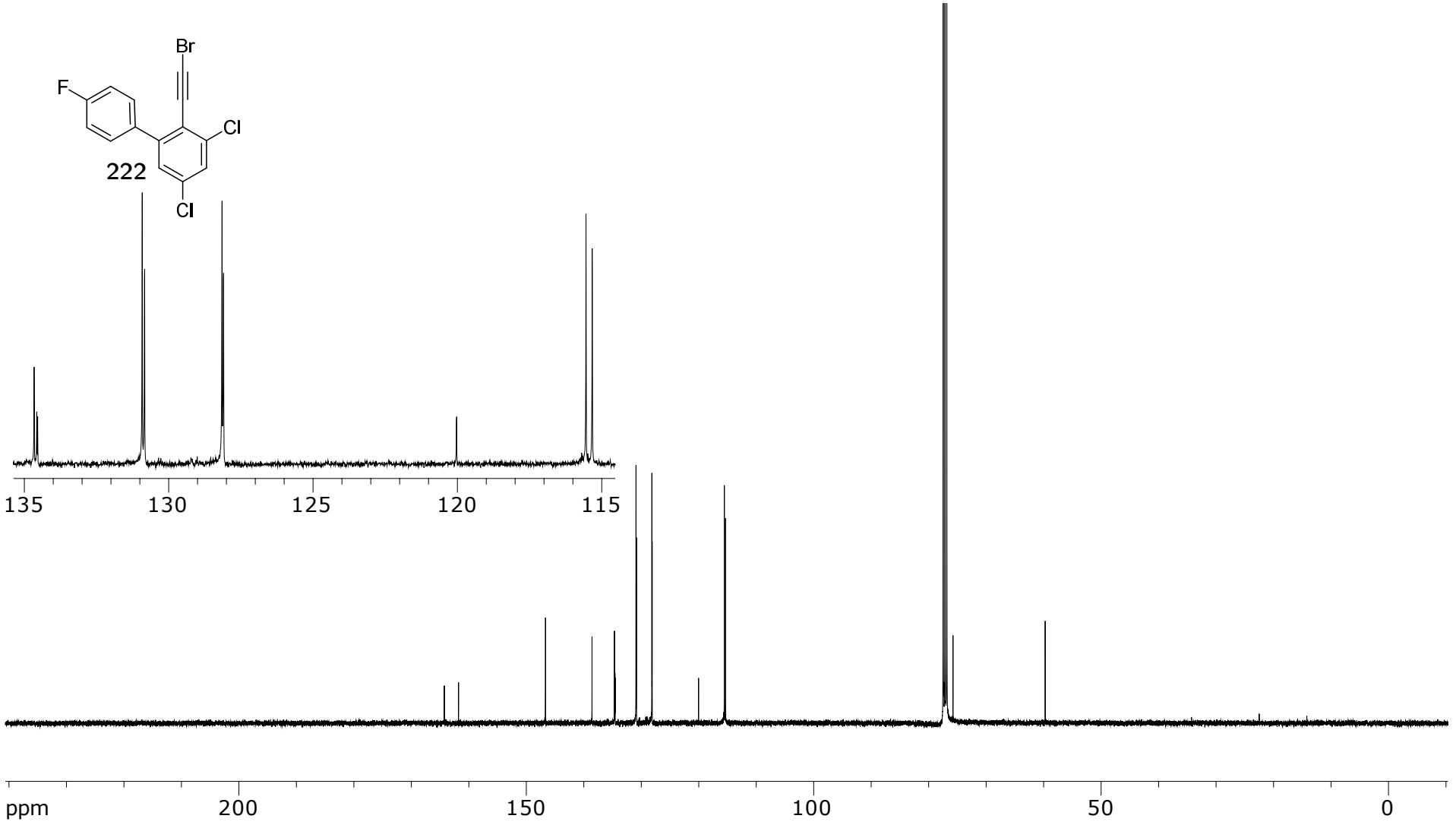

Figure A.96: 100 MHz ^{13}C NMR of **222** in $CDCl_3$

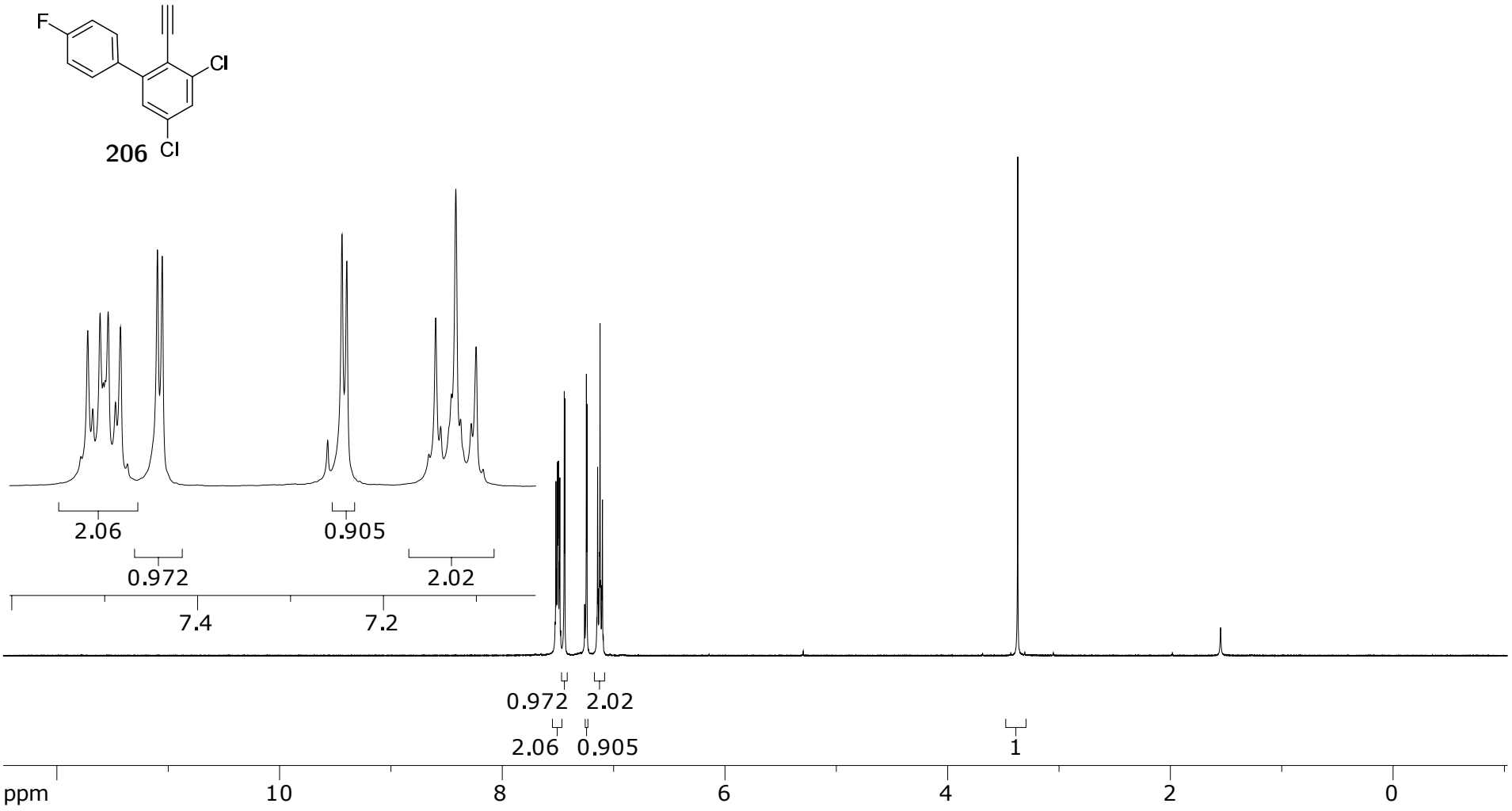

Figure A.97: 400 MHz ^{1}H NMR of **206** in $CDCl_3$

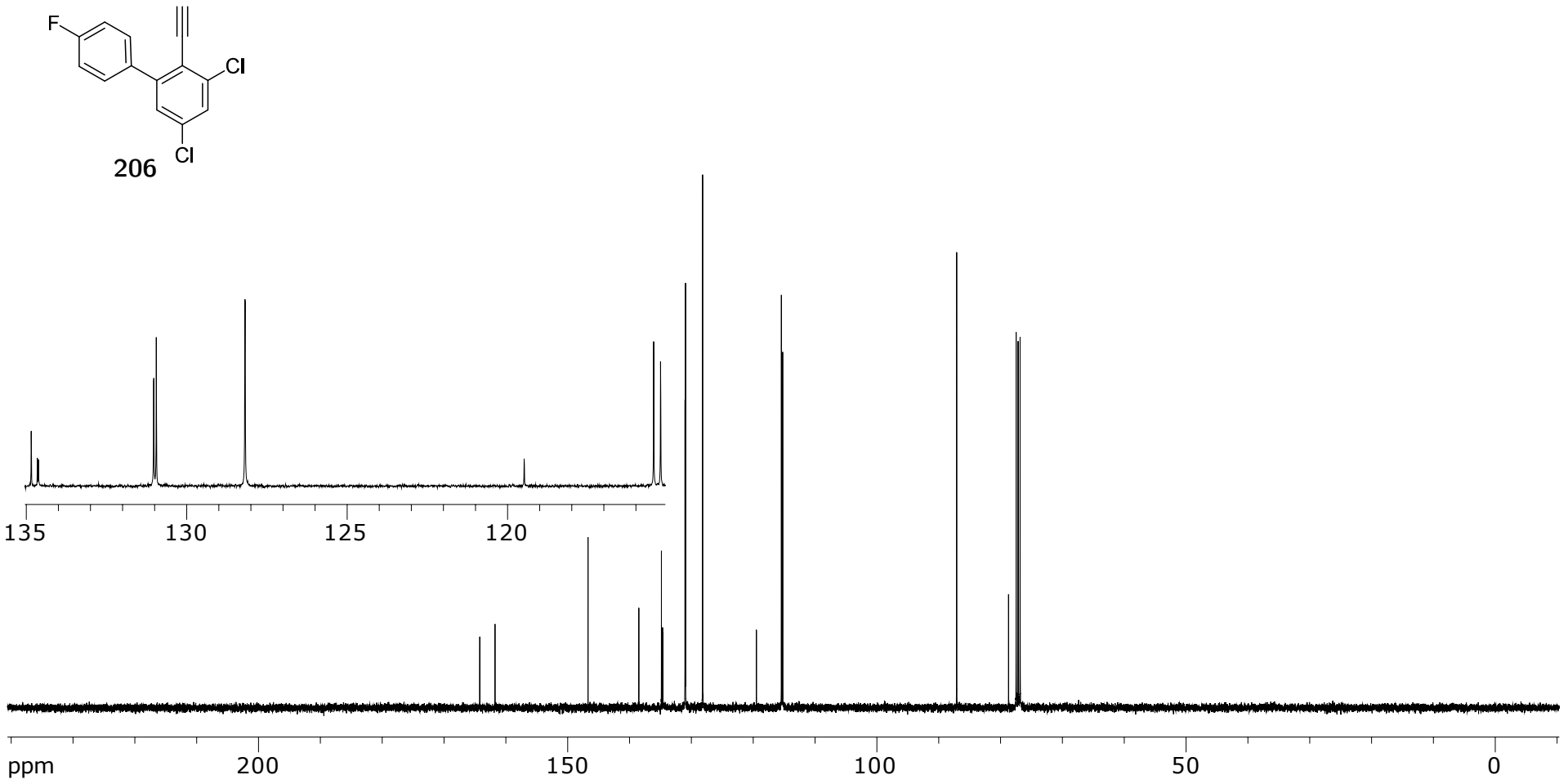

Figure A.98: 100 MHz ^{13}C NMR **206** in $CDCl_3$

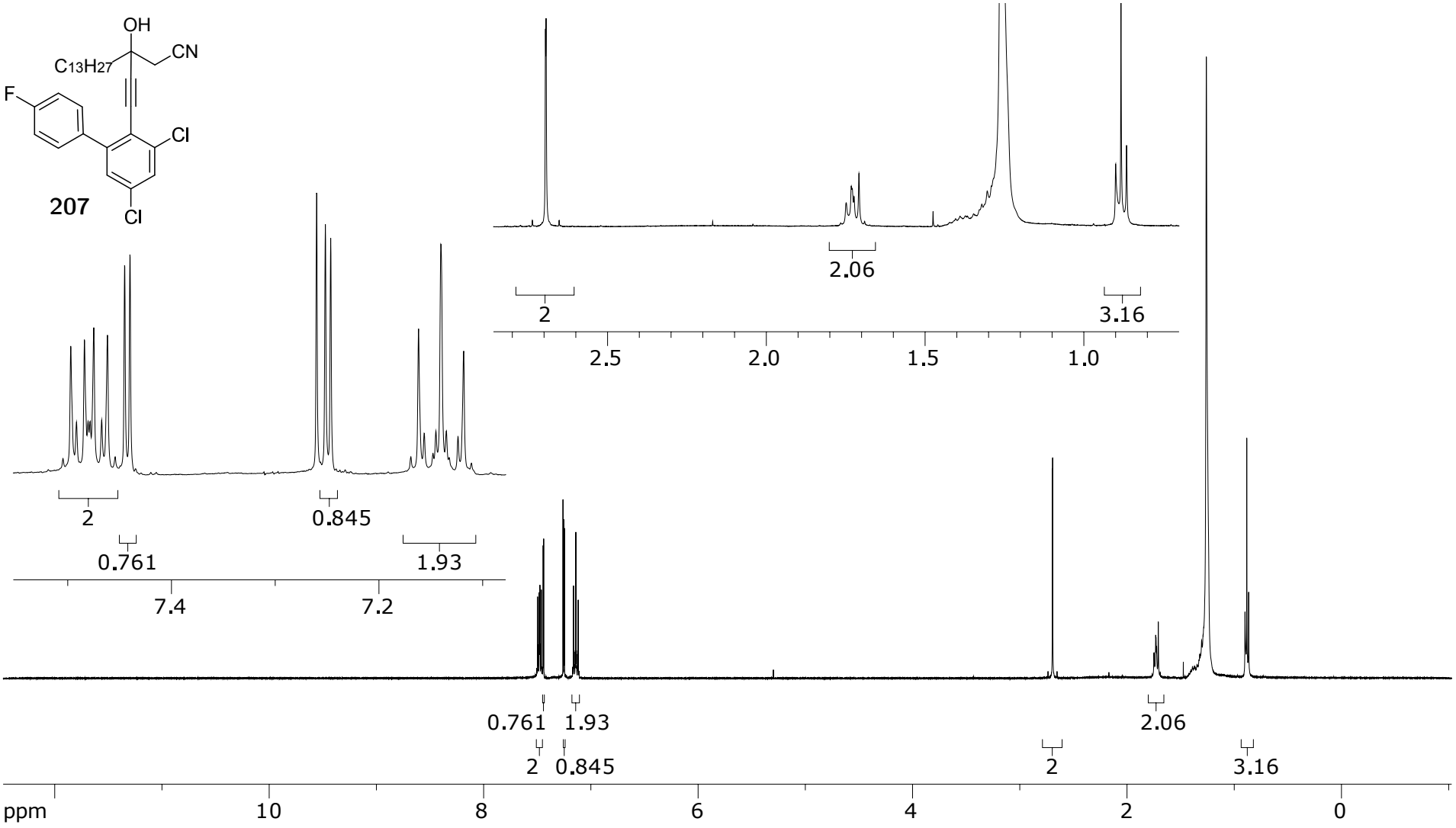

Figure A.99: 400 MHz ^{1}H NMR of **207** in $CDCl_3$

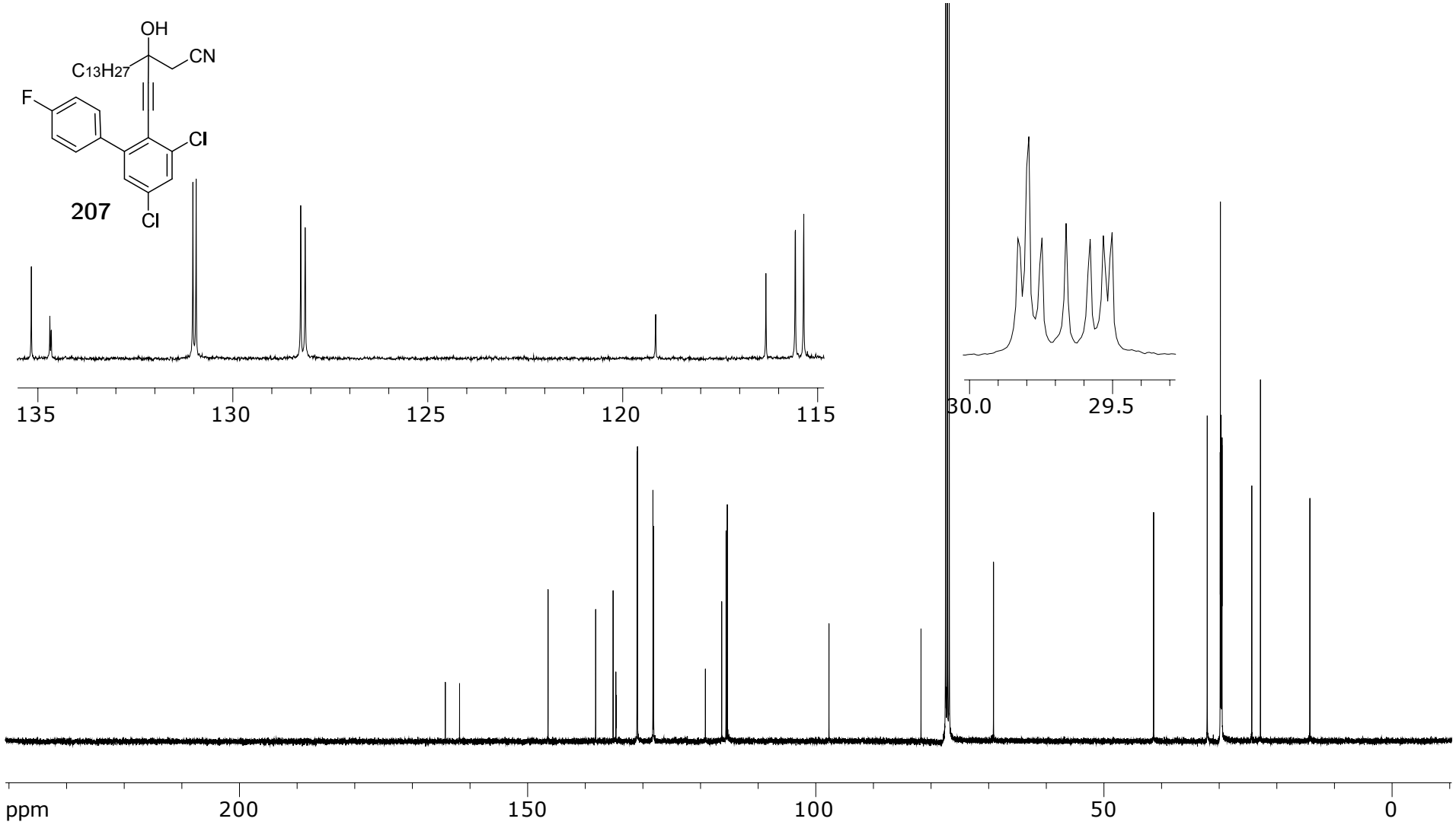

Figure A.100: 100 MHz ^{13}C NMR of **207** in $CDCl_3$

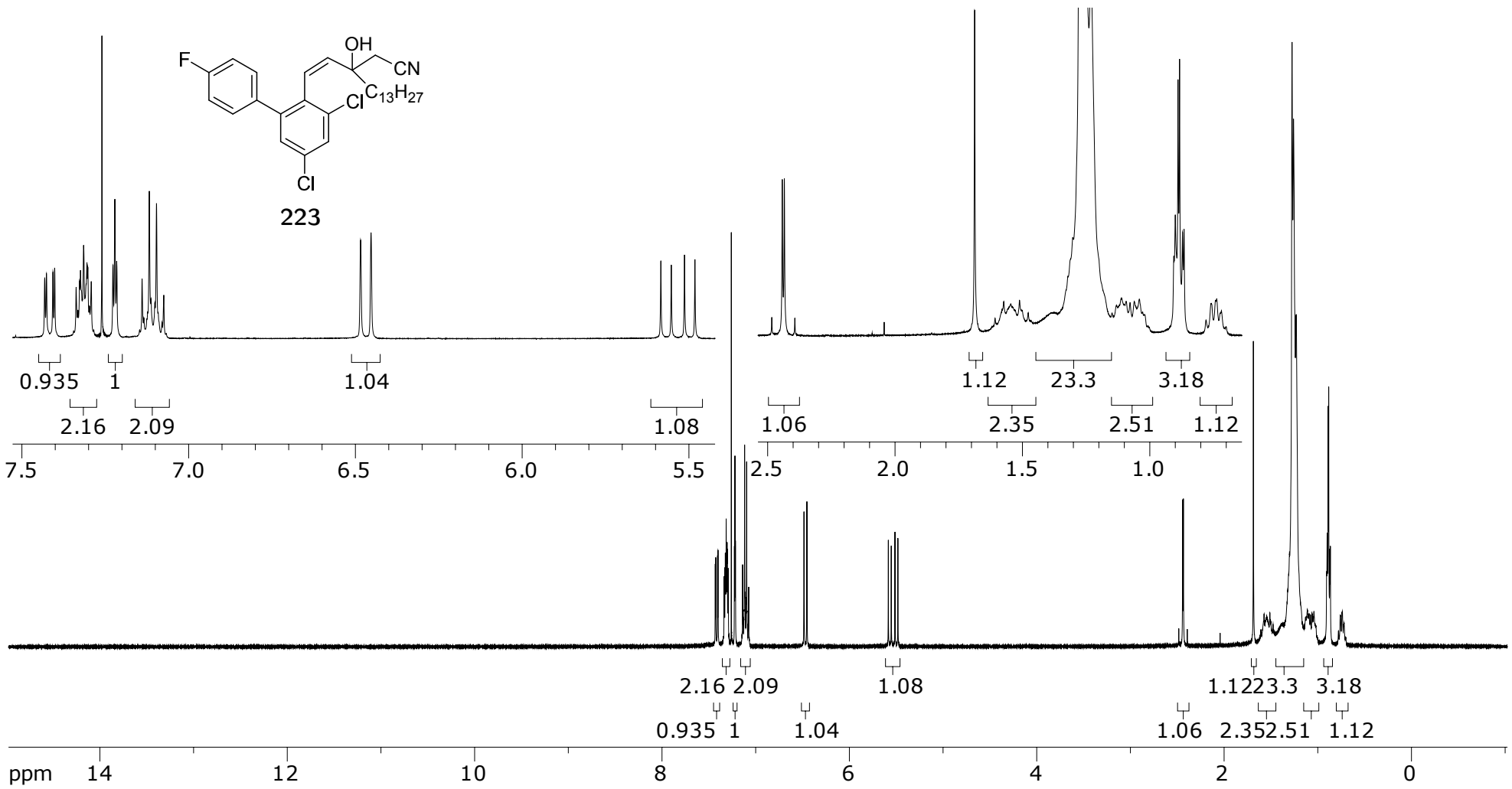

Figure A.101: 400 MHz ^{1}H NMR of **223** in $CDCl_3$

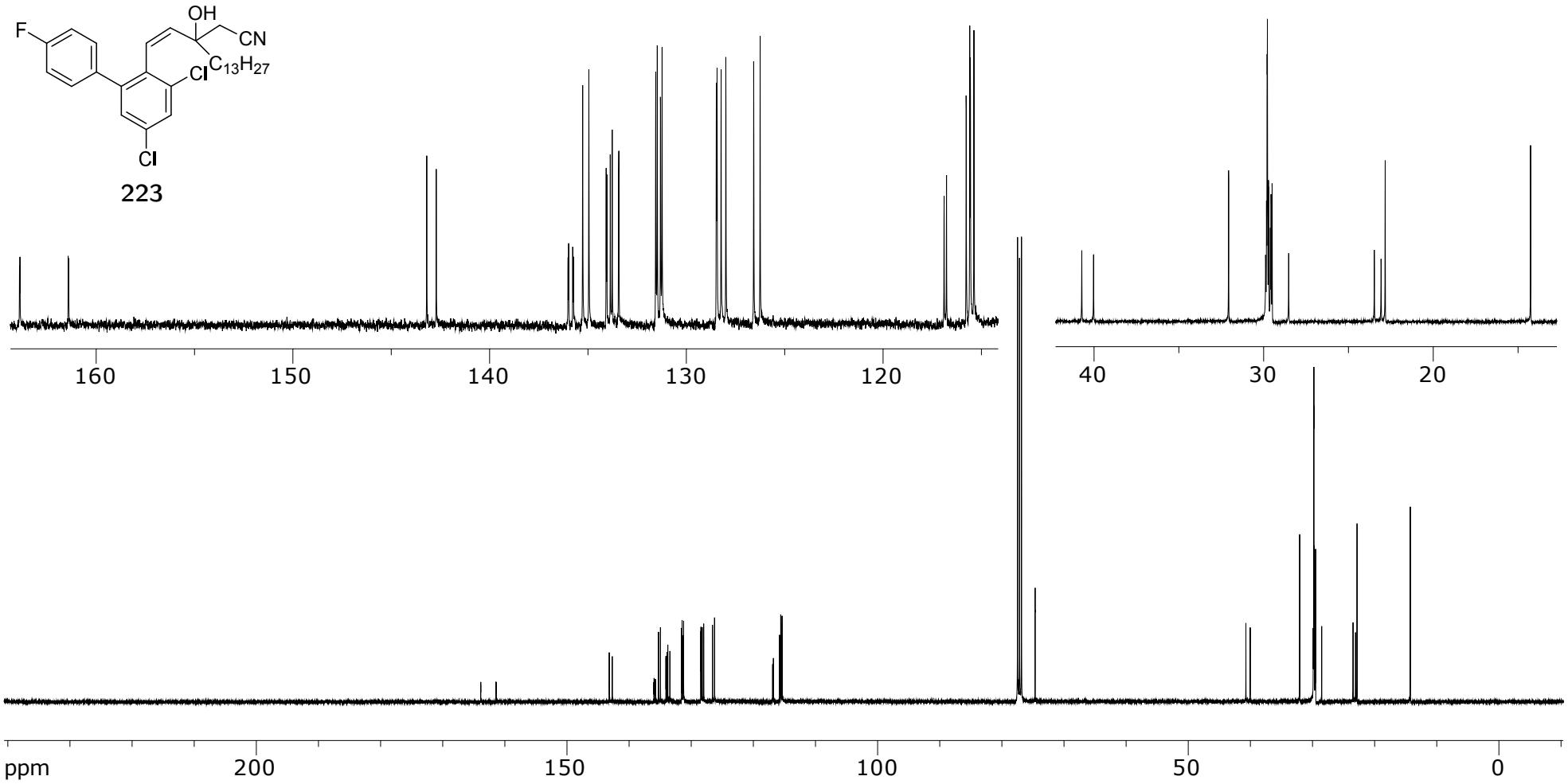

Figure A.102: 100 MHz ^{13}C NMR of **223** in $CDCl_3$

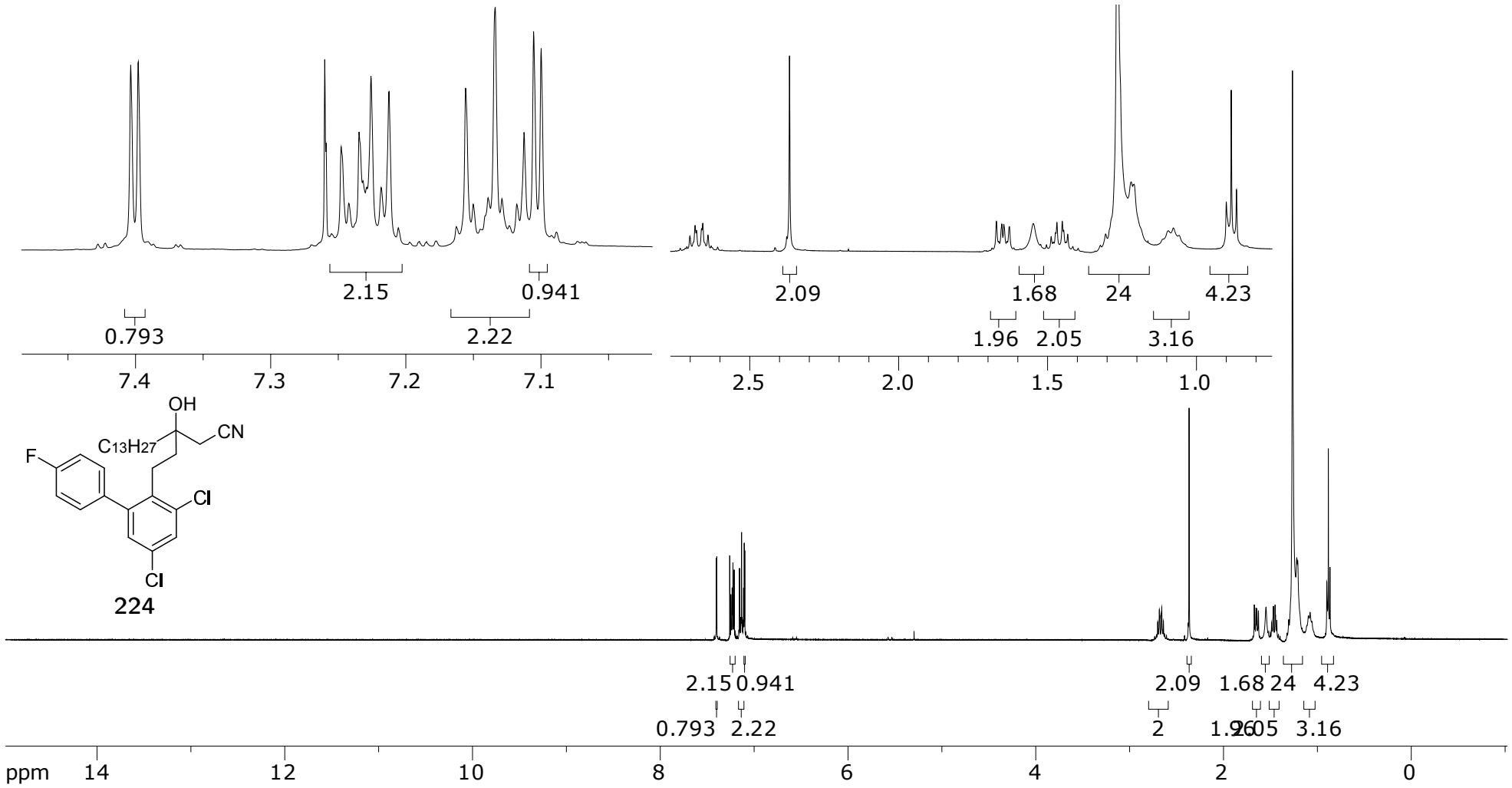

Figure A.103: 400 MHz ^{1}H NMR of **224** in $CDCl_3$

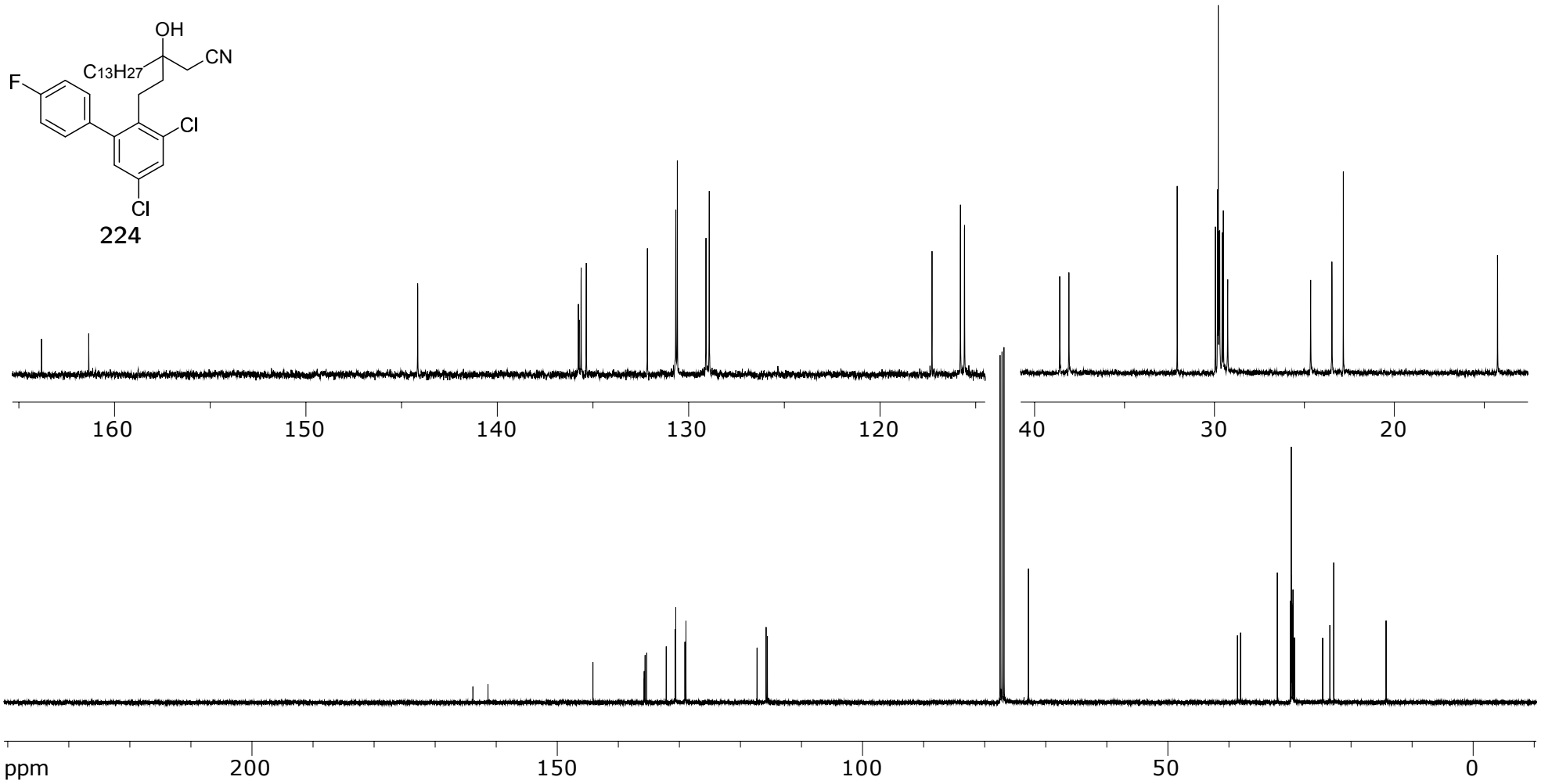

Figure A.104: 100 MHz ^{13}C NMR of **224** in $CDCl_3$

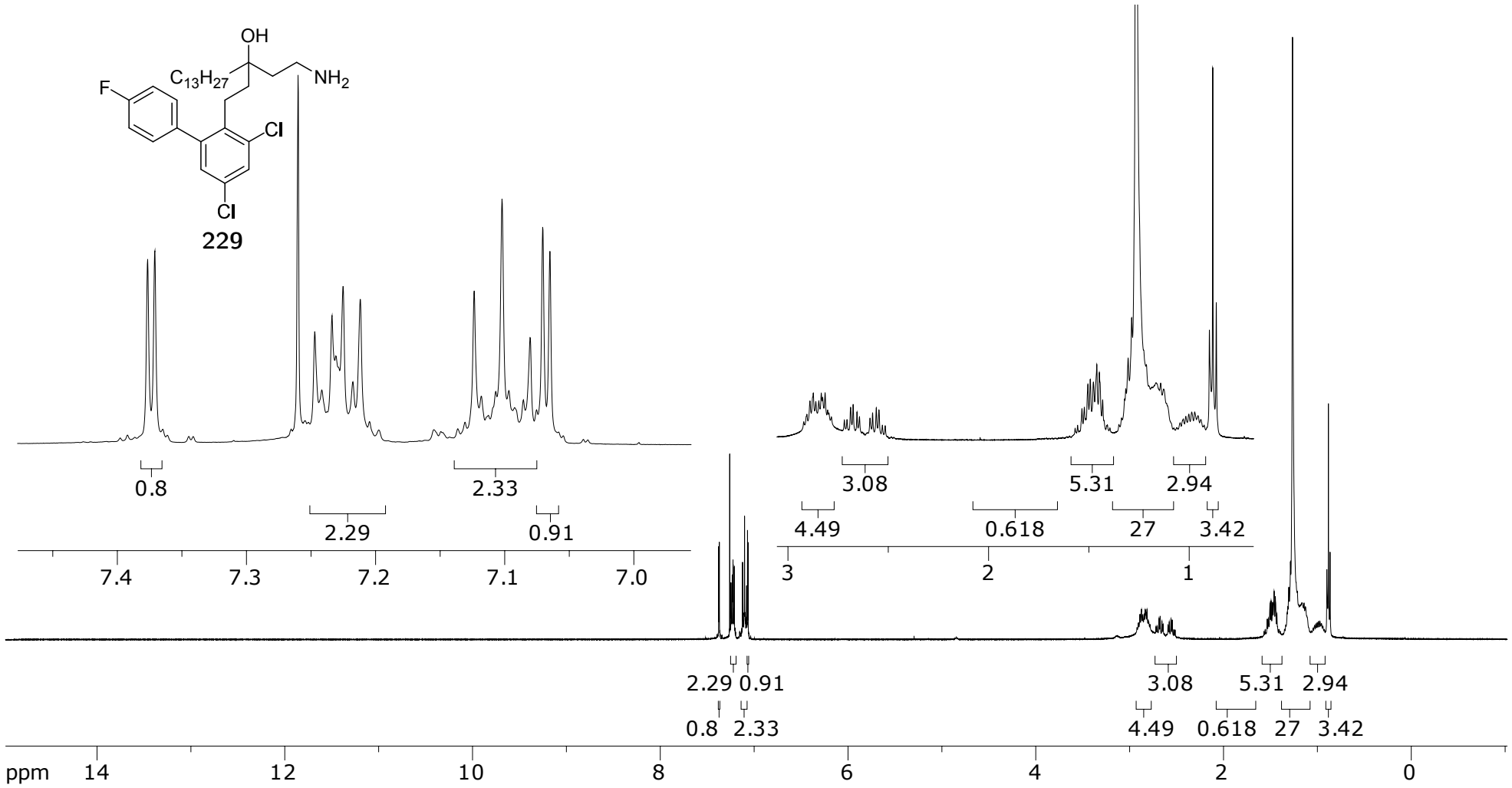

Figure A.105: 400 MHz ^{1}H NMR of **229** in $CDCl_3$

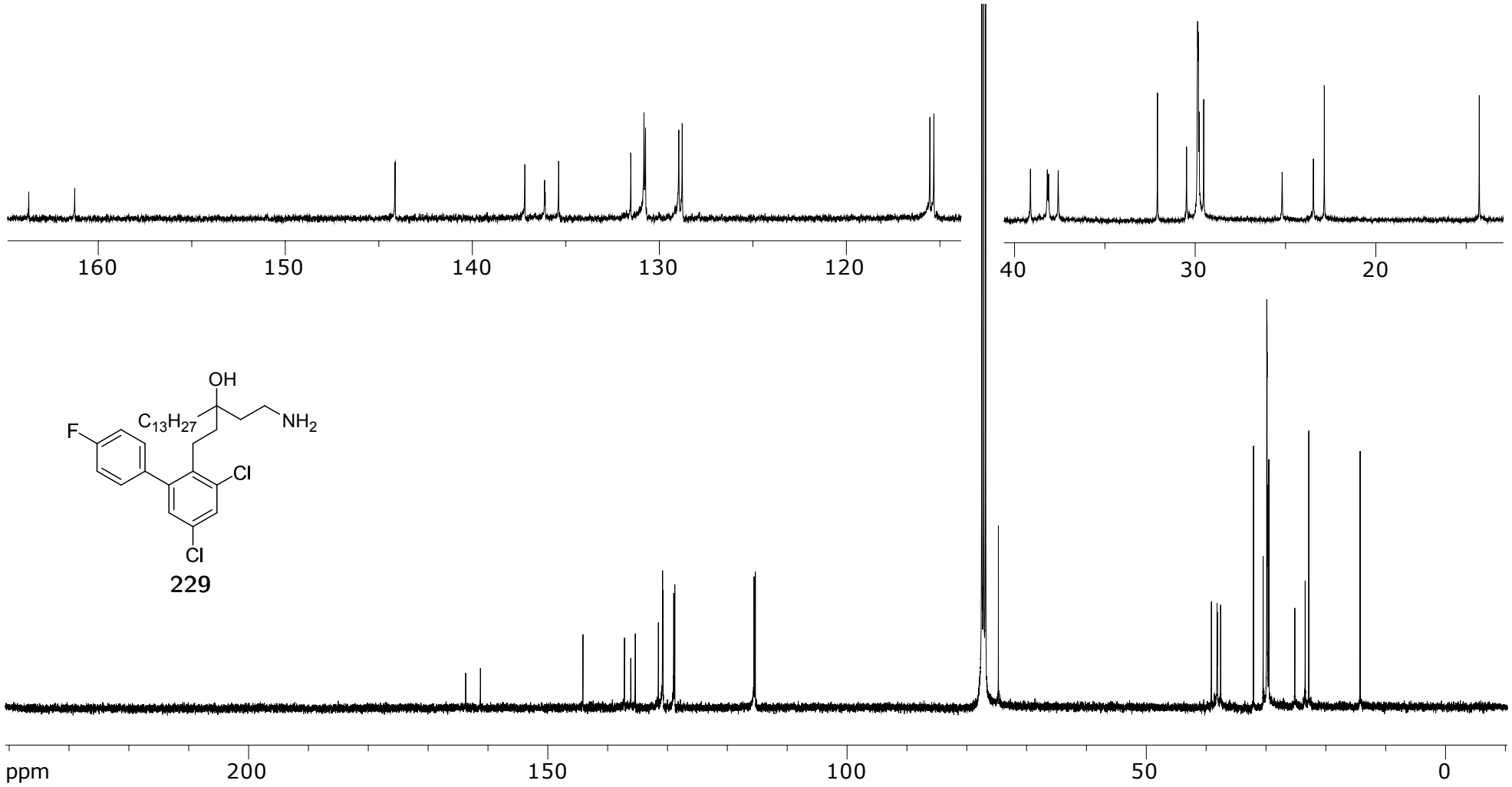

Figure A.106: 100 MHz ^{13}C NMR of **229** in $CDCl_3$

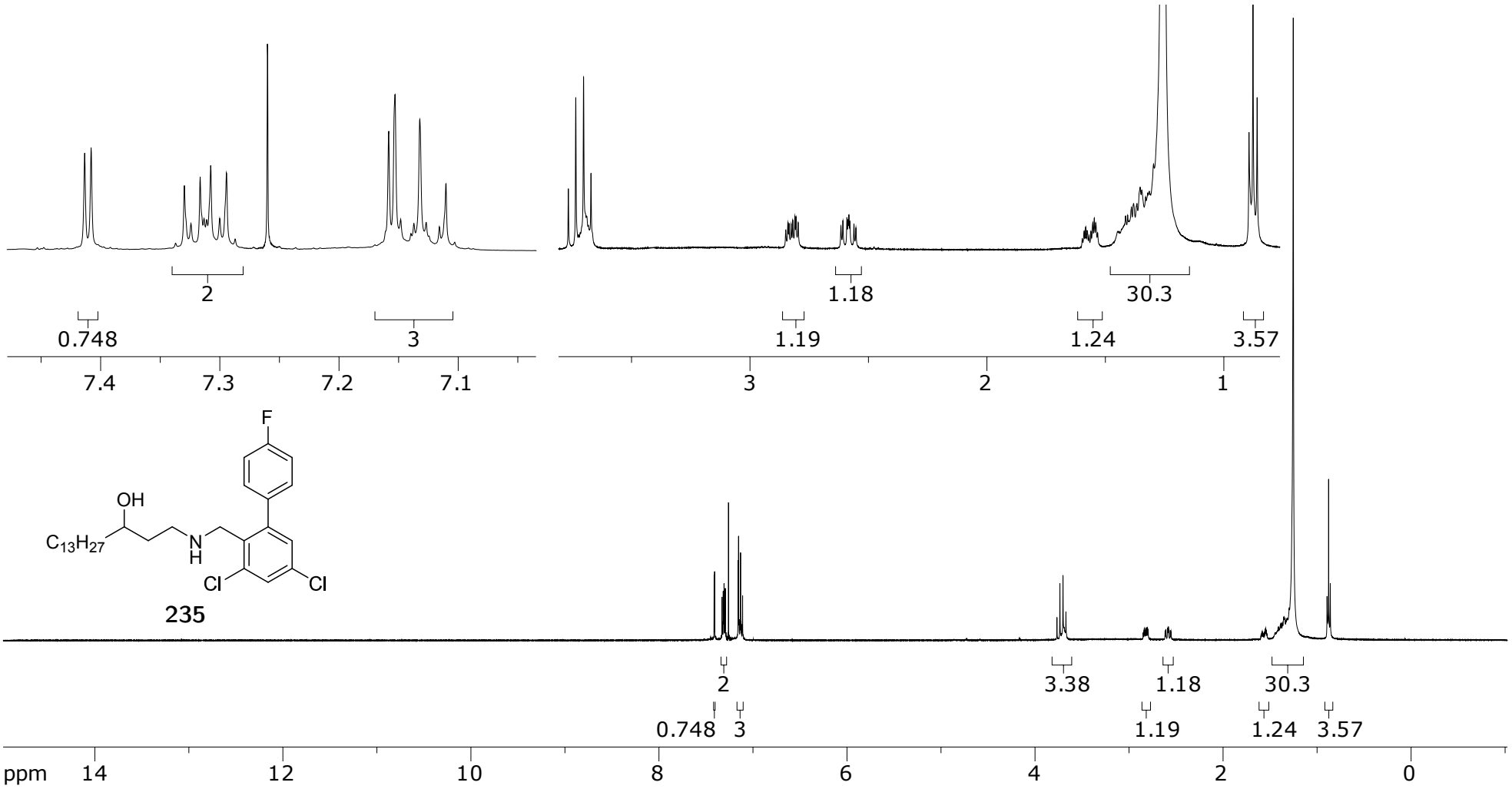

Figure A.107: 400 MHz ^{1}H NMR of **235** in C_6D6_6

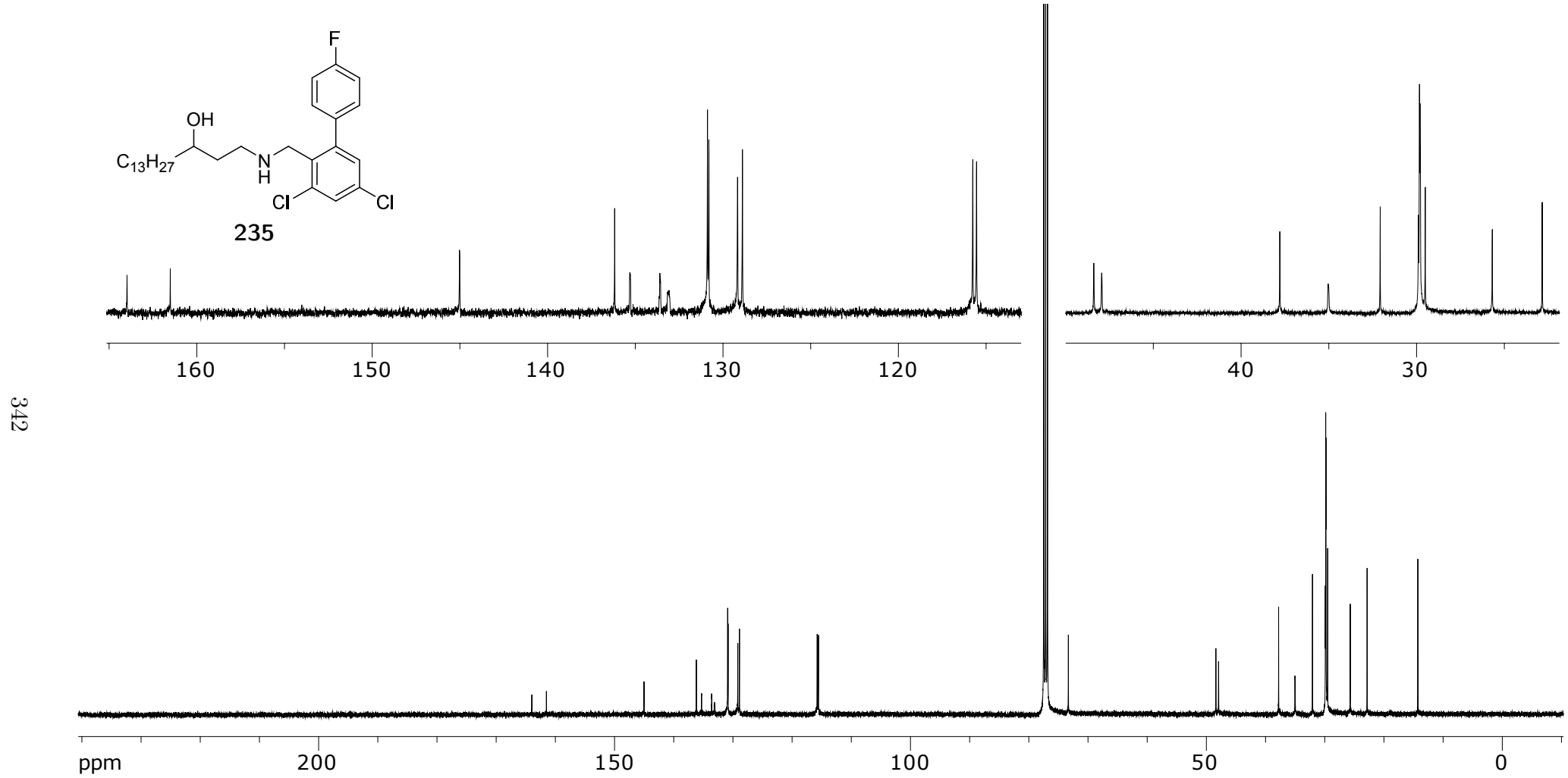

Figure A.108: 100 MHz ^{13}C NMR of **235** in C_6D6_6

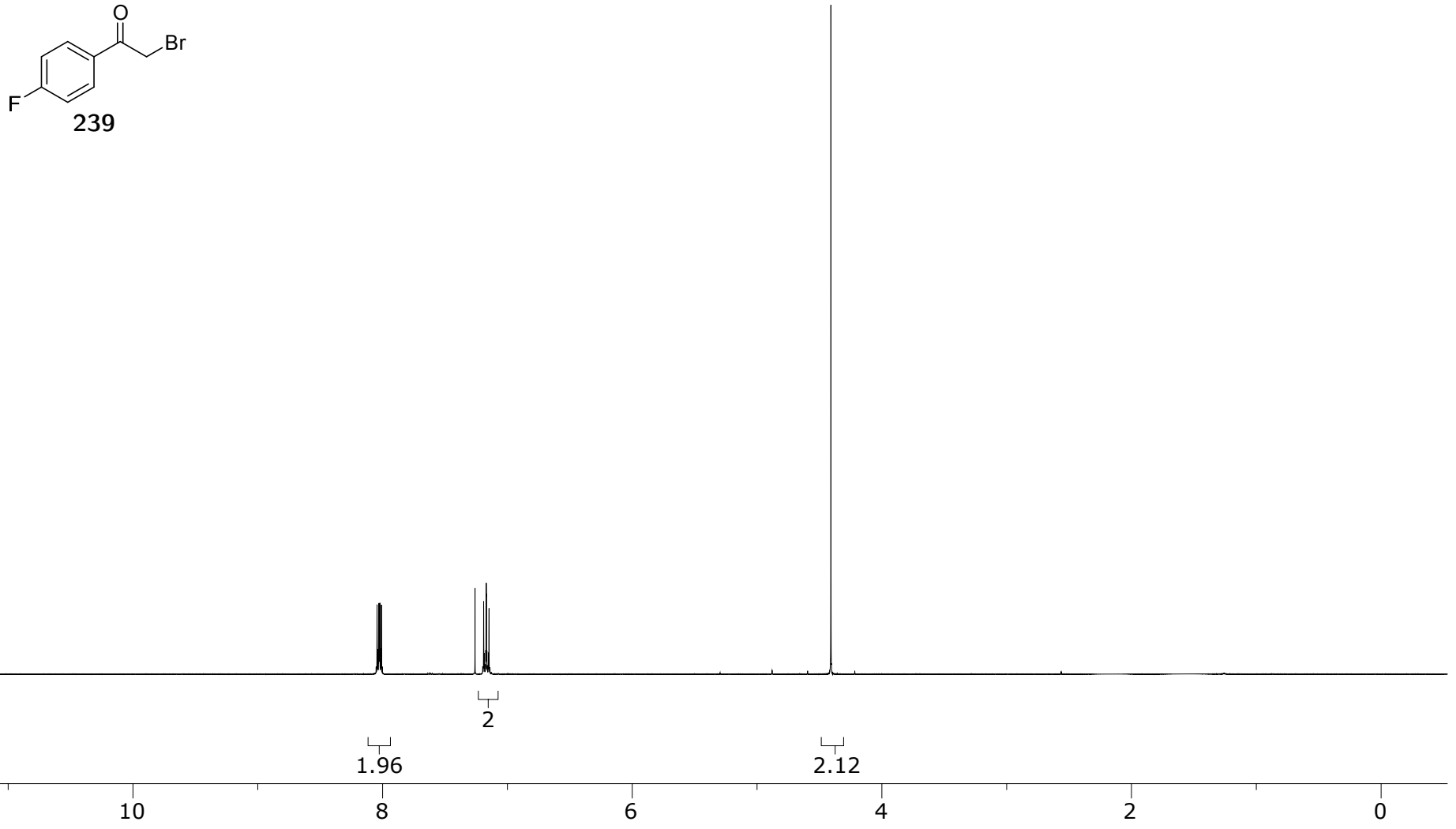

Figure A.109: 400 MHz ^{1}H NMR of **239** in $CDCl_3$

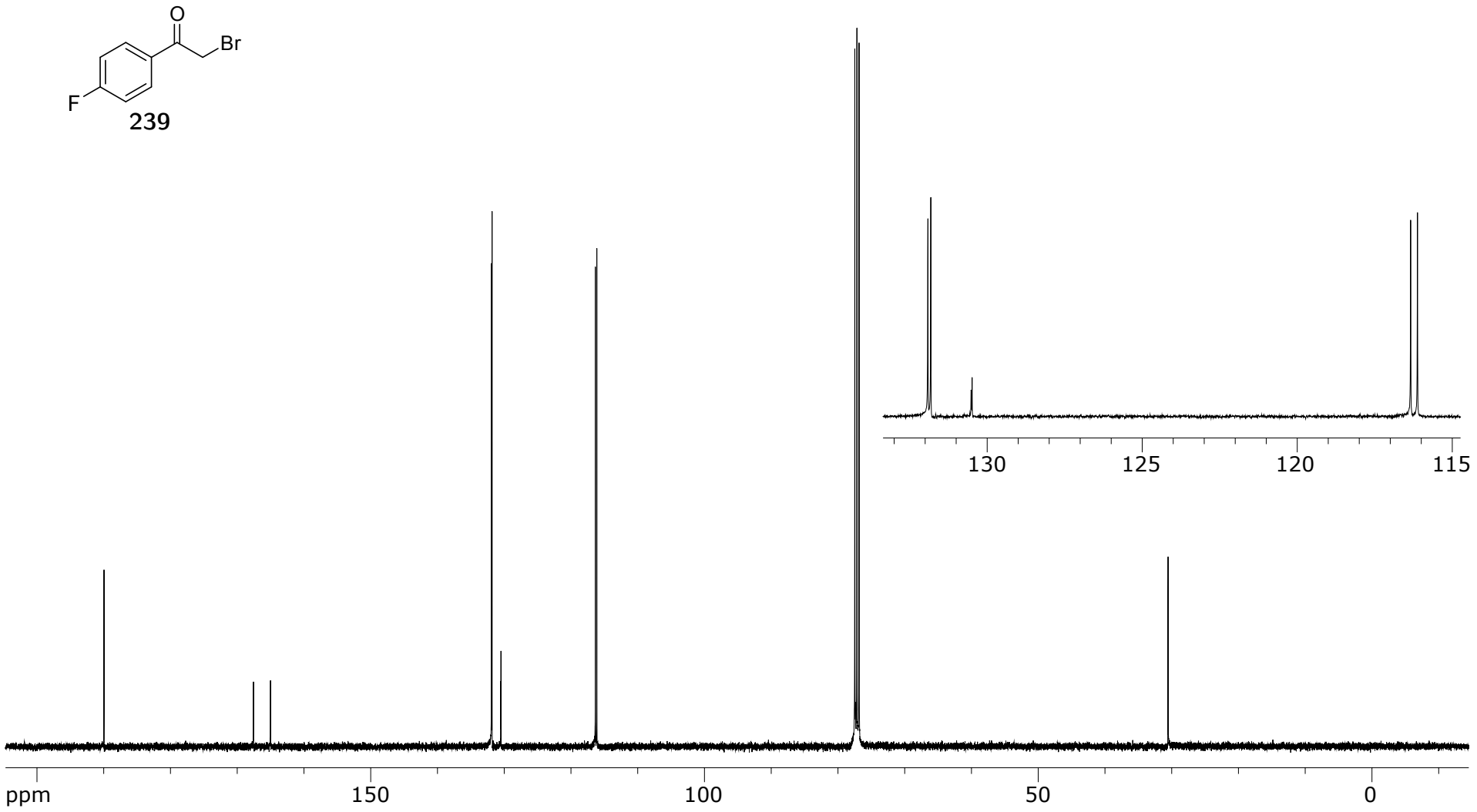

Figure A.110: 100 MHz ^{13}C NMR of **239** in $CDCl_3$

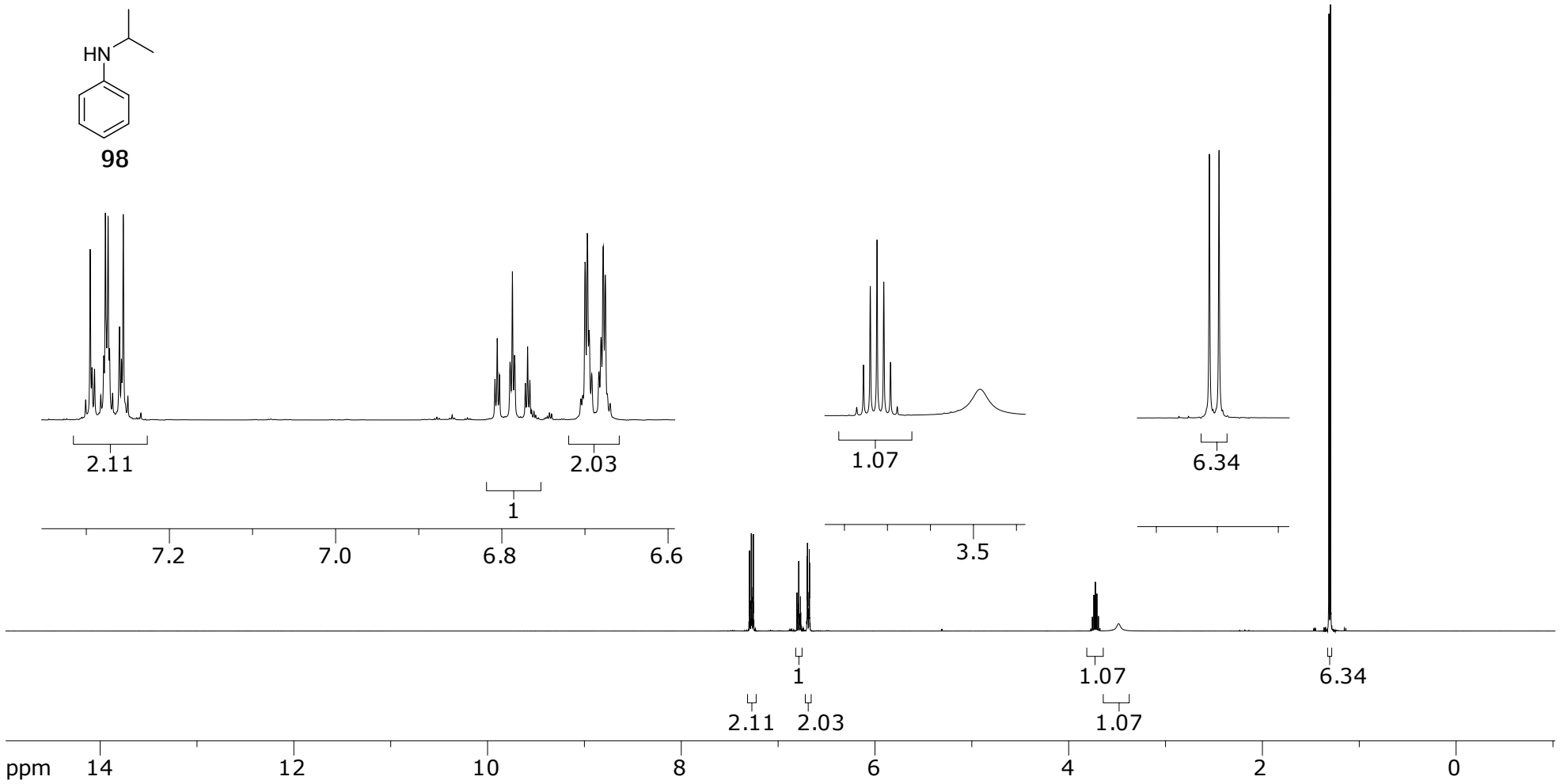

Figure A.111: 400 MHz ^{1}H NMR of **98** in $CDCl_3$

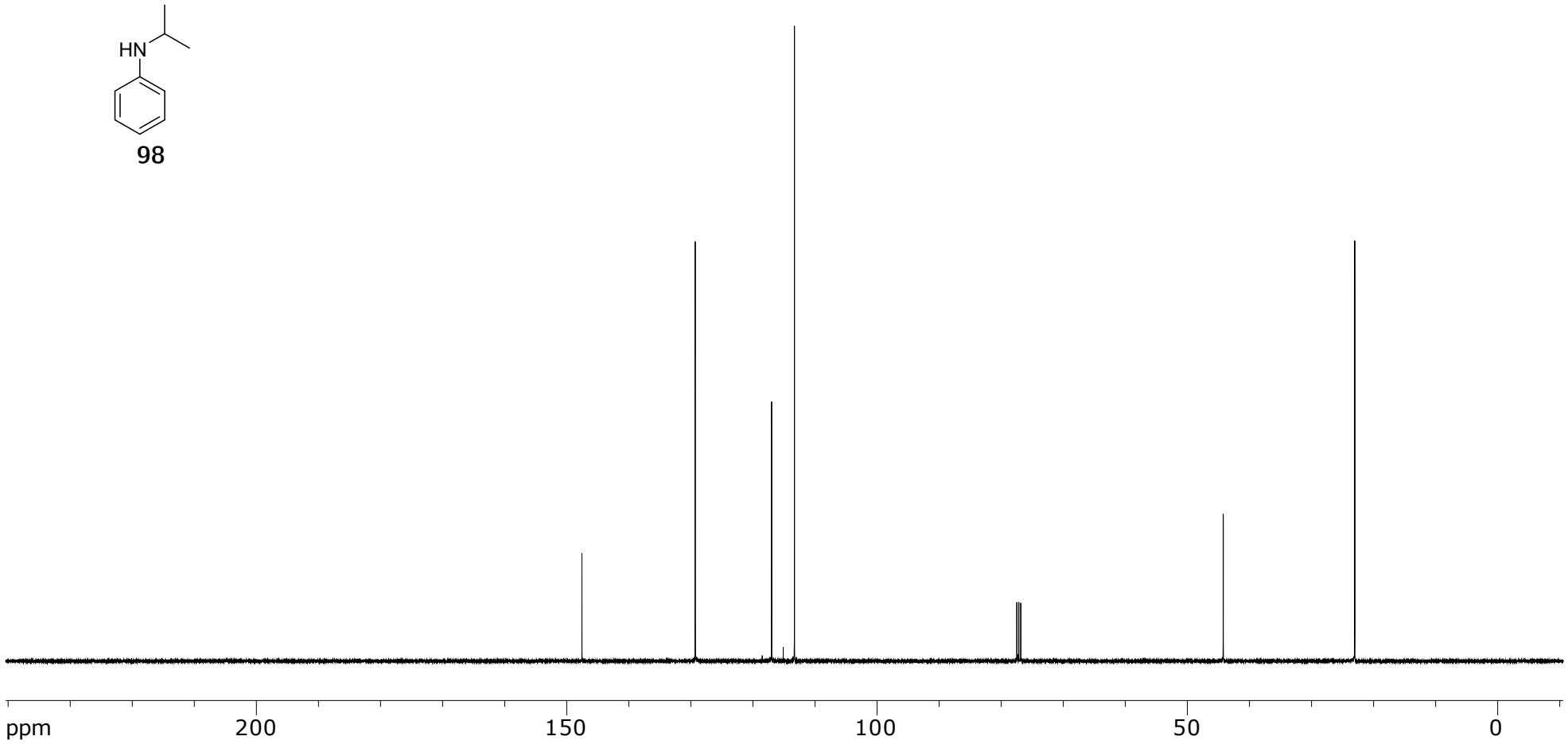

Figure A.112: 100 MHz ^{13}C NMR of **98** in $CDCl_3$

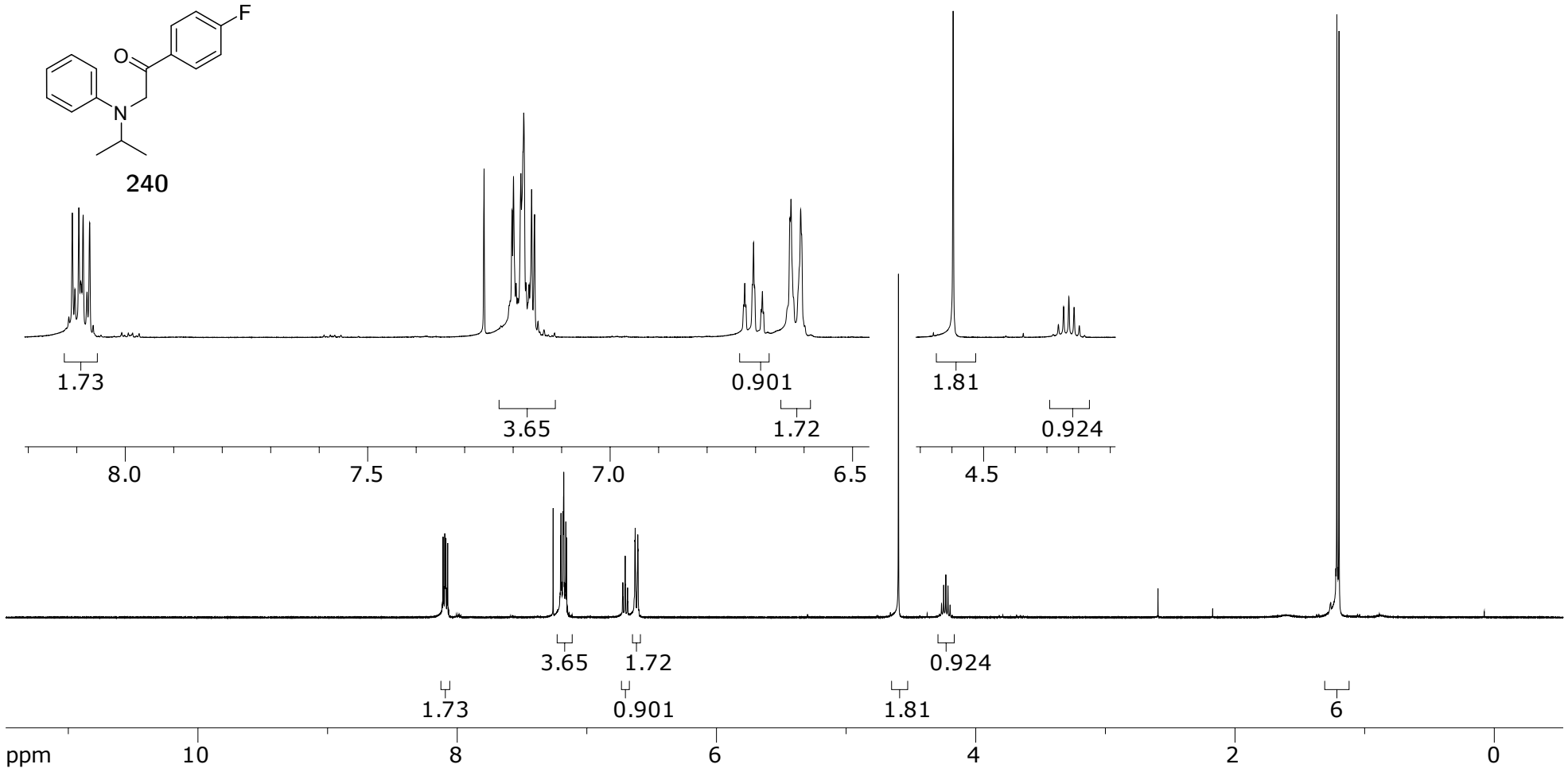

Figure A.113: 400 MHz ^{1}H NMR of **240** in $CDCl_3$

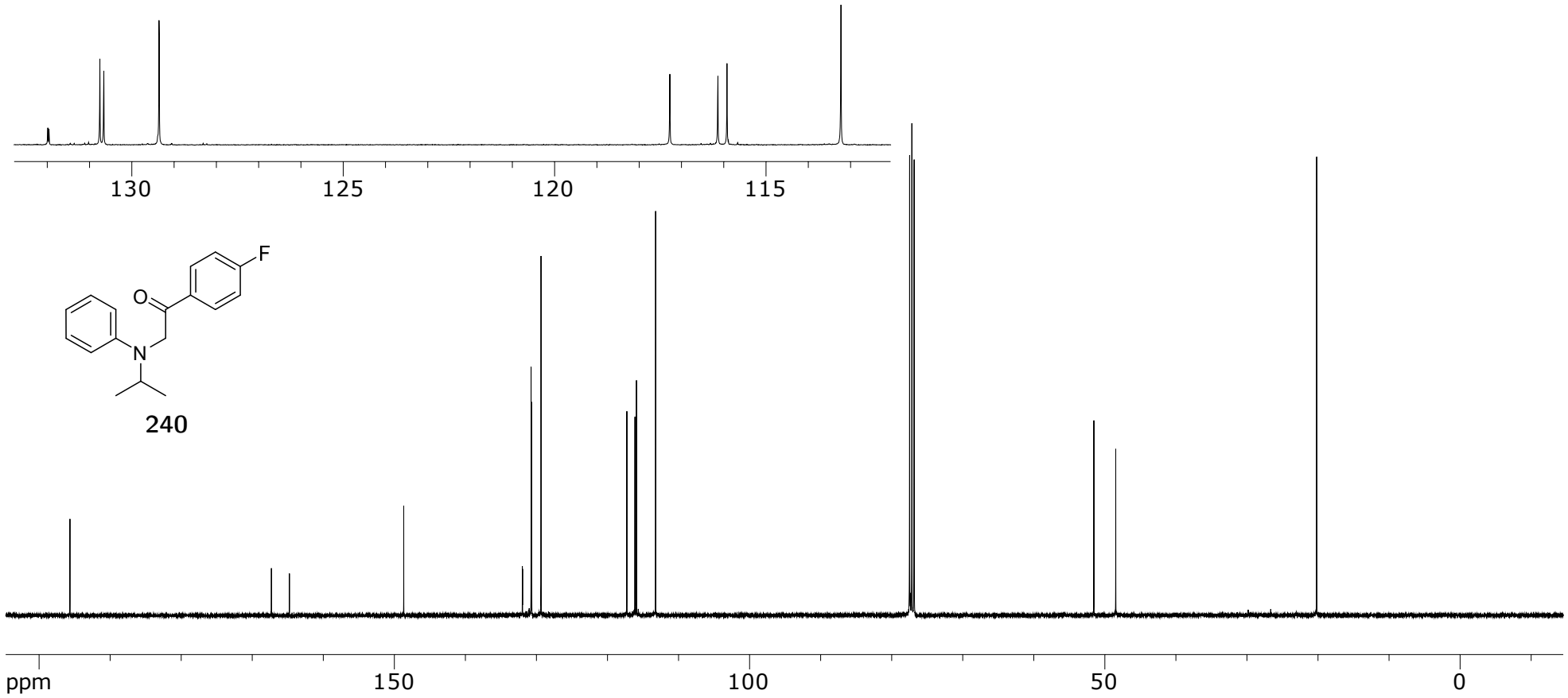

Figure A.114: 100 MHz ^{13}C NMR of **240** in $CDCl_3$

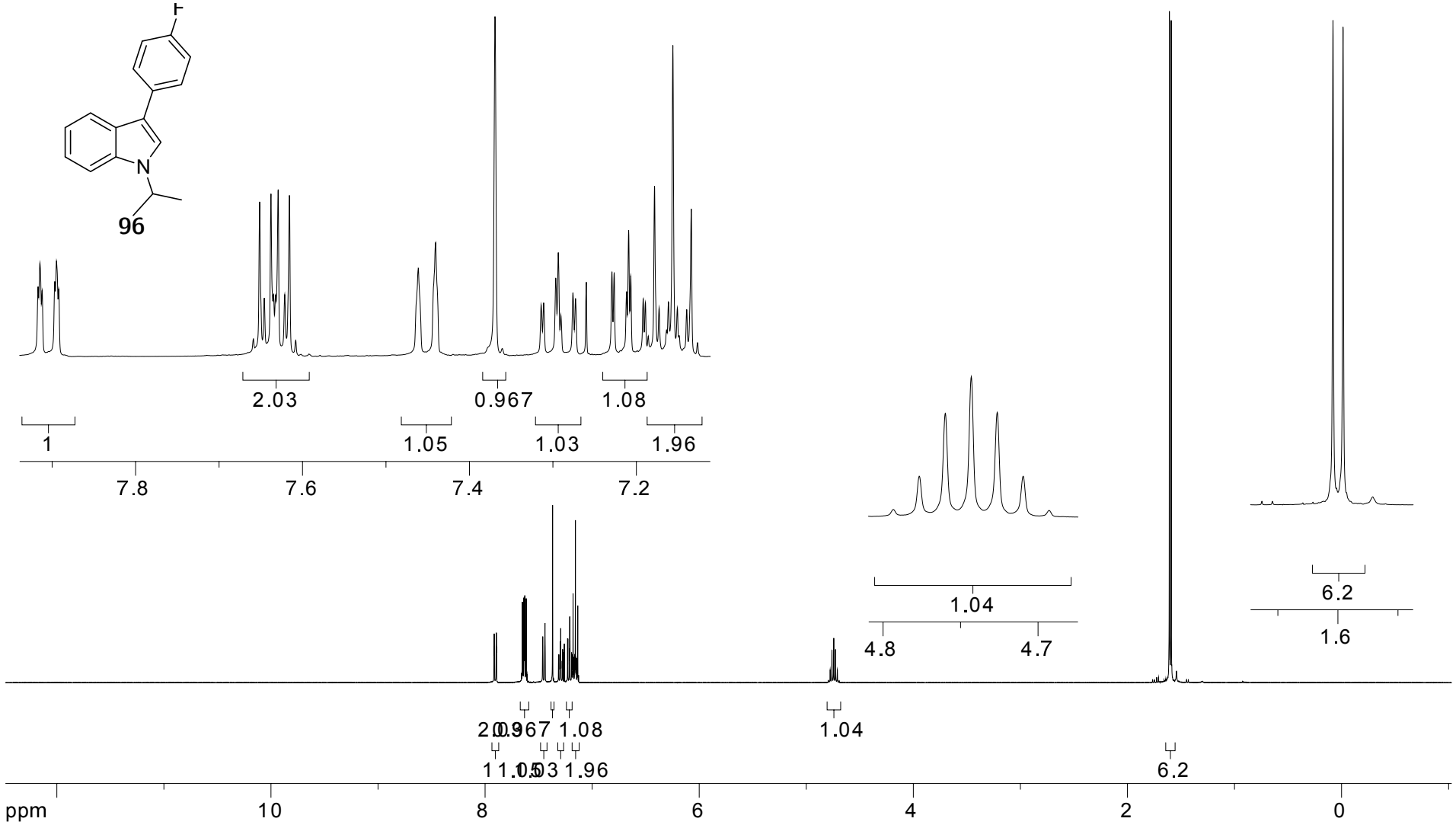

Figure A.115: 400 MHz ^{1}H NMR of **96** in $CDCl_3$

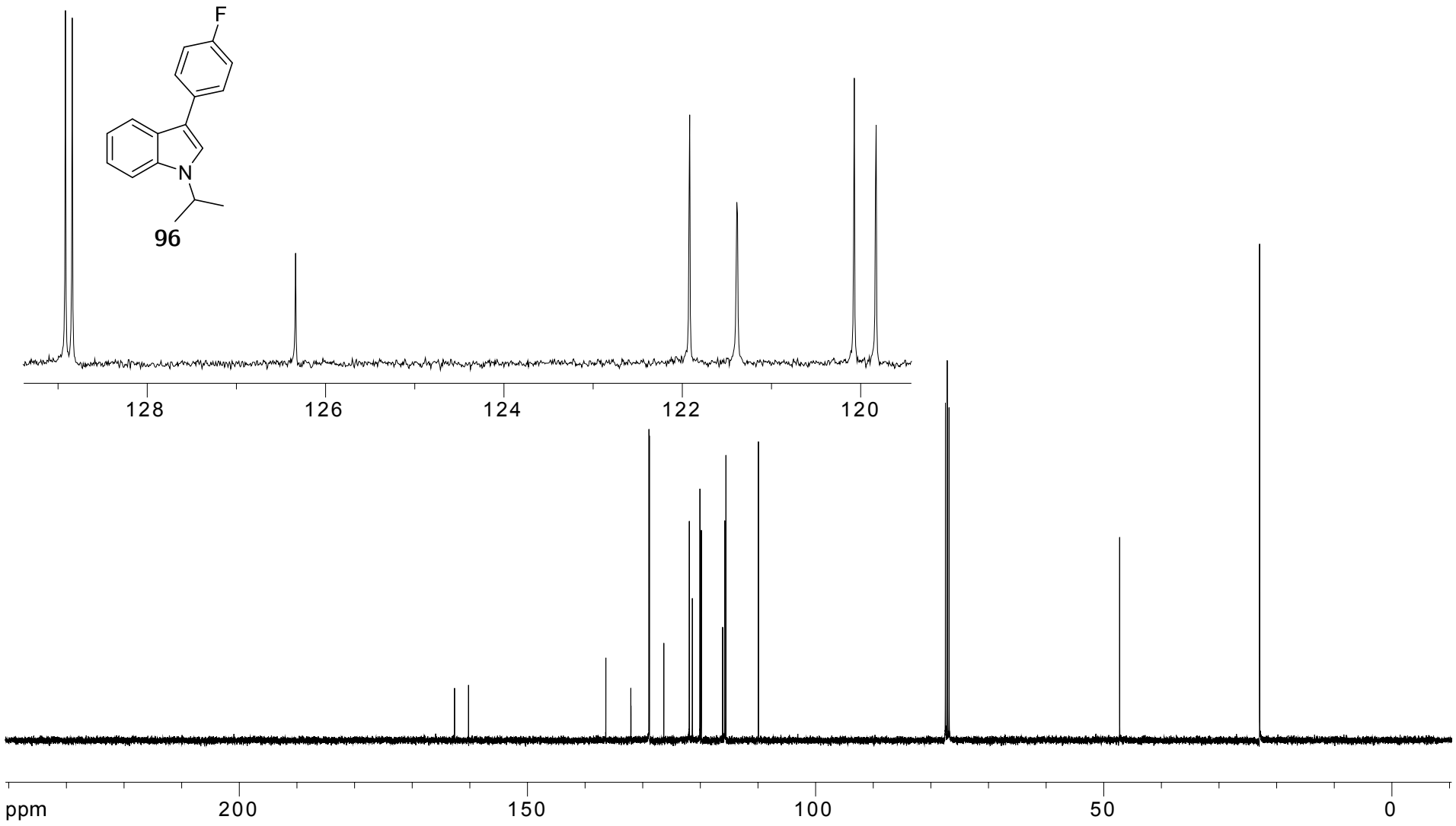

Figure A.116: 100 MHz ^{13}C NMR of **96** in $CDCl_3$

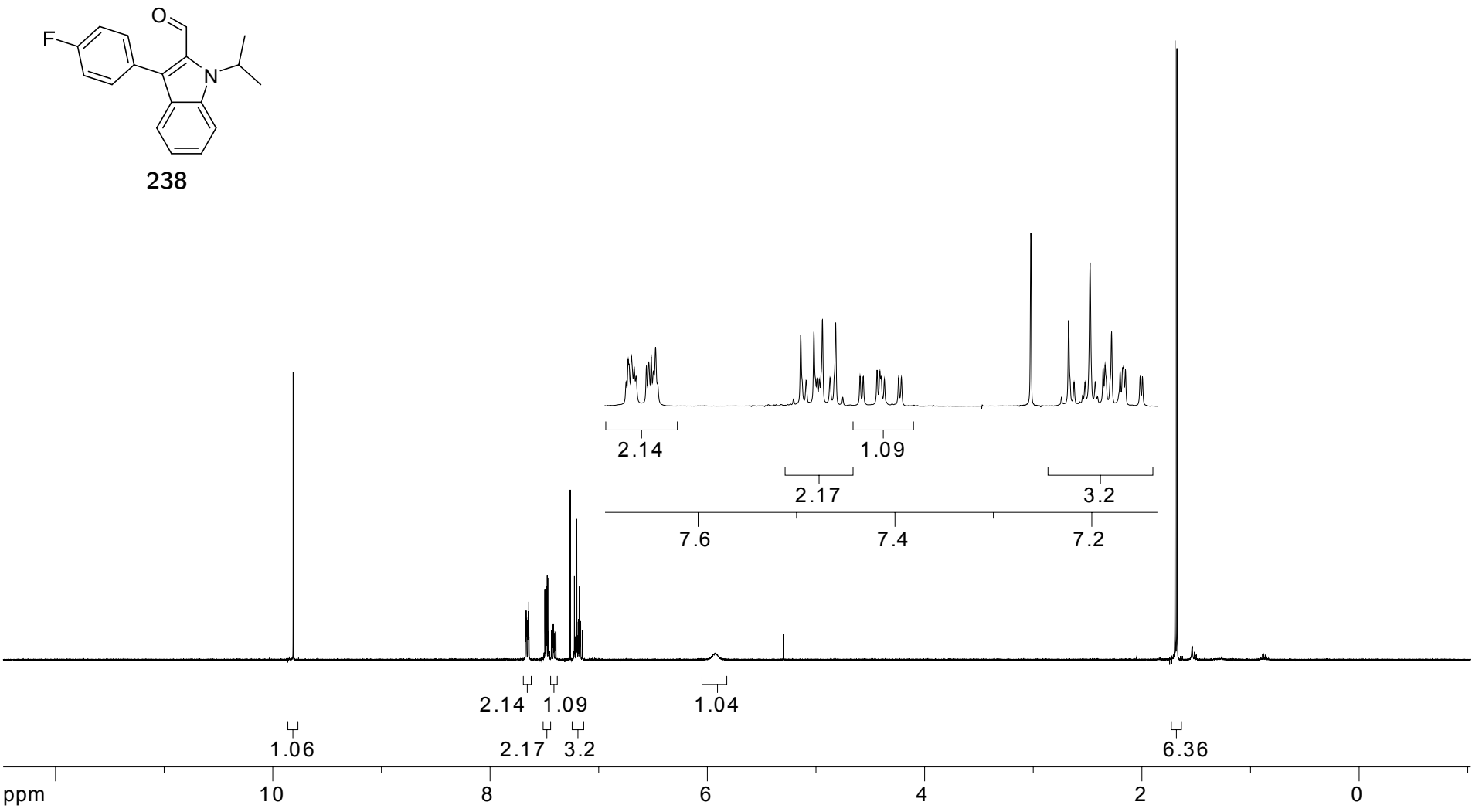

Figure A.117: 400 MHz ^{1}H NMR **238** in $CDCl_3$

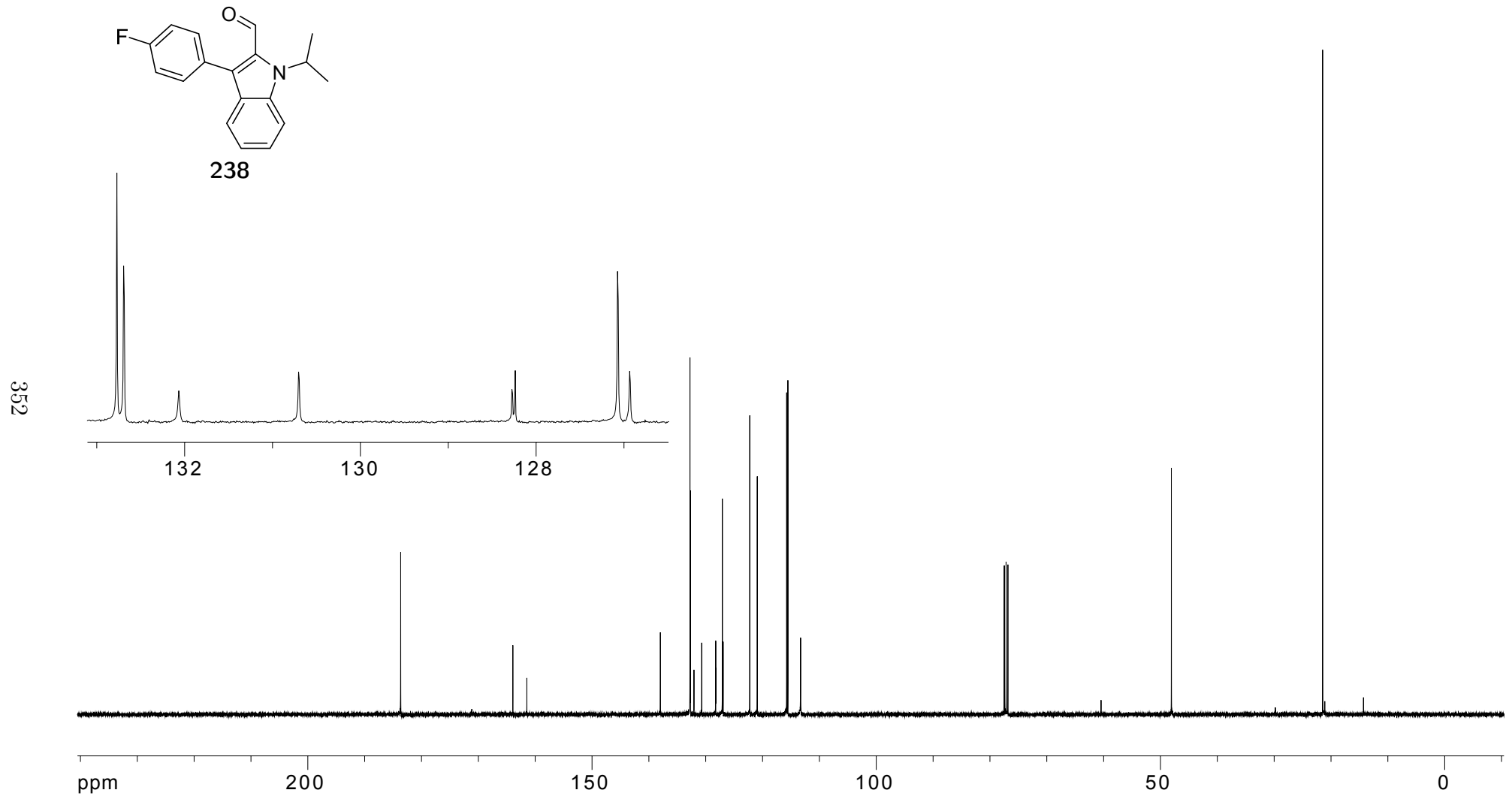

Figure A.118: 100 MHz ^{13}C NMR of **238** in $CDCl_3$

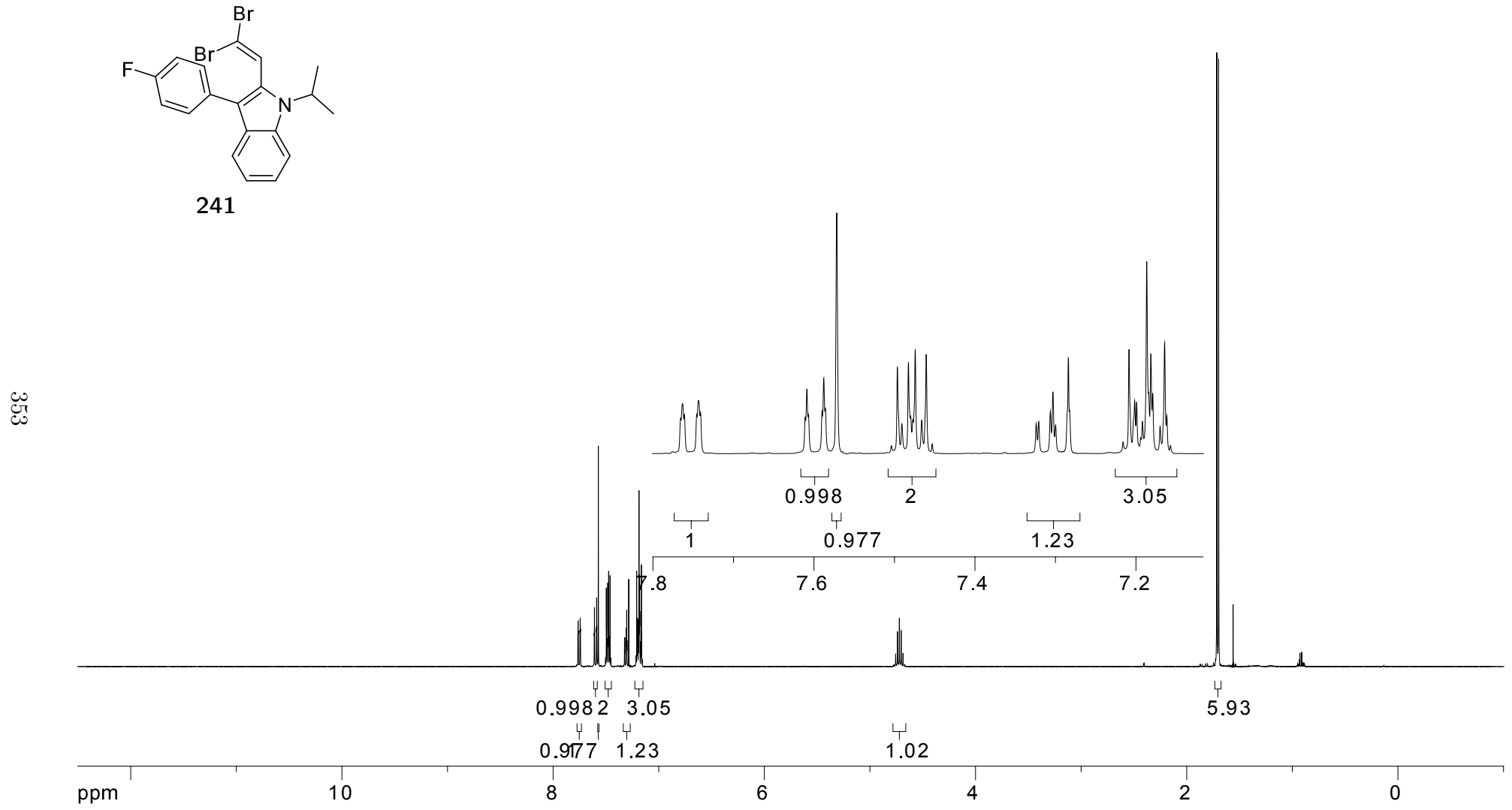

Figure A.119: 400 MHz ^{1}H NMR of **241** in $CDCl_3$

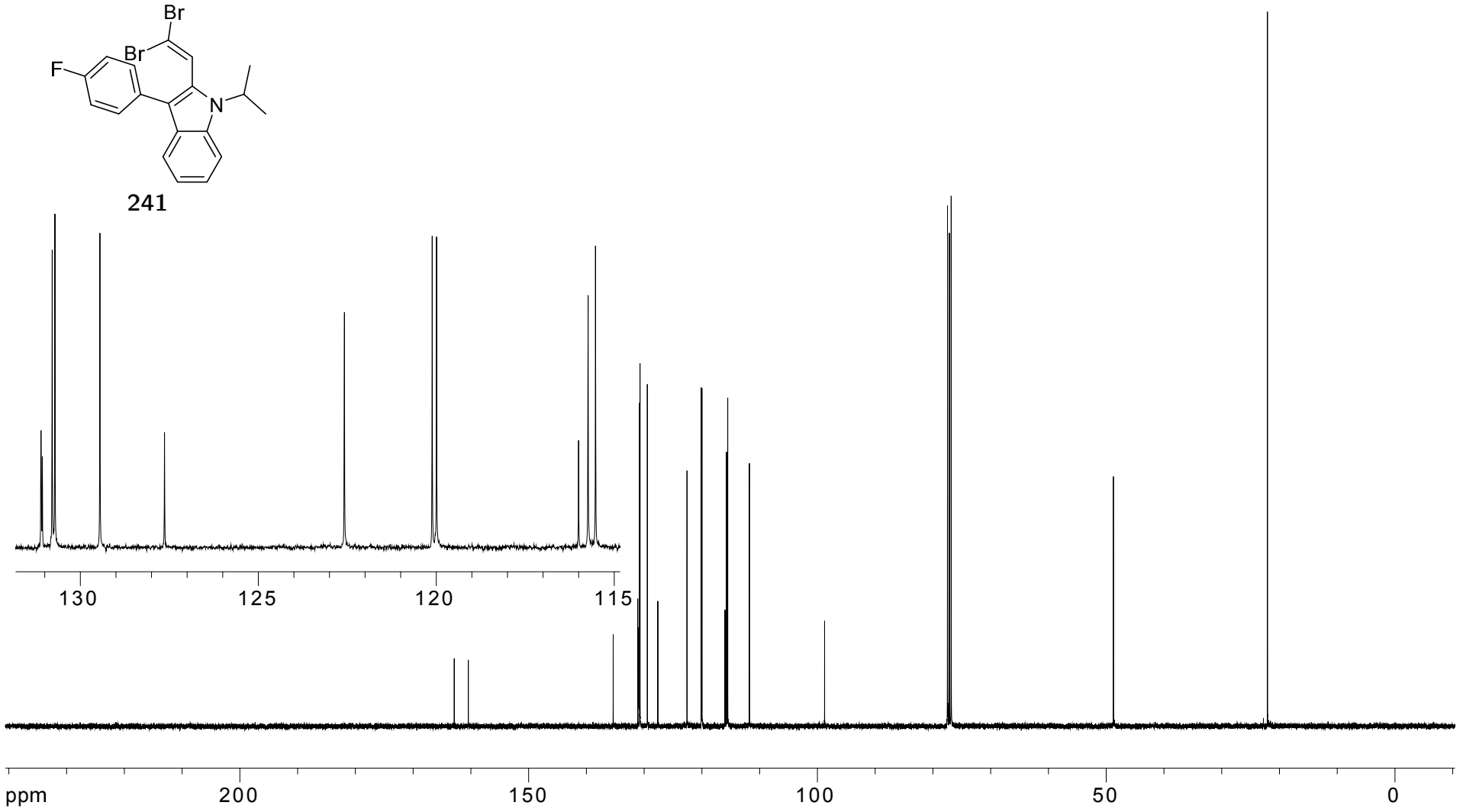

Figure A.120: 100 MHz ^{13}C NMR of **241** in $CDCl_3$

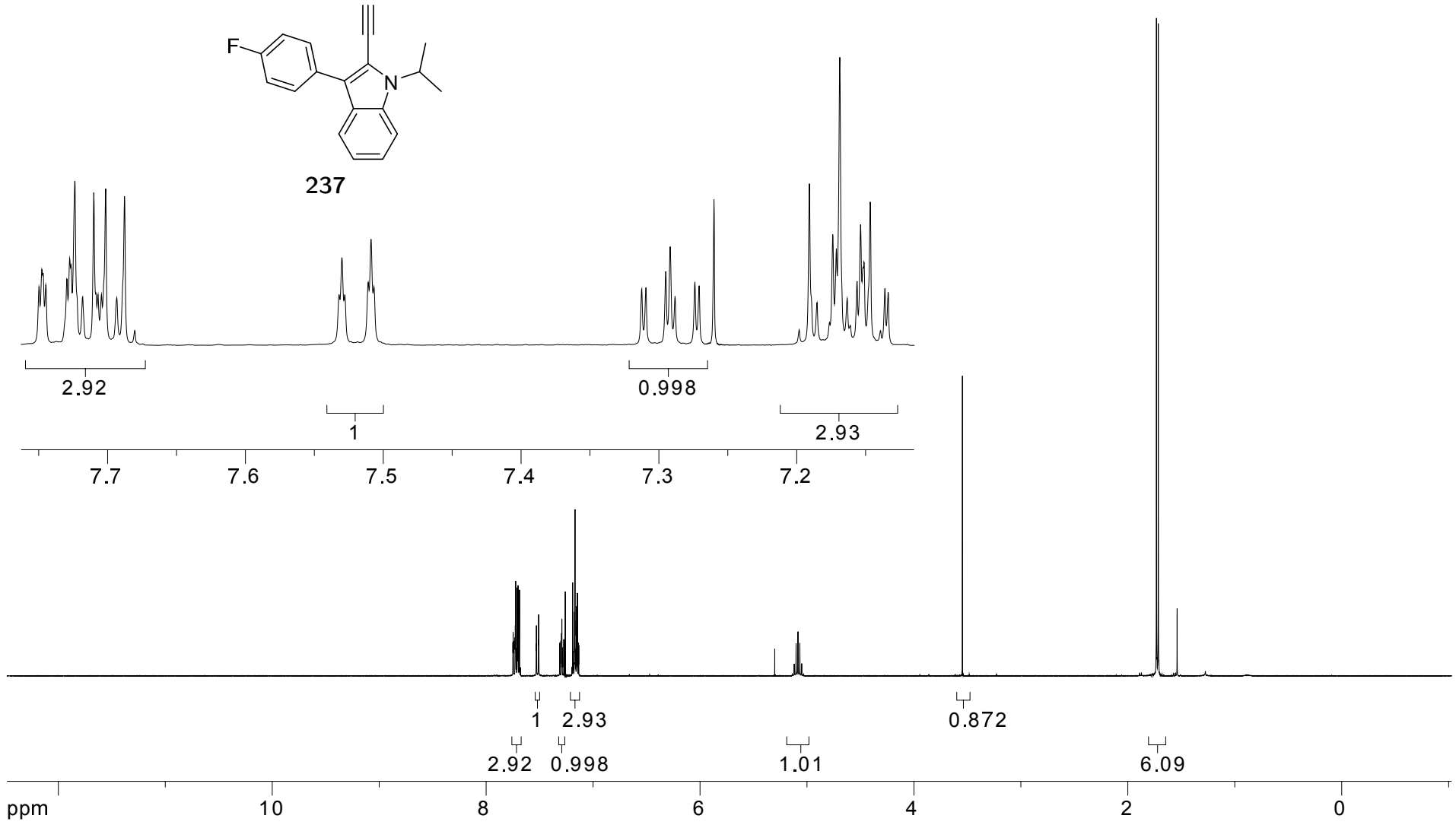

Figure A.121: 400 MHz ^{1}H NMR of **237** in $CDCl_3$

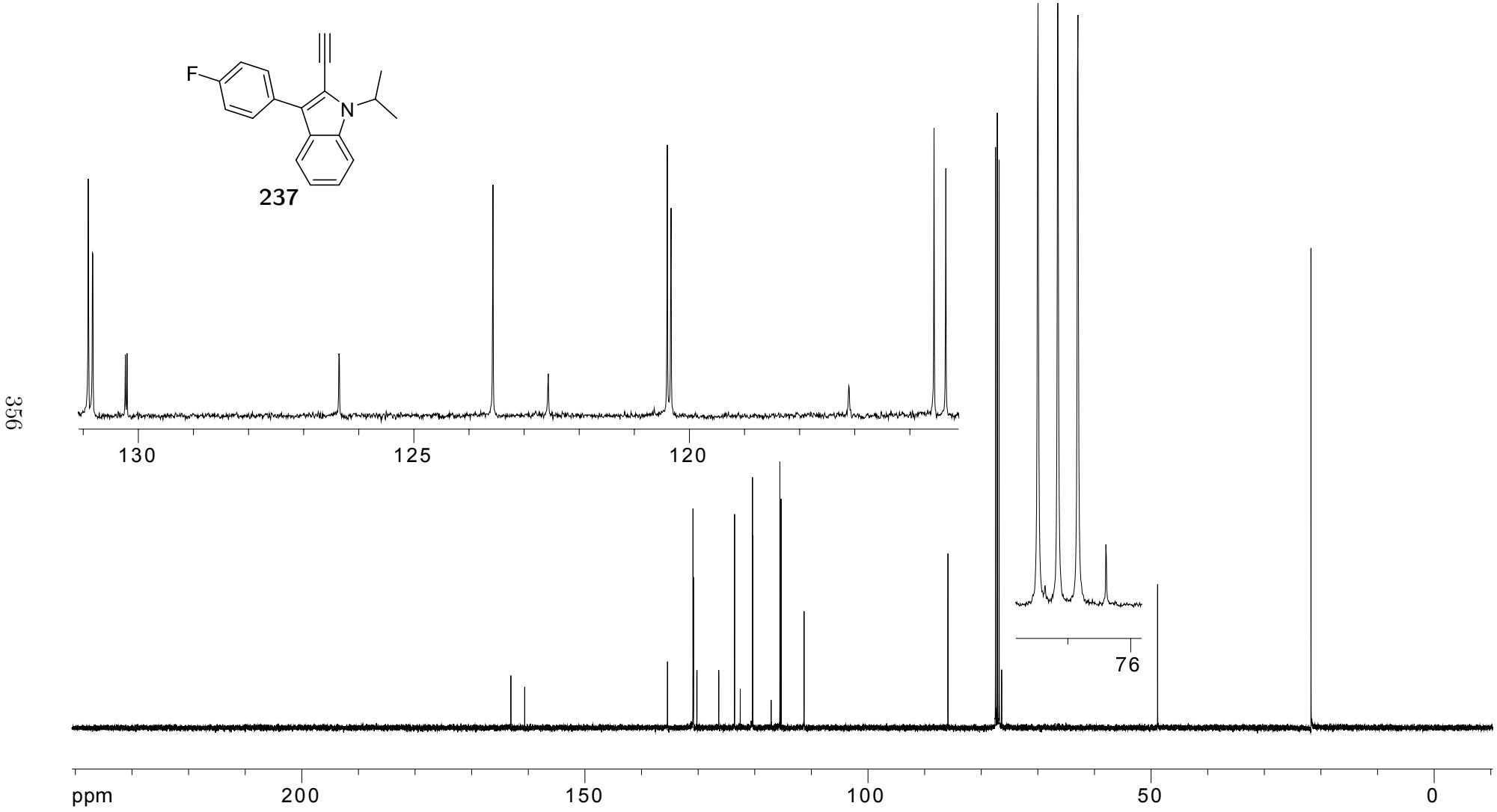

Figure A.122: 100 MHz ^{13}C NMR of **237** in $CDCl_3$

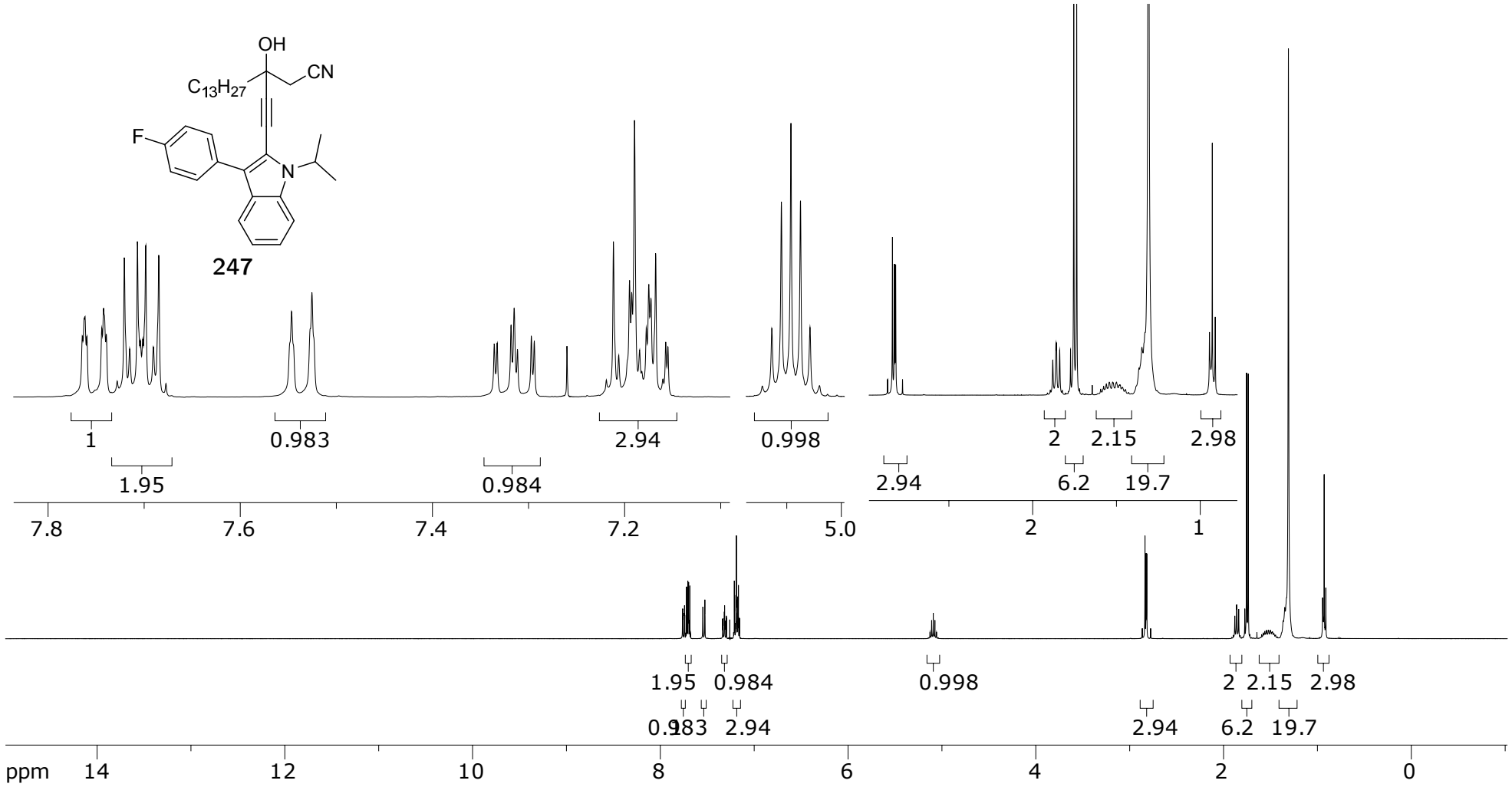

Figure A.123: 400 MHz ^{1}H NMR of **247** in $CDCl_3$

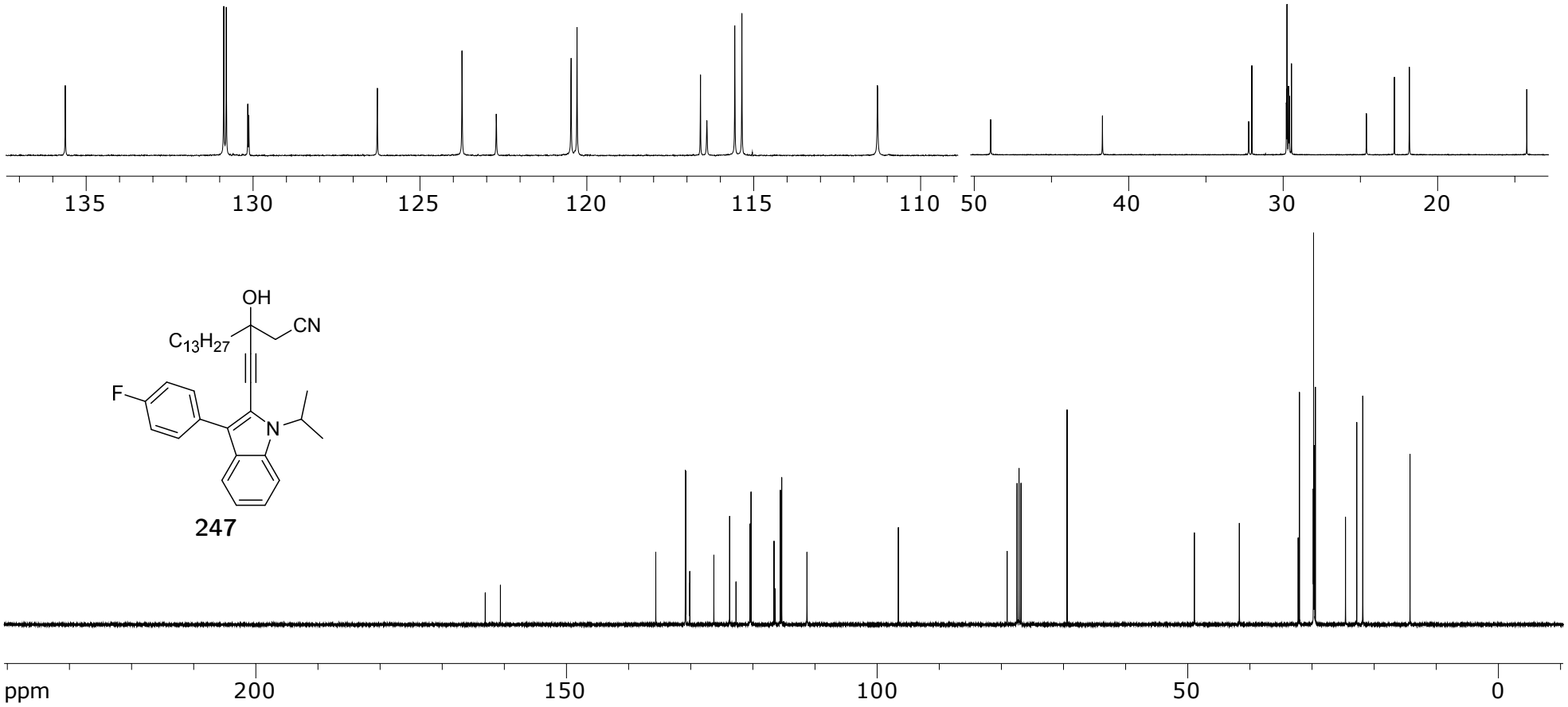

Figure A.124: 100 MHz ^{13}C NMR of **247** in $CDCl_3$

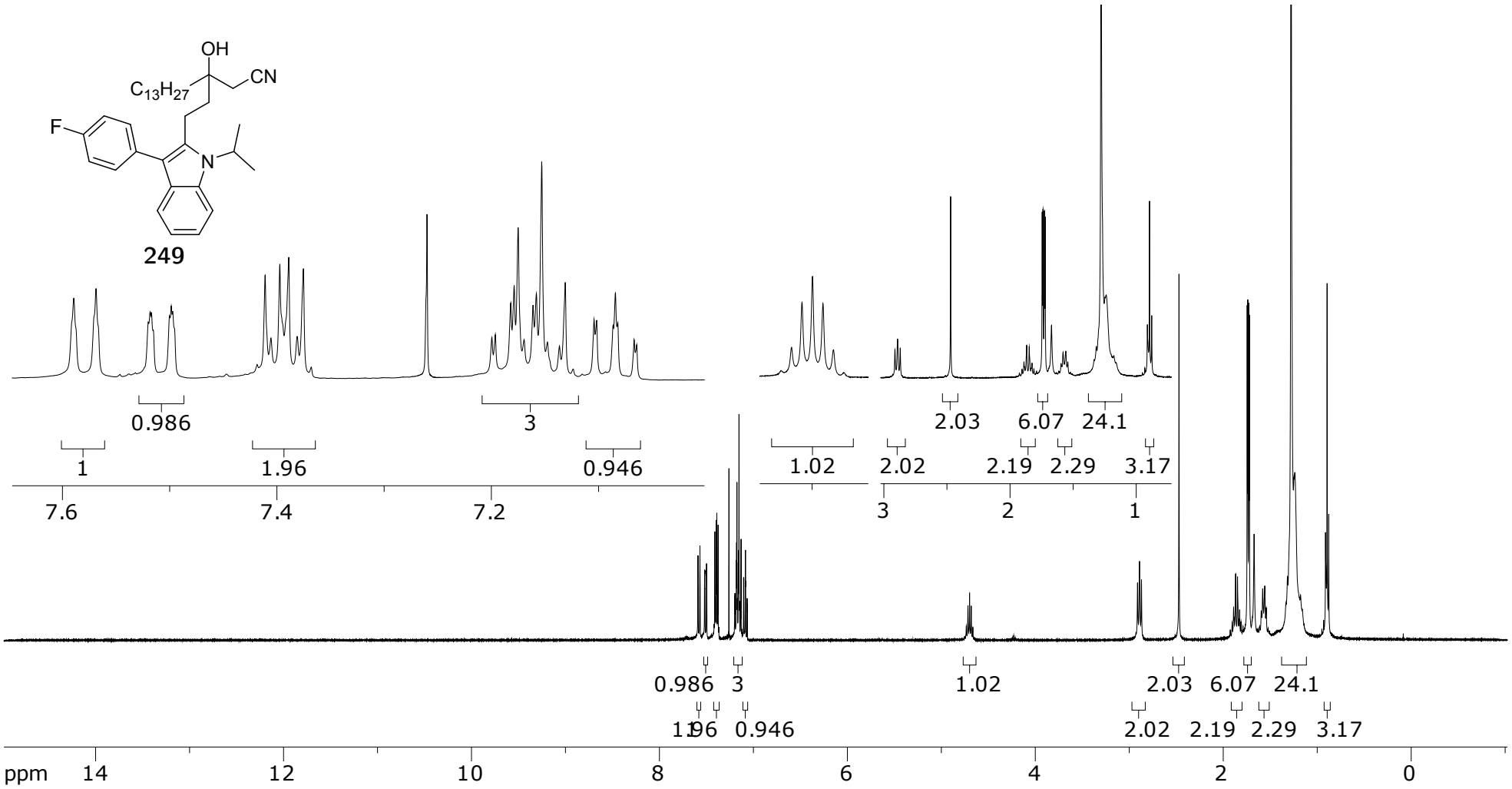

Figure A.125: 400 MHz ^{1}H NMR of **249** in $CDCl_3$

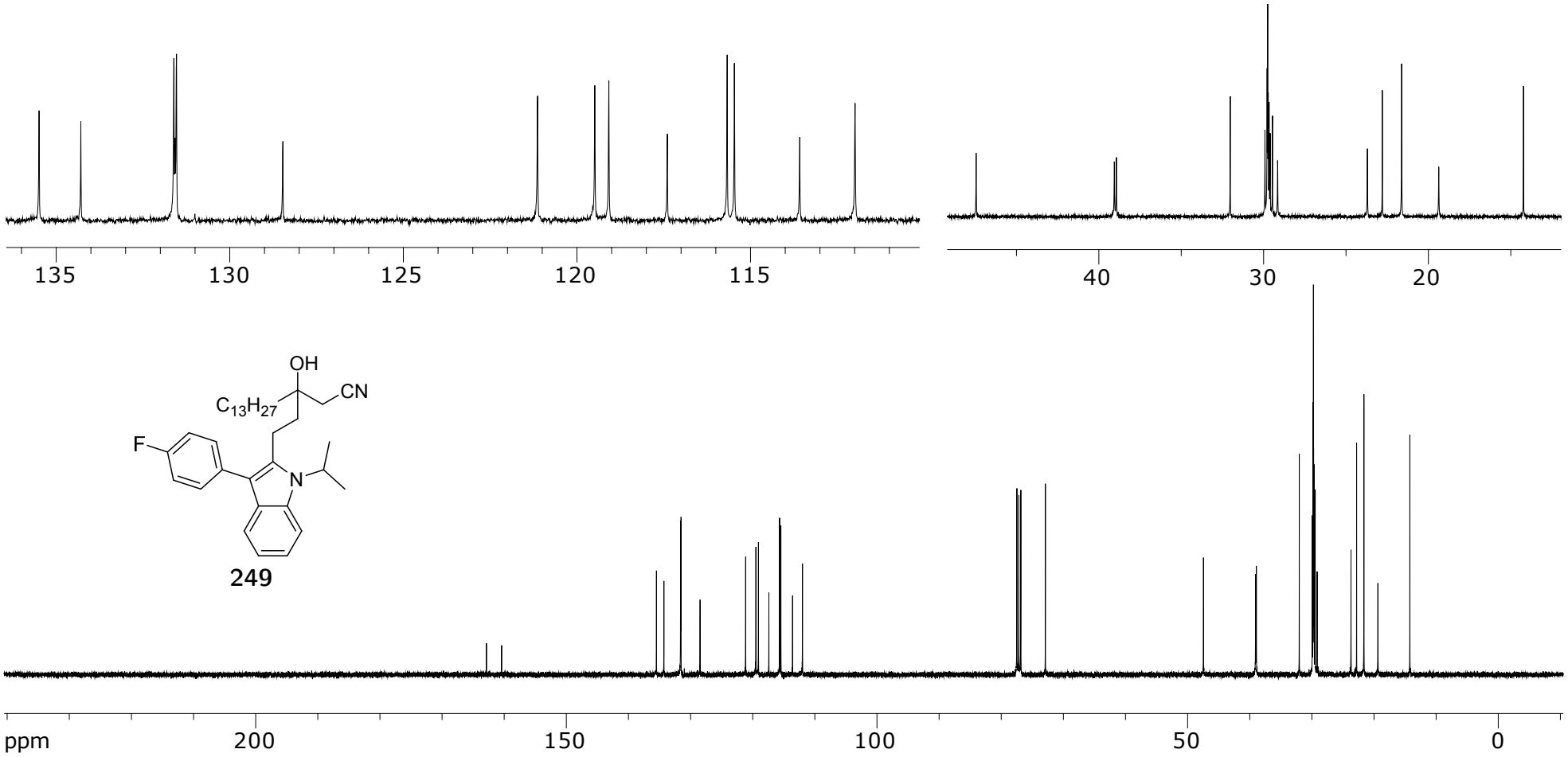

Figure A.126: 100 MHz ^{13}C NMR of **249** in $CDCl_3$

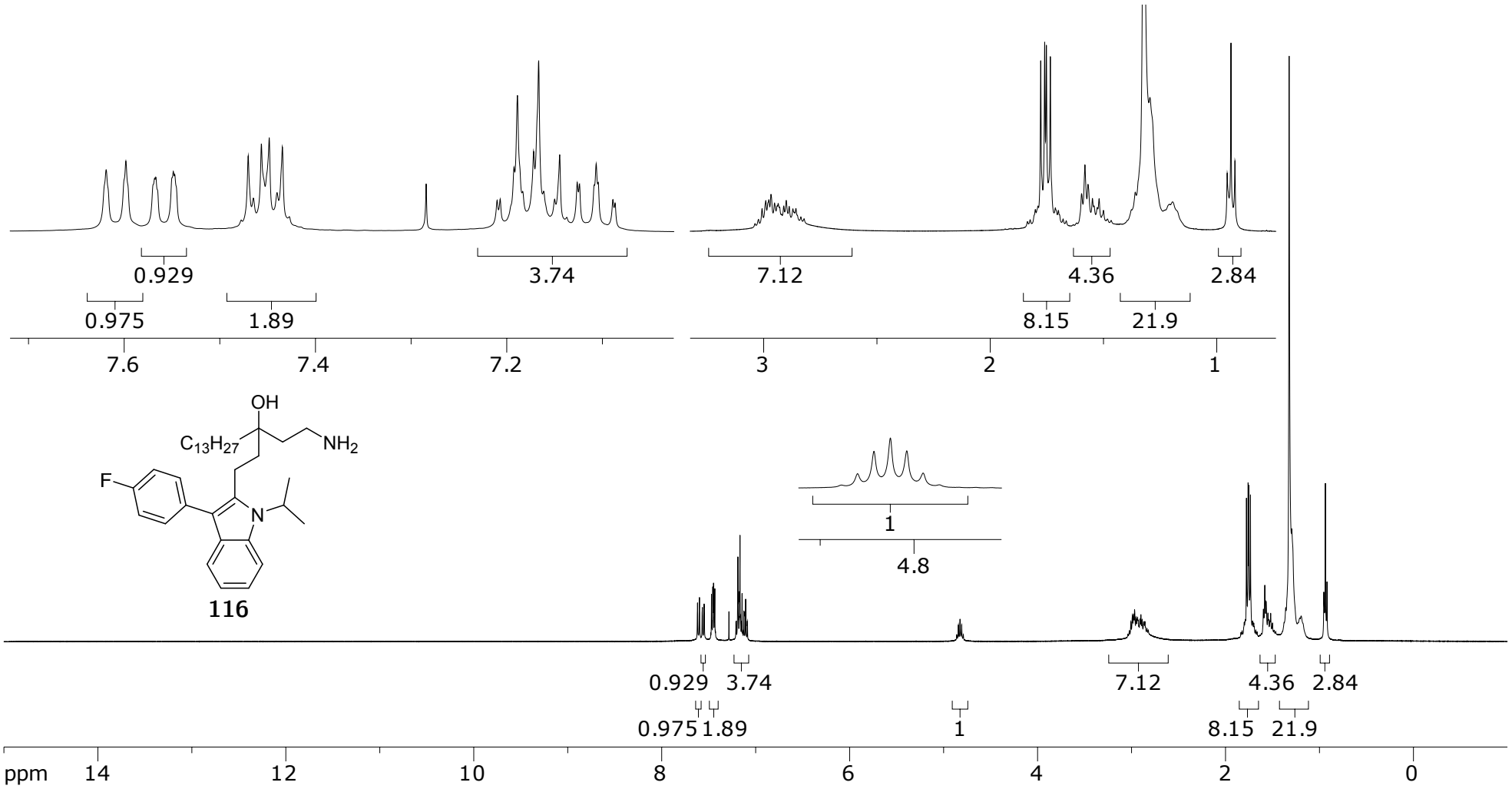

Figure A.127: 400 MHz ^{1}H NMR of **116** in $CDCl_3$

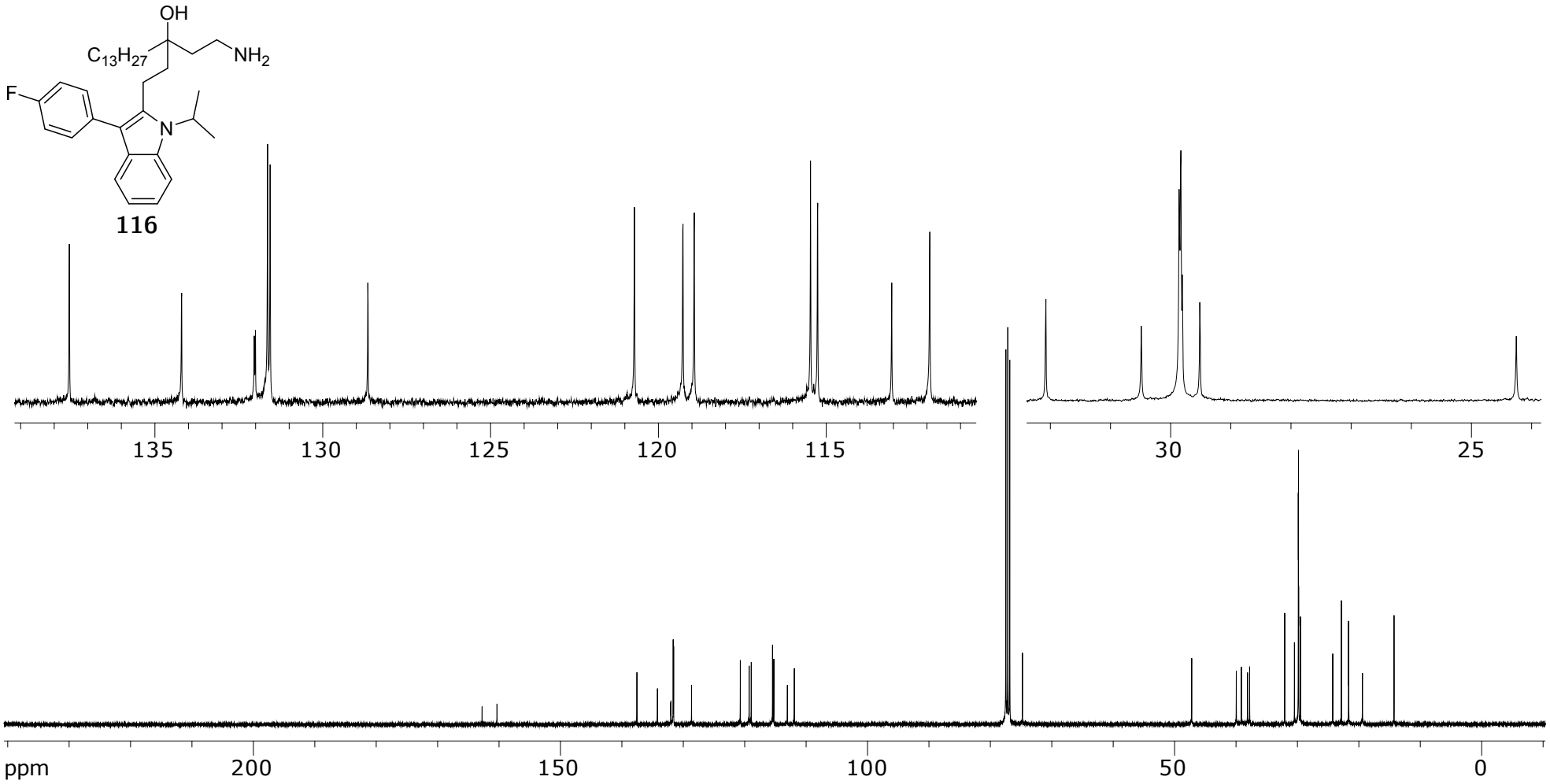

Figure A.128: 100 MHz ^{13}C NMR **116** in $CDCl_3$

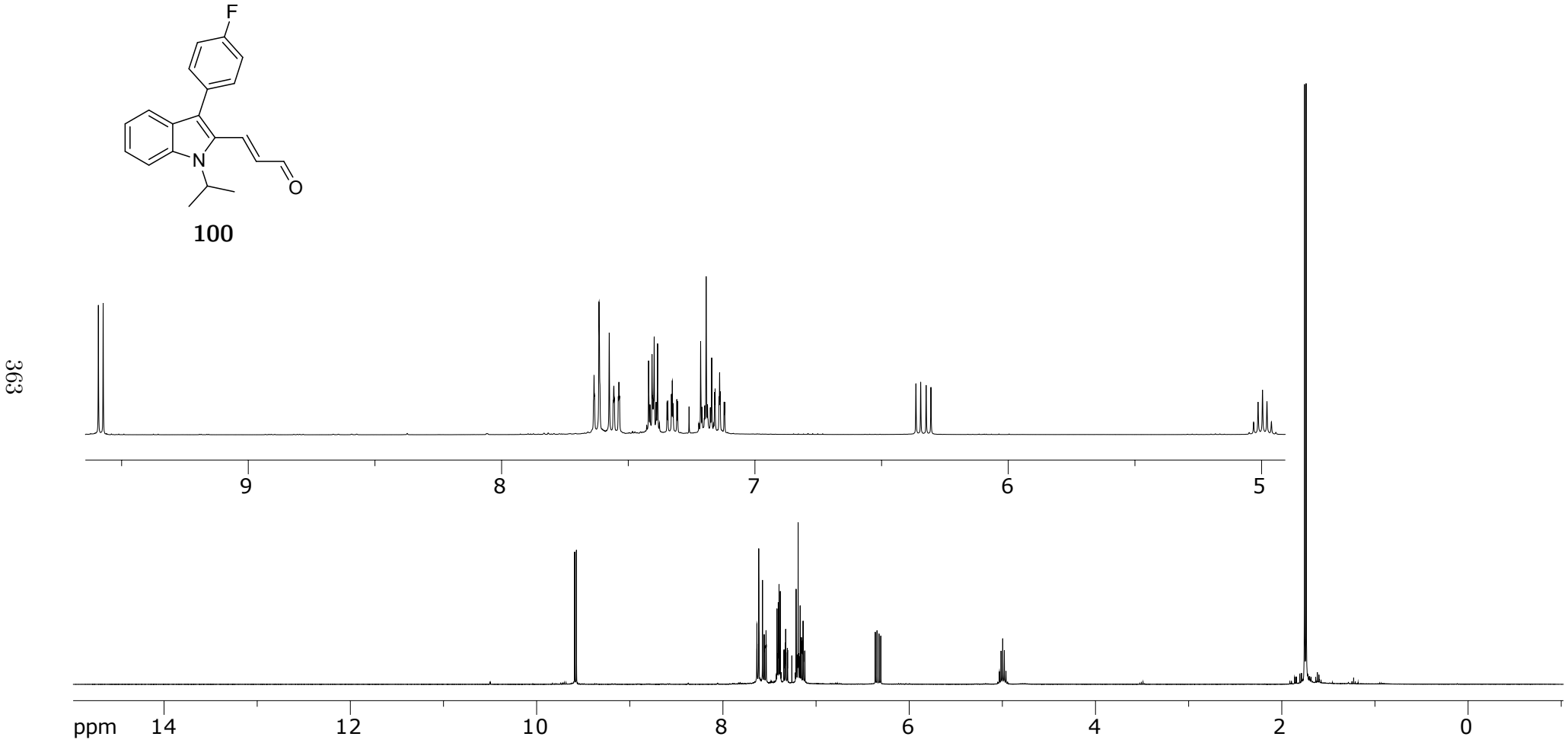

Figure A.129: 400 MHz ^{1}H NMR of **100** in $CDCl_3$

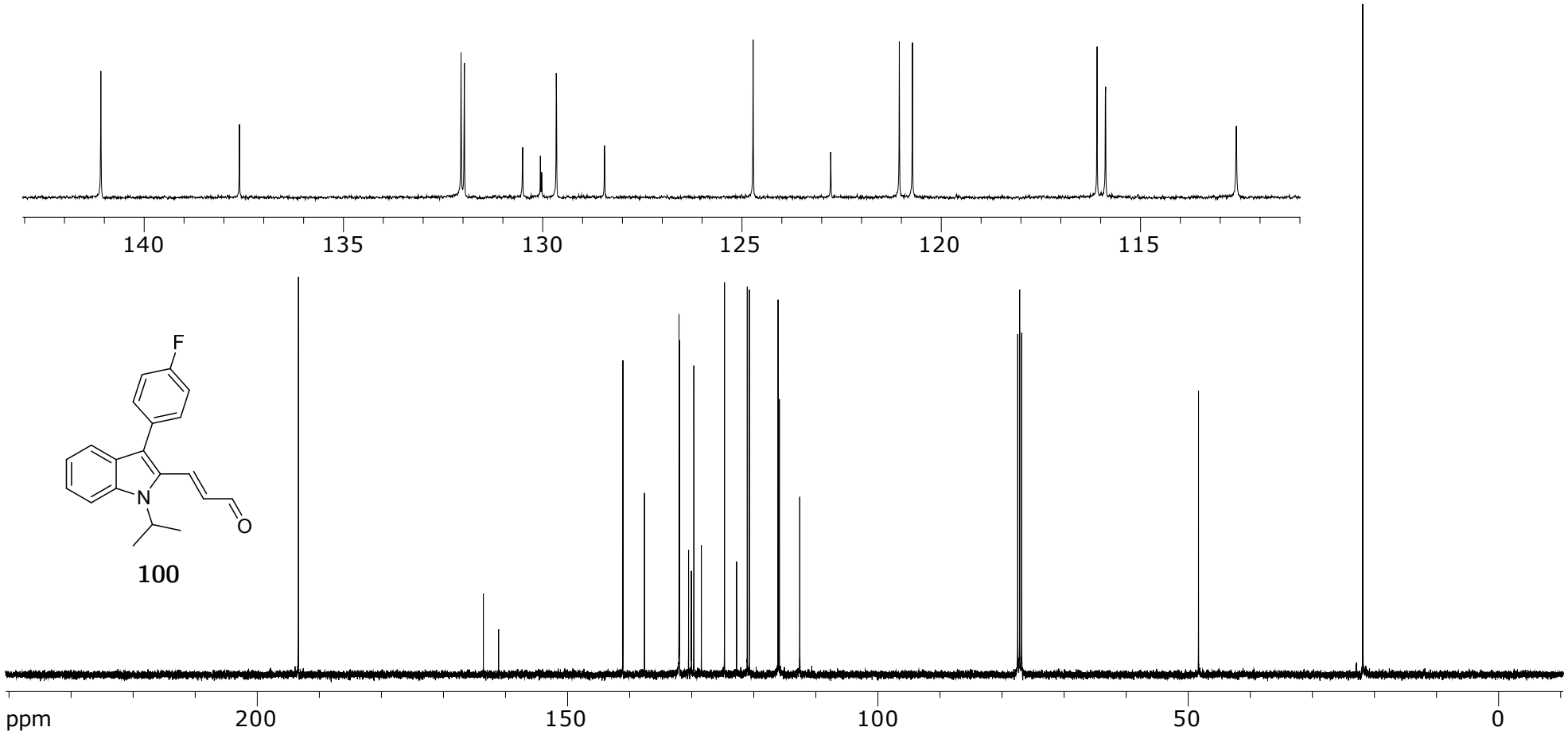

Figure A.130: 100 MHz ^{13}C NMR of **100** in $CDCl_3$

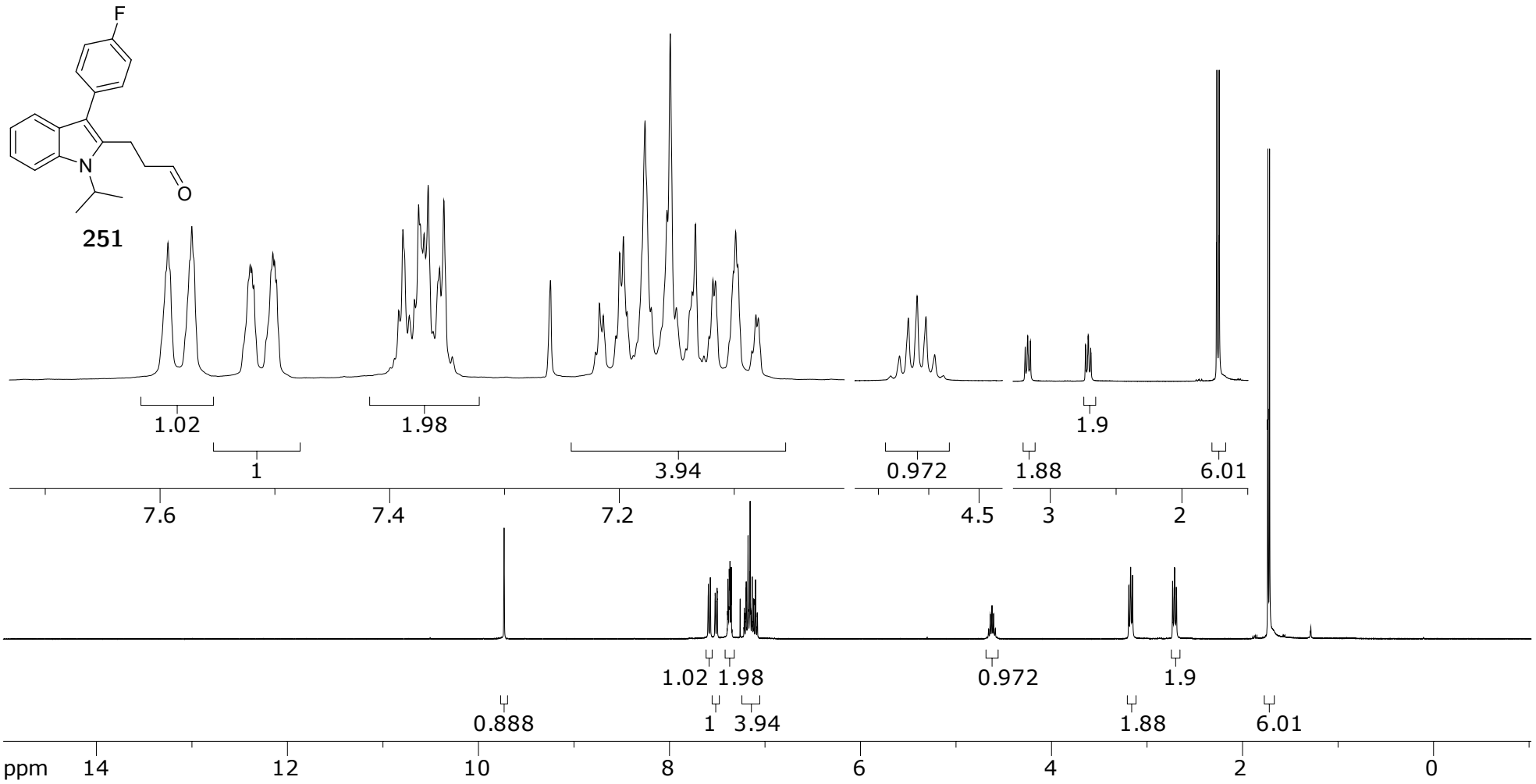

Figure A.131: 400 MHz ^{1}H NMR of **251** in $CDCl_3$

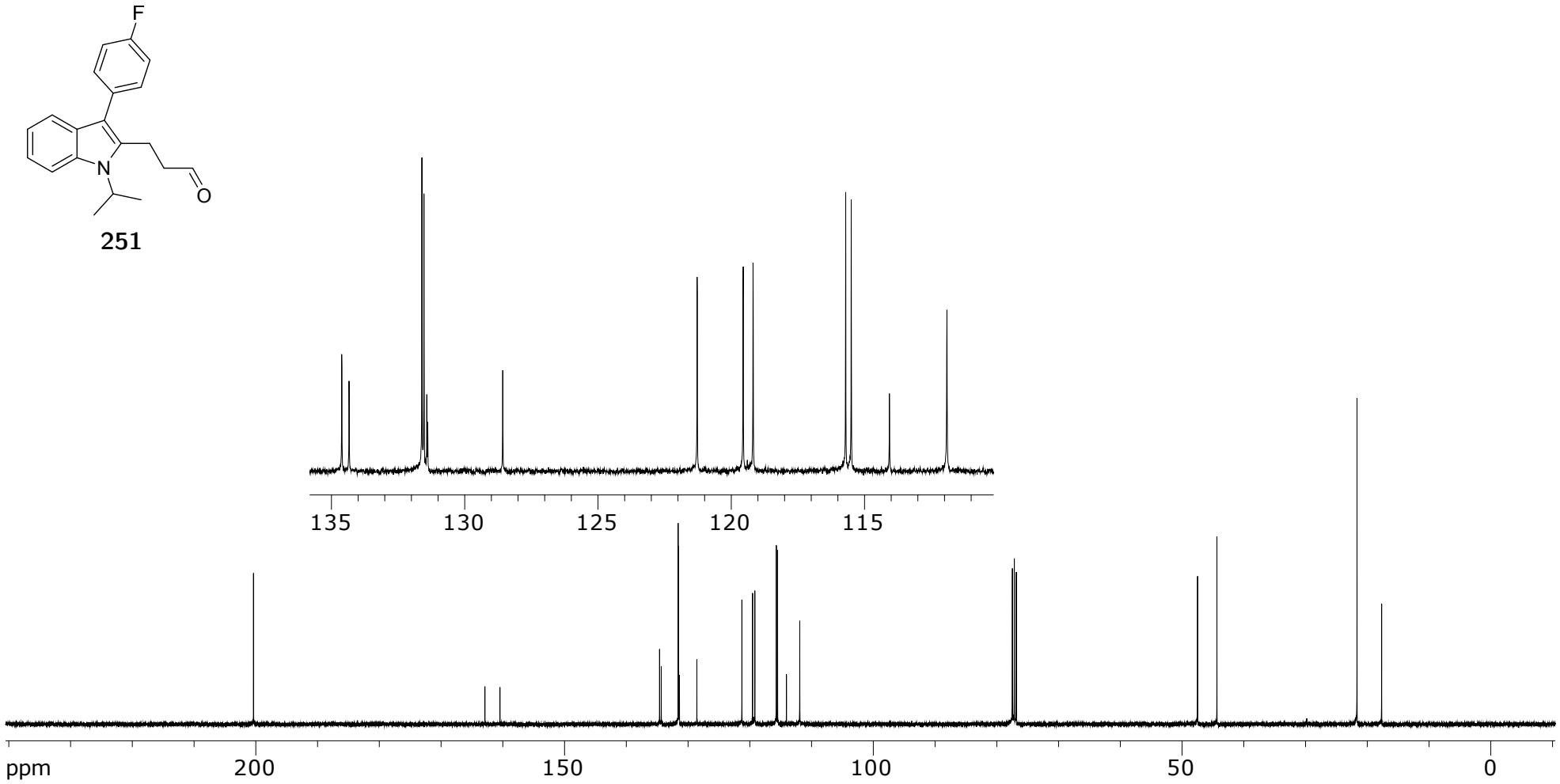

Figure A.132: 100 MHz ^{13}C NMR of **251** in $CDCl_3$

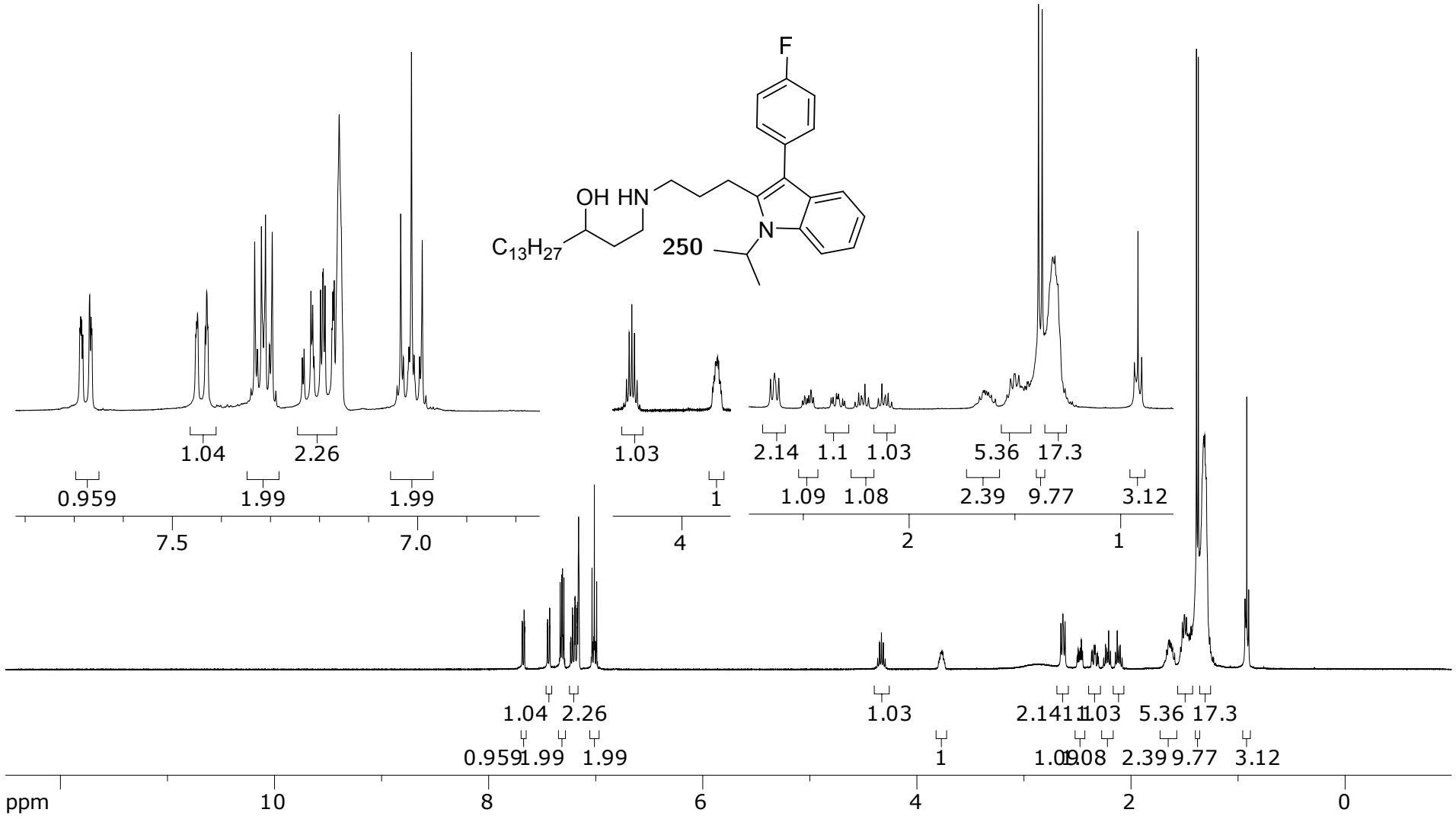

Figure A.133: 400 MHz ^{1}H NMR of **250** in C_6D6_6

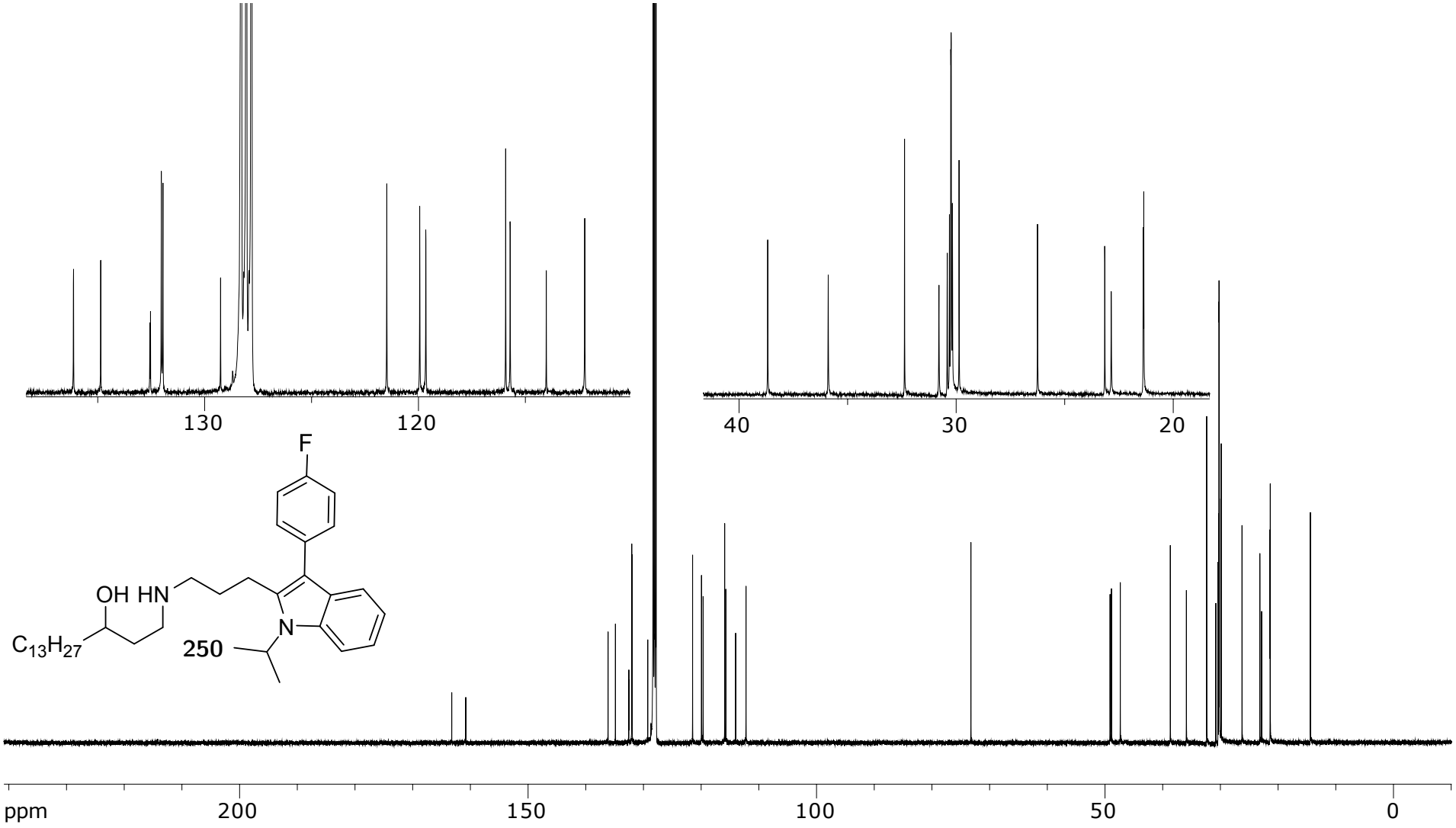

Figure A.134: 100 MHz ^{13}C NMR of **250**in C_6D6_6

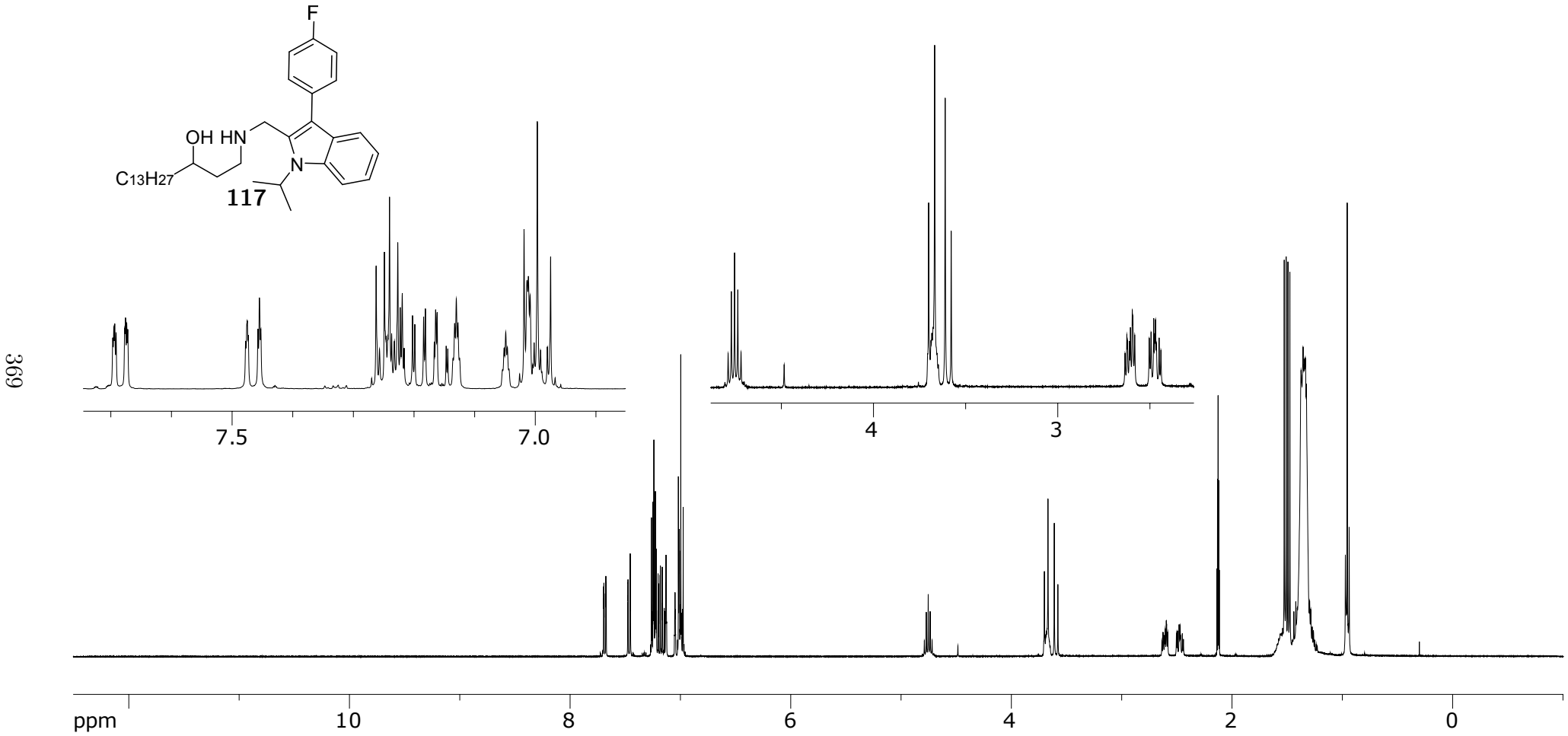

Figure A.135: 400 MHz ^{1}H NMR of **117** in $C_6D_5CD_3$

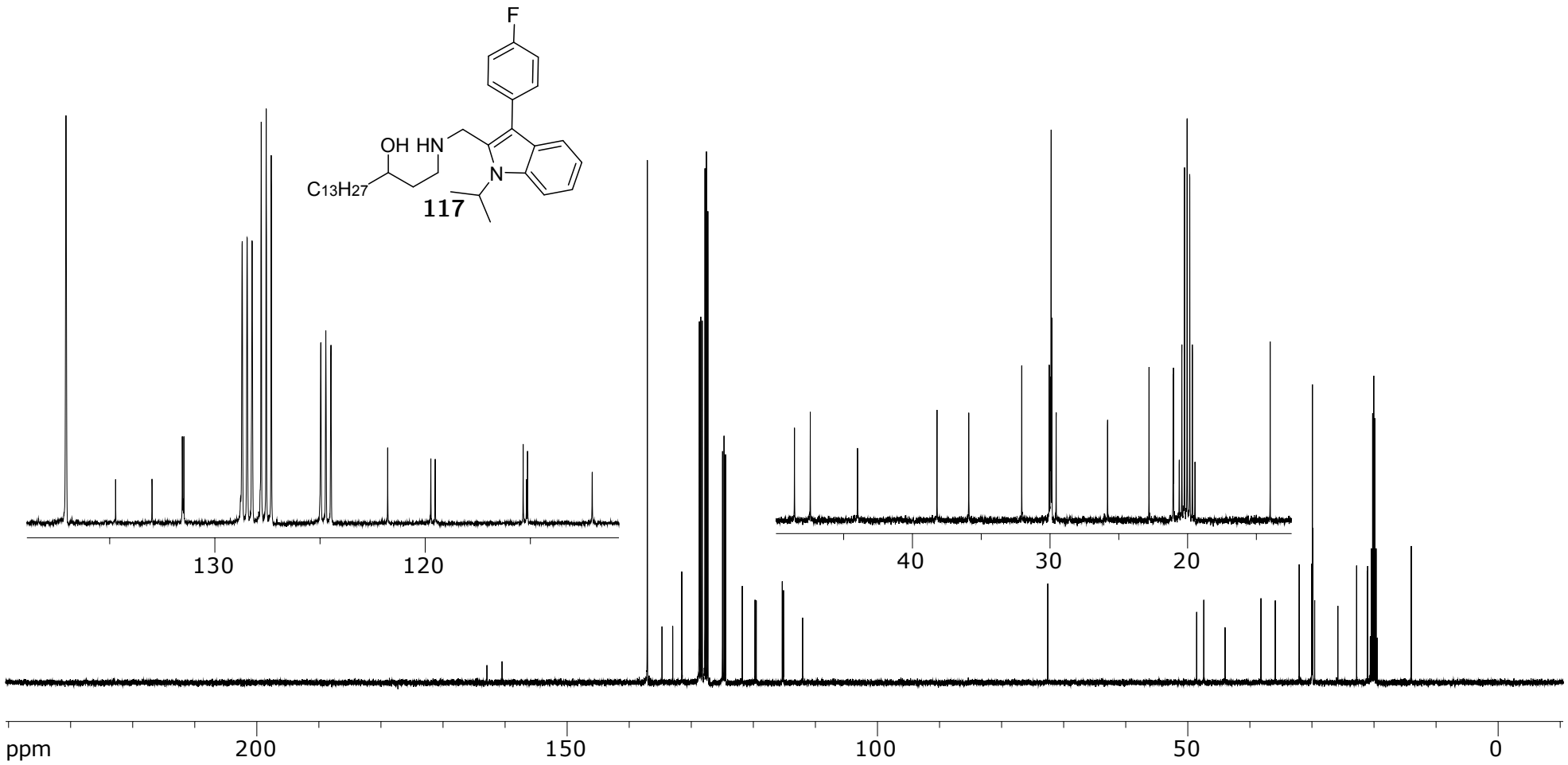

Figure A.136: 100 MHz ^{13}C NMR **117** in $C_6D_5CD_3$

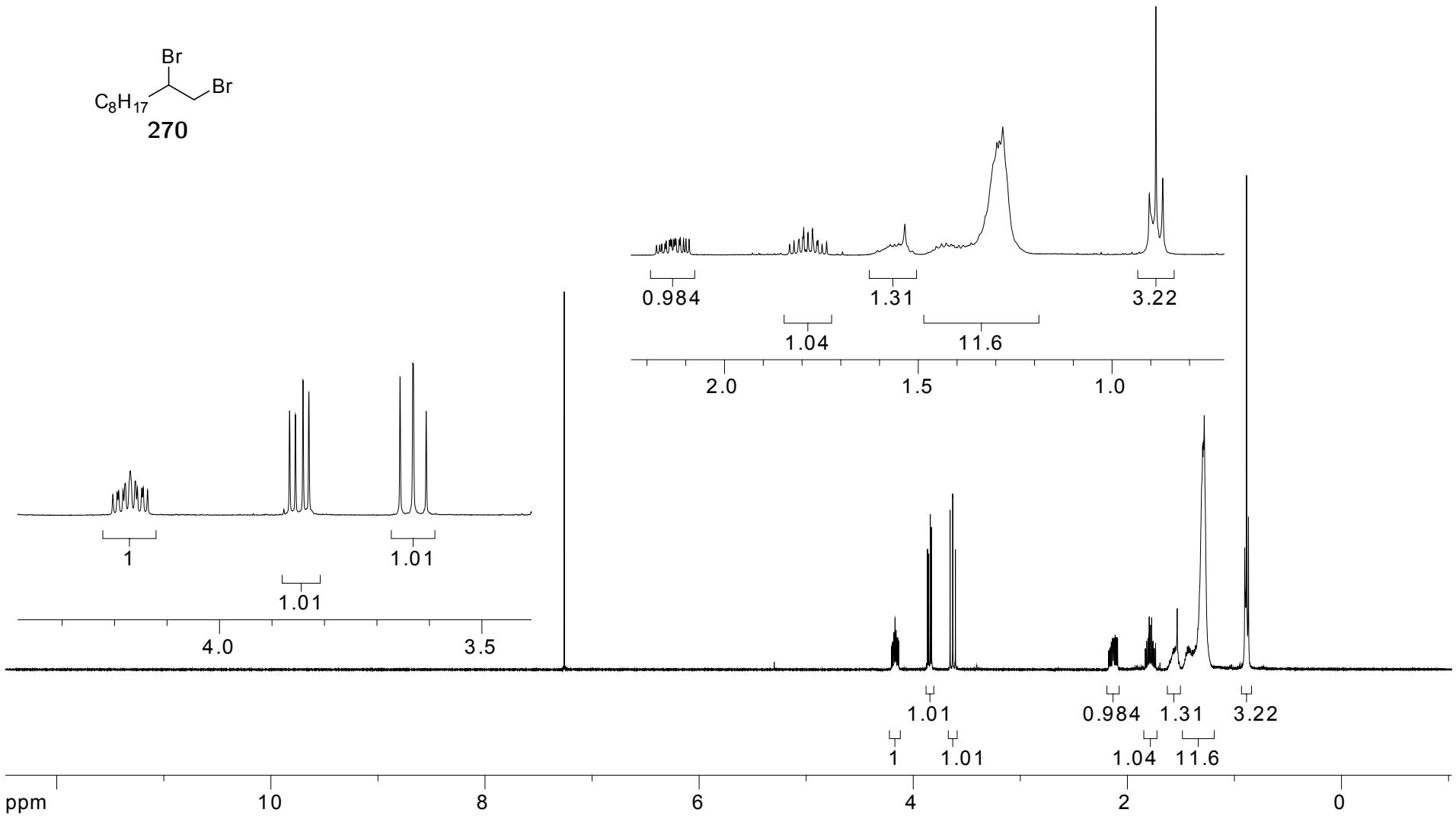

Figure A.137: 100 MHz ^{1}H NMR in $CDCl_3$ of **270**

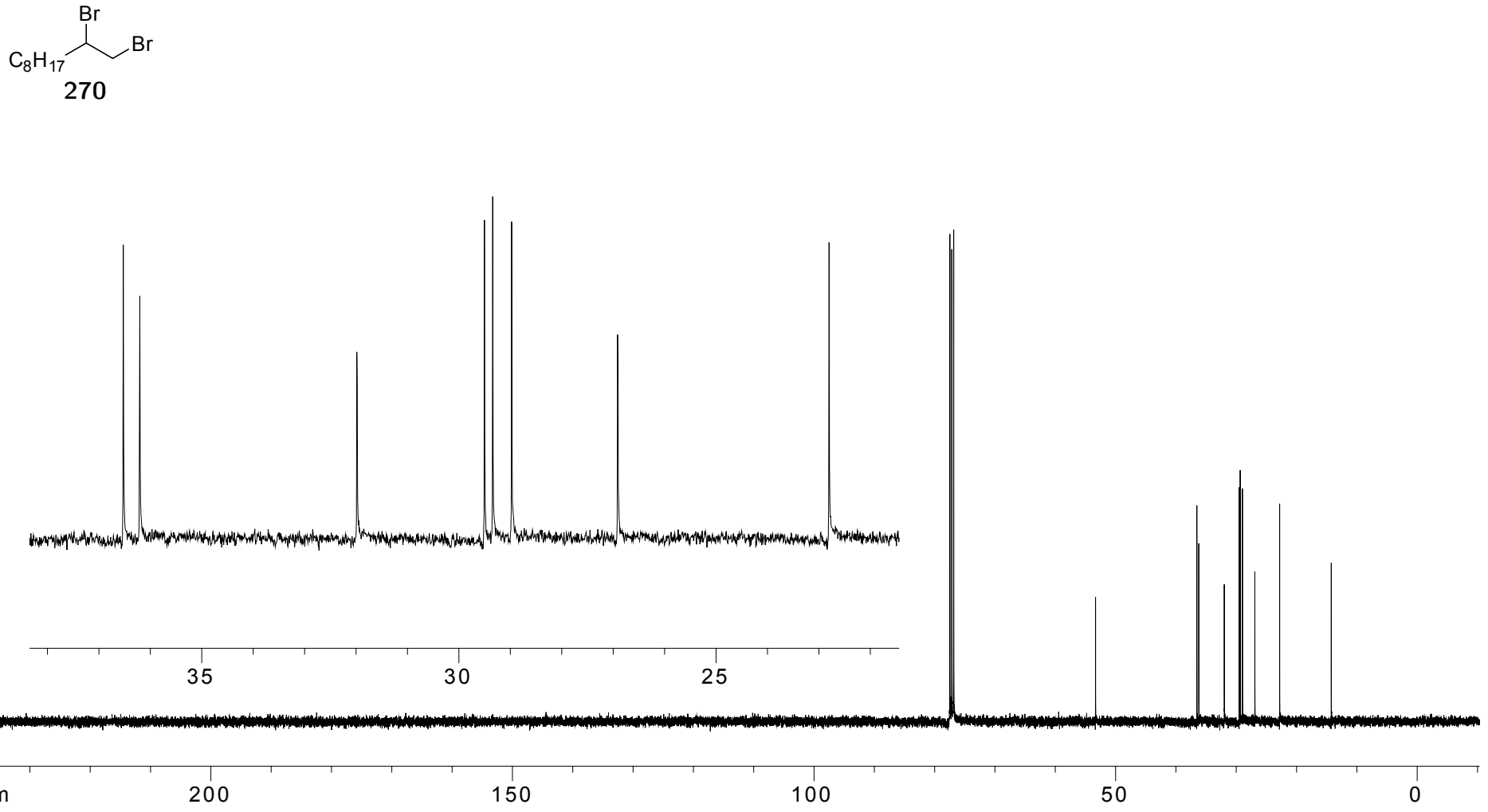

Figure A.138: 100 MHz ^{13}C NMR in $CDCl_3$ of **270**

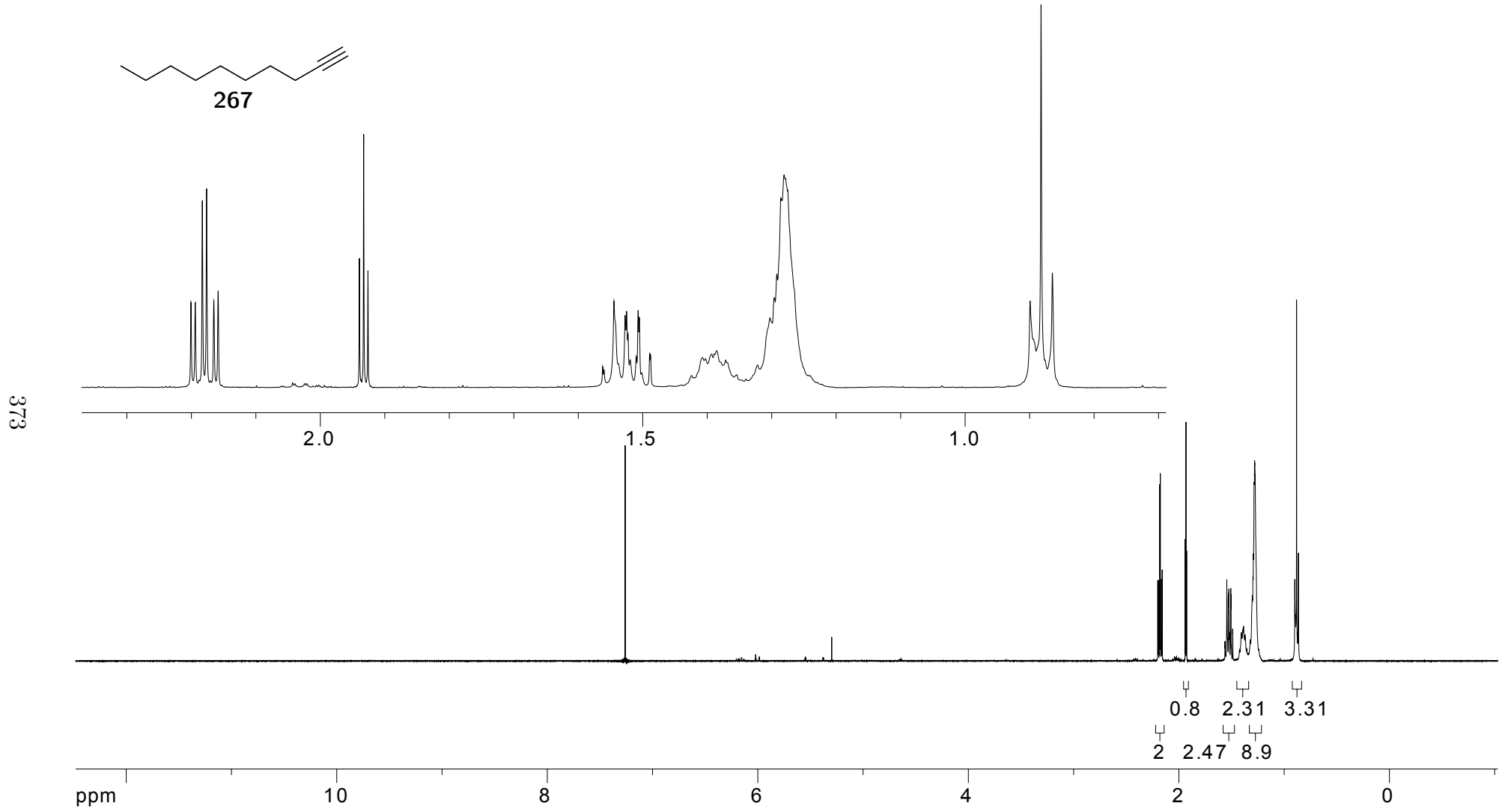

Figure A.139: 100 MHz ^{1}H NMR in $CDCl_3$ of **267**

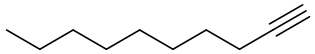

267

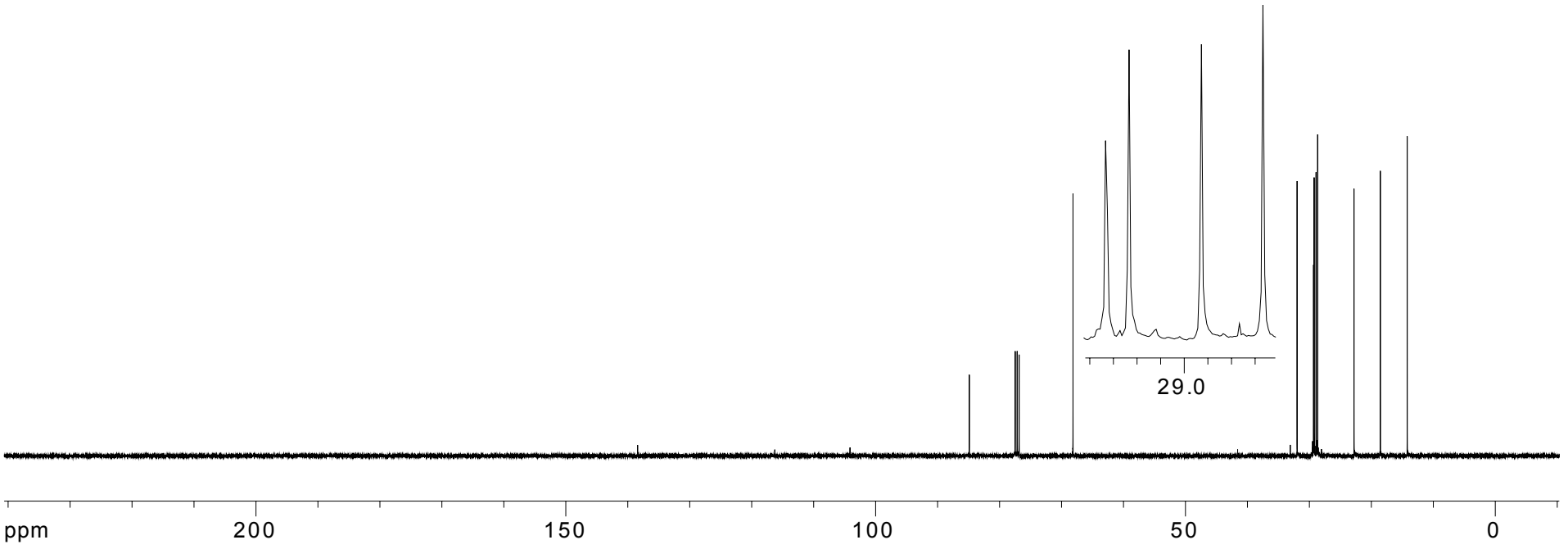

Figure A.140: 100 MHz ^{13}C NMR in $CDCl_3$ of **267**

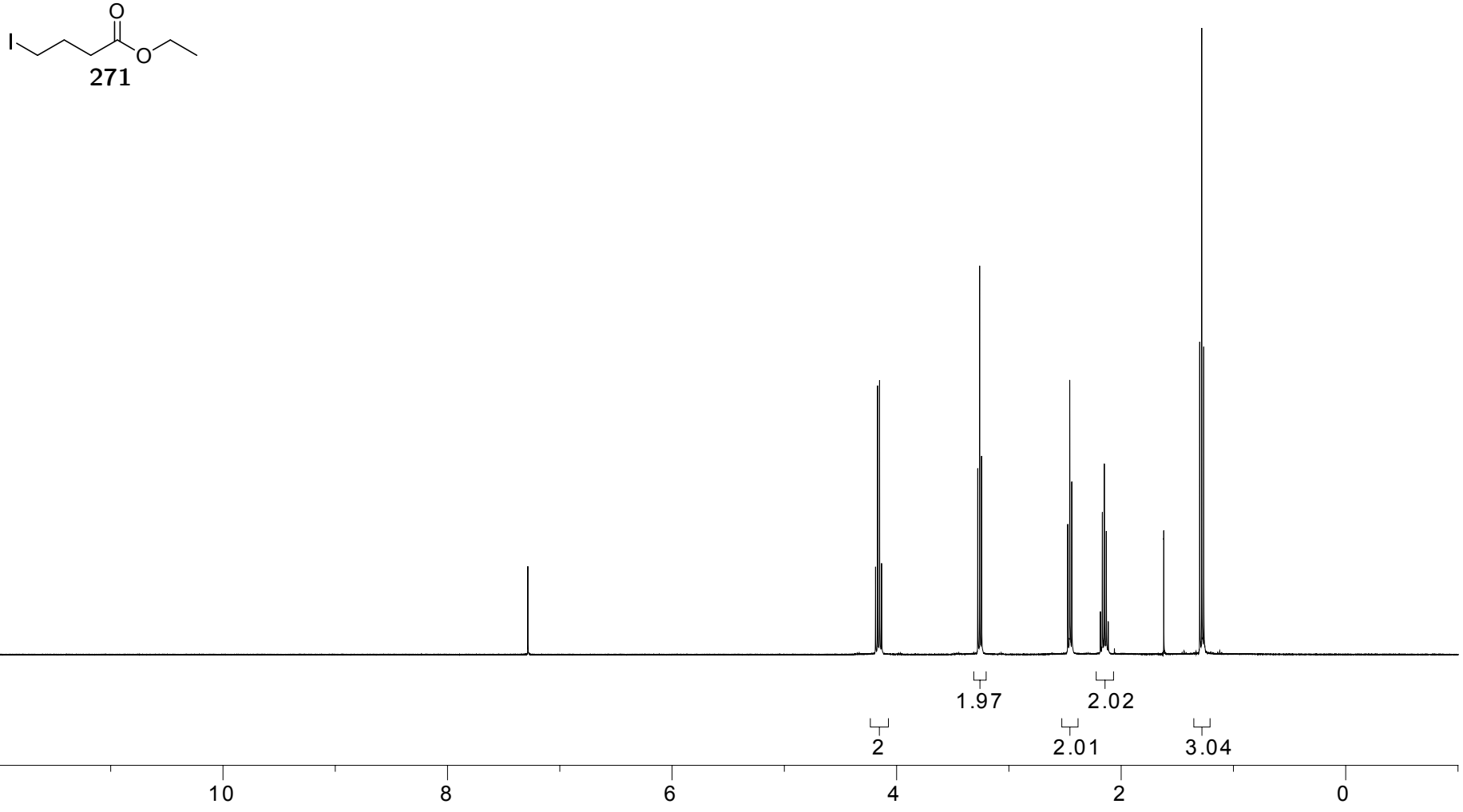

Figure A.141: 400 MHz ^{1}H NMR in $CDCl_3$ of **271**

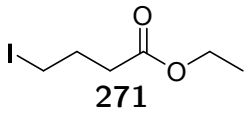

271

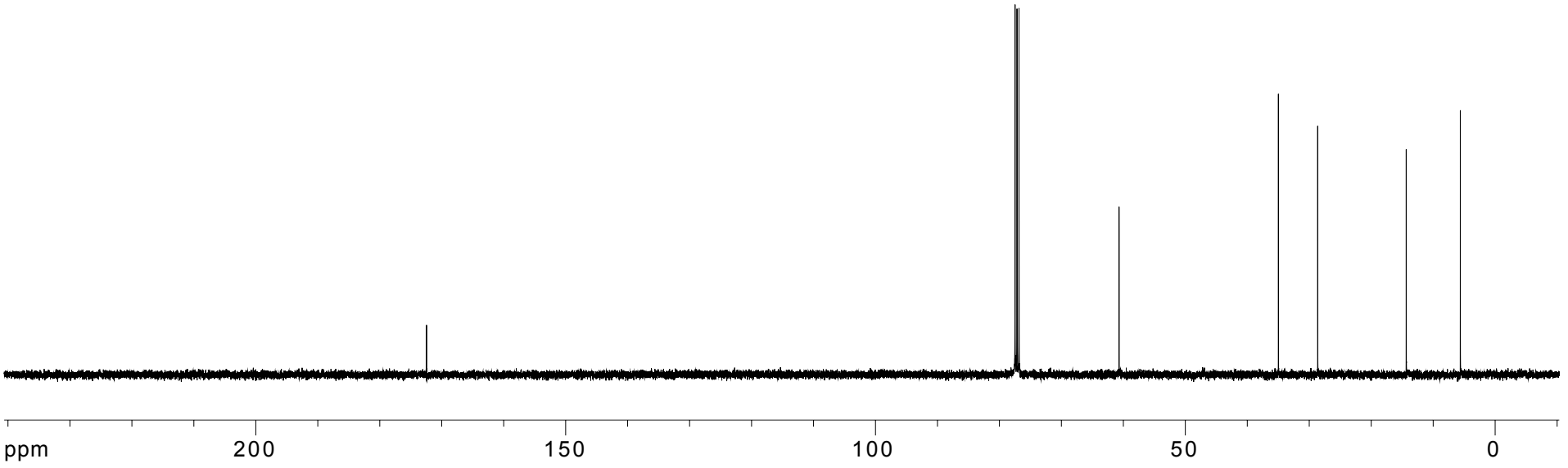

Figure A.142: 100 MHz ^{13}C NMR in $CDCl_3$ of **271**

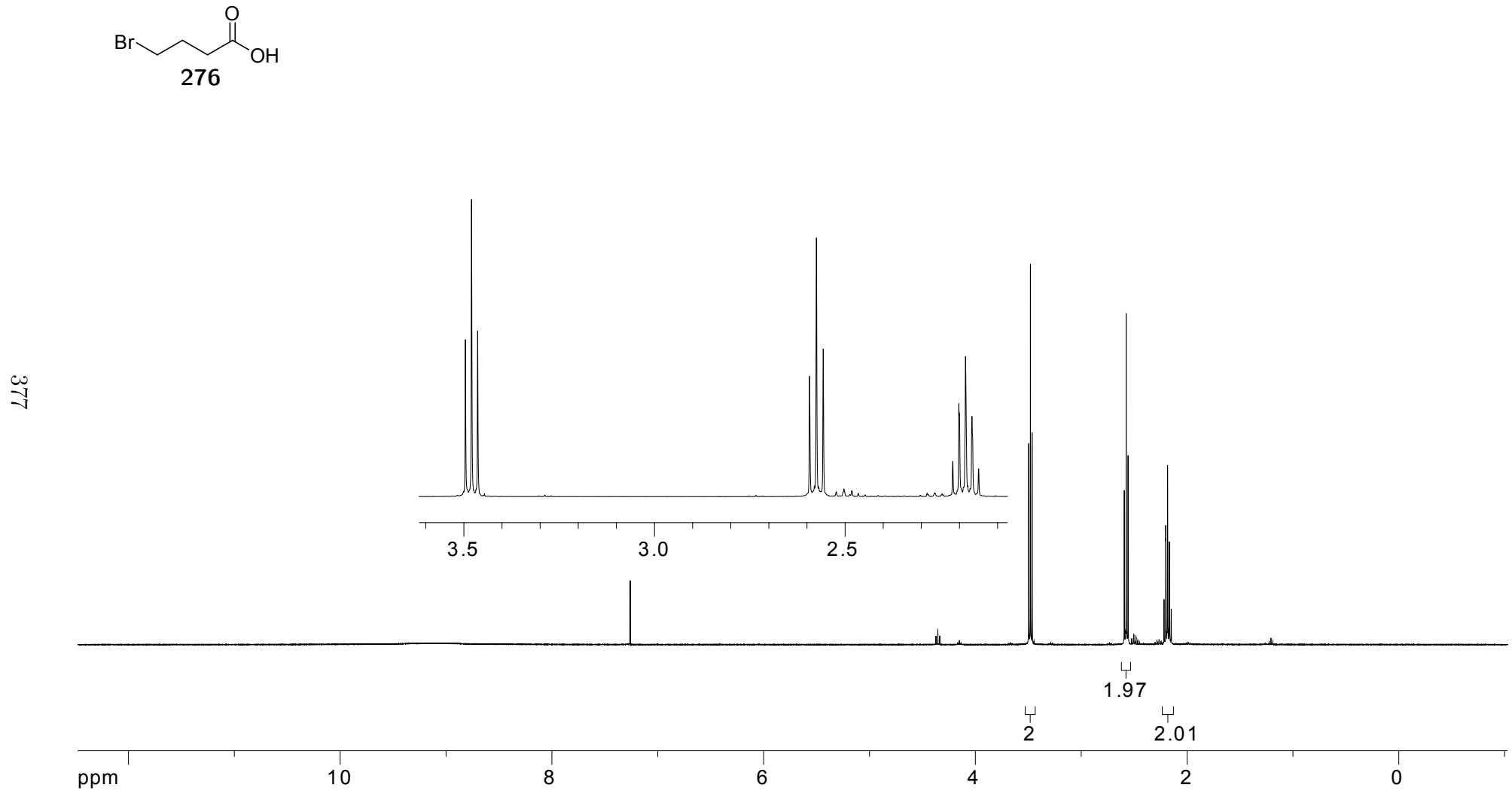

Figure A.143: 400 MHz ^{1}H NMR in $CDCl_3$ of **276**

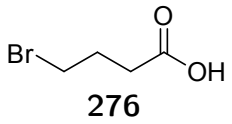

276

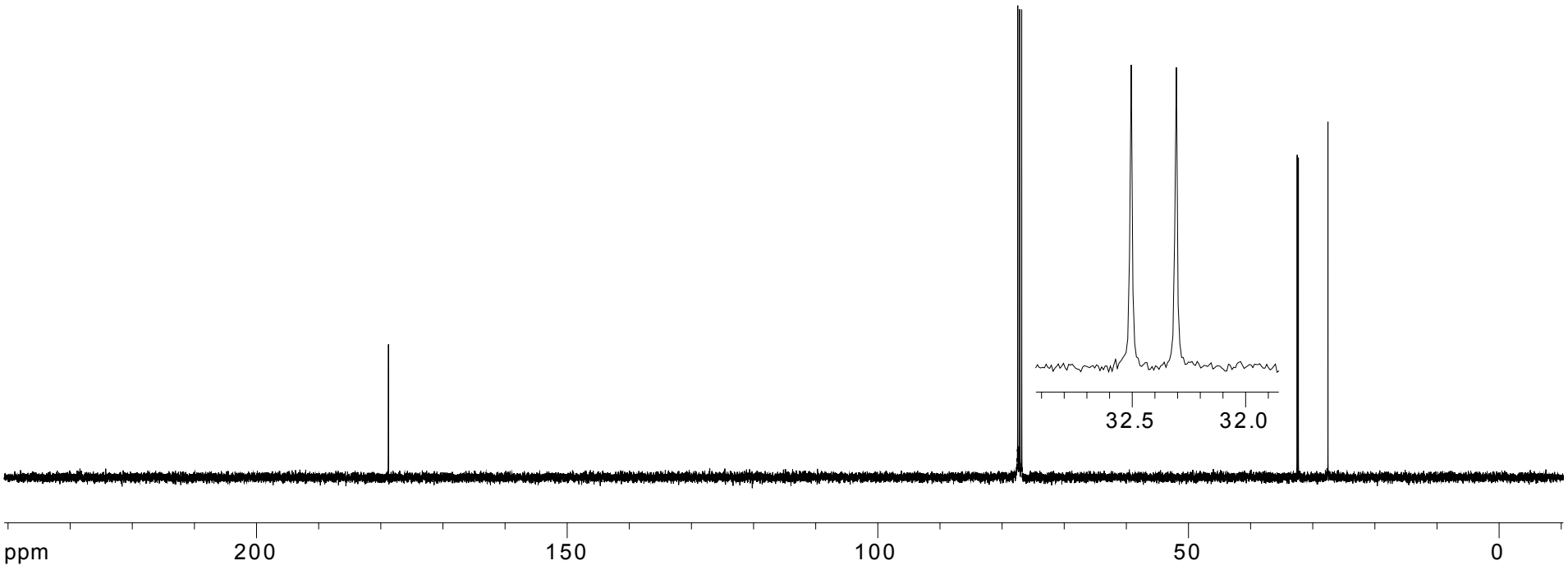

Figure A.144: 100 MHz ^{13}C NMR in $CDCl_3$ of **276**

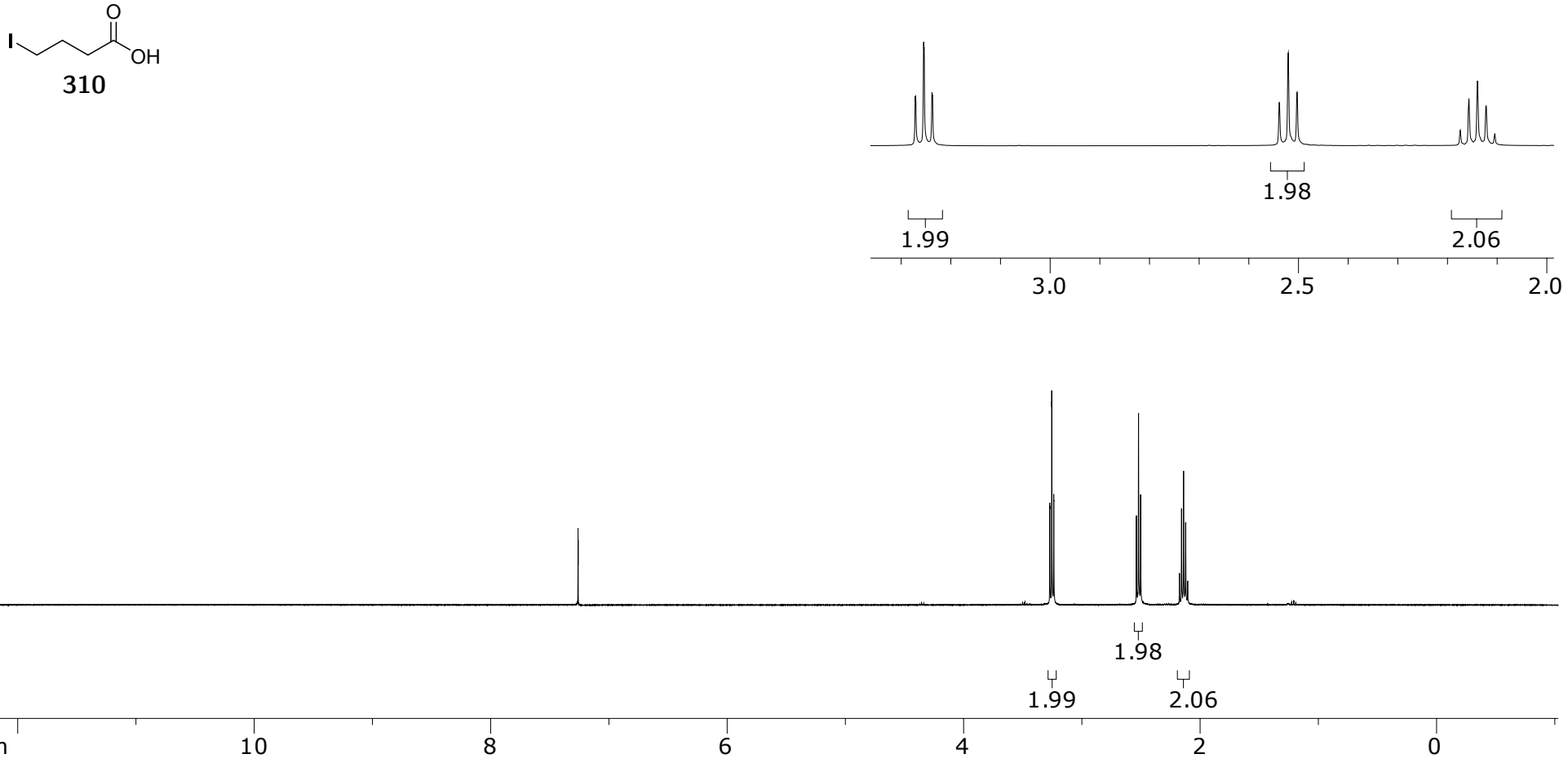

Figure A.145: 400 MHz ^{1}H NMR in $CDCl_3$ of **310**

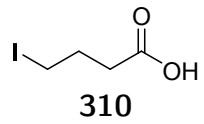

310

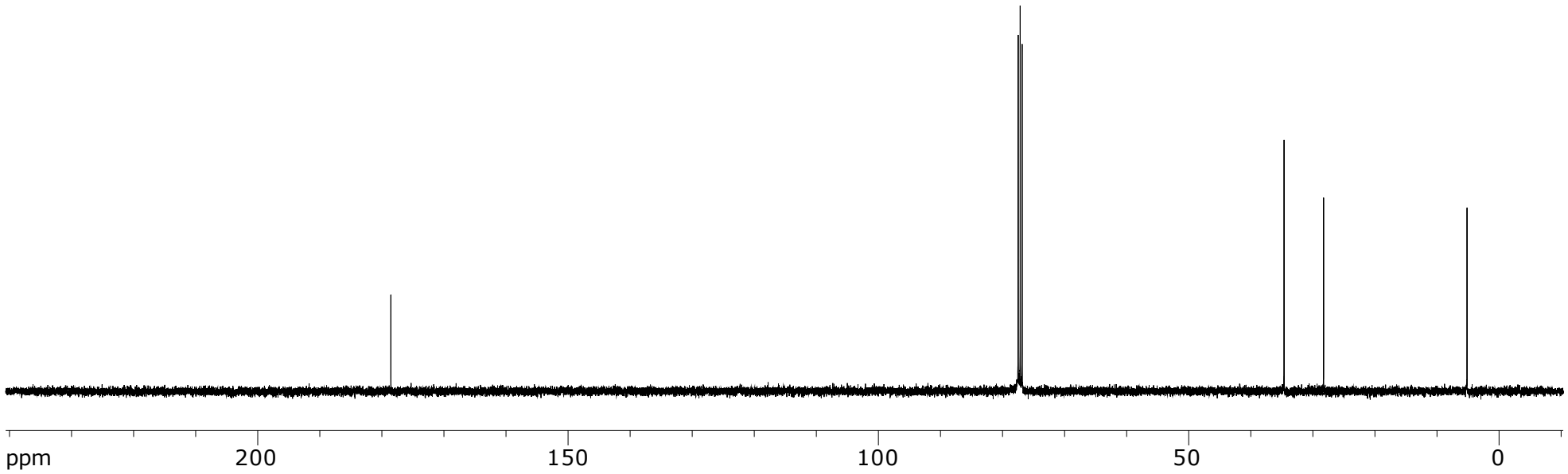

Figure A.146: 100 MHz ^{13}C NMR in $CDCl_3$ of **310**

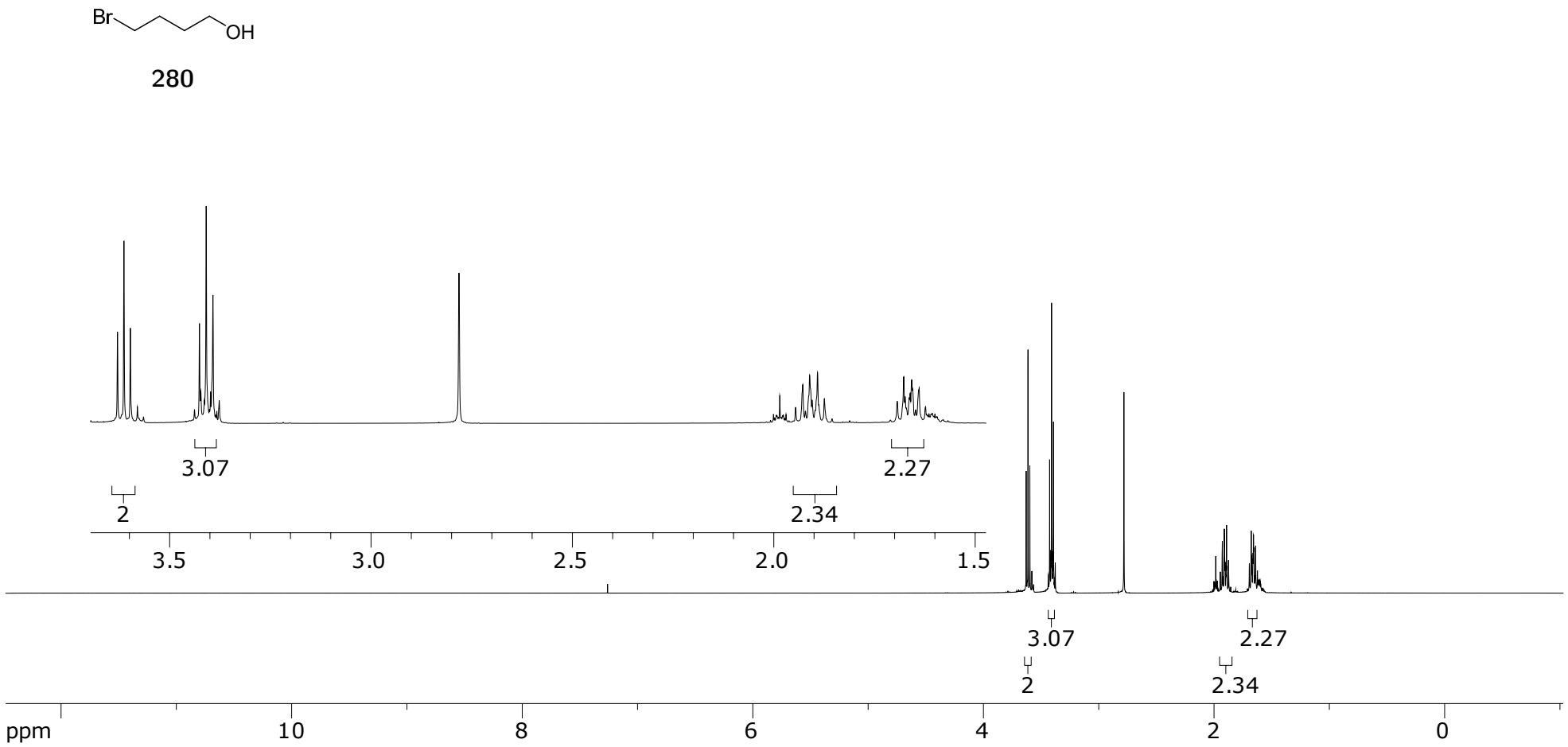

Figure A.147: 400 MHz ^{1}H NMR in $CDCl_3$ of crude **280**

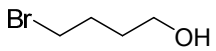

280

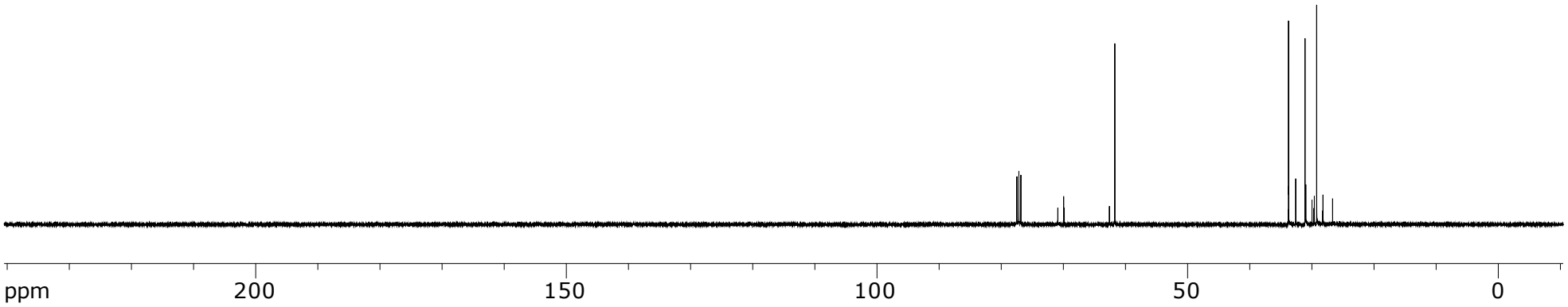

Figure A.148: 100 MHz ^{13}C NMR in $CDCl_3$ of crude **280**

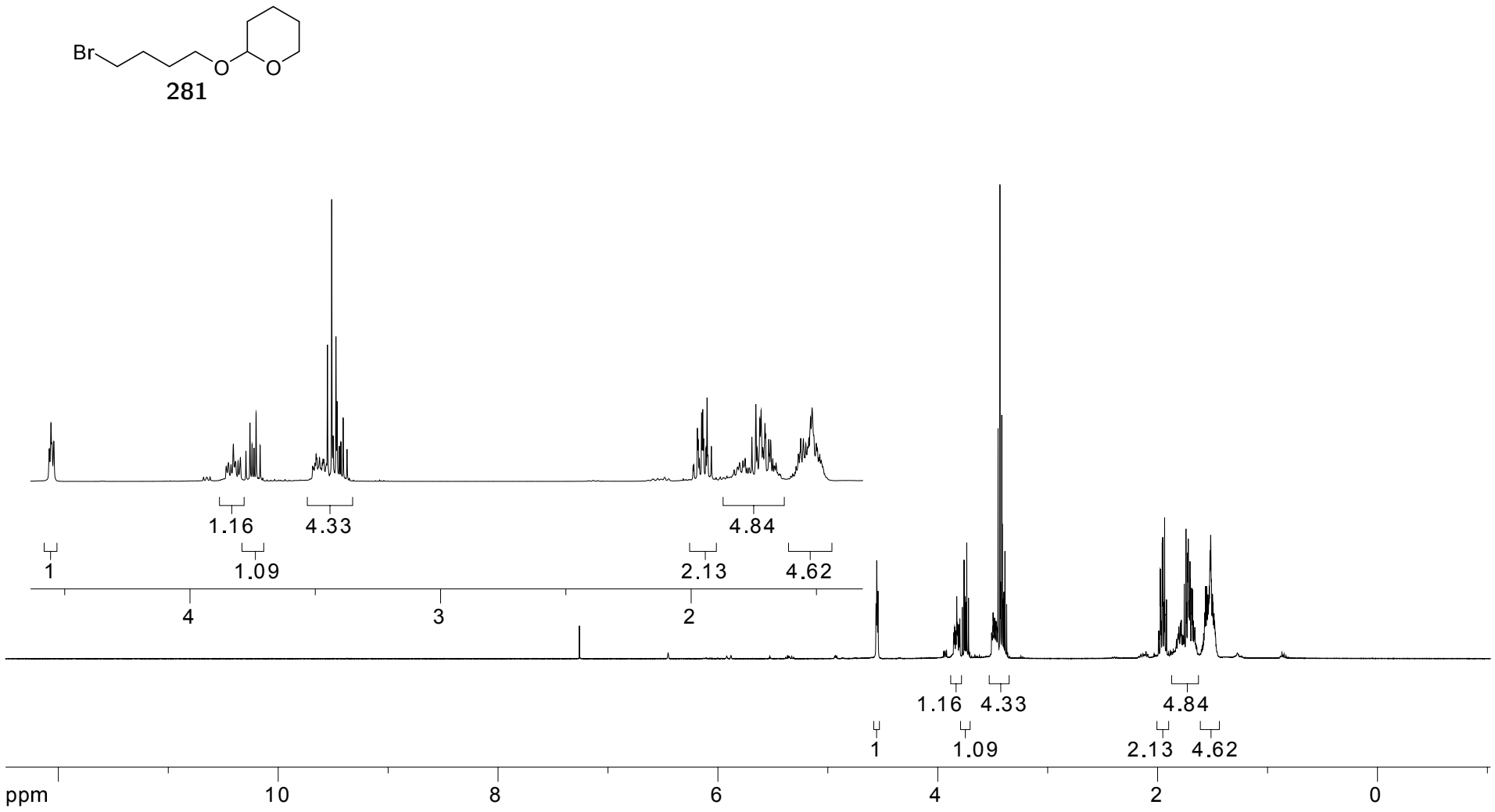

Figure A.149: 400 MHz ^{1}H NMR in $CDCl_3$ of **281**

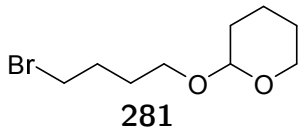

281

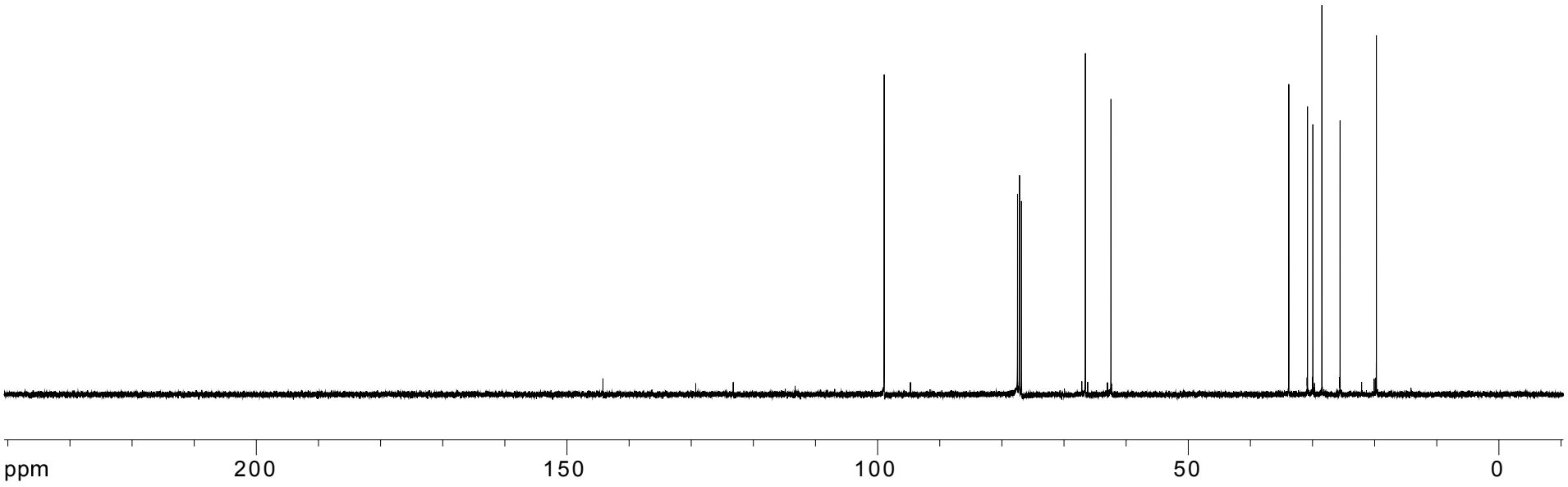

Figure A.150: 100 MHz ^{13}C NMR in $CDCl_3$ of **281**

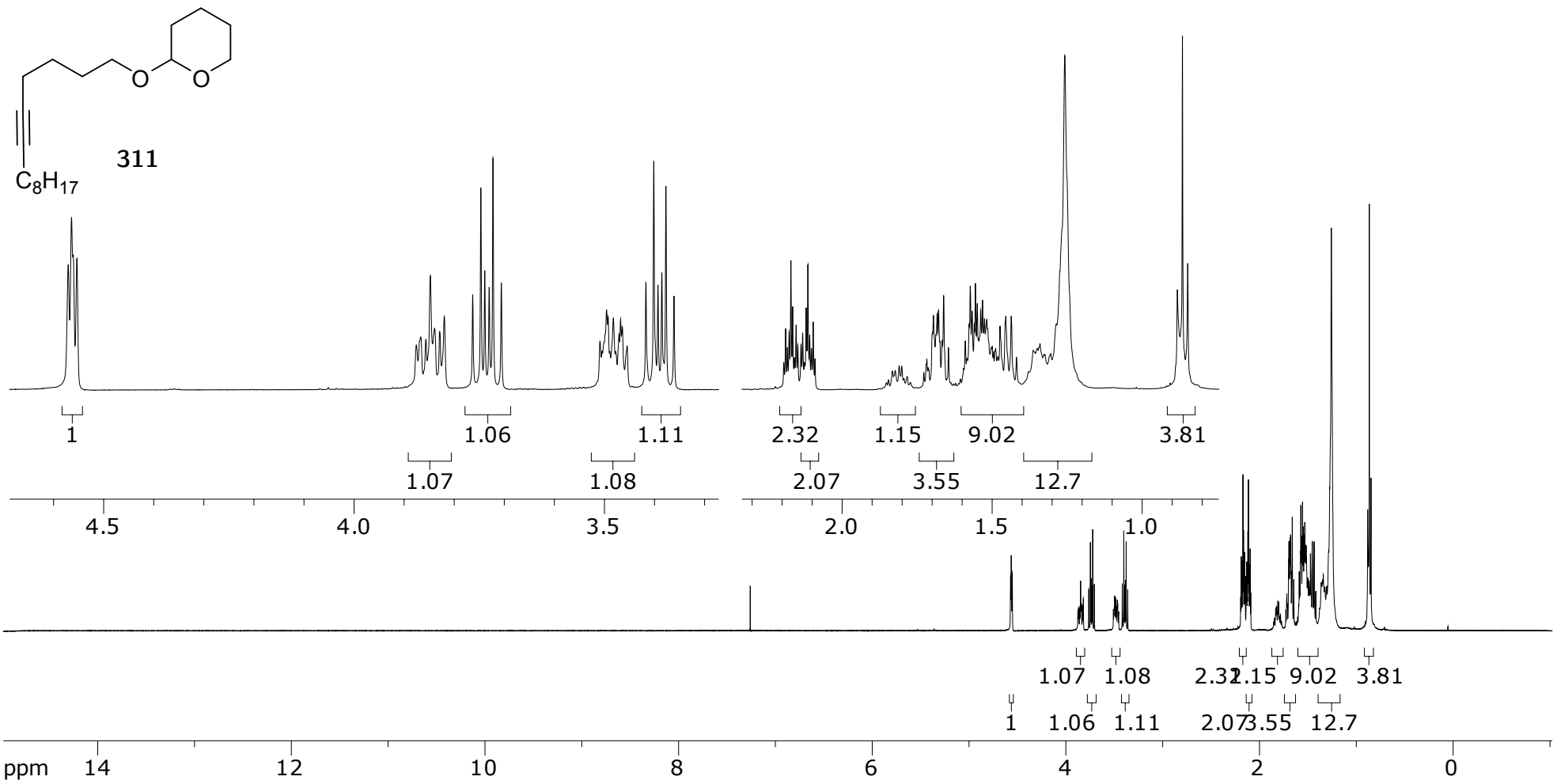

Figure A.151: 400 MHz ^{1}H NMR in $CDCl_3$ of **311**

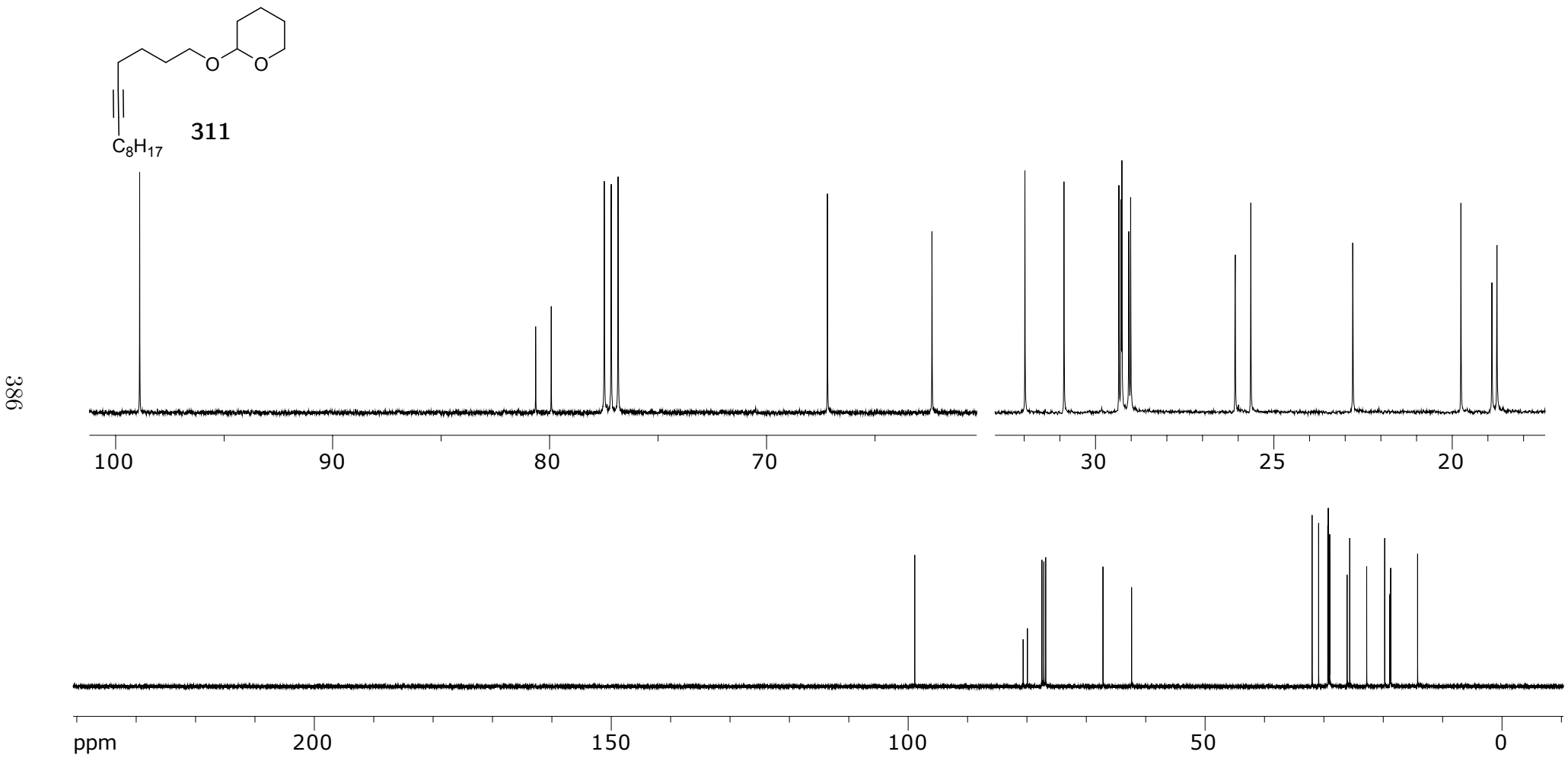

Figure A.152: 100 MHz ^{13}C NMR in $CDCl_3$ of **311**

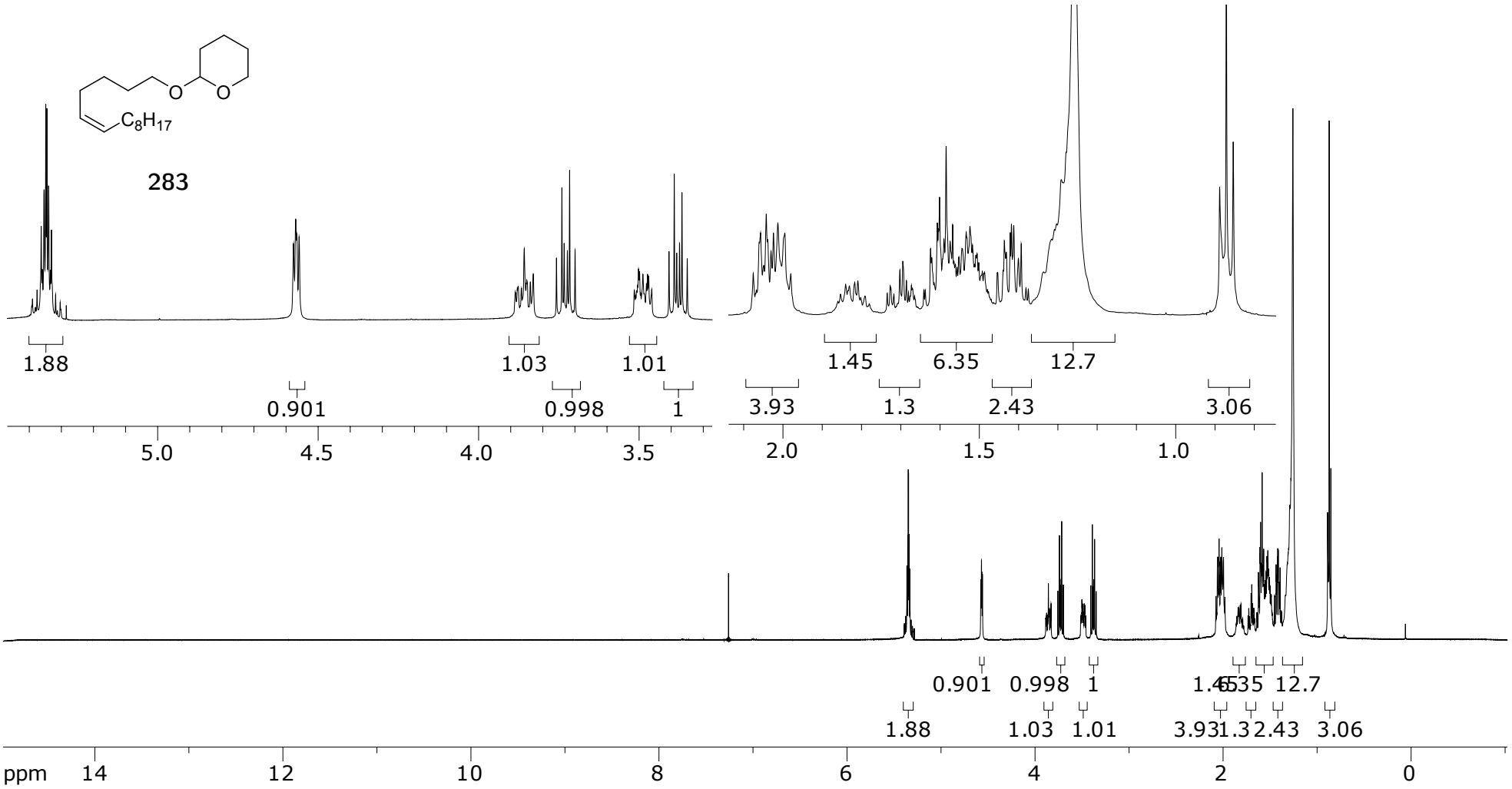

Figure A.153: 400 MHz ^{1}H NMR in $CDCl_3$ of **311**

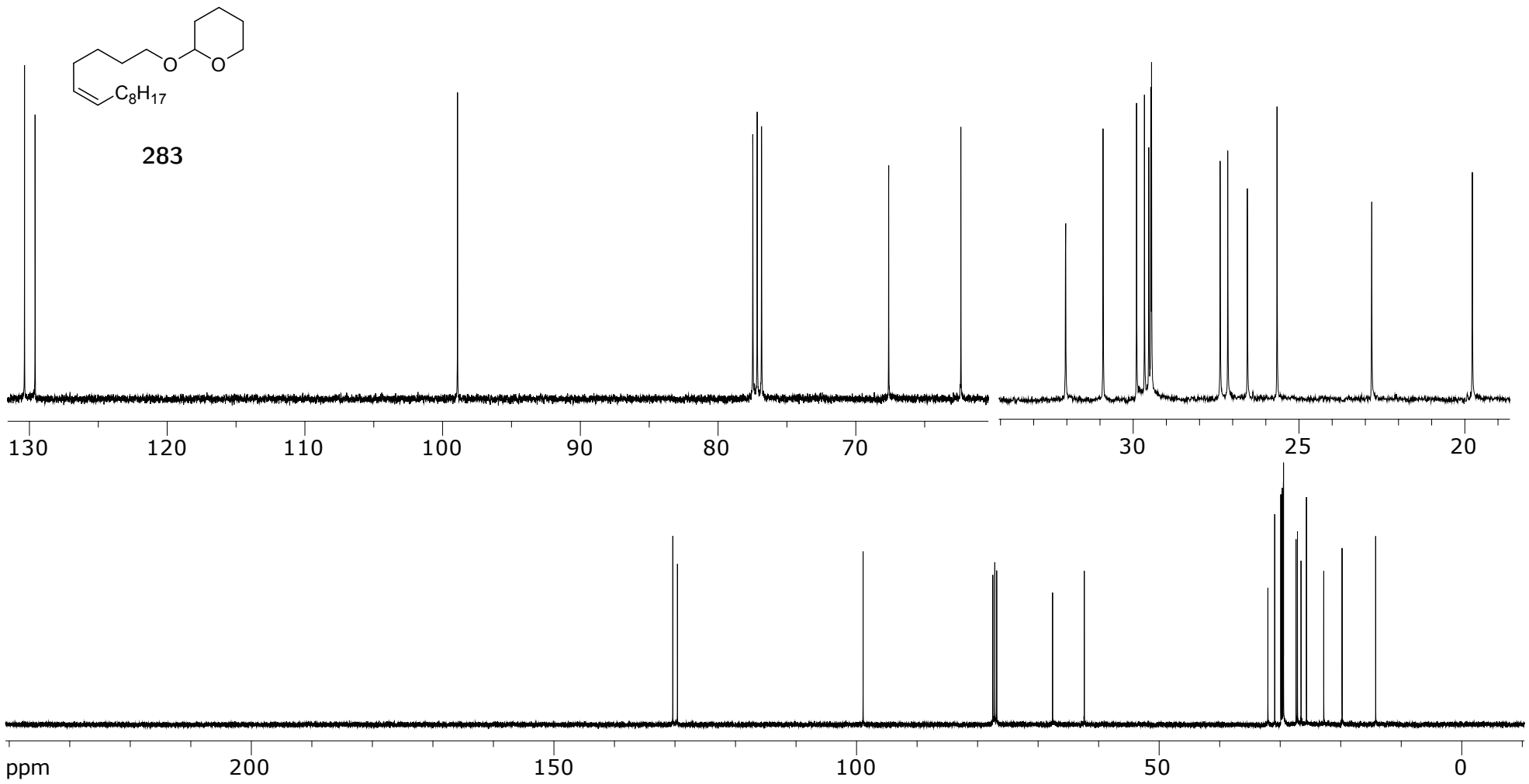

Figure A.154: 100 MHz ^{13}C NMR in $CDCl_3$ of **311**

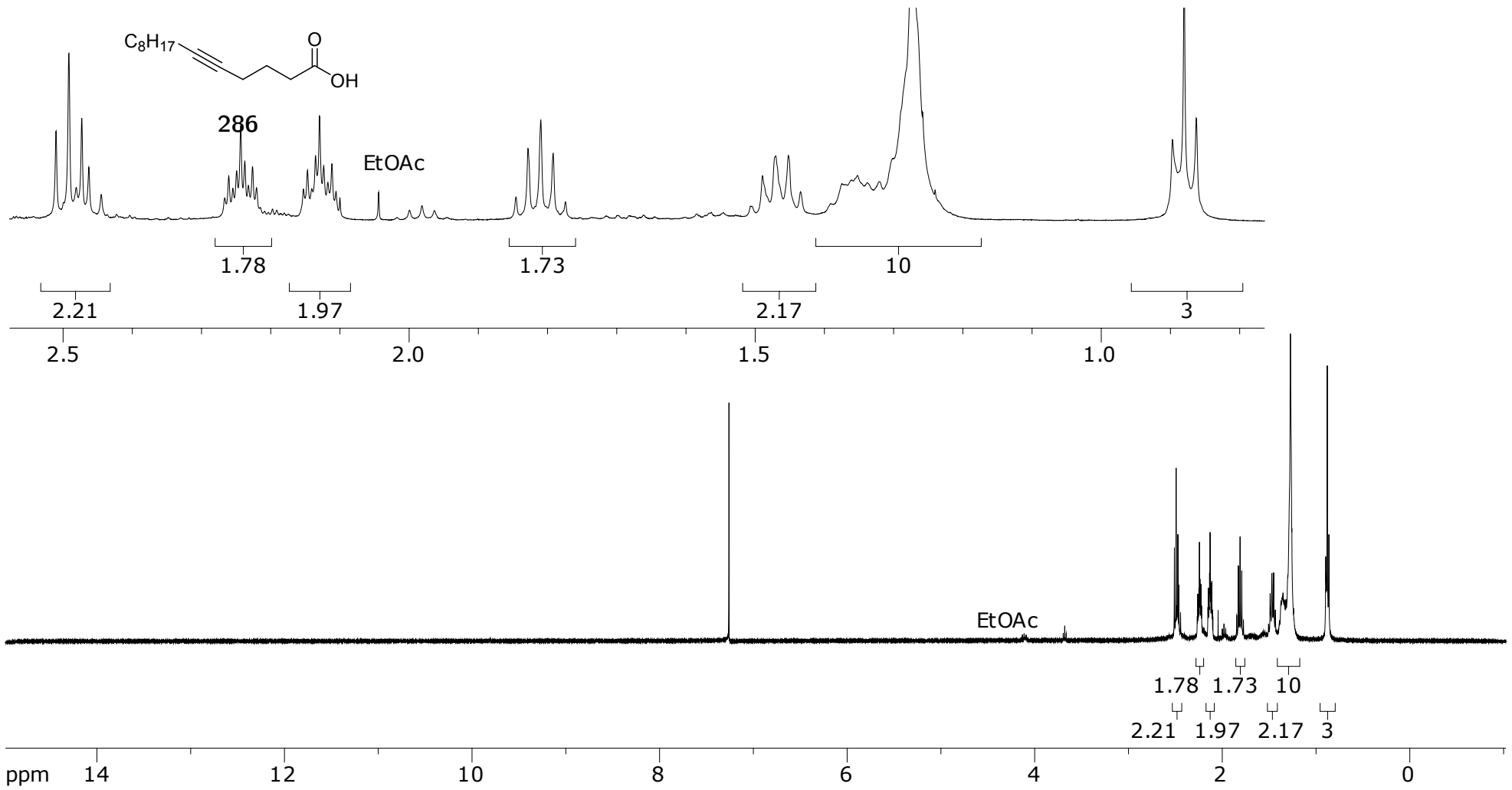

Figure A.155: 400 MHz ^{1}H NMR in $CDCl_3$ of **286**

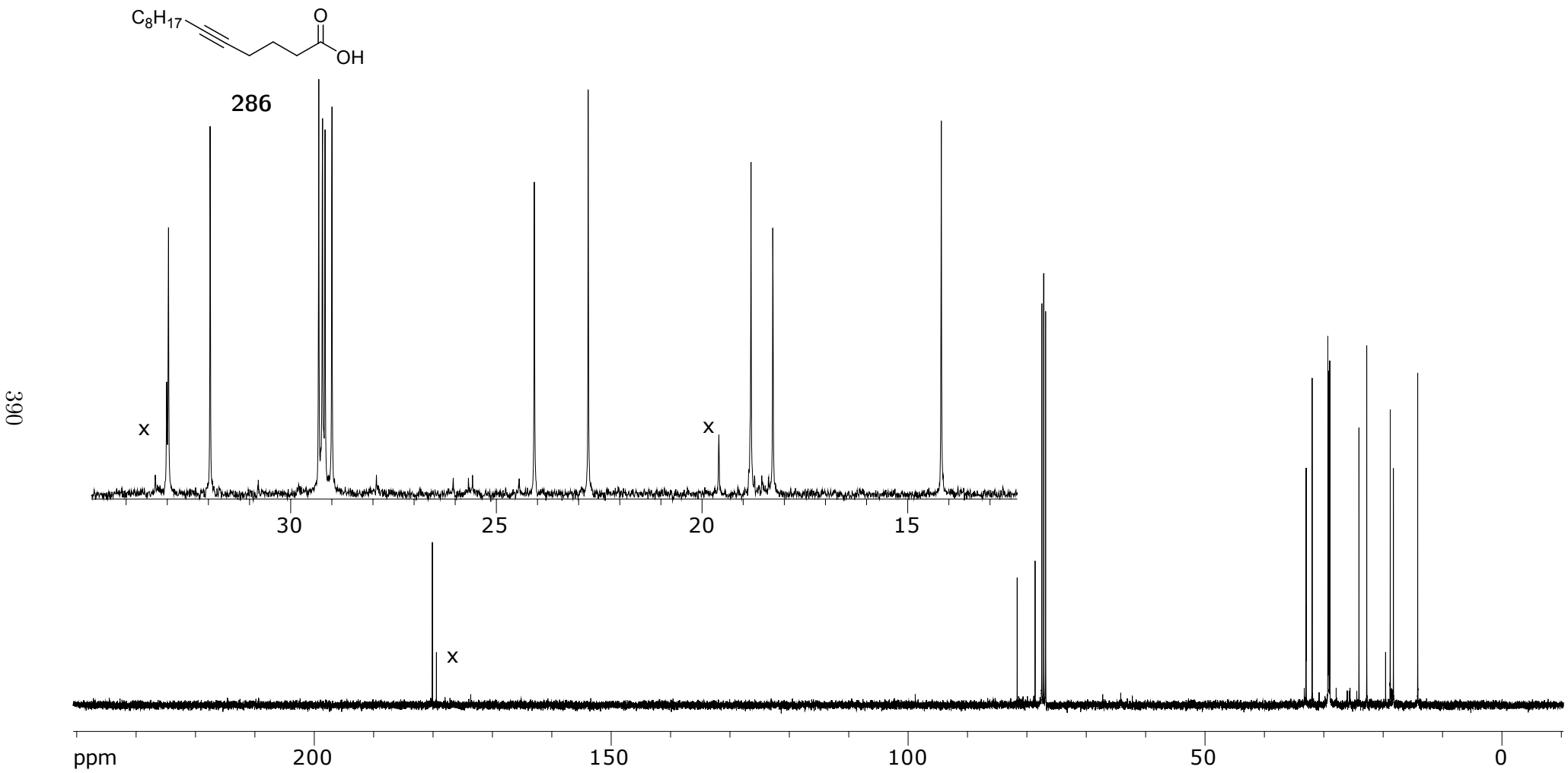

Figure A.156: 100 MHz ^{13}C NMR in $CDCl_3$ of **286**

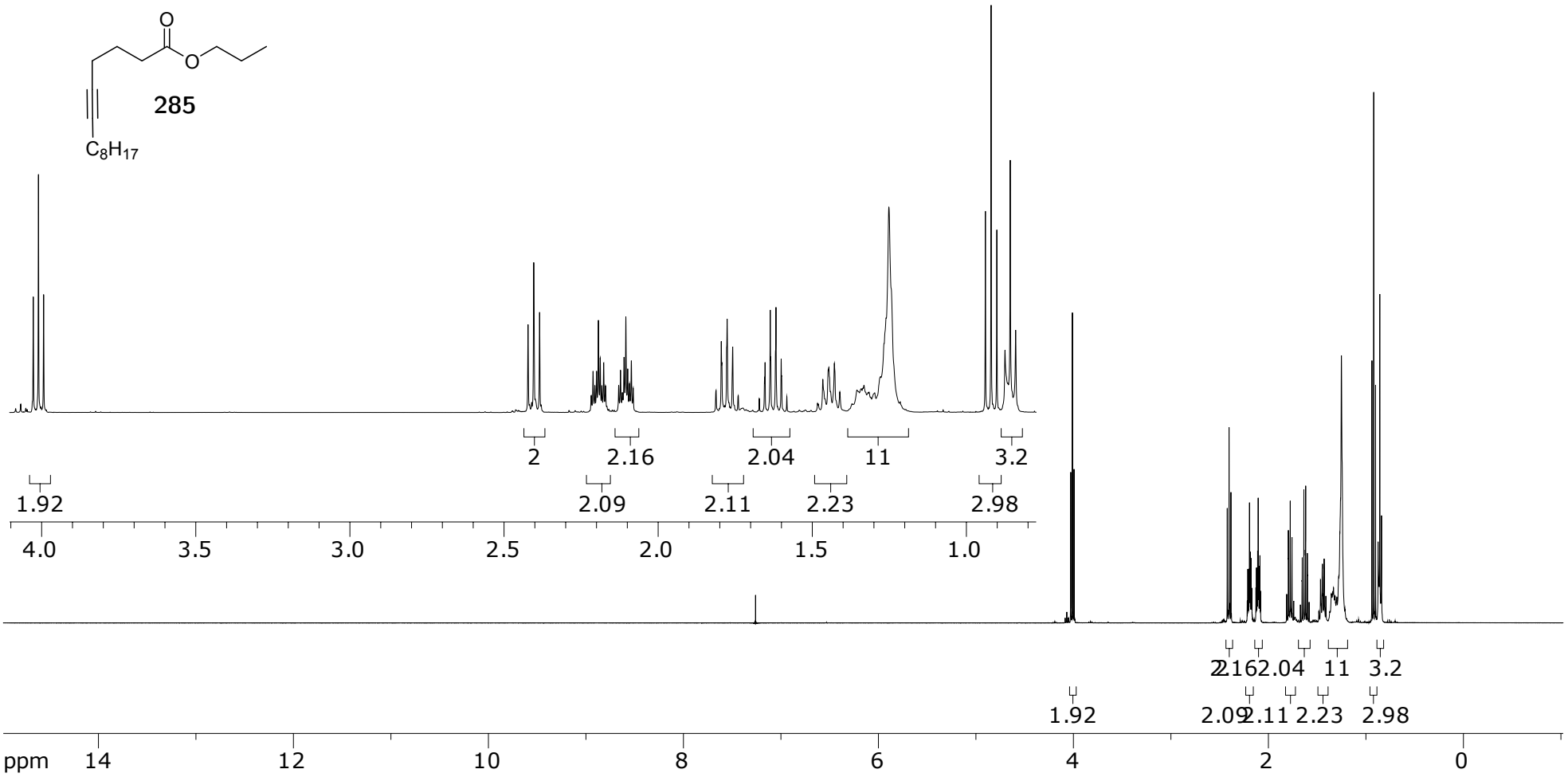

Figure A.157: 100 MHz ^{1}H NMR in $CDCl_3$ of **285**

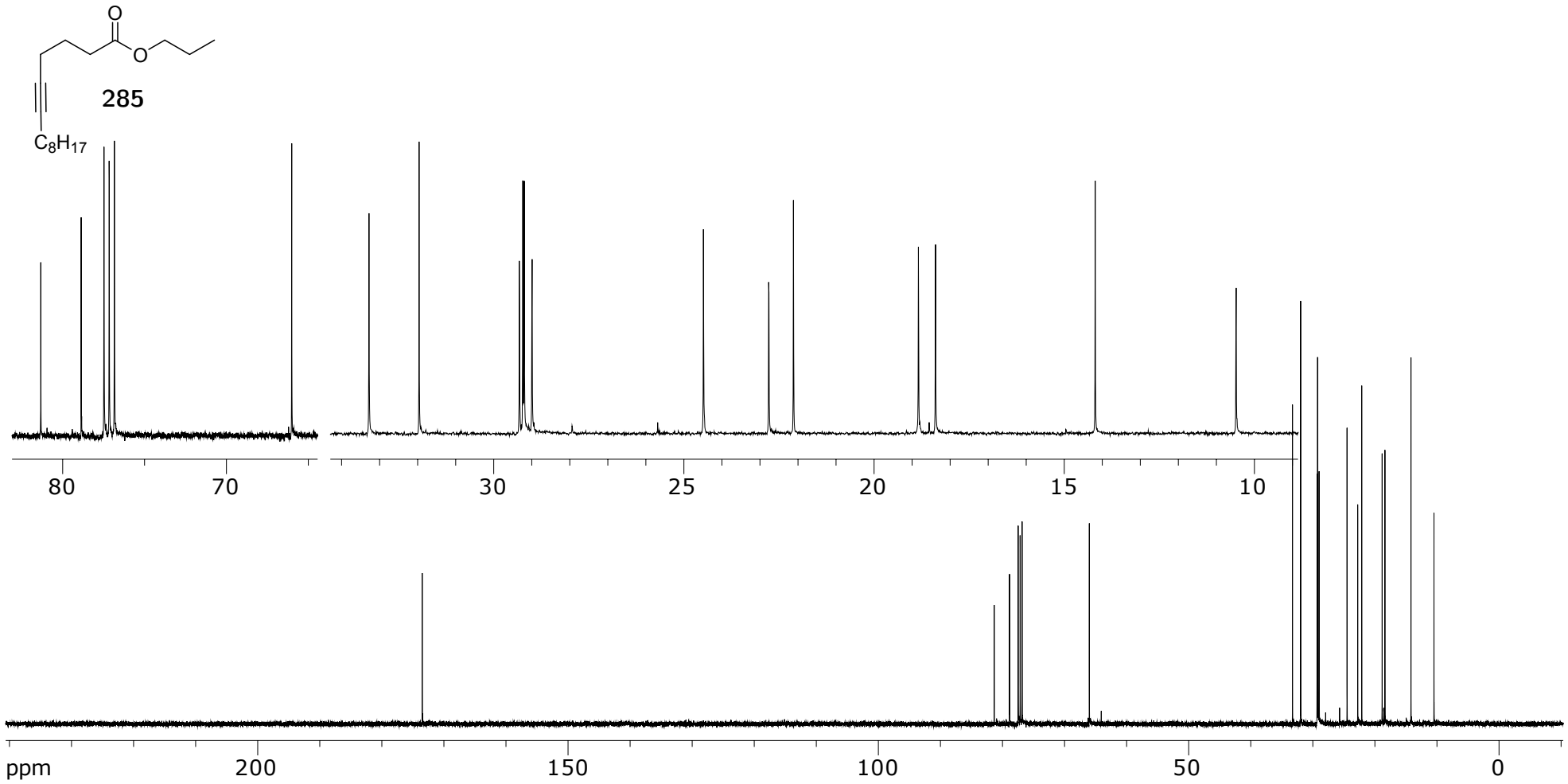

Figure A.158: 100 MHz ^{1}H NMR in $CDCl_3$ of **285**

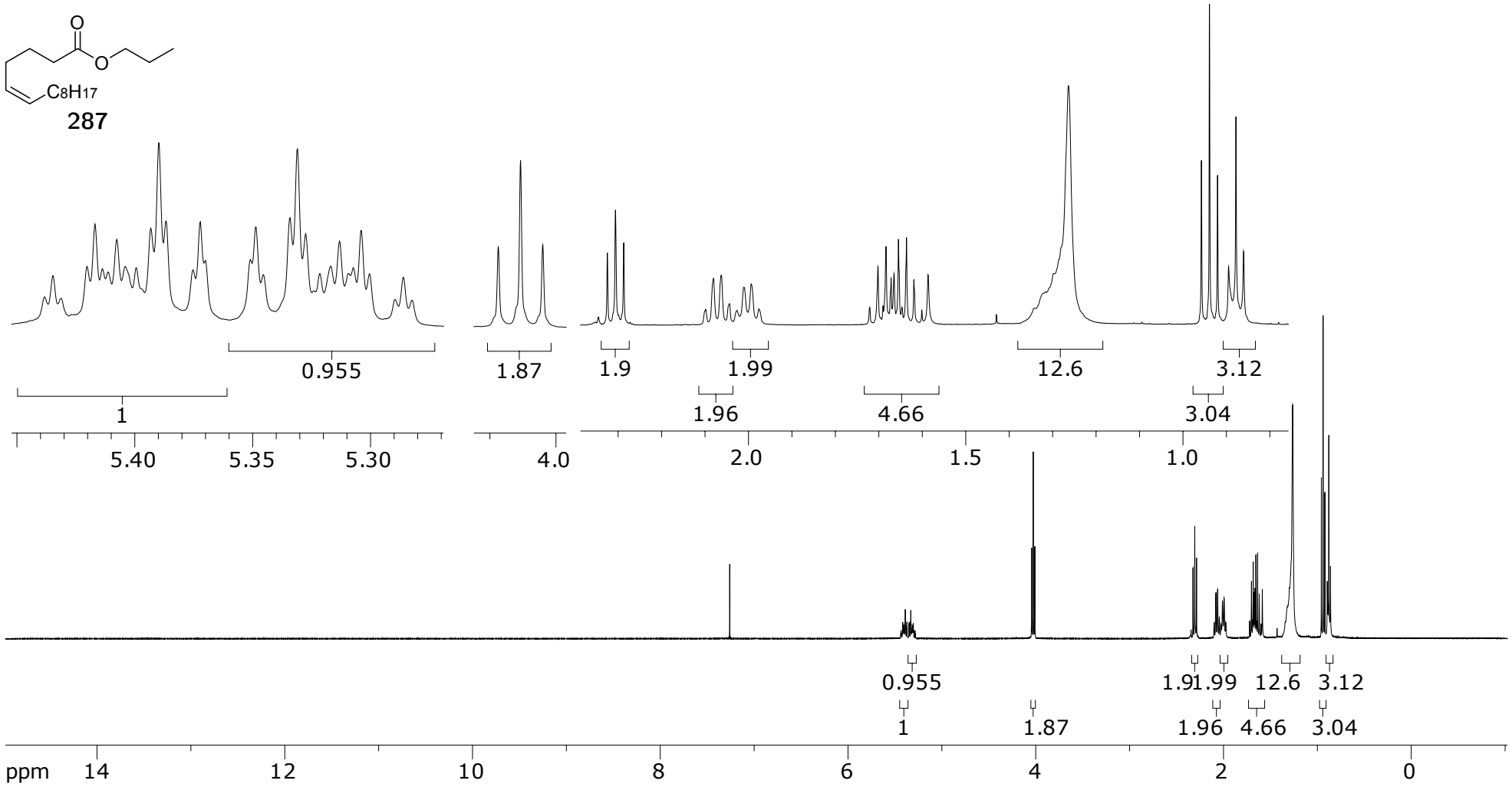

Figure A.159: 400 MHz ^{1}H NMR in $CDCl_3$ of **287**

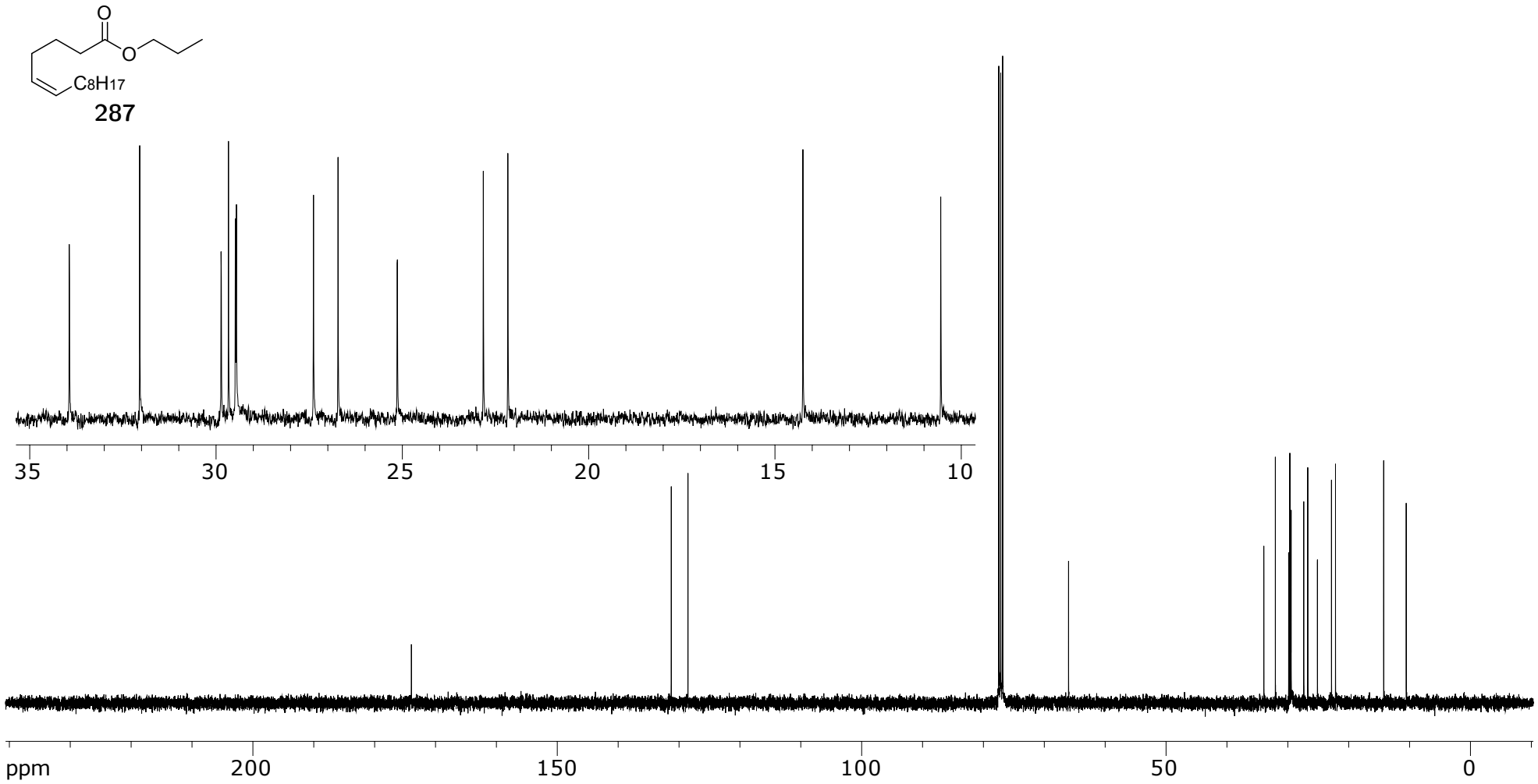

Figure A.160: 100 MHz ^{13}C NMR in $CDCl_3$ of **287**

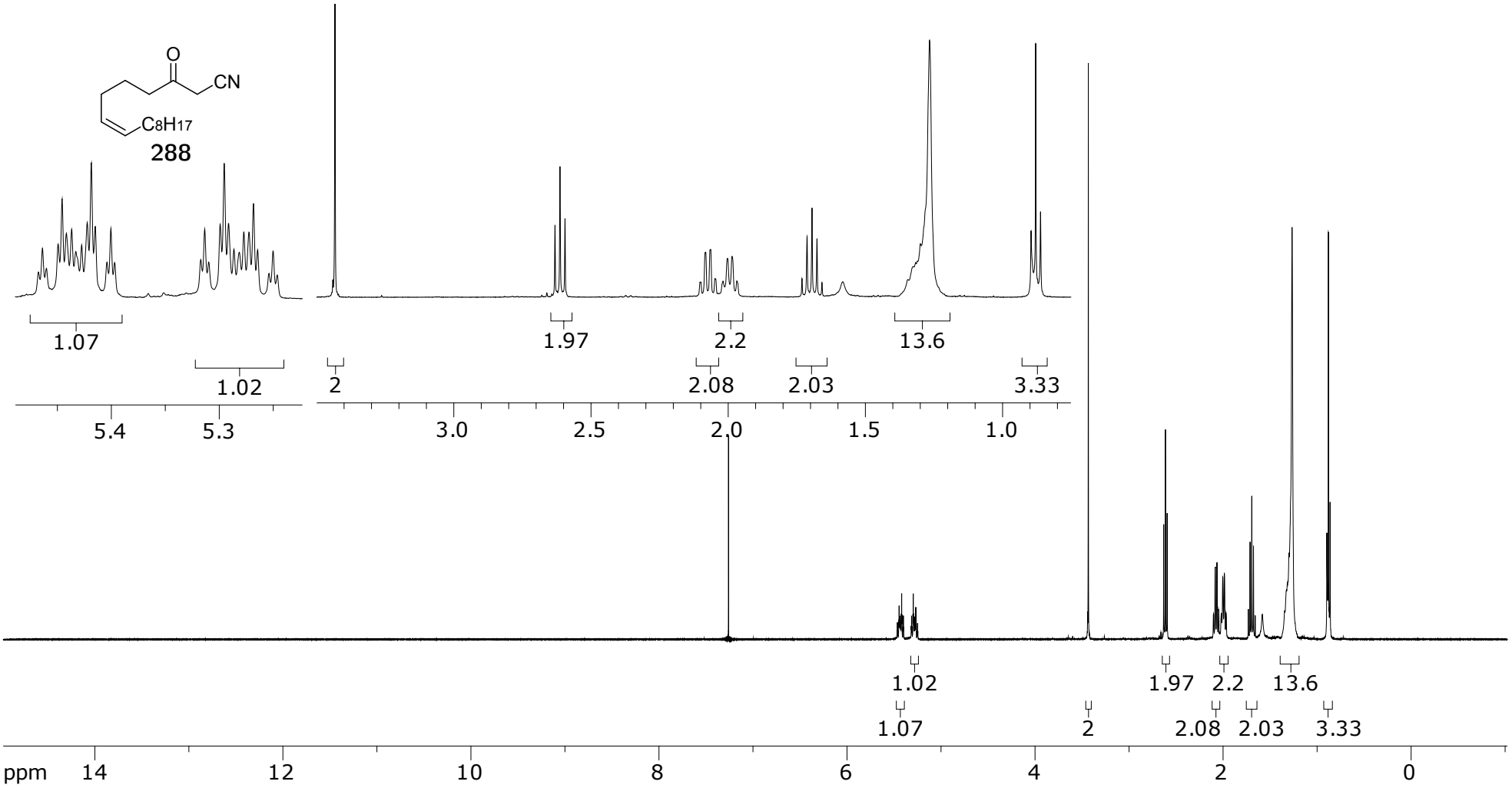

Figure A.161: 400 MHz ^{1}H NMR in $CDCl_3$ of **288**

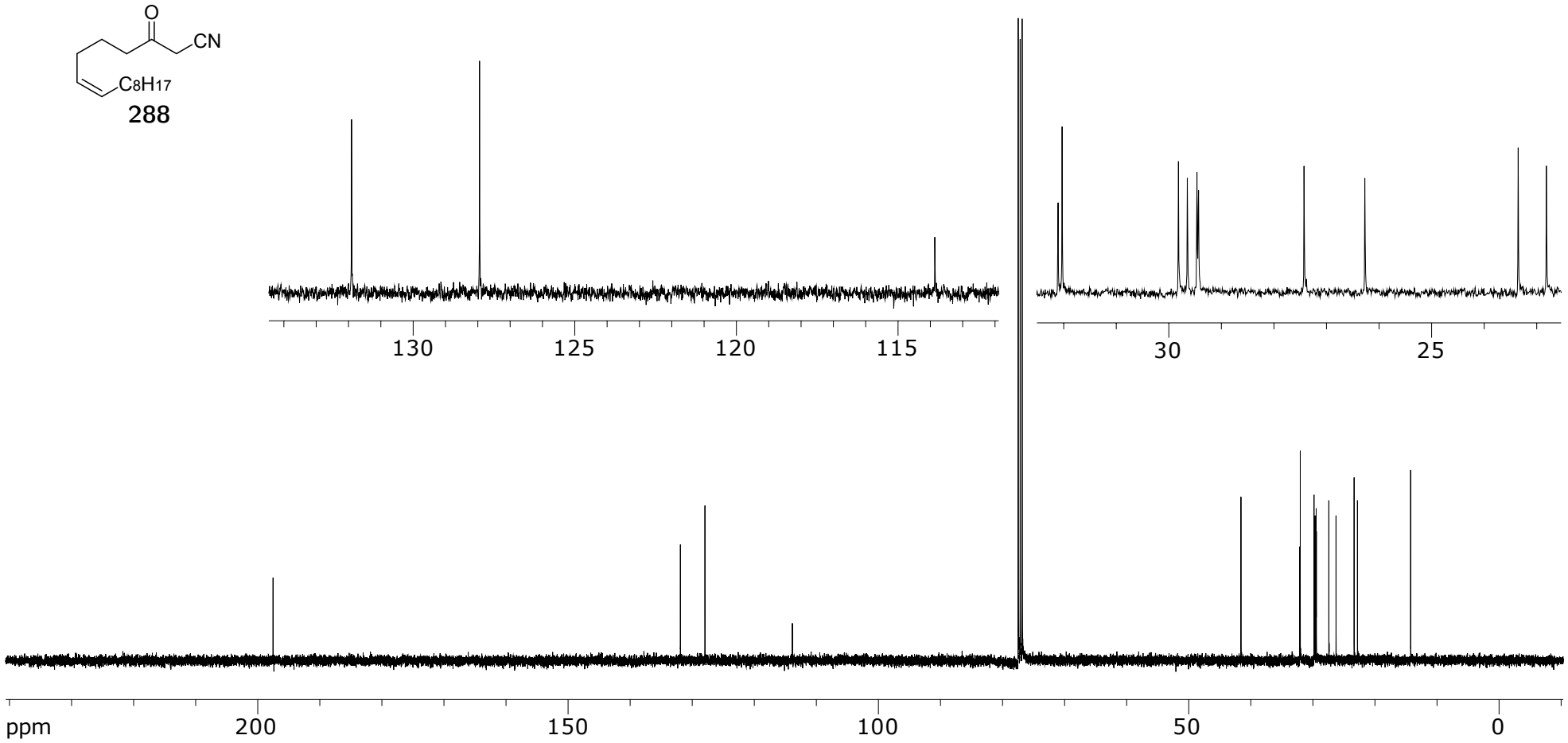

Figure A.162: 100 MHz ^{13}C NMR in $CDCl_3$ of **288**

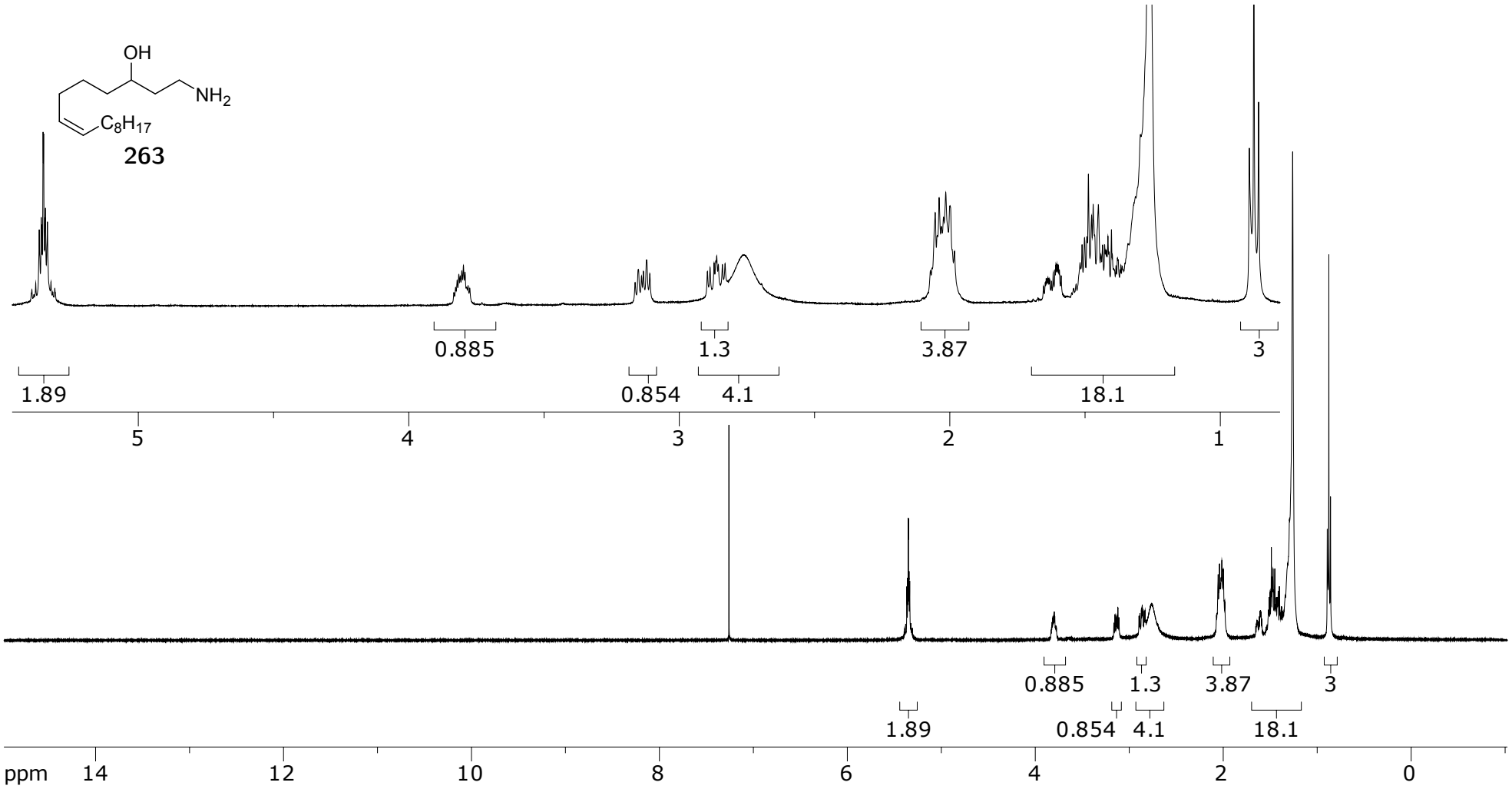

Figure A.163: 400 MHz ^{1}H NMR in $CDCl_3$ of **121**

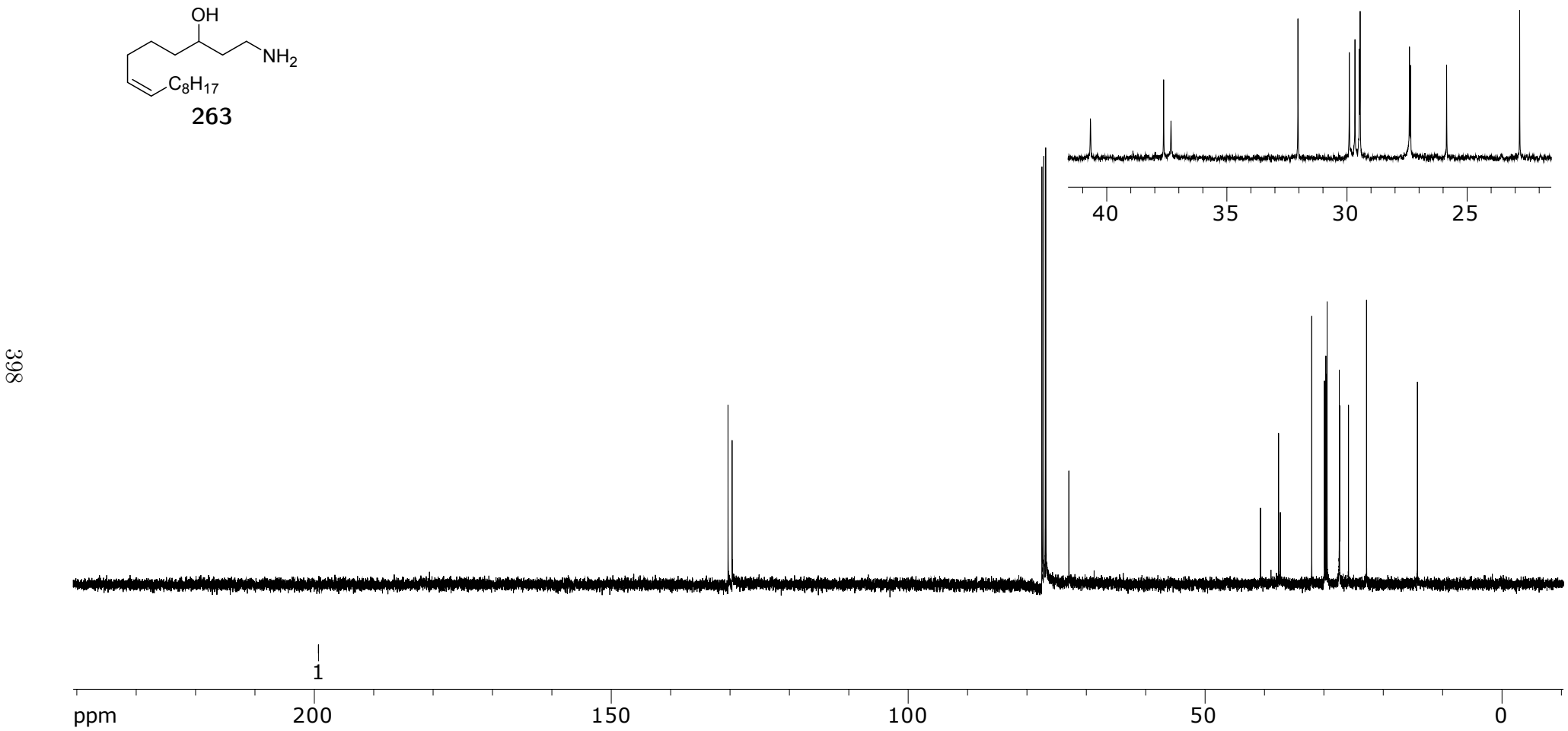

Figure A.164: 100 MHz ^{13}C NMR in $CDCl_3$ of **121**

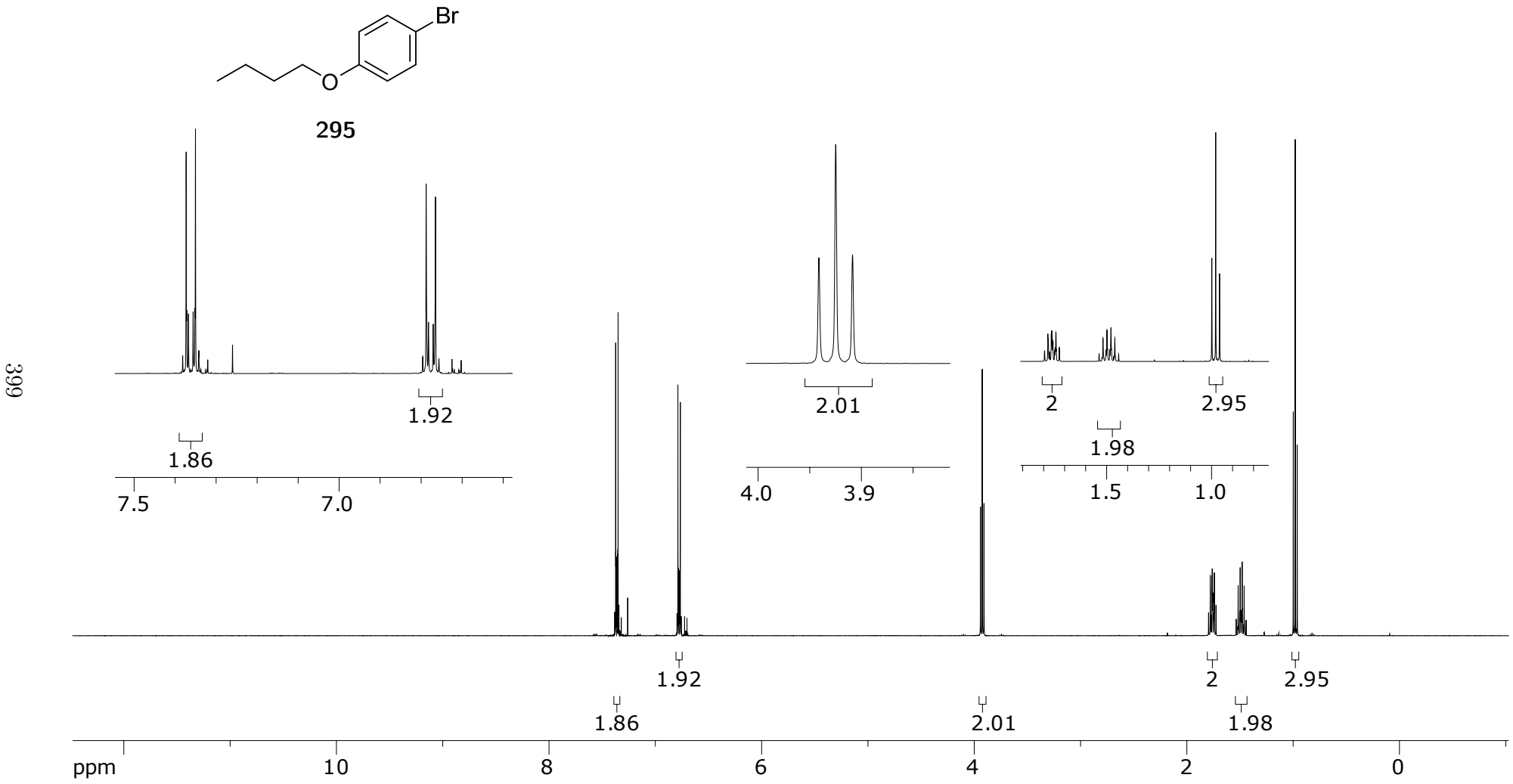

Figure A.165: 400 MHz ^{1}H NMR spectra of **295** in $CDCl_3$

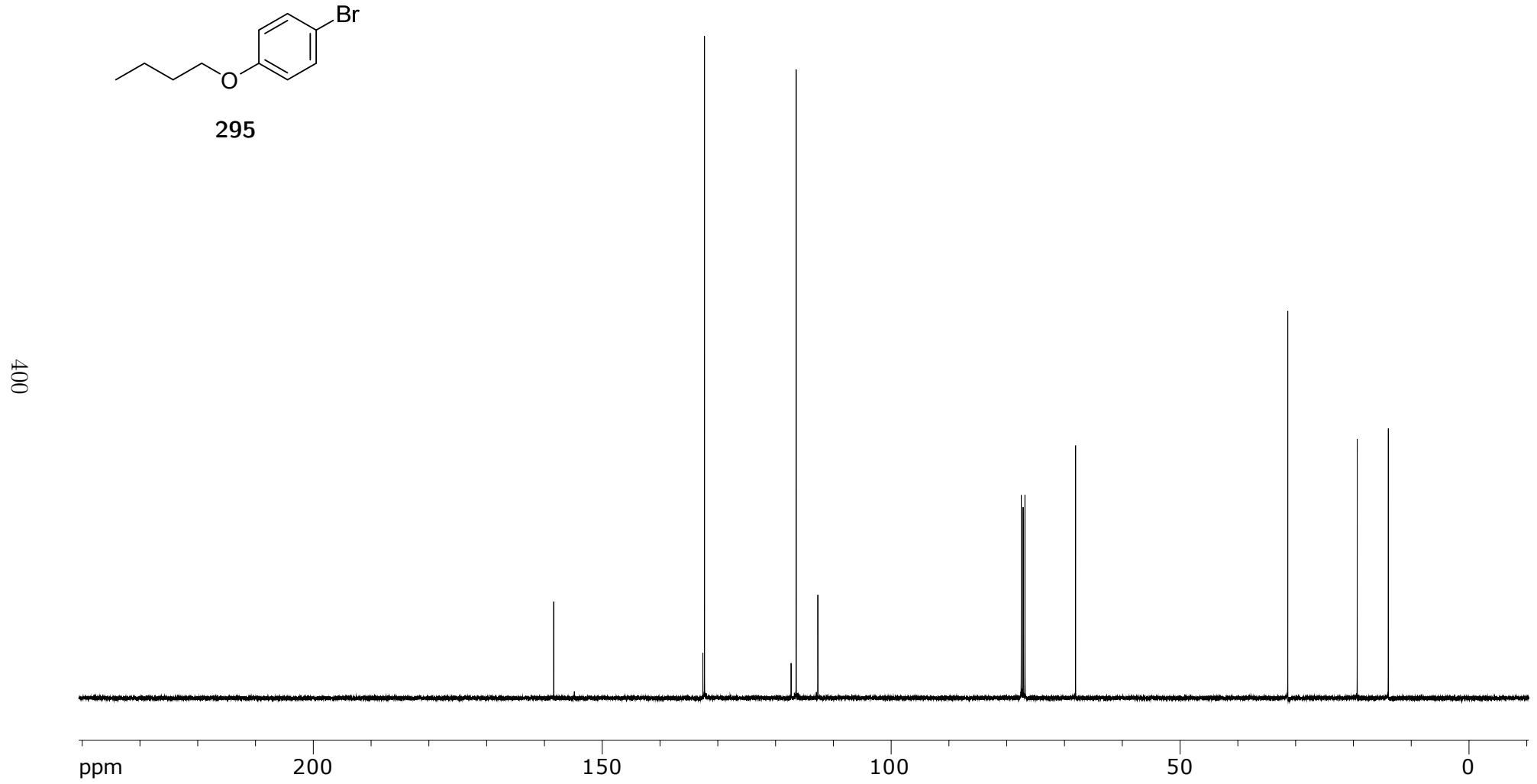

Figure A.166: 100 MHz ^{13}C NMR spectra of **295** in $CDCl_3$

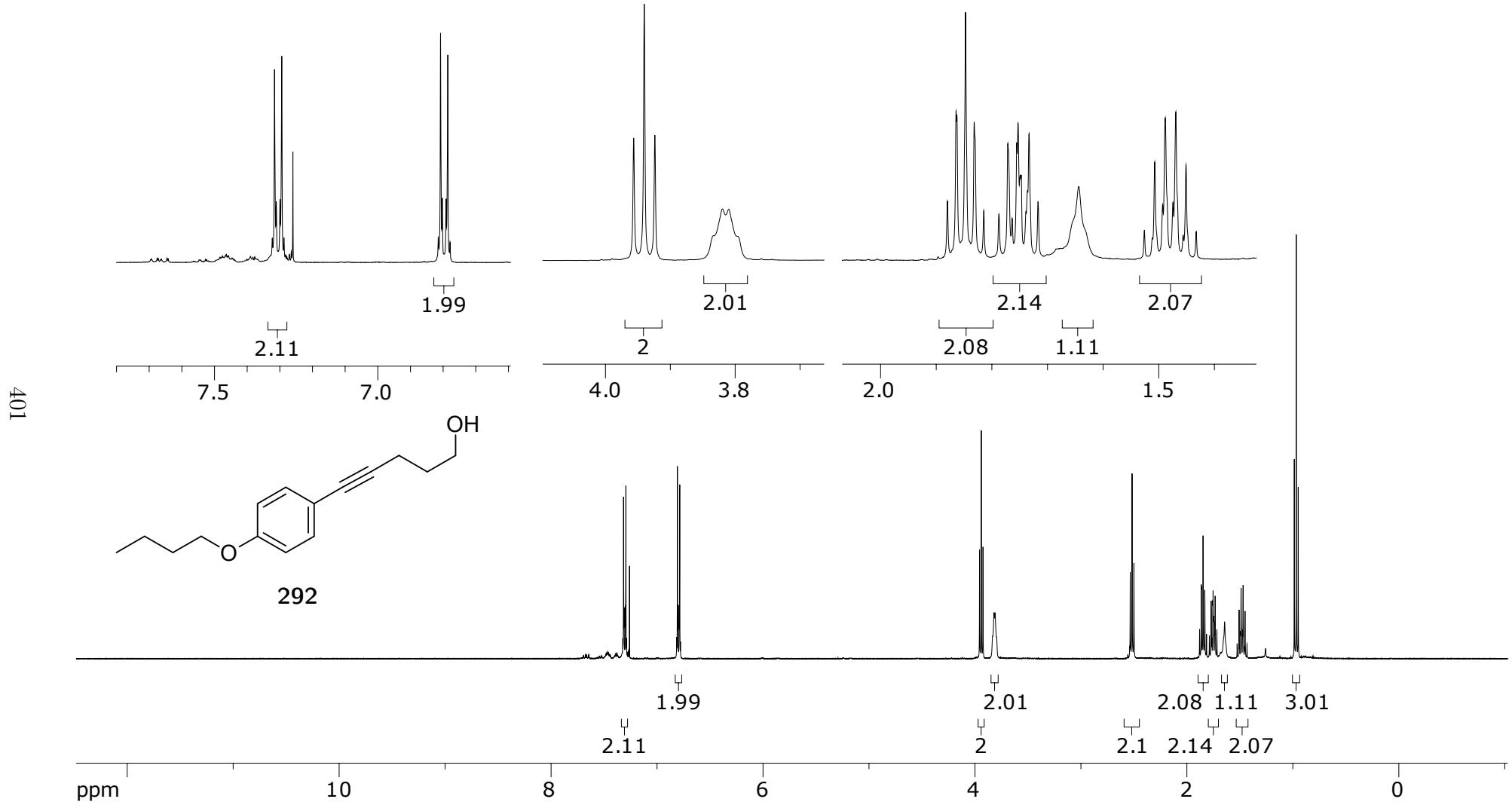

Figure A.167: 400 MHz ^{1}H NMR spectra of **292** in $CDCl_3$

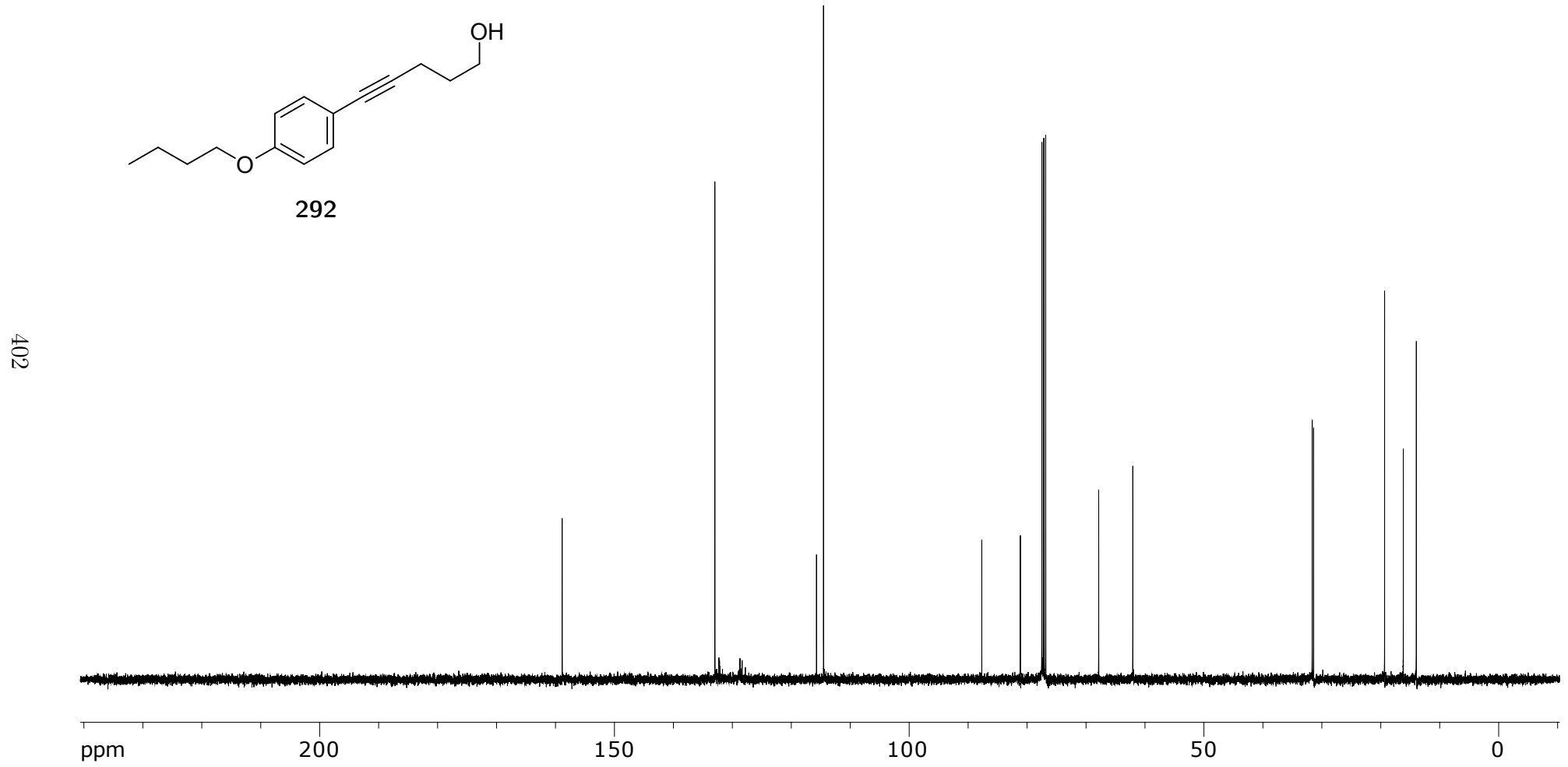

Figure A.168: 100 MHz ^{13}C NMR spectra of **292** in $CDCl_3$

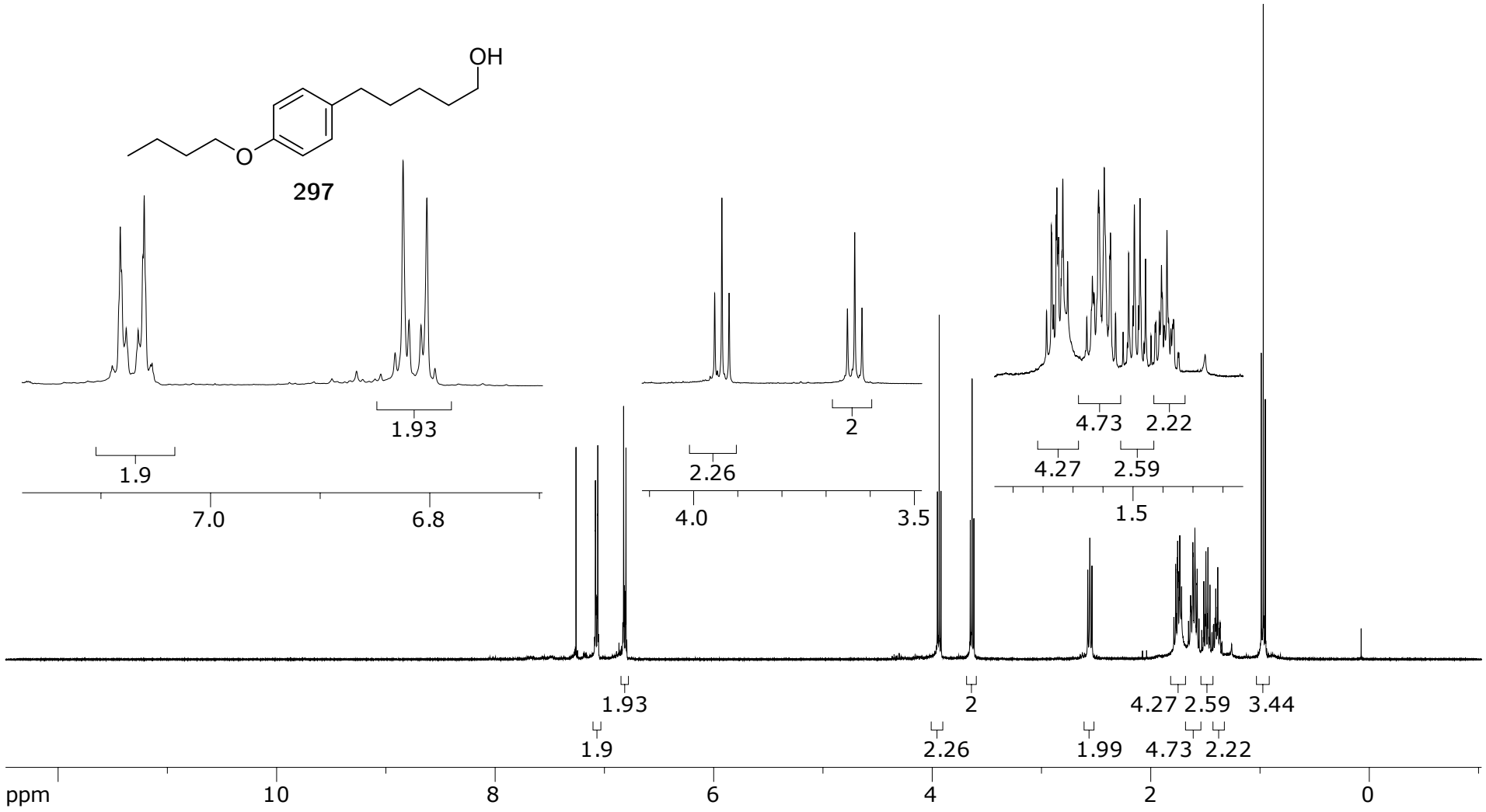

Figure A.169: 400 MHz ^{1}H NMR spectra of **297** in $CDCl_3$

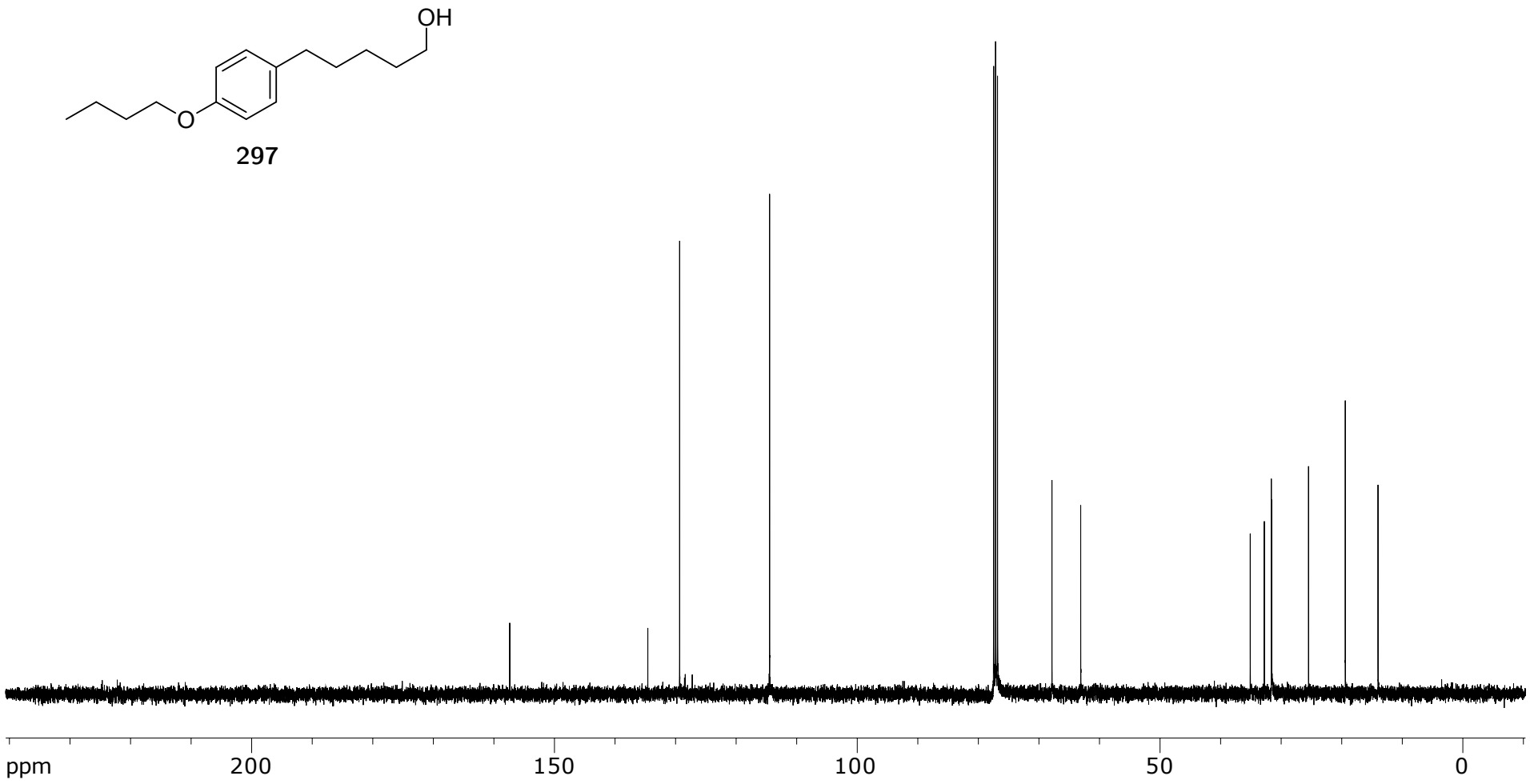

Figure A.170: 100 MHz ^{13}C NMR spectra of **297** in $CDCl_3$

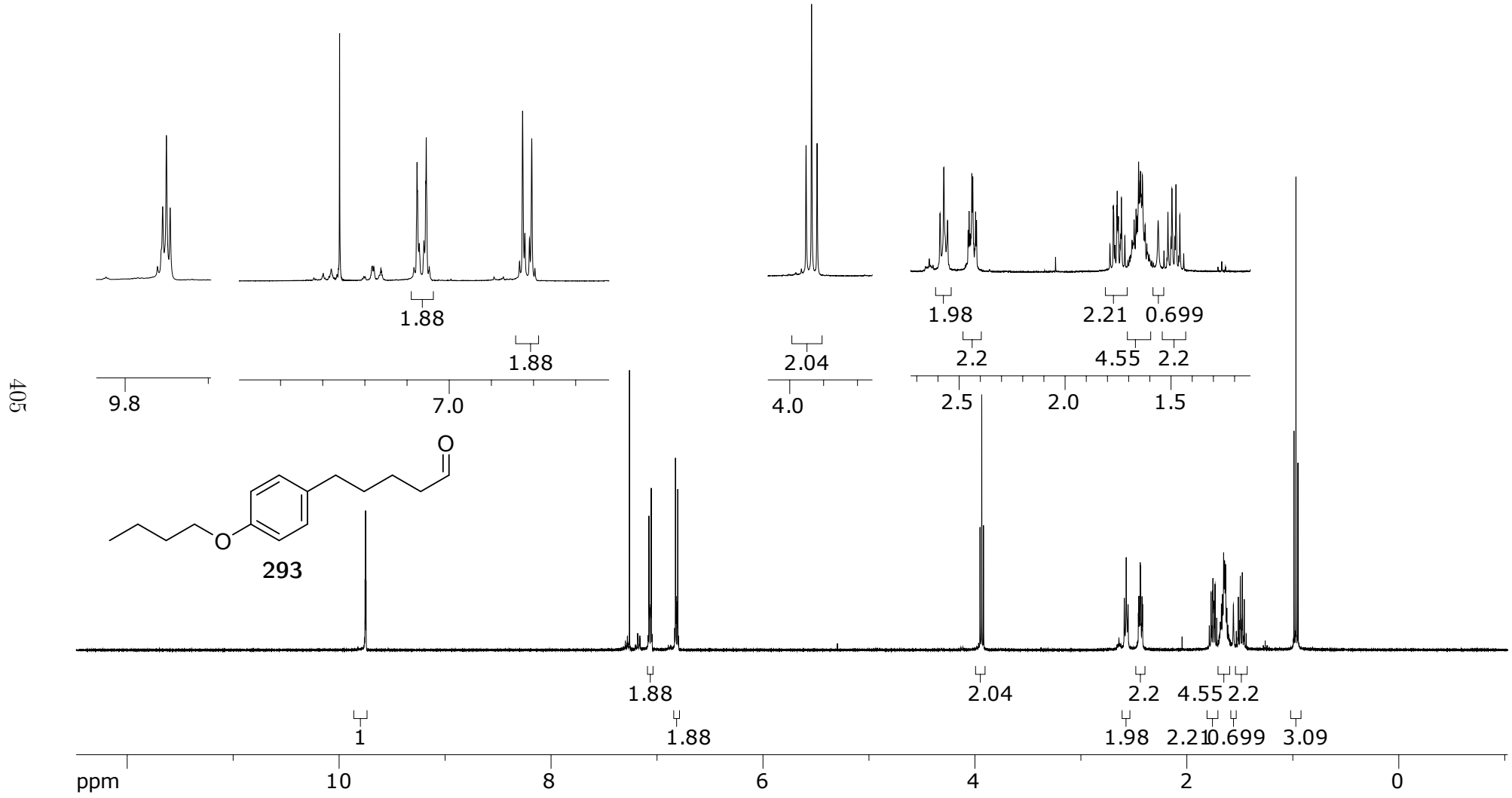

Figure A.171: 400 MHz ^{1}H NMR spectra of **293** in $CDCl_3$

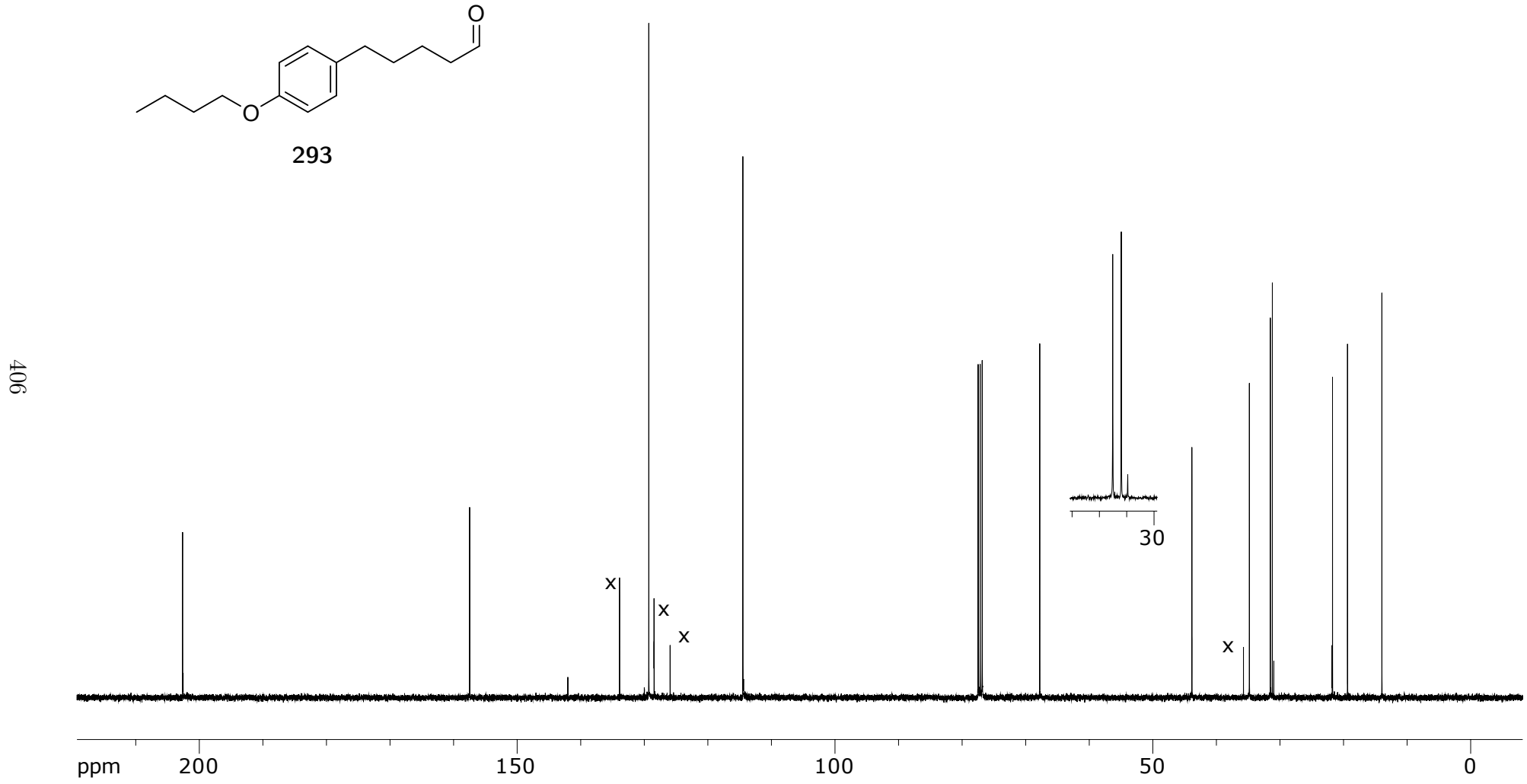

Figure A.172: 100 MHz ^{13}C NMR spectra of **293** in $CDCl_3$

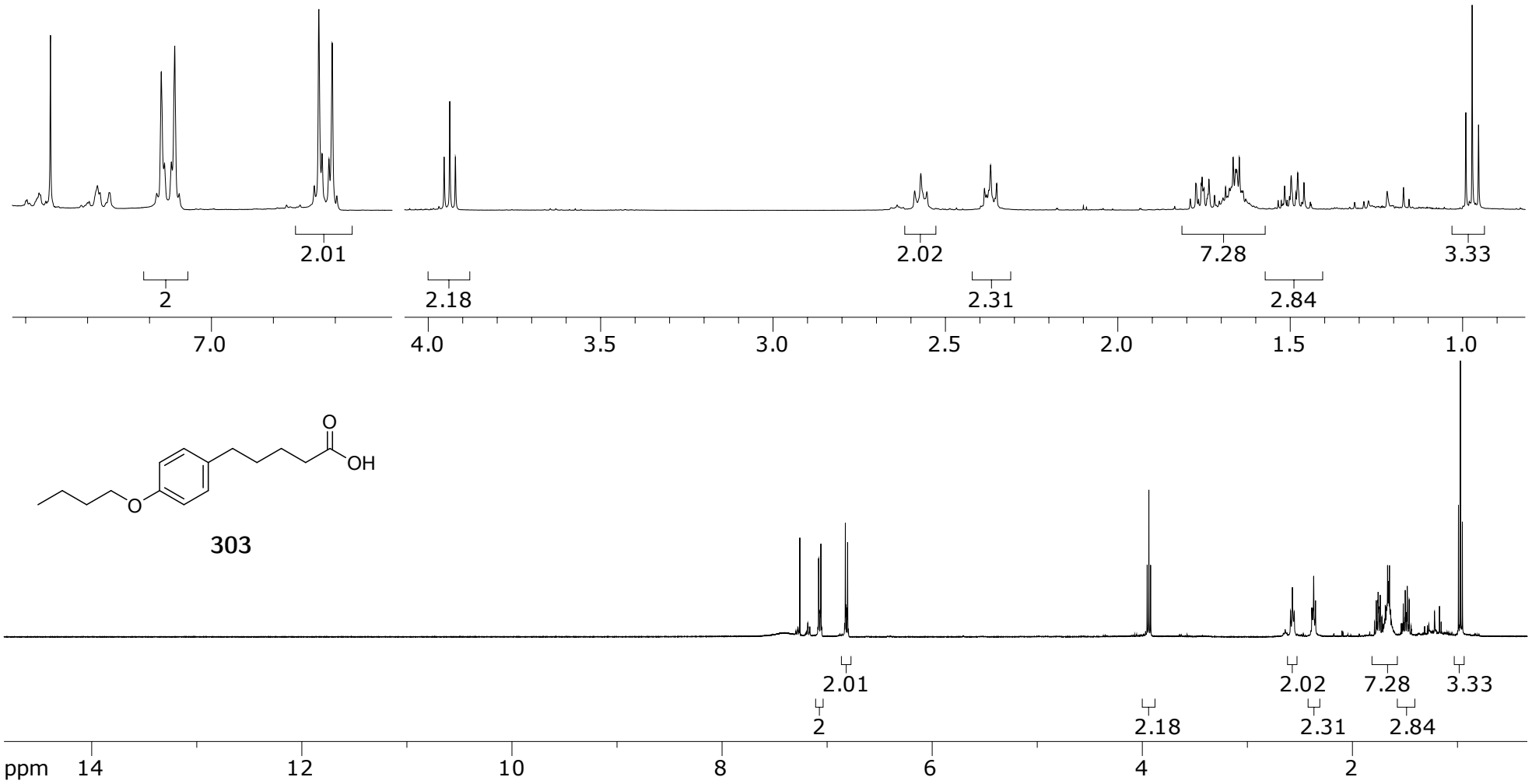

Figure A.173: 400 MHz ^{1}H NMR spectra of **303** in $CDCl_3$

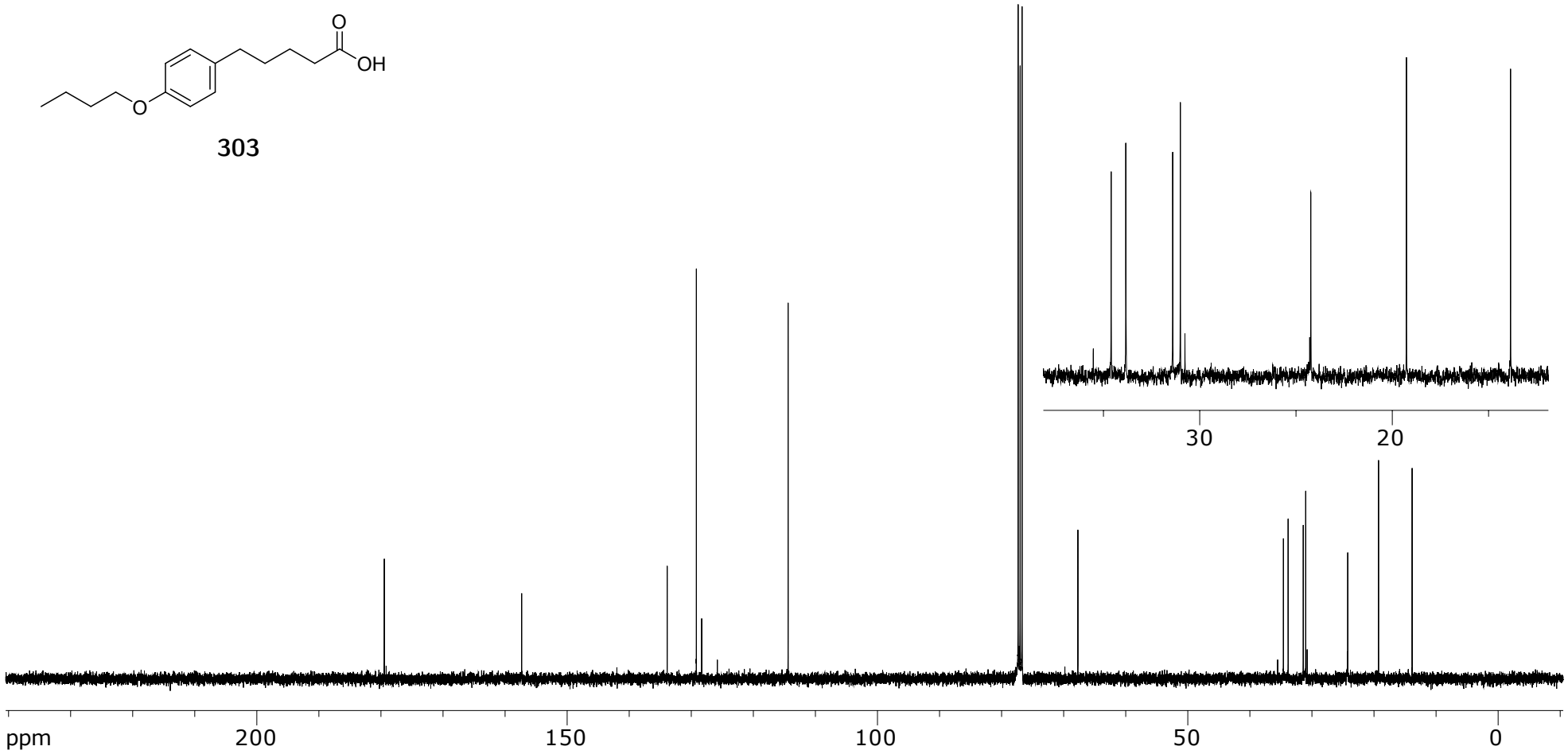

Figure A.174: 100 MHz ^{13}C NMR spectra **303** in $CDCl_3$

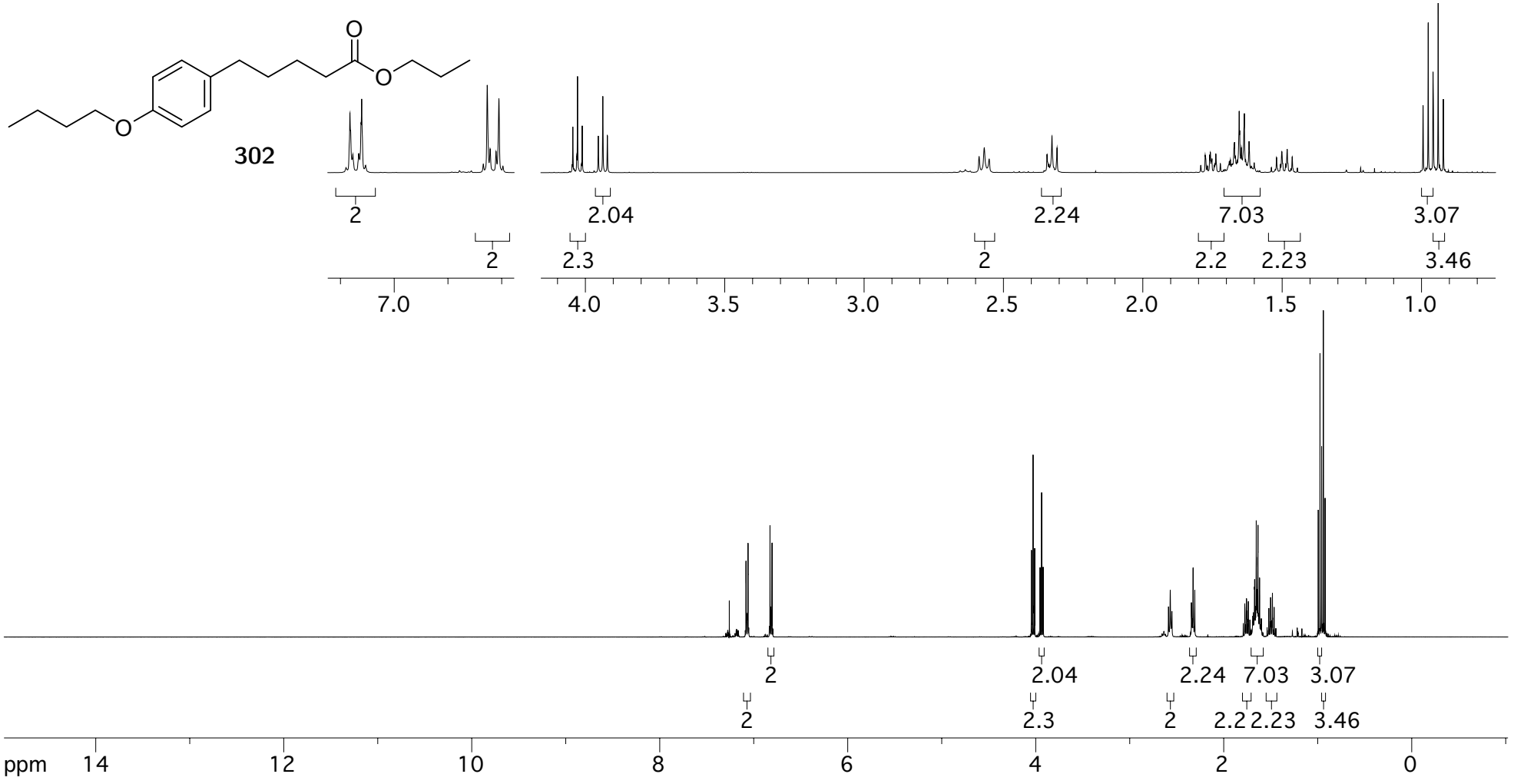

Figure A.175: 400 MHz ^{1}H NMR spectra of **302** in $CDCl_3$

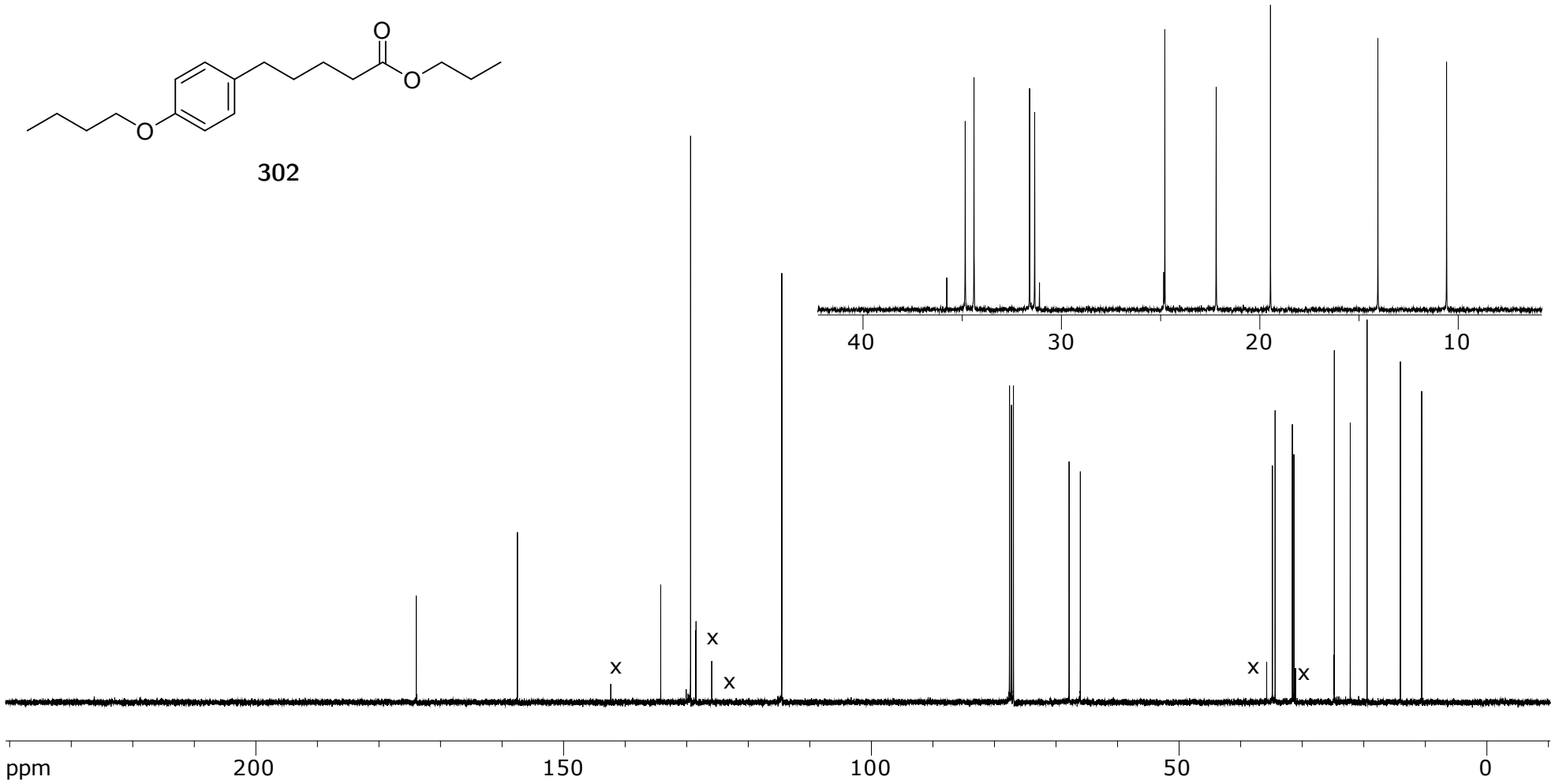

Figure A.176: 100 MHz ^{13}C NMR spectra **302** in $CDCl_3$

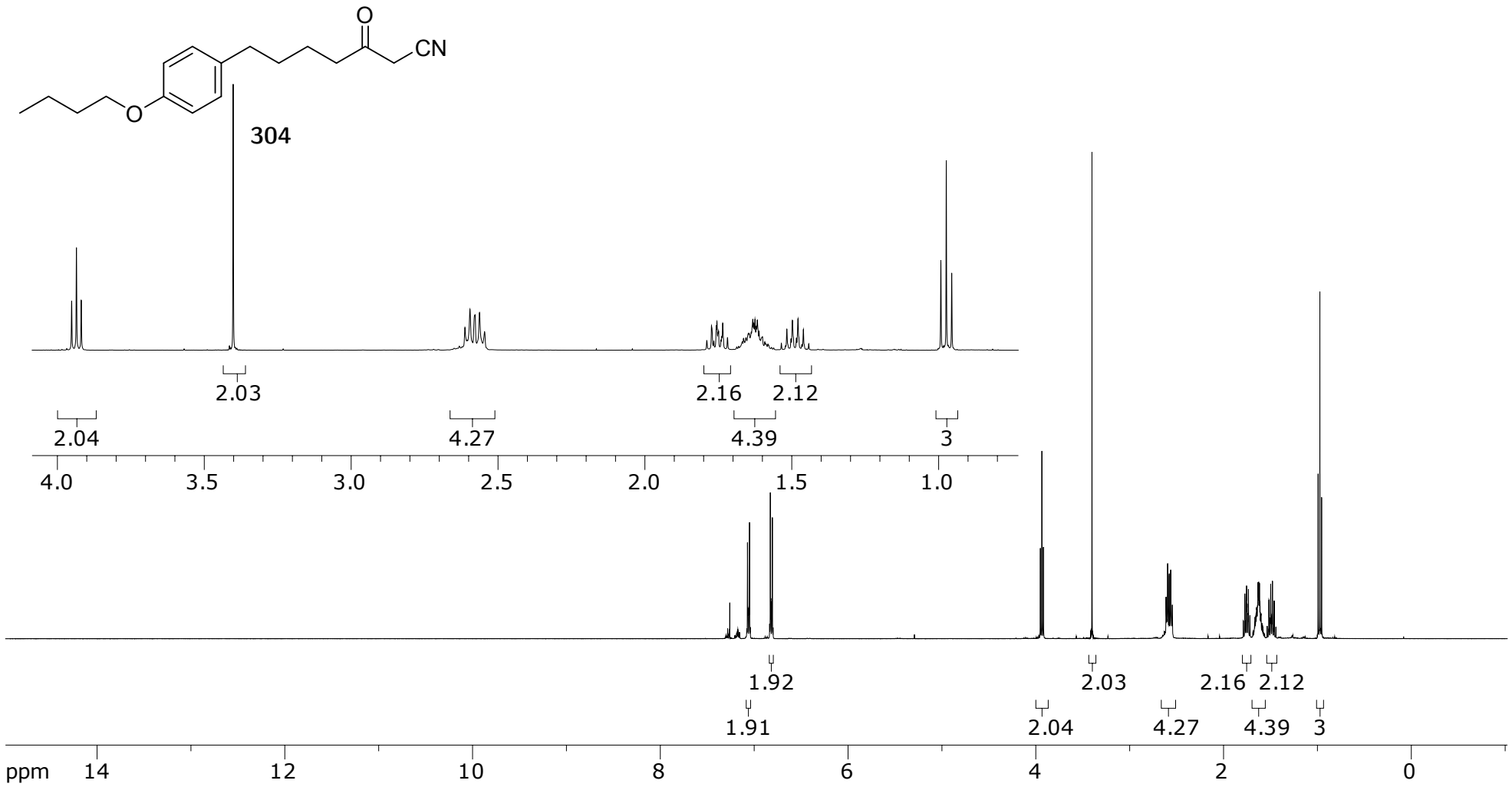

Figure A.177: 400 MHz ^{1}H NMR spectra of **304** in $CDCl_3$

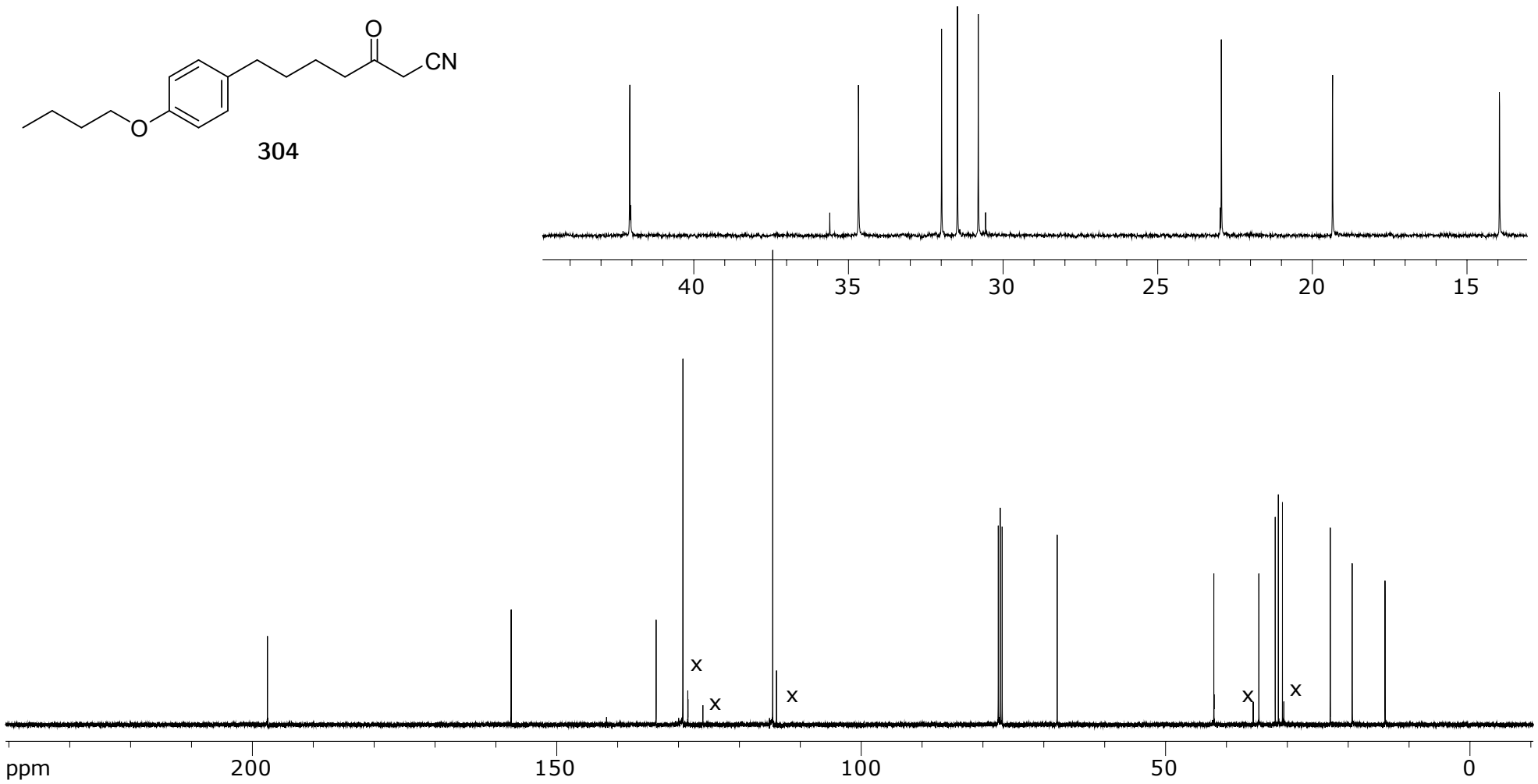

Figure A.178: 100 MHz ^{13}C NMR spectra **304** in $CDCl_3$

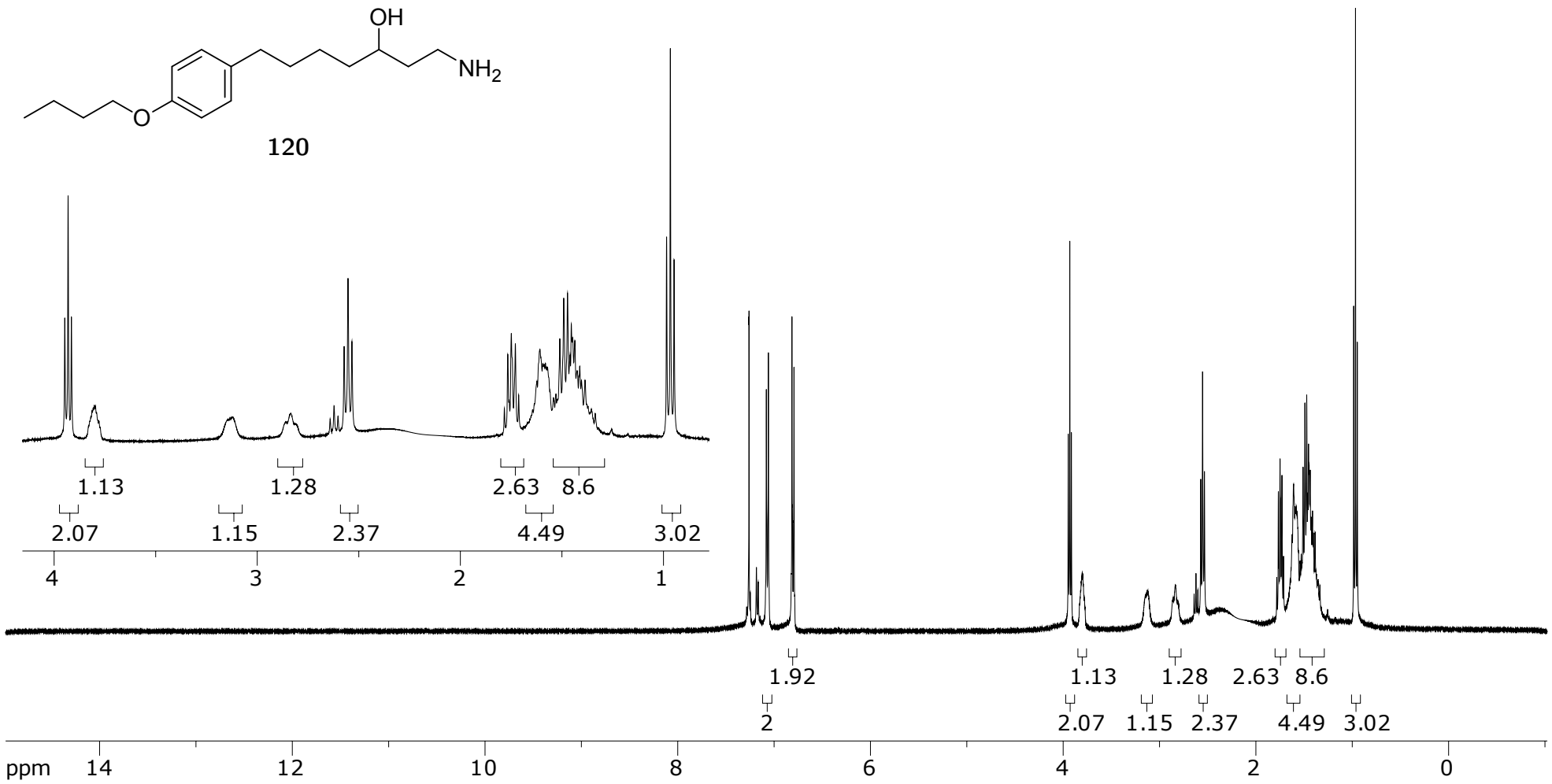

Figure A.179: 400 MHz ^{1}H NMR spectra of **120** in $CDCl_3$

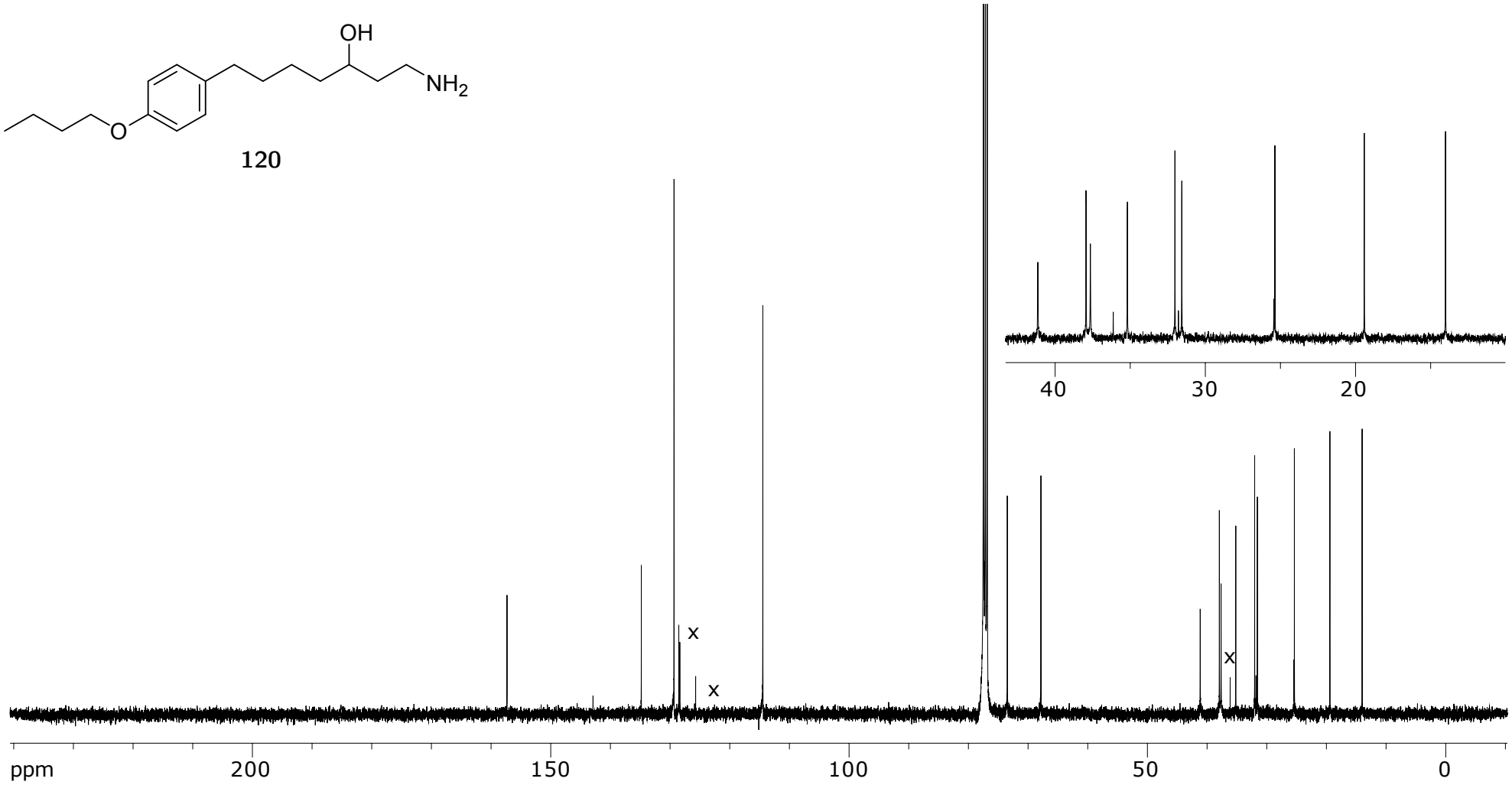

Figure A.180: 100 MHz ^{13}C NMR spectra **120** in $CDCl_3$